BCEE2

Conference Proceedings

The Second International Conference on Buildings, Construction & Enviromental Engineering

BCEE2

October 17-18, 2015 - Beirut, Lebanon

Vol. V, Sanitary, Environment & Water Resources

The 2nd International Conference of Buildings, Construction and Environmental Engineering (BCEE2-2015)

SUPREME COMMITTEE

1. **Prof. Amin D. Thamir, UOT, Iraq/ Chair**
2. **Prof. Ryiad H. Hadi, UOT, Iraq**
3. **Prof. Makram Suidan, AUB, Lebanon**
4. **Prof. Mohamed Harajli, AUB, Lebanon**
5. **Eng. Estabraq I. El-Showq, MOCH, Iraq**
6. **Eng. Ibrahem Mustafa, Mayoralty of Baghdad, Iraq**
7. **Eng. Raad A. Abdulamir, MOWR, Iraq**
8. **Eng. Fouad A. Hamid, NIC, Iraq**

INTERNATIONAL ADVISORY COMMITTEE

1. **Prof. Riadh S. Al-Mahaidi, Swinburne University, Australia/Chair**
2. **Prof. Muthana H. Al-Dahan, University of Missouri, USA**
3. **Prof. Husham Al-Mansour, National Research Council, Canada**
4. **Prof. Tom Schanz, Ruhr University Bochum, Germany**
5. **Prof. Siamak Yazdani, North Dakota State University, USA**
6. **Prof. Andrzej M. Brandt, Polish Academy of Sciences, Poland**
7. **Prof. Caijun Shi, Hunan University, China**
8. **Prof. Namir K. Al-Saoudi, Australia**
9. **Prof. Hanaa A. Yousif, University of Akron, USA**
10. **Prof. Mohamed N. Hadi, University of Wollongong, Australia**

ORGANIZING COMMITTEE

1. **Prof. Ryiad H. Hadi, UOT, Iraq / Chair**
2. **Assoc. Prof. Ghassan Chehab, AUB, Lebanon/Co-Chair**
3. **Prof. Tareq S. Hadi, UOT, Iraq/ Co-Chair**
4. **Assist. Prof. Issam Srour, AUB, Lebanon**
5. **Assist. Prof. George Saad, AUB, Lebanon**
6. **Assist. Prof. Faris H. Mohammed, UOT, Iraq**
7. **Assist. Prof. Hasan H. Joni, UOT, Iraq**
8. **Assist. Prof. Mohammed A. Mahmoud, UOT, Iraq**
9. **Ms. Zakeya Deeb, AUB, Lebanon/ Exec Admin Assist**
10. **Mr. Helmi EL Khatib, AUB, Lebanon**

LOCAL SCIENTIFIC COMMITTEE

1. **Prof. Shakir A. Salih, UOT, Iraq / Chair**
2. **Prof. Emu. Kaiss F. Sarsam, UOT, Iraq**
3. **Prof. Hussain H. Karim, UOT, Iraq**
4. **Prof. Aqeel Al-Adili, UOT, Iraq**
5. **Prof. Abdulrazzaq T. Ziboon, UOT, Iraq**
6. **Prof. Mohammed Y. Fattah, UOT, Iraq**
7. **Prof. Nabeel A. Jadoo'a, UOT, Iraq**
8. **Prof. Hisham K. Ahmed, UOT, Iraq**
9. **Prof. Abdulhameed M. Jawad, UOT, Iraq**
10. **Assoc. Prof. Shadi Najjar, AUB, Lebanon**
11. **Assist. Prof. Abbas K. Zidan, UOT, Iraq**
12. **Assist. Prof. Waleed A. Abbas, UOT, Iraq**
13. **Assist. Prof. Hasan A. Omran, UOT, Iraq**
14. **Assist. Prof. Falah H. Rahil, UOT, Iraq**
15. **Assist. Prof. Mahmoud S. Mahdi, UOT, Iraq**
16. **Assist. Prof. Maan S. Hassan, UOT, Iraq**
17. **Dr. Hussain L. Zamil, MOWR, Iraq**
18. **Dr. Suhair K. Al-Habbobi, MOCH, Iraq**
19. **Eng. Ammar M. Abdulrassol, NIC, Iraq**
20. **Assist. Prof. Nisreen S. Mohammed, UOT, Iraq / Rapporteur and Secretary**
21. **Dr. Wael Shawky Abdulsahib, UOT, Iraq / Rapporteur and Secretary**

SPONSORS OF THE CONFERENCE

Our thanks and appreciation to the supporting points of the Conference

Ministry of Higher Education and Scientific Researches, Iraq

Hanwha Engineering and Construction Bismayah Project, Iraq

Veolia For Water Technology CO. France

Fugro - Maps, Lebanon

Al-Tariq Engineering Bureau for Pile Testing Iraq

PREPARATION COMMITTEE OF THIS BOOK

1. **Prof. Aqeel Al-Adili**
2. **Dr. Wael Shawky Abdulsahib**
3. **Dr. Bassman R. Muhammad**
4. **Eng. Luay Yaly**

REVIEWERS OF THIS TOPIC

1. **Prof. Dr. Riyad Hassan Al-Anbari**
2. **Prof. Dr. Aqeel Al-Adili**
3. **Ass. Prof. Haider Alwash**
4. **Dr. Mahmoud Saleh Mahdi**
5. **Dr. Adawiya J. Haider**
6. **Dr. Adel M. Rabee**
7. **Dr. Ahmed A. H. Al-Amiery**
8. **Dr. Ali Sadiq Abas**
9. **Dr. Amer Al-Hadad**
10. **Dr. Ayad Sleeby**
11. **Dr. Azhar A. Al-Saboonchi**
12. **Dr. Faiza E. Gharib**
13. **Dr. Faris Al Ani**
14. **Dr. Ghassan Adham**
15. **Dr. Hassan Ali Omran**
16. **Dr. Hussain Musa Hussain**
17. **Dr. Jaafar S. Maatooq**
18. **Dr. Khalid A. Rasheed**
19. **Dr. Khalid Ajmee Sukkar**
20. **Dr. Maan S. Hassan**
21. **Dr. Maitham Al-Maliky**
22. **Dr. Moutaz A. Aldabbas**
23. **Dr. Sadiq Eliwy**
24. **Dr. Saleh Eysa Khassaf**
25. **Dr. Sedik A. K. Alhiyaly**
26. **Dr. Thair Shareef**
27. **Dr. Faris J. M. Alomarah**
28. **Dr. Saadi M. D. Nazal**

Table of Contents

Development of New Formula for Computing Total Sediment Loads at Upstream of Al-Shamia Barrage

Dr. Saleh I. Khassaf, Dr. Safaa K.Hashim, and M.Sc. Nasseem M. Sharba

Abstract— **This research was conducted to estimate the total amount of Sediment Load at the up-stream of Al-Shamia Barrage, which is located in the middle of Iraq within the province of Diwaniya. Twenty four cross-sections were selected along the reach of Euphrates River to study the characteristics and the rate of transport of sediments. The measured data included: cross-sections of the channel, average velocity, discharge, water surface width, slope, sediment concentration, bed material samples as well as the specific gravity of bed sediments.**

For the purpose of estimating the real and accurate amount of total sediment discharge, technical dimensional analysis has been used to find the relationship to calculate the transition sediment discharge that fit with the hydraulic conditions and properties of bed materials in the Euphrates River in the extension fact at the upstream of Al-Shamia Barrage. A new formula was obtained fit with the hydraulic conditions at the upstream of Al-Shamia Barrage and it was good formula.

Finally, the estimation of the average predicted annual total sediment discharge was made by using the new formula to be (111000) ton.

Key words: Sediments, Total load, Al-Shamia Barrage, Dimensional analysis.

List of symbols

Symbol	Quantity
B	Width of river.
C	Concentration of suspended sediment.
d_{50}	Median grain size.
Q_s	Total sediment discharge.
Q	Water discharge
Qs	Total sediment load.
R_h	Hydraulic radius.
U_*	Shear velocity.
V	Mean velocity.
V	Volume of sample.
W_1	Weight of dry filter paper.
W_2	Weight of dry filter paper + suspended sediment.
w_s	Fall velocity of particle.
ρ_s	Density of sediment.
ν	Kinematics viscosity.

1-INTRODUCTION

Sediment (sometimes called "silt" or "alluvium") is comprised of solid particles of mineral and organic material that are transported by water. In river systems the amount of sediment transported is controlled by both the transport capacity of the flow and the supply of sediment. The "suspended sediment load" refers to the fine sediment that is carried in suspension and this can comprise material picked up from the bed of the river (suspended bed material) and material washed into the river from the surrounding land (wash load). The wash load is usually finer than the suspended bed material.[7]Usually, the transport of particles by rolling, sliding and satiating is called bed-load transport, while the suspended particles are transport as suspended load transport. [9]

The suspended load may also include the fine silt particles brought into suspension from the catchment area rather than from the streambed material (bed material load) and is called the wash load. Bed load and suspended load may occur simultaneously, but the transition zone between both modes of transport is not well-defined.

There are a number of formulas to compute the total sediment load. Most of these equations have some theoretical and empirical bases. They were derived under very limited conditions of flow and sediment characteristics. All of them have shown good results when used to compute the sediment load for conditions similar to those under which they were derived. On the other hand, very poor results are obtained when they were applied for different conditions.

The most important reason for choosing this site to study is the accumulation of sediment in the up-stream of Al-shamia Barrage. The sediment was amounted to about three meters, which led to the closure of four out of six gates. There weren't any researcher studied this region in direct approach to estimate the amount of sediment.

2-Description of the Study Region

The region of this study, Figure (1) is located between the towns of Kifil and Shinafiya, extending between latitudes 31° 55' and 32° 15' N and longitudes 43° 55' and 44° 45' E. Al-shamia Barrage is located on the Euphrates river at Al-Diwaniya city in Iraq.

The maximum design discharge of this barrage is 1100 m^3/sec with water level of 22.5 m above mean sea level (a.m.s.l). Al-Shamia Barrage was constructed during 1986 to control the flow in the middle Euphrates region by using six radial gates.

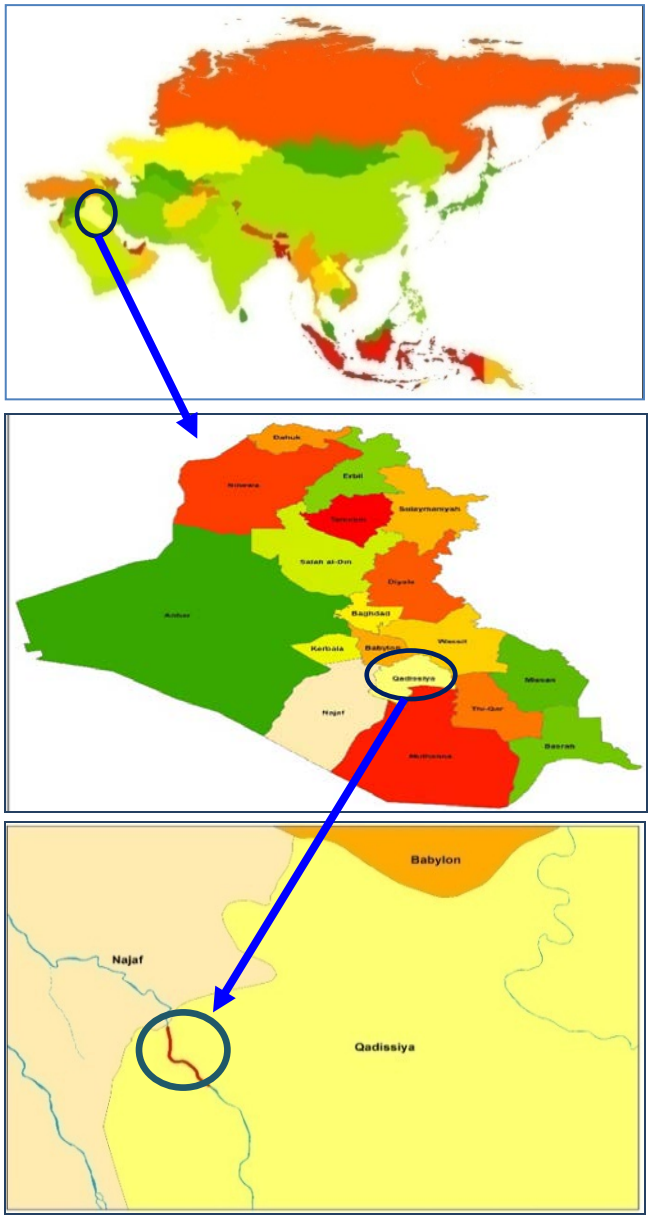

Figure (1): location of the study area

3-Field Measurement

In this study, the collected field data includes the following measurement data.

1- Data of the cross-section which can be found on the top width, the cross sectional area, and wetted perimeter of the bank as a function of depth.
2- Water discharge, temperatures, and flow velocity of the river for all the cross-sections along the considered region.
3- Representative samples of the bed sediment.
4- Representative samples of the suspended sediment.

Figure (2) shows the distribution of the sections along the search area.

Figure (2): The location of cross sections.

Tools

In this research, three devices were used; these are Acoustic Doppler Current Profiles (ADCP), Van Veen Grab Sampler, and Suspended load sampler as the work requires completing the field work.

3-1 Acoustic Doppler Current Profiles (ADCP)

The M9 has a 5-inch (13-cm) diameter Delrin housing. It has two sets of velocity measurement transducers; both in a Janus configuration – four 3.0-MHz transducers and four 1.0-MHz transducers. A 0.5-MHz vertical acoustic beam (echo sounder) provides depth data as shown in figure (3). [6]

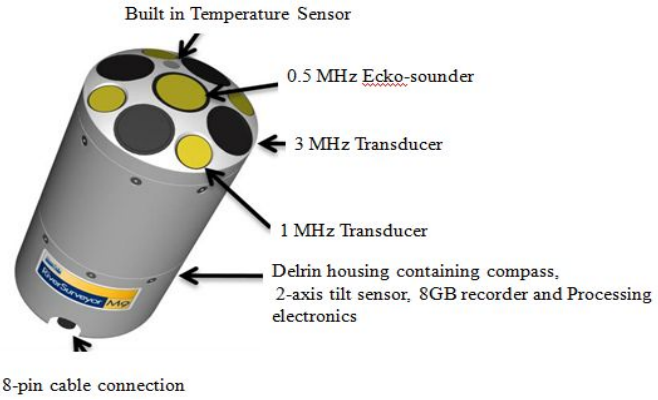

Figure (3): M9 ADCP Features [6]

The device (ADCP) is used to draw twenty-four cross-sections in the river. Thus, the discharge, velocity, area, and temperature are found for each section. SonTek River Surveyor (SRS) program starts recording all information after interconnecting with ADCP device. All information about work to computed discharge, cross-section area, and other hydraulic properties appear in (SRS) program. The observed cross-sections, discharge and velocity resulted from the program are listed in table (1).

Table (1): The cross-section area, discharge, velocity and hydraulic radius for each section.

Section number	Cross-section area (m^2)	Discharge (m^3/sec)	Velocity (m/sec)	Hydraulic radius (m)
1	133.5	31.14	0.233	1.22
2	197.8	55.4	0.28	1.77
3	117	32.29	0.276	1.5
4	126.2	57.94	0.459	2.04
5	67.8	33.14	0.489	1.15
6	96.2	31.33	0.326	1.97
7	95	33.99	0.358	1.05
8	85.6	40.92	0.478	1.64
9	176.1	36	0.204	2.27
10	93.4	28.58	0.306	2.27
11	109.7	38.61	0.352	1.46
12	89.4	34.48	0.386	1.81
13	206.7	30	0.145	2.46
14	91.6	44.34	0.484	1.15
15	68	39.7	0.584	1.16
16	214.6	53.85	0.251	2.29
17	86.4	33.98	0.393	1.39
18	129	33.8	0.262	1.56
19	245.1	62.03	0.253	3.41
20	92.5	34.99	0.378	1.17
21	132	50.45	0.382	2.21
22	83.4	33.89	0.406	1.21
23	83.8	33.96	0.405	1.21
24	244.1	57	0.234	2.83

3-2 Van Veen Grab Sampler:

The stainless steel Van Veen Grabs are made and used for taking disturbed samples from the bottom of rivers, lakes, etc. Various designs can be supplied. The smaller designs are manually controlled. The mode of operation of all Van Veen Grabs is the same [5].

After viewing the specifications, the dimensions of the device and the way currency are determined. The researcher manufactures a device that is quite similar to Van Veen Grab Sampler adopted universally from where the shape, dimensions, weight and way of working to take samples from the bottom of the river. Figure (4) and (5) shows this device.

Bed material samples are taken for sampling verticals 1/4, 1/2, 3/4 width of the river cross-section. The obtained samples are mixed together and part of the mixture is taken to the laboratory for analysis. [1]

Figure (4): Van Veen Grab after sampling

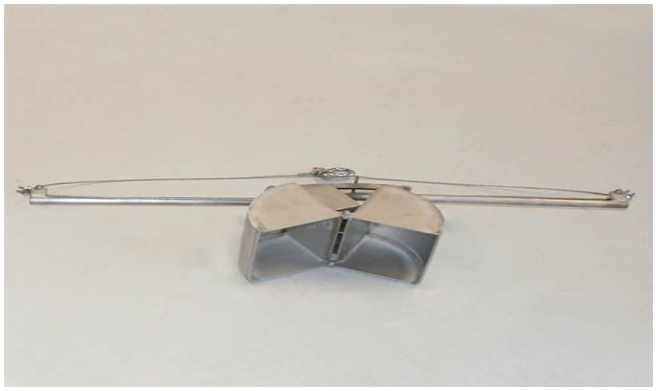

Figure (5): Van Veen Grab before sampling

3-3 Suspended Load Sampling:

In this research, the Integrated Sampler type was used to collect samples of suspended materials. The device was manufactured by the researcher as shown in figure (6) and (7). It consists of a bottle with capacity of one liter and an intake nozzle of (8 mm) in diameter. The air is escaped from long plastic tube (5 mm) diameter and there is a valve to control the entering of a mixture of suspended materials and water into the sampler.

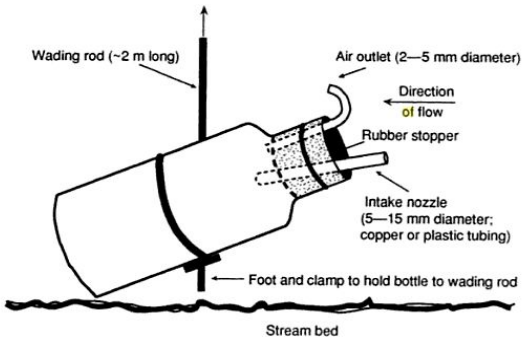

Figure(6):Sketch of the manufactured suspended sampler [4].

Figure (7): The manufactured suspended sampler.

The selection of sampling verticals at the 1/4, 1/2, and 3/4 width of a stream cross section is convenient and practical. This method provides more information concerning the distribution and discharge of sediment than the single-vertical method [3].

In this study, the sampling verticals are chosen at 1/4, 1/2, and 3/4 of the width of stream at each cross section as shown in figure (8).

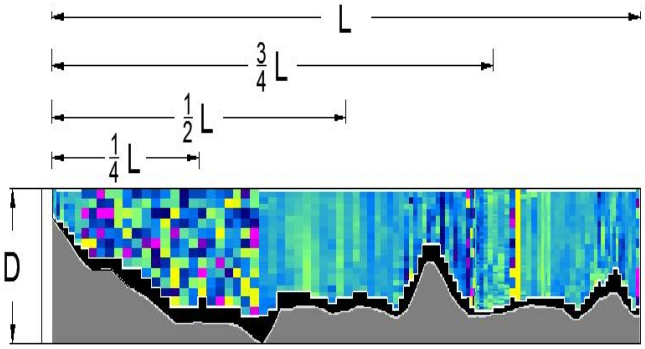

Figure (8): Selection of sampling vertical.

4- Laboratory Measurements

The laboratory work is essential for the size distribution that represents the configuration of bed materials to obtain specific gravity, texture, size, and sediment concentration.

Table (2) shows the values of a specific gravity of bed sediment material at each section. The average value of the specific gravity for all section is 2.69.

Table (2): Specific gravity of the bed sediment material.

Sec. No.	specific gravity	Sec. No.	specific gravity
1	2.62	13	2.6
2	2.65	14	2.71
3	2.67	15	2.69
4	2.69	16	2.68
5	2.68	17	2.68
6	2.68	18	2.66
7	2.6	19	2.65
8	2.69	20	2.66
9	2.65	21	2.65
10	2.72	22	2.65
11	2.68	23	2.65
12	2.69	24	2.65

4-1 Sieve Analysis

By means of sieving, a grain size distribution of the bed-material sample can be obtained, which generally shows a relation between percentages by weight versus grain size, called the gradation curve. [8]

In this research, seven sieves were used for analysis (0.84, 0.425, 0.3, 0.25, 0.212, 0.15 and 0.075) mm. Figure (9) shows the accumulative size-frequency curve for the first cross section. Table (3) shows the mean diameter of the sediment in each cross section.

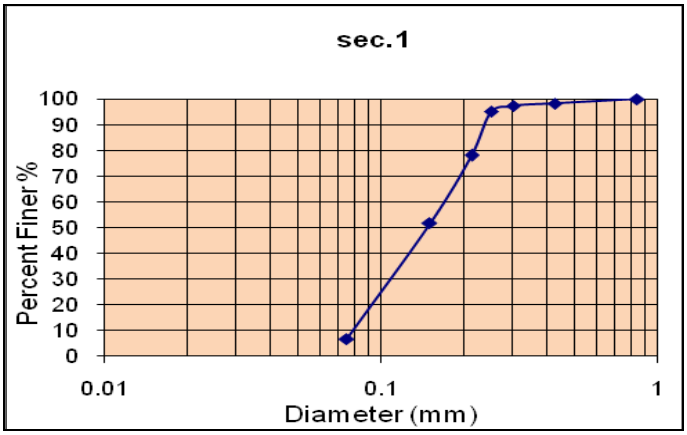

Figure (9): Size distribution curve, section No.1

Table (3): Mean sediment particle diameter

Section No.	d_{50} (mm)	Section No.	d_{50} (mm)
1	0.148	13	0.172
2	0.167	14	0.156
3	0.178	15	0.164
4	0.173	16	0.162
5	0.180	17	0.176
6	0.182	18	0.186
7	0.191	19	0.189
8	0.182	20	0.179
9	0.175	21	0.186
10	0.181	22	0.183
11	0.180	23	0.2
12	0.170	24	0.185

4-2 Sediment Concentration Measurement

Depending on two methods filtration and evaporation, the concentration of suspended sediment is usually determined in the laboratory. The second method is used when the concentration of sediment is high: it is hard and requires much time to filter a large enough volume of sample. In this research the filtration method is used.

Concentration of the suspended sediment is estimated using equation (1):

$$C = (W_2 - W_1) / V \quad \text{..... (1)}$$

Where:

C = Concentration of suspended sediment in (ppm) or (mg/l),

W_1 = Weight of dry filter paper in (mg),
W_2 = Weight of dry filter paper + suspended sediment in (mg),
V= Volume of sample (l).

5-Sediment Discharge Measurement

The measurement of sediment discharge is essential to determine the quantity of sediment load to establish or check analytical or empirical sediment transport equations. The sediment discharge can be calculated by multiplying the concentration with the flow discharge. [9]

$$Q_s = C \times Q \times 0.001 \quad \text{..... (2)}$$

Where:
Q_s = Total sediment discharge (kg/sec),
Q = Water discharge (m^3/sec).

Table (4) illustrates the calculated sediment discharge resulting from equation (3-2).

Table (4): Sediment discharge(from Eq. 2)

Section No.	Water discharge (m^3/sec)	Concentration (g/m^3)	Sediment discharge (kg/sec)
1	31.14	98	3.05
2	55.4	97	5.37
3	32.29	95	3.07
4	57.94	93	5.39
5	33.14	85	2.82
6	31.33	92	2.88
7	33.99	98	3.33
8	40.92	87	3.56
9	36	72	2.59
10	28.58	85	2.43
11	38.61	94	3.63
12	34.48	81	2.79
13	30	88	2.64
14	44.34	101	4.48
15	39.7	105	4.17
16	53.85	78	4.2
17	33.98	93	3.16
18	33.8	87	2.94
19	62.03	105	6.51
20	34.99	83	2.9
21	50.45	104	5.25
22	33.89	75	2.54
23	33.96	85	2.89
24	57	89	5.07

6-Data Used

In this research, the data used for hydraulic and sediment characteristics were collected from 24 sections in the Euphrates River distributed along the study area upstream of Al-shamia Barrage. The collected data were discharge, velocity, width, cross-sectional area, and observed suspended sediment load from the field measurements. The flow depth in study reach ranged from (1 to 5) meters, with flow ranging from (28.5 to 62) m^3/sec. The flow velocities ranges from (0.145 to 0.584) m/sec and the median sediment size (0.177) mm.

A summary of data used in the study is presented in Table (5).

Table (5): Primary data and parameters

Sec. No	1	2	3
Q_w(m^3/sec)	31.14	55.4	32.29
V (m/sec)	0.233	0.28	0.276
G_s	2.67	2.65	2.65
d_{50} (mm)	0.148	0.167	0.178
A (m^2)	133.5	197.8	117
B (m)	109.28	111.95	77.75
R_h (m)	1.22	1.77	1.5
ν (m^2/sec)	1.25×10^{-6}	1.21×10^{-6}	1.21×10^{-6}
W_s (m/sec)	0.013306	0.016724	0.018839
U_* (m/sec)	0.0424	0.051	0.047
Sec. No	**4**	**5**	**6**
Q_w(m^3/sec)	57.94	33.14	31.33
V (m/sec)	0.459	0.489	0.326
G_s	2.69	2.68	2.68
d_{50} (mm)	0.173	0.18	0.182
A (m^2)	126.2	67.8	96.2
B (m)	61.73	59.1	48.78
R_h (m)	2.04	1.15	1.97
ν (m^2/sec)	1.15×10^{-6}	1.15×10^{-6}	1.16×10^{-6}
W_s (m/sec)	0.01889	0.020065	0.020298
U_* (m/sec)	0.0548	0.0411	0.0538
Sec. No	**7**	**8**	**9**
Q_w(m^3/sec)	33.99	40.92	36
V (m/sec)	0.358	0.478	0.204
G_s	2.6	2.69	2.67
d_{50} (mm)	0.191	0.182	0.175
A (m^2)	95	85.6	176.1
B (m)	90.33	52.21	77.64
R_h (m)	1.05	1.64	2.27
ν (m^2/sec)	1.17×10^{-6}	1.15×10^{-6}	1.16×10^{-6}
W_s (m/sec)	0.020904	0.020539	0.018924
U_* (m/sec)	0.0393	0.0491	0.0578
Sec. No	**10**	**11**	**12**
Q_w(m^3/sec)	28.58	38.61	34.48
V (m/sec)	0.306	0.352	0.386
G_s	2.65	2.72	2.68
d_{50} (mm)	0.181	0.18	0.17
A (m^2)	93.4	109.7	89.4
B (m)	41.22	75.33	49.45
R_h (m)	2.27	1.46	1.81
ν (m^2/sec)	1.21×10^{-6}	1.25×10^{-6}	1.12×10^{-6}
W_s (m/sec)	0.019165	0.019211	0.018629
U_* (m/sec)	0.0578	0.0464	0.0516
Sec. No	**13**	**14**	**15**
Q_w(m^3/sec)	30	44.34	39.7
V (m/sec)	0.145	0.484	0.584
G_s	2.69	2.6	2.71
d_{50} (mm)	0.172	0.156	0.164
A (m^2)	206.7	91.6	68

B (m)	83.98	79.56	58.86
R_h (m)	2.46	1.15	1.16
ν (m^2/sec)	1.07×10^{-6}	1.15×10^{-6}	1.02×10^{-6}
W_s (m/sec)	0.019776	0.015068	0.019164
U_* (m/sec)	0.0602	0.0411	0.0413
Sec. No	**16**	**17**	**18**
Q_w (m^3/sec)	53.85	33.98	33.8
V (m/sec)	0.251	0.393	0.262
G_s	2.69	2.68	2.68
d_{50} (mm)	0.162	0.176	0.186
A (m^2)	214.6	86.4	129
B (m)	93.71	62.24	82.65
R_h (m)	2.29	1.39	1.56
ν (m^2/sec)	1.12×10^{-6}	1.04×10^{-6}	1.05×10^{-6}
W_s (m/sec)	0.017268	0.020861	0.022619
U_* (m/sec)	0.058	0.0452	0.0479
Sec. No	**19**	**20**	**21**
Q_w (m^3/sec)	62.03	34.99	50.45
V (m/sec)	0.253	0.378	0.382
G_s	2.66	2.65	2.66
d_{50} (mm)	0.189	0.179	0.186
A (m^2)	245.1	92.5	132
B (m)	71.88	79.23	59.82
R_h (m)	3.41	1.17	2.21
ν (m^2/sec)	1.02×10^{-6}	1×10^{-6}	1×10^{-6}
W_s (m/sec)	0.023429	0.021712	0.023174
U_* (m/sec)	0.0708	0.0415	0.057
Sec. No	**22**	**23**	**24**
Q_w (m^3/sec)	33.89	33.96	57
V (m/sec)	0.406	0.405	0.234
G_s	2.65	2.65	2.67
d_{50} (mm)	0.183	0.208	0.185
A (m^2)	83.4	83.8	244.1
B (m)	68.82	69.53	86.34
R_h (m)	1.21	1.21	2.83
ν (m^2/sec)	1×10^{-6}	1×10^{-6}	1×10^{-6}
W_s (m/sec)	0.02248	0.025745	0.023099
U_* (m/sec)	0.0422	0.0422	0.0645

7- Development of A New Formula:

The dimensional analysis is a good method in dealing with a complex problem if it is orderly applied. The result of dimensional analysis relies on the chosen variables. A meaningful and useful result can be obtained only if each variable selected for the analysis has a physical importance pertinent to the problem involved.

Using Buckingham's π-theorem procedure as presented in [2], the variables used for the field and the laboratory work and their relationship are as follows:

$Qs = \emptyset\ (V, R_h, d_{50}, w_s, U_*, B, \rho_w, \rho_s, \nu)$.

Or F $(Qs, V, R_h, d_{50}, w_s, U_*, B, \rho_w, \rho_s, \nu) =$ constant

The number of primary dimensions involved is 3, i.e., m = 3 (M, L, T). The total numbers of variables are 10. Therefore, the number of π-terms is (7). Thus, F $\{\pi_1, \pi_2, \pi_3, \pi_4, \pi_5, \pi_6, \pi_7\} =$ constant

Taking ρ_w, w_s, d_{50} as repeating variables, the results of the analysis are shown in Table (6).

Table (6): π parameters

π	π_1	π_2	π_3	π_4	π_5	π_6	π_7
Par.	$\frac{Qs}{\rho_w w_s d_{50}^2}$	$\frac{V}{w_s}$	$\frac{R_h}{d_{50}}$	$\frac{U_*}{w_s}$	$\frac{B}{d_{50}}$	$\frac{\rho_s}{\rho_w}$	$\frac{\nu}{d_{50} w_s}$

Then, the equation can be expressed as the following:

$$\frac{Qs}{\rho_w w_s d_{50}^2} = F\ (V/w_s)\ (R_h/d_{50})\ (U_*/w_s)\ (B/d_{50})\ (\rho_s/\rho_w)\ (\nu/d_{50} w_s)$$

The following procedure was followed to reduce the number of π-terms:

$\pi_2 \times \pi_4 = \pi_8 = (V/w_s) \times (U_*/w_s) = (U_* V/ w_s^2)$

Using the same approach, π_3 and π_7 can be combined to evaluate π_9

$\pi_3 / \pi_7 = \pi_9 = (\frac{R_h/d_{50}}{\nu/(d_{50} w_s)}) = (R_h w_s/ \nu)$

Thus, the functional relationship becomes:

$Qs/ \rho_w w_s d_{50}^2 =$ F $(U_* V/ w_s^2)\ (R_h w_s/ \nu)\ (B/d_{50})\ (\rho_s/ \rho_w)$

The final form of the formula has to be determined by the conducting of the regression analysis on the observed data. Taking into consideration that the observed data were divided into two groups, the first group consisting of sixteen sections was used to derive a new formula, while the second group (8 sections) was used to verify the new formula. The regression analysis was conducted and be found by using the following formula:

$$Qs = 32 \times 10^{-4} \rho_s\ w_s\ d_{50}\ (\frac{U_* V}{w_s^2})^{1.07}\ (\frac{R_h w_s}{\nu})^{0.32} (B) \quad \ldots (3)$$

Where:

Qs = Total sediment load (kg/sec),
ρ_s = Density of sediment (kg/m^3),
w_s = Fall velocity of particle (m/sec),
d_{50} = Median grain size (m),
U_* = Shear velocity (m/sec),
V = Mean velocity (m/sec),
R_h = Hydraulic radius (m),
ν = Kinematics viscosity (m^2/sec) and
B = Width of river (m).

The coefficient of determination of formula (3) was found to be equal (R^2=0.93). Figure (10) shows a relationship between the predicted and the observed values of sediment discharge for 16 sections. Table (7) contains the predicted and the observed values of sediment discharge.

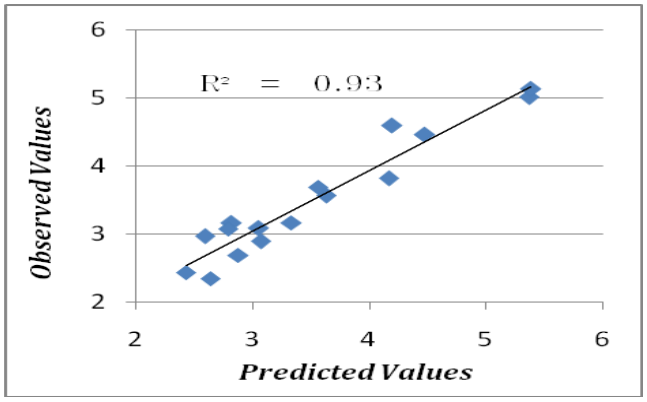

Figure (10): Observed and predicted values for (16) sections.

Figure (10) shows the well congruence between the predicted and the observed sediment discharge.

Table (7): The observed and predicted values of sediment discharge for sixteen sections for C1 to C16

Section No.	Observed values(kg/sec)	Predicted values (kg/sec)
1	3.05	3.09
2	5.37	5.01
3	3.07	2.89
4	5.39	5.13
5	2.82	3.16
6	2.88	2.69
7	3.33	3.17
8	3.56	3.69
9	2.59	2.97
10	2.43	2.44
11	3.63	3.56
12	2.79	3.08
13	2.64	2.35
14	4.48	4.46
15	4.17	3.82
16	4.2	4.59

7-1 Verification of the Proposed Formula

The sediment discharge measured and predicted of eight cross sections are listed in table (8). It demonstrates the coefficient of determination (R^2=0.94), as shown in figure (11)

With the intention of certifying the suggested formula, variables form the rest of eight cross sections along the area of study site was used. This step gives an independent certification of the precision of the new formula since there are no data used to get this proposed formula.

Table (8): The observed and predicted values of the sediment discharge for the eight sections for C17 to C24

Section No.	Observed values(kg/sec)	Predicted values (kg/sec)
17	3.16	3.04
18	2.94	2.85
19	6.51	4.65
20	2.9	3.16
21	5.25	4.13
22	2.54	3.03
23	2.89	2.99
24	5.07	4.38

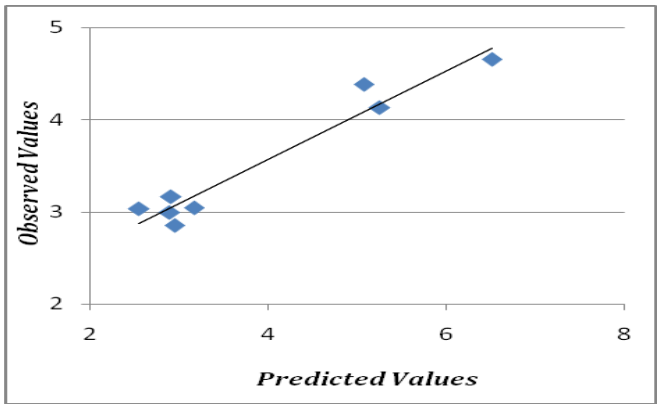

Figure (11): The Observed and predicted values for the eight sections.

A well congruence between the observed and the predicted sediment discharge can be noticed in figure (11).

8-Conclusions

Based on the results obtained in this study (Euphrates river up-stream of Al-shamia Barrage), The following conclusions can be made:

1- The sediment particle size analysis showed that the bed material of this river is composed of Sand, Silt and Clay. The large portion of bed material is sandy material, with median grain size from (0.148 to 0.2) mm.

2- A new sediment transport formula has been developed in term of five dimensionless parameters ($Qs/\rho_w w_s d_{50}^2$, $U_* V/w_s^2$, $R_h w_s/\nu$, B/d_{50} and ρ_s/ρ_w). This formula is applicable under the following conditions:

- Flow velocity (0.145 – 0.584) m/sec.
- Water discharge (30 – 60) m^3/sec.
- Concentration of suspended load (72 – 105) mg/l.
- Median grain size (0.148 – 0.2) mm.

3- The average predicted total sediment discharge in the study region is (111000) ton/year by using the new formula.

REFERENCES

[1] Adegbola, A., A., and Olaniyan, O., S.," **Estimation of Bed Load Transport in River Omi, South Western Nigeria using Grain Size Distribution Data",** Department of Civil Engineering, University of Technology, Ogbomosho, International Journal of Engineering and Technology Volume 2 No. 9,ISSN 2049-3444, 2012.

[2] Arora, K., R., **"Fluid Mechanics, Hydraulics and Hydraulic Machines"**, 1705-B, NAI SAPAK, post Box No.1106, DELHI, 2007

[3] Daryl, B. S.," **Sediment Transport Technology"**, Water Resource Publication, Forth Collins, 1976.

[4] Jamie, B., and Richard, B.**," Water Quality Monitoring - A Practical Guide to the Design and Implementation of Freshwater Quality Studies and Monitoring Programmes"**, Published on behalf of United Nations Environment Programme and the World Health Organization, UNEP/WHO, ISBN 0 419 22320 7,1996.

[5] Royal Eijkelkamp Earth Sampling Group, http.//en.eijkelkamp.com.

[6] SonTek/YSI,**" RiverSurveyor S5/M9 System Manual Firmware Version 1.0"**, CA 92121-3091, USA, 2010.

[7] UNESCO Beijing Office, and, IRTCES, **"Sediment Issues and Sediment Management in Large River Basins Interim Case Study Synthesis Report"**, International Sediment Initiative Technical Documents in Hydrology, UNESCO Office in Beijing & IRTCES, 2011.

[8] Vanoni, V. A., **"Sedimentation Engineering"**, ASCE, Manuals and Reports on Engineering Practice", No.54, ASCE, 1975.

[9] Van Rijn, L. C**.," Principles of Sediment Transport in Rivers, Estuaries and Coastal Seas"**, Aqua Publications, Amsterdam, the Netherlands, 1993.

Reduction of Scour by using Tapered Pier

* Jaafar S. Maatooq

Abstract— **The reduction of scour around bridge piers is the main target of designers . Different countermeasures methods and facilities have been adopted by researchers in field and experimental programs . The results are presented in papers and manuals for design and in field rehabilitation . This study work has been concerned by adopting a single circular tapered-shape bridge pier fixed at a center of mobile bed laboratory flume to show the advantage of this shape on reducing a scour depth around traditional circular pier . The experimental program which has been conducted was a preliminary attempt to show the percentage enhancement of local scour problem around bridge pier at clear water flow condition . The results shows that the average reduction in scour depth was 32% .**

Index Terms—**bridge piers , clear water scour , flow intensity , horseshow vortices , local scour**

I. INTRODUCTION

Recent attempts have been made to reduce scour around bridge pier , the classical one is to use rip-rap . The minimizing scour has , as well as preventing the failure of piers , another advantage that minimizing the cost of bridge by permitting smaller foundation depth . The main scour protection systems which have yield valid results are a caissons placed around the pier . The earlier study about the caisson was made by Chabert and Engeldinger,1956 tests in an experimental channel enabled them to conclude that the best system appeared to having a diameter three times the diameter of a pier , and a top elevation about half the diameter of a pier below the average natural bed . As respect to this the scour was reduced to one-third of that reached at pier without caisson [1] .

C.J. Posey [3] protected the bridge pier by means of an inverted filter extending out a distance of 1.5 to 2.5 of pier diameter in all directions . The author concluded that , a good inverted filter is necessary to prevent leaching of the bed material and the top of it should be at some distance below the mean bed level to prevent excessive exposure . More recently attempts were made to reduce scour with a circular collar around the pier , with a rectangular slot through the pier , and with a delta wing-like fine in front of the pier .

* Asst. Prof. of Hydraulic Structures Engineering ,Building & Construction Engineering ,University of Technology, Baghdad
E-mail: jaafarwes@yahoo.com : jaafarmaatooq@gmail.com

Vittal N. et. al. [6] replaces the solid pier by a group of three smaller piers angularly spaced at 120^{o} . The scour due to the group in its best orientation is compared with that of a solid cylindrical pier . The authors observed that the scour reduction is about 40% .

In present study a new type of piers were introduced by a preliminary experimental program to show its benefit on reducing the scour around bridge piers .

II. TAPERED-PIERS

This type of pier is originally suggested in the present work. Six models are presented and used in the experimental program instead of representative cylindrical pier (b=4cm) , where b, is a diameter of cylindrical pier . The first three models have the same bottom base (foundation) of a representative pier (i.e. , bB=4cm) thereby , it is tapered upward to smaller top base (bT=1.5 , 2.15 , and 2.9cm) . Whereas , the last three models have constant top base (bT=4cm) and tapered downward to smaller bottom base (bB=1.5 , 2.15 , and 2.9cm) . These models are shown in Fig.1.From this figure , it can be seen that different bases ratios may be considered as an enhancement in size of traditional cylindrical pier , at which , if appreciable reduction of scour occurs , it may be considered more reliance and greater economical than a traditional pier , so it can be adopted for bridge design . The experimental results using these models are given in Table I . As shown in this table , the scour ratio , ds/b , of cylindrical pier denoted as “original” used for comparison , where , ds, is the equilibrium scour depth which formed around pier at clear water condition . However , the ds/b(enhance) , referred to the scour ratio of tapered pier . From these results it can be concluded that , all models of tapered piers have appreciable influence on scouring process , that is reducing the scour depth as compared with original cylindrical model for the same flow situations (y=2.95cm , V=0.18338m/s) , where y and V are the flow depth and average velocity respectively and median sand particle (d50=0.575mm) . The first three models show a greater reduction of 33% , whereas , the percent reduction of the other three models is 30.7 . The average percent of this reduction was 32% . It is considered , accordingly that , the tapered piers are more efficient in reducing the scour than a cylindrical type . However , the tapered upward piers are even more efficient.

TABLE I
Experiments for Enhancement size of cylindrical pier , b=4cm

Top width b_T (cm)	Bottom width b_B (cm)	b_T/b_B	ds/b [enh.]	ds/b [ori.]	K_{tap}= ds/b(enh.)/ ds/b(ori)
1.50	4	0.375	0.595	0.993	0.559
2.15	4	0.538	0.632	0.993	0.636
2.90	4	0.725	0.768	0.993	0.773
4	2.90	1.379	0.775	0.993	0.780
4	2.15	1.860	0.663	0.993	0.668
4	1.50	2.667	0.625	0.993	0.629

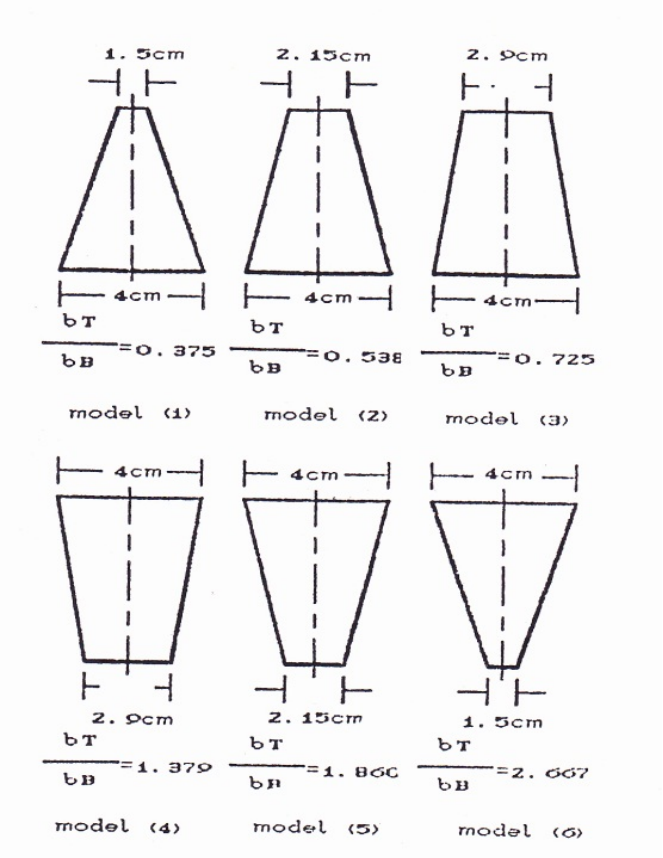

Fig.1 . Models of Tapered Piers undertaken in Experimental Program
Reduction of Scour by using Tapered Pier

III. MECHANISM OF FLOW

The reduction in scour with tapered piers may be attributed to the weakened downflow and horseshow vortices , where , the downflow is close to the upstream inclined face of a pier . The rollers consequences from the downflow can be divided into two components each has less strength than the resultant , thereby the consequence scour will be less . However , as can be seen from Fig.2 , if the tapered pier upward , the rollers of a horizontal component of the downflow will be in opposite direction of the horseshow vortices , thus , interference occurs and causes a less ability of these vortices to transport the sediment downstream . The vertical component of downflow is also weakened toward the bed because their rollers action are impinging the inclined face of pier , that is lead to less picked up sediment from a rim . When pier is tapered downward , the vertical component of downflow impinging the bed directly , and more sediments have been picked up , but its strength decreases toward the bed due to decreasing in pier size leads to reduce the scour depth compared with traditional cylindrical pier .

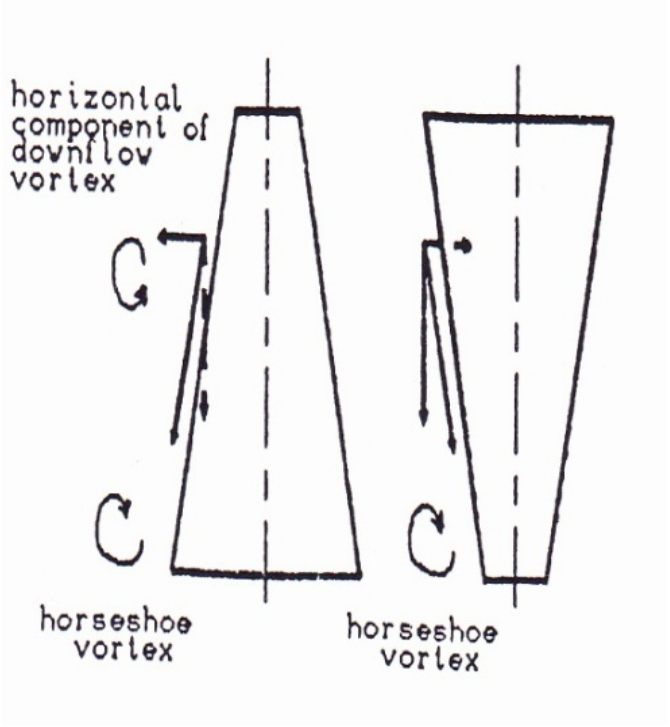

Fig.2 . Mechanism of Flow vortices around Tapered Pier

IV. SIZE ENHANCEMENT FACTOR

The base ratio , bT/bB , can be adopted as a design variable thus a new coefficient may be presented as a multiplicative factor used with a suitable equation of a scour depth around cylindrical pier , from which the reliable scour depth can be adopted for design purposes if the tapered pier is used. The results of this coefficient are listed in Table I and presented in Fig.3 with the following relationships :

$$Ktap = 0.314 + 0.664(bT/bB) \quad (1)$$

Used for bT/bB < 1.0

$$Ktap = 1.793 - 1.022(bT/bB) + 0.22(bT/bB)^2 \quad (2)$$

Used for bT/bB > 1.0

It should be noted that the enhancement size factor Ktap is restricted for circular piers and its derived formulas are covers only a small range of bases ratio , one range of flow variation , and one sediment median size . Therefore , much more data

are required to verify the validity of these formulas and hence , their uses in other conditions should only be carried out with caution .

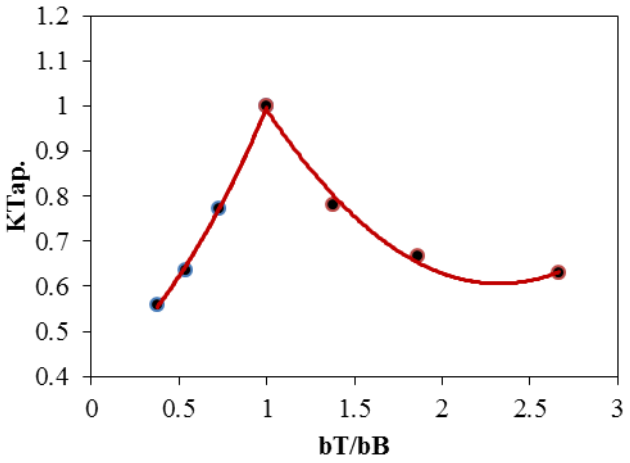

Fig.3 .The Enhancement size factor for Tapered Pier

V. CONCLUSION

The countermeasure of local scour around bridge piers is the target of the designers related to bridge foundation . A lot of enhancement methods toward this target have been presented previously by researchers via experimental programs can be found in literatures , such as riprap protection around a proposed scour hole , collar , through slot , etc . The adopted method by modification of pier configured size itself has not been presented previously . In this study a tapered pier with a specified tapered ratio

bT/bB were used in limited experimental program to show its effectiveness to countermeasure the scour depth and hole size that configured around pier . The analysis of measurement data shows that there is appreciable enhancement toward the reduction of local scour around the base of pier when replaced a traditional circular pier by a tapered pier . However , the tapered upward models piers are even more efficient where it shows a greater reduction of 33% .

REFERENCES

[1] Breusers, et. al. ,"Local scour around cylindrical piers" ,Jr. Hyd. Research , Vol.15 , No.3,1977, pp. 211-252 .
[2] Draper, N. R. , Smith H. ," Applied regression analysis "John Wiley and Sons , Inc. ,ed. ,1981
[3] Posey, C. J.,"Tests of scour protection for bridge piers", Jr. Hyd. Eng. , ASCE, Vol.100 , No.HY12 , 1974 ,pp.1773-1783 .
[4] Raudkivi, A. J. , Ettema R . ,"Clear water scour at cylindrical piers", Jr. Hyd. Eng. , ASCE , Vol.109 , No.HY3 ,1983, pp. 338-349 .
[5] Stevens, M. A. , et. al .,"Wake vortex scour at bridge piers", Jr. Hyd. Eng. , ASCE , Vol.117 , No.HY7, 1991, pp.891-904 .
[6] Vittal , N. , et. al. ,"Clear water scour around bridge pier group" , Jr. Hyd. Eng. , ASCE , Vol.120 , No.HY11 , 1994,pp.1309-1318 .

Fabrication of Nanocomposite Membrane Containing MWCNTs in Support Layer and MCM-41 in Polyamide Thin Layer for Water Purification.

Abdulkhalik K. Mahmood[a], Riyad Hassan Alanbari[b] , and Fadhil Abd Rasin[c]

[a] Kut Technical Institute, Kut, Iraq; E- mail : abdulkhalikmahmood@gmail.com. Mobile: 07801035785

[b] Building and Construction Engineering Department, University of Technology, Iraq.

[c] College of Science, Baghdad University.

Abstract_ **In this work, a new type of nanocomposite membrane containing modified multi-walled carbon nanotubes (MWCNTs) in support layer and Mobile crystalline material (MCM-41) in thin film was developed. A thin film containing 0.05 % of MCM-41 was deposited on the polysulfone support layer containing (0.0, 0.05, and 0.4 w/w %) of MWCNTs, by interfacial polymerization. MCM-41 nanomaterial was synthesized by chemical reaction using TEOS as silica source. Particle and pore size distribution were determined by (N_2) gas adsorption, and specific surface area was conducted by BET test and found to be 958m^2/gm. MWCNTs were modified by acid method and characterized by Raman test. Membranes were studied by SEM, AFM, and ATR FT-IR, morphological study showed that modified MWCNTs and MCM-41 were dispersed and well bounded in the polymer matrix, the synthesized membranes showed an increase in the surface roughness's, hydrophlicity and zeta potential by addition 0.05% of MCM-41. A comparison between synthesized conventional nanocomposite membrane without nanomaterial and a new nanocomposite membrane containing (0.4 w. % MWCNTs and 0.05 % MCM-41) are shown, that the pure water flux was increased from (36 L/m^2.h) to (61 L/m^2.h), which means that there is an increase of water flux about (69.4 %). Integration of MCM-41 in thin film was contributed in an increase in water flux about (47.2 %), while embedded MWCNTs in support layer was contributed an increase of (22.2 %).This proves that the type of support layers influences the membranes permeability. The salt rejection of new developed membranes were found to be 97.51 – 97.57 % for NaCl, and 98.59 -98.65 %for Na_2 SO_4 of concentration (2000mg/L) and transmembrane pressure (TMP) 15 bars, this means that addition of nanomaterials not affected the selectivity of the membranes. Also the new membranes save TMP by (43.7 %) and this is the main objective of this work, to decrease the release of gasses and saving energy to reduce the global warming.**

Keyword (fabrication, nanocomposite, MWCNTs, MCM-41, Purification)

1. Introduction

Nowadays, Integration of nanoparticle in the design and synthesis of new materials has been an area of intense research [1]. Such materials have added a prevalent importance in many areas of science and technology due to their significant changes in properties such as mechanical, thermal, and magnetic as compared to untreated polymers [2].Thus, one of the latest applications includes the incorporation of nanoparticles into polymeric membranes in order to improve the performances of the membranes such as permeability, selectivity, mechanical strength, and hydrophilicity. The introduced nanoparticles to polymer membranes might be silica, Fe_3O_4, ZrO_2, TiO_2, Al_2O_3, and modified multi-walled carbon nanotubes (MWCNTs).

L.Reingders, (University of Amsterdam 2009) discussed the development of nanocomposites of organic polymers and TiO_2 or amorphous SiO_2 nanoparticles [4].

Eun-Sik Kim *et al*. (2012) synthesized a new type of thin-film nanocomposite (n-TFN) by the interfacial polymerization of a support layer

containing acid modified multi-walled carbon nanotubes (MWNTs) and a thin-film layer containing nano-Ag particles. They concluded that MWNTs at 5.0 % (w/w) in the support layer and nAg particles at 10 %(w/w) in the thin-film layer were enhanced the pure water permeability of the n-TFN membrane by 23% and 20%, respectively, compared to 0 wt. % of these components in their respective layers[5].

Jun Yin *et al.* (2012) synthesized a thin-film nanocomposite (TFN) membrane containing porous MCM-41 silica nanoparticles (NPs) by the in situ interfacial polymerization (IP) process. By a comparison between the membranes with non-porous silica NPs(S-TFN) and with the porous MCM-41 NPs (M-TFN), they suggested that the internal pores of MCM-41 NPs contributed significantly to the increase of water permeability [6].

Mengru Bao, Guiru Zhu, *et al.* (2013) synthesized mono dispersed spherical mesoporous nanosilicas by the hydrothermal method. Mono dispersed spherical mesoporous nanosilica–polyamide TFC RO membranes were obtained via interfacial polymerization. With increased silica loading, water flux increases from (19 L/h·$m^{2)}$ to (53 L/h·m^2) and all solute rejection rates exceed (96 %) [8].

Although progress has been made on the synthesis of nanocomposite membranes with various nanomaterials, reports of water treatment with membranes containing a combination of different nanomaterial's are not widely studied. The successful incorporation of two nanomaterials' MWCNTs in support layer and MCM-41 in thin layer is expected to produce a nanocomposit membrane with enhanced permeability, selectivity, and reduced bio fouling potential during filtration. Such a nanohybrid membrane is the special topic in our research that would combine the unique properties of each component.

2. Experimental Work

2-1 Materials

Polysulfone support layers were containing (0.0, 0.05, 0.4 % w/w) MWCNTs were synthesized perversely, (data not shown here, minimum and optimal values of MWCNTs in support layers), Cetyltrimethyl ammonium bromide (CTAB, 95%, Aldrich) was used as surfactant and tetraethyl orthosilicates (TEOS, 98%, Sigma-Aldrich) was used as silica source for the synthesis of MCM- 41, in addition to Sodium Hydroxide (NaOH, Molar mass 39.9971 g mol^{-1}). M-phenyl diamine (MPD, 99%, Aldrich) and trimesoylchloride (TMC, 98.5%, Aldrich) were monomers used in the IP process. All chemicals were ACS reagents grade .Deionized (DI) water produced by Millipore DI system from local market(18.2 MΩ.cm) was used for solution preparation and filtration study. NaCl, Na_2SO_4 for salt solution preparation were used.

2-2 Membrane Synthesis

2-2-1 Synthesis of MCM-41 Nanomaterials.

Different methods have been used to synthesize these types of materials. In majority of these methods the cationic surfactant cetyltrimethylammoniumbromide (CTAB) has been used as the Structure-directing agent (template) and tetraethylorthosilicate (TEOS) have been used as the sources of silica. To remove the organic template, usually the simplest way is the calcination process.

The MCM-41 nanomaterials were synthesized by two different methods as follow.

First method:-

3.5 ml of sodium hydroxide solution of two molarity (NaOH, Aldrich) and 480 ml of deionized water were mixed for ten minute, then 1.0 gram of cetyltrimethylammoniumbromide (CTAB) was added to the mixture with stirring at 500 rpm, and the mixture was heated to 80 ^{0}C for 30 minute. At that time, a 5 ml of tetraethylorthosilicate (TEOS) was added drop-wise to the prepared solution. After 2 hours of stirring, a white slurry mixture formed, and then the mixture was for 10 minute centrifuged at 10,000 rpm and washed twice with deionized water. The product was dried at room temperature and heating in air at 550 C^0 for 4 hours for calcination process. The final product (MCM-41) was stored in a desiccator.

Second method:-

A 1.36 g of CTMABr was dissolved in 76 g of deionized water in a 250 ml flask at room temperature under constant stirring (500 rpm). Then, 10.9 g of aqueous ammonia (25 wt. %) was added to this solution and stirred for 10 min. At last 6.67 g of TEOS was added drop wise with high speed stirring to obtain the final gel of composition ratio SiO2: CTMABr: NH_4OH: H_2O:of 1:0.12:2.5:150. The stirring was continued for 2 hours. The resultant solution was transferred into a 100 ml Teflon-lined bomb and aged for a week at 105°C in a hot box. The product (white precipitate) was recovered by filtration, washed thoroughly with distilled water and methanol and dried at 100°C overnight. Removal of the template was accomplished by calcination in air at 540 ^{0}C for 6 hours followed by cooling to room temperature. The product was afterwards characterized with different techniques such as X-Ray Diffraction (XRD), Nitrogen Adsorption-desorption, BET, SEM and AFM

2-2-2 Synthesis of Nanocomposite Membranes

The TFN membrane was hand cast by conventional interfacial polymerization [6]. A support layer containing (0.0, 0.05, and 0.4 % w/w MWCNTs) taped on a glass plate was soaked in 2.0 % w/w1, 3-phenylenediamine (MPD, ≥99%) (Sigma–Aldrich, St. Louis, MO, USA) in aqueous solution for 10 min. Excess solution was removed with a rubber roller and the glass plate was placed in 0.1. % w/w1, 3, 5-benzenetricarbonyl trichloride (TMC, >98%) (sigma- Aldrich, USA) in n-hexane for 3 min. MCM-41 was mixed with the TMC solution and dispersed in an ultrasonic bath for 10 min prior to interfacial polymerization. The concentration of MCM-41 in the thin-film layer was fixed at 0.05wt. % to obtain the properties and performance capability reported in literature [6]. The properties and membrane performance of TFC membranes (containing 0 % w/w MCM-41 in the thin-film layer and 0% w/w of MWCNTs in support layer) were compared with TFN membranes (containing 0.05wt. % MCM-41 in the thin-film layer and different ratio of MWCNTs in support layers as mentioned above). Fabricated TFN membranes were cured in an oven at 60–70 ^{0}C for 10 min. and stored in DI water at 4 ^{0}C. Finally, a 47 mm diameter circular membrane was cut from the fabricated sheet for further performance tests.

3. Result and Discussion

3-1 Characterization of Synthesized MCM-41 NPs.

MCM-41 was synthesized by chemical reaction and characterized through examination of morphology, specific surface area and particle size distribution. Figure 1 shows the pore diameter distribution of MCM-41 nanoparticles, while BET analysis showed very high surface areas for the synthesized MCM-41. As it is clear from table 1, which shows the physical properties of material. The material had shown a hexagonal array of uniform mesopores with sizes ranging from 2 to 10 nm with high surface area about 958 m^2/gm.

Table 1 Physical properties of synthesis MCM-41

sample	a_0 (nm)	S_{BET} (m^2/gm)	V_{meso} (cm^3/gm)	dp (nm)	Wt (nm)
MCM-41	4.03	958	0.67	3.13	0.9

The SEM and AFM for MCM-41 show that the material had near spherical shape. The size of particle was about 100nm. Highly ordered hexagonal array as shown in Figure 2. Which is agrees with the values usually reported for MCM-41 synthesis [11] - [12] - [13] - and [14].

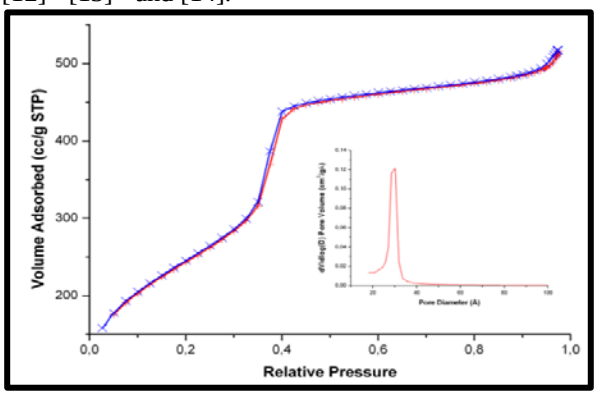

Fig. 1 Pore diameter distribution of synthesized MCM-41

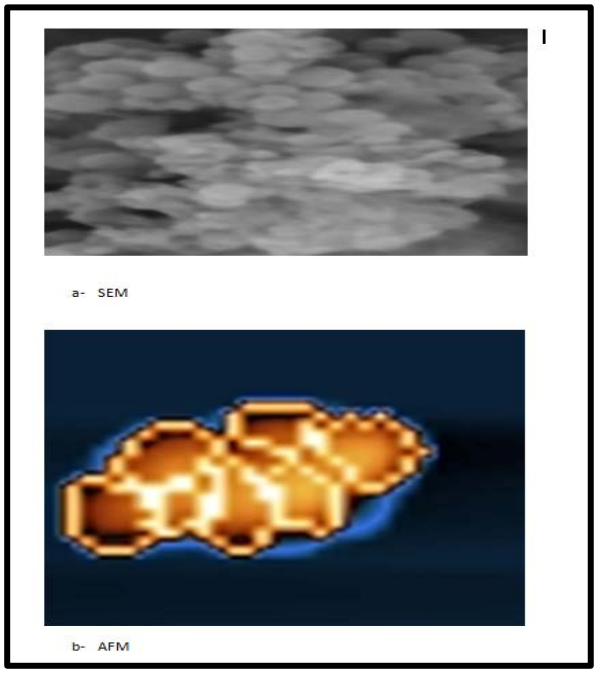

Fig. 2 SEM and AFM images of synthesis MCM-41

3-2 XRD Test

Typical X-ray diffraction patterns of MCM-41usually show four peaks indicating the long range order present in this material [23]. The repeating distance a_0 between two pore centers can be calculated by using the following formula [23] - [24]: $a_0 = (2/\sqrt{3})\ d_{100}$. Then, the pore diameter can be achieved from this value by subtracting 1.0 nm which is an approximate value for the pore wall thickness [23] (in worth mentioning that this value was obtained by other worker [25] to have a value of ~0.92 nm).The XRD patterns of the synthesized samples was obtained at the following conditions: X-

ray Tube: Cu (1.54060 A) Voltage: 40.0 kV Current: 30.0 mA Scan Range: 00.0000 <-> 25.0000 deg. Step Size: 0.2000 deg. Count Time: 1.20 sec. as shown in figure 3. In this figure five peaks appeared due to the calcinations of the MCM-41, which is also responsible to pores shrinkages.

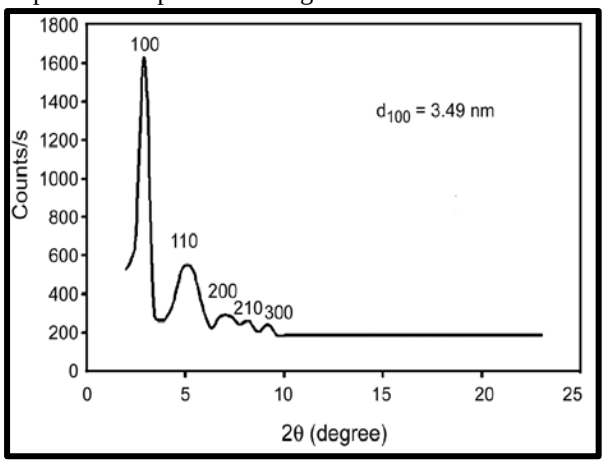

Fig. 3 The XRD spectrum of the synthesized sample of MCM-41.

3-3 Characterization of TFN membrane.

The prepared four nanocomposite membranes were characterized by measuring the hydrophilicity of membranes (measuring contact angle and zeta potential), surface morphologies, cross sections and roughness by (SEM and AFM), and measuring the performance of the membranes by evaluating the pure water flux and salt rejection.

The types of membranes are:-

1- TFC (thin film composite membrane)
2- 0.05TFN (nanocomposite membrane containing 0.05 % w/w MCM-41 in thin layer).
3- 0.05TFN0.05 (nanocompsite membrane containing 0.05 % w/w MWCNTs in support layer and 0.05 % w/wMCM-41 in thin layer.
4- 0.05TFN0.4 (nanocomposite membrane containing 0.4 % w/w MWCNTs in support layer and 0.05 % w/w MCM-41 in thin layer.

3-3-1 Contact Angle and Zeta Potential.

The contact angle and zeta potential of syntheses membranes are presented in table 2. The contact angle of membranes are decreased by adding small amount of MCM-41 to thin layer from (64±1.2 for TFC to 36±1.8 for 0.05TFN0.4), which mean that an increase in hydrophilicity of membranes will take place upon the addition of the pores MCM-41 to thin layer. The embedded MCM-41 NPs can be exposed on the membrane surface. Therefore, the membrane surface hydrophilicity may increase because of the hydrophilic properties of MCM-41 NPs. Embedding with porous MCM-41 NPs; the membrane surface could even become more hydrophilic due to the capability of the hydrophilic pores to imbibe water via capillary effects. This is consistent with the result by Jeong *et al.* [14], who observed that the contact angle of membrane surface decreased with increasing zeolite concentration and attributed this to the super-hydrophilic property of zeolite.

The zeta potentials of membrane surfaces were calculated from the tangential steaming potential measurements (Models: Brook haven nano Brook zeta plus- USA) and presented in table 2.

The zeta potential of TFC (-5.6 mv ±0.2) increased by addition of pores MCM-41 to (-7.8±0.0.25mv) for 0.4NTF0.05, this is similar to the results of other researchers [6]. MCM- 41 NPs carried negative charge at pH 5.8. And some embedded NPs may be exposed to the membrane surface as discussed above. The surface NPs in direct contact with the electrolyte may exert additional negative charge on the surface.

Table 2 Contact angle and zeta potential for nanocomposite membranes.

Type of membrane	Contact angle (degree)	Zeta potential (mv)
TFC	64±1.2	-5.6±0.2
0.05TFN	38±2.5	-7.2±0.3
0.05TFN0.05	37±1.4	-7.4±0.16
0.05TFN0.4	36±1.8	-7.8±0.25

3-3-2 SEM, AFM Analysis.

The surface morphology and cross section of the synthesized nanocomposite membrane containing MWCNTs in support layer and MCM-41 in thin layer were investigated by SEM, the surface images of (TFC and 0.05TFN0.05) are presented in Figure 4. While the cross section of nanocomposite membranes (0.05NTF0.05, 0.05TFN0.4) are depicted in Figure5. The pores structure of MCM-41 that makes defects in the thin layer and the macro voids causes by the MWCNTs in support layers expected to increase the permeability and pure water flux of nanocomposite membrane.

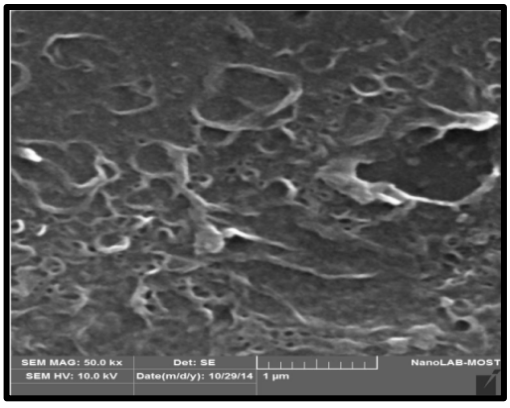

a

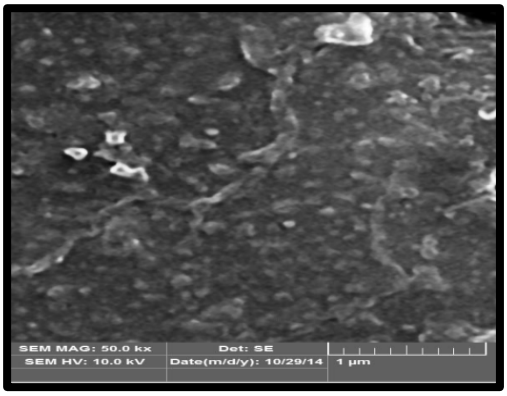

b

Fig. 4 SEM images of surface morphology of a- TFC, and b- TFN containing 0.05 % MCM-41 and 0.05 MWCNTs.

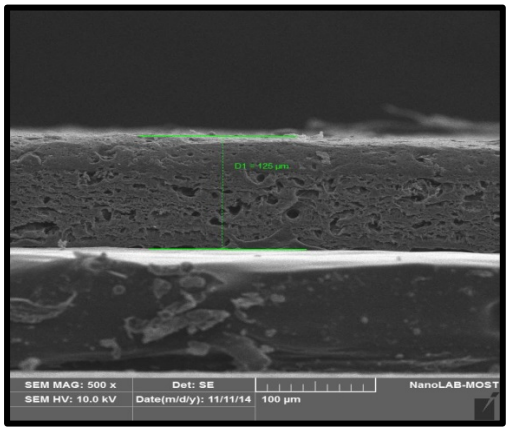

a- Cross section of TFN containing 0.05% MWCNTs in support layer+ 0.05%MCM-41in thin layer

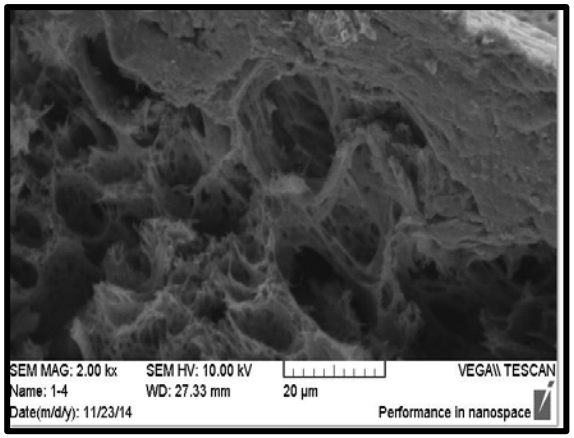

B-Cross section of TFN containing 0.4% MWCNTs in support layer+ 0.05%MCM-41 in thin layer

Fig. 5 SEM image shows the cross section of TFN containing a- 0.0.05 % MWCNTs in support layer+ 0.05%MCM-41in thin layer, and b- 0.4% MWCNTs in support layer+ 0.05%MCM-41 in. thin layer

The surface roughness of membranes were characterized by AFM and tabulated in table 3. The roughness of TFC which expressed by the term RMS (5.90nm) are increased to (41.19 nm) by addition 0.05 % of MCM-41 to polyamide thin layer, these increases of roughness are due to migration of MCM-41 to the surface of polyimide thin layer during interfacial polymerization. The decreases of contact angles and the increase of roughness are due to embedding MCM-41 into thin layer. Both will contribute to increase the hydrophilicity of nanocomposite membrane, and expected to increase the pure water flux, shown in table 2. The 3d spectra of the surfaces and roughness's of three types of syntheses membranes (TFC, 0.05TFN, 0.05TFN0.05) are presented in Figure 6.

Table 3 Roughness of the different types of nanocomposite membranes

Type of membrane	Min nm	Max nm	Peak to Peak nm	RMS nm	Average roughness nm
TFC	-44.97	45.73	90.7	5.901	3.64
0.05TFN 0.05	-207.6	140.6	348.3	41.68	27.9
0.05TFN 0.4	-165.1	176.8	341.9	41.17	31.0

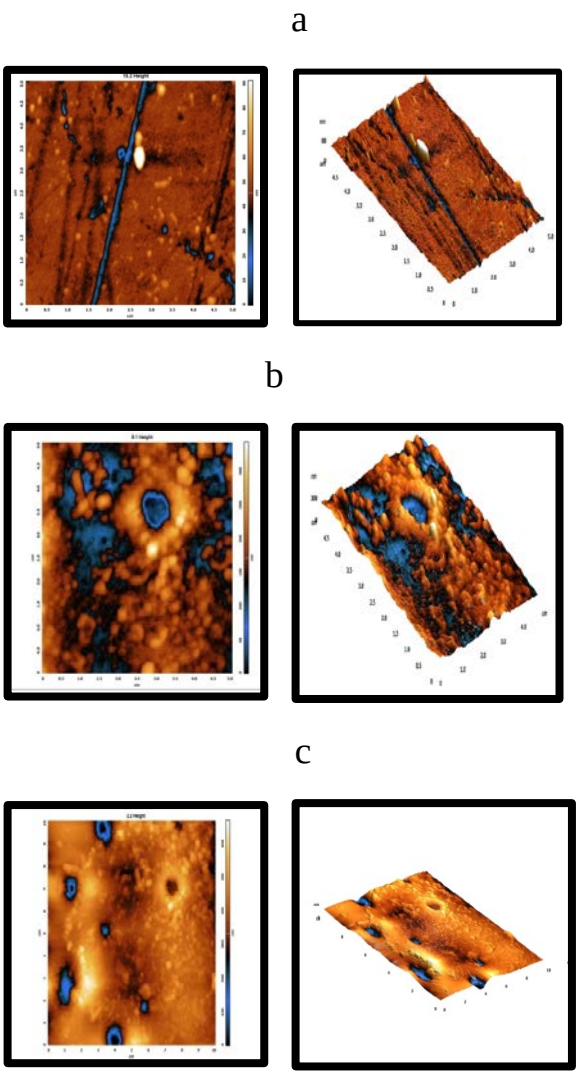

Fig. 6 AFM images shows the surface morphology and roughness of the a- TFC membrane, b- TFN containing 0.05 %MWCNTs in support layer+ 0.05 %MCM41 in thin layer, and c - TFN containing 0.4 % MWCNTS in support layer + 0.05% MCM-41 in thin layer

3-3-3 Permeability Test and Salt Rejection.

The permeability and salt rejection test for membranes are conducted by using high pressure cross flow filtration system. Three samples of each type of membranes (TFC, 0.05TFN, 0.05TFN.05, 0.05NTF0.4) were compressed for 2 hours at pressure 20 bars. Then the pure water flux and salt rejection were measured for solutions of 2000mg/L of NaCL, and Na_2SO_4. Figure7 shows the pure water flux for nanocomposite membranes containing MWCNTs in support layer and MCM-41in thin file.

From the Figure 7, it was shown that at pressure 16 bars, the pure water flux for TFC was increased from 36L/m^2.h to 61L/ m^2.h by adding 0.05 % by weight of MCM-41 to thin film and a 0.4% MWCNTs to support layer, *i.e* an increase about (69.4%) of pure water flux.

The increases of pure water flux due to the addition of two types of nanomaterials to traditional TFC membrane can be explained upon the following observation. The addition of MCM-41 nanomaterial to polyamide thin layer result in an increase about 47.2% of pure water flux, while the addition of MWCNTs to support layer result in an increase of 22.2% of pure water flux. This good proof that the support layer material influences the performance of nanocomposite membrane.

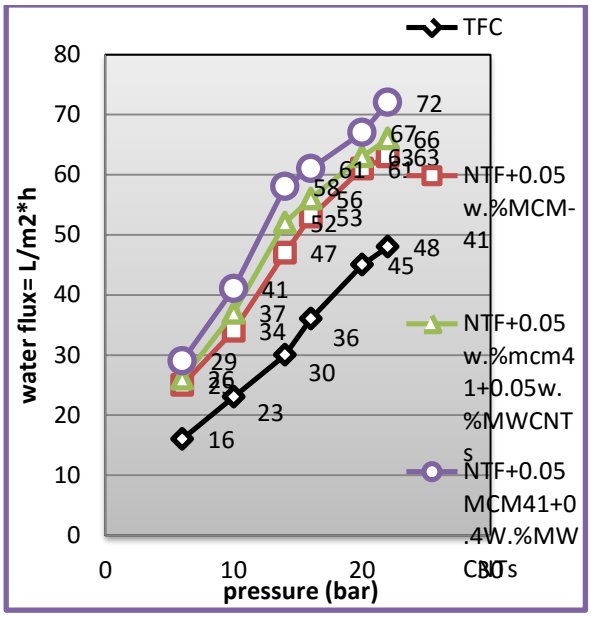

Fig. 7 Pure water flux for nanocomposite membrane (Flow rate 160 L/h).

Figure 7, showed that the performance of conventional TFC membrane at 16 bars was 36 L / m^2.h, can be obtained by the nanocomposite membrane containing 0.4 % MWCNTs at support layer and 0.05 % MCM-41 in thin layer at pressure less than 9 bars 38 L /m^2.h. In other words, this mean that a decreases of 7 bars in the required pressure, and saving of 43.7% of the needed energy. The main objective of this work is to decrease the emission of gasses and saving energy to reduce the global warming.

To study the effect of the flow on the pure water flux and salt rejection, the permeability test was conducted in two other flows 140 and 120L/h.

Figures 8 and 9 depicted the pure water flux for membranes at flow 140 and 120L/h respectively. It was clear that the performance of pure water flux of the membranes were decreased with decreasing the flow while the salt rejections were not affected by this decreasing.

Salt rejections of the synthesized nanocomposite membranes containing MWCNTs and MCM-41 nanomaterials were in the range 97.51 – 97.57% for NaCl solution and 98.59- 98.65% for Na_2SO_4. These results are nearly the same as that of TFC a membrane, which means the addition of nanomaterials, not affected the selectivity of the membranes and agree with results of other researchers [13]-[19].

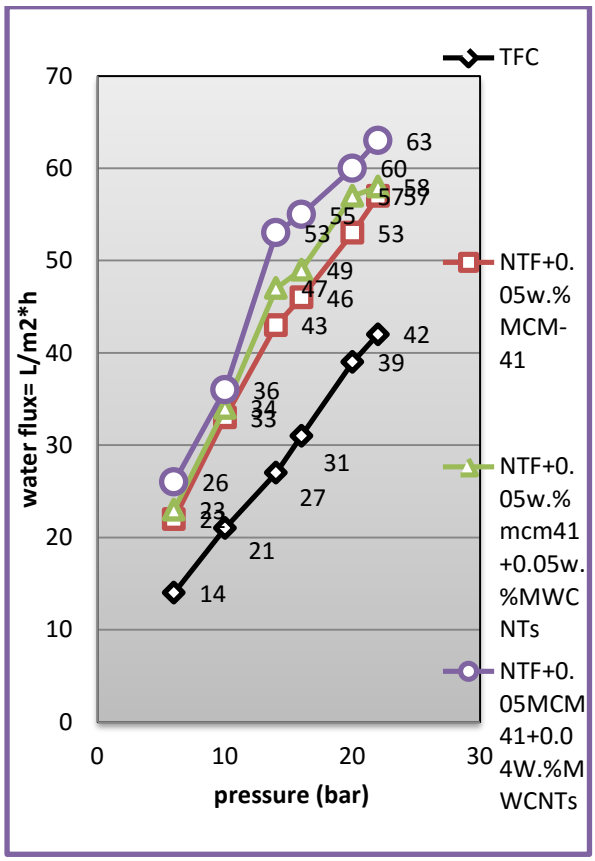

Fig. 8 Pure water flux for nanocomposite membrane at a flow of 140L/h.

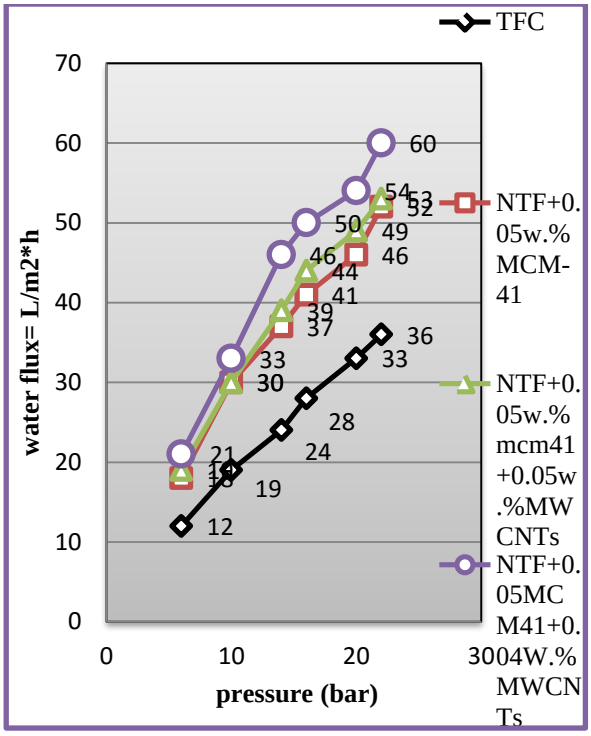

Fig. 9 Pure water flux for nanocomposite membrane at flow of 120L/h.

Table 4 Shows the percentage of salt rejection of nanocomposite membranes.

Type of membrane	NaCl % rejection	Na_2SO_4 % rejection
TFC	97.58	98.70
0.05TFN	97.51	98.65
0.05TFN0.05	97.57	98.59
0.05TFN0.4	97.53	98.63

4. Conclusions

A new type of nanocomposite membrane containing MWCNTs in support layer and MCM-41 in thin film was developed. A thin film containing 0.05 % of MCM-41 was deposited on the polysulfone support layer containing (0.0, 0.05, and 0.4 %) of MWCNTs, by interfacial polymerization. morphology study showed that the modified MWCNTs and MCM-41 were dispersed and well bounded in the polymer matrix, the synthesized membranes showed an increase in the surface roughness's, hydrophlicity and zeta potential by addition 0.05% of MCM-41. A comparison between synthesized conventional

nanocomposite with the a new nanocomposite membrane containing (0.4 % MWCNTs and 0.05 % MCM-41) reveals that the pure water flux was increased from 36 $L/m^2.h$ to 61 $L/m^2.h$, with an increase of 69.4 % in the water flux. Integration of MCM-41 in thin film was contributed an increase of 47.2 % in water flux, while embedded MWCNTs in support layer was contributed an increase of 22.2 %. This proves that the type of support layers influences the membranes permeability. The salt rejection of new developed membranes were found to be in the range of 97.51 – 97.57 % for NaCl, and 98.59 -98.65 % for $Na_2 SO_4$ with salt solution concentration of 2000mg/L and TMP at 15 bars, i.e the addition of nanomaterials did not affect the selectivity of the membranes. The new membranes of TMP save 43.7 % of the needed energy.

5. References

(1) Law Yong Ng, Abdul Wahab Mohammad, "Polymeric Membranes Incorporated with Metal/Metal Oxide Nanoparticles: A Comprehensive Review". Desalination 308(2013)15-33.

(2) M. Hosokawa, K. Nogi, M. Naito, T. Yokoyama (Eds.), "Nanoparticle Technology Handbook", First ed., Elsevier B.V., AE Amsterdam, 2007.

(3) J. Schaep, C. Vandecasteele, R. Leysen, W. Doyen, "Separation and Purification Technology" 14 (1998) 127.

(4) L. Reijnders, "The Release of Tio_2 and Sio_2 Nanoparticles from Nanocomposites". Journal of Polymer Degradation and Stability 94 (2009)873-876.

(5) Eun-Sik Kim, Geelsu Hwang, Mohamed Gamal, "Development of Nanosliver and Multi-Walled Carbon Nanotubes Thin –Film Nanocomposite Membrane for Enhanced Water Treatment". Journal of Membrane Science 394-395 (2012).

(6) Jun Yin, Eun-Sik Kim, John Yang, Baolin Deng, "Fabrication of a Novel Thin Film Nanocomposite (TFN) Membrane Containing MCM-41 Silica Nanoparticles (NPs) for Water Purification", Journal of Membrane Science 423-424(2012).

(7) Xin Liu, Saren Qi, Ye Li, "Synthesis and Characterization of Novel Antibacterial Silver Nanocomposite Nano filtration and Forward Osmosis Membranes Based on Layer-by-Layer Assembly". Journal of Water Research 47(2013) 3081-3092.

(8) Mengru Bao, Guiru Zhu et al., "Preparation of Mono Dispersed Spherical Mesoporous Polyamide Thin Film Composite Reverse Osmosis Membranes via Interfacial Polymerization". Desalination 309(2013) 261-266.

(9) Seongpil An, Min Wood Lee, Bhavanaa N. Joshi, "Water Purification and Toxicity Control of Chlorophenols by 3D Nanofiber Membranes Decorated with Photo Catalytic Titania Nanoparticles". Journal of Ceramics International 40(2014)3305-3313.

(10) S.A.AL Malek, M.N. Abu Seman and et al., "Formation and Characterization of Polyether Sulfone Using Different Concentration of Polyvinylpyrrolidone". Journal of Desalination 288(2012)31-39.

(11) S.pevzner, O. Regev, "Thin Film of Mesoporous Silica: Preparation and Characterization, Current Opinion in Colloid and Interface Science". 4(2000)420-427.

(12) Xiaolei Qu, Pedro J.J, "Application of Nanotechnology in Water and Wastewater Treatment". Water Research 47(2013)3931-3946.

(13) Siriat Kasemset, Alberto Lee et al., "Effect of Polydopamine Deposition Condition on Fouling Resistance, Physical Properties, and Permeation Properties of Reverse Osmosis Membranes in Oil/ Water Separation". Journal of Membrane Science 425-426(2013)208-216.

(14) Byeong-Heon Jeong, Eric M.V.Hoek "Interfacial Polymerization of Thin Film Nanocomposite: A New Concept for Reverse Osmosis Membranes". Journal of Membrane Science 294(2007)1-7.

(15)Soumitra Kar, R.C.Bind, "Carbone nanotube membranes for desalination and water purification: challenges and opportunities". Nano today (2012)7, 385-389.

(16)- A.L. Ahmad, A.A. Abdulkarim, "Resent Development in Additives Modification of Polyether Sulfone Membrane for Flux Enhancement". Chemical Engineering Journal 223 (2013)246-267.

(17) Christopher A. Crock, Adam R. Rogensues, "Polymer Nanocomposites with Grapheme-Based Hierarchical Fillers as Materials for Multifunctional Water Treatment Membranes". Journal of Water Rsearch 47(2013) 3984-3996.

(18) Reza Sepahvand, Mohsen Adeli et al., "New Nanocomposites Containing Metal Nanoparticles, Carbon Nanotube and Polymer". J. Nanopart Res (2008) 10:1309–1318.

(19)Gaurav S. Ajmani et al., "Modification of Low Pressure Membranes with Carbon Nanotube Layers for Fouling Control". Journal of Water Research 46 (2012)5645-5654.

(20) Rasel Das et al., "Carbone nanotube membranes for water purification, a bright future in water desalination". Journal of Desalination 336(2014)97-109.

(21)L. Brunet et al., "Properties of Membranes Containing Semi-Dispersed Carbon Nanotubes". Environmental Engineering Science Journal, Volume 25, Number 4, 2008.

(22) Stefan Balta et al. "Anew Outlook on Membrane Enhancement with Nanoparticles: the Alternative of ZnO". Journal of Membrane Science (2011).

(23) Mesoporous MCM-41 Materials: Control of Porosity and Morphology", Micropo. Mater. **27**, 207-216, 1999.

(24) Emerson SC, Klocke DJ, "Foam Reduction during Synthesis of MCM-41", US Patent 5,538,711 (Jul 23, 1996).

(25) Dong X, Wang L, Zhou J, Yu H, Sun T, "Preparation of Nano- Polyethylene Fibers Using TiCl4/MCM-41 Catalytic System", Catal Commun, **7**, 1-5, 2006.

Properties Study of a Polysulfone Support Layer Membrane Containing Multiwall Carbon Nanotube for Water Purification.

Abdulkhalik K.Mahmood[a] , Fadhil Abd Rasin[b], and Riyad Hassan Alanbari[c]

[a] Kut Technical Institute, Kut, Iraq; E- mail : abdulkhalikmahmood@gmail.com. Mobile: 07801035785

[b] College of Science, Baghdad University

[c] Building and Construction Engineering Department, University of Technology, Iraq.

Abstract_ **In this research, we describe the preparation, characterization, evaluation of performance, and study of mechanical properties of polysulfone support layer membranes containing modified MWCNTs. The membranes were prepared by wet phase inversion method in which the acid oxidized multi walled carbon nanotubes (MWCNTs) embedded in polysulfone support layer as matrix polymer. The oxidized MWCNTs were added by a low mount (0.0, 0.05, 0.1, 0.2, 0.4, 0.6 and 1.0 wt. %). Raman spectra were used to identify that carboxyl croup attached to MWCNTs after acid treatment. A SEM and AFM spectrum were used to study the morphology, surface roughness, and the dispersion of nanotubes in membrane. Large macro void were appeared in support layer by addition of low amount of MWCNTs. The membranes were characterized for water up take, contact angle, surface roughness, permeability, and mechanical properties. The results indicated that the addition of 0.4w. % of MWCNTs to the polysulfone support layer were enhanced the water uptake, hydrophilicity (by measuring contact angles) and roughness of the membrane due to migration of functionalized MWCNTs to membrane surface during the phase inversion process. The permeability test show an increase of pure water flux about (53%) at TMP 4 bars. The salt rejection for polysulfone support layer was not calculated since the nanopores of polysulfone structure did not allow significant salt rejection. Polysulfone support layer containing 0.4w. %MWCNTs suffered from weak stress preventing exploitation of the mechanical properties of the CNTs. transfer, the membranes tensile strength was not improved while the elongation decreased about (25.8%) compared with support layer without MWCNTs.**

Keyword (Polysulfon, MWCNTs, Support layer, Purification)

1. Introduction

The shortage of clean water is one of the most problems facing the development of world economy. Furthermore, the presence of various contaminants such as natural organic component, heavy metals, industrial dyes, produced by products materials and microorganisms are worsen the mater, nowadays, there are a tendency towards the membrane technology for producing a clean drinking water[1].

Regardless of all materials used in membranes, the common goal of scientists and technology is to create membrane with low cost materials, low operation powered, stable flux, high permeability and excellent rejection of fouling materials.

Carbon nanotube shows higher mechanical and electrical properties that make them attractive for emerging a new composite material. Recent studies have considered the properties and advantages of polymer CNT composites.

L.Brunt et al. (2007) study the properties of membrane containing semi-dispersed carbon nanotubes. They concluded that after addition of 0.4w% of MWCNT the asymmetric structure of the membrane, the permeability, and the hydrophobicity were not changed, but the roughness increased. The tensile strength of the composite membrane was not improved while the elongation to frailer decreased because of a lack of dispersion of nanotubes. The new composite membrane did not indicate any antibacterial effect due to the presence of CNT [2].

Vahid Vatanpoura et al. (2011) fabricated and characterized of novel antifouling membrane prepared from oxidized MWCNT and polyether sulfone nanocomposite. They indicated that blending MWCNT to PES matrix cause to increasing hydrophilicity and water flux of membrane. The results confirmed that the surface roughness of membrane plays an important role in

anti- bio-fouling resistance of MWCNTs membrane [3].

Eun Sik et al. (2012) developed a new nanocomposite membrane containing nano silver and MWCNTs. This study demonstrated that the addition of 5.0w% of MWCNTs to support layer and 10w% of nAg to thin film were enhance the permeability by 23% and 20%, respectively, compared to 0 wt. % of these components in their respective layers and anti-bio-fouling properties of thin-film nanocomposite membranes[4].

Cauravs S. Agmani et al. (2012) studies the Carbon nanotubes (CNTs) with different physiochemical properties, layered onto low pressure membranes and tested for antifouling properties, using natural surface water with high fouling potential. They concluded that membranes modified with the largest diameter pristine multi walled CNTs (MWCNTs) were most effective in controlling membrane fouling [5].

Rasel Das et al. (2014) comprehensively reviewed molecular modeling and experimental aspects of CNT membrane fabrication and functionalization for the desalination of both sea and brackish water. They present the current problems and future challenges in water treatments [6].

The aim of our research are to fabricate a polysulfone support layer containing different ration of modified MWCNT to enhance the pure water flux , salt rejection and study the effect of addition of MWCNT on the mechanical properties of the membrane. The membrane morphology and roughness were characterized by SEM, AFM, Raman, and ATR FT-IR. The hydrophilicity of the membrane was evaluated by measuring contact angle and water up take. Mechanical properties were evaluated by tensile strength, modulus of elasticity, and elongation. The pure water flux and salt rejection were evaluated by high pressure cross flow filtration system.

2. Experimental work

2-1 Materials

Polysulfon (PSU, Sigma-Aldrich) pellets, density 1.24 g/ml at 25 °C, average Mw ~35,000 purchased from sigma –Aldrich USA. Used as polymer and N, N- dimethylformamide, colorless liquid, odor fishy, ammoniac, molar mass 73.09 g/ mole (DMF, 99.8%, Aldrich) were used as solvent for the casting solution to make the support layer. Poly (vinyl pyrolidone) (PVP, 25kDa) used as additive was purchased from local market. Carbon nanotube, multi-walled(Sigma-Aldrich, appearance form: solid, , multi-walled≥98% carbon basis, O.D. × I.D. × L 10 nm ± 1 nm × 4.5 nm ± 0.5 nm × 3-~6 μm). Also sulfuric acid (H_2SO_4) (ACS reagent, Fisher Scientific, USA) and nitric acid (HNO_3) (ACS reagent, BDH Chemicals, Canada) were used for modification of MWCNT. All chemicals were ACS reagents grade. Deionized (DI) water produced by Millipore DI system from local market (18.2 MΩ.cm) was used for solution preparation and filtration study.

2-2 Membrane Preparation

2-2-1 Modification of Carbon Nanotube.

The surface of the MWCNTs was treated with strong acid i.e. concentrated H_2SO_4 and HNO_3 to introduce hydrophilic functional groups. Acid-treated MWCNTs are known to have carboxyl groups on their surfaces showing good dispersion in polar organic solvents. For this purpose we used two methods.

First method:-

To prepare 5 grams of modified MWCNTs. 2000 gm of a mixture of sulfuric acid and nitric acid were prepared with a mixing ratio $3H_2SO_4$: $1HNO_3$ (wt:wt) and mixed with 5 gm of MWCNTs and stirring at 300 rpm for 24 hours at room temperature (23±1 ^{0}C). ; the MWCNTs were collected by repeated filtration using a 0.2 μm polytetrafluoroethylene (PTFE) membrane (Whatman®) and washing with DI water until the result reached pH neutrality. The final product was washed four times with methanol (CH3OH) (ACS reagent, Fisher Scientific, USA) and then DI water, and dried overnight at 50 C^0 [4].

Second method:-

To prepare 5 gm of modified MWCNTS. A 500 ml of 3M HNO_3/H_2SO_4 (1/3, v/v) were mixed with 5 gm of raw MWCNTs and sonicated for 1 h. then the mixture were reflex in an oven for 12 h. at temperature 127 C$^{0.}$ The solution was then diluted with 2 liters of deionized water and filtered through a 0.45μm membrane. The modified MWCNTs were rinsed with deionized water to reach to neutral PH [3].

2-2-2 Preparation of the Polysulfone, MWCNT Support Layer.

Polysulfone support layers with and without MWCNTs were prepared using the phase inversion casting method [3]. 15 gm of Polysulfone pellets were heated in an oven at 150 ^{0}C for 5 hours to degassed, and then dissolved in 85 gm of N, N-dimethylformamide (DMF) for the 15.0 wt. % concentrated solution. 1.0 wt. % of polyvinyl pyrrolidone (PVP) was added to the polysulfone solution as additive.

The mixture was stirred at (500r/min.) constantly at 50 ^{0}C for 24 h. The function of stirrer is to make sure that the polymer (PSU) and solvent (N-N DMF) can be mixed well in order to form a homogeneous solution. The thermometer measured the temperature during the mixing process. The processing temperature should be controlled in a

suitable and optimum temperature range by the heater. The casting solution was kept in the dark to reduce the amount of bubbles in the solution. Nonwoven polyester fabric was used to add strength to the membrane. The casting solution was deposited on the nonwoven fabric; the coated fabric was fixed onto a glass plate and the solvent was evaporated for 1 min to achieve a uniform surface of the support layer. A stainless steel knife was used for membrane casting. The thickness was determined to be approximately 200 µm. The glass plate was transferred into a water bath at room temperature (23 ± 1.0^0 C) for 1 h to remove residual solvents. The casted membrane was rinsed with DI water (18.2 MΩ. cm) and stored in DI water at 4 ^{0}C. For polysulfone support layer containing different ratio of modified MWCNTs, Predetermined amounts of MWCNTs (0 –1.0 wt. %) were added to the polysulfone casting solution. seven samples were prepared (0.0, 0.05, 0.1, 0.2, 0.4, 0.6, and 1.0 %) to study the optimal tensile strength and enhanced membrane performance. Note that membranes marked as 0.05 wt. % MWCNTs refer to membranes prepared in a casting solution in which the content of the MWCNTs with respect to (PSU +N-N DMF) was 0.05 wt. %.

2-3 Characterization of the Membrane Surface.

2-3-1 Contact Angle Measurement

The contact angle is defined as the angle made by the intersection of the liquid/solid interface and the liquid/air interface. For example, a contact angle of zero degrees will occur when the droplet has turned into a flat puddle; this is called complete wetting. The simplest way of measuring the contact angle is with a goniometer, which allows the user to measure the contact angle visually. A 5-µl of distilled water was placed onto dry membrane in air and the contact angle was measured. The average contact angle for distilled water was determined in a series of five measurements for each of the different membrane surfaces. Multiple droplets can be deposited in various locations on the sample to determine heterogeneity.

2-3-2 Water Uptake Measurement

Water uptake is an important factor in determining the effectiveness of the support layer of the prepared n-TFN membranes [4]. The water uptake of the MWNT support layers was determined by the gravimetric method. Ten pieces of MWCNT support layer (10 *10 mm) were immersed in DI water for 24 h, removed from the water and dabbed with filter paper to remove excess water on the surface, and weighted. Samples were dried at room temperature for 24 h and weighted again. The water uptake ratio of the sample was calculated with Eq. (1):

$$U = [(W_W - W_d) / W_d] * 100 \qquad \text{Eq. (1)}$$

Where Ww is the wetted weight, W_d is the dried weight of the MWCNT support layer samples and U is the water uptake ratio.

2-3-3 Mechanical Properties of Polysulfon Support Layer.

This experiment were conducted at room temperature (23±1^0C) using a tensile testing machine (Instorn model 4500, canton, MA) with an extension rate of 1mm/minute. The main parameters of interest are tensile strength, elastic modulus, and a percentage of elongation. All membrane coupons investigated (at least five specimens per composition).each specimens 63.5mm length and 3.3 mm width.

2-3-4 Permeability test

The experiments were carried out at room temp. (23±1^0C). The cross flow high pressure filtration system as shown in fig.1 was used to conduct the test. A 47 mm diameter (effective surface area 12.56 cm^2) membrane coupon was tested and three specimens for each composition. Carbon nanotube embedded PSU support layer membranes were characterized by measuring the pure water flux, and salt rejection. Each membrane was initially pressurized at 6 bars for 30 min, and then the pressure was lowered to the operating pressure of 0.5 - 4 bars. The water flux, Jw (kg/m^2 h) was calculated by the following:

$$J = \frac{M}{\Delta t \, .A} \qquad \text{Eq. (2)}$$

Where M (kg) was the weight of permeated water, A (m^2) was the membrane area and Δt (h) was the permeation time. Permeates were collected over a given period and weighed. The experiments were carried out at 23±1 ^{0}C.

Fig. 1 High pressure cross flow filtration system used for evaluation of performance and salt rejection.

2-3-5 Characterization of the Morphology of Membrane

The membrane structure and properties were characterized by SEM, AFM, and FTIR. A scanning electron microscope directly provides the visual information of the cross-sectional morphology of the membrane. (SEM, Tescan Vega 111- Czech) from Ministry of Science and Technology-Baghdad. The membranes were cut into small pieces and cleaned with filter paper. The pieces were immersed in liquid nitrogen for 60–90 s and were frozen. Frozen fragments of the membranes were broken and kept in air for drying. The dried samples were gold sputtered for producing electric conductivity. After sputtering with gold, they were viewed with the microscope at 17 kV.

Atomic force microscopy was used to analyze the surface morphology and roughness of the prepared membranes. The AFM device was (Spm Ntegra NT-MOT) from Ministry of Science and Technology-Baghdad. Small squares of the prepared membranes (approximately 1 cm^2) were cut and glued on glass substrate. The membrane surfaces were imaged in a scan size of 5μm×5μm. The surface roughness parameters of the membranes, which are expressed in terms of the mean roughness (Rm), the root mean square of the Z data (RMSz) and the mean difference between the highest peaks and lowest valleys.

FTIR spectra were used to characterize presence of functionalized groups in multi walled carbon nanotubes structure and presence of these groups in prepared MWCNT/PSU membranes.

3. Result and discussion

3-1 Functionalization of MWCNT.

Acid –treated MWCNTs are known to have carboxyl groups on their surfaces showing good dispersion in polar organic solvents. Raman and Fourier- transform infrared spectroscopy (FTIR) tests were used to identify introduced functional group onto the surface of acid treated MWCNTs; Raman spectroscopy (Raman seutera Raman microscope, Bruker com. Germany) offers several advantages for microscopic analysis. Since it is a scattering technique, specimens do not need to be fixed or sectioned. Raman spectra can be collected from a very small volume (< 1 μm in diameter); these spectra allow the identification of species present in that volume. Water does not generally interfere with Raman spectral analysis. Thus, Raman spectroscopy is suitable for the microscopic examination of minerals, materials such as polymers and ceramic. Fig. 2 shows the Raman spectra of two modified samples of MWCNTs material, the approach used in this spectrum is hyperspectral imaging or chemical imaging, in which thousands of Raman spectra are acquired from all over the field of view. The data can then be used to generate images showing the location and amount of different components.

Raman spectra of MWCNTs show three peaks intensity at 1350 cm^{-1}, 1560 cm^{-1} and 2650 cm^{-1} and the intensity ratio of 1350 cm^{-1} and 1580 cm^{-1} for raw MWCNTs about 0.72[25].The extent of the modification or defect in MWCNTs can be evaluated by the intensity ratio of 1350 cm^{-1} and 1580 cm^{-1}. From the Fig. 2, we can extract the intensity ratio are 1.2 and 1.3 for the two samples respectively. It is clear that the two samples have a higher intensity ratio (or more structural damage), which indicates the acid-oxidation treatment would cause a significant structural damage on MWCNTs and thus decrease the electrical conductivity of MWCNTs. It indicates these two functionalization methods cause significant structure changes of MWCNTs and would give rise to the loss in the conductivities of MWCNTs

3-2 Characterization of Polysulfone Support Layer.

The support layers were characterized by water up take, contact angle, SEM, AFM, Raman and ATR-IR test.

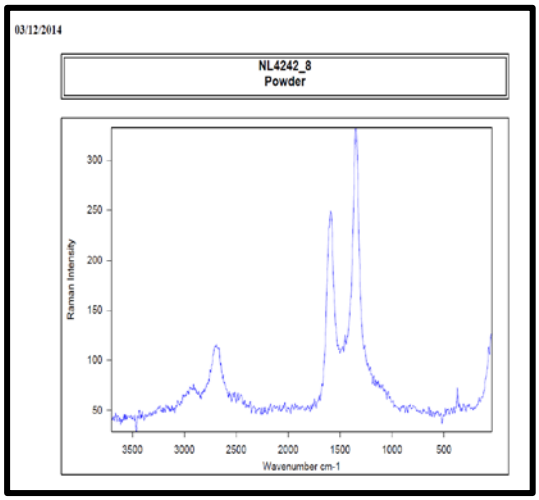

a- Modified MWCNTs prepared by method (2), intensity ratio = 1.21.

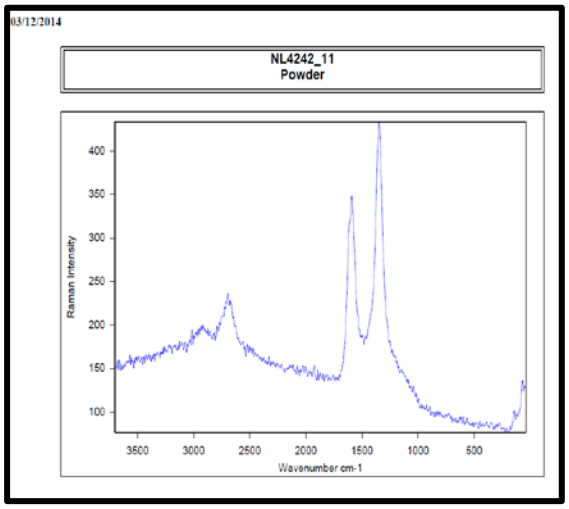

b- Modified MWCNTs prepared by method (1), intensity ratio = 1.32

Fig. 2 Raman spectra of acid modified MWCNTs for two samples a, and b

3-2-1 Water Uptake Measurement.

Water uptake is an important factor in determining the effectiveness of the support layer of prepared TFN membranes. Fig. 3 shows the water uptake ratio of MWCNTs support layers with different MWCNTs loading. As shown from the fig. 3 the water up take of polysulfone support layer equal 8% while the water uptake of polysulfone support layer containing 0.4w.% MWCNTs increased to 32%. This means an increase about 300% of water uptake, this cause a higher diffusivity and an increase of permeability of membrane.

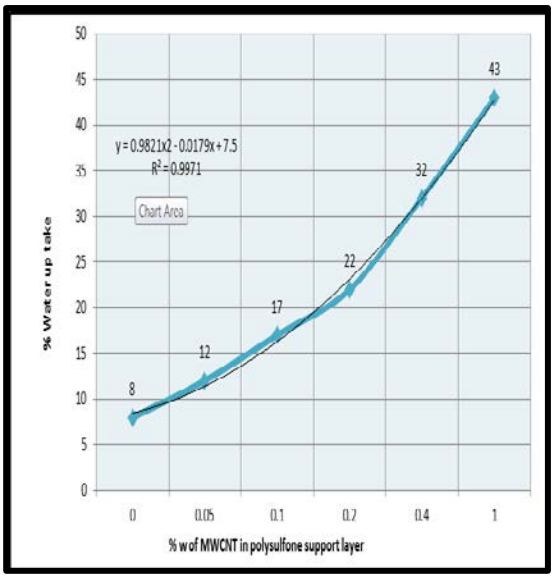

Fig. **3** Water uptake for polysulfone support layer containing MWCNTs.

3-2-2 Contact Angle.

Contact angles of the MWCNTs support layers are shown in the fig. 4. The contact angles of the support layers decreased by increasing the percentage of embedded MWCNTs. A decrease in the contact angle reflects an increase in the hydrophilicity, therefore the hydrophilicity of support layers increased with an increase in wt. % of MWCNTs. Contact angle ($34.14^0 \pm 1.65$) of the 1.0wt. % MWCNTs support was relatively hydrophilic compared to the contact angle (68.730 ± 1.2) of a pure polysulfone support layer. The increase in hydrophilicity could be due to the tunnel structure of the tubules and the acid modification of the MWCNTs [3].The support layer can affect the quality of the thin –film layer. This can directly influence the membrane permeability. Higher hydrophilicity can increase water uptake and water diffusivity causing increased membrane permeability. The hydrophilicity of membrane was improved with an increase of MWCNTs amount. It can be explained by the fact that during the phase inversion process, hydrophilic MWCNTs transfers freely to the membrane/ water interface to decrease the border energy [3]-[16]-[17].

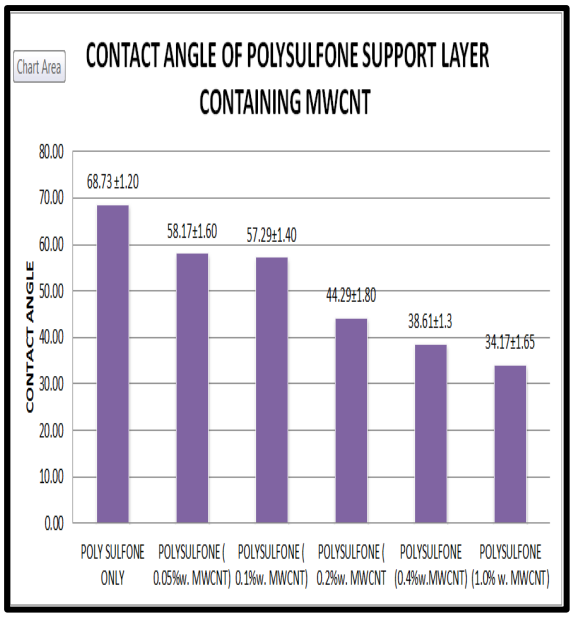

Fig. 4 Shows the contact angle for polysulfone containing MWCNTs.

The movement of MWCNTs to the surface of composite membranes was clear when the top and the bottom surface photographs of prepared membranes were matched. By increasing amount of mixed multi-walled carbon nanotube in PSU, the membrane top surface became blacker. Furthermore, color of bottom surface of membrane (glass side) was very lighter than top surface, demonstrating movement of functionalized MWCNTs to the top-layer surface of membrane.

3-2-3 Morphology and Surface Roughness of Polysulfone Support Layers.

SEM images of top-layer of prepared polysulfone support layers show at first by increasing of oxidized MWCNTs, the size of top-layers pores enhanced until 0.4 w.% of MWCNT and again reduced by further increase of MWCNT amount. This order of pore size and porosity change must cause an increase of pure water flux of the membranes when test for water performance later. The water permeation of membranes is usually controlled by two factors; hydrophilicity and the pore size and structure of the membrane. The hydrophilic groups of MWCNTs surface improve the hydrophilicity of membrane surface (see Fig. 3). This increase in hydrophilicity results an increase in water flux. In addition, the increase in pore size leads to increasing water permeation through the membranes. Increasing water flux up to 0.4 w.% of functionalized MWCNTs content can be attributed to improvement of membrane hydrophilicity due to functional groups of carbon nanotube and increase of the pore size of top-layer causing the more exchange rates between solvent and non-solvent during the phase inversion. However, when the MWCNTs amount exceeds 0.4 w. %, the high density of MWCNTs in the casting solution leads to an increase in the viscosity of solution [14] - [15]. This will hinder the exchange between solvent and non-solvent during the phase inversion and slow down the precipitation of the membrane. Also, the density of MWCNTs in the membrane is so large that the steric hindrance and electrostatic interactions among the MWCNTs and between the MWCNTs and the polymer chains cause to cluster the MWCNTs during phase inversion. Therefore, a less porous membrane was created in 1.0 w. % of MWCNTs.

The cross-section of the prepared polysulfone support layer with and without MWCNTs membranes were observed using scanning electron microscopy (SEM). The cross-section images of membranes prepared from (0, 0.2, and 0.4 w. %) MWCNTs are shown in Fig 5. The membrane prepared from polysulfone without MWCNT (Fig. 5 a) exhibits a typical asymmetric structure and developed macro-voids and dense thick top-layer. The membranes prepared by 0.2 w. % MWCNTs/PSU (Fig. 5 b) and 0.4wt% MWCNT/PSU (Fig. 3-4 c) demonstrated the strong change in sub-layer and skin layer morphology. The porosity of top-layer and sub-layer were increased. Very large macro-voids appeared in sub-layer by addition of low amount of functionalized multi walled carbon nanotubes. This result may be explained by the fast exchange of solvent and non-solvent in the phase inversion process due to the hydrophilic MWCNTs.

The AFM topography images for different compositions of MWCNTs/PSU are shown in Fig. 6. In these images, the brightest area presents the highest point of the membrane surface and the dark regions indicate valleys. The images indicate that the roughness is increased by adding (0.05, 0.2, 0.4w. %) MWCNTs to polysulfone support layer. Next, in 1.0 w. % roughness extremely decreases. The roughness parameters are presented in Table 3-1, which obtained from probing three randomly chosen AFM images.

3-2-4 ATR-IR test for polysulfone support layer.

Polysulfone support layer containing different ratio of surface modified MWCNTS (0.0, 0.2, and 0.4% wt.) were characterized by ATR-FT-IR spectra. These spectra are presented in fig. 7. The surface functional groups of acid modified MWCNTs were generated through the oxidation process

Table 1 Roughness of polysulfone support layer containing different ratio of MWCNTs.

Type of membrane	Min nm	Max nm	Peak to Peak nm	RMS nm	Average roughness nm
PSU only	-58.73	60.99	119.735	12.49	8.587
PSU+ 0.05w.%MWCNTs	-97.61	88.92	186.539	21.46	21.761
PSU+0.1w.% MWCNTs	-45.14	47.14	92.28	27.16	29.32
PSU+0.2w.% MWCNTs	-54.18	56.87	111.05	33.14	32.15
PSU+0.4w.% MWCNTs	-66.80	65.11	131.91	38.34	39.45
PSU+1.0w.% MWCNTs	-46.50	29.83	76.33	9.738	7.586

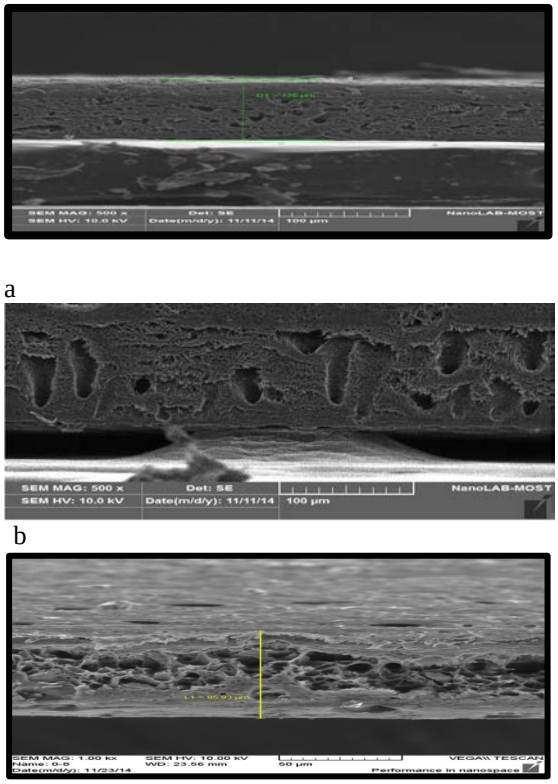

a

b

c

Figure 5 SEM shows the cross section of polysulfone support layer containing a- 0.0w.% MWCNTs b- 0.2w.%MWCNTs c- 0.4w.%MWCNTs

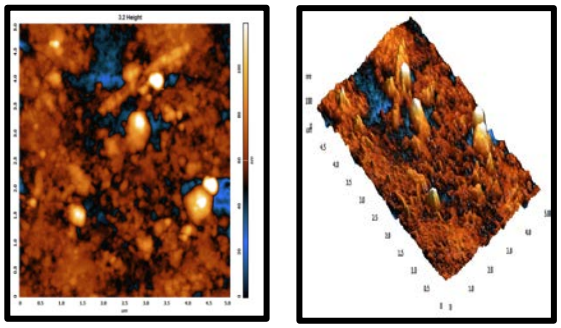

a-Polysulfone support layer only

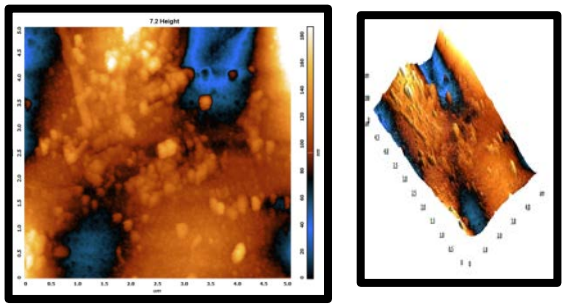

b - Polysulfone +0.05w. % MWCNTs

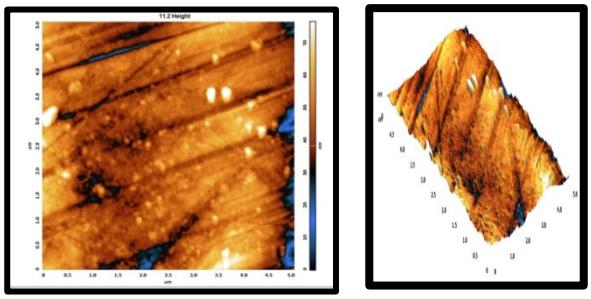

c- Polysulfone + 1.0w.% MWCNTs

Fig. 6 Shows AFM for polysulfone support layer containing MWCNTs

. The C-O-C symmetric stretching vibration at 1240 cm^{-1}, conjugation of C=O with C=C at 1670 cm^{-1}, the C=O stretching vibration at1715cm^{-1}, and the carboxylic acid group including the peak corresponding to the hydroxyl group at 3350 cm^{-1} were increased with the increase in MWCNTs loading. The C-O-C stretching increases should be expected with an increase in the carbon source, such as an addition of MWCNTs, and carboxylic groups would be increased in the acid modification process [15], [18]. It is expected that the polysulfone support layer containing higher amount of MWCNTs become more hydrophilic (fig. 3). This conforms that the affinity between the MWCNTs and the polysulfone matrix might be

stronger than other types of nanocomposite membrane.

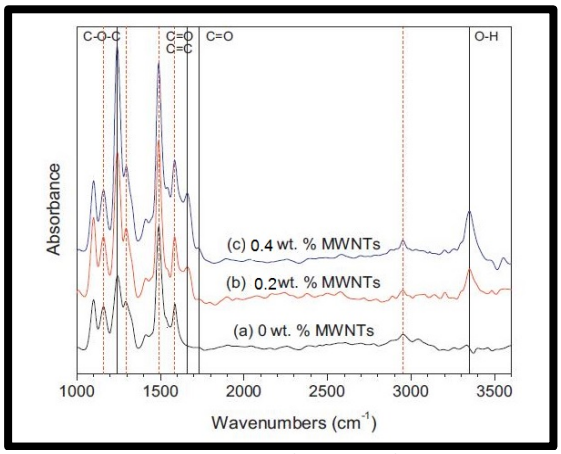

Fig. 7 ATR FT-IR spectra for polysulfone support layer containing different ratio of MWCNTs. red dashed line for polysulfone matrix and black solid line for MWCNTs.

3-3 Mechanical Property**.**

This test was conducted in laboratory of the advanced material department in ministry of science and technology in Baghdad. Five samples for each type of membrane were tested for tensile stress and percentage of elongation (mean ± standard deviation, n=5). The impacts of CNTs on the mechanical properties of the membranes are shown in table 2.

Table 2 Mechanical properties of the support layer with and without MWCNTs.

Specimen	Tensile stress Mpa	Elongation %
Polysulfone only	4.67±1.2	6.66±1.3
Polysulfone+ 0.05w.% MWCNTs	4.92±0.8	5.12±1.18
Polysulfone + 0.2w.% MWCNTs	4.68±1.35	5.10±0.6
Polysulfone + 0.4w.% MWCNTs	4.63±1.5	4.94±1.4
Polysulfone+ 1.0w.%MWCNTs	4.69±0.9	4.90±1.1

The polysulfone support layer containing MWCNTs shows decreases in elongation. As shown in the table above for support layer containing 0.4w. % MWCNTs there is no improvement in tensile stress but decreases in elongation about (25.8%) when compared with support layer without MWCNTs.

According to SEM pictures, the nanotubes are dispersed moderately in the membrane and coated with the polymer but the degree of disaggregation and interfacial bonding is not extended enough to achieve an efficient transfer of mechanical properties of CNTs to membranes.

Our polysulfone support layer containing MWCNTs suffered from weak stress preventing exploitation of the mechanical properties of the CNTs. transfer, a better dispersion could potentially be achieved with longer mixing time and sonication of the nanotubes in the solvent. These results agree with others literatures [2].

3-4 Permeability Test and Salt Rejection.

The permeability tests were conducted at room temperature (23±1 ^{0}C). Three coupons for each type of polysulfone support layer containing (0, 0.05, 0.1, 0.2, 0.4wt. %) MWCNTS with diameter 4.7cm were tested; first the membranes were compressed at 6 bars for 0.5 h. using deionized water then the pure water flux was measured for solution of 2000mg/l of NaCl. The pure water fluxes are increased by increasing the percentage of MWCNTs in polysulfone support layer as shown in fig. 7, by adding 0.4w. % MWCNTs to polyslfone support layer the water flux increased from 318L/m^{2}h to 487 L/ m^{2}h. That means an increase about 53% of pure water flux. The salt rejection for polysulfone support layer was not calculated since the nanopores of polysulfone structure did not allow significant salt rejection.

Not: - the performance of membrane contains 1.0w. % of MWCNTs was not conducted because of high viscosity of casting solution and formation of clusters of MWCNTs, which causes defects in the samples.

1. Conclusion

Polysulfone support layer show an enhancement to water uptake, hydrophilicity, surface roughness and permeability when small amount of modified MWCNTs were embedded in. SEM and AFM spectra show that large macro voids were created in polysulfone structure due addition of MWCNTs and their migration to the surface of membrane during phase inversion casting.

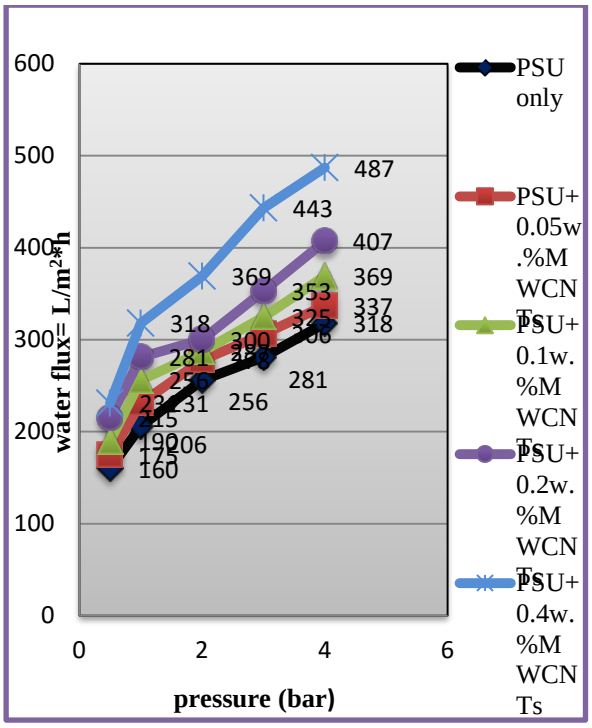

Fig. 7 Water flux for polysulfone support layer containing different ratio of MWCNTs. Flow 40L/h.

It was found that at optimal amount of MWCNTs addition 0.4w.%, the pure water flux of membrane increased from 318L/m^2.h to 487 L/m^2.h at TMP of 4 bars, that mean an increase about 53% of water flux. The salt rejection for polysulfone support layer was not calculated since the nanopores of polysulfone structure did not allow significant salt rejection. Mechanical properties of polysulfone support layer embedded with modified MWCNTs show no change in tensile stresses limit of membranes and a decrease of elongation about 25.8%.

References

(1) Peng Gao, Zhaoyang Liu, Minghang, "Multifunctional graphane oxide-TiO2 microsphere hierarchical membrane for clean water production". Journal of applied catalysis B: Environmental 138-139 (2013)17-25.

(2) L. Brunet et al., "properties of membranes containing semi-dispersed carbon nanotubes". Environmental engineering science journal, volume 25, number 4, 2008.

(3) Vahid Vatanpour, Sayed Siavash et al, "Fabrication and characterization of novel antifouling membrane prepared from oxidized multi walled carbon nanotube/ polyether sulfone nanocomposite". Journal of membrane science 375(2011)284-294.

(4) Eun-Sik Kim, Geelsu Hwang, Mohamed Gamal, "Development of nanosliver and multi-walled carbon nanotubes thin –film nanocomposite membrane for enhanced water treatment". Journal of membrane science 394-395 (2012).

(5) Gaurav S. Ajmani et al., "Modification of low pressure membranes with carbon nanotube layers for fouling control". Journal of water research 46 (2012)5645-5654.

(6) Rasel Das et al., "Carbone nanotube membranes for water purification, A bright future in water desalination". Journal of desalination 336(2014)97-109.

(7)Venkata K.K and et al., "Application of carbon nanotubes technology for removal of contaminates in drinking water". A review, journal of science of the total environment 408(2009) 1-13.

(8) Reza Sepahvand , Mohsen Adeli and et al. , "New nanocomposites containing metal nanoparticles, carbon nanotube and polymer", J Nanopart Res (2008) 10:1309–1318.

(9) Law Yong Ng, Abdul Wahab Mohammad, "Polymeric membranes incorporated with metal/metal oxide nanoparticles: A comprehensive review". Desalination 308(2013)15-33.

(10) M. Hosokawa, K. Nogi, M. Naito, T. Yokoyama (Eds.), "Nanoparticle Technology Handbook", First ed., Elsevier B.V., AE Amsterdam, 2007.

(11) J. Schaep, C. Vandecasteele, R. Leysen, W. Doyen, "Separation and Purification Technology" 14 (1998) 127.
(12)- Richard W.Baker, "Membrane technology and applications", John Wiley and Sons Ltd, 2nd Edition, 2004.

(13) Mark Wilf, Ph.D. Tetra Tech, "Membrane types and factors affecting membrane performance", Advanced membrane technologies Stanford University, May 07, 2008.

(14) M. Sun, Y. Su, C. Mu, Z. Jiang, "Improved antifouling property of PES ultrafiltration membranes using additive of silica-PVP nanocomposite", Ind. Eng. Chem. Res. 49 (2010) 790.

(15) S.-H. Liao, C.-C. Weng, C.-Y. Yen, M.-C. Hsiao, C.-C.M.Ma, M.-C. Tsai, A. Su, M.-Y.
(16) Youngbin Baek, Jihyun yu, and et al, "Effect of surface properties of reverse osmosis membranes on biofouling occurrences under filtration condition". Journal of membrane science 382(2011)91-99.

(16) E. Celik, H. Park, H. Choi, H. Choi, "Carbon nanotube blended polyether sulfone membranes for fouling control in water treatment", Water Res. 45 (2011) 274.

(17) M. Sun, Y. Su, C. Mu, Z. Jiang, "Improved antifouling property of PES ultrafiltration membranes using additive of silica-PVP nanocomposite", Ind. Eng. Chem. Res. 49 (2010) 790.

(18) A.L. Ahmad, A.A. Abdulkarim, "Resent development in additives modification of polyether sulfone membrane for flux enhancement", chemical engineering journal 223 (2013)246-267

(19) S.A.AL Malek, M.N. Abu Seman and et al., "Formation and characterization of polyether sulfone using different concentration of polyvinylpyrrolidone". Journal of desalination 288(2012)31-39.

(20) Xiao lei Qu, Pedro J.J, "Application of nanotechnology in water and wastewater treatment". Water research 47(2013)3931-3946.

(21) Siriat Kasemset, Alberto Lee, and et al., "Effect of polydopamine deposition condition on fouling resistance, physical properties, and permeation properties of reverse osmosis membranes in oil/ water separation". Journal of membrane science 425-426(2013)208-216.

Disposal of Sludge from Water Treatment Plants in the Manufacturing of Building Blocks (Bricks)

Ghaydaa Y. rasheed, Shaimaa T. Kadhum
University of Technology

Abstract - **Annually a huge amounts of sludge are generated from water treatment plants in Iraq, which are being either returned to River and this causes increase in mineral ions concentrations spatially Aluminum ion resulting from coagulants which added to sedimentation tank and these minerals have negative impacts on human health and its accumulation in the body causes many diseases like Alzheimer disease, or are eliminated by landfill in soil and this will affect the plants and groundwater by leaching. For these reasons it is necessary to find another way to get rid of this sludge, and this research is about using this sludge as a raw material in brick manufacturing offering an alternative safe method for its elimination. The sludge was burned at 550^{0}c and mixed at (10, 20, 30 %) with soil of Al-Nahrawan factory and each type of mixture burned at a variety of burning temperature (850,950, 1000, 1050^{0}c), means 12 types of brick and 36 samples produced, and for comparison purpose another 8 samples of brick was made without adding the sludge ash and burned with the same temperatures. The final tests on all the samples have shown that the physical properties of these samples match the Iraqi standards specifications (IQS 25/1988 (UDC: 591.44:6:1) for building bricks). Regarding the chemical properties there is a relative increase in the concentrations of minerals oxides of aluminum, calcium, magnesium and potassium in relation to Iraqi standards in general, but it was found that mixing the sludge ash in (10%) with soil and with a burning temperature of (1000^{0}c) will result in a building brick that is fully identical to the Iraqi standard specifications class (A) without any harmful environmental effects or increase in cost , if compared with cost that used to remove the effect of sludge on environment.**

Keywords: soil, coagulant, sludge, brick manufacturing

I. INTRODUCTION

Water industries globally consider coagulation is one of the major treatment unit used to improve overall treatment efficiency and cost effectiveness for water and wastewater treatment [(1), (2)]. The coagulation process itself generates most of the waste solids. Generally a metal salt (aluminum $^{+++}$ or iron $^{+++++}$) is added as the primary coagulant [(3), (4)]. These metal residual in treated water is undesirable for aesthetic reasons, but also because of a possible link between aluminum and neurological effects such as Alzheimer's disease, children mental retardation, and the common effects of heavy metals accumulation [(5), (6)].So that, the coagulation sludge disposal methods should be considered.

In Iraq, the sludge discharged into rivers and this lead to accumulative rise of aluminum concentration in river water, aquatic organisms, and human bodies. For this reason, it became necessary to reuse these sludge in another fields especially industry.

Some scientists used the inorganic environmental hazardous contaminants material in sludge for production of building materials which bound as mineral to the material and utilization of sludge reduces mining of raw material for production of building material [(7)]. Andersone used incinerator sludge ash as a clay substitute during the manufacturing of bricks and he found that the process improves the ceramic properties and product strength of the resulting construction materials [(8)]. While in Egypt, water treatment plant sludge used with clay with different mixing proportions and with different firing degrees, and they found that 50% was the

optimum sludge addition to produce brick from sludge – clay mixture with properties superior to those available in the Egyptian market [9]. Another researchers used the produced sludge from wastewater treatment plants in brick manufacturing [10], as in Taiwan a research was performed about using the produced sludge from wastewater treatment plants in brick manufacturing and they noticed that the addition of 20% sludge and with burning temperature 960-1000^{0}c the compressive strength being within the Chinese standard specifications and gives a good quality brick [11].

Also the industrial wastes were used in building units manufacturing such as the waste of a paper factory. These waste were used with 40-50% and mix with 15-20% lime without burning and high pressure (10 Mpa) were supplied. The compressive strength were tested after 3, 7, and 28 days and it have been noticed the increase of strength with time even arrived (20.5 Mpa) after 28 days [12]. Another researchers used the olive mill wastewater in building bricks manufacture by mixing it with clay and the results of this study showed a significant increase in the volume shrinkage (10%) and the water absorption (12%), while the tensile strength remained constant. The maximum plasticity index value was found when incorporating 23% of olive mill wastewater. This rate either maintained the physical and mechanical properties of brick or improved them [13]. In our country Iraq, a lot of researches have been done to study the probable beneficial effect of many types of additives to the soil on brick quality for example adding lime to the soil to produce brick [14], but there was no study have been done about using the producing waste from water and wastewater treatment plants in brick manufacturing.

II. MATERIALS PREPARATION

Settled sludge from coagulation basin of Wathba treatment plant (north east of Baghdad) which gets its supply of water from Tigris River is used. The station use aluminum sulfate (alum) in purification process with 1% proportion. Sludge contain a proportion of water and for drying sludge has been put in containers exposed to air for evaporation, and for drying the rest of water it has been put in ovens with 110^{0}c for one day. Three samples of dried sludge were taken, the physical properties were studied and the average value was taken as shown in Table (1), also the chemical properties were studied as shown in table (2). The second step was removing of organic materials by burning at 550^{0}Cfor one hour. Samples of burnet sludge were taken and the physical and chemical properties were studied as shown in table 1, and table 2 to know the changes that happen due to burning. Table (3) shows the standard methods for the physical and the chemical experimental test of burnt sludge, unburnt sludge, and soil.

Burnt sludge were crushed and passed throw sieve 75mm and the passing were used in brick manufacturing.

Soil of Al-Nahrawan factory were analyzed to find the physical and the chemical properties as shown in Tables 1 and Table 2. Also a hydrometer test was made to know some of soil characteristics and the results proved it ranging between silt and clay with varying percentages 60 % clay and 40 % silt as shown in figure (1). Then soil were dried at 110^{0}c for one hour to get rid of water content, crushed, and used the passing throw sieve 75mm in brick manufacturing.

TABLE 1

THE PHYSICAL PROPERTIES OF THE BURNET SLUDGE, UNBURNT SLUDGE AND THE SOIL

Test	Type of material		
	Soil	Unburnt sludge	Burnt sludge
Water Content (WC)	12%	100%	2.6%
Liquidity limit	30	26.7	NON
Plasticity limit	14.8	NON	NON
Plasticity index	16	26.7	NON
Soil type	Sand – Silt Clay	Sand	Sand

TABLE 2

THE CHEMICAL PROPERTIES OF THE BURNT SLUDGE, UNBURNT SLUDGE AND THE SOIL

Test	Type of material			
	Soil	Unburnt sludge	Burnt Sludge	Iraqi standard specification
pH	7.6	7.2	7	--------
EC	1120	1090	1140	--------

Test	Type of material			
	Soil	Unburnt sludge	Burnt Sludge	Iraqi standard specification
(µm/cm)				
TDS %	560	540	540	--------
OM %	5.6	16.7	2.6	--------
CL %	0.071	0.0177	0.62	--------
SO_4^- %	0.25	0.205	0.2	≤ 0.3%
CO_3 %	0.7	0.5	0.4	--------
SO_4^- %	0.537	0.537	0.43	--------
AL_2O_3	1.89	20	10	--------
PbO %	0.0003	0.0008	0.0006	5.0 mg/l
CdO %	0.000013	0.000014	0.00001	1.0 mg/l
CaO %	7.9	10.6	7.76	0.1 %
MgO %	1.5	0.63	0.52	0.03 %
K_2O %	0.13	0.07	0.056	0.03 %
Na_2O %	0.4	0.04	0.032	0.03 %
MnO %	0.06	0.068	0.032	--------

TABLE 3

STANDARED TEST METHODS OF THE PHYSICAL AND THE CHEMICAL PROPERTIES OF THE SOIL, BURNT SLUDGE, AND UNBURNT SLUDGE.

Test	Symbol	Unit	specification
Water content	Wc	%	ASTM* D2216 -92 -COE L1 DOD†† 2-V:1
Atterberg limits	L.L – P.L	%	AST M D4318-95 : CODE 111 :DOD- V111
Sieve analysis	----------	---------	ASTM D422 - 63 –COE V:DOD -2-111,2-V;CSSS 47.4
Hydrometer test	----------	----------	ASTM D 422 - 63 ; CSSS† 47.3 ; COE VCSSS.47.2
pH	pH	----------	ASA** 1996 Ch 16 :16.2.1
Electrical conductivity	Ec	(µmoh/cm)	ASA 1996 Ch 14
Dissolved salts	TSS	%	ASA 1996 Ch 14:18.2.2
Organic material	O.M	%	ASTM D2974, D297 ; D2974 – SI –AEA 1984 ;29-4.2; CSSS 44.3
Carbonate	CO_3	%	ASA 1996 Ch 16; CSSS 14.2 and 44.6
Sulphite	SO_3	%	ASA 1996 Ch33
Gypsum	$CaSO_4.2H_2O$	%	ASA 1996 Ch33
Chloride	Cl	%	ASA 1996 Ch31
Sodium	Na	%	ASA 1996 Ch19
Potassium	K	%	ASA 1996 Ch19
Mineral content	---------	---------	EPA†* –SW 846 -200.,;ASA 1996 : Ch 18-30

Notes:

*ASTM = American Society for Testing and Material (ASTM 1996) [15]

**ASA = American Society for Agronomy /Soil Science Society of America – Method of soils Analysis, part-1996[16]

†CSSS= Canadian Society of soil Science (Carter 1993) [17]

††DOD = U.S. Department of the Army Navy, and Air Force 1987. [18]

†*EPA= USEPA (1986) [19]

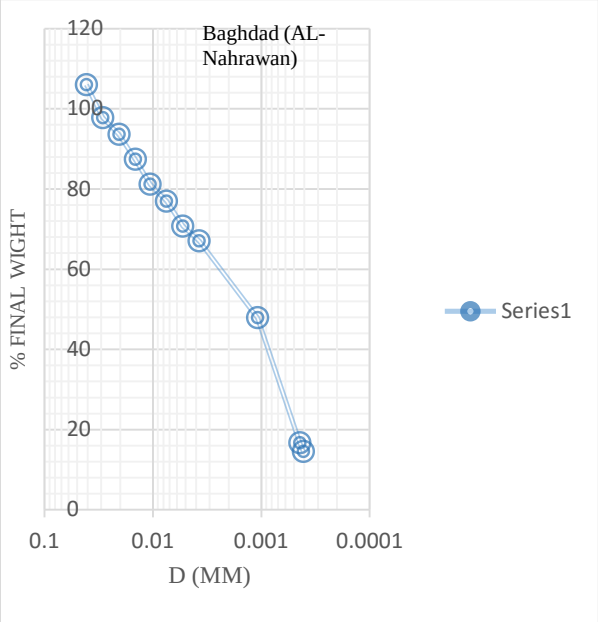

Fig. 1: Hydrometer test results

III. SAMPLES PREPARATION

A wooden templates with height, length, and depth (8*12*12 cm) dimensions viz. half brick were manufactured and each template were surrounded with aluminum bond to increase durability and bears pressure.

The work was divided into two parts. The first part was manufacturing of building units consist of (10, 20, and 30%) of burnt sludge (prepared previously), and (90, 80, and 70%) of soil and mixed with 17% water. Then were casted and a pressure of (1045 N/cm^2) was applied for consolidation. For each percentage, 12 samples were manufactured, means 36 samples. These samples were left in air for 7 days for

drying and shrinkage to facilitate samples extraction from templates. After that, these samples were left for another 7 days for drying. For get rid of water content they were put in oven at 110^0C temperature for 24 hours. After that, every four samples of the same mixing proportion were exposed to different burning temperatures (850, 950, 1000, and 1050^0C) and for all percentages. The burning process was mad in the structural lab in the University of Technology. Table (4) shows the quantities of soil and burnt sludge which used in brick manufactured.

TABLE 4

QUANTITIES OF THE SOIL AND THE SLUDGE USED IN BUILDING UNIT (BRICK) MANUFACTURING

Type of brick	Percentage (%)			Plasticity index (P.I)	Weight (gm)			Total solid weight(gm)	Added water volume (ml)
	Sludge	Soil	Water		Sludge	Soil	Water		
1	10	90	17	15.9	230.4	1682	392.5	1912.4	
2	20	80	17	15.5	460.8	1451.7	392.5	1912.4	392.5
3	30	70	17	15.1	691.2	1221.2	392.5	1912.4	392.5
4	0	100	17	16	-----	1912.4	392.5	1912.4	392.5

The other part included production of 8 samples of brick manufactured from soil and 17% water and by the same previous method of molding and drying, also every two samples were burned in a different temperatures of burning (850, 950, 1000, and 1050^0C) for comparison.

IV. DISCUSSION OF THE RESULTS

A. CHEMICAL PROPERTIES OF SOIL AND SLUDGE

As shown in Table (2), pH value of sludge ash sample was 7 which is less than that of unburnt sludge and soil, and that indicate neutrality of sludge ash due to treatment of` sludge by burning and so decrease its activity. Also, we notice the similarity between soil's contents and sludge's contents and the percentages of their metals are convergent except for aluminum and calcium as their concentrations in sludge are higher than in soil and these concentrations decrease after burning of sludge at 550^0C as a treatment, also high temperatures caused oxidation of metals and decrease leaching. When we compare the percentages of metals in burnt sludge with Iraqi standard specifications [20], we notice that aluminum, calcium, magnesium, and potassium percentages more than specifications. During manufacturing of bricks, sludge ash and soil will burn at temperatures over than 850^0C and till 1050^0C and at these temperatures metal oxides will form and leaching value will decrease.

B. PHYSICAL PROPERTIES OF SOIL AND SLUDGE

Water content have great effect on atterberg limits and especially the plasticity of the soil. Soil with plasticity index (PI) range between (0-0.5) consider as non-plastic, (PI) range between (15-30) slightly plastic, and (PI) greater than (35) consider as highly plastic [21]. Table (1) showed that (PI) for soil was (16) and consider slightly plastic, and it was (26.5) for unburnt sludge, while the sludge ash were considered as non-plastic. From Table (4), we can notice that the plasticity index values of sludge ash and soil mixtures are consider as slightly plastic for all mixing percentages, and there was no significant reduction in the plasticity index of soil by the addition of sludge ash. PI decrease with the increase of the added sludge ash percentage.

C. ABSORPTION OF WATER

Work has been done to determine the amount of water absorbed by bricks and the rate of absorption, in an attempt to arrive at some scientific basis for grading bricks according to their resistance to the penetration of water [22]. Figure (2) shows the results of percentages of absorption for all types of bricks with different proportions of sludge and burning temperature and we notice increase percentages of absorption with increase the percentage of the added

sludge ash to soil, and decrease with increase of burning temperatures.

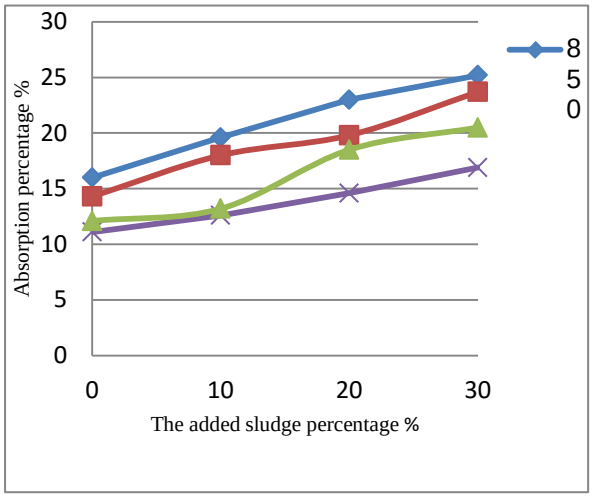

Fig. 2: Relationship between sludge ash and percentages of absorption of water

The correlation between brick mixture contents have a great role in ability absorption. From the above, it shows that plasticity index PI decrease as sludge ash added increase and so the correlation between sludge ash and soil will decrease. Whenever percentage of the added sludge ash increase, the sludge ash ability of adhesion to mixture will decrease and so the pours in brick will increase and as a result of this the absorption ability of brick will increase. According to the Iraqi specification [20], set 20% absorption as brick type (A), 24% brick type (B), (26%) brick type (C). From figure (2) we notice that all bricks with different percentages of the added sludge have less than 20% absorption at burning temperatures 1000^0C and 1050^0C so considered as brick type (A), and proportions of mix (0, 10, and 20%) at 950^0C and proportions of mix (0, 10%) at 850^0C are type (A), and the rest are type (B).

D. EFFLORESCENCE

Efflorescence is a powdery deposit of salts which forms on the surface of bricks and mortar. It is usually white but efflorescence may be yellow, green or brown. Salts enter the wall from various sources. New bricks seldom contain soluble salts but mortar and concrete have relatively high soluble salt contents [23]. When these salts have a high percentages of SO_4, It will affect the cement mortar. Iraqi specification classified the mild efflorescence as type (A) and the moderate efflorescence type (B). The efflorescence results were mild to none. Therefore, all the produced samples of bricks classified as type (A). Going back to Table (2), we can notice that the percentage of SO_4 soluble in acid within the specification and the percentage of dissolved salts in soil, sludge, and ash are within the standard specification.

E. LOSS ON IGNITION

Sludge was burned at 550^0C to remove the organic materials. From Table (2), we notice the decreasing in organic material after burning from 16.7% to 2.6 %, while the soil have 5.6% organic materials. Figure (3) shows the relationship between the percentage of the added sludge ash and the percentage of loss by ignition with all different temperatures and the increase in the added sludge ash will decrease the loss by ignition of the brick. In this research we notice that all the results of loss by ignition are less than (20%) and within the Iraqi standard specification [20] except brick of no addition of sludge and with 850^0c burning temperature is consider higher than of specification.

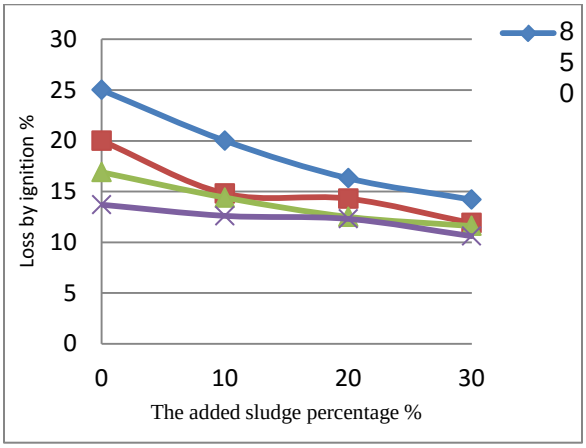

Fig. 3: relationship between percentage of sludge added and percentage of loss on ignition

F. COMPRESSIVE STRENGTH

Bricks vary in compressive strength due to the differing qualities of raw material and the method of firing. Compressive strength test is consider one of the most important tests of building units. Figure (4) Shows that the compressive strength of brick depends

on the percentage of the added sludge ash to mixture and on the temperature of burning, and the best percentage of the added sludge ash which give brick with the best compressive strength is (10%) of the weight of brick. With 950^0Call percentages of the added sludge give compressive strength values within the limits of brick type A according to Iraqi specification.

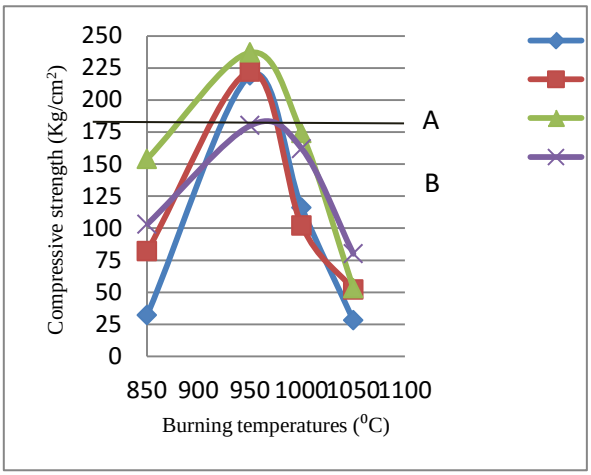

Fig. 4: Relation between compressive strength and the added sludge percentage

V. ECONOMICAL VIEWPOINT

This research have practically proved the success of using the waste of water treatment plant in brick manufacturing and the produced brick met the Iraqi specification and also gave the opportunity of disposal of the sludge in environment friendly way. Wathba plant disposed the sludge by draining it directly into Tigris River and that pose a threat to the health of people by exposing them to the heavy elements in direct and indirect ways. To study the economic feasibility of using the waste of water treatment plant in brick manufacturing we should begin from the inside of Wathba plant. The produced sludge from settling basins must be dried and that requires build an opening basins (50m x 10m) approximately and this a necessary step for any required treatment. The quantity of sludge differs depending on seasons and turbidity which it approximately 1000 NTU in winter with sludge quantity about 22 Ton/ day, while it approximately 40 NTU in Summer with sludge quantity about 3 Ton/day. In addition to these costs there is a transport cost from Wathba plant to brick factory and the cost of consuming the burning furnace which used basically in brick manufacturing. The Feasibility consist of sludge transport and furnace consuming if we consider the cost of draying basin construction is a basic step for any water treatment plant. The small extra cost of sludge disposal by using it in brick manufacturing in comparison to the transport only cost of the landfill method of sludge disposal can be justified easily given the benefit of avoiding the large environmental pollution caused by the landfill method.

VI. CONCLUSIONS

From the results of this study we can conclude the following:

1- Burning of sludge at 550^0c as a treatment decrease the percentage of organic materials and chemicals in it. But, the percentages of aluminum, calcium, magnesium, and potassium consider above the Iraqi specifications.

2- All mixtures of sludge ash and soil with different percentages of the added sludge consider slightly plastic and there is no significant reduction in the plasticity index of soil by the addition of sludge ash.

3- All bricks with different percentages of the added sludge have less than 20% absorption of water at burning temperatures 1000^0c and 1050^0c so considered as brick type (A), and proportions of mix (0, 10, and 20%)at 950^0c and proportions of mix (0, 10%) at 850^0c are type (A), and the rest are type (B).

4- All the produced samples of bricks classified as brick type (A) according to Iraqi specification.

5- All the produced samples of bricks with different percentages of the added sludge and different burning temperatures have loss of ignition values less than 20% and within limits of Iraqi specification.

6- With regard to compressive strength, brick with 10% sludge ash and with all burning temperatures is classified as brick type (A).

REFERENCES

[1] Jia Q. Jiang. The role of coagulation in water treatment. Current opinion in chemical engineering. Volume 8, May 2015, pages 36-44.

[2] Mohammed, H.A.M., Abvzaid, N.S., and AARIF, H.A.M. Coagulation of polymeric wastewater discharged by a chemical factory .waters 33, (1998) , NO. 2-521-529.

[3] EPA. Water treatment residuals management for small systems. Water research foundation (2009).

[4] Schulz, C.R. and Okun, D.A, (1992) Surface water Treatment for communities in developing country John Wiely & Sons, New York.

[5] IWA Water Wiki. Coagulation and flocculation in water and wastewater treatment. 2010. www.iwawaterwiki.org.

[6] Prakhar. P.E.and K.S.Arup. Donnan Membrance process. Principles & Application in Coagulant Recovery from water Treatment plant Residuals. Lehigh University. Beth/chem.PA 18015 (1998).

[7] Lubarski, V., Levlin,E., and Koroleva,E., Endurance test of aluminous Cement produced from water treatment sludge. (1996) Vatten, 52 (1), 39-42.

[8] Anderson, M., R .G., Skerratt, J.P. Thomas, and S.D. Clay (1996) case study Involving Fluidized Bed in Brick Manufacture. Water Science and Technology .Volume 34, Number 314.PP.507-515.

[9] Ramadan, M.O; Fouad, H.A; Hassanain, A.M; Reuse of water Treatment plant sludge in Brick Manufacturing. Journal of Applied Sciences Research .4 (10):1223-1229. (2008) Egypt.

[10] Alleman, J.E., and Berman, N.A. Constructive sludge management: biobrick, J. Env. Eng., 110(2), 301-311(1984).

[11] Weny, C.H.,Lin,D.F., Chiany, P.C., Utilization of sludge as brick materials . Advances in Environmental Research 7(2003) 679-685 (Taiwan). http://www.elsevier.com/locate/aer.

[12] Mymrin, V.,Ferreira,A.m.c.,Gardolinski, J.E.; Guimaraes, B.; Okiomoto,M.L.L.(2009) paper production sludge Application for producing of new construction Materials proceeding of the 11th international conference on non-conventional Materials and Technologyies (NOCMAT 2009) 6-9 September , Bath, UK, Brazil.

[13] Mekki, H.; Nderson, M.; Benzina,M; and Ammar,E.; V alorization of Olive mill wastewater by its incorporation in buildings bricks. Journal of Hazardous Materials Vol.158 issues 2-3 October 2008 pages (308-315). Tunisia.

14- القس دز رائد متي, محمد عبد الحسن, نسرين ابراهيم, سوسن فؤادز. تأثير حبيبات الكلس المتواجدة في التربة على خواص الطابوق الطيني. مجلس البحث العلمي/ مركز بحوث البناء/ ت.ب 102/ 1985.

[15] American Society of Agronomy. Methods of soil analysis part 1 .Physical and mineralogical properties, including statistics of measurement and Sampling. (1965) Madison, W1.

[16] American Society of Testing and Materials (1996) Annual book of ASTM .Standards. Philadelphia, PA.

[17] Carter, M.R., ed. Soil sampling and methods of analysis .Candian Soc.Soil Sci., Lewis Publisher, Boca Raton, Ann Arbor,London , (1993)Tokyo.

[18] Department of the Army, Novy, and Air Force.Materials testing , Field Manual 5-530,U.S.Army Engineer School, Fort Bslvoir, VA (1987).

[19] U.S. Environmental Protection Agency. Test methods for evaluation of solid waste. U.S. Environmental Protection Agency. Office of Solid waste and Emergency Response, Washington, DC. (1986).

20- المواصفة القياسية العراقية رقم 24.25 لسنة 1988 لخصائص الطابوق الفيزيائية وللاملاح الذائبة في الماء. الجهاز المركزي للتقييس والسيطرة النوعية/ وزارة التخطيط.

[21] Wary, W.K. Atterberg limits. Chapter &: Measuring engineering properties of soil, Prentice-Hall. (1985) Englewood cliffs, N.J.

[22] Civil Construction Tips. Properties of bricks – hardness, compressive strength, absorption, frost resistance, efflorescence. January 7, 2011. Copyright © Civil Construction Tips

[23] AZO MATERIALS. Brick Walls and Brickwork – Efflorescence. June 11, 2013. www.azom.com

Noise Acoustic Pollution In Tikrit University Buildings

Abbas Hadi Abbas
envabbas@yahoo.com
Mob.07702646694

Asst.prof. Riyadh M. Mahmood
alsaleem1962@yahoo.com
Mob. 07706273109

Abstract

The present era is representing a noise era with excellence because of the spreading of communications media, music and visuals on a large scale, causing a state of negative disturbing and annoying, especially in buildings that need a large amount of relative calm, such as hospitals, libraries, schools and universities. In our research paper that has been selected (University of Tikrit) campus to make the measurements realistic and true to some vital buildings which are representing of selected classrooms to see how much the amount of acoustic noise affecting the functioning of the teaching process in those buildings, and also in the building reading halls of central library and several cafeterias inside university campus .It was observed that most of the buildings at the university suffers from an unacceptably high level of noise emitted from many sources .The results showed that the noise levels need for more attention to this phenomenon where it was found that the noise from the surrounding buildings exceeded all acceptable standards, as well as the ambient noise on the campus of colleges emitted from different sources continuously .

In this paper several criteria are studied to identify those specifications. These criteria are represented by the outdoor and indoor noise sources of classrooms and also the manner of measurement of direct mathematical calculations, as well as properties that affect the receipt of the concept of lecturer diction , including the Signal to noise ratio (SNR) and the distance between the Lecturer and students . It has been recommended, that it can be obtained a quiet classrooms using modern technology (construction materials, proper equipment, and design appropriate), as well as to give more attention to treat the noise sources with appropriate recommendations to reduce it like the noise emitted from diesel electrical generators , traffic nose and loudspeaker of cafeterias.

Key words: Noise, internal sources, external sources, voices.

1. Introduction

Noise enters all our facilities and become a problem for the comfortable of humans. Factories, streets, outer roads, and stations or airports, noise has crept into our life and without feeling in spite of the human tendency to adapt [1].

Continuous exposure to noise leads to loss of hearing with age and the estimated number of people from the age group (50-60 years) who have lost their hearing partially or totally are tens of millions of people and expected to increase the proportion of these people for the present generation of young people when they reach that age because of the increased exposure to noise compared to generations before them [2].

Noise pollution effects the understanding of lectures in the classrooms also effects on workers and students (customers) in restaurants and cafeterias. Hence the need to conduct a survey of noise pollution in the Tikrit University.

In this research, the field work included noise measurements and other field measurements for a number of buildings at the University of Tikrit included cafeterias, classrooms, and the central library. The following is a description of the equipment and tools used in this study as well as field work:

a. Digital Sound Level meter: In this study, sound level meter model 407 730 from the production of Extech Instrument Company as shown in Figure (1) is used to measure the noise.

Figure (1) sound level meter

b. Measuring tape: used to measure the distances between sound sources and recipients.

2. Fieldwork

Included measurements of noise pollution for a number of halls, restaurants (cafeterias) and number of classrooms in the University of Tikrit, as shown below:

1. Reading halls in the Central Library:
   A. Hall No.(1) with dimensions: (25 × 25 × 3) m.
   B. Hall No. (2) with dimensions: (25 × 25 × 3) m.
2. Faculty of Agriculture:
   A. Cafeteria (boys) with dimensions (15.7 × 11.5 × 2.5) m.
   B Cafeteria (girls) with dimensions (13.2 × 6.5 × 2.5) m.
3. Cafeteria of the Faculty of Pharmacy with dimensions: (18 × 17.5 × 2.9) m.
4. Student Center Cafeteria at the university with dimensions :(31 × 24 × 4.5) m.
5. Classroom at the Faculty of Law Department No. (2) with dimensions of: (14.5 × 8 × 4) m.
6. Classroom at the Faculty of Political Sciences No.(1) with dimensions of: (14.5 × 8 × 4) m .

2.1. Mathematical equations:

2.1. Sound pressure level (SPL) is a logarithmic value of the ratio between the instantaneous sound pressures effective to the acoustic pressure quadrate. The equations are listed below [3], [4].

SPL = 20 Log $\frac{P}{P_o}$ …….(1)

SPL = 20 Log $\frac{P}{2*10^{-5}}$

SPL: sound pressure level dB (A).

P: acoustic pressure effective.

Po: acoustic pressure quadrate, hearing threshold ($2 * 10^{-5}$ Pa).

2. 2. Equivalent Continuous Noise Level (Leq):

Leq = 10 Log [($t_1 * 10^{L_1/10} + t_2 * 10^{L_2/10} + t_3 * 10^{L_3/10} + t_4 * 10^{L_4/10}$ …..) / T] ……. (2)

Leq: the alleged equivalent continuous sound dB (A).

t1, t2, t3 ...: the time required for each particular sound pressure level (h).

L1, L2, L3, sound pressure level each time dB (A).

T: total time (hours) [5].

2. 3. Sound Pressure Level at Distance:

SPL = Lw – 20 Log r – 11 (For absorbent Ground) ……. (3)

SPL = Lw – 20 Log r – 8 (For Non - absorbent Ground) ……..…… (4)

SPL: sound pressure level at a certain distance dB (A).

Lw: sound pressure level ((measurement device)) dB (A).

r: distance (radius) m[6].

Constant depends on the type of land Are absorbent or non-absorbent of sound.

Drop = 20 Log $\frac{Far}{Near}$ ……. (5)

Drop: reduction in the intensity of sound pressure level dB (A).

Near: the distance from the noise source to the point where the subject noise measuring device (m).

Far: The distance away from the noise source (m)[7].

Professor voice at a certain distance = voice professor at the measurement - the reduction site..... (6)

2.4. To measure verbal conceptual, we are using the speaker-to-noise ratio (SNR):

SNR = voice Professor at a certain distance - the existing noise level in the classroom [8] …. (7)

2.5. Find the outcome of the two source of noise:

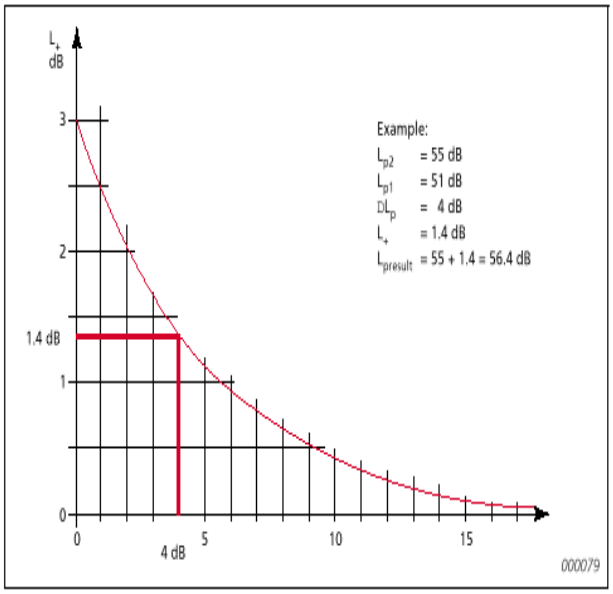

Fig. (2) Curve to create the effect of more than one source of noise on the final outcome.

The outcome of the noise (SPL) for two or more sources are not worth the simple combination of forced exporters to noise levels, but it is taking the difference between the noise level b dB (A) then extracted the increment from the curved shown in Fig. (3)[9][10].

3. Measurements tables.

Table (1) the noise level in the reading hall number (1) - Central Library.

The time From ---To	The number of the readers students	The case of diesel generator near the library	Noise inside the hall dB (A)	Noise equivalent dB (A)	Acceptable limit Leq dB (A)
9:00-11:00	39	Operated	60.6	57.99	30-45
11:00-12:30	35	Operated	55.4		
12:30-2:30	28	Operated	52.2		

Table (2) the noise level in the reading hall number (2) - Central Library.

The time From ---To	The number of the readers students	The case of diesel generator near the library	Noise inside the hall dB (A)	Noise equivalent dB (A)	Acceptable limit Leq dB (A)
8:45-11:00	19	Operated	48.3	49.03	30-45
11:00-12:30	20	Operated	51.0		
12:30-2:30	11	Operated	47.9		

Table (3) the noise level in the cafeteria (No.1) of the College of Agriculture.

The time From --To	Number of workers exposed Noise	Acoustic pollution sources	No.	Case Operating	Internal Noise level dB (A)	Exposure time Hour	Leq dB(A)	Notes
8:30-10:30	4	People (customers)	12		62.8	2	77.32	
		Loud speaker	1	x				
		Air Conditioner	1	x				
		TV	1	x				
		Fan	3	x				
		External noise level rate dB (A)	55.9	x				
10:30-12:30	2	People (customers)	14		77.8	2		
		Loud speaker	1	x				
		Air Conditioner	1	x				
		TV	1	x				
		Fan	3	x				
		External noise level rate dB (A)	67.2	x				
12:30-2:30	2	People (customers)	22		80.0	2		
		Loud speaker	1	x				
		Air Conditioner	1	x				
		TV	1	x				
		Fan	3	x				

		External noise level rate dB (A)	77.6	x				

Table (4) the noise level in the cafeteria (No.2) of the College of Agriculture.

The time From --To	Number of workers exposed Noise	Acoustic pollution sources	No.	Case Operating	Internal Noise level dB (A)	Exposure time Hour	Leq dB(A)	Notes
8:30-11:30	2	People (customers)	17		61.4	3	78.43	
		Loud speaker	1	x				
		Air Conditioner	2	x				
		TV	1	x				
		Fan	3	x				
		Cloning device	1	x				
		External noise level rate dB (A)	53.0	x				
11:30-1:30	2	People (customers)	28		81.8	2		
		Loud speaker	1	x				
		Air Conditioner	2	x				
		TV	1	x				
		Fan	3	x				
		Cloning device	1	x				
		External noise level rate dB (A)	76.6	x				
1:30-3:00	2	People (customers)	25		79.9	1.5		
		Loud speaker	1	x				
		Air Conditioner	2	x				
		TV	1	x				
		Fan	3	x				
		Cloning device	1	x				
		External noise level rate dB (A)	78.1	x				

Table (5) the noise level in the cafeteria of the College of Pharmacy.

The time From --To	Number of workers exposed Noise	Acoustic pollution sources	No.	Case Operating	Internal Noise level dB (A)	Exposure time Hour	Leq dB(A)	Notes
8:30-10:30	11	People (customers)	10		70.7	2	78.16	Cafeteria close to street traffic for vehicles
		Loud speaker	1	x				
		Air Conditioner	5	x				
		TV	1	x				
		Fan	5	x				
		External noise level rate dB (A)	67.8	x				
10:30-12:30	11	People (customers)	70		80.8	2		
		Loud speaker	1	x				
		Air Conditioner	5	x				
		TV	1	x				
		Fan	5	x				
		External noise level rate dB (A)	79.5	x				
12:30-2:30	11	People (customers)	25		78.1	2		
		Loud speaker	1	x				
		Air Conditioner	5	x				
		TV	1	x				
		Fan	5	x				
		External noise level rate dB (A)	80.3	x				

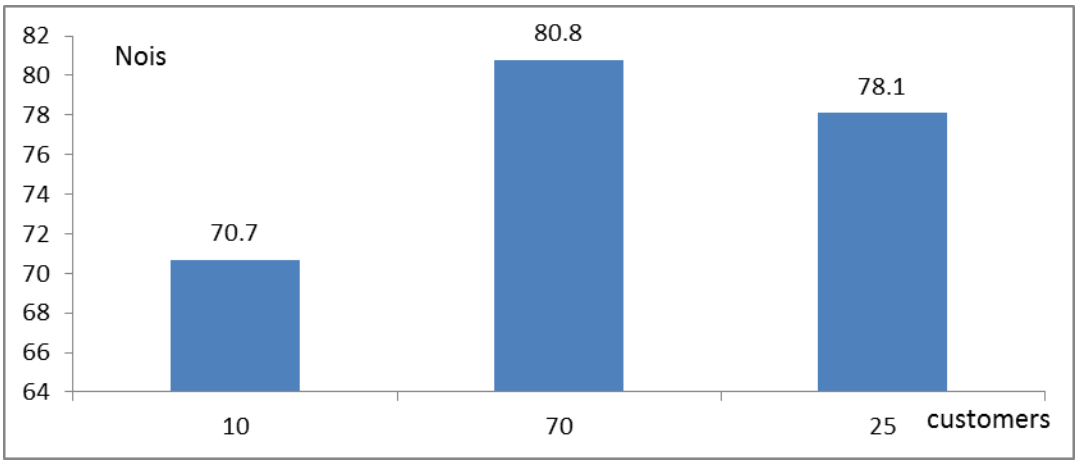

Fig.3. The relationship between the customers and the noise in the cafeteria of the College of Pharmacy.

Table (6) the noise level in the cafeteria of the Student Center.

The time From --To	Number of workers exposed Noise	Acoustic pollution sources	No.	Case Operating	Internal Noise level dB (A)	Exposure time Hour	Leq dB(A)	Notes
8:30-10:30	5	People (customers)	31		63.3	2	79.22	
		Loud speaker	2	x				
		Air Conditioner	5	x				
		TV	2	x				
		Fan	18	x				
		Billiards	4	x				
		External noise level rate dB (A)	71.6	x				
10:30-12:30	5	People (customers)	95		82.89	2		
		Loud speaker	2	x				
		Air Conditioner	5	x				
		TV	2	x				
		Fan	18	x				
		Billiards	4	x				
		External noise level rate dB (A)	77.6	x				
12:30-2:30	5	People (customers)	70		77.5	2		
		Loud speaker	2	x				
		Air Conditioner	5	x				
		TV	2	x				

		Fan	18	x				
		Billiards	4	x				
		External noise level rate dB (A)	81.3	x				

Table (7) the noise level at the Faculty of Law classroom No.(2).

The time From - -To	Number of students	Acoustic pollution sources (All works)	No.	Professor Voice dB (A)	Internal noise level busy by students dB (A)	Leq dB(A)	External noise level dB (A)	Internal noise level Unoccupied and without work devices dB (A)	Damping Noise walls, windows and door dB (A) (All are Not matching)	SNR dB(A) Distance from the Professor (3 meters)
8:30-10:30	96	Air Conditioner	1	**65.3**	**58.6**		**75.4**	**58.6**	**16.8**	**-8.86**
		Fan	2							
11:00-1:00	96	Air Conditioner	1	**69.0**	**60.9**	**59.4**	**77.6**	**60.9**	**16.7**	**-7.46**
		Fan	2							
1:00-2:00	65	Air Conditioner	1	**62.8**	**56.4**		**73.9**	**56.4**	**17.5**	**-9.16**
		Fan	2							

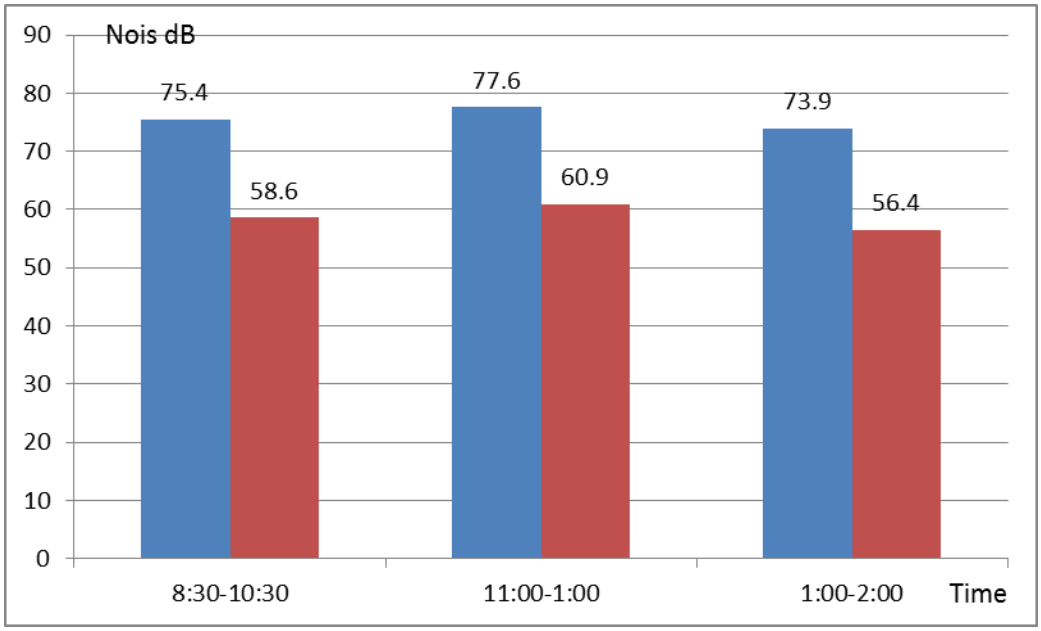

Fig.4. The relationship between time and noise at the Faculty of Law classroom No.(2).

Table (8) the noise level at the Faculty of Political Sciences classroom No.(1).

The time From - -To	Number of students	Acoustic pollution sources (All works)	No.	Professor Voice dB (A)	Internal noise level busy by students dB (A)	Leq dB(A)	External noise level dB (A)	Internal noise level Unoccupied and without work devices dB (A)	Damping Noise walls, windows and door dB (A) (All are Not matching)	SNR dB(A) Distance from the Professor (4 meters)
8:30-10:30	25	Air Conditioner	1	**79.9**	**73.4**		**79.9**	**73.4**	**6.5**	**-5.54**
		Fan	2							
10:30-12:30	20	Air Conditioner	1	**78.4**	**71.9**		**78.5**	**71.9**	**6.6**	**-5.54**
		Fan	2			**72.11**				
12:30-2:30	18	Air Conditioner	1	**71.8**	**70.6**		**77.5**	**70.6**	**6.9**	**-10.84**

		Fan	2							

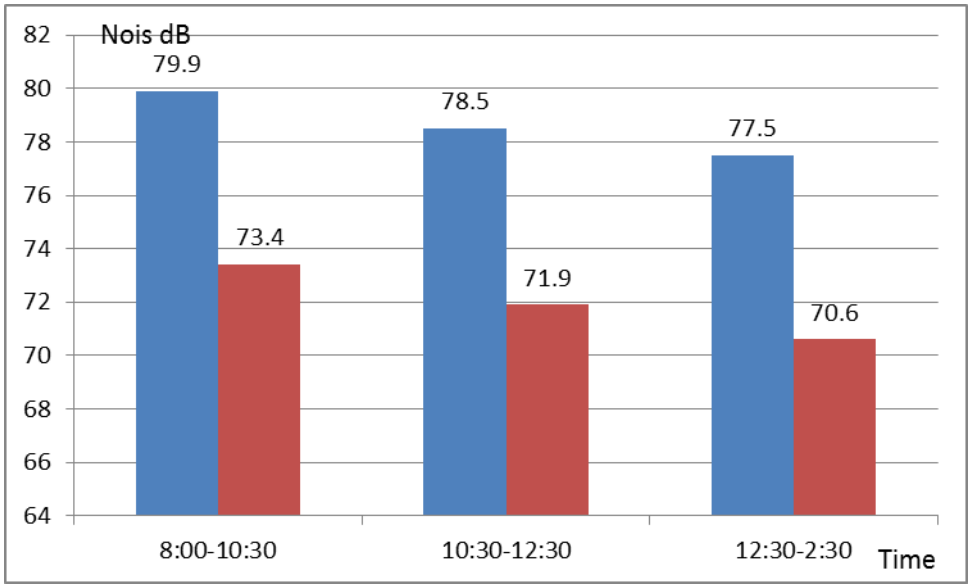

Fig.5. The relationship between time and noise at the Faculty of Political Sciences classroom No. (1)

4. Results and discussion.

Noise in the cafeterias results from internal and external sources. The internal noise includes: talking while eating, and noises from operating electrical devices such as sound speakers which launches loud music, TVs, fans, and air-conditioners. While external sources is represented in all the sources that surround the restaurant besides electrical diesel generators. Noise level in the cafeteria is directly proportional to the number of diners and the time of the day. It was noticed that (12:30 - 2:30PM) recorded the highest level of noise where this period represents the peak of the noise. There is also a direct correlation between the numbers of customers with the internal noise level of the cafeteria.From Table 5 and figure (3), It can be noticed that high level of noise was monitored in the period (10: 30- 12:30PM) with noise level of 80.8 dB (A), which approves the presence of the largest number of customers (70 customers). Besides that, 5 electrical fans were operated which contributed to maximize the noise in a substantial increase in the internal noise pollution. As for the external noise to the cafeteria of Faculty of Pharmacy, the resultant of the noise comes from two main sources: first customers gathered in front of the entrance of the cafeteria and second the traffic noise where the cafeteria is located close to the street. To compare the results with the determinants described in the table (4) and (5) and (6) – we noted that the equivalent noise level in the cafeteria was 78.16 (dB A) which is higher than the allowable limits, while it be noted that (11) workers exposed to equivalent noise level of (78.16 dB (A)) which is within the acceptable limits.Tables (7) and (8) shows results obtained for classroom of Law Department No. (2) and classroom No.(1) of the of Political Science Department. Results (A) showed that the noise level of the two classrooms were 59.4 and 72.11 dB respectively and at least 18 students were exposed to this level of noise and when comparing with specifications, it is clear that the noise level of the classrooms are off limits and the exposure of students in the two classrooms is within acceptable limits. The external noise of classrooms of Law Department classroom No.(2) and (1) of the of

Political Science Department of the periods set out in tables above are 75.4, 77.6 , 73.9 dB (A), and 79.9, 78.5,77.5 dB (A). And internal noise level 58.6, 60.9, 56.4 dB (A), and 73.4, 71.9, 70.6 dB (A). Thus, the noise damping of the two classrooms of 16.8 , 16.7 , 17.5 dB(A) and 6.5, 6.6 , 6.9 dB (A) respectively, as shown in figures (4) and (5).

5. Conclusions and recommendations.

5.1. Conclusions

1. Noise level recorded in reading halls in the Central Library and cafeterias was higher than the allowable limits and that there is direct proportion between the number of readers and the level of noise in the halls.

2. Internal noise level in classrooms is higher than the permissible limits, and the sound damping ratio of the walls, doors and windows is less than the engineering specifications.

3. The speaker-to-noise ratio SNR in classrooms is low except for students sitting the front rows. This affects hearing and understanding the lecture by recipient students.

4. Diesel generators effected directly to the infiltration of noise to reading halls in Central Library and , cafeterias and classrooms.

5.2. Recommendations

1. Noise pollution must be taken into consideration when designing any building from architectural point by choosing the function of that room (reading room, cafeteria. Sports hall, classrooms), which provides the lowest level of reverberation time .

2. Acoustic insulation of walls, ceilings and floors must be taken into consideration in the design and implementation of any building in, and using doors and windows that provide better damping of external noise .

3. The landscaping work around the buildings is suitable environmental solution which prevents the transmission and reduction of the noise.

4. Develop a soundproof barriers for diesel generators at the University to prevent the transmission of noise to the halls and buildings .

5. Not using amplifiers and recorders with high votes in the cafeterias.

6. Studying the traffic noise pollution within the campus and its impact on the buildings at the University.

6. References:

(1) Bjorkman, E. & Rylander, R. (1980) Laboratory annoyance and different traffic noise sourses. Journal of Sound and Vibration, 70, 333-341.

(2) S. K. Jha, Rupak Kumar Deb., Vinay Chandra Jha ,and Iqbal Ahmed Khan (2010) (Effect of Illumination and Cross Ventilation in Classroom on academic performance of the students) International Journal on Emerging Technologies 1(1): 46-52(2010)

(3) Glass, D. & Signer, J. (1972) Urban Stress: Experiments on Noise and Social Stressors. New York: Academic Press.

(4) Paulo Henirque, Trombetta Zanin and Andressa Maria Coelho Ferreira (2009) (Field Measurement of acoustic Quality in University Classroom) , Journal of Scientific & Industrial Research Vol. 68 ; PP.1053 – 1057 .

(5) ZHNG JON, and GENG Ya – ni (2008) (Study on Environmental Noise of Baoji University of Arts and Science (Old Campus))- Journal of Baoji University 2008.

(6) Dave Guckelberger (2003) (A new Standard for a coustics in Classroom. Jouranal of Engineers Newsletter. Volume 32 No.1 .

(7) Michel Vallet and Zahram Karabiber (2002) (Some European Policies Regading a coustical comfort in Educational Building). The Journap

of The Institutte of Noise Control Engineering of USA Vol.50 No.2 .

(8) Pamela Woolner and Elaina Hall (2010) (Noise in School): A Holistic Approach to The Issue. International Journal of Env. Rws, 7 , 3255 – 3269 , www.mdpi.com/Journal/ijerph .

(9) Dafrozah Samagwa ,Stelyust Mkoma and Clevery Tungaraza (2009)(Investigation of Noise pollution in Restaurant in Morogora Municipality ,Tanzania , South Africa)

(10) Michel Vallet and Zerhan Karabiber (2002) (Some European policies regarding acoustical comfort in educational buildings).Noise Control Engineering Journal. Vol. 50, No. 2.pp 58-62

Modeling Water Harvesting System Using Soil Water Assessment Tool (SWAT) (Case Study in Iraq)

Imzahim Abdulkareem Alwan [1], Ibtisam R.Kareem [2], and Mahmood J. Mohamed[3]

Abstract— Estimation of runoff volume and analyzing quantity of water is needed to aid the engineers and researchers for knowing the quantity of water harvesting and determined the potential of utilization the collection water for irrigation or drinking and other uses.

The main objective of this study is to estimate the runoff volume for Wadi-Al Naft watershed with an area of (8820km^2), which is located inter the geographic coordinates ($45^\circ\ 00'\ 00''$to $46^\circ\ 00'\ 00''$) E, ($33^\circ\ 00'\ 00''$ to $34^\circ\ 00'\ 00''$) N at the North-East of Diyala city in Iraq republic , by using Soil Water Assessment Tool (SWAT).

SWAT requires three basic data for delineating the basin into sub basins, a digital elevation model (DEM), soil map and land use/land cover (LULC) map.

Soil Conversation System (SCS) was used with Geographic Information System (GIS) to develop the land use, soil type and soil texture maps from Landsat-8 (ETM+) satellite image. Also, Digital Elevation Model (DEM) is used to delineate the watershed and for computing watershed properties.

Index Terms— **Runoff, Water harvesting, Land sat 8, SWAT , case study-Iraq**

I. INTRODUCTION

Rainwater harvesting (RWH) refers to collection of rain falling on earth surfaces for beneficial uses before it drains away as Runoff. The concept of RWH has a long history. Evidences indicate domestic RWH having been used in the Middle East for about 3000 years and in other parts of Asia for at least 2000 years. Collection and storage of rainwater in earthen tanks for domestic and agricultural uses is very common in the world, since historical times. The main purpose of hydrologic model is to estimate the amount of surface runoff, sub surface runoff, water stored in the soil, and the changing of them through the seasons.

Manuscript received July 6, 2015; accepted August 16, 2015.

[1] Professor, Building and Construction Engineering Department, University of Technology, Baghdad, Iraq. (corresponding author: e-mail: mzahim74@yahoo.com

[2] Asst. Professor, Building and Construction Engineering Department, University of Technology, Baghdad, Iraq. (e-mail: **m-_bajalan@yahoo.com**

[3] M.Sc. in Geomatics Engineering. (e-mail:. mahmoodjasim2004@yahoo.com

(II) SCS CURVE NUMBER METHOD

SCS Curve Number (CN) is method for estimating direct runoff volume response from rainstorms was developed to fill technological niche in the 1950. Since then, use of the CN method has extended to other applications, and user experience and analysis have redefined numerous features of the original technology (Hawkins, et al, 2008). Its popularity is rooted in its convenience, its simplicity, is authoritative origins, and its responsiveness to four readily grasped catchment properties: soil type, land use/treatment, surface condition, and antecedent condition (Ponce and Hawkins, 1996). SCS Curve number method is an infiltration loss model, although it may else account for interception surface storage losses through its initial abstraction feature. As originally developed, the method is not intended to account for evaporation and evapotranspiration (long-term loses) (Ponce and Hawkins, 1996).

Watersheds have a certain group of soil and fair pasture cover can be classified by various curve numbers. These curves are the relationship obtained between rainfall and runoff, such that, (Chow, 1964):

$$F/S = Q/P \quad (1)$$

Where:

F=P-Q: is actual retention (mm).

S: is potential retention (mm).

Q: is actual runoff (mm)

P: is potential runoff that is total rainfall (mm).

Initial abstraction, I_a, is all losses before runoff begins. It included water retention in surface depression and intercepted by vegetation, infiltration, and evaporation as shown in figure (1).

I_a : is subtracted from rainfall P in equation(1) yields:

$$(P - Ia - Q) / S = Q / (P - Ia) \quad (2)$$

Solving for Q yields

$$Q = \frac{P-0.25s}{P-Ia+s} \quad (3)$$

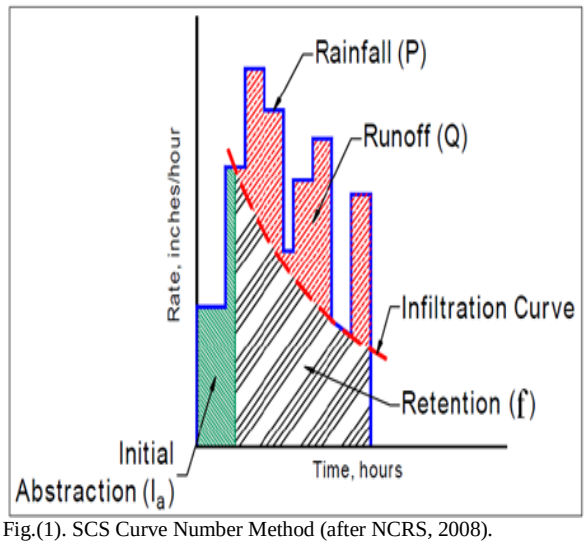

Fig.(1). SCS Curve Number Method (after NCRS, 2008).

(III) WADI-Al NAFT WATERSHED.

Wadi –Al- Naft watershed located in the north east of Iraq republic. It lies in the north of Diyala City between (45˚ 00′ 00″ to46˚ 00′ 00″) E and (33˚ 00′ 00″ to34˚ 00′ 00″) N along Land sat 8 track (36, 37) path and (168) row. The watershed area is about 8820 km². Figure (2) illustrated of the study area.

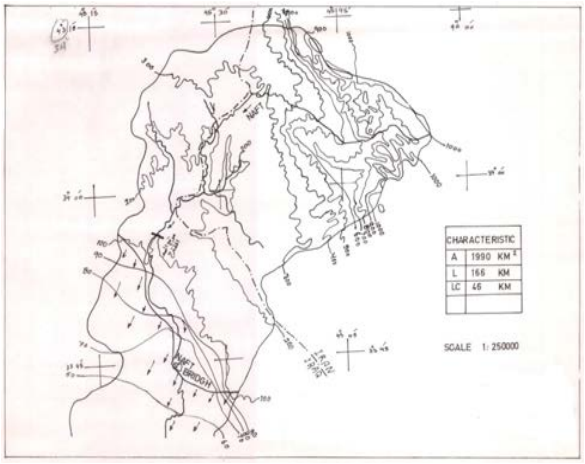

Fig. (2): Location of Wadi- Al- Naft in Iraq [Ministry of Water Resources in Iraq]

(IV) Data Collection

Climate Data.

Climate data (rainfall, minimum and maximum temperature, relative humidity, solar, wind speed) was obtained from Iraq Meteorological Organization and Seismology at Kanaqin station, and the Website http://www.fao.org/landandwater/aglw/cropwat.stm) for the period (2000 to 2014).The geographic location of Diyala Governorate imposed a dry and warm summer for the period June, July, and August, with temperature of 31.5 °C as an average summer temperatures for the studied period. The city is usually windy during winter. This season extends from December till February. However, the temperature in the winter season is about 7.6 °C. The average relative humidity for summer and winter are 25.5% and 65.6% respectively, while the evaporation reached 329.5 mm in summer and 53 mm in winter where the average wind speed in winter 1.2 m/sec and little bit more in summer 1.8 m/sec. Sunshine duration reaches 5.1 hour and 10.6 hour in winter and summer respectively.

Land use/land cover and Soil digital maps

The land use (LU,LC) and Soil properties of study area can be obtained from satellite imagery; Land sat 8 and the Website(http://seamlessUSGS. Gov/Website/seamless/viewer.Htm). Three Land sat images; acquired in 08 Feb 2015, were used to cover the study area. These images were geometrically and atmospherically corrected and digitized in GIS software. Then, these images were mosaic processed and the study area masked up from the mosaic image. Thematic mapping of different (LULC), soil classes were achieved through supervised classification using technique of (GIS) software. According to exploratory soil map of Iraq 1960 and Land-use map [Ministry of Industry and Minerals, State Establishment of Geological Survey and Mining, 1994] at scale 1,000,000. Analyzing texture of soil was done using Soil Water Characteristics Software (SPAW) Figure(3); This program estimates soil water tension, conductivity and water holding capability based on the soil texture, organic matter, gravel content, salinity, and compaction.

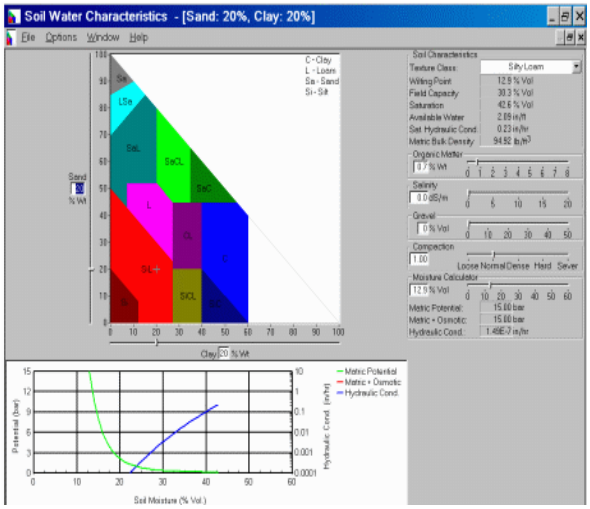

Fig.(3): SPAW model for soil water characteristic solutions.

(V)Runoff Modeling by Soil Water Assessment Tool (SWAT)

The model selected for the application to the Wadi Al Naft watershed, is the Soil and Water Assessment Tool (SWAT) version (2012) and it was operated through the interface Arc SWAT developed by the United. State Department of Agriculture and Texas A & M University 2012 . It simulates the different surface and ground hydrological components as

well as crop yields. SWAT has been used extensively by future water in various places and important modifications, improvements and extensions have been developed. A distributed rainfall-runoff model – such as SWAT – divides a catchment into smaller discrete calculation units for which the spatial variation of the major physical properties are limited and hydrological processes can be treated as being homogeneous. The total catchment behavior is a net result of manifold small sub-basins. The soil map and land use map within sub-basin boundaries are used to generate unique combinations, and each combination will be considered as a homogeneous physical property, i.e. Hydrological Response Unit (HRU). The water balance for HRUs is computed on a daily time step. Hence, SWAT will subdivide the river basin into units that have similar characteristics in soil and land cover and that are located in the same sub-basin. SWAT divides rainfall into different components which include evaporation, surface runoff, infiltration, plant uptake, lateral flow and groundwater recharge. Surface runoff from daily rainfall is estimated with a modification of the SCS curve number method from the United States Department of Agriculture Soil Conservation Service (USDA SCS) and peak runoff rates using a modified rational method (Neitsch et al., 2005).

(V) Digital Elevation Model (DEM) of study area

Digital elevation models map of the study area (Wadi Al-Naft) is loaded from the Website of Landsat8 www.usgs.glovis.com , showed in the Figure (4).

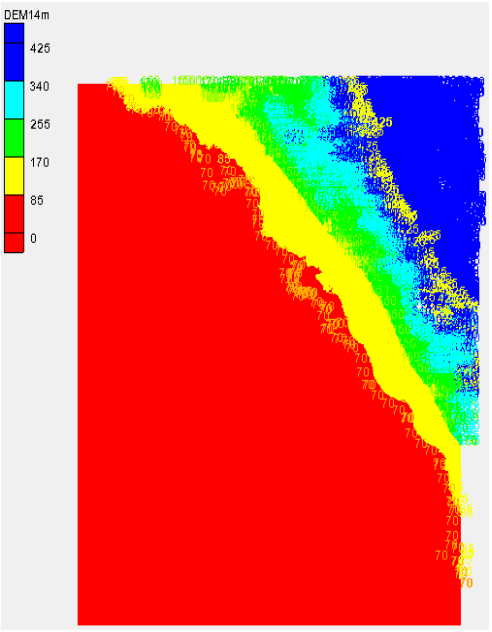

Fig. (4): Digital Elevation Model of Wadi- Al-Naft.

First step required to build a SWAT model is defining the elevation related properties such as: elevation above sea level, slope, aspect, stream flow network, and distance to nearest stream, and dividing the basin in sub-catchments. Within SWAT the number of sub-catchment to be included in the study, based on a minimum area of each sub-catchment, it depends on the nature of the demonstration case, an appropriate threshold value is somewhere between 1000 and 5000 ha. A lower value provided too much detail in the flat areas, while a higher value resulted in sub-catchments that were too large in the mountainous areas. Optimal sizes of sub-catchments were obtained by using a threshold value of 3000 ha and manually adding more details in the mountainous areas, resulting in 103 sub-catchments. The final layout can be seen in Figure (5).

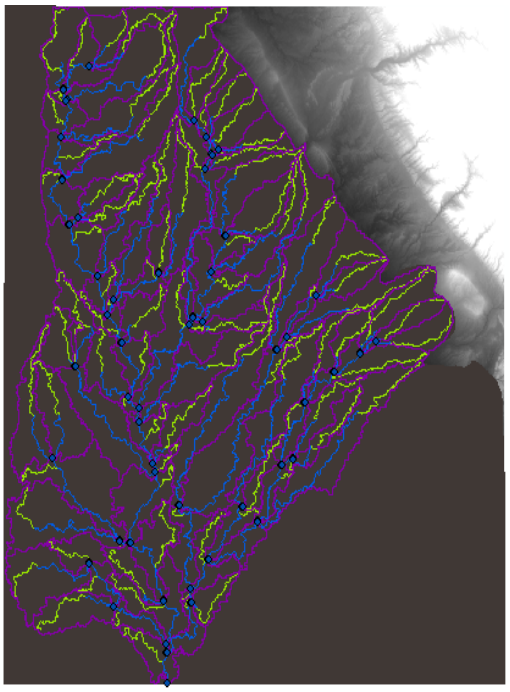

Fig. (5): Watershed Delineation.

(VI) Hydrologic Response Unit (HRU) Analysis

The rainfall has a monsoonal seasonal pattern, with using commands from the HRU Analysis menu on the Arc SWAT Toolbar. These tools allow users to load land use and soil layers into the current project, evaluate slope characteristics, and determine the land use/soil/slope class combinations and distributions for the delineated watershed and each respective sub watershed. The datasets can be ESRI grid, shape file, or geo database feature class format. Once the land use and soil datasets have been imported and linked to the SWAT databases, the user specifies criteria used in determining the HRU distribution. One or more unique land use/soil/slope combinations (hydrologic response units or HRUs) can be created for each sub basin. The Land Use/Soils/Slope classification and Overlay tool allows the user to load the land use and soil datasets and determine land use/soil/slope class combinations and distributions for the delineated watershed(s) and each respective sub-watershed. The datasets can be ESRI grid, shape file, or geo database feature class. Vector data

sources are automatically converted to grid, the format required by spatial analyst to compute cross-tabulated areas between land use and soil data sets. The land use and soil datasets must be in the same projection as the Digital Elevation Model, (DEM) used in the watershed delineation. Slope characterization is based upon the DEM defined in the watersheds delineation.

(VII) Results and Discussion

In order to simulate the average runoff events in the catchment area of 103 basins with net area of the watershed 5565 Km^2 the season 2000-2014 was selected with total rainfall depth 2373 mm which represent the average rainy seasons during the study period 2000-2014.

When dividing the watershed into number of sub basin (103), with minimum elevation 17, maximum elevation 425 and mean elevation 51.54 m. These properties were computed from DEM file with spatial resolution 14 m. figure (6) & (7) showed the hydrologic unite response (HUR) soil, Land use, slope distribution and reclassified.

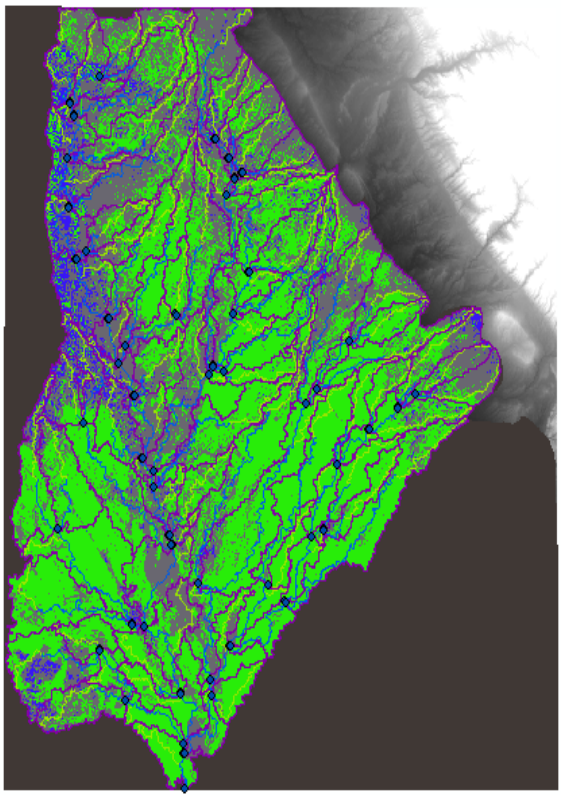

Fig.(6): Land use reclassified.

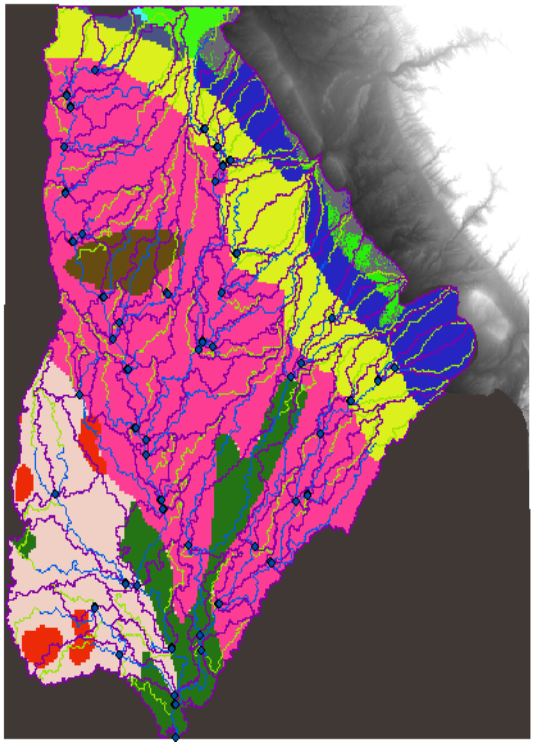

Fig. (7): Soil reclassified.

Curve Number values range between (60 to 90) and the total net runoff for the period 2000-2014 exactly 782030m3; as shown in Table (1).

Table 1: Annual total runoff of study area.

Year	Total runoff(m^3)
2000	8294
2001	12079
2002	37957
2003	204
2004	1072
2005	2014
2006	883
2007	2000
2008	2247
2009	610
2010	2150
2011	2625
2012	2910
2013	693
2014	2465
Total sum	782030

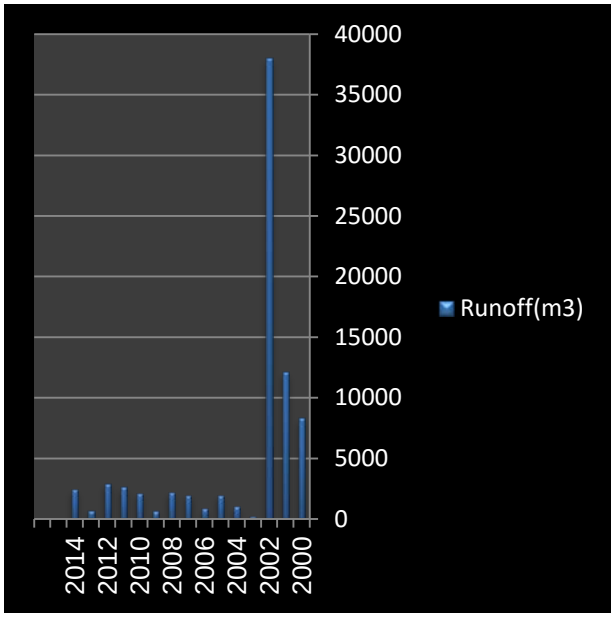

Fig. (8): Annual runoff volumes for the period (2000-2014).

(VIII) Conclusions.

According to the results the following conclusions may be drawn from the present study which is applied SCS-CN method was successfully used to estimate surface runoff for the study area using Soil Water Assessment Tool,(SWAT). This method considers the relationship of Land cover type and hydrologic soil group, which together make up the curve number. The annual average runoff overall the net area of watershed 5565 km^2 for the period 2000-2014 is estimated to be about (782030 m^3)

Without computed the percolation water and the quantity of water that contribution for recharge ground water and evaporation water. Finally soil water assessment tool (SWAT) software able to prediction the next annual quantity and quality of water by generating weather data and all parameter required.

References

[1]. Al-Ansari, N.A. (2013) "Management of water resources in Iraq: Perspectives and prognoses". Journal of Engineering, **5**, 667-684.

*J.G.Arnold and J.R.Williams (2012) "soil and water assessment tool theoretical", Agricultural Research Service Black land Research Centre-Texas Agrilife Research.

[2] . Arnold, J.G., J.R. Kiniry, R. Srinivasan, J.R., Williams, E.B. Haney and S.L. Neitsch, 2011. Soil and Water Assessment Tool – Input/output file documentation – version 2009, Texas Water Resources Institute, College Station, Technical Report no. 365

[3] .Anderson, James R., 1971, Land use classification schemes used in selected recent geographic applications of remote sensing: Photogram Eng., v. 37, no. 4, p. 379-387.

[4] . Barzinji, Khalid T. M., 2003, "Hydrologic Studies for Goizha-Dabashan and Other watersheds in Sulymaniah Governorate", M.Sc. Thesis, College of Agricultural, University of Sulymaniah.

[5] .Bhawan, P. & Nager, A., 2001, "Concepts and Practices for Rainwater Harvesting", Ministry of Environment & Forests, Govt. of India, Delhi-110 032

[6] .Bedient, Philip B. and Wayne C. Huber, 1992, "Hydrology and Floodplain Analysis", 2nd, Addison-Wesley Publisher company, USA.

[7] .Chen, L , and Michael. H Young, 2006,"Green Ampt Infiltration Model for Sloping Surfaces", Water Resources Research, Vol. 42.

[8] .Chow, Ven Te, 1964, "Handbook of Applied Hydrology", McGraw-Hill Company, New York.

[9] . Oweis, T. and Hachum, A. (2006) "Water harvesting and supplemental irrigation for improved water productivity of dry farming systems in West Asia and North Africa". Journal of Agricultural Water Management, **80**, 57-73.

[10] . Dhiman, S.C. & Gupta, S,2011."Rain water Harvesting and Artificial Recharge" Central Ground Water Board Ministry of Water Resources New Delhi.

[11] .Website metadata from satellite image http://glovis.usgs.gov.

[12] .Linsley, Ray K., Max A. Kohler and Joseph L. H. Paulhus, 1988, "Hydrology for Engineering", SI Metric Edition, McGraw-Hill Published Company, London.

[13] . Ministry of Industry and Minerals, State Establishment of Geological Survey and Mining map, 1994.

[14] . Ministry of water resource Iraq, Topographic map,1982.

[15] .Najmi, K. 2008, "Rainwater Harvesting " Journal earth science India: popular issue.

[16].National Committee on Plasticulture Applications in Horticulture (NCPAH) , 2010,"Farm pond lined with plastic film" Ministry of Agriculture (MOA), Govt. of India.

[17] .NRCS, National Resources Conservation Service, 2008, "Curve Number Rainfall-Runoff: Professional Applications", Assembly Center Columbus, Ohio.

[18] .Siegert, K. (1994) Introduction to water harvesting: Some basic principles for planning, design and monitoring. Water Harvesting for Improved Agricultural Production. Proceedings of the FAO Expert Consultation, FAO, Cairo

[19] .SCS, Soil Conservation Service, 1986, "Urban Hydrology for Small Watersheds", Technical Release 55.

[20] . Raghunath, Hassan M., 2006, "Hydrology: Principles, Analysis, Design", 2nd, New Age International Publishers, Delhi.

[21] .Contributions from Agric. Res. Serv., USDA, in cooperation with the College of Agric. and Home Economics, Agric. Res. Center, Washington State Univ., Pullman, WA 99164. Scientific Paper no. 6911. Received 10 June 1985.

[22] .(Ministry of Water Resources of Iraq, agro-Ecological Zones Map scale 1:1800.000 AGRO

[23]. Prinz, D. (1996) Water harvesting: Past and future. In: Pereira, L.S., Ed., *Sustainability of Irrigated Agriculture. Proceedings, NATO Advanced Research Workshop, Vi- meiro*, 21-26.03, Balkema, Rotterdam, 135-144.

[24]. Van Liew, M. W., J. G. Arnold, and D. D. Bosch. 2005. Problems and potential of auto calibrating a hydrologic model. *Trans. ASAE* 48(3): 1025-1040.

Preparation and Characterization PVC/PS/PVA Hollow Fiber Nano-filtration Composite Membranes

[1]Rana J. Kadhim, [2]Talib Albyati, [2]Zainab Shneen, [2]Qusay F. Alsalhy, [3]S. Simone, [3]Alberto Figoli, [3]Enrico Drioli
[1]Building and Construction Engineering Department, University of Technology, Baghdad, Iraq
[2]Membrane Technology Research unit, Chemical Engineering Department, University of Technology, Baghdad, Iraq
[3] Institute on Membrane Technology (ITM-CNR), Calabria University, Cosanza, Italy

Abstract:-

Nano-filtration composite hollow fiber membranes (NF) was synthesized by using dip- coating method in order to use it for the separation of NaCl and $CaCl_2$ from salt solution. Effects of poly (vinyl alcohol) (PVA) concentration in coating solution on the morphology and separation performance of the NF hollow fiber composite membrane was studied. Cross-sectional structure of the NF membranes was characterized by using scanning electron microscope (SEM). The permeation and rejection results demonstrated that the NF membranes had a significant ability to the separation of NaCl and $CaCl_2$ from salt solution. From the experimental work it was found that the permeation flux and solute rejection results of the NF membranes prepared from different concentration of PVA (0.5, 1, and 1.5 wt% PVA solution) and dip- coating process for 90 minute at 60 ºC could be considered as a good candidate for the separation of NaCl and $CaCl_2$ from salt solution with good performance.

Keywords: NF membranes; Composite NF membranes; Rejection performances; phase inversion; polysulfone; poly(vinyl alcohol)hollow fiber membrane

Introduction

Nano-filtration membranes (NF) have several properties that give to their worth for application in industry. For example, plurality of the NF membranes have molecular weight cut-off of about 200-1000 Dalton, which is go between the traditional reverse osmosis (RO) membranes and the ultrafiltration (UF) membranes [1,2]. Based on the Stokes-Einstein relationship, NF membrane is assumed to have a pore size ranged from 1 nanometer to a few nanometers in diameter. Moreover, most NF membranes are either positively or negatively charged according to their materials, and the membrane charges properties have important roles in the permeability and rejection of charged solutes [3]. Besides, NF can be operated at low pressures (i.e., 0.5 to 3 MPa), which is fascinating for industry due to the reduction of operation cost and give comfortable membrane system maintenance.

There are many methods employed in the synthesis of composite NF membranes, for example, vapor deposition, plasma-initiated and photo-initiated polymerization, radiation and atom transfer radical polymerization, dip coating and vacuum coating method, interfacial polymerization, electron beam irradiation, resin-filled chelating, and in situ amines cross-linking [4-17]. Nanofiltration membranes consist of an active layer, determining the separation properties, and a support structure, giving mechanical strength. The active layer may be integrally connected to the support structure, such as membranes prepared via immersion precipitation process [18, 19]. This type of membrane has distinct pores in the nanometer range at the skin layer. The active layer can also be an extra coating layer on a tailor-made support structure. The characteristics of the coating material determine the separation properties of the membrane. Several studies describe the use of PVA polymer, as coated active layer thanks also to its antifouling properties [21, 22], for NF membrane applications.

Gohil et al. [20] reported the coating of PVA onto the polysulfone (PSF) ultrafiltration membrane and studied their NF performance. From the analysis of flux and rejection data it may be concluded that membranes prepared from17% PSF, 1% PVA, with MA solution concentration of 0.2% (w/w) cured at a temperature of 125 ± 2 °C for 30 min give the optimum balance of flux and rejection (R).

Jegal et al. [23, 24] have also prepared NF composite membranes by coating micro-porous PSF support membrane by blending PVA and sodium alginate solutions. The results show that under an operational pressure of 0.6 MPa, water fluxes of NF-1, NF-2 and NF-3 are 4.1, 6.0 and 26.5 l/m^2 h, respectively, while the retentions of Na_2SO_4 are78, 94 and 94%, respectively.

Kim et al. [25] found that the antifouling performance of commercial NF membranes has been enhanced by coating of poly (vinyl alcohol) (PVA) solution on the membrane surface [25]. the results of the

permeation tests, the surface charge and the surface roughness of the NF and RO membranes. By coating the NF membrane with neutral PVA, the rejection rate of the salts was increased. However, in the case of the RO membrane, the rejection rate decreased. Those results explained by the size exclusion and the Donnan exclusion theory. For the NF membrane which is more porous than the RO membrane, the salt rejection can be affected more by size exclusion than by the Donnan effect. However, in the case of the RO membrane, which has a very dense top layer, a decrease in the negative charge on the RO membrane surface by the PVA coating occurs. The surface charge and the surface roughness decreased.

In this study, it is reported the preparation of composite PVA-NF membranes by dip-coating of PVA on the poly(vinyl chloride) (PVC) hollow fibers which was prepared in previous work [26] and the characterization of the produced membrane. Finally the performance of the novel PVA composite hollow-fibers has been tested for evaluating both flux and solute rejection.

Experimental

Materials

Poly(vinyl chloride) (PVC)/polystyrene (PS) hollow fiber membrane was used as a support material given by Membrane Technology Research Unit, Chemical Engineering Department, University of Technology, Iraq [26]. PVA (Mw =75-79 kg/mol), and fatty alcohol polyoxyethylene ether (AEO_9) used as a coating materials were obtained from Sigma–Aldrich Chemical Co.

Composite membrane preparation

Three types of PVC/PS hollow fiber membranes prepared in previous work were selected: 1) PVC1 [PVC-3% PS]; 2) PVC2 [PVC-6% PS]; 3) PVC3 [PVC-9% PS], [26]. At room temperature, three types of the coating solutions were prepared; PVA was dissolved in distilled water at 85-90°C with agitation by magnetic stirrer until the PVA dissolved completely in water. Then, PVA aqueous solution was cold to room temperature. After that AEO_9 was mixed with the PVA solution until the coating solution became homogeneous. AEO_9 has been added to the PVA solution to decrease the solution interfacial tension with PVC/PS hollow fiber membrane surface. PVC/PS hollow fiber membranes were coated by immersion in the coating solution for 10s by using dip-coating method. The PVA-coated hollow fiber composite membranes then were dried at room temperature. The final PVC/PS/PVA hollow fiber composite membranes with the selective layer on the outside of the support hollow fiber membrane were obtained after heat treatment in an oven at 60°C temperatures for 90 min as shown in Table 1.

Scanning electron microscopy (SEM) observations

Fibers cross-sections, inner and outer surfaces and thickness of the PVA layer morphology was observed by using SEM (Quanta FENG 200, FEI Co., Hillsboro, Oregon USA) .

Measurements of permeation flux and solute rejection

A schematic diagram of the NF experiments rig is given in Figure 1. For each NF composite hollow fiber type, three modules were tested. The performance tests for the prepared membrane were carried out under trans membrane pressure of 1 MPa at 25 °C. The retentate was re-circulated to the feed tank, while the permeate solution was collected to calculate the permeation flux and solute rejection during the NF experiments as shown in Figure 1. The pure water and solutes permeability (PWP) were calculated using the following formula:[24]

$$PWP = \frac{Q_w}{\Delta P\, A_s} \qquad (1)$$

Where, PWP is the permeability of membrane (l/ (m^2 h bar)), Q_w the volumetric flow rate (l/h), ΔP the transmembrane pressure drop (bar), and A_s is the effective surface area of the membrane (m^2), NF tests were performed using the OUTSIDE/IN configuration. NaCl and $CaCl_2$ solution with concentration of 500 mg/l was used for determining the composite NF membranes rejection, R(%), which was calculated using the following formula:[24]

$$R(\%) = \left(1 - \frac{C_p}{C_f}\right) \times 100\% \qquad (2)$$

Where C_f and C_p are the solutes concentrations in feed and permeate solution respectively. The concentration of NaCl and $CaCl_2$ were measured by using a conductivity meter (model DDS 307) measuring range is 0-2 × 10^5 .

Results and Discussion

Structure characteristic of the PVA composite NF membrane

The SEM cross-section of the composite PVC/ PS hollow fiber membranes, at two different magnifications, is shown in Figure 2. The SEM pictures show a thin active PVA layer with a compact surface on a finger-like hollow fiber UF support membrane. Figure 3 shows SEM images of the hollow fiber membranes prepared from 6 wt.% PS with different coating solutions A) 0.5 wt.% PVA; B) 1 wt.% PVA; C) 1.5 wt.% PVA. The thickness of the PVA coated layer is strongly dependent

on the concentration of PVA in coated solution as shown in figure 3. In fact, at higher PVA concentration it can be noticed that the thickness of the PVA coated layer increases and this is obviously due to the increased of PVA content in coated solution. [27,28]

Table 1:- PVC/PS/PVA Composite NF Membrane Preparation Conditions

Membrane no.	Membrane type	Treatment method	The coating solution PVA/AEO_9/H_2O (wt %)	Heat treatment	
				Temp. (°C)	Time (min)
1	PVC 1a	Dip-coated	1.5/0.5/98	60	90
2	PVC 1b	Dip-coated	1.5/0.5/98	60	90
3	PVC 1c	Dip-coated	1.5/0.5/98	60	90
4	PVC 2a	Dip-coated	1/0.5/98.5	60	90
5	PVC 2b	Dip-coated	1/0.5/98.5	60	90
6	PVC 2c	Dip-coated	1/0.5/98.5	60	90
7	PVC 3a	Dip-coated	0.5/0.5/99	60	90
8	PVC 3b	Dip-coated	0.5/0.5/99	60	90
9	PVC 3c	Dip-coated	0.5/0.5/99	60	90

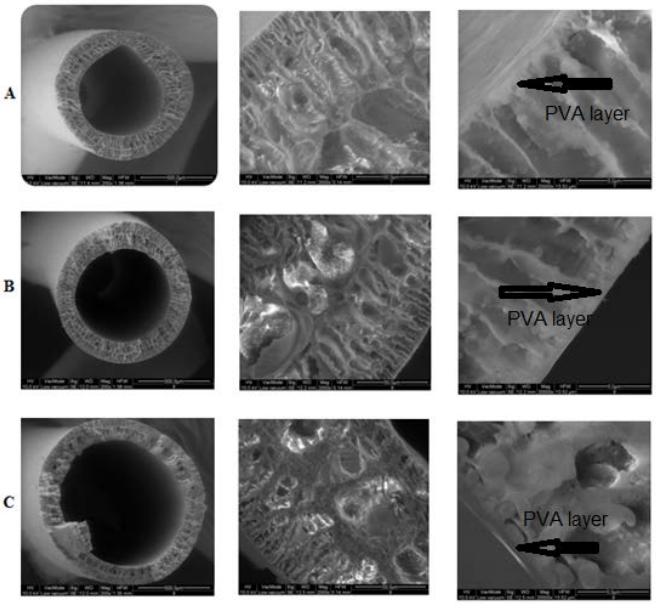

Figure 2:- SEM images of the Composite NF membranes with 0.5% PVA coating solution; A) PVC; B) PVC; C) PVC

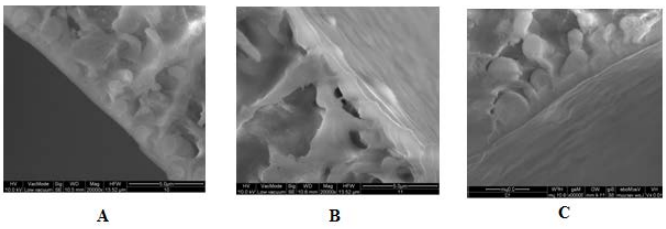

Figure 3:- SEM images of the hollow fiber membranes prepared from 6% PS with different coating solution, A) 0.5% PVA; B) 1% PVA; C) 1.5% PVA

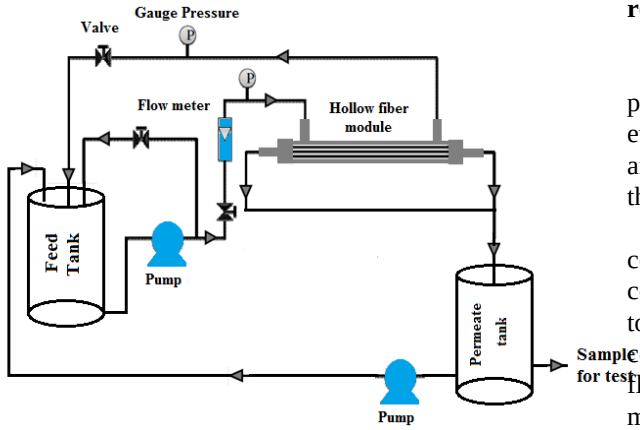

Figure 1:- schematic diagram of the NF experiments set-up

Effect of PVA concentration in coating solution on rejection and flux of composite NF membranes

The performance of the composite NF membranes prepared with dip-coated process was determined by evaluating flux of individual solutes (NaCl, and $CaCl_2$) and their rejection from aqueous solution as shown in the Figures 4 - 8.

Figure 4 shows the pure water permeability of composite NF membranes with different PVA concentrations .The pure water flux increased from 8.5 to 13 (kg/m^2 h bar) for PVC1 with increase of PVA concentration from 0.5 to 1.5 wt.%, whereas permeation flux increased from 12.5 to 15 (kg/m^2 h bar) for PVC2 membrane. Moreover, permeation flux increased from 9.6 to 13.2 (kg/m^2 h bar) for PVC3 membrane. This difference in permeation flux of the three types of

composite membrane is attributed to the thickness of the selective layer, which increases with the increase of PVA concentration.[28]

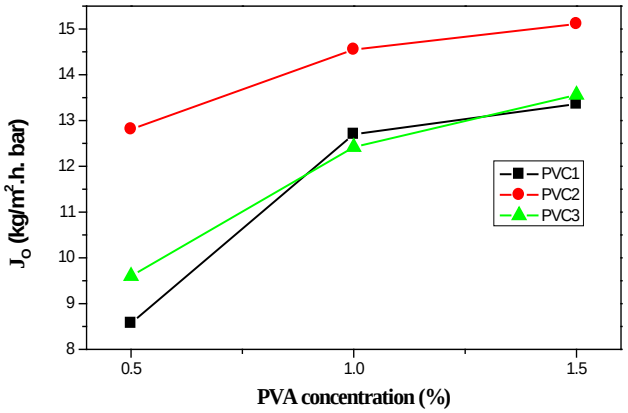

Figure 4:- Pure water permeability of different composite nanofiltration membranes

Figure 5 and 6 show the effect of PVA concentrations on the NaCl and $CaCl_2$ permeability of composite nano filtration membranes. In Figure 5 when PVA concentration changed from 0.5 to 1.5 wt.%, the flux of $CaCl_2$ solution was increased from 5 to 10.5 (kg/m^2 h bar) for PVC1 and the maximum increasing was for the PVC2 where the permeation flux increased from 8.5 to 11.5 (kg/m^2 h bar). For PVC3 the permeation flux increased from 6.7 to 10.4 (kg/m^2 h bar) with increase of PVA concentration.

From Figure 6 it can be noticed that when PVA concentration increased from 0.5 to 1.5 wt%, the flux of NaCl solution was increased from 4.5 to 11.5 (kg/m^2 h bar) for PVC1, whereas permeation flux increased from 6.5 to 12.5 (kg/m^2 h bar) for PVC2. Moreover, the permeation flux of PVC3 was increased from 4.5 to 11.1(kg/m^2 h bar). The reason of the phenomenon in both Figures 5 and 6 belong to the thickness increasing of the coating layer with the increase of PVA concentration due to the increase of cross-linking degree of the membrane surface, which results in higher permeation flux and also due to the affinity of PVA to water [28, 29].

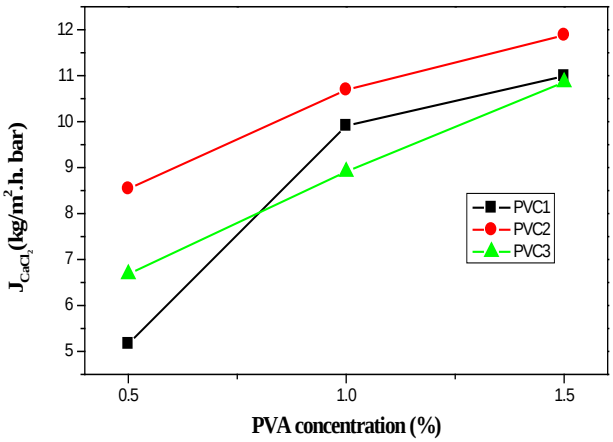

Figure 5:- $CaCl_2$ solution permeability of different composite nano filtration membranes at 0.5 wt% PVA concentration

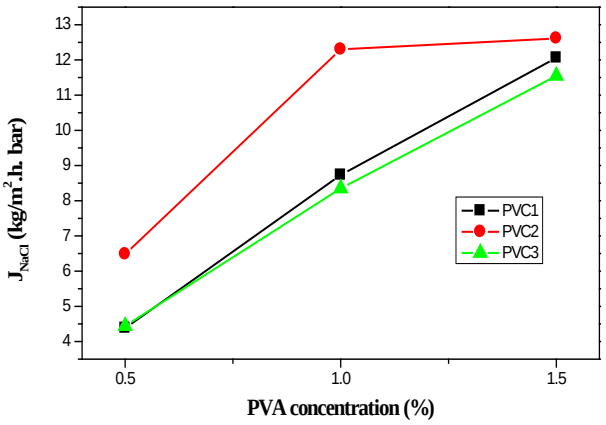

Figure 6:- NaCl solution permeability of different composite nanofiltration membranes at 0.5 wt% PVA concentration

Effect of PVA concentration on rejection of composite NF membranes

The effect of PVA concentrations on the NaCl rejection of three types of composite nano filtration membranes is represented in Figure7. It can be seen that when PVA concentration increased from 0.5 to 1.5 wt%, the rejection decreased between 98% and 94% for three types of composite membranes., the viscosity of coated solution is directly relevant to PVA concentration [27, 28]. The rejections began to decrease when PVA concentration exceeded 1 wt%, which might result from the increase of cross-linking degree of the membrane surface [29].

Figure 8 illustrates the effect of PVA concentrations on the $CaCl_2$ rejection of composite nano filtration membranes. In histogram of Figure 8 it can be noticed

that when PVA concentration increased from 0.5 to 1.5wt%, the rejection increased between 73% and 93.1% for all composite NF membranes. This is due to the thickness of the selective layer increased with the increase of PVA concentration, which results in higher rejection [29]. In addition, the increasing of PVA concentration leads to reduce the pore diameter of the membrane surface which contributed in higher rejection and lower permeation flux.

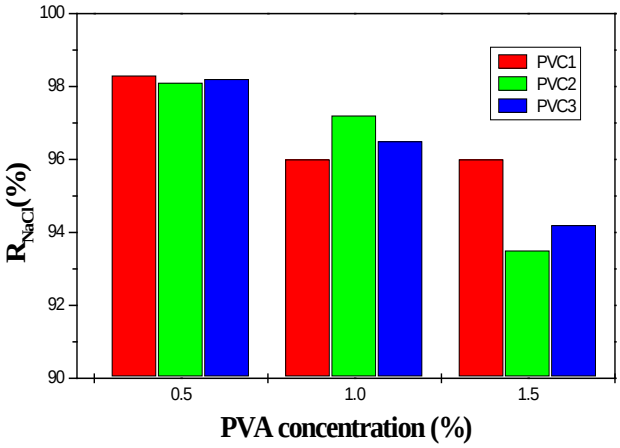

Figure 7:- Effect of PVA concentrations on the NaCl rejection of composite nanofiltration membranes

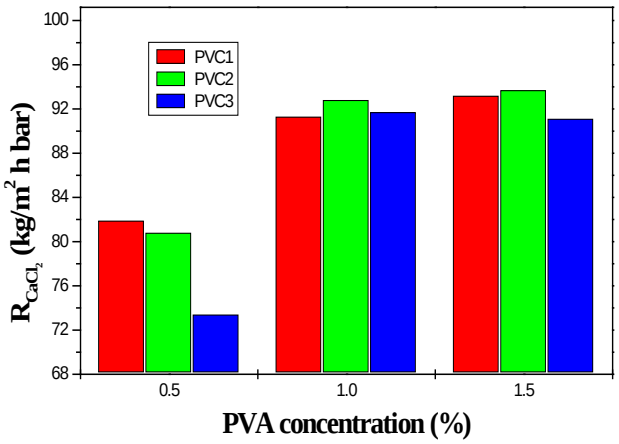

Figure 8:- Effect of PVA concentrations on the $CaCl_2$ rejection of composite nanofiltration membranes

Conclusions

The coating solution with different concentrations of PVA is considered as a good candidate for the synthesis of composite NF membrane. Moderate performance have been obtained from the composite NF membrane prepared from 0.5 to 1.5 wt.% PVA coating solution by dip-coating process for 90 min at 60 ºC and cross-linking with PVC/PS membranes. The thickness of the coated layer of the composite NF membranes is increased with increase of PVA concentration. The difference in performance for three NF membranes is attributed to the difference in structural morphology of the membranes. Also, it can be conclude that the rejection and permeation flux of three types of composite NF membranes were affected by concentration of PVA in coated solution and results to increase of permeation flux and decrease of solutes rejection with increase of PVA concentration. The order of their rejections is $CaCl_{2<}$ NaCl. The membrane has a high rejection to monovalent and divalent salts and can be used to water purification.

References

[1] T. Tsuru, M. Miyawaki, H. Kondo, T. Yoshioka, and M. Asaeda,"Solvent Resistant Nanofiltration Membranes", Sep. Purif. Technol., 32, 105 (2003).

[2] C. K. Diawara, "Characterization of ion transport in the active layer of RO and NF Polyamide membranes"Sep. Purif. Rev., 37, 303 (2008).).

[3] N. Mattias, L. Frank, T. Gun, and O. Kain,"Preparation and characterization of a novel Nanofiltration Membrane", Sep. Purif. Technol., 60, 36 (2008).

[4] H. Yanagishita, D. Kitamoto, K. Haraya, T. Nakane, T. Tsuchiya, N. Koura, Preparation and pervaporation performance of polyimide composite membrane by vapor deposition and polymerization (VDP), J. Membr. Sci. 136 (1997) 121–126.

[5] Y. Hayakawa, N. Terasawa, E. Hayashi, T. Abe, Plasma polymerization of cyclic perfluoroamines and composite membranes for gas separation, J. Appl. Polym. Sci. 62 (1996) 951–954.

[6] Zhi-Ping Zhao, Jiding Li, Dan-Xia Zhang, Cui-Xian Chen, Nanofiltration membrane prepared from polyacrylonitrile ultrafiltration membrane by low-temperature plasma, I. Graft of acrylic acid in gas, J. Membr. Sci. 232 (2004) 1–8.

[7] B. Bae, B.-H.Chun, H.-Y. Ha, I.-H. Ohc, D. Kim, Preparation and characterization of plasma treated PP composite electrolyte membranes, J. Membr. Sci. 202 (2002) 245–252.

[8] T. Yamaguchi, S. Nakao, S. Kimura, Plasma-graft filling polymerization: preparation of a new type of pervaporation membrane for organic liquid mixture, Macromolecules 24 (1991) 5522–5527.

[9] M. Ulbricht, Hans-Hartmut Schwarz, Novel high performance photograft composite membranes for separation of organic liquids by pervaporation, J. Membr. Sci. 136 (1997) 25–33.

[10] R. Zhigong, L. Guixiang, T. Sugo, J. Okamoto, Gas-phase and liquidphase pre-irradiation grafting of Aac onto LPPE and HDPE films for pervaporation membranes, Radiat. Phys. Chem. 39 (5) (1993) 421.

[11] H. Yanagishita, D. Kitamoto, K. Haraya, T. Nakane, T. Okadab, H. Matsuda, Y. Idemoto, N. Koura, Separation performance of polyimide composite membrane prepared by dip coating process, J. Membr. Sci. 188 (2001) 165–172.

[12] J. Peterson, K.-V.Peinemann, Novel polyamide composite membranes for gas separation prepared by interfacial polycondensation, J. Appl. Polym. Sci. 63 (1997) 1557–1563.

[13] W. Morgan, Condensation Polymers: By Interfacial and Solution Methods, Interscience, New York, 1665, pp. 19–64.

[14] H. Yanagishita, J. Arai, T. Sandoh, H. Negishi, D. Kitamoto, T. Ikegami, K. Haraya, Y. Idemoto, N. Koura, Preparation of polyimide composite membranes grafted by electron beam irradiation, J. Membr. Sci. 232 (2004) 93–98.

[15] Anagi M. Balachandra, Gregory L. Baker1, et al., Preparation of composite membranes by atom transfer radical polymerization initiated from a porous support, J. Membr. Sci. 227 (2003) 1–14.

[16] Guangling Pei, GuoxiangChenga, Qiyun Du, Preparation of chelating resin filled composite membranes, and selective adsorption of Cu(II), J. Membr. Sci. 196 (2002) 85–93.

[17] XuTongwen, Yang Weihua, A novel positively charged composite membranes for nanofiltration prepared from poly(2,6-dimethyl-1,4- phenylene oxide) by in situ amines cross-linking, J. Membr. Sci. 215 (2003) 25–32.

[18] T. He, M.H.V. Mulder, M. Wessling, H. Strathmann, Preparation of composite hollow fiber membranes. Co-extrusion of dense hydrophilic coating onto porous hydrophobic support structures, J. Membr. Sci. 207 (2002)143–156.

[19] W.R. Bowen, T.A. Doneva, H.B. Yin, Polysulfone-sulfonatedpoly(ether ether) ketone blend membranes: systematic synthesis and characterization, J. Membr. Sci. 181 (2001) 253–263.

[20] J.M. Gohil, P. Ray, Polyvinyl alcohol as the barrier layer in thin film composite nanofiltration membranes: preparation, characterization, and performance evaluation, J. Colloid Interface Sci. 338 (2009) 121–127.

[21] N. Li, Z. Liu, S.G. Xu, Dynamically formed poly(vinyl alcohol) ultrafiltration membranes with good anti-fouling characteristics, J. Membr. Sci. 169 (2000) 17–28.

[22] X.L. Ma, Y.L. Su, Q. Sun, Y.Q. Wang, Z.Y. Jiang, Enhancing the antifouling property of polyethersulfone ultrafiltration membranes through surface adsorptioncrosslinking of poly(vinyl alcohol), J. Membr. Sci. 300 (2007) 71–78.

[23] J. Jegal, N.W. Oh, D.S. Park, K.H. Lee, Characteristics of the nanofiltrationcompositemembranes based on PVA and sodium alginate, J. Appl. Polym. Sci. 79(2001) 2471–2479.

[24] J. Jegal, N.W. Oh, K.H. Lee, Preparation and characterization of PVA/SA composite nanofiltration membranes, J. Appl. Polym. Sci. 77 (2000) 347–354.

[25] I.C. Kim, K.H. Lee, Dyeing process wastewater treatment using fouling resistant nanofiltration and reverse osmosis membranes, Desalination 192 (2006) 246–251.

[26] Qusay F. Alsalhy, Hollow fiber ultrafiltration membranes prepared from blends of poly (vinyl chloride) and polystyrene, Desalination 294 (2012) 44–52

[27] H.-Y. Zhu, L. Xiao, Z.-X. Liu, Influence of solvent treatment on the properties and structure of chitosan films, Polym. Mater.Sci. Eng. 20 (2) (2004) 110–113 (in Chinese).

[28] Hongwei Sun, Guohua Chen, Ruihua Huang, CongjieGao, A novel composite nanofiltration (NF) membrane prepared from glycol chitin/poly(acrylonitrile) (PAN) by epichlorohydrin cross-linking, Journal of Membrane Science 297 (2007) 51–58.

[29] J. Miao, G.-H.Chen, C.-J.Gao, A novel kind of amphoteric composite nanofiltration membrane prepared from sulfated chitosan (SCS), Desalination 181 (2005) 173–183.

Groundwater and Seawater Intrusion Simulation at Basrah Coastal Aquifer (Aug. 2015)

Ammar Ashour Akesh Al-Suraifi .

***Abstract*— A simulation models to characterize groundwater flow and seawater intrusion in Um-Qasr coastal aquifer was constructed and calibrated by applying a 3-D SEAWAT model. SEAWAT was used for simulating the spatial and temporal evolution of hydraulic heads and solute concentration of groundwater in the southern part of Iraq at Basrah (Um-Qasr region). The work in this research was aimed to define the behavior of the seawater intrusion in the region and to assess its outcomes by applying the variable-density model using the 3-D finite difference discretization. In this way it was planned to clarify when and where most of seawater intrusion occurred and to predict its future behavior along the region. This model is a fully coupled flow and transport model, capable of simulating variable-density effects on groundwater flow. For calibration purpose, a comparison between the results of the simulation model and the actual observation data from 12 observation wells was done. The simulation result gave good agreement at comparison with actual observations with less parameters adjustments. Accordingly, the calibrated model was used for prediction of future changes in water levels and seawater transport in the aquifer for planning period of 20 years. The pumping from the aquifer was considered at continues to increase from the same pumping wells assuming that there are no new water resources for Um-Qasr city. The final simulation results show that seawater intrusion would occur in the aquifer at high levels if the current rates of groundwater pumpage continue with increase at its current rate with future.**

I. INTRODUCTION

Saltwater intrusion refers to the movement of salty water into freshwater aquifers (figure 1). Saltwater intrusion has been a major groundwater resource problem in coastal environments for decades. Many coastal states which depend upon groundwater are particularly affected. Increasing population in these areas and resulting groundwater consumption has added to the problem as the saltwater intrusion moves further inland in response to pumping. This critical problem requires proper studies and management to protect groundwater resources. Seawater intrusion is caused by decreases in groundwater levels or by rises in seawater levels. When fresh water pumped out rapidly, the height of the freshwater will lowered forming a cone of depression. According to Ghyben-Herzberg theory [1] the salt water rises 40 feet for every 1 foot of freshwater depression and forms a cone of ascension. Intrusion can affect the quality of water not only at the pumping well locations, but also at other well locations, by increasing salinity of the groundwater; (Figure 1).

The Um-Qasr aquifer on Arabian Gulf coast is a good example for seawater intrusion problem. Basrah province is in critical situation that requires immediate efforts to improve the water situation in terms of quality and quantity were demand greatly exceeds water supply. If uncontrolled pumping is allowed to continue the aquifer, which is the primary source for the Um-Qasr region, will become unusable as a source of fresh municipal water and most agricultural extraction will be too saline for crop irrigation [2]. Um-Qasr located in the south east of Iraq in Basrah province and its contain important and largest port in Iraq which is depends mainly on groundwater for fresh water supplying. More than 77 wells on Um Qasr aquifer. The study area locates between (779030)E and (3323445)N, area of (39.2 km2). Its borders, Khur Al-Zubair from the east, Safwan area from the north and west, and Kuwait from the south (figures 2). The population of Um-Qasr is 56433 person [3]. Um-Qasr coastal aquifer met with the seawater intrusion problems such as ports location, industrial, dense population, arid and water scarcity, and more wells in the future to digging to supply Irrigation water for planed Basrah vegetation belt projects for that it is a good example for studying seawater intrusion problem.

2. HYDROGEOLOGICAL SETTING OF THE STUDY AREA

Groundwater in the study area occurs in an unconfined aquifer of alluvial deposits, which are composed mainly of sand and silts. The principal direction of the groundwater flow is from the south-west to the north east towards the Khur Al-Zubair lagoon. The hydraulic gradient is consistent with the topography, steep in the east, and gentle in the west. Basrah governorate /South of Iraq is characterized by hot, dry climate and high wind velocity in summer, and cold, humid and little to moderate rainfall in winter. In general, the study area located within semi-arid zone with average annual precipitation of 151 mm/y [climate data].

3. METHODOLOGY

This research outlined the development and applications of a simulation flow and transport models for Um-Qasr aquifer. The development of the simulation model (using seawater intrusion model SEAWAT) followed the characterization step. In this step, models were constructed and used for model development. Simulation models were applied to the study area in two stages. Current year simulation was used in the first stage and then the predication simulation be

applied at second stage to predicate the seawater intrusion with future pumping for the study area using calibrated simulation modeling.

4. Flow-Transport Simulation Model

The groundwater flow and salinity transport in Um-Qasr aquifer was simulated using the SEAWAT model [4]. SEAWAT uses a modified version of MODFLOW [5] to solve the variable density, groundwater flow equation and MT3DMS [6] to solve the solute-transport equation. To minimize complexity and runtimes, the SEAWAT model uses a one-step lag between solutions of flow and transport. This means that MT3DMS runs for a time step, and then MODFLOW runs for the same time step using the last concentrations from MT3DMS to calculate the density terms in the flow equation. For the next time step, velocities from the current MODFLOW solution are used by MT3DMS to solve the transport equation.

5. Conceptual Model Features

A conceptual model was constructed to simulate the variable density groundwater flow in the Um-Qasr aquifer with the following data: Total effective area of 39.1 km^2; The total period of simulation was 21 years from 2014 until 2034; and Model max. thickness of 35 m. A conceptual and hydro-geological 3-dimentional and cross-sectional model for Um-Qasr aquifer is shown in figures (3) and (4). In all this area, the coastal aquifer is unconfined and composed of one layer of dunes sand, gravel, silt, with interaction of clay and loam.

5.1. Spatial Model Discretization

A finite difference grid was developed to adequately discretize the model domain; this was according to guideline indicating in models instruction [7]. For the Um-Qasr aquifer a regularly spaced, finite-difference model grid was constructed so that the y-axis represent the north and x-axis represent the east as shown in figure (5). The grid consists of 120 rows and 120 columns, regularly spaced grid in horizontal and longitudinal directions. A one cell (layer) in the vertical direction with variable thickness (ΔZ) according to the surface topographic and corresponds with land surface elevation, based on a compiled topographic contour map was used. The bottom of the layer is set at an elevation of 20 m below sea level to insure all the wells at full penetration within the model. The total number of model regularly spaced cells is 14400 cells. Each cell is 53.4 × 51.9 m in the horizontal plane. The horizontal extend for the whole model is 6.4 km east zone from the sea and 6.1 km in the north direction.

5.2. Boundary and Initial Conditions

The boundary conditions of the model domain depend on many considerations, such as domain extent, stratigraphy, water bodies and physical features within the study area. There are three types of flow boundary conditions: i) specified head, ii) specified flow, and; iii) head-dependent flow.
And three types of boundary conditions are generally associated with the contaminant-transport equation [8], [9], [10]: i) the Dirichlet (or first-type), ii) Neumann (or second-type), and; iii) Cauchy (or third-type).

For Um-Qasr model, the boundary conditions were set as below:

Constant head and concentration was specified to the model cells along the coast (east side). The specified constant concentration of sea side salinity determined from samples tests was 40000 mg/l which represent the average concentrations for one year seasons. A reference density of 1025 kg/m^3 and 1000 kg/m^3 was used for seawater and fresh water respectively. For heads setting, the simulation was performed using a present day constant mean sea level of zero meters.

To represent the lateral flow of groundwater from the inland perimeter of the model, the western side represents the flow side due to fact that the water level at this boundary is higher than the water level inside the model domain. On the other hand, a drop in water levels in the model area reverses the flow from outside towards inside. Constant head boundary conditions were assigned to the western boundary of the model with a specified salt concentration. The constant concentration and head was calculated from the available water levels and TDS contour maps at that boundary during the year of observation. The final value of heads was adjusted during the mode first run and set to about 3.7 m above mean sea level. The lower end of the model represents the base of the aquifer. A Neumann-type of no-flux boundary conditions was assigned to the bottom of the aquifer. A Neumann-influx boundary condition was assigned at the land surface, and the recharge package was used to represent the recharge of the aquifer. The recharge concentrations are calculated from proportions of rain and return irrigation flow where the rain water TDS are estimated about 10 mg/l, and return flow TDS for R.O. units was about 4000 mg/l . The northern and the southern boundaries were assumed to be no flow boundaries, since the flow lines are parallel to them as shown in figure (8).

Initial conditions (heads and concentrations) were specified using the measured heads and concentration data. Twelve monitoring wells distributed over the study area were selected to measure (over a period of one year) the initial and historical groundwater levels and salt concentrations (6 for head and 6 for concentration). These values then used for calibration proposes. Figure (6) shows the local distribution for observation wells. In the monitoring process, different devices such as level, tape, sounder and GPS were used to measure the groundwater level monthly for the period (April, 2012; March, 2013). Table (1) shows the initial hydraulic head and TDS concentration for observed wells for the year 2012.

5.3. Wells and Recharge Flow

More than 77 pumping wells are indicated and represented in the model domain (figure 7). For future model simulation the well withdrawal estimation was done according to the available data of population, population growth, number of wells, and groundwater abstraction within 2012-2014 which is estimated to be increase at a rate of (2%).

The recharge package in SEAWAT (RCH) is used to apply surface recharge from rainfall to the model with a specified low salt concentration taken as (10mg/l). The sources of the recharge are rainfall and return flow. The average rate of

recharge applied on the model was in the order of 0.414 mm/day. Direct recharge from rainfall is considered by far the principle source of recharge in the Um-Qasr aquifer. Review of the previous studies and literature indicates varying estimates of recharge from rainfall. Most of the recharge estimates made for the study region specified recharge with different coefficients according to the amount of rainfall [11] and as follow:

Recharge = 0.2 × (annual rainfall intensity) ≈ 0.2 × (151) = 30.2 mm/yr.

For estimating the recharge from return flow, one type of return flow was considered in the estimation which is the return flow from reverse osmoses treatment units (R.O.). There is no return flow from irrigation due to the irrigation at study area done by trickling methods [field data]. Within the study area, the majority of the stressed areas (high wells concentrations) are located in the eastern part near Um-Qasr port (Figure 7). Total numbers of wells that are used for R.O. units are 47 well; these units receive approximately 23500 m^3 of water daily. The return flow is estimated to be around 25% from treated water volume. This yields an annual return flow from these wells as follows:

Annual total quantity of water withdrawal to wells within the study area is about $6.1x10^6$ m^3 as obtained from the field database. The assumed annual losses are about 25% or $1.52x10^6$ m^3. This lost quantity is assumed to percolate down to recharge the aquifer.

5.4. Modeling Time Discretization

The first simulation period for the basic groundwater flow model was 365 days to reflect a one year of time starting from the year 2012 until 2013. For future prediction simulation, the period for the groundwater flow and transport model was 7,300 days to reflect a 20 years of time starting from the year 2014 until 2033.

The 20-year simulation period is divided into 20 stress periods. For each stress period, the average hydrologic conditions for that period are assumed to remain constant. For one year simulation period the stress periods taken as four parts to represents the difference source/sinks within the seasons of the year and further temporal discretization is introduced in the form of time steps within each stress period. The length of the flow time steps was in the range of 10-30 days and the transport time step was assigned to start with (1) day and increased by a multiplier factor of (1.2), were these values represent the best and suitable values for practical operation of the model.

5.5. Aquifer Parameter and Modeling Data for Study Area

Hydraulic aquifer parameters are estimated from field works and laboratory testing for more than 60 soil samples and from results of aquifer pumping tests carried out in the Um-Qasr region [12]. The field works conducted in this study includes detailed field surveys to investigate all study area characteristics. Many soils and water samples were collected to analyze the characteristics and TDS values. Modern devices for topographic and water levels measurements were used such as total station, modern GPS, TDS measurement device, sounder. Two pumping tests were executed at different zones and 12 selected wells were used for continues observations of heads and concentrations within two years for calibration and for verification. The field surveys that were conducted in Um-Qasr aquifer started, April 2012 till December 2013.

According the field survey, the values of hydraulic conductivity (K) was mostly within a range of 60-80 m/day. The pumping test results gave K values of (65.7 and 66.8) m/day for the two sites as calculated from the two pumping test results evaluation. Specific yield values are estimated to be about 0.2-0.3 while specific storativity was about 10^{-4} m^{-1} [13]. Some of Um-Qasr hydraulic parameters that are difficult to estimate by pumping or lab tests such as vertical permeability (K_v) and longitudinal and transvers dispersivities (αL and αT) were estimated from soil properties standards tables or from other researches done at state of Kuwait [14], [15], [16].

The groundwater levels at present state are found at about 10-8 m depth from land surface, which approximately is 1m above sea level. Depth to water levels of the coastal aquifer varies between 8 meters in the low land area along the shoreline, and about 11 m along the western border. Table (2) summarizes Um-Qasr input parameters to SEAWAT model.

6. Simulation Model Results

After completing the calibration and verification for the flow-transport simulation model, the developed model was then used to simulate the groundwater levels, concentration, flow, saltwater-freshwater transition zone and movement at the current year (2013) and then will be used for 20 future years (2014-2034) predication results for Um-Qasr aquifer. On the basis of the calibrated model and the investigated / assumed temporal pumping stress, the transient changes in groundwater levels and of the TDS distribution will be simulated for current year (2013). This period was divided into 4 pumping stress periods, with 3 flow time step for each stress period as shown below:

For practical model operation, transport time step was selected as 3 days and the Strongly Implicit Procedure (SIP) solver was used for flow calculation and the finite difference method was used for solving the transport.

Total simulation time	One year simulation (12 months)											
Stress Periods	stress period 1 (1.Apr. - 30.Jun)			stress period 2 (1.Jul. - 30.Sep.)			stress period 3 (1.Oct. - 30.Des.)			stress period 4 (1.Jan. - 30.Mar.)		
Time steps	Apr.	May.	Jun.	Jul.	Aug.	Sep.	Oct.	Nov.	Dec.	Jan.	Feb.	Mar.

6.1. Groundwater Levels, Concentration and Flow

The simulated results for steady state groundwater levels are shown in figure (8). It's clear from the figure (8) that the initial water level changes linearly from the sea to the west border of 1m head in average. Figure (9) show the steady state simulated TDS concentrations for Um-Qasr aquifer for year 2013 which show the variation in salinity distribution for the aquifer. Figure (10) show the initial steady state groundwater flow directions for Um-Qasr aquifer at year 2013. Under natural conditions, groundwater flow direction in the Um-Qasr region is towards the sea (Khor Al-Zubair). However, pumping over many years as illustrated in production simulation has significantly disturbed natural flow patterns. Large cone of depression have formed in the east and south where water levels are below mean sea level, including inflow of seawater towards the major pumping centers.

6.2. Saltwater-Freshwater Transition Zone and Groundwater Movement

The estimated extent of the seawater wedge from seawater intrusion modeling at the end of year 2013 is presented in figure (11). It is considered that the extent (wedge) of seawater intrusion is represented by isoline 10000 mg/l of TDS concentrations. It is clear from the above results that most of affected area by seawater intrusion is located in the east of Um-Qasr region at Um-Qasr port wells.

Figure (12) shows the velocity vector distribution in Um-Qasr region for year 2013. It is clear from this figure that the discharge to the sea is very low, which means that there is overexploitation from this area. Also, the velocity is high near the wells at middle of the area, due to the high abstraction rates. On the other hand, the velocity is high in landward direction near the sea-shore due to high rate of pumping.

7. Simulation Predication Runs

In order to demonstrate the effect of future changes of groundwater pumpage on seawater intrusion, the pumpage from the aquifer were estimated to use the calibrated model for calculations of future changes in water levels and salinity concentrations in a period of another 20 years, within 2014-2034. The pumping from the aquifer considered continues to increase from the same pumping wells at a population increasing rates of 3%, assuming that there are no new water resources for Um-Qasr city.

Table 3 and figure 13 show amount of abstracted water from the aquifer for the proposed state**.** The predicated simulation was carried out for 20 years using the obtained first run results of year 2013 as initial conditions. The results of the first run were used as initial conditions for transient simulation of stressing aquifer by pumping during 2014-2034.

Figures 14 and 15 show the future changes in the predicted water levels and TDS concentrations corresponding to the extent of seawater intrusion in aquifer through the simulation years (2014-2034) for the suggested case throughout the simulation periods.

8. Summary and Conclusions

Simulation of variable density of groundwater flow coupled to solute transport for Um-Qasr aquifer was formulated using SEAWAT. The conceptual model was constructed at the first step with all its features, (boundary and initial conditions, recharges, simulation periods, aquifer and modeling parameters), the sensitivity analysis and calibration for the model was then done to develop an accurate integrated simulation model. The results of the sensitivity analysis shows that the model was very sensitive to changes in recharge rate, well pumping and hydraulic conductivity and less sensitive to specific yield and dispersivity. The model gave good results for changes in salinity in the aquifer. This result shows that seawater intrusion is accrued in port wells at eastern parts of Um-Qasr area. SEAWAT model was applied to examine how far inland seawater transition zone has moved since intrusion began. The numerical model was applied to test the overall impact on the aquifer with future pumping. The suggested pumping increases continuously from $6.1x10^6$ m^3/y to reach about $8.8x10^6$ m^3/yr in the year 2034 and at a rate of 3%. It is predicted that between years 2015 and 2034, the simulation induces a considerable quantity of seawater intrusion especially in the eastern part. Model results indicate extent of the isoline (TDS concentration = 10000 mg/l) at aquifer of additional 1.5 km in the eastern part. According to the results of simulation, a seawater intrusion rate of 250 m/year can be concluded. On the other hand, the simulation results indicate that, in year 2034 the total inflow from the sea is estimated to be $7.2x10^6$ m^3/yr, where the discharge to the sea for the same year is estimated to be about $3x10^6$ m^3/yr. Figures 16 show the three dimensional simulations model output results for the extent of seawater intrusion in the Um-Qasr aquifer at years (2015, 2024 and 2034).

References

[1] Reem Fathi Saleh Sarsak, 2011, Numerical Simulation of Seawater Intrusion in Response to Climate Change Impacts in North Gaza Coastal Aquifer Using SEAWAT, A thesis presented for the degree of M.Sc., in Water and Environmental Engineering, Faculty of Graduate Studies, at An-Najah National University, Nablus, Palestine.

[2] CENTRAL ARIZONA SALINITY STUDY,PHASE I, Technical Appendix-A.

[3] Tokyo Engineering Consultants Co., Ltd. and NIPPON KOEI CO., LTD, The Feasibility Study on Improvement of the Water Supply System In Al-Basrah City and Its Surroundings in The Republic of Iraq, INTERIM REPORT, JAPAN INTERNATIONAL COOPERATION AGENCY (JICA), 2006.

[4] Visual MODFLOW Premium, Demo Tutorial, Waterloo Hydrogeologic, (2000).

[5] J.M. McDonald and A.W. Harbaugh, "A Modular Three-Dimensional Finite-Difference Ground-Water Flow Model", in Techniques of Water Resources Investigations, U.S.G.S., Book 6. Reston, VA: U.S. Geological Survey, 1988.

[6] Anna Buseman-Williams, David Farrell and Alexander Sun, SOFTWARE VALIDATION TEST PLAN AND TEST REPORT FOR MODULAR THREE-DIMENSIONAL MULTISPECIES

TRANSPORT MODEL (MT3DMS) VERSION 4.5, Center for Nuclear Waste Regulatory Analyses, 2005. Zheng, C.M. and P.P. Wang. "MT3DMS: A Modular Three-Dimensional Multispecies Transport Model for Simulation of Advection, Dispersion, and Chemical Reactions of Contaminants in Groundwater Systems; Documentation and User's Guide." Contract Report SERDP-99-1. Vicksburg, Mississippi: U.S. Army Engineer Research and Development Center. 1999.

[7] Thomas E. Reilly and Arlen W. Harbaugh, " **Guidelines for Evaluating Ground-Water Flow Models",** Scientific Investigations Report - 5038. U.S. Department of the Interior, U.S. Geological Survey, (2004).

[8] Chan-Hee Park, SALTWATER INTRUSION IN COASTAL AQUIFERS, Ph.D. thesis, in Civil and Environmental Engineering, Georgia Institute of Technology, (2004).

[9] Yuan Ding and Yong Peng, " CONTAMINANT TRANSPORT IN COASTAL AQUIFERS", Final Report, New Jersey Department of Environmental Protection, Division of Science, Research and Technology, Trenton, New Jersey, 2009.

[10] Reilly, T. E. , System and boundary conceptualization in groundwater flow simulation, U.S. Geological Survey techniques of water resources investigations, Book 3, Chapter B8, 26p, (2001).

[11] Al-Aboodi, A.H.A, OPTIMAL GROUNDWATER MANAGEMENT IN TEEB AREA, MISSAN PROVINCE, USING GENETIC ALGORITHM TECHNIQUE, A thesis presented for the degree of phD., College of engineering, University of Basrah, (2011).

[12] ASTM Standard Test Method (Field Procedure) for Withdrawal and Injection Well Tests for Determining Hydraulic Properties of Aquifer Systems, D 4050 – 96 (Reapproved 2002).

[13] BUCCA Water Production Treatment Plant and Storage, Design Analysis Report, by Areebel Co.. CAMP BUCCA-UM QASR, IRAQ, 2008.

[14] A. Mukhopadhyay and M. Al-Otaibi, " NUMERICAL SIMULATION OF FRESHWATER STORAGE IN THE DAMMAM FORMATION, KUWAIT", The Arabian Journal for Science and Engineering, Volume 27, Number 2B, 2002.

[15] M. Al-Rashed, A. Mukhopadhyay, M. Al-Senafy, and H. Ghoneim, " CONTAMINATION OF GROUNDWATER FROM OIL FIELD WATER DISPOSAL PITS IN KUWAIT", The Arabian Journal for Science and Engineering, Volume 35, Number 1B, 2010.

[16] A. Mukhopadhyay, J. Al-Sulaimi, and J.M. Barrat, "Numerical Modeling of Groundwater Resource Management Options in Kuwait", Groundwater, 32(6), pp. 917–928, (1994).

[17] Rohit R. Goswami and T. Prabhakar Clement, "Laboratory-scale investigation of saltwater intrusion dynamics", WATER RESOURCES RESEARCH, VOL. 43, W04418, doi:10.1029/2006WR005151, 2007.

[18] Reem Fathi Saleh Sarsak, 2011, Numerical Simulation of Seawater Intrusion in Response to Climate Change Impacts in North Gaza Coastal Aquifer Using SEAWAT, A thesis presented for the degree of M.Sc., in Water and Environmental Engineering, Faculty of Graduate Studies, at An-Najah National University, Nablus, Palestine.

Table (1) Initial hydraulic heads and concentrations for observed wells in the study area

Well No.	Hydraulic head elev.(m)	TDS Concentration (mg/l)
Ob1	0.6	7440
Ob2	1.71	4210
Ob3	1.50	4500
Ob4	2.40	3500
Ob5	1.45	4900
Ob6	0.75	4970
C1	0.58	7473
C2	1.45	4574
C3	2.25	3551
C4	1.20	6119
C5	1.70	4213
C6	0.80	4895

Table (2) Original aquifer parameters assigned for Um-Qasr aquifer

Parameter	Value	Remarks
Hydraulic conductivity K_{xy}	66 m/d	Estimated from field pumping test
Hydraulic conductivity K_z	50 m/d	From other data for Kuwait [15] and from soil properties standards tables
Total porosity	0.30 %	Estimated from soil samples test
Effective porosity	0.28 %	Estimated from soil samples test data
Specific yield	0.25	Estimated from field pumping test
γ_s: Average soil dry density	1.77 Kg/m^3	Estimated from soil samples test
α_L : longitudinal dispersivity	15 m	From other data for Kuwait [15] and from soil properties standards tables
α_T : transverse dispersivity	1.5 m	Estimated from longitudinal dispersivity [17]
α_v : vertical dispersivity	0.15 m	Estimated from longitudinal dispersivity [17]
fluid viscosity for water	0.001 kg.m/sec	Typical value
g : gravitational acceleration	9.81 m/sec^2	Typical value
ρ_w : density of fresh water	1000 $kg.m^{-3}$	Typical value
ρ_s : density of sea water	1025 $kg.m^{-3}$	Estimated from samples test
Sea water concentration	40000 mg/l	Estimated from samples test

Table 3: Abstraction prediction amounts from Um-Qasr aquifer.

Stress period no.	Period length	First case Abstraction ($x10^6$ m^3/yr)	Stress period no.	Period length	First case Abstraction ($x10^6$ m^3/yr)
1	2014 - 2015	6.171	11	2024 - 2025	7.404
2	2015 - 2016	6.242	12	2025 - 2026	7.547
3	2016 - 2017	6.367	13	2026 - 2027	7.691
4	2017 - 2018	6.493	14	2027 - 2028	7.834
5	2018 - 2019	6.617	15	2028 - 2029	7.995
6	2019 - 2020	6.743	16	2029 - 2030	8.156
7	2020 - 2021	6.868	17	2030 - 2031	8.317
8	2021 - 2022	6.993	18	2031 - 2032	8.477
9	2022 - 2023	7.118	19	2032 - 2033	8.639
10	2023 - 2024	7.261	20	2033 - 2034	8.799

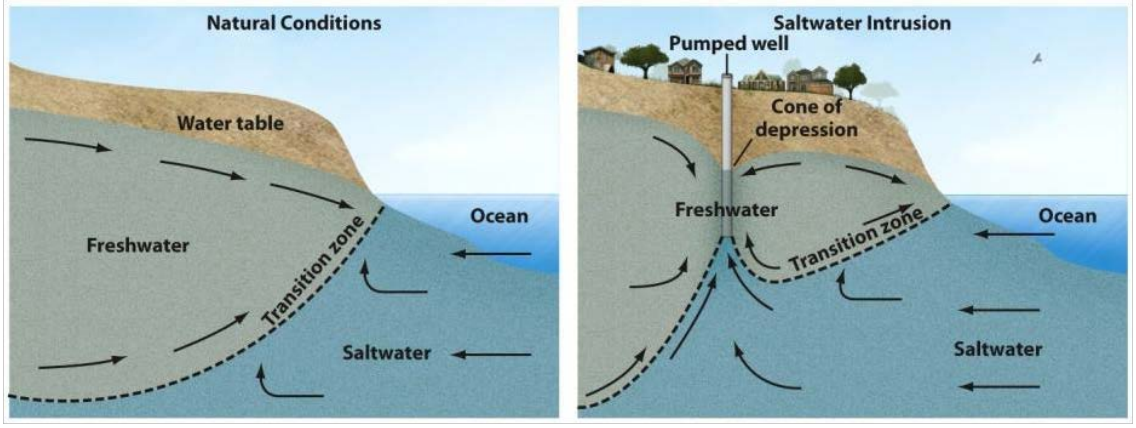

Figure (1): (a): Natural Conditions of freshwater/seawater interface, (b): effect of pumping into freshwater/seawater interface.[1]

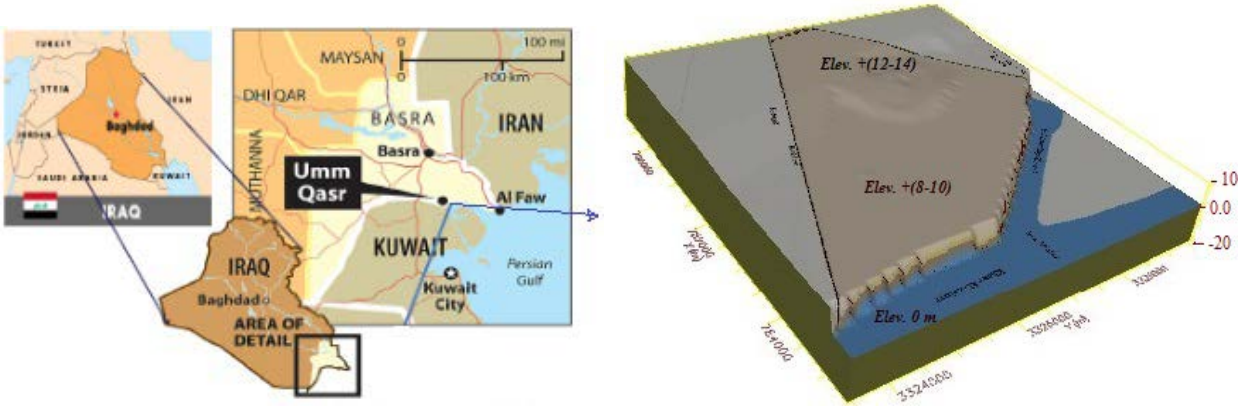

Figure (2) Location map of the Um-Qasr region

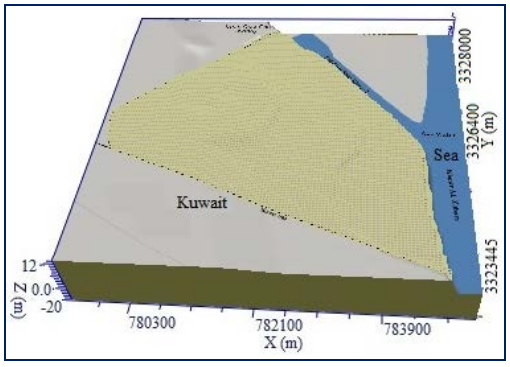

Figure (3) Conceptual model for Um-Qasr aquifer

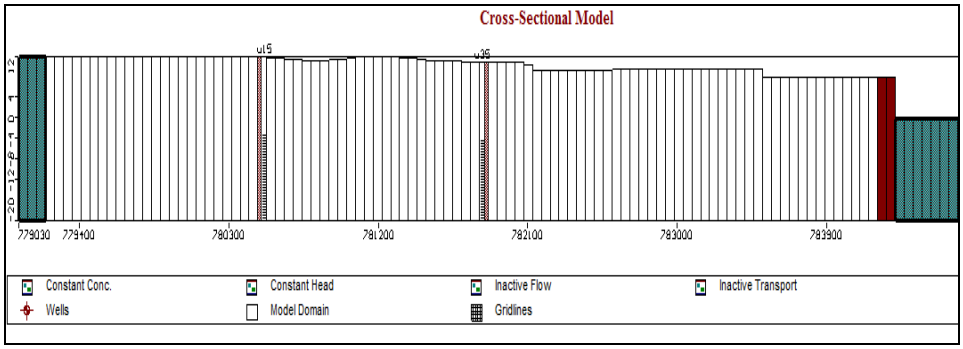

Figure (4) Cross sectional model for Um-Qasr aquifer

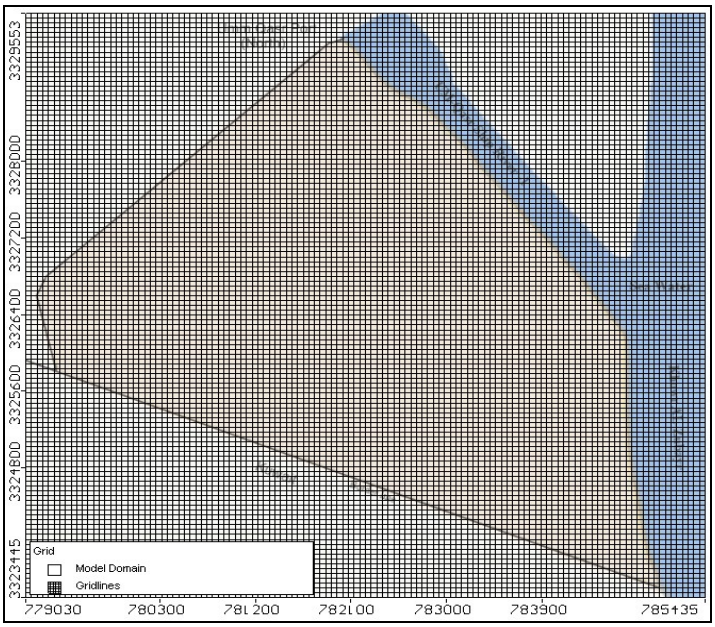

Figure (5) Finite difference grids for Um-Qasr aquifer

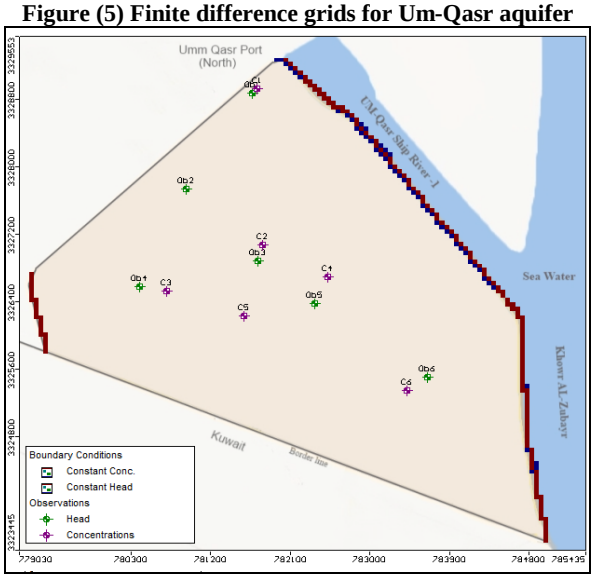

Sea Side

Figure (6) Boundary conditions and monitoring wells distribution in Um-Qasr aquifer

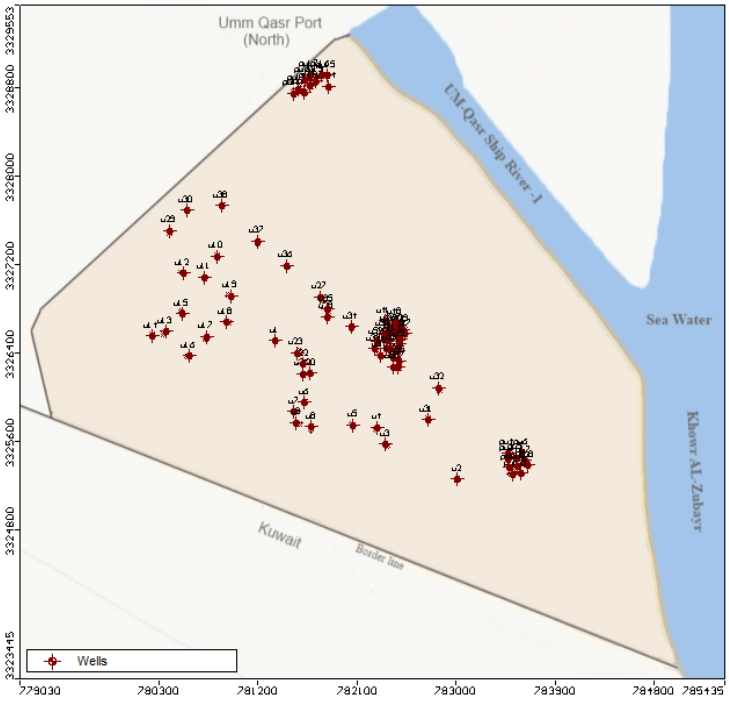

Figure (7) Distribution of existing wells in the study area.

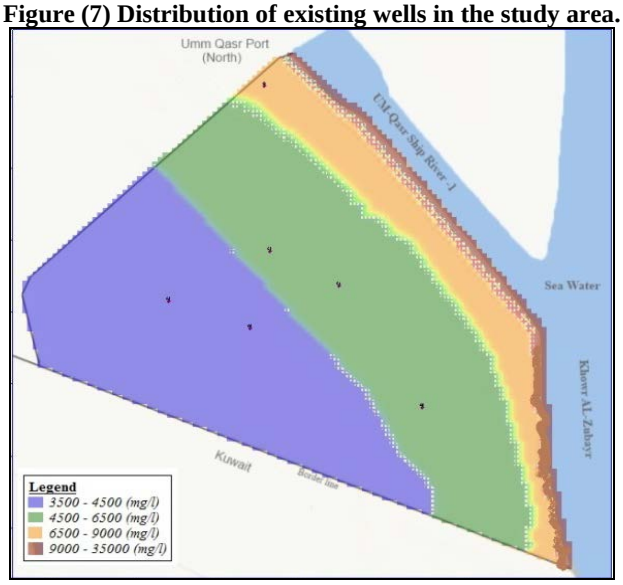

Figure (9) The steady state simulated TDS concentrations for Um-Qasr aquifer at year 2013.

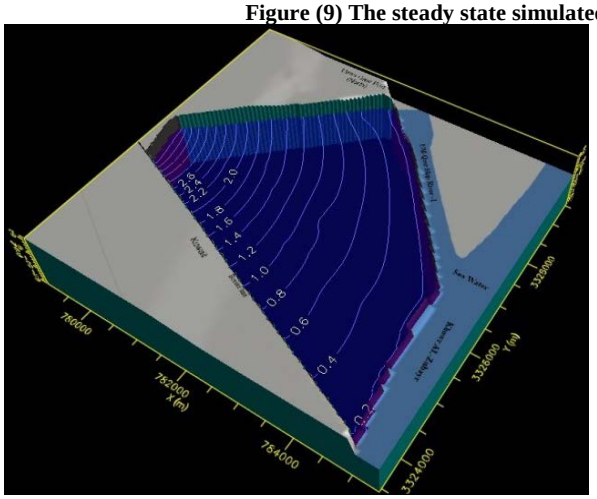

Figure (8) Initial or steady state groundwater levels contours for Um-Qasr aquifer.

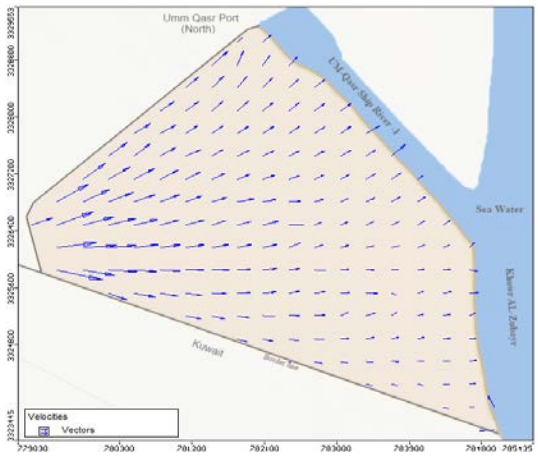

Figure (10) Initial Groundwater flow directions at year 2013.

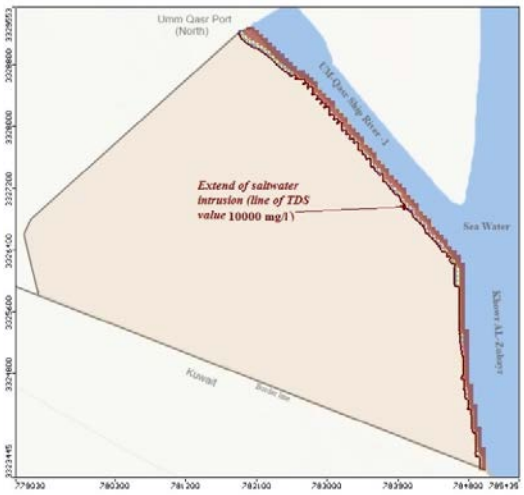

Figure (11) Isolines of calculated 10000 (mg/l) TDS concentration by SEAWAT at year 2013 along Um-Qasr aquifer.

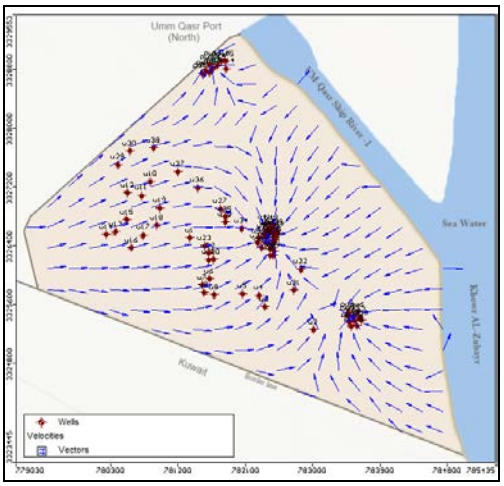

Figure (12) The calculated velocity vector distribution in Um-Qasr aquifer by SEAWAT at year 2013.

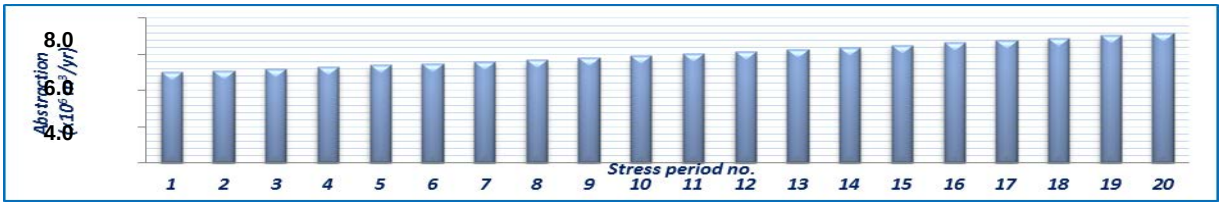

Figure 13: Proposed future pumping schemes increasing rates from the Um-Qasr aquifer.

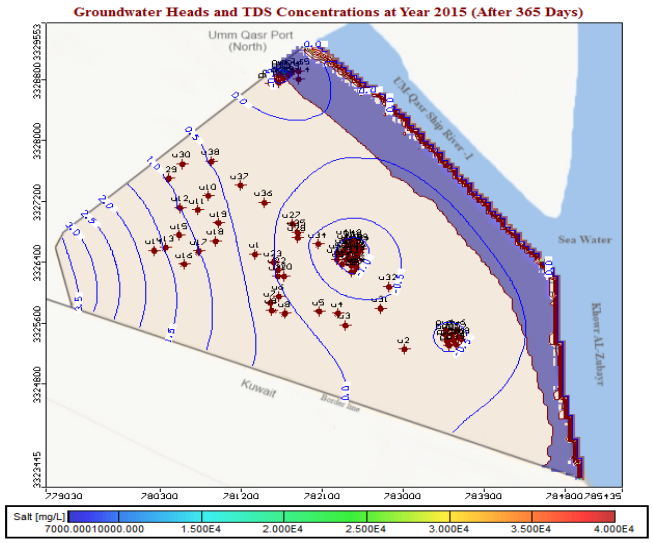
Groundwater Heads and TDS Concentrations at Year 2015 (After 365 Days)
Umm Qasr Port (North)
UM Qasr Ship River -1
Sea Water
Khawr AL-Zubayr
Kuwait
Border line
Salt [mg/L]
7000.00010000.000
1.500E4
2.000E4
2.500E4
3.000E4
3.500E4
4.000E4

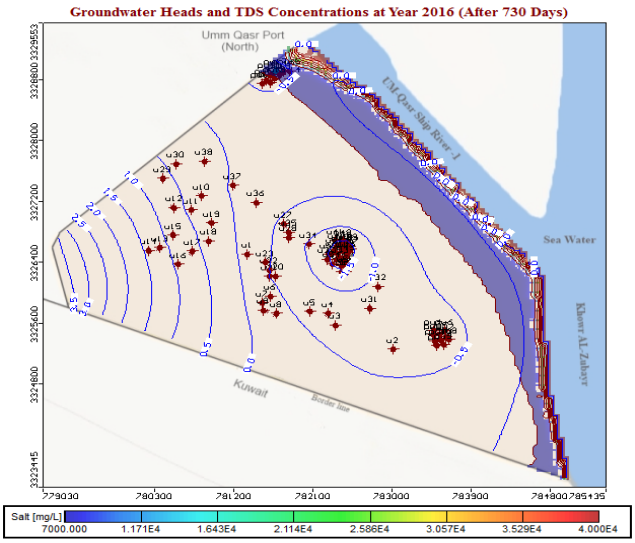
Groundwater Heads and TDS Concentrations at Year 2016 (After 730 Days)
Umm Qasr Port (North)
UM Qasr Ship River -1
Sea Water
Khawr AL-Zubayr
Kuwait
Border line
Salt [mg/L]
7000.000
1.171E4
1.643E4
2.114E4
2.586E4
3.057E4
3.529E4
4.000E4

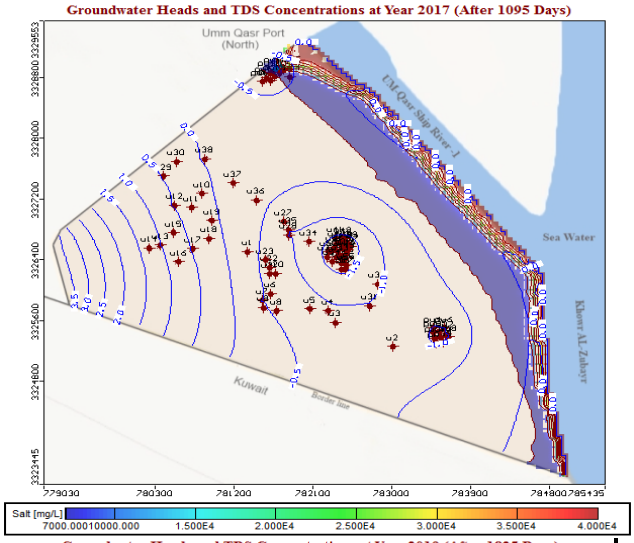
Groundwater Heads and TDS Concentrations at Year 2017 (After 1095 Days)
Umm Qasr Port (North)
UM Qasr Ship River -1
Sea Water
Khawr AL-Zubayr
Kuwait
Border line
Salt [mg/L]
7000.00010000.000
1.500E4
2.000E4
2.500E4
3.000E4
3.500E4
4.000E4

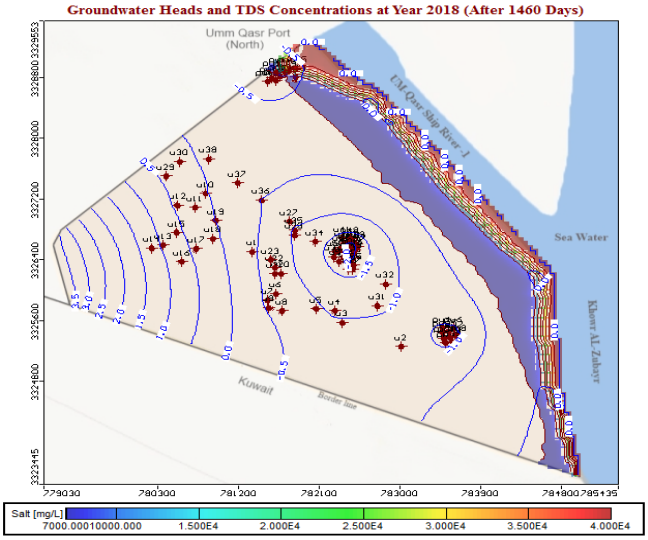
Groundwater Heads and TDS Concentrations at Year 2018 (After 1460 Days)
Umm Qasr Port (North)
UM Qasr Ship River -1
Sea Water
Khawr AL-Zubayr
Kuwait
Border line
Salt [mg/L]
7000.00010000.000
1.500E4
2.000E4
2.500E4
3.000E4
3.500E4
4.000E4

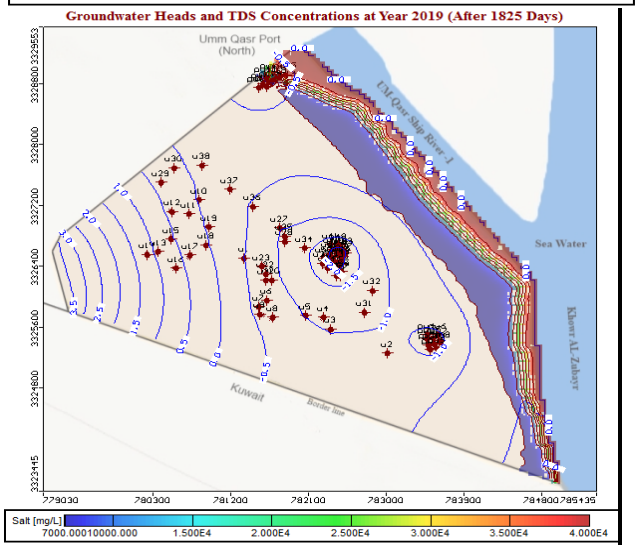
Groundwater Heads and TDS Concentrations at Year 2019 (After 1825 Days)
Umm Qasr Port (North)
UM Qasr Ship River -1
Sea Water
Khawr AL-Zubayr
Kuwait
Border line
Salt [mg/L]
7000.00010000.000
1.500E4
2.000E4
2.500E4
3.000E4
3.500E4
4.000E4

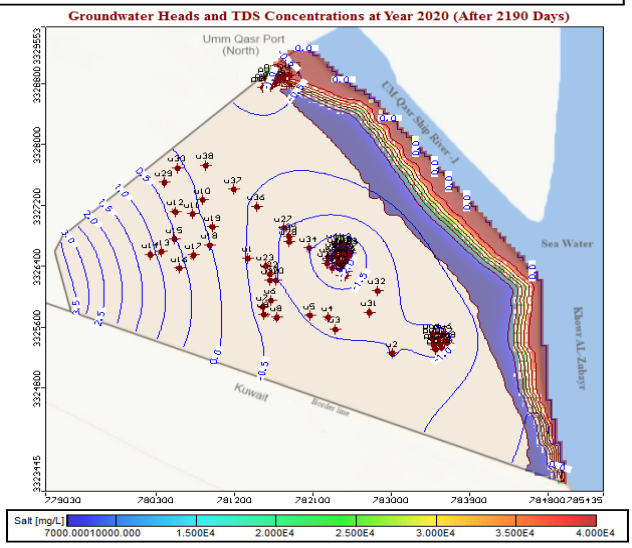
Groundwater Heads and TDS Concentrations at Year 2020 (After 2190 Days)
Umm Qasr Port (North)
UM Qasr Ship River -1
Sea Water
Khawr AL-Zubayr
Kuwait
Border line
Salt [mg/L]
7000.00010000.000
1.500E4
2.000E4
2.500E4
3.000E4
3.500E4
4.000E4

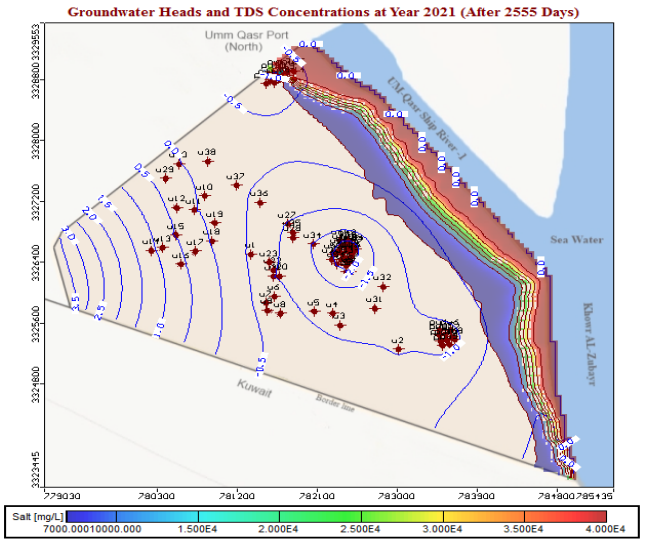
Groundwater Heads and TDS Concentrations at Year 2021 (After 2555 Days)
Umm Qasr Port (North)
Um Qasr Ship River -1
Sea Water
Khowr Al Zubayr
Kuwait
Salt [mg/L]
7000.00010000.000
1.500E4
2.000E4
2.500E4
3.000E4
3.500E4
4.000E4

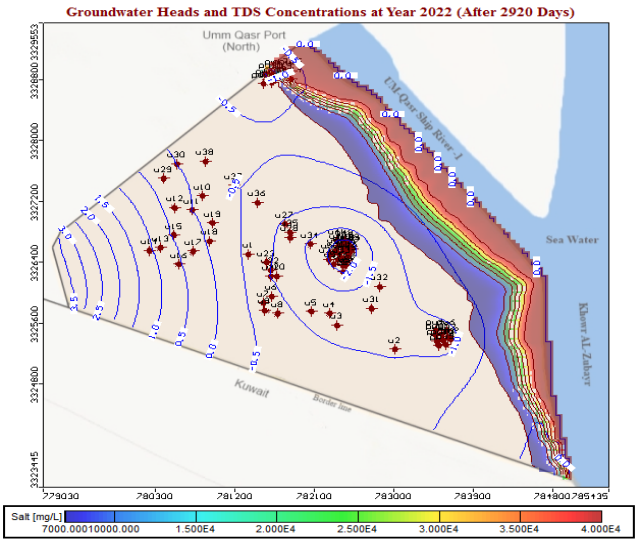
Groundwater Heads and TDS Concentrations at Year 2022 (After 2920 Days)
Umm Qasr Port (North)
Um Qasr Ship River -1
Sea Water
Khowr Al Zubayr
Kuwait
Salt [mg/L]
7000.00010000.000
1.500E4
2.000E4
2.500E4
3.000E4
3.500E4
4.000E4

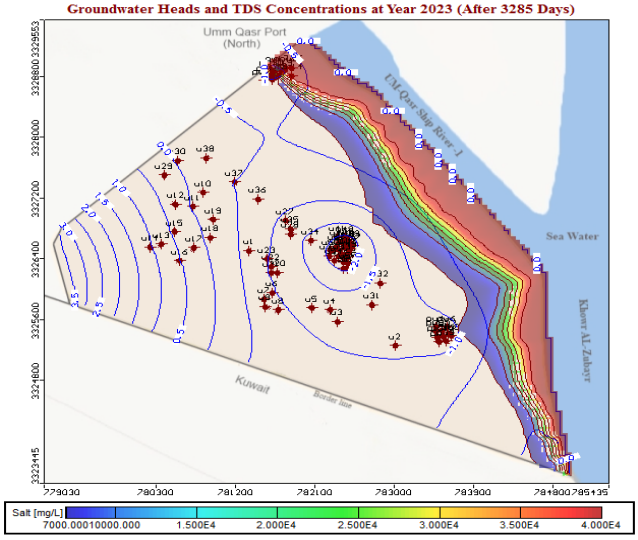
Groundwater Heads and TDS Concentrations at Year 2023 (After 3285 Days)
Umm Qasr Port (North)
Um Qasr Ship River -1
Sea Water
Khowr Al Zubayr
Kuwait
Salt [mg/L]
7000.00010000.000
1.500E4
2.000E4
2.500E4
3.000E4
3.500E4
4.000E4

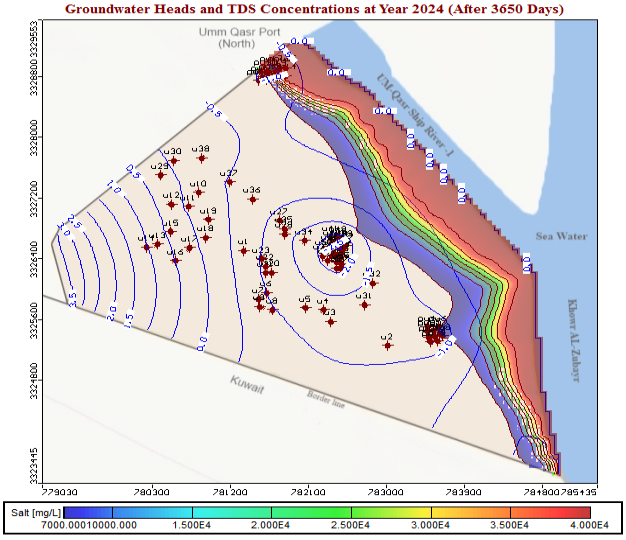
Groundwater Heads and TDS Concentrations at Year 2024 (After 3650 Days)
Umm Qasr Port (North)
Um Qasr Ship River -1
Sea Water
Khowr Al Zubayr
Kuwait
Salt [mg/L]
7000.00010000.000
1.500E4
2.000E4
2.500E4
3.000E4
3.500E4
4.000E4

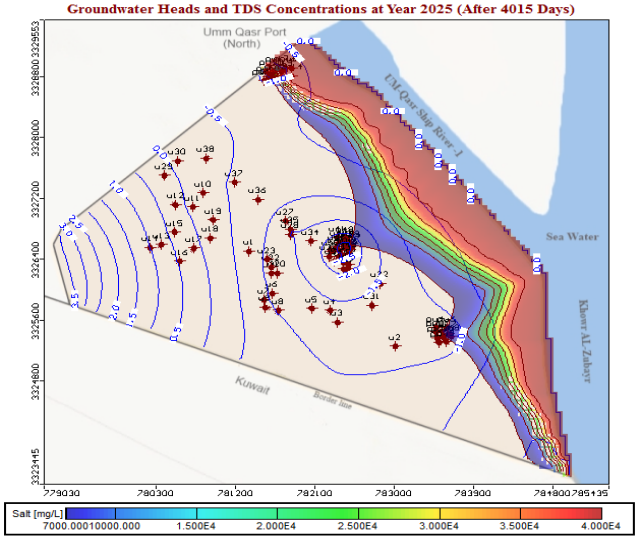
Groundwater Heads and TDS Concentrations at Year 2025 (After 4015 Days)
Umm Qasr Port (North)
Um Qasr Ship River -1
Sea Water
Khowr Al Zubayr
Kuwait
Salt [mg/L]
7000.00010000.000
1.500E4
2.000E4
2.500E4
3.000E4
3.500E4
4.000E4

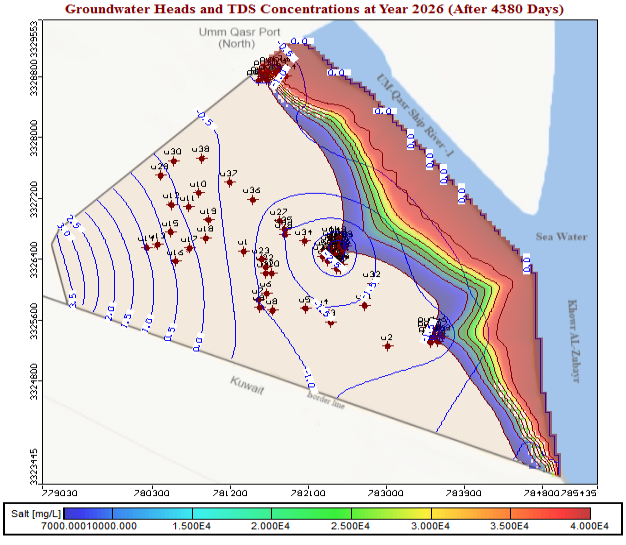
Groundwater Heads and TDS Concentrations at Year 2026 (After 4380 Days)
Umm Qasr Port (North)
Um Qasr Ship River -1
Sea Water
Khowr Al Zubayr
Kuwait
Salt [mg/L]
7000.00010000.000
1.500E4
2.000E4
2.500E4
3.000E4
3.500E4
4.000E4

Groundwater Heads and TDS Concentrations at Year 2027 (After 4745 Days)

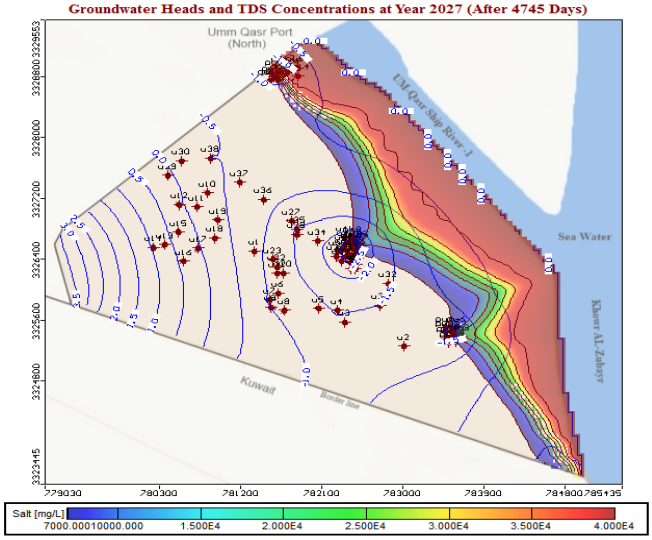

Groundwater Heads and TDS Concentrations at Year 2028 (After 5110 Days)

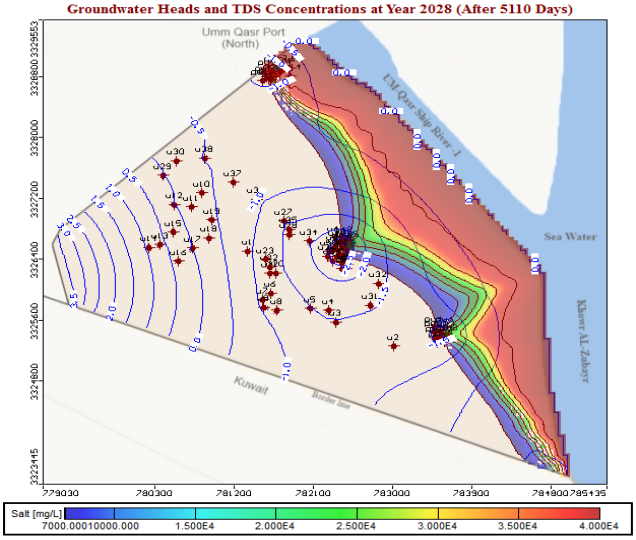

Groundwater Heads and TDS Concentrations at Year 2029 (After 5475 Days)

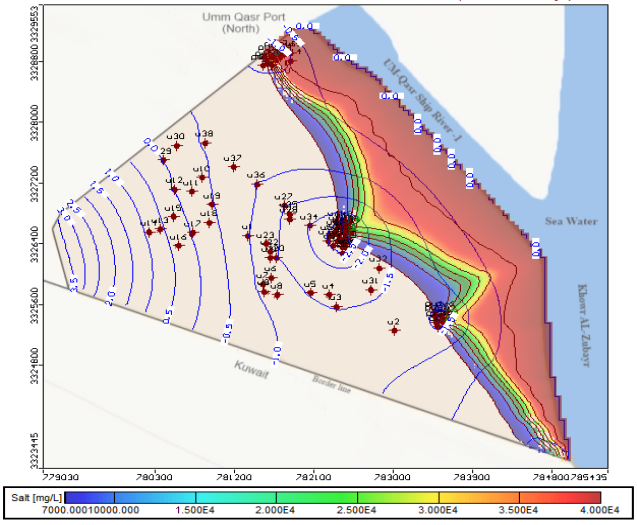

Groundwater Heads and TDS Concentrations at Year 2030 (After 5840 Days)

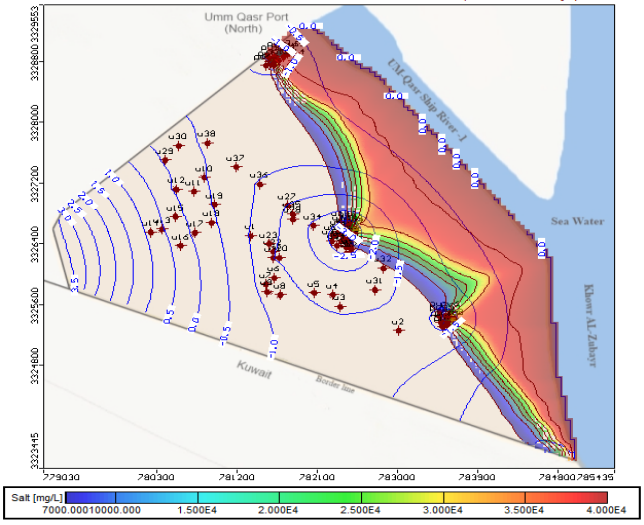

Groundwater Heads and TDS Concentrations at Year 2031 (After 6205 Days)

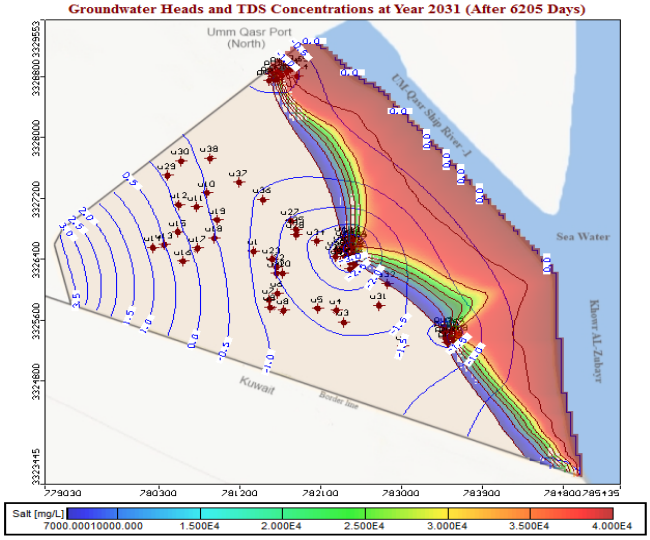

Groundwater Heads and TDS Concentrations at Year 2032 (After 6570 Days)

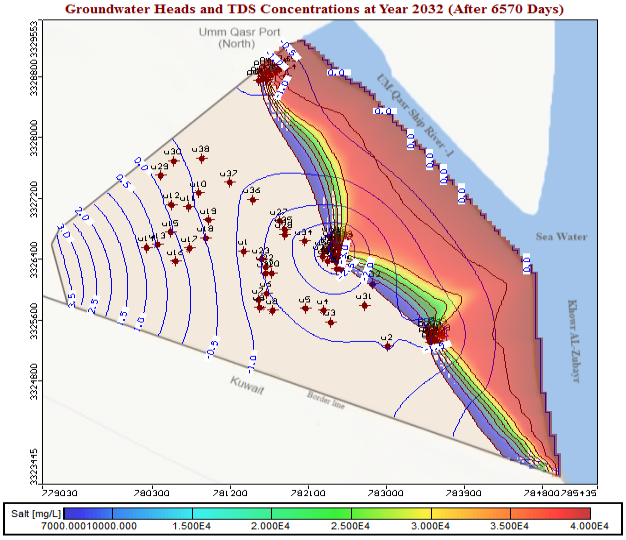

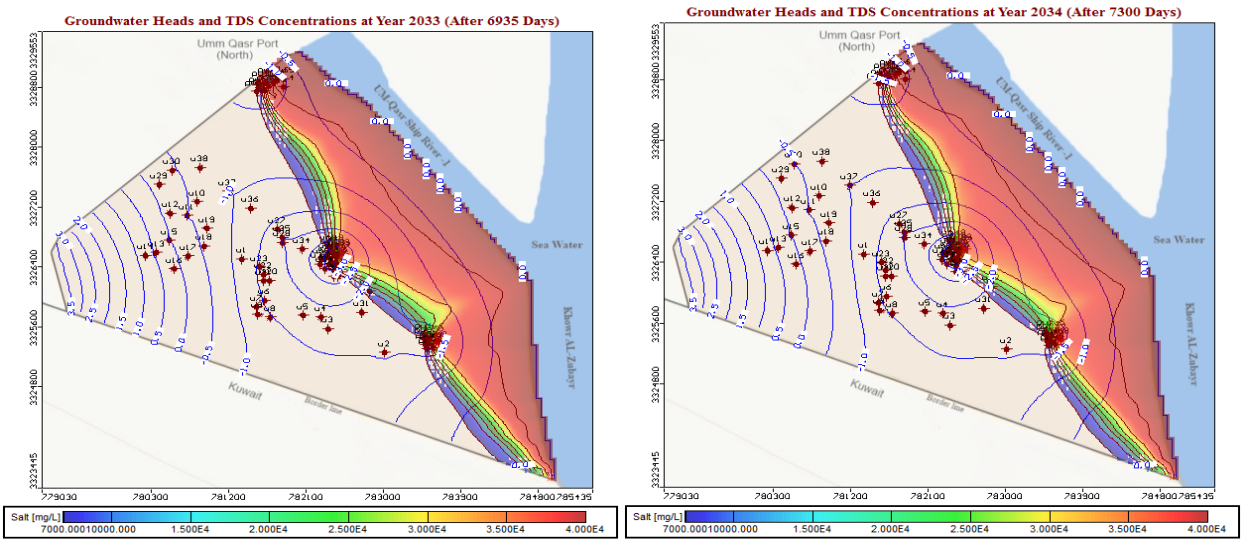

Figure 14: Predicted contour lines of groundwater levels and extent of TDS concentration (more than 7.0 kg/m^3) in Um-Qasr-aquifer in (2015 – 2034).

Figures 15 show the extents of seawater intrusion in the Um-Qasr aquifer cross-sections in specified years for the period (2014 to 2033).

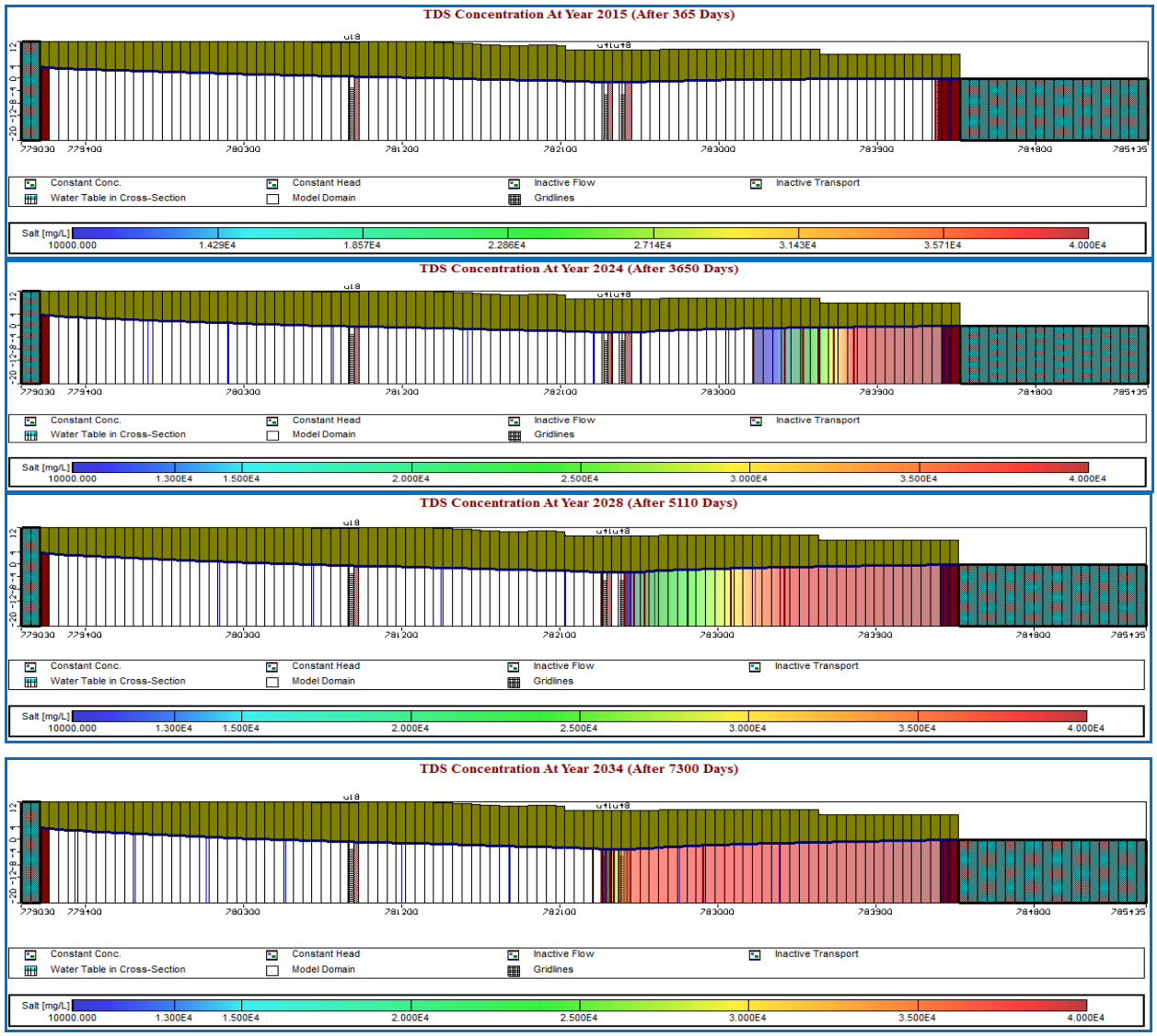

Figure 15: Simulated extent of TDS concentration (more than 10.0 kg/m^3) in Um-Qasr aquifer cross-section in (2015-2034) for the first scenario.

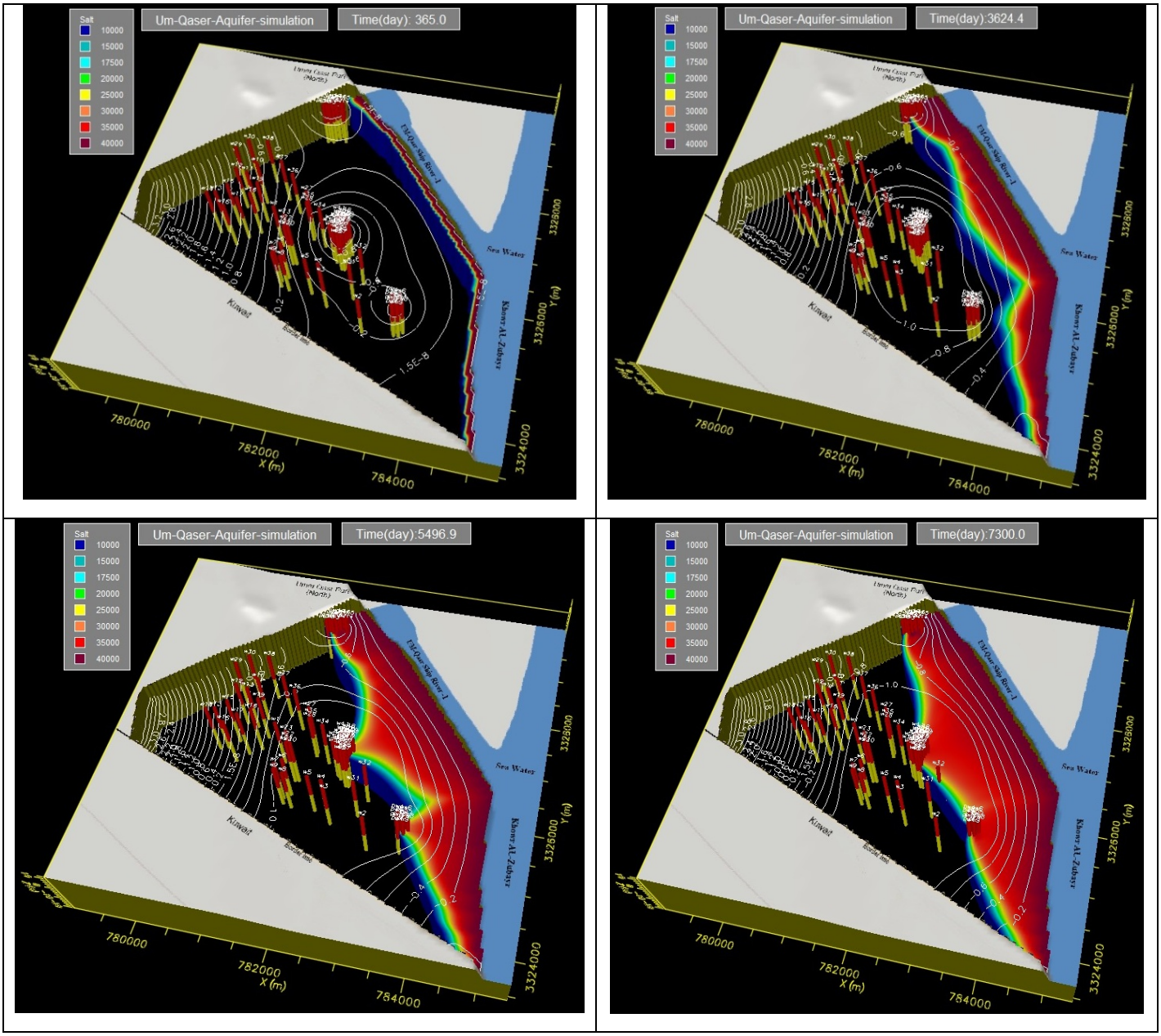

Figure 16: 3-D Simulated seawater intrusion in Um-Qasr aquifer after (365, 3650, 5490 and 7300) days.

Comparing between Moving Bed Biofilm Reactor and Conventional Activated Sludge System in Al-Rustamiyah WWTP (May 2015)

Walaa S. Mizeel, Prof. Dr. Mudhaffar S. Al-Zuhairy, and Dr. Zainab Bahaa

***Abstract*—In this research, presents the comparing between the Conventional Activated Sludge systems (CAS) and Moving Bed Biofilm Reactor (MBBR). An experimental campaign has been carried out at Al-Rustamiyah WWTP in Baghdad (Iraq); on a pilot plant consist of five reactors in series with Anoxic MBBR-1, Aerobic MBBR-2, Aerobic MBBR-3, Outlet chamber and the Flocculation part with dosing unit, that were operated continuously at different organic loading rates. The MBBR tank was filled with suspended carriers (AnoxKaldnes K_5), with a 50% filling ratio. The obtained results showed a good treatment ability of the MBBR system, referring to the organic matter removal, the average BOD_5 removal efficiencies for CAS and MBBR were 91% and 88% respectively. On the contrary the COD removal efficiency resulted alike (89% for both systems). The results demonstrate the higher treatment capacity of the MBBR addressing such system as an effective technology for the upgrading of overloaded wastewater treatment plants.**

***Index Terms*— Moving bed biofilm reactor, Al-Rustamiyah wastewater treatment plant WWTP, Efficiency**

I. INTRODUCTION

Today because of increased flow and organic loading many wastewater treatment plants are being expanded to provide addition capacity. The secondary treatment of the WWTP is usually accomplished by biological processes that can be classified as being either suspended or attached growth process. The conventional and mostly used suspended growth system is represented by the classical and well known activated sludge process (AS). Indeed, this process can present some shortcomings when exposed to increased hydraulic and organic loads. To increase the performances of an existing CAS system it would be necessary to increase the amount of biomass inside the aerobic reactor [1]. In the last years, the idea to combine the two different processes (attached and suspended biomass) by adding biofilm carriers, usually plastic carriers, into the aeration tank for biofilm attachment and growth has been proposed. A Moving Bed Biofilm Reactor (MBBR) is a compilation of these two technologies [2].

The MBBR was developed in Norway at the Norwegian University of Science and Technology in co-operation with a Norwegian company Kaldnes Miljøteknologi (now Anox Kaldnes AS). The first MBBR was installed in 1989. Currently, there are more than 500 large scale wastewater treatment plants based on MBBR process in operation in 50 different countries all over the world.

The Moving Bed Biofilm Reactor (MBBR) is a highly effective biological treatment process that was developed on the basis of conventional activated sludge process and biofilm process. It is a completely mixed and continuously operated Biofilm reactor, where the biomass is grown on small carrier elements that have a little lighter density than water and are kept in movement along with a water stream inside the reactor. The movement inside a reactor can be caused by aeration in an aerobic reactor and by a mechanical stirrer in an anaerobic or anoxic reactor [3].

Types of moving bed technology

1- Pure MBBR process: the biomass is growing chiefly on carriers that move freely in the reactor.
2- Hybas (Hybrid Biofilm Activated Sludge) processes: The biomass is growing on carriers that move freely in the reactor and act as suspended activated sludge [3].

II. CONVENTIONAL ACTIVATED SLUDGE PROCESS

Clark and Gage developed the activated sludge process at the Lawrence experiment station in Massachusetts [4] but the

Walaa S. Mizeel
M.SC. in Environmental Engineering/ Department of Building and Construction Engineering, University of Technology, Baghdad, Iraq.
walaasaadbest@yahoo.com
Prof. Dr. Mudhaffar S. Al-Zuhairy
President of Southern Technical University – Iraq
mshz005@yahoo.com
Dr. Zainab Bahaa
Department of Building and Construction Engineering, University of Technology, Baghdad, Iraq
zbm_asr@yahoo.com

conception of activated sludge process was discovered by Ardern and Lockett (1914). In this type of wastewater treatment, the microorganisms responsible for treatment are maintained in liquid suspension by appropriate mixing methods. The activated sludge process was so named because it involved the production of an activated mass of microorganisms capable of stabilizing a waste under aerobic condition [5].

The object of this experimental study was to Evaluate and compare the performance of a pilot plant moving bed biofilm reactor and conventional activated sludge (CAS).

III. MATERIALS AND METHODS

IV. EXPERIMENTAL SET-UP

TABLE I
COMPARING BETWEEN ACTIVATED SLUDGE PROCESS AND MOVING BED BIOFILM REACTOR

no.	Conventional Activated sludge (CAS)	Moving bed biofim reactor (MBBR)
1	Area required is more.	Less Area Required Compared to any other Process.
2	Final result dependent on the biomass separation. MLSS to be maintained.	Final result less dependent on the biomass separation. No MLSS to be maintained (Self Controlling Biomass)
3	Very sensitive to shock loads and varying loads. Process gets easily disturbed and takes several days to re-stabilize.	Very high resilience to shock loads and varying loads. In the unlikely event of destabilization, the plant returns to normal in a matter of few hours
4	Activated Sludge Process capital cost is low	MBBR cost is low

The experiments of comparing were conducted between conventional activated sludge the technology that using in South Al-Rustamiyah WWTP and Moving bed biofilm reactor the pilot plant was built at South Al-Rustamiyah WWTP located on the banks of Diyala River south of Baghdad city. It is one of the oldest sewage treatment plant projects in the Iraq. The total capacity of the project (175,000 m^3/day) and distracts sewage into the Diyala River after treatment.

Components of South Al-Rustamiyah WWTP:

- Screen
- Main lift
- Grit chamber
- Pre-Aeration tanks
- Primary clarifier tank
- Aeration tanks
- Secondary clarifier tanks
- Chlorine Contact Tanks

V. THE PILOT PLANT (MBBR)

The pilot plant (MBBR) consists of, the type of pilot plant is Hybas.

- Screen (coarse & fine) the bar spacing in the coarse screen 10 mm, the perforation for fine screen ∅ 3mm.
- Tank divided to five parts in series, the first part MBBR-1(Anoxic) with anoxic mixer, the second MBBR-2 (Aerobic), the third part MBBR-3 (Aerobic), the fourth part Outlet chamber and the Flocculation part with dosing unit and flocculation mixer.
- Final clarifier with dia. 1.5m, high 2m, water volume 3.53m^3 with sludge recycle.
- Drum filter which polyester filter cloth 10µm opening, the separated solids are collected in a separate channel inside the drum and taken out.

Reactors in series can provide greater treatment capacity. The process consists of an anoxic tank followed by the aeration tank where nitrification occurs. Nitrate produced in the aeration tank is recycled back to the anoxic tank. Because the organic substrate in the influent wastewater provides the electron donor for oxidation reduction reactions using nitrate, the process is termed substrate denitrification. The inlet arrangement for influent raw wastewater will be given at the top of tank. To control discharge in and out pilot plant and dissolved oxygen there is a flowmeter for inflow, outflow and a device for dissolved oxygen control. A sketch of moving bed biofilm reactor is shown in Figure 1 and some key parameters are listed in Table II. Characteristics of the AnoxKaldnes K_5 plastic media are presented in Table III.

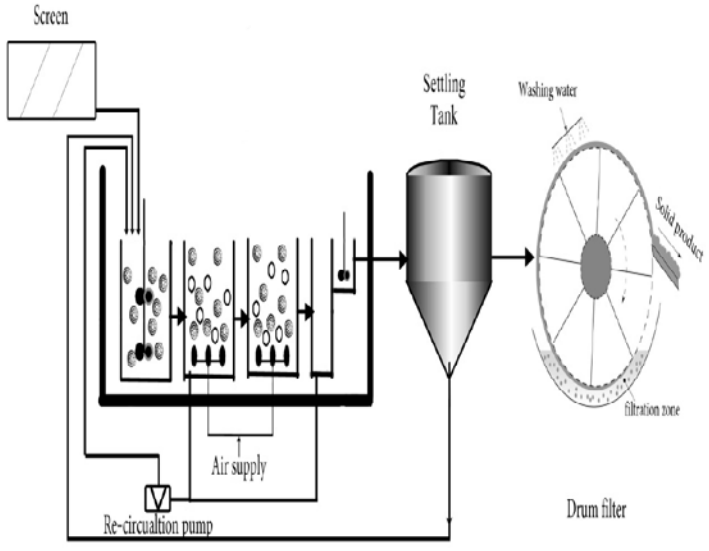

Fig. 1 Schematic diagram of MBBR system

TABLE II
TECHNICAL DATA FOR THE MOVING BED BIOFILM REACTOR

Parameter	Anoxic reactor	Aerobic reactor	Aerobic reactor	Outlet chamber	Flocculation
Volume m^3	4.5	2.25	3	1.5	0.18
Water volume m^3	4	2	2.5	1	0.1
Media volume m^3	2	1	1.5	-	-
Filling ratio with carriers%	50	50	50	-	-
Flow rate m^3/hr	1.5	1.5	1.5	1.5	1.5
Flow direction	Up-flow	Up-flow	Up-flow	Up-flow	Up-flow
HRT hr	3	1.5	2	1	0.12

TABLE III
CHARACTERISTICS OF ANOXKALDNES K_5 THE USED CARRIER

Type	AnoxKaldnes K5
Material	Polyethylene
Shape	Chips
Density	0.95 g cm^{-3}
Diameter	25 mm
Thickness	4 mm
Specific biofilm surface area m^2/m^3	800

VI. Sampling and analysis

Samples were collected from influent and effluent for the both system and analysed at the same time during April 2014 to July 2014. Temperature, dissolved oxygen and pH were measured in each reactor. Procedures followed for analysis have been in accordance with the Standard Methods for Examination of Water and Wastewater [6].

VII. RESULTS AND DISCUSSION

VIII. BIOCHEMICAL OXYGEN DEMAND (BOD5)

In Figure 2 the effluent concentrations of the BOD_5 for CAS and MBBR were in the ranges 7-34 mg/L, 5-64 mg/L respectively. Some values exceeded the standards when compared with the Iraqi National Standards set by the Regulation 3 at 2012. Due to the microorganisms growth on the carriers are still not achieved because the microorganisms need some days to grow and acclimate as shown in previous studies [7]. Aeration plays a vital role on the microbial growth and development, as well as its stability on the carriers and its movement throughout the reactor. Aeration supplies the microbial oxidation with oxygen and also enhances the turbulent intensity of fluid, which are important for the efficiency of wastewater treatment [8]. Therefore, it is important to provide suitable aeration rate for the stable operation of MBBR. At the period from 13th to 28th of May the pilot plant faced problem, high concentration level of oxygen because malfunction of automatic control that providing oxygen not work, which led to the buoyancy of the bacteria on the surface of the clarifier tank and that in turn effect on the removal efficiency and this was agreed with other previous studies Shrestha, (2013) [9].

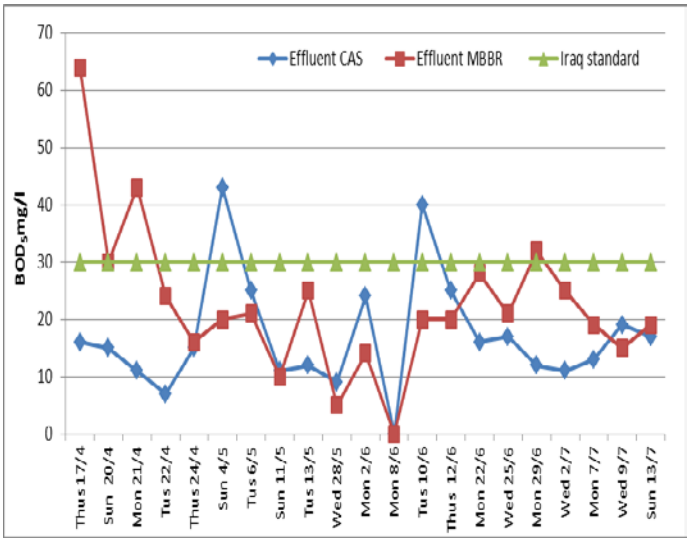

Fig.2 Effluent BOD_5 concentrations for both systems

In Figure, 3 it can be observed that the removal efficiency rate of BOD_5 in MBBR system was higher than that of CAS in 2nd phase due to the optimum operation and the enhancement in performance with time. This explains the microorganisms growth and multiply in the MBBR system. The average removal efficiency was 91% to MBBR and 86% for CAS. Similar results were obtained by [7] who pointed out in his study that at BOD_5 load of about 150-200 mg/L, filling ratio of plastic elements in MBBR reactor was 40%. The BOD_5 removal efficiencies were 78% and 90% for AS and MBBR respectively.

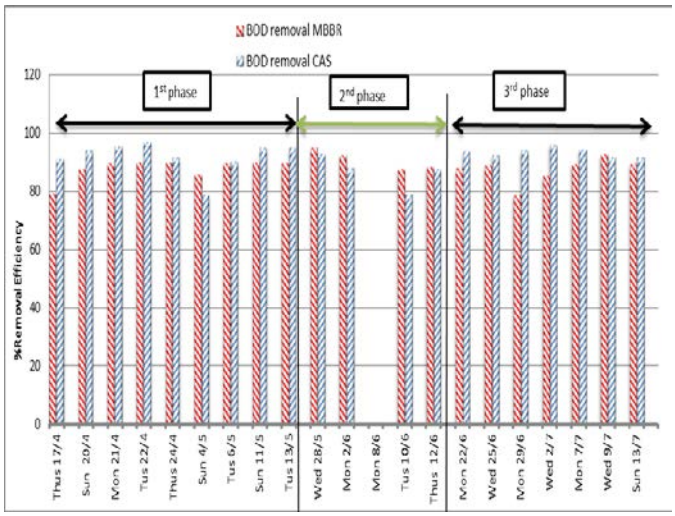

Fig. 3 BOD_5 removal efficiency % for both systems

IX. CHEMICAL OXYGEN DEMAND (COD)

Figure 4 present the variation with time of influent and effluent COD for CAS and MBBR process, respectively. The influent concentrations of COD were highly fluctuated and ranged between 357 to703 mg/L for CAS and 331 to 839 mg/L for MBBR. In spite of the high range of the inlet COD, characterized by a maximum concentration of 839 mg/L, the effluent COD concentrations were almost constant with an average value of approximately 47 mg/L for both systems as shown in Figure 4. It is important to highlight that the COD concentrations at the outlet are always under the Iraqi standard limit equal to 100 mg /L.

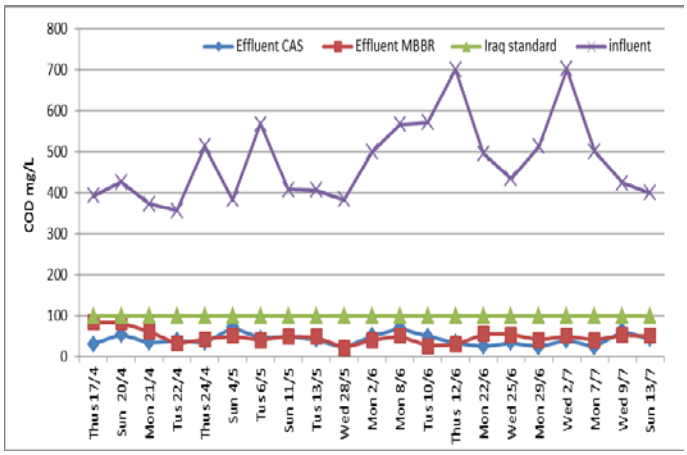

Fig. 4 Effluent COD concentrations for two systems

The behavior of both systems is also shown in terms of removal efficiency (Figure 5). In particular, both systems showed good removal efficiencies in each experimental phase. These results are committing with Di Trapani et al. (2010) [10], and Shrestha, (2013) [9] who reported that COD removal was not significantly affected by the different operating conditions. Except in the period ranging from the 17th - 21th of April, probably related to a sharp increase in the inlet COD concentration for MBBR because of the grit chamber was out of service at that time and the period 22th June to 9th July due to breakdown diver. The breakdown was affected on the growth of biomass on the carrier.

The average COD removal efficiencies for the CAS and the MBBR were very similar with average values 90.3% and 88.5% respectively in the overall experimental period. This result agrees with the findings of other work (Andreottola et al., 2000) [11] who reported that the average efficiencies for tot COD removal were 76 % for MBBR and 84 % for AS and the limited performance of the MBBR was not the specific biomass activity but the biomass concentration.

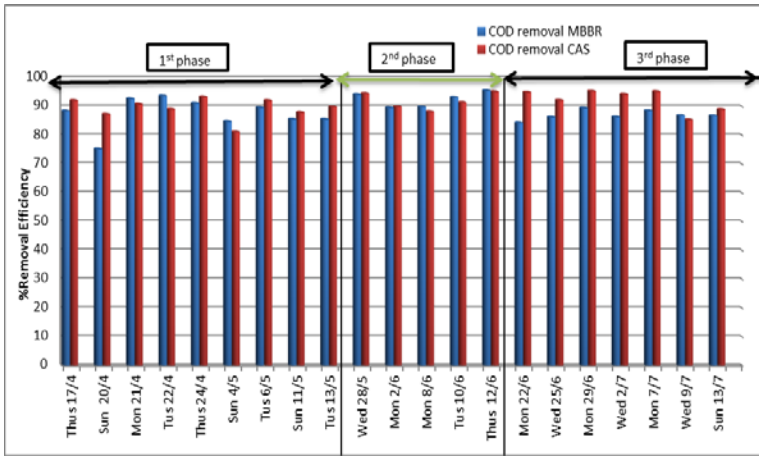

Fig.5 COD Removal Efficiency % for CAS and MBBR

X. CONCLUSION

- In terms of BOD5, particularly in the first and latter phases, the performances of the two systems were almost comparable, suggesting that the attached biomass in MBBR did not give an extra contribution to the removal process due to operation problem. On the other hand, in the second phase, the MBBR showed a better performance respect to the CAS reached to 95% and 88% to CAS removal efficiency.
- The performance of CAS and MBBR systems shows good removal of pollutants from wastewater according to measured parameters (COD) with average removal efficiency reached to 90.3% , 88.5% to CAS and MBBR systems, respectively.
- The different aeration rates influenced the biomass development on the carriers, its stability on the carriers and movement of the carriers throughout the reactor.
- At higher aeration rate the biomass on the carriers was easily washed off due to the stronger turbulence.
- It was concluded that (MBBR) can be an excellent alternative for upgrading and optimizing existing municipal wastewater treatment plants.

ACKNOWLEDGMENT

I wish to express my deep gratitude to my supervisors Prof. Dr. Mudhaffar S. Al-Zuhairy and Dr. Zainab Bahaa Mohammed for their valuable time, guidance and encouragement invaluable remarks and fruitful discussion throughout the preparation of my thesis.

REFERENCES

1- Qiqi, Y., Qiang, H. and Ibrahim, H.T.: Review on Moving Bed Biofilm Process. Pakistan Journal of Nutrition vol.11 (9), pp. 804-811. 2012.
2- Randall, C. W. and Sen, D.: Full-Scale Evaluation of an Integrated Fixed-Film Activated Sludge (IFAS) Process for Enhanced Nitrogen Removal. Water Science and Technology Journal, vol. 33 (12), pp. 155–162, 1996.
3- Borkar, R.P, Gulhane, M.L. and Kotangale, A.J.: Moving Bed Biofilm Reactor – A New Perspective in Wastewater Treatment. Journal of Environmental Science, Toxicology and Food Technology vol. 6 (6), pp. 15 – 21, 2013.
4- Metcalf, L. and Eddy, H.P.: Sewerage and Sewage Disposal. McGraw-Hill Book Company, Inc., New York and London 1930.
5- Metcalf, L. and Eddy, H.P.: Wastewater Engineering: Treatment and Reuse. 4th Edition McGrawHill 2004.
6- APHA, WWA & WEF,: Standard Methods for Examination of Water and Wastewater. 21st Edition, American Public Health Association, Washington, D.C., 2005.
7- Abdul-Majeed, A.M., Alwan, H.H., Baki, M.I., Abtan, F.R. and Sultan, H.I.: Wastewater Treatment in Baghdad City Using Moving Bed Biofilm Reactor (MBBR) Technology. Engineering and Technology Journal, vol.30 (9), pp.1550 – 1561, 2012.
8- Li, S.R., Cheng, W., Wang, M. and Chen, C.: The flow patterns of bubble plume in an MBBR. Journal of Hydrodynamics, Ser. B, vol. 23 (4), pp. 510-515, 2011.
9- Shrestha, A.: Specific Moving Bed Biofilm Reactor in Nutrient Removal from Municipal Wastewater. M.Sc. Thesis, University of Technology, Sydney, 2013.
10- Di Trapani, D., Mannina, G., Torregrossa, M. and Viviani, G.: Comparison between Hybrid Moving Bed Biofilm Reactor and Activated Sludge System: A Pilot Plant Experiment. Water Science and Technology, vol. 61(4), pp. 891 – 902, 2010.
11- Andreottola, G., Foladori, R., Ragazzi, M. and Tatàno, F.: Experimental Comparison between MBBR and Activated Sludge System for the Treatment of Municipal Wastewater. Water Science and Technology, vol. 41(4-5), pp. 375 – 382, 2000.

12-

The Efficiency of Electrocoagulation in the Treatment of Turbid Water

Prof. Dr. Riyad H. Al-Anbari ,and Prof. Dr. Jabbar H. Al Baidhani

Abstract: The main aim of the present study is to test the ability of electrocoagulation process in treating of turbid raw water. In this study, an electrolytic cells device was manufactured and used to perform the experimental work. Many sets of experiments have been conducted to find the efficiency of electrocoagulation process in treating of raw water. It was found the electrocoagulation is very effective in removing water turbidity up to 97% depending on the voltage rate.

In addition because of the large number of variables associated with the electrocoagulation process so the present study aimed to differ from previous studies by finding a dimensionless function to describe and to know the effect of each variable clearly on the electrocoagulation process.

Keywords: electrocoagulation, water, turbidity, current, voltage

Introduction:

The surface water from rivers often contains suspended particles of clay, silt, sand, various organic, and inorganic dissolved solids and other materials, which manifest themselves in turbidity, dissolved solids and other chemical parameters. The conventional treatment method consists of coagulation by the addition of metal salts to destabilize the colloidal particles followed by flocculation, sedimentation, filtration, and disinfection. This method of treatment has certain drawbacks like handling large quantities of chemicals, accuracy of dosing, feeding of chemicals and production of large volume of sludge casing environmental problem of alum disposal to receiving water bodies **Donald Mills (2000)**.

Many researchers have been focused on performance of electrocoagulation in water treatment. **Vik et al. (1984)** have studied the process of electrocoagulation, which was followed by filtration as a possible alternative technique to the conventional process. **Balmer and Fouilds (1986)** have indicated that electrocoagulation can be used successfully in decreasing of turbidity in oil emulsion.

They have found that the using of iron anode gives 100% oil removal efficiency with zero residual water turbidity. **Donini et al (1990)** referred that the produced sludge can be reduced by (50 -70) percent with water treatment by electrocoagulation**. Paul (1996)** had treated river water of various turbidities in an electrolytic cell. His results indicated that the electrocoagulation gives very good reduction of water turbidity from (400- 900) J.T.U to about 2 J.T.U. **Donald Mills (2000)** has interesting study on electrocoagulation process to treat raw water sources. He applied low voltage direct current (D.C) on the cells to produce iron hydroxide flocculent. He concluded that high removal percent of water turbidity could be achieved by using this process. **Vivian Robinson (2000)** showed that the water with turbidities in the range of 197 N.T.U and 400 N.T.U can be reduced by the process of electrocoagulation to less than 0.50 N.T.U. **Rahmani AR (2008)** investigated removal of turbidity from raw water using electrocoagulation under different voltage rates with three types of electrodes and he found that in 20 minutes the removal efficiency of turbidity was 93, 91,and 51 percent for Al, Fe, and St electrodes respectively**. Malakootian et al (2009)** studied the efficiency of electrocoagulation in removal of water hardness with aluminum sheet electrode and their results showed that the removal efficiency of water hardness reached to 95.6 % by electrocoagulation process. **Ümran et al (2009)** used electrocoagulation with iron electrode to remove fluoride from synthetic water. They have found that highest treatment efficiency was obtained for the largest current density. **Solak et al (2009)** used electrocoagulation process in removal of suspended solids and turbidity by using aluminum and iron electrodes which were run in serial and parallel connection systems. Their results showed that the removal efficiency of suspended solids was to be 99.86 to 99.86%.**S.Perez et al (2011)** studied the removal of water turbidity from three sources by electrocoagulation process with aluminum and iron electrodes .Based on their results it was possible to eliminate the turbidity of river water. **Mikko Vepsäläinen (2012)** used electrocoagulation to treat surface water that contained high concentration of natural organic matter. Also he investigated the effect of the main parameters, like current density, pH, etc. on the efficiency of electrocoagulation process. According to results of their study, Fe(II) can be effective in some special applications such as sulphide removal. **Sri et al (2012)** evaluated the effects of various operating parameters on turbidity removal using electrocoagulation. They found that the turbidity removal efficiency increased with increase in applied voltage from 50 % to 5 V to 99% to 25 V. **Soidat et al (2012)** studied the factors that affect the energy consumption and efficiency of electrocoagulation process used for removal of turbidity from petrochemical wastewater and they found that the maximum turbidity removal efficiency was 97.43%.**Ville et al. (2013)** have attempted to review studies that conducted mainly during 2008- 2011 which are concerning of electrocoagulation applications. They have found that the costs of electrocoagulation vary generally depending on the type of solution to be treated, but in general

*** Faculty Member/ University of Technology/ Building and Construction Eng. Dep. Baghdad/Iraq /Telephone No. 009647801214977/e-mail: riyadhassan2003@yahoo.com**
**** Faculty Member Babylon University/College of Eng. Babylon/Iraq/Telephone No.009647818374670/e-mail: jabbaralbaidhani@yahoo.com**

they found that the electrocoagulation has low water treatment cost typically around 0.1- 1.0€/m^3 and 0.4- 4.0 kWh/m^3.

Briefly stated the goals of the present study are to provide laboratory data by manufacturing equipment (electrolytic cells device) to provide necessary experimental information regarding the performance of electrocoagulation process and also to undertake theoretical analysis which leads to derive relationship concerned with the dimensions and arrangement of electrolytic cells required in operation of electrocoagulation process and these above goals have been completely differed from previous studies.

Theory of Electrocoagulation:

Electrocoagulation provides an alternative for the removal of pollutants from water, and wastewater. The process involves the application of a direct current to sacrificial electrodes, usually aluminum or iron plates and /or rods, inside a processing reactor **(Paul A.B.1996)**.

Chemical Reactions in Electrocoagulation Process:

The following aluminum electrode reactions occur in this process **(Robinson Vivian 2001**):

Anode: $Al^0 = Al^{3-} + 3e^-$ ---------- (1)

Cathode: $3H_2O + 3e^- = 3OH + 1.5\ H_2$ --- (2)

Additionally, the anode will be dissolving chemically in water

$Al^0 + 3H_2 + 3H_2O = Al(OH)_3 \downarrow + 1.5\ H_2$ ---- (3)

For an iron sacrificial electrode, the simplified electrode reactions are:

Anode:

$Fe \rightarrow Fe^{+2} + 2e^-$ ---------- (4)

$(4\ Fe^{+2} + O_2 + 2H_2O \rightarrow 4Fe^{+3} + 4OH^-$-------- (5)

$Fe^{+3} + 3OH^- \rightarrow Fe(OH)_3 \downarrow$ ---------- (6)

Cathode:

$2H_2O + 2e^- \rightarrow 2OH^- + H_2$ ---------- (7)

In electrocoagulation process, an electric current is incorporated to neutralize, valence, and particulate charges thereby allowing contaminants such as colloidal particulates, oils, and dissolved metals to be precipitated and removed from stable suspensions and emulsions. The cathode reaction is very important for two reasons: it provides gas micro-bubbles, which assist flotation of the oily flocs so forming a surface scum, which can be skimmed off; and hydroxide ions are produced which help to maintain the local pH conditions sufficiently alkaline to enable the formation of ferric hydroxide flocs. The nature of (Fe^{+3}) in water is complex, due to a series of aquo – complexes as a function of pH: $Fe(H_2O)_6^{3+}$, $Fe(H_2O)_5\ (OH)^{2+}$, $Fe(H_2O)_4(OH)^{2+}$, $Fe(H_2O)_3$, $Fe(H_2O)_2\ (OH)^-_4$ etc. **(Malik, et al 1983)**.

Clearly, for effective flocs formation one must operate in the region of insolubility of $Fe(OH)_3$. This is even more complicated in practice as the composition of the species in a ferric salt solution also depends on the concentration, temperature, mode of operation, age and type of anions present. The reactions at the anode generating aluminum/iron ions as a coagulating agent as well as gas bubbles. The well-known properties of the aluminum / iron ions as a coagulating agent cause them to combine with the pollutants **(Malik, et al 1983)**

Dimensional Analysis:

A dimensional analysis of the problem will provide a general evaluation in the form of dimensionless terms, which assist in studying the performance of electrocoagulation process in treating water with various levels of initial turbidity, and flow conditions. The following variables should be considered:

$$F_8(Da,d,S,l_a,R,T_i,W,H_1,H_2,V_0,I,\eta_{AP},v,a,F,n_1,n_2,Q,t_0,t_t,T_0,t_1,t,t_2,K,\rho,\mu,g,pH) \quad (8)$$

Where:

Da= anode diameter (L), d= distance between the electrodes(L), S= spacing between the electrolytic cells(L), l_a= the active length of anode and cathode(L), also it approximately represents the device width, R= the device hydraulic radius= A_d/P_d, where A_d and P_d are device area, and parameter respectively (L), T_i= the device thickness , hence T_i is approximately = D_c where D_c= cathode diameter (L),W= width of device (L),H_i= length of upper part (L),H_2= length of lower part(L),V_0= volume of electrolytic cell device (L^3),i= the acting current (amp), η_{AP}= applied over potential in volts, v= valency of anode (Ex. Fe^{2+}), a= atomic weight of iron(56),F =Faraday constant (96500 C ; C= Coulombs),n_1= number of cell,n_2= number of cathode holes, Q = turbid and /or polluted flow rate through the electrolytic cells device (L^3T^{-1}), t_0 =hydraulic detention time (V_0/Q), t_t= charging time or (electrolysis time),(T),T_0= initial turbidity of water (NTU) ,T=residual turbidity of water (NTU),G= velocity gradient for flocculation process (T^{-1}), t_1, t, t_2= rapid, slow, and settling times respectively (T) ,K= conductivity of raw water to be

treated (μs/cm), ρ= mass density of water (M/L^3), μ=water viscosity (M/L.T), g= acceleration due to gravity (L/T^2), and pH=free hydrogen ion concentration in water to be treated.

It worth to say that the researchers could not find previous works which are related to the above aforementioned variables which are definitely different in their units (geometrical, time, mass) units as well as physical- chemical and electrical units. However to simply the problem, one can separate the variables which have not units similar to that of repeating variables units namely (mass, length, and time) in an independent groups with the addition of Da, d, and t_1 as a complementary parameters to perform a dimensional analysis for such group. On the other hand, the other parameters can be collected in another group that permits dimensional analysis easily.

Eq. (8) can be now split in two groups of variables. The first group is:

$$\mathbf{F9\ (i, \eta_{AB}, v, a, F, n_1, n_2, T0, T, K, pH, Da, d, t_1)} \text{ ---------- (9)}$$

The expected dimensionless terms for the parameters of this group are:

$$\mathbf{F_{10}\ (i / \eta_{AP}, d/A, K, it_1/F, n_1/n_2, T/T_0, pH)} \text{ ---------- (10)}$$

Eq. (10) could be written in new symbols in the following form:

$$\mathbf{F_{11}\ (\eta_{IR} / \eta_{AP}, it/F, n_1/n_2, T/T_0, pH)} \text{ ---------- (11)}$$

The term T/T_0 could be called the remaining turbidity ratio of water treated by coagulation.

The parameters of the second group are:

$$\mathbf{F_{12}\ (S, l, R, T_i, W, H_1, H_2, V0, Q, t_0, t_t, G, t_1, t, t_2, \rho, \mu, g)} \text{ ---------- (12)}$$

To make dimensional analysis of the second group parameters, Pi-Theorem is used .With the selection of R,t_0, and ρ as repeating variables, the problem reduces to:

$$\mathbf{F_{13}\ (S / R, l / R, T_i / R, W / R, H_1 / R, H_2 / R, V_0 / R.W.T_i, V_0 / Qt_1, t_1/t_2, G.t_0, t_1/t_0, t/t_0, t_2/t_0, \rho.V_0/\mu.t_0.W.T_i, 1/g.R(V_0/t_0.1/W.T_i)^2)} \text{ ---------- (13)}$$

With combination of aforementioned two groups of variables and with delimitation of some dimensionless parameters and after simplification the derived equation may be restated as:

$$\mathbf{F_{14}\ (\eta_{IR} / \eta_{AB}, i\ t_t /F, T/T_0, pH, t_t/t_0, t_1/t_0, t_2/t_0, R_e, F_r)} \text{ ---------- (14)}$$

It is worth to note that the dimensional analysis with experimental work helped in finding a dimensionless equation which has described the remaining turbidity in terms of other pertinent parameters of electrocoagulation process.

Equipment and Procedure:

The experiments used are the electrical device, flow meter, pH meter, conductivity meter, flocs tester (Jar testing device), turbidity-meter.

Design consideration for Electrolytic cells:

The device and its electrolytic cells are shown in Plate (1) . The device consists of a ladder series of electrolytic cells containing (carbon steel) anodes and stainless – steel cathodes. Application of low –voltage direct current (D.C) to the cells produce iron hydroxide flocculent. Water flows through the ladder of cells by ways of a labyrinth of holes in the cathode in order to assure turbulence inside the device. Each electrolytic cell contains an iron anode of (18 mm) in diameter, and the anodes used in this study are of low carbon steel (LCS) composition as mentioned by **Donald Mills (2000).**

The electrolytic cell device as shown in Plate (1) is constructed to achieve a narrow gap of about 2mm as studied by **Donald Mills (2000)** between the central anode and the surrounding cathode. D.C voltage up to (14 Volts) is maintained between anode and cathode as the water to be treated flows through the labyrinth of cells. The electric field produced in the annular space between anode and cathode by the D.C voltage ranges between (3000 and 6000) V/m.

The experiments were done in a laboratory pilot plant as shown in Fig. (1). the plant consists of two storage tanks, pump, flow meter and stainless – steel electrical device with its power supply. The two storage tanks are connected to the bottom of the device via a section of (20 mm) galvanized steel pipe, which represent the device water supply pipe. The supply pipe section contains a gate valve of (20 mm) in order to control the water flow through the cell. Each storage tank has a dimension of (0.5x0.5x0.5) m.

During runs, a fraction of the inlet water is returned to the top of tanks by pumping it through a (12.7 mm galvanized steel pipe to assure water mixing along the tanks height to assist in regulating flow which passes through the device cells. Centrifugal pump with characteristics of (0.60-2.4) m^3/hr capacity, (2850 rpm), axial flow unit with a single-phase motor

of (2.5) hp, and a head of (9.0 m) to (32m) is to supply the water to be treated through the electrocoagulation apparatus. The inlet flow rates used were in the range of (0.029 to 1.90) m^3/hr and the returned flow fraction was adjusted to obtain the desired inlet flows. Under these conditions, the average electrolysis times of the process water in the device approximately ranged between (0.10 and 9.35) min. Under these conditions, the average electrolysis times of the process water in the device approximately ranged between (0.10 and 9.35) min.

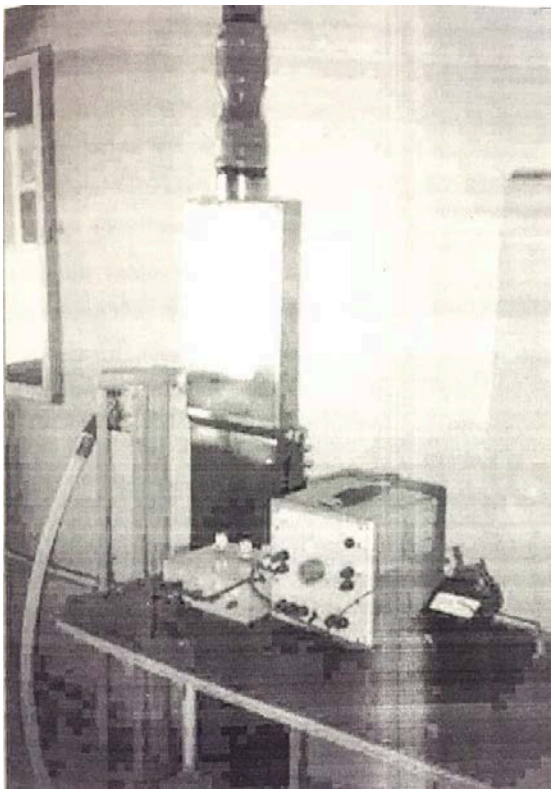

Plate (1): The Electric Cells Device Used

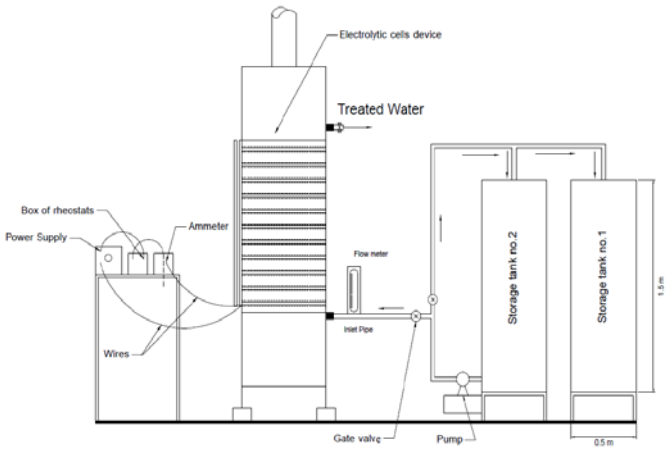

Fig. (1): The Arrangement of Pilot Plant Units

The power supply:

One of the main part of the pilot plant used is the power supply, a variable – regulated power supply (4-40) V was used to provide electric current to the cells of electrocoagulation device. A resistance box that had three rheostats of 5,100 and 200 ohms respectively was used to regulate the current density.

Experimental Work:

The following sub-sections give a description of the techniques used in this study.

Experiments of natural Stream Water Turbidity:

Since the research objective is to evaluate the electrocoagulation process with various natural turbidity levels, the first set of experiments is done with the process of electrocoagulation with turbidity of Euphrates river water at the study region. Turbidity values were used in a range of (2.5 to 22.5) N.T.U.

Jar Testing:

Since the major goal of the present study is to test the ability of electrical cells in generation of ferrous ions as an effective coagulant to remove turbidity, and then to show this fact of electrically coagulation generation via the device used, Jar testing is used.

Experimental Studies:

In order to provide the main aim of the present study, the experimental works are divided into two main studies:

Study No.1 (Natural Water Turbidities)

One of the major objectives of this study is to present a new continuous flow electrocoagulation process capable of producing domestic water with relatively low turbidity. It was firstly started with experiments, which used natural river turbidities a wide range of levels, which ranged from 2.5 N.T.U to 22.5 N.T.U .

Study No.2 (Synthetic Water Turbidities)

One part of this study is to get the efficiency of electrocoagulation process in treating of water with high levels of synthetic turbidities with the same pilot plant units.in this study, particular concentrations of the river clay suspension were used to produce synthetically turbid water in the range of (25 -90) N.T.U. This range of turbidity is prepared by mixing kaolinite clay with tap water. A required weight of kaolinite to prepare a specific turbidity is soaking in 1 liter of tap water for

24 hours and then diluted in the feed tank. Then it was obtained a relationship between turbidity and weight of kaolinite clay.

Results and Discussion:

In the design of electrolytic cells device, which was arranged to study the efficiency of electrocoagulation process in the treatment of water. The use of electrolytic cells device has been found to be effective in treating water .The effectiveness of electrocoagulation process however is presented through the results of the experimental study with the effects of currents, electrolysis time, rapid mixing, slow mixing, and settling times verses the reduction of turbidity.

Presentation of Results:

It was decided to adopt the reaming turbidity ratio as a dimensionless parameter used as a criterion in assessing the hydraulic and environmental performances of coagulation process in water treatment with electrolytic cells device.

Figs. (2); and Figs. (3) Present the variation of the remaining turbidity ratio (T/T_0) with the variation of (m/ρ) values. The values of (T/T_0) tend to decrease as (m/ρ) values increase. The analysis of results in these figures shows the rate of decrease in the remaining turbidity ratio is appreciable for the range of current from (1to3) amperes when detention time is increased from(2.8 to 7.42) min. Above this range of currents the rate of decrease in the remaining turbidity ratio seems to be insignificant. The values of (T/T_0) are equal to 0.025 and 0.085 could be reached with (m/ρ) values of $9.40x10^{-5}$, and $2.85x10^{-5}$ respectively. In other words the removal efficiency of water turbidity is ranged between (91.5 to 97.5) % by using electrocoagulation process.

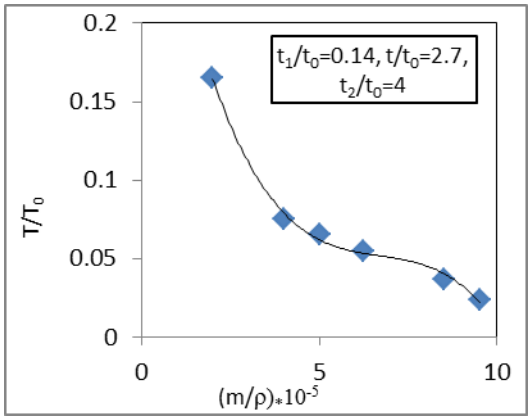

Fig. (2): Variation of Residual Turbidity Ratio with Iron Dosage Ratio (t_0=7.42 min., T_0=20.5 N.T.U)

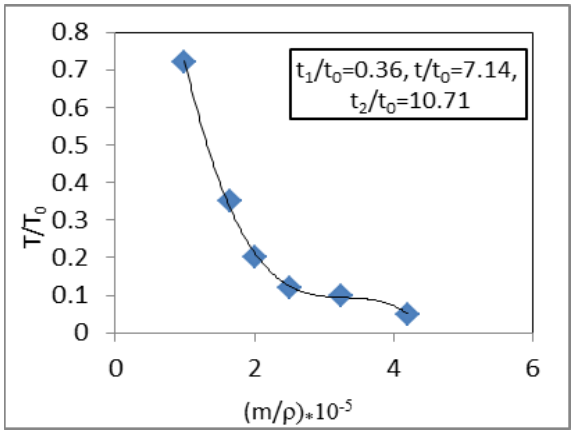

Fig. (3): Variation of Residual Turbidity Ratio with Iron Dosage Ratio (t_0=2.80 min., T_0=20.5 N.T.U)

Fig.(4) illustrates the effect of rapid mixing time ratio (t_1 /t_0) for constant values of detention time (t_0), initial turbidity (T_0), slow mixing time (equal to 20 min),and settling time (equal to 30 min). This figure reveals that a value of 0.65 as a remaining turbidity ratio (T/T_0) could be obtained when rapid mixing time is increased from (1 to 2) with (m/ρ) value of $0.58x10^{-5}$.

Examining the results of Fig. (5) Indicates that a value of (T/T_0) of 0.8 could be decreased to a value of 0.45 when the value of slow mixing time is increased from (20 to 30) min. In addition, the value of T/T_0 equal to (0.063) or (93.7 % removal efficiency) could be obtained with a value of (m/ρ) of ($2.9x10^{-5}$).

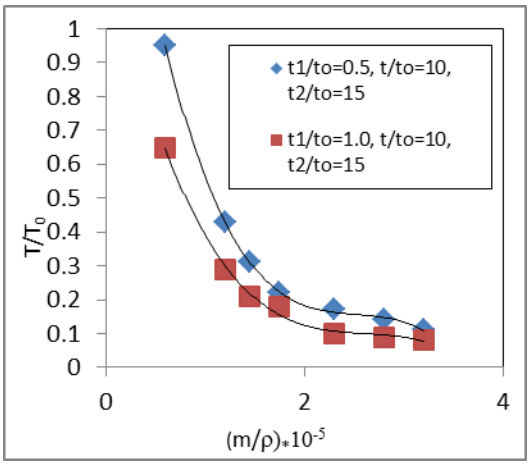

Fig. (4): Effect of Rapid Mixing Time Ratio on Residual Turbidity Ratio (t_0=2.00 min., T_0=8.50 N.T.U)

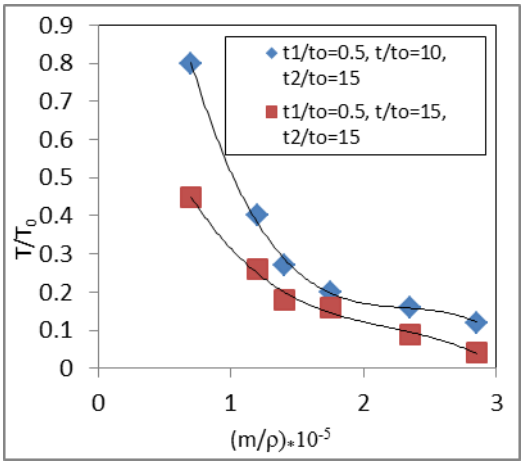

Fig. (5): Effect of Rapid Mixing Time Ratio on Residual Turbidity Ratio (t_0=2.00 min., T_0=10 N.T.U)

Fig.(6) shows under wide range of slow mixing time values with a constant values of 1 min., and 30 min, for rapid mixing time, and settling time respectively. This figure shows the effects of electrocoagulation process in decreasing of the remaining turbidity with the increasing of slow mixing time. The figure is presented to assert the efficiency of electrocoagulation in reduction of water turbidity due to increasing of flocculation time. The effects of increasing in flocculation time assists in in increasing of flocs production, which leads to more efficient settling.

Fig. (7) Shows the variation of (T/T_0) with the increasing of slow mixing time under a detention time of (2.07) min and this time was controlled by dividing the volume of electrolytic cells device by the flow of water to be treated . The figure indicates that the (T/T_0) values decrease with both increasing of slow mixing time, and detention time. The effects of increasing of detention time is significant for low range of

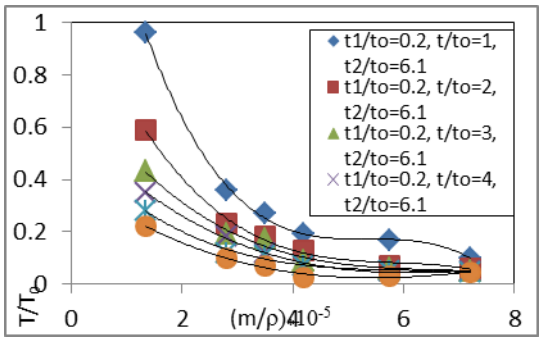

Fig. (6): Effect of Slow Mixing Time Ration on Residual Turbidity Ratio (t_0=4.90 min., T_0=13.50 N.T.U)

current from (1 to 3) amperes. Then the rate of decreasing in turbidity becomes low. In this figure, the slow mixing time is 1 min. and settling time is 30 min.

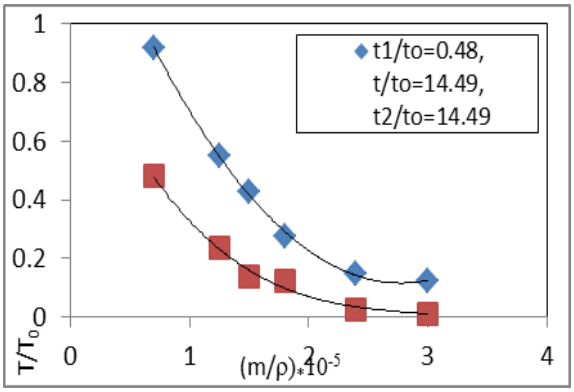

Fig. (7): Effect of Slow Mixing Time Ration on Residual Turbidity Ratio (t_0=2.07 min., T_0=16 N.T.U)

It is worthy to say here that the researchers could not find previous works which are related to the same above aforementioned variables which are early presented in dimensional analysis technique so it was difficult to compare with other results in the literature .But in general the obtained results of present study are in a good agreement with previous studies of the range of turbidity removal. Also the present study and other previous studies are confirmed that the electrocoagulation process can be considered as an effective alternative technique in water treatment.

Conclusions:

1- The relation describes the efficiency of electrocoagulation based on process of dimensional analysis is:

$$T/T_0 = 0.073 + e^{(0.60 - 0.69\ m/\rho - 3.04\ \eta_{IR}/\eta_{AP} - 0.02\ t_1/t_0)}$$

The above relation was developed by using the experimental data of studies No. 1 and No. 2, and then the nonlinear regression of Statistica program was used to find the required relation.

2- The removal efficiency of turbidity with electrocoagulation process is increased with increasing of iron dosage (m) under different inlet flow conditions. In general the removal efficiency of turbidity by using electrocoagulation process was ranged between (91.5 to 97.5%) depended on values of the operating parameters used.

3- The rate of production of ferric ions is controlled by the rate of electric current. This can be conveniently adjusted to match the required ion dosage in relation to turbidity removal ratio.

4- For certain current the increase in electrolysis time or (detention time) increases the efficiency of turbidity removal ratio as shown in the presented figures. For low range of electric current in the order of (1-3) amperes the

effects of increasing in electrolysis time is significant. Above this rang these effects seem to be no appreciable.

5- The recommended operating current required for the electrocoagulation process to reduce water turbidity was in the range of (2-3) amp .For the range of current from 1 to 3 amp, the range of decrease in remaining turbidity ratio is high.

References:

1. Donald Mills : A New Process For Electrocoagulation. Journal of AWWA, Vol. 92, issue 6, USA, 2000.

2- Donini, J. C. et al.: Electrocoagulation- Some Basic and Operating Characteristics" , Proc. 11th Intl. Coal Preparation Congress, Tokyo, 1990.
3- L. M. Balmer and A.W. Foulds: Separating Oil from Oil- in- Water Emulsions by Electroflocculation/Electrocoagulation. Journal of Filtration and Separation , Vol. 23, No. 6, 1986.

4- Mikko Vepsäläinen: Electrocoagulation in the treatment of industrial waters and wastewater. Ph.D. Thesis, Mikkeli , Finland, 2012.

5-M. Malakootian, N. Yosefi: The Efficiency of Electrocoagulation Using Aluminum Electrodes in Removal of Hardness from Water. Iran J. Environ. Health. Sci. Eng. ,Vol. 6, No. 2, pp 131 - 136 ,Iran 2009.

6-Malik P.,Matov B.,Nagits V.: Continuous Apparatus for Purification of Grape Juice by Electrocoagulation. Sadovostvoi Vinodelie Moldavii (1):39-10, 1984.

7- Paul A. B.: Electrolytic Treatment of Turbid Water in Package Plant .In 22 and WEDC Conference, New Delhi, 1996.

8-Rahmani AR: Removal of Water Turbidity by Electrocoagulation Method. J Res Health Sci, Vol.8, No. 1, pp. 18-24, Iran, 2008.

9- Rabinson Vivian: A New Technique for the Treatment of Wastewater.Enviro 2000- Ozwater Ozwaste Conference, Darling Harbour, Sydney, 2000.

10-Soidat Olanipekun Giwa, Suna Ertunc, Mustafa Alphaz, and Hale Hapoglu: Electrocoagulation Treatment of Turbid Petrochemical Wastewater. International Journal of Advances in Science and Technology, Vol. 5, No. 5, Turky, 2012.

11-Solak M., Kilic M., Huseyin Y., Sencan A.: Removal of Suspended Solids and Turbidity from Marble Processing Wastewater by Electrocoagulation: Comparison of Electrode Materials and Electrode Connection Systems. J Hazard Mater.Vol. 172, No. 1,Epub, 2009.

12-S. Perez, J,B. Morales, R.M. Felix, and O.M. Hernand: Evaluation of the Electro-Coagulation Process for the Removal of Turbidity of River Water, Wastewater and Pond Water. Rev. Mex. Ing. Quim, Vol. 10, No. 1, Maxico abr. 2011.

13-Sri M. A., Sudha Goel:Optimizing :Electrocoagulation of Drinking Water for Turbidity Removal in a Bach Reactor. 2012 international conference on environmental science and technology IPCBEE, Vol. 30, Singapore 2012.

14-Ville Kuokkanen, Toivo Kuokkanen, Jaakko Rämö, Ulla lassi: Recent Applications of Electrocoagulation in Treatment of Water and Wastewater – A Review. Green and Sustainable Chemistry,3, 89-121,2013.

15-Vik, E. A. et al.: Electrocoagulation of Potable Water. Water Res. , 18:1355, 1984.

16-Ümrann Tezcan Ün, A. Savas Koparal, and Ülker Bakir Öğüteveren: Electrocoagulatin Process for the Treatment of Drinking Water. Thirteen International Water Technology Conference, IWTC, 13, Hurghada, Egypt, 2009.

DETERIORATION OF WATER QUANTITY AND QUALITY IN IRAQ DUE TO STORAGE

Ala Hassan Nama
College of Engineering - University of Baghdad
alhasnam@hotmail.com

***Abstract*—Iraq is currently facing a serious water shortage problem. This problem is expected to be more severe in the future where the supply is predicted to be decreased up to about 50% of the currently estimated demand.**

Construction of dams to store water have a big benefits but the process of water storage has negative effects in the quantity and quality of the store water, where the most effective factor is the evaporation which leads to lose considerable amount of water every year that may affect and deteriorate the water quality via increasing the concentration of the pollutants and increasing the salinity of water.

This research aims to examine the effect of storage level on the volume of water losses and water quality in the reservoirs, lakes and marshes in Iraq at different storage conditions.

The mass conservation low was applied to determine the water and salt budget considering the geometrical properties and hydrological conditions of each reservoir, lake or marsh.

The results show that the volume of water loss due to evaporation is about 7%, 18% and 26% of the volume of the stored water at the condition of minimum, average and maximum storage level, respectively. According to these conditions the TDS concentration of the stored water was increased to about 11%, 20% and 34%, respectively. Therefore, it is important to get maximum benefit of all the available water during the period of high flow

It is very important to try to consistency with the nature and stimulate the activities that depend on the exploitation of water resources during the periods of high flow and development of the sectors that do not depend on the exploitation of large amounts of water during the periods of high evaporation and low flow.

The effects of storage water on the rivers morphology and the impact of storage plan on the deterioration of water qualities and its impact on the salinization of arable lands and deterioration of water consuming sectors should be studied.

***Key Words*—**Reservoirs, evaporation losses, salinity, water deterioration.

I. INTRODUCTION

The Water scarcity in Iraq becomes a big problem due to many reasons, namely that Iraq had built many dams on the Euphrates and Tigris tributaries. However, the water shortage forms a real problem in some parts of Iraq as a large part of the country is desert. But the existing water conveyance networks have also suffered from lack of maintenance or by being destroyed during the war. According to the International Federation of Red Cross and Red Crescent Societies [1], only 32 percent of the Iraqi population has access to clean drinking water, and only 19 percent has access to a good sewage system, and the proportion of rainfall in Kurdistan 600-1200 millimeters per year in the rest of Iraq is less than 200 millimeters per year, lack of rainfall in Kurdistan mountains which led to lack of water that feed groundwater and springs and artesian wells. Iraq consumes 90% of its water in agriculture.

Water resources in Iraq has made a tremendous wealth of Iraq and one of the richest countries in the world in this vital area which is sponsor of the refreshment of the country and achieve high levels of prosperity. In Iraq, it is not confined to these two great wealth rivers (Tigris and Euphrates) and their tributaries, but the large number of lakes and marshes scattered in various rivers. There are six main reservoirs and lakes located on these two rivers and on their tributaries. Whereas, the main Marshes (ALHammar, ALHuwizah and ALQurna) located in southern part of Iraq

The climate of Iraq is very hot at summer where the temperature ranging from (45-50 ^{0}C) and that's leads to evaporate a large amount of water which consequently effecting the quality of water causing increase of water salinity.

The objective of this research is to compute the amount of water loss due to evaporation from Iraqi reservoir, lakes and marshes and to determine its effect on the water quality.

The mathematical and analytical methodologies can be adopted for currying out this study based on the following steps; reviewing the related literatures and previous studies, collecting the geometric, hydrological, metrological, water quality data and design and operation data (for the reservoir and marshes), obtaining the area and storage-elevation curves of the considered reservoirs, computing the monthly evaporation losses from the considered reservoirs according to different storage conditions, computing the change in water quality of the considered reservoirs according to different storage conditions, analyzing and discussing the results and extracting the main conclusions and presenting the necessary recommendations.

II. Materials and Methods

A. *Area of Study*

Six reservoirs (Al-Mosul, Dokan, Al-udhaim, Darbandikan, Hemrin and Haditha), two lakes (Tharthar and Habbaniah) and three marshes (Al Qurna, Al Hammar and Al Huwizah) were taken in consideration which represent the main water bodies in Iraq.

The geometrical characteristics of the considered reservoirs, lake and marshes can be summarized in Table I and the area and storage-elevation curves are as shown in Fig.s 1 to 11, [2].

Table I. Geometrical characteristics of the examined water bodies [2].

Water body	Location		Maximum water level (m.a.m.s.l)	Normal water level (m.a.m.s.l)	Minimum water level (m.a.m.s.l)
	Easting	Northing			
Al-Mosul dam	36.63^0	42.82^0	338	330	300
Dokan dam	35.95^0	44.95^0	515	511	469
Al-udhaim dam	34.57^0	44.52^0	143	131	118
Darbandikan dam	35.11^0	45.70^0	493	485	434
Hemrin dam	34.11^0	44.97^0	107	104	92
Haditha dam	34.21^0	42.36^0	150	147	112
Tharthar Lake	34.18^0	23.54^0	65	48	40
Habbaniah Lake	34.27^0	23.18^0	51	48	43
Al Qurna Marsh	47.13^0	31.21^0	6	0	0
Al Hammar Marsh	46.49^0	30.50^0	5	3	0
Al Huwizah Marsh	47.41^0	31.29^0	7	4	1

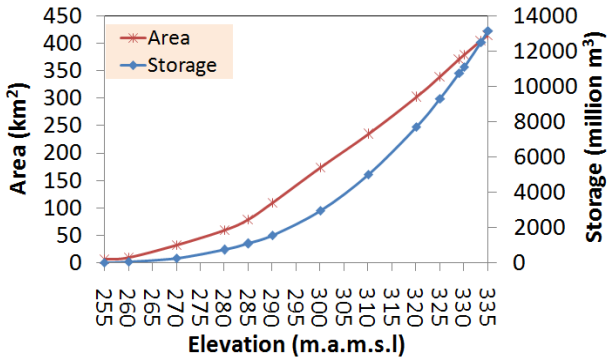

Fig. 1. Area and storage - elevation curve of Al-Mosul Dam, [2].

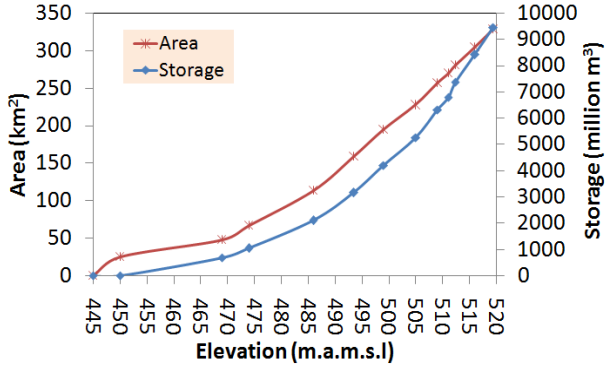

Fig. 2. Area and storage - elevation curve of Dokan Dam, [2].

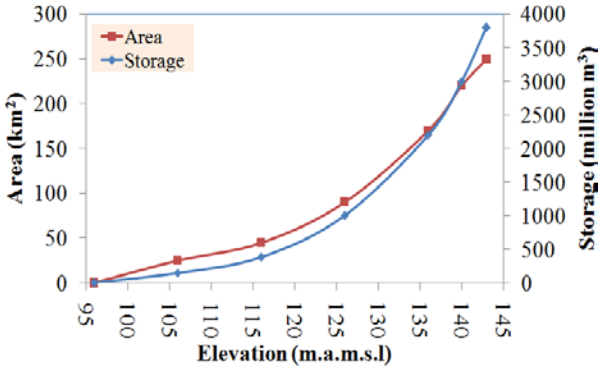

Fig. 3. Area and storage - elevation curve of Al-udhaim Dam, [2].

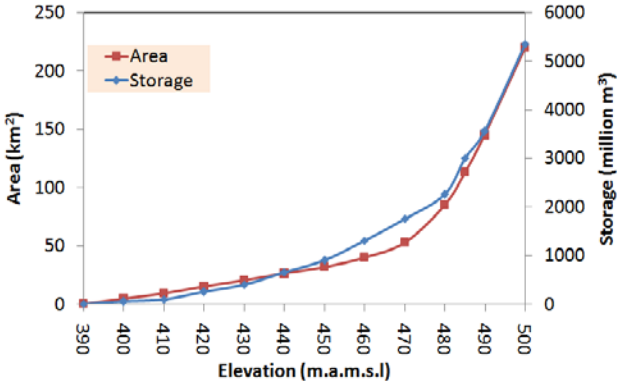

Fig. 4. Area and storage - elevation curve of Darbandikan Dam, [2].

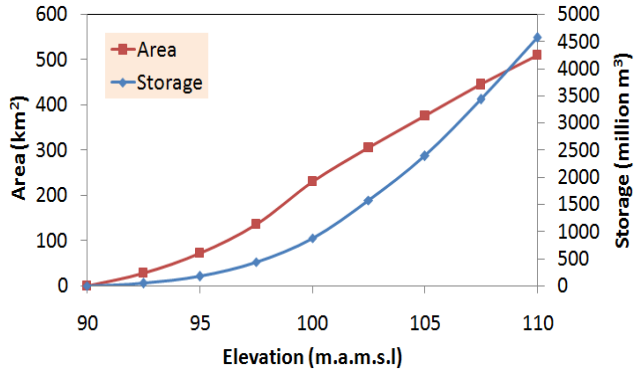

Fig. 5. Area and storage - elevation curve of Hemrin Dam, [2].

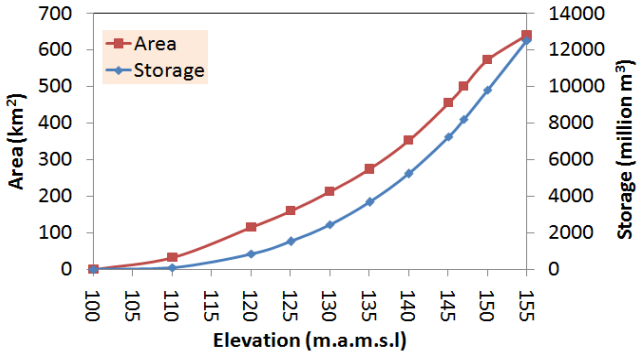

Fig. 6. Area and storage - elevation curve of Haditha Dam, [2].

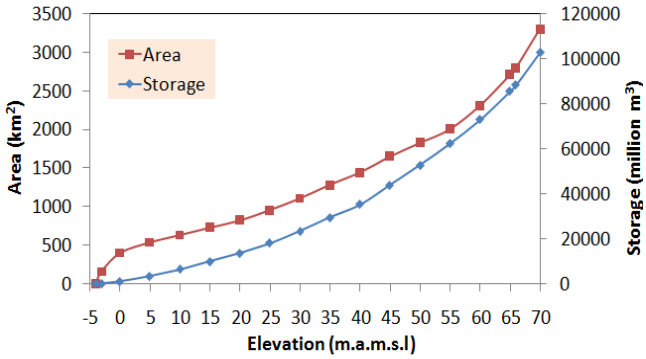

Fig. 7. Area and storage - elevation curve of Tharthar Lake, [2].

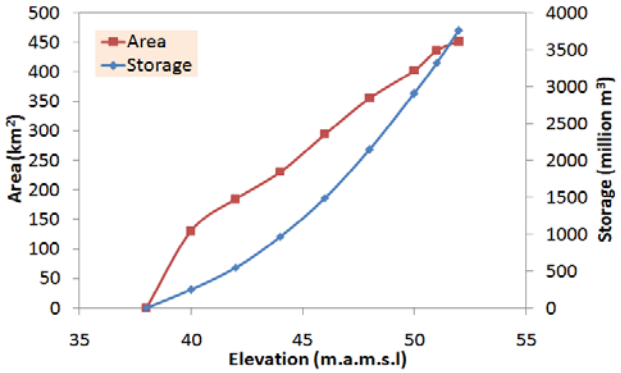

Fig. 8. Area and storage - elevation curve of Habbaniah Lake, [2].

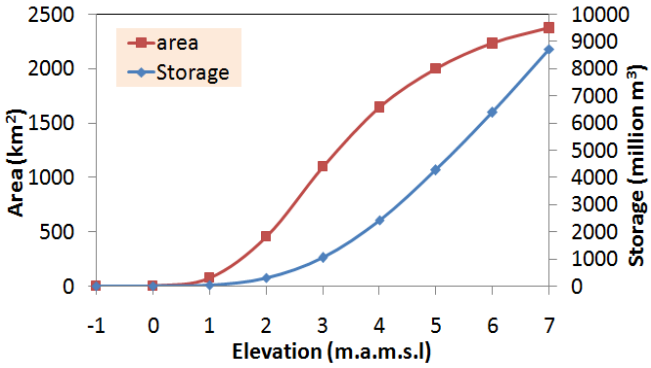

Fig. 9. Area and storage - elevation curve of Al Qurna Marsh, [2].

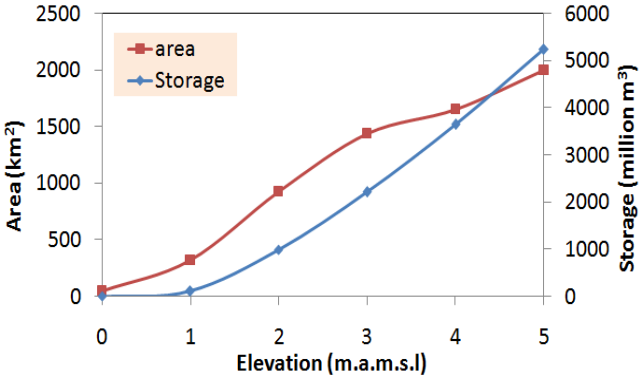

Fig. 10. Area and storage - elevation curve of Al Hammar Marsh, [2].

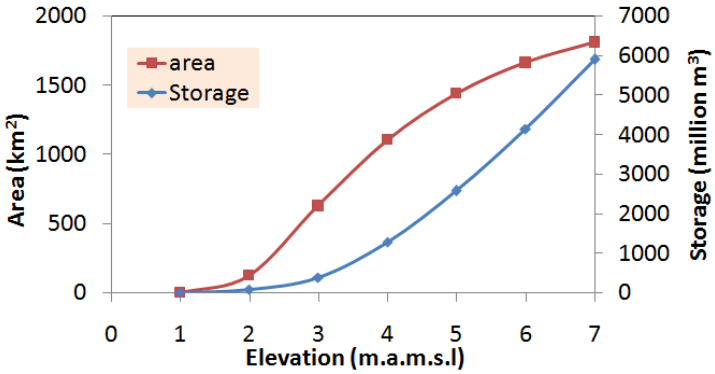

Fig. 11. Area and storage - elevation curve of Al Huwizah Marsh, [2].

The monthly evaporation data of the considered reservoirs, lake and marshes is as listed in Table II. [5].

Total dissolved solid (TDS) data were adopted as a salinity indicator to evaluate the deterioration. The recorded mean monthly concentrations of the TDS for the considered reservoirs, lakes and marshes are as listed in Table III, [4].

Table II. Monthly evaporation rate of the examined water bodies [4]

Water body	Evaporation rate (mm)											
	Month											
	1	2	3	4	5	6	7	8	9	10	11	12
Al-Mosul dam	300	500	900	1400	2500	3500	4000	3600	2600	1500	700	300
Dokan dam	400	600	900	1400	2400	3500	4100	3700	2500	1600	700	400
Al-udhaim dam	300	500	900	1400	2500	3500	4000	3600	2600	1500	700	300
Darbandikan dam	400	600	900	1400	2400	3500	4100	3700	2500	1600	700	400
Hemrin dam	670	960	1580	2180	3550	4480	4870	4320	3340	2300	1090	700
Haditha dam	670	960	1580	2180	3550	4480	4870	4320	3340	2300	1090	700
Tharthar Lake	856	1200	1800	2300	3100	3900	4800	4300	3200	2400	1500	1000
Habbaniah Lake	856	1157	1810	2335	3149	3852	4779	4310	3206	2371	1470	978
Al Qurna Marsh	480	700	1300	2000	3100	4700	4800	4300	3300	2200	1100	600
Al Hammar Marsh	520	800	1400	2100	3300	4700	4600	4100	3400	2500	1200	700
Al Huwizah Marsh	540	800	1300	2000	2800	3800	4200	3900	2800	1700	1000	600

Table III. Mean monthly TDS rate (ppm) for the examined water bodies [3].

Water body	Mean monthly TDS (ppm)											
	Month											
	1	2	3	4	5	6	7	8	9	10	11	12
Al-Mosul dam	247	249	247	247	226	210	212	201	204	220	232	240
Dokan dam	187	178	223	199	190	179	147	141	163	150	203	200
Al-udhaim dam	400	413	415	375	380	370	372	363	344	354	369	394
Darbandikan dam	264	265	255	245	200	189	202	212	224	258	230	236
Hemrin dam	400	413	415	375	380	370	372	363	344	354	369	394
Haditha dam	615	571	597	573	574	547	605	638	627	643	638	645
Tharthar Lake	1440	1490	1504	1457	1378	1202	1269	1341	1355	1454	1412	1326
Habbaniah Lake	968	918	865	919	904	911	918	1015	976	1154	1112	1235
Al Qurna Marsh	1558	1048	1661	1106	1038	863	736	827	886	820	893	1005
Al Hammar Marsh	1870	1348	1880	1356	1300	1288	1236	1264	1317	1320	1330	1380
Al Huwizah Marsh	625	600	437	500	525	850	1000	875	862	1000	875	750

B. Method

The evaporation losses from the reservoirs, lakes and marshes, were computed according to the area and storage-elevation curves, Fig.s 1 to 11, and the monthly evaporation data considering a pan coefficient of 0.7, Table II, with storage water level stepped one meter from the minimum to maximum water level for each reservoirs, lakes and marshes.

The increase in evaporation rate affects water quality due to the increase in the salinity of water. The salt mass balance equation, Eq. 1, was used to calculate the increase in salt mass due to water evaporation from water bodies. The increase in TDS value was computed for the storage cases of minimum, average and maximum.

$$TDS_{i+1} = \frac{S_i \times TDS_i}{S_i - Ve_i} \qquad \ldots\ldots\ldots\ldots\ldots\ldots\ldots \quad 1$$

Where:

S is storage volume (L^3)

Ve is evaporation volume (L^3), which is (water surface area (L^2)× evaporation(L)).

i is month index (i= 1 to 11)

III. RESULTS

The computed evaporation losses from the reservoirs, lakes and marshes were as shown in fig.s 12 to 22. Accordingly, the computed TDS concentrations in these water bodies were as listed in Table IV.

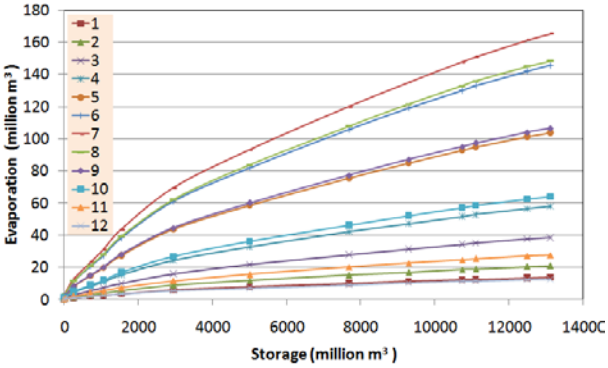

Fig. 12. Estimated evaporation losses from Al-Mosul Dam.

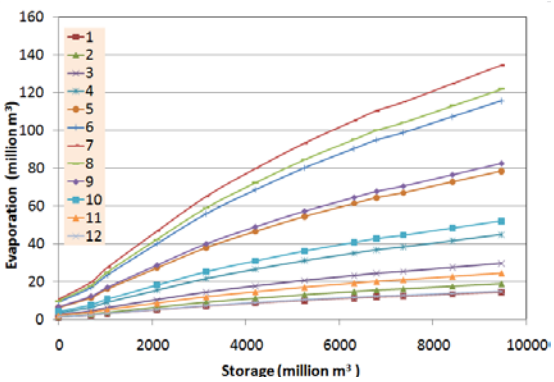

Fig 13. Estimated evaporation losses from Dokan Dam.

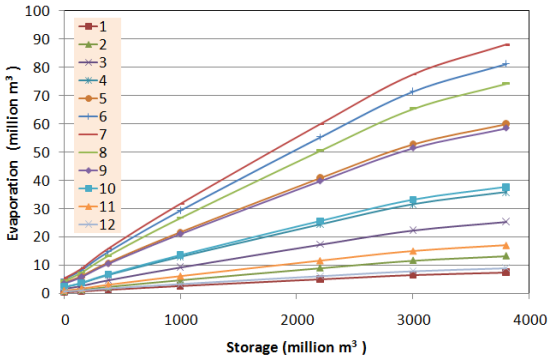

Fig. 14. Estimated evaporation losses from Al-Udhaim Dam.

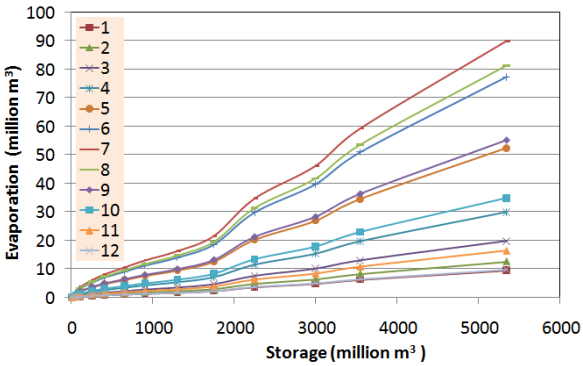

Fig. 15. Estimated evaporation losses from Darbandikan Dam.

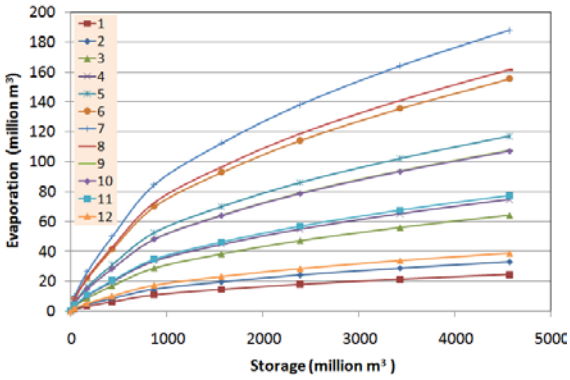

Fig. 16. Estimated evaporation losses from Hemrin Dam.

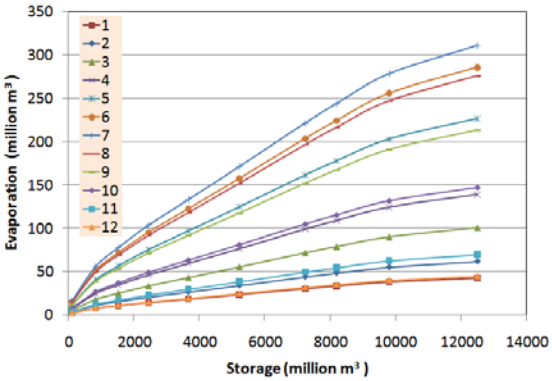

Fig. 17. Estimated evaporation losses from Haditha Dam.

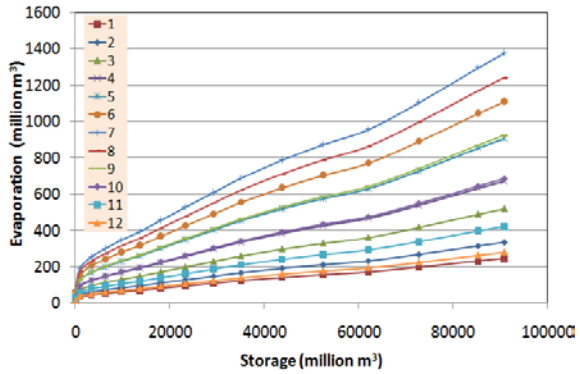

Fig. 18. Estimated evaporation losses from Tharthar Lake.

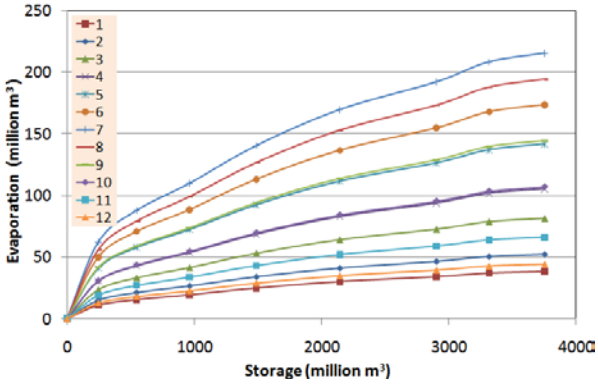

Fig. 19. Estimated evaporation losses from Habbaniah Lake.

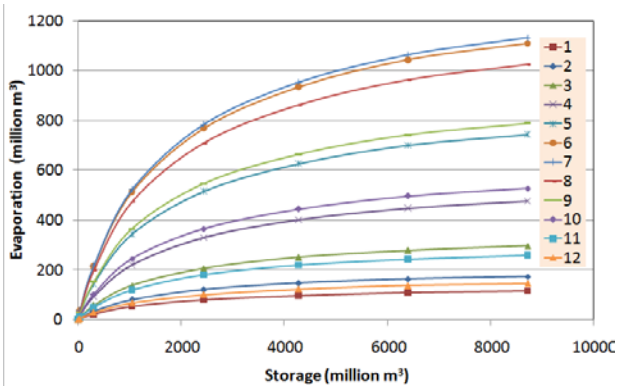

Fig. 20. Estimated evaporation losses from Al Qurna Marsh.

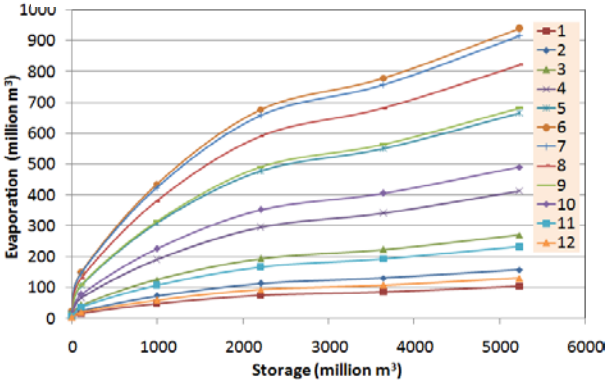

Fig. 21. Estimated evaporation losses from Al Hammar Marsh.

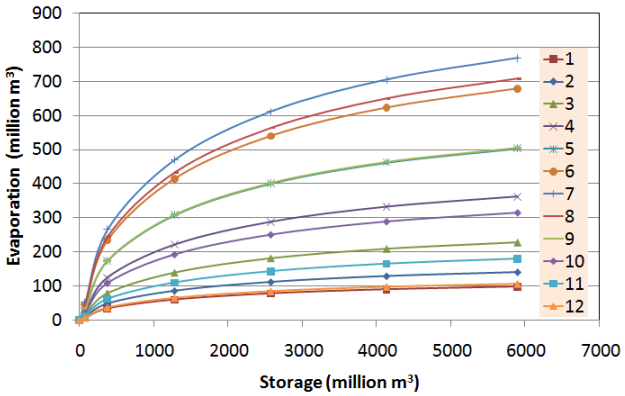

Fig. 22. Estimated evaporation losses from Al Huwizah Marsh.

Table IV. Estimated mean monthly TDS (ppm) for the examined water bodies.

Water Body		Month											
		1	2	3	4	5	6	7	8	9	10	11	12
Al-Mosul Dam	Min.	250	253	255	258	246	237	243	227	222	231	237	242
	Ave.	251	254	259	263	254	249	261	239	232	236	237	244
	max.	257	264	279	321	367	364	424	360	295	272	252	249
Dokan Dam	Min.	190	182	230	209	208	205	172	162	179	160	209	203
	Ave.	191	183	232	211	212	211	178	169	183	161	209	227
	max.	193	184	235	214	229	236	202	189	197	168	212	206
Al-udhaim Dam	Min.	422	447	476	457	494	498	537	506	450	438	407	419
	Ave.	425	450	464	437	480	473	501	460	424	408	401	416
	max.	456	502	585	627	1096	2105	3569	1780	895	614	462	452
Darbandikan Dam	Min.	269	271	264	259	222	220	242	249	248	275	237	240
	Ave.	269	272	265	260	221	222	244	255	257	276	238	240
	max.	284	288	282	272	227	222	253	262	267	290	249	251
Hemrin Dam	Min.	418	440	461	436	492	519	541	502	438	415	396	412
	Ave.	425	502	551	531	562	572	632	582	527	497	445	424
	max.	438	501	528	509	548	583	618	551	447	443	445	449
Haditha Dam	Min.	630	592	635	626	662	658	749	773	723	707	667	663
	Ave.	636	600	649	645	701	712	805	819	756	728	675	669
	max.	642	608	664	666	743	768	880	883	799	754	686	675
Tharthar Lake	Min.	1460	1524	1556	1519	1455	1273	1361	1425	1434	1529	1473	1364
	Ave.	1481	1547	1597	1579	1533	1367	1496	1553	1504	1573	1482	1368
	max.	1491	1563	1622	1608	1578	1426	1571	1622	1555	1607	1500	1380
Habbaniah Lake	Min.	1077	1059	1100	1253	1443	1700	2086	2103	1584	1609	1350	1399
	Ave.	1116	1119	1202	1440	1767	2263	3544	3061	1941	1825	1440	1456
	max.	1245	1333	1298	1426	1731	2050	2951	2687	1793	1731	1410	1425
Al Qurna Marsh	Min.	1580	1072	1718	1153	1096	914	789	879	938	862	932	1034
	Ave.	1602	1088	1764	1199	1155	981	868	958	983	887	937	1037
	max.	1613	1099	1791	1221	1189	1024	911	1000	1017	906	949	1046
Al Hammar Marsh	Min.	1896	1379	1945	1414	1373	1364	1326	1343	1394	1388	1387	1420
	Ave.	1923	1400	1996	1470	1446	1465	1457	1464	1462	1428	1396	1424
	max.	1936	1414	2028	1497	1489	1528	1530	1529	1511	1459	1413	1436
Al Huwizah Marsh	Min.	634	614	452	521	554	900	1072	930	912	1052	913	771
	Ave.	643	623	464	542	584	967	1179	1013	957	1082	918	774
	max.	647	629	471	552	601	1008	1238	1058	989	1105	930	781

IV. CONCLUSION

Reservoirs, lakes and marshes are expected to affect water quality and quantity for millions of downstream users. About 170 km^3 of water evaporates from the world's reservoirs every year, more than 7% of the total amount of freshwater consumed by all human activities.

Results of studying the effect of storage on water losses because of evaporation from reservoirs, lakes and marshes in Iraq with minimum, average and maximum storage conditions show that the volume of losses because of evaporation is 7%, 18% and 26% of the storage volume at these storage conditions, respectively.

Increase of salinity is another risk made worse by evaporation from reservoirs and changes to flows downstream. High salt concentrations are poisonous to aquatic organisms and corrode pipes and machinery. The results of this study show that the process of water storage affect water quality of reservoirs, lakes and marshes through increasing the TDS to 11%, 20%, and 34% for the minimum, average and maximum storage conditions.

Storage of water change the timing, amount and chemical composition of a river's flow, leading to dramatic changes to groundwater-storing floodplains and wetlands. It is trapped river-borne nutrients; it can lead to the growth of toxic algaes. Water stored for months or even years behind major reservoirs may become lethal to most life in the reservoirs and in the rivers for long distances below the reservoirs. It also leads to riverbed deepening for tens or even hundreds of kilometers below the reservoir. Riverbed deepening can lower the groundwater along a river, threatening vegetation and local wells in the floodplain and requiring crop irrigation in places where there was previously no need.

Accordingly, it recommend to consider these negative effects before taking a decision to construct any other dam, study the variation of evaporation loss according to the reservoirs and lakes rules curve, study the two dimensional distribution patterns of salt mass within the reservoir and lakes and studying the effect of water loss from reservoirs on the ecological of rivers.

REFERENCES

[1] IFRCRCS (International Federation of Red Cross and Red Crescent Societies), 2008. "Iraq: Response to Humanitarian Crisis- Final Report" MDRIQ002 , 30 April 2008.

[2] MoWR (Ministry of Water Resources), 2006. "Technical Data for Dams, Reservoir and Main Control Structures with Mean Monthly flow-Rates and Water Quality for Main Water Reservoirs (1976 to 2005)" unpublished Report, Water Control Center, Baghdad-Iraq.

[3] MoWR (Ministry of Water Resources), 2013. " unpublished Recorded Data" National Center of Water Resources, Baghdad-Iraq.

[4] MoT (Ministry of Transportation), 2013. " Unpublished recorded data" Iraqi Metrological Organization and Seismology, Baghdad-Iraq.

Improving the Water Use Efficiency of AL- Hussainiyah Irrigation Project

Mahmoud S. Mahdi, Building and Construction Eng. Dept./University of Technology-
Linoxer@Gmail.com
Haider. H. Alwash -- University of Technology, Baghdad-Iraq
Layth S. Al-Khafaji, - University of Karbala, Karbala-Iraq

***Abstract*— Irrigation efficiency is one of the most important inputs for agricultural production, since water scarcity is turning into a severe problem worldwide, affecting mainly arid and semi-arid region. Recently, there is an increase in the need to produce more output per unit of water, which means it is required to increase the Water Use Efficiency (WUE).**

Al-Hussainiyah Irrigation Project in the province of Karbala- Iraq is one of the most important irrigation projects in the central region of Iraq, which suffers from a deficiency of water.

The objective of this study is to improve the WUE of Al-Hussainiyah Irrigation Project through evaluating the present state of agriculture and deficit in water resources during the drought season and reducing the effect of this deficit on the total yield.

This objective was achieved through correlating the deficit irrigation with yield reduction and estimating the WUE for seven crops (Maize, Cotton, Small Grain, Summer Vegetable, sunflower, Sesame and Alfalfa) under different irrigation deficit levels (5, 10, 15, 20 and 25%) as a function of all crop growth for heavy soil.

All the required data were collected from number of related Iraqi ministries. CROPWAT 8.0 software was used to solve the model and test its application sensitivity by changing deficit levels. The results of the model show that the yield reduction of Maize is the highest, whereas the Cotton has the less yield reduction for all deficit levels. The estimated WUE for the considered crops show that the maximum WUE obtained at different deficit level for each crop.

Key Words*— *Efficiency, deficit, yield and Irrigation.

I. INTRODUCTION

Water resource management is the activity of planning, developing, distributing and managing the optimum use of water resources, it is a sub-set of water cycle management. Ideally, water resource management planning has regard to all the competing demands for water and seeks to allocate water on an equitable basis to satisfy all uses and demands. As with other resource management, this is rarely possible in practice.

To ensure food security the water must be wisely used in order to enhance food production while save water as much possible or in other words to increase water use efficiency, So the only tool to overcome this phenomenon is the enhancing of water use efficiency, it is also called water productivity.

Deficit irrigation is one management practice of maximizing Water Use Efficiency (WUE) for higher yields per unit of irrigation water applied. The expectation is that the loss in yield after water stress is justified by the benefits gained through diverting the saved water to irrigate other valuable crops.

Waseem, 2010, [10], Estimated reference crop evapotranspiration (ET_0) through CROPWAT 8.0 from limited climatic data and comparing the result with that of full set of climatic data under temperate conditions of Kashmir in India The results revealed that the ET_0 estimated from limited data i.e. daily air temperature with annual mean wind speed (0.625 m/s) through CROPWAT have good agreement with that of ET_0 estimated from full set of climatic data. A. Dominguez et al., 2012, [2] developed a methodology (Optimized Regulated Deficit Irrigation (ORDI)) for determining the stress level that can be applied to each growth period for maximum yield for the simulation of maize in Castilla-La Mancha (Spain). The result was for low water stress conditions, deficit irrigation should be applied during the initial and vegetative development stages. Abdul Amir, 2012, [1] determined the water requirement and water use efficiency of corn under different irrigation treatments (deficit irrigation concept) under middle of Iraq conditions (Baghdad). The field and crop water use efficiencies values reduced when deficit irrigation was applied at vegetative growth stage, and increased when deficit irrigation was applied at seedling, flowering and grain maturity stages in comparison with full irrigation treatment. Aysar, 2013, [4], studied five models for estimating the potential evapotranspiration for Al-Hussainiyah Irrigation in Iraq. It is found that Penman Monteith (PM) model produced the most reliable estimates compared to Penman -FAO-24 model (PF).

II. THEORETICAL BACKGROUND

A. Reference Crop Evapotranspiration (ET_0)

Estimation of ET_0 is important in irrigation management and development. ET_0 depends on climatic parameters and can be computed from weather data. The Penman Monteith method of estimating ET_0 is expressed in equation (1), [3]

$$ET_O = \frac{0.408(R_n - G) + \gamma \frac{900}{T+273} U_2 (e_s - e_a)}{\Delta + \gamma(1 + 0.34U_2)} \quad \ldots\ldots\ldots \quad (1)$$

Where, ET_o is the reference crop evapotranspiration (mm d^{-1}), R_n is the net radiation at the crop surface (MJ m^{-2} d^{-1}), G is the soil heat flux (MJ m^{-2} d^{-1}), T is the average air temperature ($^{\circ}C$), U_2 is the wind speed measured at 2 m height (m s^{-1}), (e_s- e_a) is the vapour pressure deficit (kPa) The symbol γ denotes the psychrometric constant (kPa/ $^{\circ}C$), Δ is the slope of the vapour pressure versus temperature curve (kPa/ $^{\circ}C$), λ is the latent heat of vaporization (MJ kg^{-1}).

B. Crop Water Requirements and Irrigation Water Demand

Crop consumptive use or actual evapotranspiration is usually calculated from the following equation:

$$ETc = ET_0\ K_c \quad \ldots\ldots\ldots\ldots\ldots\ldots \quad (2)$$

Where, ET_C is crop consumptive use rate in mm/month, ET_0 is the reference evapotranspiration, and K_c is crop coefficient. On the other hand, information about farm irrigation efficiency (IE) is necessary to transform ET as a net Irrigation Water Requirement (NIWR) into gross irrigation water requirement (GIWR) as, [8]:

$$GIWR = \sum_{t=1}^{n} \frac{ET_C\ (NIWR)}{IE} \quad \ldots\ldots\ldots\ldots\ldots\ldots \quad (3)$$

Where, t varies from 1 to n months of the plant life-cycle. Multiplying gross irrigation requirement by the irrigated area gives the Total Irrigation Water Requirement TIWR for cropped area as follows:

$$TIWR = \sum_{t=1}^{n} \sum_{j=1}^{r} GIWRjt\ Ajt \quad \ldots\ldots\ldots\ldots \quad (4)$$

where, the GIWR is the amount of irrigation water per unit of area for each crop (j) in month (t), and (A) is the cropped area of each crop j in month t. The discharge requirements at the head of main canal can be expressed as:

$$QT = \frac{TIWR}{CE} \quad \ldots\ldots\ldots\ldots\ldots\ldots \quad (5)$$

where, CE = conveyance efficiency, expressed as a percentage, QT = total discharge applied the project head regulator, $m^3\ sec^{-1}$.

C. Water USE Efficiency

Water use efficiency (WUE) is a broad concept that can be defined in many ways. For farmers and land managers, WUE is the yield of harvested crop product achieved from the water available to the crop through rainfall, irrigation and the contribution of soil water storage equation (6), [11]. The yield is the crop yield in kg/ha and the irrigation requirement in m^3/ha.

$$WUE = \frac{\text{Yield}}{\text{Irragation Requirment}} \quad \ldots\ldots\ldots\ldots\ldots \quad (6)$$

D. Deficit Irrigation

Deficit irrigation (DI) has been defined as follows:"Deficit irrigation is an optimization strategy in which irrigation is applied during drought-sensitive growth stages of a crop. DI maximizes irrigation water productivity, which is the main limiting factor [5].

Doorenbos and Kassam, 1979 empirically derived yield-response factors (K_y) for individual growth stages and also for the total growing period and are given by:

$$\frac{Ya}{Ym} = K_y\left(1 - DI * \frac{ET_a}{ET_m}\right) \quad \ldots\ldots\ldots\ldots\ldots\ldots \quad (7)$$

Where, Ym: Maximum expected yield that results from applying full irrigation level for each growth stage of the crop life in kg/ha, Ya: Expected actual yield in kg/ha, K_y: yield response factor of the crop for growth stage which reflects the sensitivity of the growth stage to water deficit, ET_m: Maximum crop evapotranspiration at growth stage, ET_a: Actual crop evapotranspiration at each stage, DI: level of the suggested irrigation.

III. Study Area

Al-Hussainiyah Irrigation Project is located on the right side of the Euphrates river in the provinces of Babel and Karbala in Iraq and extends between latitudes N 32° 36' to 32° 48' and longitudes E 43° 55' to 44° 17 '. The monthly average of the climatic parameters for the study area during the period 1990 to 2012 are as shown in Table (I).

The present cropping pattern data were collected from Directorate of Agriculture in Karbala Governorate. Agricultural divisions in the study area contains three divisions: City center, Own and AL-Hussainiyah. There are three agricultural seasons, winter, summer, and perennial. The main winter crops are wheat, barley, and winter vegetable. Maize and summer vegetables are the dominant summer crops, while the orchards, palms and alfalfa are the dominated perennial crops.

The response of yield to water supply is quantified through the K_y which relates relative yield decrease to relative evapotranspiration deficit, this approach and the calculation procedures for estimating yield response to water were published in the FAO Irrigation and Drainage Paper No. 33. The values of the yield response factor, K_y, for the crops of Al-Hussianiyah Irrigation Project as suggested by FAO are listed in Table (II) [6].

The crop coefficient (K_C) integrates the effect of characteristics that distinguish a specific crop from the reference crop. The K_C, Table (III), and the planting and harvesting data, Table (IV), for the cropping patterns in Al-Hussianiyah Irrigation Project is recommended by the Ministry of Irrigation (MoI) for the central zone of Iraq [7].

Soil physical parameters data, such as soil texture, soil depth, infiltration rate, and the available soil moisture and bulk density, Table (V), are required to calculate the total available water in the root zone and thus the irrigation schedule. These data have been gathered from Allen et. al., 1998 [3] and Ministry of Water Resources, 2013 [9].

Table (I). The monthly average of the climatic parameters during the period 1990 to 2012.

Climatic parameter	Jan	Feb	Mar	Apr	May	Jun	Jul	Aug	Sept	Oct	Nov	Dec
Air temperature (C^0)	10.5	13.2	17.8	24.4	30.2	34.7	37.0	36.7	32.5	26.1	17.5	12.1
Rainfall (mm)	16.9	13.9	10.2	12.3	1.9	0.0	0.0	0.0	0.4	2.8	9.6	14.1
Max. air temperature (C^0)	16.1	19.1	24.0	31.3	37.6	42.2	44.5	44.4	44.4	33.9	24.1	18.1
Min. air temperature (C^0)	4.8	7.4	11.5	17.6	22.8	27.2	29.5	29.0	24.6	18.2	11.0	6.2
Evaporation (mm)	59.2	92.0	170.0	237.1	329.4	408.4	438.2	395.8	301.0	201.8	100.4	61.5
Relative humidity (%)	74.3	61.2	50.1	43.1	34.8	29.0	30.5	32.3	37.3	46.4	61.2	71.6
Sun shine duration (hr/day)	5.9	7.0	7.8	8.3	9.4	10.9	11.2	10.9	10.0	8.1	7.1	6.0
Wind speed (m/sec)	1.7	2.0	2.3	2.4	2.4	3.1	3.2	2.5	1.9	1.5	1.3	1.4

Table (II). K_Y for the crops of Al - Hussianiyah Irrigation Project *[6]*.

	K_y			
Crops	**Initial**	**Development**	**Mid-season**	**Late**
Maize	0.4	0.4	1.3	0.5
Cotton	0.2	0.5	0.5	0.25
Sunflower	0.4	0.6	0.8	0.8
Sesame	0.4	0.6	1.25	0.8
Small grain	0.4	0.6	1.25	0.8
Summer vegetables	0.8	0.4	1.2	1
palms	0.8	0.8	0.8	0.8
Alfalfa	0.7	0.9	0.8	0.7

Table (III). K_C for the crops of Al - Hussianiyah Irrigation Project *[7]*.

ID	Crops	Jan	Feb	Mar	Apr	May	Jun	Jul	Aug	Sept	Oct	Nov	Dec
1	Maize	0.00	0.00	0.58	0.82	1.08	0.80	0.00	0.00	0.00	0.00	0.00	0.00
2	Cotton	0.00	0.00	0.00	0.54	0.64	0.80	0.98	0.82	0.49	0.00	0.00	0.00
3	Sunflower	0.00	0.00	0.58	0.68	0.84	1.02	0.49					
4	Sesame	0.00	0.00	0.00	0.00	0.52	0.70	0.94	0.75	0.40	0.00	0.00	0.00
5	Small grain	0.00	0.00	0.00	0.55	0.67	0.90	1.00	0.60	0.00	0.00	0.00	0.00
6	Summer vegetables	0.00	0.00	0.58	0.67	0.79	0.93	0.95	0.76	0.46	0.00	0.00	0.00
7	Orchards and palms	1.00	1.05	1.05	1.00	0.95	0.95	0.85	0.85	0.80	0.80	0.85	0.95
8	Alfalfa	1.10	0.98	0.94	0.92	0.90	0.89	0.89	0.89	0.89	0.89	0.94	1.14

Table (IV). Planting and harvesting Date *[MoI, 1982]*.

Id	Crops	Planting date	Harvesting date
1	Maize	11/March	5/July
2	Cotton	1/April	10/September
3	Sunflower	21/ March	31/July
4	Sesame	1/May	10/ September
5	Small grain	6/April	15/August
6	Summer vegetables	21/March	30/ September
7	Orchards and palms	Perennial	
8	Alfalfa	Perennial	

Table (V). Main soil characteristics *[3] and Ministry of Water Resources, 2013]*.

	Soil name	Heavy (clay)
1	Total available soil moisture (mm /meter)	200
2	Maximum rain infiltration rate (mm /day)	40
3	Maximum rooting depth (cm)	900
4	Initial soil moisture depletion (as % TAM)	0
5	Initial available soil moisture (mm /meter)	200

IV. Correlation of Deficit Irrigation with Yield Reduction

The fundamental goal of deficit irrigation for this research is to increase water use efficiency, either by reducing irrigation adequacy or by eliminating the least productive irrigations. The CROPWAT 8.0 Software was used to solve the model by using Schedule module. The ET_c reduction per stage is the CROPWAT option which is selected for irrigation timing, and irrigation is always done for refilling soil to Field Capacity (FC). This means that the percentage of ET_c is focused on stage. There are eight crop types (Maize, Cotton, Sunflower, Sesame, Small grain, Summer vegetables, Alfalfa and palms) in the considered project during summer season, while the soil of the project is heavy and the following input data were required to run the model are: Climatic Parameters**,** Cropping patterns, K_y for each crop, K_C **,** Crop planting and harvesting date and physical and chemical properties of the soil.

IV Maximum Net Revenue Optimization Model

A linear mathematical model was used to find the maximum net revenue. This model includes an objective function equation (8) and a set of linear constraints include water, land and non-negative, equations (9) to (11) respectively. The implemented objective function aims to maximize the net revenue of the farmer by allocating different areas for each crop and getting the optimum local cropping pattern. The model took in consideration the available land, the available water, different suggested levels of deficit irrigation, the crop cost of production, and the net revenue.

$$\text{Max } Z = \Sigma[Ai \times Ni] \quad \ldots\ldots\ldots\ldots \quad (8)$$

Wher: Z = Total net income of the agricultural area (USD), Ai = Area of crop i (ha), Ni = Net income of crop i (USD), i = Index of crop type and Net income Ni = Total income – Total cost of production, Total income = Yi × Pi. Where, (Yi) is the crop yield of crop i in area (ton/ha), and (Pi) is the crop price of crop i in area ($/ton).

$$\Sigma (Ai*Wi) \leq CE* TAWS \quad \ldots\ldots\ldots\ldots\ldots \quad 9)$$

Where: Ai = Area (ha) allocated for crop i, Wi= Volume of water (m^3) needed to produce crop "i" per hectare in one month under different Model 1 scenarios, TAWS = Total available irrigation water for supplying during drought season (m^3) (2008) and CE= Conveyance efficiency, expressed as a percentage (unitless).

$$\Sigma Ai \leq TA \quad \ldots\ldots\ldots\ldots\ldots \quad (10)$$

Where TA = Total available agricultural land (ha) **.**

$$Ai \geq 0 \quad \ldots\ldots\ldots\ldots\ldots \quad (11)$$

V Sensitivity Analysis

In order to analysis the sensitivity of the model, Six scenario for each crop were used. They were based on changes in different deficit irrigation levels. The following suggested six scenarios were used to test the sensitivity of the model.

1- Irrigate at critical depletion (full irrigation) (S0).
2- Irrigate at given ET crop reduction per stage (5% for all stage) (S1).
3- Irrigate at given ET crop reduction per stage (10% for all stage) (S2).
4- Irrigate at given ET crop reduction per stage (15% for all stage) (S3).
5- Irrigate at given ET crop reduction per stage (20% for all stage) (S4).
6- Irrigate at given ET crop reduction per stage (25% for all stage) (S5).

V. Result Analysis and Discussion

A. *Estimation of (ET_0)*

After defined the main climatic parameters, Results of estimating the ET_0 are obtained by applying the CROPWAT software and they were as shown in Table (VI).

The values of ET_0 are found to be low during the period from Jan. to April and increase during May to September. It reached maximum value of 320.65 mm in July, while the minimum monthly value takes place during January with 47.23 mm, and declined during October to December. This variation in ET_0 values is attributed to combined effects of temperature, sun shine hours, radiation, wind speed and humidity.

Table (VI). Input Climate data and estimated ET_o for AL-Hussainiyah project

Country Iraq — Station AL Hussainiyah
Altitude 28 m. — Latitude 32.00 °N — Longitude 44.00 °E

Month	Min Temp	Max Temp	Humidity	Wind	Sun	Rad	ETo
	°C	°C	%	m/s	hours	MJ/m²/day	mm/month
January	4.7	16.1	74	1.6	5.9	10.9	47.23
February	7.4	19.1	61	1.9	6.6	13.7	67.48
March	11.5	24.0	51	2.3	7.8	17.9	120.77
April	17.6	31.3	43	2.4	8.4	21.1	171.03
May	22.8	37.6	34	2.4	9.4	23.8	230.54
June	27.2	42.2	29	3.0	10.8	26.2	288.10
July	29.4	44.5	30	3.2	11.1	26.4	320.65
August	28.9	44.4	32	2.5	10.8	24.9	278.32
September	24.6	40.4	37	1.9	9.9	21.4	202.80
October	18.2	33.9	46	1.5	8.1	16.2	137.33
November	11.0	24.1	61	1.3	7.2	12.6	75.05
December	6.2	18.1	72	1.3	6.0	10.3	48.77
Average	17.5	31.3	48	2.1	8.5	18.8	1988.08

B. Deficit Irrigation and Yield Reduction

The CROPWAT 8.0 Software was used to solve the model by using Schedule module. There are eight crop types (Maize, Cotton, Sunflower, Sesame, Small grain, Summer vegetables , Alfalfa , palms) in the considered project during summer season. These results were used to find the relationships between deficit irrigation and yield reduction for each crop considering of heavy soil, Table (VII). The SPSS Table Curve 2D V5.0 software were used for this purpose Fig. (1).

Table (VII). Estimated yield reduction (%) and total Gross irrigation (mm) for Heavy soil.

Crop		Maize	Cotton	Sunflower	Sesame	Small grain	Sumer Vegetable	Alfalfa	Palms
S0	Yield reduction	0.0	0.0	0.0	0.0	0.0	0.0	0.0	0.0
	Total Gross mm	1082.0	1689.9	1139.7	1372.2	1345.9	1960.7	2738.9	2437.7
S1	Yield reduction	5.9	3.8	3.9	5.9	5.2	6.3	5.8	3.7
	Total Gross mm	907.1	1331.9	1028.1	1333.3	1160.1	1841.0	2361.0	2244.6
S2	Yield reduction	13.1	8.6	9.3	10.2	10.6	10.6	11.3	8.2
	Total Gross mm	1010.0	1456.6	1194.6	1183.1	1263.9	1665.3	2590.2	2442.6
S3	Yield reduction	15.6	11.2	12.0	154.2	14.4	15.5	15.7	11.3
	Total Gross mm	778.4	1108.0	935.2	989.0	981.0	1542.5	2294.5	2076.6
S4	Yield reduction	23.9	14.8	17.7	18.7	17.0	20.7	20.3	16.3
	Total Gross mm	832.4	1159.0	1013.7	1037.3	1014.0	1514.6	1925.2	2163.2
S5	Yield reduction	32.1	20.3	22.7	24.7	23.9	25.6	26.0	17.6
	Total Gross mm	865.7	1210.7	698.4	1073.9	1048.1	1445.2	2008.7	1674.1

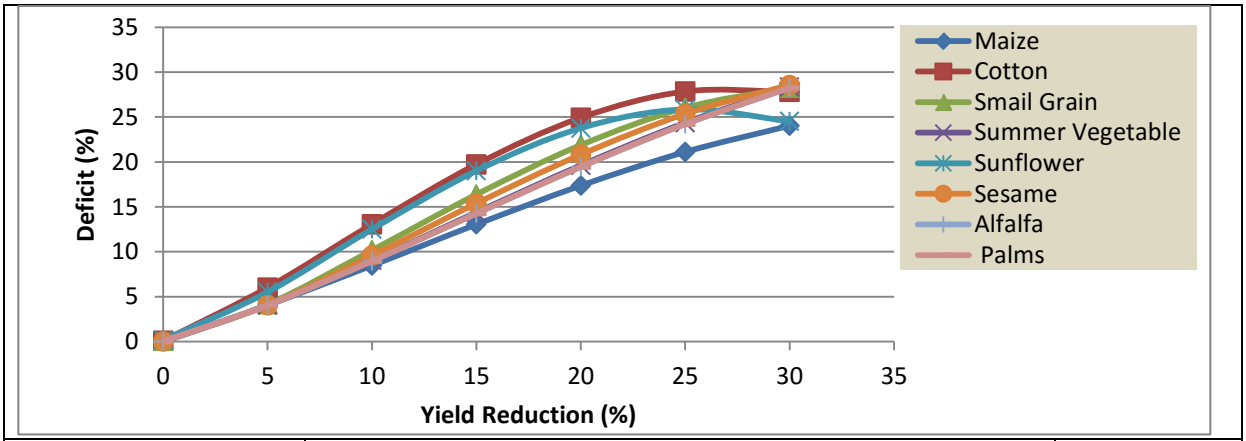

Crop type	Obtained relationshipes	R^2
Maize	$y = a + bx^{1.5} + cx^{2.5} + dx^{0.5}$ a=0.0123, b=0.2255, c=-0.0035, d=0.7696	0.9910
Cotton	$y = a + bx^{1.5} + cx^{2.5} + dx^{0.5}$ a=0.08713, b=0.4362, c=-0.0097, d=0.7120	0.9958
Sunflower	$y = a + bx^{1.5} + cx^{2.5} + dx^{0.5}$ a=0.15535, b=0.467, c=-0.011, d=0.3384	0.9889
Sesame	$y = a + bx^{1.5} + cx^{2.5} + dx^{0.5}$ a=0.0078, b=0.3222, c=-0.0053, d=0.3355	0.9983
Small Grain	$y = a + bx^{1.5} + cx^{2.5} + dx^{0.5}$ a=0.0836, b=0.3799, c=-0.0070, d=0.0936	0.9921
Summer Vegetable	$y = a + bx^{1.5} + cx^{2.5} + dx^{0.5}$ a=-0.0256, b=0.2652, c=-0.0037, d=0.5845	0.9993
Alfalfa	$y = a + bx^{1.5} + cx^{2.5} + dx^{0.5}$ a=0.0253, b=0.2578, c=-0.0035, d=0.6028	0.9995
Palms	$y = a + bx^{1.5} + cx^{2.5} + dx^{0.5}$ a=-0.0334, b=0.1685, c=0.0022, d=2.0358	0.9995

Fig. (1) shows that there are different relationships between deficit irrigation and yield reduction applying the range of deficit from 5 to 25% and there are two sets of crops appear clearly when increasing the level of irrigation deficit. The reason for this is due to the difference in the sensitivity of these crops for deficit irrigation.. The first group includes cotton and sunflower, while the second group includes maize, sesame, small grain, summer vegetable, alfalfa and palms. The percentage of yield reduction of the first group was less than that of the second group for the deficit irrigation less than 25%. While, when applying deficit greater than 25% the yield reduction increase must rapidly to be very high. The yield reduction of the Maize was the highest at any level of irrigation deficit, while cotton gave less yield reduction

To calculate water use efficiency of crops for heavy soil, equation (6) was used. Table (VIII) lists the estimated water use efficiency of consider eight crops. The estimated WUE for the seven crops in the heavy soil show that the maximum value of WUE obtained at different irrigation deficit level for each crop. The maximum values of WUE were obtained at deficit irrigation level of 15% for all the studied crops except Sunflower which was at 25% of irrigation deficit.

Table (VIII). Water use efficiency of the Crops in heavy soil.

ID	Crops	Deficit irrigation (%)	Yield Reduction (%)	Yield (ton/ha)	Irrigation Requirement (m^3/ha)	WUE (Kg/ m^3) *10^{-2}
1	Maize	0	0	2.612	10826	24.127
		5	5.9	2.457	9070	27.099
		10	13.1	2.269	10108	22.455
		15	**15.6**	**2.204**	**7784**	**28.321***
		20	23.9	1.987	8323	23.882
		25	**32.1**	**1.773**	**8657**	**20.486****
2	Cotton	**0**	**0**	**1.24**	**16900**	**7.337****
		5	3.8	1.192	13319	8.956
		10	8.6	1.133	14566	7.780
		15	**11.2**	**1.101**	**11079**	**9.938***
		20	14.8	1.056	11590	9.115
		25	20.3	0.988	12107	8.162
3	Sunflower	0	0	0.8	11397	7.019
		5	3.9	0.7688	10281	7.477
		10	**9.3**	**0.7256**	**11946**	**6.073****
		15	12	0.704	9352	7.527
		20	14.8	0.6816	10137	6.723
		25	**22.7**	**0.6184**	**6984**	**8.854***
4	Sesame	0	0	0.8	13723	5.829
		5	5.9	0.752	13332	5.646
		10	10.2	0.718	11830	6.072
		15	**15.2**	**0.678**	**9890**	**6.859***
		20	18.7	0.650	10373	6.270
		25	**24.7**	**0.602**	**10738**	**5.609****
5	Small grain	0	0	0.7	13460	5.200
		5	5.2	0.663	11601	5.720
		10	**10.6**	**0.625**	**12640**	**4.950****
		15	**14.4**	**0.599**	**9810**	**6.108***
		20	17	0.581	10140	5.729
		25	23.9	0.532	10481	5.082
6	Summer vegetables	0	0	6.92	19606	35.295
		5	**6.3**	**6.484**	**18409**	**35.222****
		10	10.6	6.186	16652	37.151
		15	**15.5**	**5.847**	**15425**	**37.908***
		20	20.7	5.487	15147	36.228
		25	25.6	5.148	14450	35.629
7	Alfalfa	**0**	**0**	**27**	**22779**	**118.530****
		5	3.7	26.001	20691	125.663
		10	8.2	24.786	19702	125.804
		15	**11.3**	**23.949**	**15665**	**152.882***
		20	16.3	22.599	16089	140.462
		25	17.6	22.248	16780	132.586

* Maximum WUE

** Minimum WUE

VI. CONCLUSIONS

It is important to find studied solutions for the problem of water scarcity during the drought seasons which can help the farmers to overcome this problem and to maximize the benefit of using the available water through maximize the water use efficiency.

The results of this study show the ability of using the deficit irrigation techniques for increasing the water use efficiency and increasing the cultivated areas which can treat the environmental damages produced due to drought in addition to the economic benefit of the increase in water use efficiency.

Study of the relationship between the level of irrigation deficit and the yield reduction for the considered seven crops (Maize, Cotton, Small Grain, Summer Vegetable, sunflower, Sesame and Alfalfa) cultivated in heavy soil under different irrigation deficit levels (5, 10, 15, 20 and 25%) shows that this relation highly affects the water use efficiency which computed according to the climate conditions of the study area and the characteristics of the cultivated crops.

Analysis of the results of this study shows that each crop has its own nonlinear relationship between deficit irrigation level and yield reduction which different from those of other crops. Maize has the highest yield reduction percentages for all deficit irrigation levels, while the Cotton has the less percentages. The maximum WUE can be obtained at different deficit irrigation level for each crop.

REFERENCES

[1] Abdul Amir Salih Thejel, and Adnan Shubar Falih, 2012 " Management of Corn Irrigation to Increase Water USE Efficiency in Middle of IRAQ" Journal of Diyala Agricultural Sciences 0.4 (1): 62-75.2012.

[2] A. Dominguez, J.A.de Juan, J.M. Tarjuelo, R.S. Martinez, A.Martinez-Romero, 2012. "Determination of optimal regulated deficit irrigation strategies for maize in A semi-arid environment ", Journal of Agricultural Water Management 110 (2012) 67– 77.

[3] Allen, R.G., Perira, Raes D. and Smith, M., 1998. "Crop Evapotranspiration, Guide lines for Computing Crop Water Requirements", Irrigation and Drainage Paper No. 56, Food and Agriculture Organization of the United Nations.

[4] Aysar Tuama AL Awadi, 2013. " Optimal Water Allocation Management of Al-Hussainiyah Irrigation Project with GIS Support ", MSc. Thesis, Building and Construction Engineering Department, Water and Dams Branch, University of Technology, Iraq.

[5] English, M.J., 1990. "Deficit irrigation. Analytical framework. Journal of Irrigation and Drainage", Engineering Division, ASCE 116 (3), 399±412.

[6] FAO, 1986. "Yield response to water", Irrigation and Drainage Paper 33, Food and Agriculture Organization of the United Nations (FAO), Rome, Italy, pp.193 .

[7] MoI (Ministry of Irrigation), 1982. "General Scheme of Water Resources, and Land Development in Iraq", Volume III, Books 1 and 2

[8] MoI (Ministry of Irrigation), “Design Manual for Irrigation and Drainage “ State Organization for Land Reclamation, General Establishment for Design and Research, and Pencol Engineering Consultant, 1983., Baghdad, Iraq.

[9] Ministry of Water Resources, Directorate of Water Resources in Karbala Province, Technical Department, 2013, "Unpublished Data about the Available Water Releases of Al-Hussainiyah Irrigation Project during (2006-2012) ", in Karbala, Iraq, (in Arabic).

[10] Waseem Raja, 2010. " Validation of CROPWAT 8.0 for Estimation of Reference Evapotranspiration using Limited Climatic Data under Temperate Conditions of Kashmir ", Research Journal of Agricultural Sciences 2010, 1(4): 338-340.

[11] White, G. F., 1961. "The Choices of Use in Resource Management". Natural Resources journal, 1, #1, pp. 23-40.

The Treatment of Grey water Discharged from AL-Sadeer Hotel in Baghdad

Lec. Rana Jawad Kadhim

Assit. Lec. Faaeza Ahmed Abd Ulkareeam

Building and Construction Engineering Department, University of Technology,

Baghdad, Iraq

Abstract:-

This research aims to investigate the physical, chemical, and biological characteristics of grey water discharged from Al-Sadeer Hotel and propose feasible methods of treatment to render it fit for reuse.

Samples were directly collected from lavatory in Al- Sadeer Hotel starting from November 2013 and terminating in March 2014. The values of TSS for grey water had a mean of 391.1mg/L and a range of 200-670mg/L. The COD values ranged between 140-350mg/L with a mean of 230.35mg/L. The pH values averaged 7.28 with a range of 6.4 - 7.9. Total coliform counts generally were high and exceeded our dilution ranges ($>10^6$cfu/100mL).

The proposed treatment methods for grey water include: coagulation and flocculation, sedimentation, filtration and chlorination.

Ten runs were performed to treat the grey water. Polyelectrolyte of 10mg/L was as the optimum dose of a primary coagulant.

The results obtained from above experiments show removal efficiency of suspended solids of about (62.32 – 100%) and chemical oxygen demand of about (60.71 – 89.9%).

Physical, chemical, and biological parameters for the effluent of grey water from above treatment methods are: TSS (0-60mg/L), pH (7.5-8.3), COD (20-110mg/L), and TC (23-80cfu/100mL). These parameters satisfy for the agriculture reuse quality regulations set in the USEPA and Jordanian standards.

Key words:- grey water, AL-Sadeer Hotel, TSS, COD , Coliform counts , Polyelectrolyte.

Introduction:-

Grey water is the output from bathtubs, showers, sinks, floor drains and washing machines, which although no longer clean, is not as contaminated as toilet water. This water can be relatively easily treated on-site for reuse in non-potable contexts such as toilet flushing and garden irrigation. By intercepting grey water before it goes to the septic tank or the municipal wastewater system, and providing some treatment (in certain cases, no treatment may be required) the water may be reused to irrigate plants. With a little additional treatment, the water also may be used for toilet flushing [3].

Advantages and Disadvantages of Grey water Reuse

Advantages:

- Domestic grey water use is that it replaces or conserves potable water use, and can reduce the cost of potable water supply.
- Appropriately applied, grey water may contain nutrients (e.g. phosphorus and nitrogen from detergents), benefiting plant growth and resulting in more vigorous vegetation.
- Offers potential cost reductions for regional sewage treatment facilities, removing grey water from residential wastewater drainage to sewer decreases the flow through the sewer and the treatment plant and enables the existing infrastructure to service more connections.[12]
- Offers potential energy savings over centralized sewerage alternatives where grey water reuse applications require limited or no treatment, and where the grey water otherwise would have to be pumped to centralized treatment plant and treated.

- Grey water could supply most, if not all, of the irrigation needs of a domestic dwelling landscaped with vegetation in a semi-arid region.
- In addition to application for outside irrigation, grey water can also be used for toilet flushing, and if treated in advanced secondary or tertiary level, can also be used for a wide range of domestic water uses including bathing, showering, and laundry [16].

Disadvantages:

- Grey water may contain sodium and chloride, or other chemicals that can be harmful for some sensitive plant species. Additionally; grey water is alkaline (high pH) and shouldn't be used to irrigate acid-loving plants.[11]
- Concern regarding the public health implications of grey water reuse, and the need for research to determine the risks of grey water reuse.
- Cost of treatment and diversion/transfer pipe and pumps [2].

There are essentially three different grey water streams; they are [4].

- **Bathroom Grey water** (bath, basin, and shower) – contributes about 55% of the total grey water volume.
- **Laundry Grey water** – contributes about 34% of the total grey water volume..
- **Kitchen Grey water** – contributes about 11% of the total grey water volume.

Grey water can be contaminated in three ways due to the addition of waste materials: (1) contaminated by microorganisms which may be pathogenic, (2) chemically polluted by dissolved salts such as sodium, nitrogen, phosphates and chloride or by organic chemicals such as oils, fats, milk, soap and detergents, (3) physically polluted by particulates of dirt, food, lint, sand, etc [15].

The composition of grey water mainly depends on quality and type of available water supply and building activities. Cooking habits as well as amount and type of soap and detergent used significantly determine the level of contamination [17].

Physical Characteristics:- [10].

- Temperature
- Suspended Solids

Chemical Characteristics

- pH
- Biological and Chemical Oxygen Demand (BOD,COD)

Microbial Characteristics of Grey water

Fecal contamination of greywater, traditionally expressed by fecal indicators such as fecal coliforms, strongly depends on the age distribution of the building members. Average concentrations are reported to be around 10^3–10^6 cfu/100 ml. However, contamination can be as high as 10^7–10^8 cfu/100 ml in laundry or shower grey water**[**8**].**

Grey water Quantity

Grey water production is dependent on sanitary standards, awareness of the need for water conservation, and water availability. Grey water volume also varies with lifestyle, occupants' size, age of residents, eating habits and detergents used [17].

Various studies have indicated that the amount of grey water generated per person per day varies from 25 to 45 gallons (96 to 172 liters) [8].

When availability increases, the production of grey water increases, but it seldom exceeds 100 liters per person per day in developing countries. In industrialized countries, grey water production is normally in the range of 100-200 liters per person per day (the highest are reported from the USA and Canada) and sometimes exceeds 200 liters per person per day. In new housing developments in Europe, where awareness of the need for water conservation is promoted, the per capita daily grey water production is less than 100 liters [17].

Application Range and Quality Requirements for Grey water Reuse

grey water reuse and disposal applications have not received a great deal of consideration by regulatory authorities. Few countries have developed grey water-specific regulations, such as some north American states (Arizona, New Mexico, California, New Jersey), Australia (Queensland, New South Wales). Most countries

have no grey water-specific regulations but more general standards for residential wastewater management. [7].

treatment of the grey water is dependent on the intended use and the respective quality requirements. These quality requirements for process water should be oriented towards the intended use. In general, process water from grey water recycling plants should be hygienically /microbiologically safe, colorless and almost free from suspended matter. Even following several days of storage, no odor emissions from the process water should occur [9].

Based on scientific investigations, the quality aims have been tested and proved and are thus recommended for application in the areas of toilet flushing, laundry, agriculture, and direct discharge into surface waters.

Toilet Flushing

United States Environmental Protection Agency (USEPA) published "Guidelines for Water Quality" that describes the treatment stages, water quality requirements and monitoring tools. According to the EPA, reclaimed water used for toilet flushing should undergo eventual filtration and disinfection [15].

The EPA and European Union (EU) guidelines and Japanese targets for toilet flushing are shown in Table (1).

Table (1) Water quality requirements for toilet flushing.

Parameter	USEPA guidelines [15]	EU guidelines [9]	Japanese targets [14]
pH (unit)	6-9	--	5.8-8.6
BOD_5(mg/L)	<10	<5	--
Cl_2 residual	≥1	--	Detected
Total coliform (cfu/100ml)	--	<500	<1000
Fecal coliform (cfu/100mL)	0	<100	--

Laundry

The quality requirements for process water listed in Table (2) are recommended for laundry activities. Studies made with treated grey water, which fulfill the quality aims listed in Table (1), have also shown that from a hygienic / microbiological aspect, there is no difference between clothes washed with treated grey water and those washed with drinking water following drying [5].

Agricultural Reuse

The quality requirements for irrigation water are regulated by the USEPA (1992). These quality requirements refer to the hygienic, microbiological and some chemical aspects of irrigation water in agriculture, gardening, landscaping as well as in parks and sport facilities [6].

Table (3) provides a summary of water quality parameters of concern with respect to their significance in water reuse systems, as well as approximate ranges of each parameter in raw grey water and reclaimed water.

Table (2) Summary of water reuses standards in the United States and some Arab Countries:

Country	Ref.	Type of use	pH (unit)	TSS (mg/L)	BOD_5 (mg/L)	COD (mg/L)	Cl_2 residual (mg/L)	MPN coliforms (cfu/100mL)
U.S.A	(15)	food crops, surface irrigation and orchards	6-9	<30	<30	--	1	<200
Jordan	(13)	crops eaten cooked	6-9	50	30	100	0.5-1	200
Palestine	(18)	fodder & landscape irrigation	6-9	50	60	200	--	1000
Kuwait	(15)	crops eaten raw	-	10	10	40	1	100
Oman	(15)	Surface irrigation	6-9	30	20	--	--	<1000

Table (3) Summary of Water Quality Parameters of Concern for Water Reuse [1and 15]

Parameter	significance for water reuse	Typical range of bathroom water	Treatment goal in reclaimed water
pH	Measure of the alkalinity-acidity of water that may have negative effects on plants and soil structure	6.1-8.4	6-9
TSS	Measure of particles. Can be related to microbial contamination. Can interfere with disinfection. Clogging irrigation system. Clogging plumbing reuse system.	(34-380) mg/L	(<5-30) mg/L
BOD_5	Organic substrate for microbial growth. Can favor bacterial re-growth in reuse systems and microbial fouling.	(45-330) mg/L	(<10-45) mg/L
COD		(90-660) mg/L	(<20-90) mg/L
Total coliforms	Measure of risk of infection due to potential presence of pathogens. Can favor bio-fouling in storage tank.	(10^4-10^7) cfu/100mL	(<1-200) cfu/100mL
Chlorine residual	To prevent bacterial re-growth. Excessive amount of free chlorine can damage some sensitive crops.	0	(0.5-1) mg/L

Results and Discussion

Research aims at investigating the physical, chemical, and biological characteristics of grey water discharged from AL-Sadeer hotel, then feasible methods of treatment to render it fit for reuse will be identified. the experimental results of grey water characterization, laboratory tests, and pilot plant tests and compares the effluent of pilot plant with water reuse standards by using graphical representation. Grey water samples for the characterization study were collected on a weekly basis starting from November 2013 and terminating in March 2014. Samples were collected from lavatory in maintenance department of the hotel. At the first stage, (where the laboratory tests were carried out on raw grey water only) grey water samples were taken immediately after the grey water producing event, kept in wet ice at 4°C during transportation and delivered to the testing laboratories within 24 hours. Samples were marked using waterproof labels and noted in hard-cover. Twenty liters sample was collected from the site in plastic container in the second stage. In this stage the laboratory tests were achieved on both raw and treated grey water. Sample was transported to the laboratory during half-hour. Once in the laboratory, a portion was analyzed immediately for total coliforms, as well pH. If the remainder of the sample could not be analyzed immediately, the sample was kept at 4^oC for further analysis for COD and TSS. Laboratory tests included:

1. pH was determined with pH meter instrument using standard calibration solutions.
2. Total suspended solids (TSS): using Standard Method for Examination of Water and Wastewater, twentieth edition, according to 2540 D [American Public Health Association].
3. COD: using Standard Method**,** twentieth edition, according to 5220 B
4. Residual Chlorine: using Standard Method, twentieth edition, according to 4500-Cl
5. Total Coliforms: using Standard Method, twentieth edition, according to 9221B and 9221C

Ten runs were performed to treat the grey water to render it fit for agriculture reuse. It was treated by filtration only in two runs and treated by coagulation and flocculation, sedimentation, and filtration in four runs. Chlorination was added to treatment processes in the last four runs.

pH Values

Values for pH a range of 6.4 to 7.9. The mean ranges likely reflect the use of pH water. Fig. (1) shows the time plot pH values

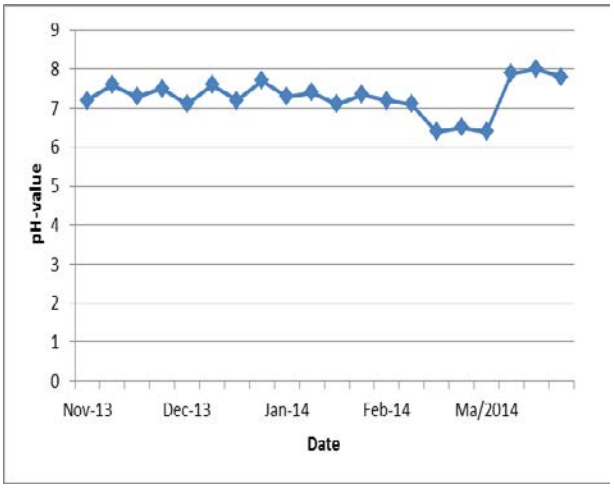

Fig. (1) pH variation with Date.

Total Suspended Solids (TSS)

Temporal fluctuations in total suspended solids (TSS) are presented in Fig. (2). The TSS values (range: 200-670mg/L). This Fig. shows relatively high TSS values over the winter period which may be due to small grey water quantity discharged from the source. Typical grey water TSS values as reported in table 3, range from 34-380 mg/L Thus, the range of TSS values was higher than typical range of grey water.

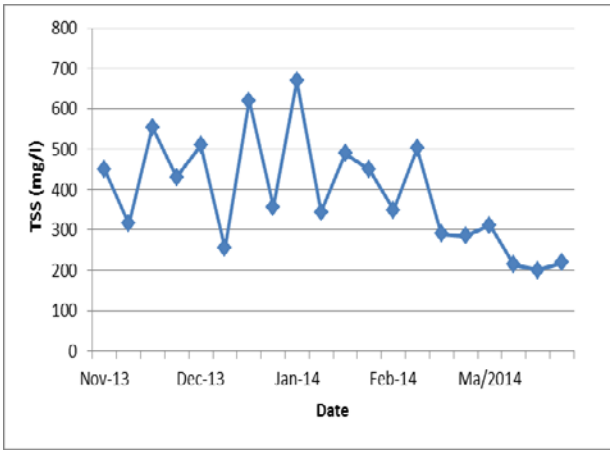

Fig :- (2) Time plot total suspended solids (TSS).

Chemical Oxygen Demand (COD)

Fig. (3) shows the fluctuation of the chemical oxygen demand (COD) over the entire monitoring period. The mean of COD values were230.35 mg/L (range: 140-350 mg/L). Typical COD values for grey water as reported in table 3, range from 90-660 mg/L. Therefore, the COD values can be considered within the typical range.

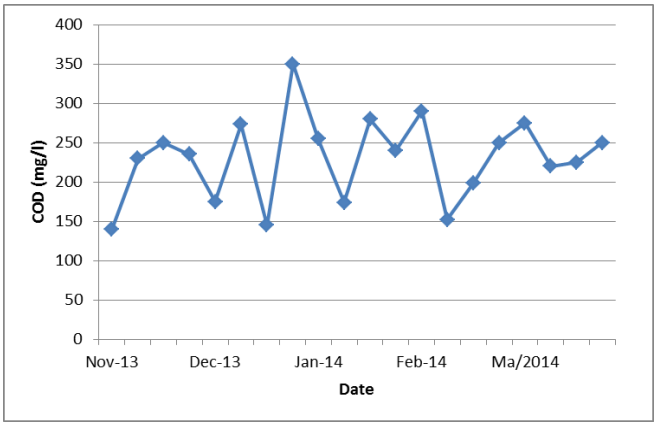

Fig. (3) Time plot chemical oxygen demand (COD).

Total Coliforms (TC)

Monthly sampling for coliforms (just in Feb.. and March for 2014) included test for total coliforms (TC). Values for TC generally exceeded maximum countable colonies (TNTC means Too Numerous to Count) and often exceeded $>10^6$ cfu/100mL. Grey water samples typically ranged between 10^4-10^7 TC per 100mL (Table 3). The two results of total coliforms test are shown in Fig. (4).

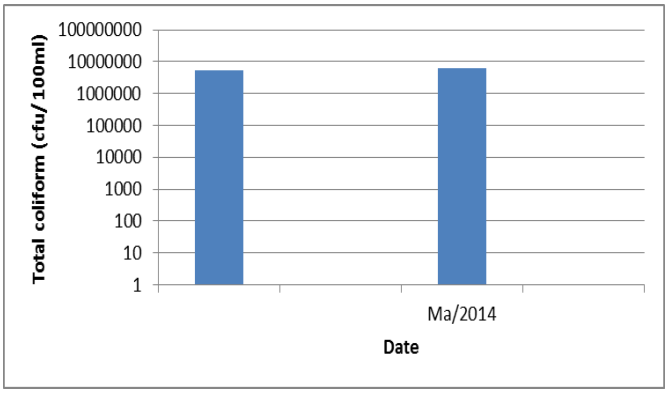

Fig. (4) Total coliforms content in grey water collected in two months

The Pilot Plant Tests

The characteristics of grey water used in the pilot plant. The optimum chemical dose of

coagulant (cationic polyelectrolyte) obtained from the jar test was 10mg/L.

pH-value

Upper and lower limits of Jordanian effluent standards concerning pH are the same limits for the USEPA effluent standard. The pH values of effluent of grey water range from 7.5 to 8.3 units. This refers to nonexistence of great variations in the pH values.

Fig. (5) shows that the pH values for all results of pilot plant fall between the recommended standard ranges of 6-9.

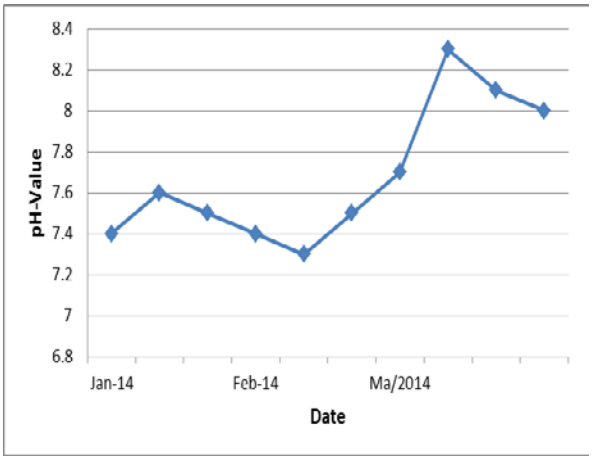

Fig. (5) Comparison between the pH values of effluent and pH effluent standards

Total Suspended Solids (TSS)

Fig. (6) compares between the effluent of pilot plant on one side and Jordanian and the USEPA standards concerning TSS concentrations on the other side.

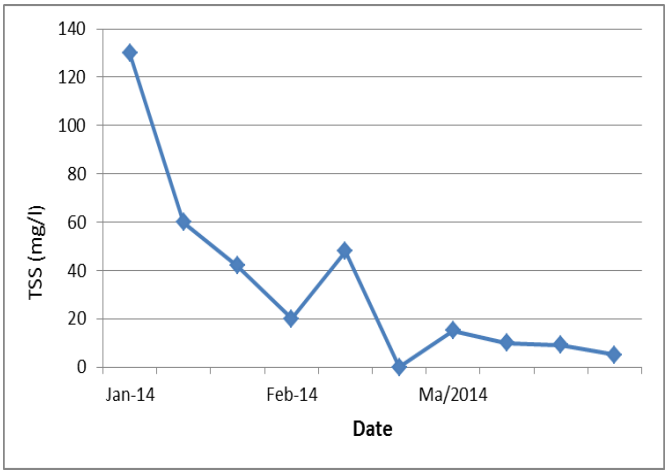

Fig. (6) Comparison between TSS values of pilot plant and TSS values of Jordanian and USEPA effluent standards.

Chemical Oxygen Demand (COD)

Fig. (7),it can be observed that all results of chemical oxygen demand (COD) of the reclaimed water are below the limit of Jordanian effluent standard for irrigation reuse (100mg/L) except the first run, which exhibited a consistently higher COD. This was the property with a treating greywater for these runs by filtration only without addition of polyelectrolyte to the influent of greywater. But when polyelectrolyte was added to the influent at 5mg/L and 10mg/L as coagulant dose, the reduction in COD concentration happened, and the effluent agrees with water reuse standard.

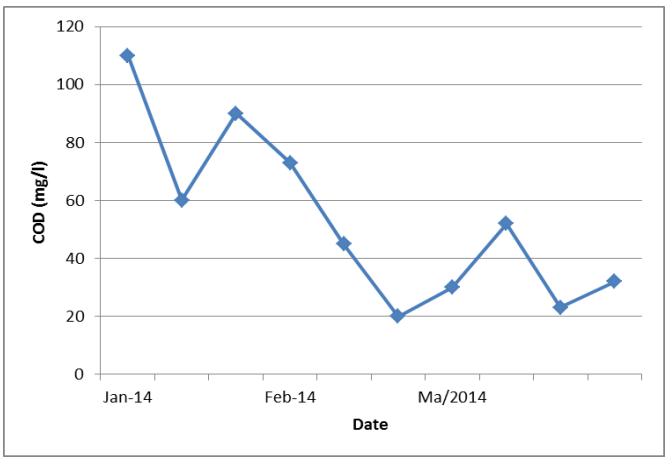

Fig. (7) Comparison between COD values of pilot plant and COD Jordanian effluent standard for irrigation water.

Total Coliforms (TC)

Reclaimed water sampling was carried out on a four runs for total coliforms only as indicator of organism analysis in effluent of grey water. The biggest risk to health from the recycling of grey water is from the presence of biological contaminants, rather than chemical parameters. Fig. (8) illustrates that the total coliforms range of (23-80cfu/100mL), and the USEPA and Jordanian standards for total coliforms in reclaimed water are less than 200cfu/100mL. Therefore, all the samples fell well within standard specifications. These results refer to the good disinfection of grey water that was carried out by adding calcium hypochlorite $Ca(OCl)_2$.

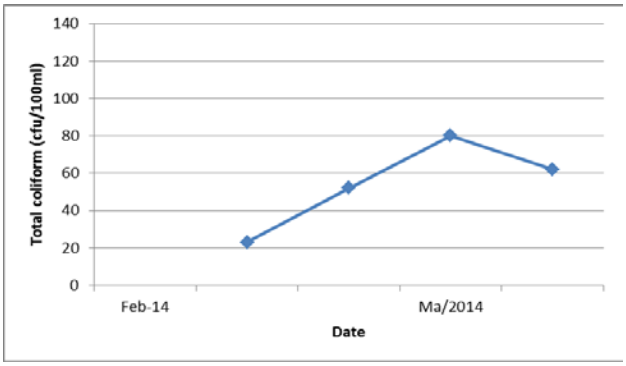

Fig. (8) Comparison between total coliforms of pilot plant and the USEPA and Jordanian standards for total coliforms in reclaimed water.

Conclusions:-

1. Values determined in this paper indicate that grey water quality shows low variability, except in TSS. The parameters of influent grey water are: TSS (200-670mg/L), pH (6.4-7.9), COD (140-350mg/L), and TC (5.2-6.1 log number/100mL).
2. The results obtained from experiments show that the removal efficiency of suspended solids is about (62.32 – 100%) and chemical oxygen demand about (60.71 – 89.9%) by using 10mg/L of polyelectrolyte as the optimum dose of a coagulant and when sand depth in filter is equal to 60cm.
3. Physical, chemical, and biological parameters for the effluent of grey water are: TSS (0-60mg/L), pH (7.5-8.3), COD (20-110mg/L), and TC (23-80cfu/100mL). These parameters are acceptable when compared with standard wastewater irrigation guidelines (eg., USEPA and Jordanian standards).
4. Filtration of grey water is not enough to make it meet the agriculture reuse quality regulations. But coagulation and flocculation (by using polyelectrolyte), sedimentation, filtration, and chlorination are adequate treatment processes to use grey water for irrigation.

References:-

1- Boal D. Christova, P. Lechte and R. Shipton, (1995), "Installation and Evaluation of Domestic Greywater Reuse Systems", Victoria University of Technology, Victoria, Australia**.**

2- Capital Regional District (CRD 2004), "Greywater Reuse Study Report", Program report FE-88 SCIRO Molecular science.

3- Center for the Study of the Built Environment (CSBE, 2003) "Greywater Reuse in Other Countries and Its Applicability to Jordon", Project funded by Ministry of Planning in Jordon.

4- Department of Health in Western Australia, (2005), "Code of Practice for The Reuse of Greywater in Western Australia", published by the website (www.health.wa.gov.au).

5- Friedler E., R. Kovalio and N. I. Galil, (2005), "On-site Greywater Treatment and Reuse in Multi-story Buildings", Journal of Water Science and Technology, Vol.51, No.10.

6- INWRDAM, (2003), "Greywater Treatment and Reuse", Tufileh, Jordan, Inter-Islamic Network on Water Resources Development and Management (INWRDAM), published by the Ministry of Planning in Jordan.

7- Jefferson, B., A. Palmer, P. Jeffrey, R. Stuetz and S. Judd, (2004) "Greywater Characterizations and Its Impact on The Selection and Operation of Technologies for Urban Reuse", Journal of Water Science and Technology, Vol. 50, No.2.

8- Jenkins Joseph C., (2005), "The Humanure Handbook", A guide to compositing human manure, published by Jenkins Joseph Inc., 3th edition.

9- Karl, Friedrich, (2005),"Greywater Recycling", Editing by fbr-expert group, information sheet H201, published by the website (www.fbr.de),1th edition.

10-Morel, A. and Stefan Diener, (2006), "Greywater Management in Low and Middle-Income Countries," Swiss Federal Institute of Aquatic Science and Technology, Switzerland.
11-NSW, (2000), "Greywater Reuse in Sewered Single Domestic Premises", New South Wales, Australia.
12-Pilipenko, Polina, (2007), "Cationic Polyelectrolytes as Primary Coagulants for Municipal Wastewater Treatment", Thesis for the degree doctor engineering, Norwegian University of Science and Technology, Faculty of Engineering Science and Technology, Department of Hydraulic and Environmental Engineering.
13-Scott, C.A., N.I. Faruqui, and L. Raschid-Sally, (2005), "Wastewater Use in Irrigated Agriculture". International Water Management Institute (IWMI), Patancheru, India, and International Development Research Centre (IDRC), Ottawa, Canada.
14-Suzuki Yutaka, Masashi Ogoshi, Hiroki Yamagata, Masaaki Ozaki, and Takashi Asano, (2003). "Large Area and On-site Water Reuse in Japan", Public Works Research Institute, Minamihara , Tsukuba, Japan.
15-USEPA (2004), "Guidelines for Water Reuse". U.S. Environmental Protection Agency report.
16-Veneman, P.L.M. and Bonnie Stewart, (2002), "Greywater Characterization and Treatment Efficiency", University of Massachusetts, State of Boston.
17-WHO (2006), "Excreta and Greywater Use in Agriculture", Guidelines for the safe use of wastewater, excreta and greywater, Vol.4.
18-Zimmo Omar and Gigi Petta, (2005), "Prospects of Efficient Wastewater Management and Water Reuse in Palestine", Birzeit University, West Bank-Palestine.

Upgrading of an Existing Iraqi Sewage Treatment Plant to Achieve Nitrogen and Phosphorus Removal

Dr. Aumar N. Al-Nakeeb, Walaa K. Al-Janabi and Moaid M. Ismaeel

***Abstract*— A typical design accomplished by German consultants (H&F) had been considered for many Iraqi wastewater treatment plants in eighties. This design was analyzed by using GPS-X 6.1 software to evaluate nitrogen and phosphorus removal and the results show that the effluent quality exceeds the new acceptation limits for streams disposal. Therefore, two sets of modifications examined by using the same software to upgrade the removal efficiency for both nitrogen and phosphorus within biological treatment units. The results show the ability to achieve nitrogen removal biologically while the accepted limit of phosphorus could not reached biologically because of limited available space.**

***Key words* — Wastewater; Treatment Plant; BNR; ASM.**

I. Introduction

Upgrading the existing Sewage Treatment Plants (STP) may be necessary to meet the recent more restricted effluent quality. The inability of STP may result from inadequate plant design capacity and increased hydraulic or organic loading rate caused by a change in wastewater flow or effluent characteristics [1], [2], [3], [4]. As the space available at a STP is limited, processes are required which can accommodate the need for increased treatment capacity and/or improvement of effluent quality without requiring much more space [5].

In many cases, the upgrade of STP by expanding the reactor volume is either impossible or economically not feasible, because of not only the high construction cost of the new reaction tanks, but also the higher operational costs caused by aeration and carbon demand at conventional nitrification / denitrification [6]. When untreated wastewater arrives to the plant, most nitrogen is present in the ammonia form, which can be removed in a two-step procedure. In the first step ammonia is oxidized to nitrate in aerobic conditions, this process is called nitrification and can be described by the following simplified chemical reacting scheme [7]:

$$NH_4^+ + 1.5O_2 \rightarrow NO_2^- + H_2O + 2H^+ \quad (1)$$

$$NO_2^- + 0.5O_2 \rightarrow NO_3^- \quad (2)$$

That is, the ammonia is firstly oxidized to nitrite and then to nitrate. The bacteria involved in these reactions require oxygen to perform the process. The nitrates are then converted to nitrogen by denitrification. This process occurs in anoxic environment, i.e., oxygen is mainly present as nitrate and the responsible bacteria respires the oxygen as nitrate instead of dissolved oxygen. The following simplified reaction scheme shows the basic process [7]:

$$2NO_3^- + 2H^+ \rightarrow N_2 + H_2O + 2.5O_2 \quad (3)$$

By nitrification and denitrification, nitrogen is removed from wastewater biologically. This means that anoxic zones are necessary for denitrification, whereas aerobic zones are necessary for nitrification. Anoxic zones can be placed either at the beginning of the tank (pre-denitrification) or at the end of the process (post-denitrification). [7]

In the last few years, there has been considerable progress in the area of mathematical modeling of sewage treatment processes. The turning point is undoubtedly the release of IAWQ Activated Sludge Model No.1. [8]. In fact, it is now possible to simulate the entire sewage works from head works to the effluent disinfection. A significant part of coding is spent on developing routines for file I/O, menus, graphics and numerical solutions. To alleviate these problems and to bring efficient, high-power computing into the reach of practicing engineers, the General Purpose Simulator (GPS-X) was created utilizing the new low-cost, high-power workstation platform which has become available in the last few years. GPS-X is both a modeling environment for any type of dynamic process, and an extensive, modifiable library of most of the process models available today in this filed.

GPS-X considered several models to describe the biological process in the activated sludge plant. The developments in the family proposed by the International Water Association (IWA) represent a major contribute:

- ASM1, the Activated Sludge Process Model No.1 [9] can be considered as the reference model since this model triggered the general acceptance of the biological process modeling. ASM1 was primarily developed to describe the removal of

Dr. Aumar N. Al-Nakeeb is with the Building & Construction Engineering Department, University of Technology (UOT), Baghdad, Iraq. Phone: +964-770-375-1751; e-mail: aumar.alnakeeb@gmail.com.

Walaa K. Al-Janabi is with the Building & Construction Engineering Department, University of Technology (UOT), Baghdad, Iraq. e-mail: walaakll@yahoo.com.

Moaid M. Ismaeel is with the Building & Construction Engineering Department, University of Technology (UOT), Baghdad, Iraq. e-mail: moaid.mohammed60@yahoo.com.

organic compounds and nitrogen with simultaneous consumption of oxygen and nitrate as electron acceptor. The model, furthermore, aims at yielding a good description of the sludge production. COD (Chemical Oxygen Demand) was adopted as the measure of the concentration of organic matter.

- ASM2, the Activated Sludge Process Model No.2 [10] extends the capabilities of the ASM1 to the description of bio-phosphorus.
- ASM2d, the Activated Sludge Process Model No.2d [11] is built on the ASM2 model adding the denitrifying activity of PAOs1 to allow a better description of the dynamics of phosphate and nitrate.
- ASM3, the Activated Sludge Process Model No.3 [12] was also developed for biological nitrogen removal, with basically the same goal as the ASM1. The major difference between the ASM1 and the ASM3 models is that the latter recognizes the importance of storage polymers in the heterotrophic activated sludge conversion.

All of these models have been used to reach the aim of this study to verify possible solutions to upgrade the existing design of Al-Mada'in Sewage Treatment Plant (STP) to achieve nitrogen and phosphorus removal from the treated wastewater.

II. STP DESIGNED PROCESS DESCRIPTION

Al-Mada'in is one of the Bagdad governorate cities, have a design population of (100,000 capita), located about (30 km) in the south east of Baghdad city on the east bank of Tigress river. The STP had been under construction during preparing of this study in November 2012. The designed and under construction STP treatment units are described in GPS-X 6.1 diagram that shown in figure (1), basic design data are shown in table (1) and other design data are shown as GPS-X 6.1 plate in figure (2) (where principle data have been highlighted).

TABLE 1

Basic design data of Al-Mada'in STP.

Parameter	Unit	Influent	Effluent
Dry Weather Flow Average Peak Minimum	m^3/h	 828 1,904 343	
Wastewater generation rate per capita	L/capita/d	250	
TSS rate per capita	g/capita/d	90	
BOD_5 rate per capita	g/capita/d	60	
Equivalent Inhabitants		79,480	
TSS	mg/L	360	30
COD	mg/L	520	100
BOD_5	mg/L	240	20
TKN – TN	mg/L	40	12
NH3-N	mg/L	20	
NO3-N	mg/L	< 1.0	
TP	mg/L	8	2
pH		6.5 – 8.0	7.0 – 8.0

Parameter	Unit	Influent	Effluent
Wastewater Temp.: Design Maximum Minimum	°C	 20 35 15	

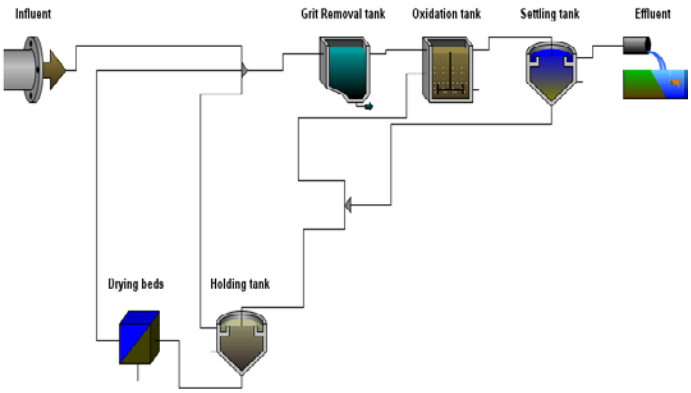

Fig.1. GPS-X 6.1 modelling and simulation of Al-Mada'in designed STP treatment units.

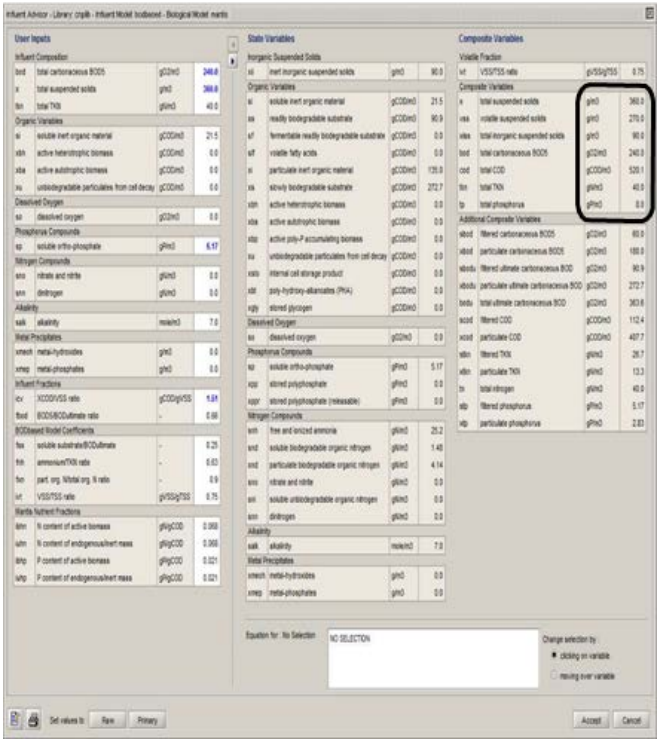

Fig. 2. GPS-X 6.1 plate of the STP design data.

III. ORIGINAL DESIGN SIMULATION

Peak flow has been indicated as hourly flow because it has been considered as the peak flow reaching the plant only during for few hours a day. Figure (3) shows the estimated daily variation of flow issued according to standard curves [7].The liquid temperature of sewage, in Iraq, during the year is expected to be as shown in figure (4).

The suitability of the original design has been verified for the Nitrogen and Phosphorus removal in according to effluent

limit by using GPS-X 6.1 software. The design STP consists of (4) aeration basins, each in capacity of (2,080 m^3), for a total available volume of (8,320 m^3). Each of them equipped with (4) surface aerators with installed power of (22 kW) per each, and no other equipment are previewed for this verification process. Peak values of the simulation results correspond to the effluent of a typical day after (120) days of process stabilization have been shown in table (2) and presented in figure (5), in which the peak values correspond to peak flow during the day. Results show that TSS effluent value is always very close to the limits (30 mg/L) and values related to total Nitrogen and Total phosphorus are always higher than accepted limits.

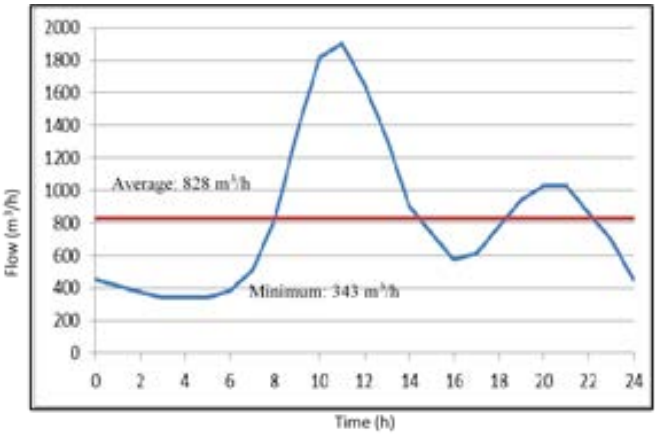

Fig. 3. Estimated daily variation of influent flow to the STP.

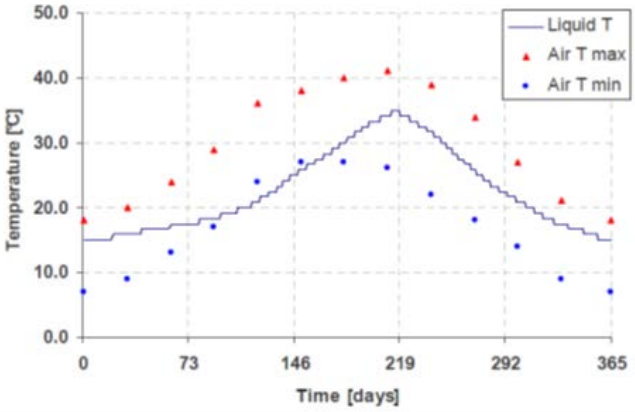

Fig. 4. Sewage liquid temperature during the year.

TABLE 2

Peak values of GPS-X simulation results for some effluent parameters with variable temperatures of original STP.

Parameter (mg/L)		GPS-X Simulation at			
	Treated effluent limits	15°C	20°C	30°C	35°C
TSS	30	28.4	28.2	28.0	28.0
COD	100	54.1	53.2	51.8	51.2
BOD_5	20	8.98	8.05	6.48	5.79
Total N	12	20.0	20.1	20.2	20.2
Total P	2	3.46	3.70	3.97	4.06

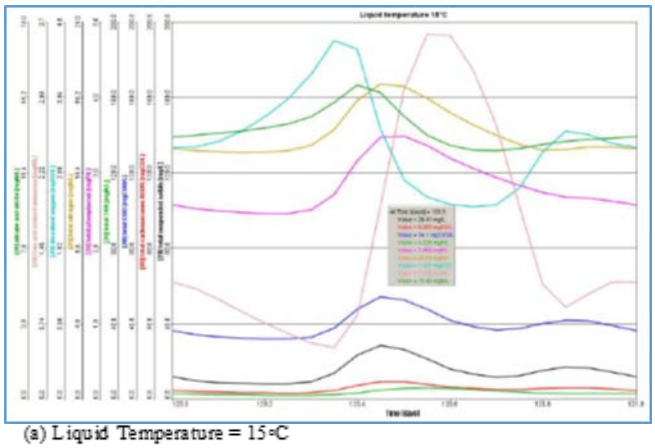

(a) Liquid Temperature = 15◦C

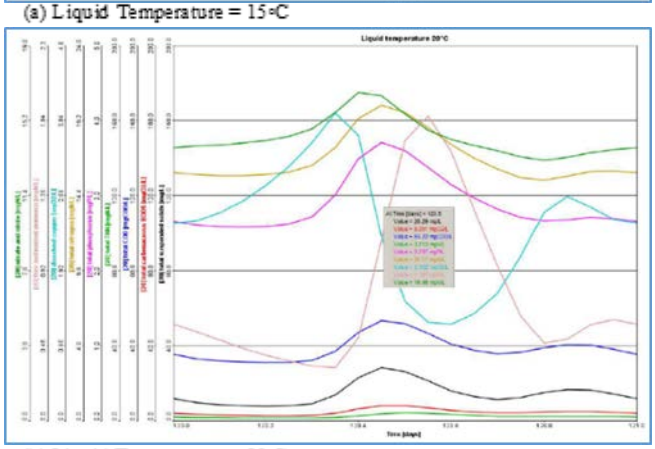

(b) Liquid Temperature = 20◦C

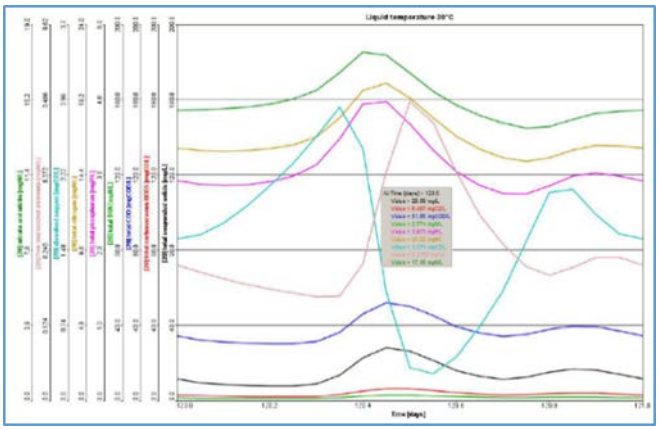

(c) Liquid Temperature = 30◦C

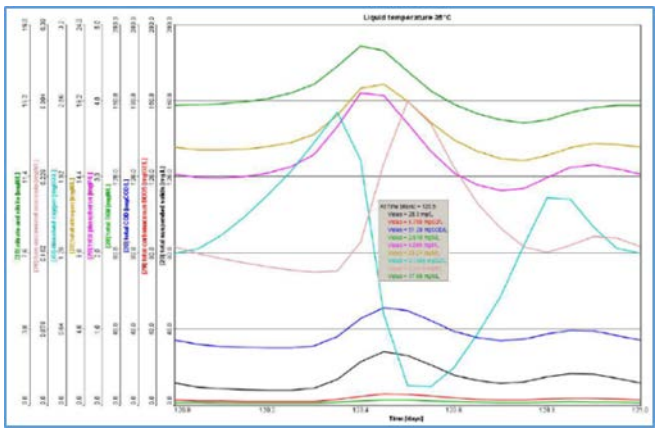

(d) Liquid Temperature = 35◦C

Fig. 5. Designed effluent parameters with variable temp.

IV. PROPOSED DESIGN MODIFICATIONS

Due to the results obtained, the original design of aeration basins is not suitable to achieve acceptable Nitrogen and Phosphorus removal. Therefore different solution has been studied to determine solution according to the guideline that minimum modifications must be done respect to the original design. The solution is summarized in the following two sets of modifications:

A. FIRST SET OF MODIFICATIONS

1) Keep the same plant dimension of the original aeration basins for the new biological basins,
2) Decrease the dimensions of the inclined wall at the bottom of the basin from 2×2m to 1×1m in order to increase the total usable volume from (8,320 m^3) to (9,128 m3) (+9.7%),
3) Increase the water depth in the oxidation basins from (3.0 m) to (3.23 m), keeping the same absolute level of the foundations (27.85 m) and increasing the top water level (from 30.85 m to 31.08 m). The usable volume will be increased to (9,849 m^3) (additional +8.7%, for a total of+18.4% respect to the original design),
4) Keep a total of (16) surface aerators (4 per each nitrification basin), checking their sizing according to oxygen requirement,
5) Check the obtained concentration of Phosphorus at the outlet and take further decisions according to checked value,
6) Increase the side water depth in the secondary clarifiers in order to increase the efficiency of clarification and consequently reducing the TSS in the effluent. In total the water depth in the secondary clarifier will be increased by 0.25 m (from 2.55 m to 2.8 m). All these solutions will surely reduce the TSS in the effluent.
7) Raising the water level in the inlet works by 0.25m to satisfy the hydraulic requirements.

The biological treatment of municipal wastewater is typically based on the activated sludge process, i.e. on the use of suspended biomass capable to oxidize organic compound. Organic nitrogen and ammonium can be also oxidized to nitrate (nitrification process) by ensuring additional aeration capacity and the adequate sludge retention time for the selection of slow growing nitrifying biomass. The proposed increase of volume of aeration tank will surely increase the performance of Nitrogen removal. Results obtained from GPS-X simulation by using the same plant layout which shown in figure (1) are illustrated in table (3) and figure (6).

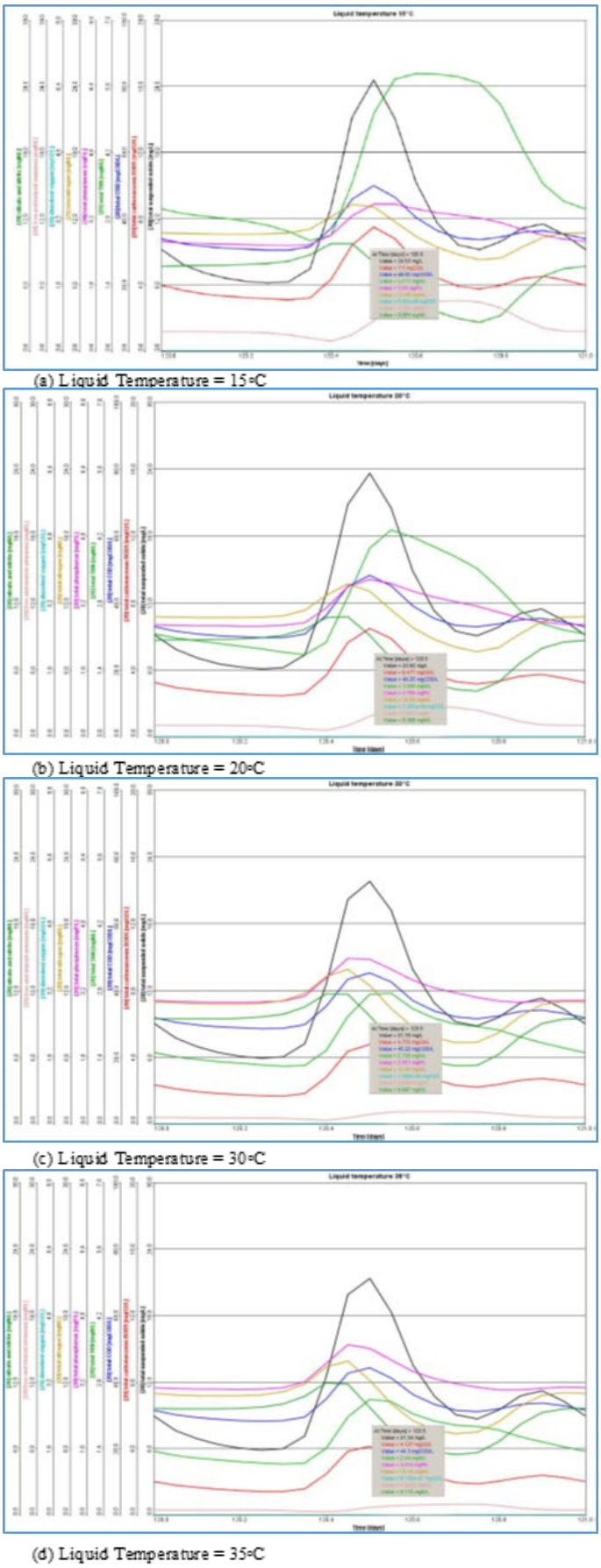

Fig. 6. Modified effluent parameters with variable temp.

TABLE 3

Peak values of GPS-X simulation results for some effluent parameters with variable temperatures of first modified design layout.

Parameter (mg/L)		GPS-X Simulation at			
	Treated effluent limits	15°C	20°C	30°C	35°C
TSS	30	24.5	23.6	21.7	21.3
COD	100	49.9	48.2	45.2	44.3
BOD_5	20	7.50	6.47	4.77	4.12
Total N	12	13.0	13.0	12.4	12.1
Total P	2	3.55	3.76	3.95	4.01

B. SECOND SET OF MODIFICATIONS

In order to reduce the concentration of nitrogen in the treated effluent, it is possible to introduce an anoxic tank in which the nitrate will be used instead of oxygen for the oxidation of readily biodegradable organic matter (denitrification process). The nitrate will be consequently converted to nitrogen gas and released to the atmosphere. For an optimal denitrification process, the presence of readily biodegradable COD is mandatory and can be satisfied by internal sources. For this project, the introduction of a pre-denitrification step has been adopted, which is based on the utilization of readily biodegradable matter coming with the influent.

During normal biological degradation processes marginal amounts of phosphorus are used for the biomass growth, concentration of Phosphorus at the outlet will be checked before taking further decisions. Accordingly the following further modifications have been considered:

1) Separate each aeration basin in two adjacent zones, the first of pre-denitrification (volume equal to one fourth of volume) and the second nitrification (three fourth of volume),
2) Make use of the existing side feeding channels for the nitrate recirculation required in pre-denitrification.
3) Add a total of (12) submersible recirculation pumps (2 duty + 1 stand-by per each aeration basin) in order to push the nitrate flow from the side channel into the denitrification tank, complete with check valve, fixing and lifting system for maintenance,
4) Add a total of (4) vertical mixers for denitrification (one per each tank) in order to keep in suspension the mixed liquor in the denitrification tank,
5) Increasing the capacity of each surface aerator to 30 kW to compensate for the reduction in their number to 9.

The design summarized in the figure (7) has been modeled in the GPS-X 6.1 software. Table (4) summarized the main design value that presented in the proposed layout showed in figure (8). Simulation results correspond to the effluent of a typical day after (120) days of process stabilization have been presented in figure (9).

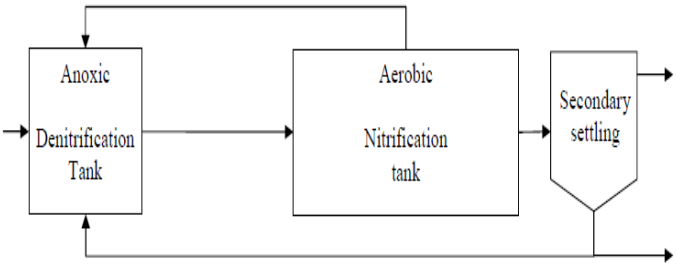

Fig. 7. Proposed modification diagram for Nitrification – Denitrification process.

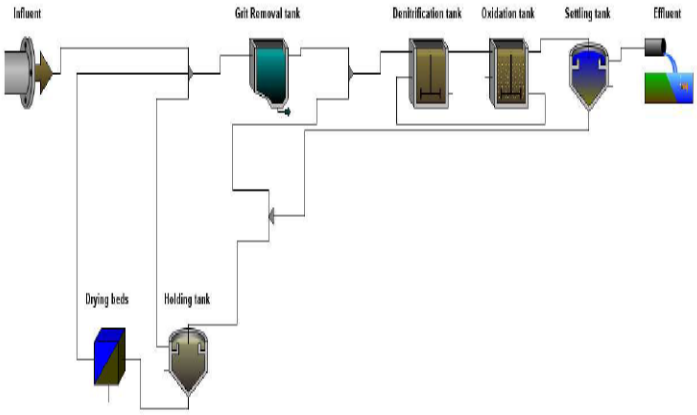

Figure. 8. GPS-X 6.1 modeling and simulation for proposed design layout.

The obtained results show that all values are under limits except values related to Phosphorus. By considering the small space available for the biological tank and the civil works already started at site, the obtained results can be considered the best that could be done with small modifications to the original design. In addition, due to big dilution in the receiving water body which is Tigris River, the exceeding of the average and peak values of effluent Phosphorus limit of (2.0 mg/L) can be accepted.

If the proposed solution could not be considered acceptable, then bigger volumes of biological tanks will be needed (with big changes respect to the original design and available area), or chemical precipitation of Phosphorus will be needed by using ALUM preparation and dosing system.

The design parameters of modified treatment units have been discussed below:

TABLE 4

Main Modified Design Parameters.

Design Parameter	Unit	Value
Total Basin Volume	m^3	9,849
Nitrification tank Volume	m^3	2,462
Denitrification tank Volume	m^3	7,387
HRT tot	H	11.9
MLSS	kg/m^3	4
Sludge recycle ratio		1
Nitrate recycle ratio		2

TABLE 5

Peak values of GPS-X simulation results for some effluent parameters with variable temperatures of second modified design layout.

Parameter (mg/L)		GPS-X Simulation at			
	Treated effluent limits	15°C	20°C	30°C	35°C
TSS	30	25.3	24.4	22.5	21.7
COD	100	51.0	49.2	46.0	44.7
BOD_5	20	7.91	6.73	4.95	4.21
Total N	12	6.73	5.99	4.99	4.69
Total P	2	3.33	3.69	4.01	4.09

- The simulations in GPS-X have been run considered the simultaneous operation of the (16) surface aerators, with installed and adsorbed power, and oxygen transfer capacity per each are (22 kW), (17 kW), (39.1 kgO_2/h) respectively. The total oxygen transfer capacity is (625.6 kgO_2/h) that also guarantee the oxygen transfer requirement calculated during the peak loadings of (424 kgO_2/h). The presence of still a small amount of dissolved oxygen in the effluent, together with low value of ammonia nitrogen confirms that the transferred oxygen is enough to perform a good nitrification.
- The run considered the nitrate recirculation rate equal to (200%) of average flow rate, therefore recirculation will be performed by means of (8) duty pumps + (4) stand-by, each with pumping capacity of (210 m^3/h).
- The Simulations of two secondary clarifiers with (30 m) diameter and water height increased to 2.8 m confirm that there is no accumulation of suspended solids in the secondary settling tank and the value of TSS in the effluent is always under the admissible limits.
- For the recycled activated sludge (RAS), the proposed pumps (2 duty + 1 in standby, each with (450m^3/h of pumping capacity) will allow to obtain the designed recycling ratio of (828 m^3/h) (100% of the average influent flow) with a good safety margin.
- The wasted activated sludge (WAS) will be transferred to the holding tanks by gravity. Considering the sludge production of (3400 kg/d) and estimating a concentration of (8 kg/m^3) at the bottom of the secondary clarifier, an average WAS flow rate of (425 m^3/d) will be transferred to the holding tanks.
- The wasted activated sludge will go by gravity to the two holding tanks, each in capacity of (700 m^3), for thickening prior to the discharge on the drying beds.

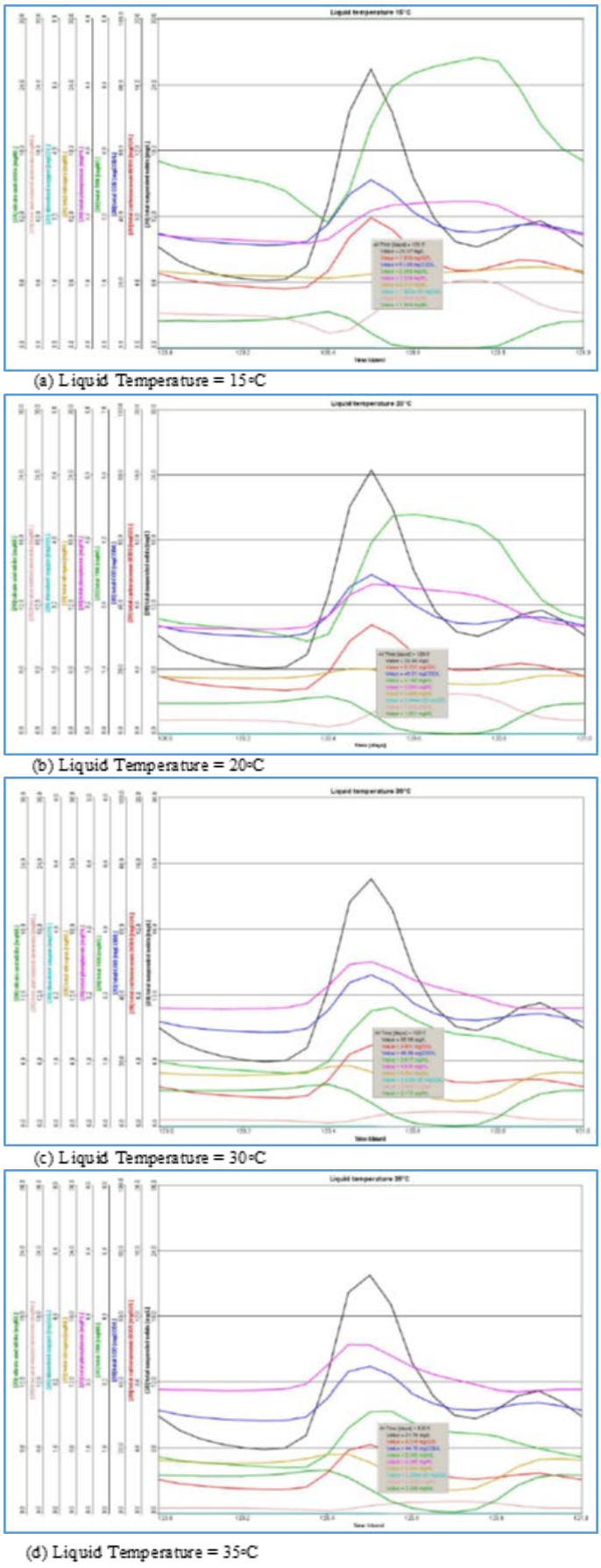

Fig. 9. Modified effluent parameters with variable temp.

V. CONCLUSION

Due to the fact that the original design of aeration tanks is not suitable to achieve acceptable Nitrogen and Phosphorus removal, few small modifications have been proposed in order to reach acceptable values of Nitrogen and Phosphorus removal efficiency, together with the guideline to make as much as possible smallest variations to the original civil works already started at site.

Results found with GPS-X (Hydromantis) simulation software are good enough to consider the proposed modification acceptable, in fact, Nitrogen effluent values are always under limits and, notwithstanding the average and peak values of effluent Phosphorus are a little exceeding the limit of 2 mg/L, due to the big dilution of Phosphorus inside the receiving river.

If the proposed solution could not be considered acceptable, then bigger volumes of biological tanks will be needed (with big changes respect to the original design and available area), or chemical precipitation of Phosphorus will be needed by using ALUM preparation and dosing system.

REFERENCES

[1] Bub, S., Einfeldt, J., Günter, H., Werner, T. Upgrading of wastewater treatment plants to achieve advanced standards concerning nutrient removal. Water Sci. Technol., 1994, 29 (12): 49-58.

[2] Qasim, S. R. Wastewater Treatment Plants, Planning, Design and Operation, 2nd Ed., Technomic Publishing Co., Lancaster, PA, 1999.

[3] WEF. Upgrading and Retrofitting Water and Wastewater Treatment Plants. McGraw-Hill, N. Y. USA, 2005.

[4] Mahvi, A. H., Rahimi, Y. and Mesdaghinia, A. R. Assessment and upgrading of Khoy wastewater treatment plant. Pak. J. Biol. Sci., 2006, 9 (7): 1276-1281.

[5] Brinch, P. P., Rindel, K. and Kalb, K. Upgrading to nutrient removal by means of internal carbon from sludge hydrolysis. Water Sci. Technol., 1994, 29 (12): 31-40.

[6] Rosenwinkel K.-H, Beier M., Phan L.-C and Hartwig P. Conventional and Advance Technologies for Biological Nitrogen Removal in Europe. Water Practice & Technology, 2009, Vol 4 No 1, IWA doi: 10.2166/WPT.2009.014.

[7] Meltcalf & Eddy Inc. Wastewater Engineering: treatment, disposal and reuse. McGraw Hill, 2002.

[8] Henze, M., Grady Jr., C.P.L., Gujer, W., Marais, G.v.R., and Matsuo, T. Activated sludge Modle No.1. IAWPRC Task Group on Mathematical Modeling for Design and Operation of Biological Wastewater Treatment, IAWPRC, London, England, 1987.

[9] Henze, M., Grady Jr., C.P.L., Gujer, W., Marais, G.v.R., and Matsuo, T. Activated Sludge Process Model No. 1. Scientific and Technical Report 1, IAWQ. London, UK, 1987.

[10] Henze, M., Grady Jr., C.P.L., Gujer, W., Marais, G.v.R., and Matsuo, T. Activated Sludge Process Model No. 2. Scientific and Technical Report 3, IAWQ. London, UK, 1995.

[11] Henze, M., Gujer, W., Mino, T., Matsuo, T. M., Wetzel, C., Marais, G. V. R. and van Loosdrecht, M. C. M. Activated Sludge Process Model No. 2d. Water Science and Technology, 1999, 39(1):165–182.

[12] Gujer, W., Henze, M., Mino, T. and van Loosdrecht, M. C. M. Activated Sludge Process Model No. 3. Water Science and Technology, 1999, 39(1):183–193.

Determination of Discharge Coefficient of Rectangular Broad-Crested Weir by CFD

Assist. Prof. Dr. Shaymaa Al-Hashimi, Assist. Prof. Dr. Sadeq A. Sulaiman, and Dr. Huda M. Madhloom

Abstract— **The hydraulic characteristics of flow over rectangular broad-crested weirs with varying upstream shape were studied. A large number of these studies are physical model tests of rectangular weirs. In this study, Computational Fluid Dynamic (CFD) model together with laboratory model of rectangular broad-crested weir were used to improve the performance of broad crested weirs. The performance of broad crested weir was improved by introducing an upstream face slope, varying from 90 to 23 degree in order to reduce the effect of flow separation. Analysis of numerical results showed that introducing an upstream slope face to square edge broad crested weir improved the performance and gave higher values of discharge coefficient. Two empirical equations were obtained to estimate the value of discharge coefficient in terms of effective head to crest height ratio, and upstream slope face of weir with high correlation coefficients of 0.976 and 0.985. The discharges performances obtained from CFD analyses were compared with the observed results for various upstream face slopes. The results obtained from all face slopes are in a good agreement.**

***Index Terms*— CFD, Laboratory Model, Rectangular Broad-Crested Weir, Discharge Coefficient**

1. INTRODUCTION

Broad crested weirs are defined as structures where the streamline run parallel to each other over the weir crown, and the crest of the weir is horizontal [Bos, 1976]. In most layouts of broad crested weirs also the hydrostatic pressure is fully accomplished in the middle of crest. However in cases where the weir length is too small it might be that the hydrostatic pressure is not fully accomplished [Hager, 1986]. The broad crested weir is in addition to irrigation systems used for highways, railroad and for hydropower structure. Also an application as a simple discharge measurement structure is possible. An important feature of boarded crested weir is the up and downstream side slope angle, which may vary between a vertical end and a ramped slope. Sloping embankment have a higher discharge capacity compared to a traditionally broad crested weir with vertical faces [Fritz and Hager, 1998]. The discharge characteristics for vertical face weirs with square edge or rounded entrance are extensive analyzed by [Azimi and Rajaratnam (2009)]. First investigations on discharge capacity of broad crested weir were made by [Bazin in 1898]. An extensive series of experiment were conducted by [Hager and Schwalt (1994)] for evaluating the flow feature over a broad crested weir. Earlier work involving flow modeling over a rectangular broad crested weir has been conducted by [Sarker and Rhodes (2004)] who investigated a weir experimentally as well as numerically (used code Fluent V.4.4.7). Good agreement was found in the above mentioned case for the upstream water level (stated as excellent), whereas all other numerical results, like rapidly varied flow profile over the crest, differ slightly from the results of the physical model study. [Hargreaves et al (2007)] used the volume of fluid method (Fluent V6.2) to compute the discharge also over a vertical faced broad crested weir. This paper shows the application of computation fluid dynamic CFD model to estimate free surface flow over broad crested weir with different sloping of upstream face. In the current paper, the commercial program Fluent is used to obtain flow field and pressure distribution over a broad crested.

Manuscript received March 20, 2015; this paper has been reviewed for publication in the conference July 25, 2015 and final accepted is August 20, 2015.

The University of Al-Mustansiriyah; Engineering College, Civil Engineering Dept., Baghdad, Iraq (shyabed@yahoo.com, shyabed1976@gmail.com)

2. THEORETICAL ASSESSMENTS

The broad crested models are based on the following assumptions: flow upstream of weir is steady, sub-critical and two dimensional; the effects of flow surface tension and viscosity are eliminated. For rectangular broad crested weir assuming the critical flow on the weir crest, the equation for flow rate is written as (Boiten, 2002):

$$q = C_D \times \frac{2}{3} \times H_e \sqrt{\frac{2}{3} g H_e} \qquad \text{…….. (1)}$$

where,

q = flow rate over the weir per unit width,

CD = dimensionless weir discharge coefficient,

He = effective upstream head above crest including approach velocity head,

$$= H_1 + \frac{q^2}{2g(P_1 + H_1)^2} \quad ,$$

H1 = upstream head above crest,

P1 = weir height, and

g = acceleration due to gravity.

For a free flow over broad crested weir with square upstream corner, a functional relationship can be written as follows:

$f(q, H_e, P_1, g, \alpha, \upsilon) = 0$ …….. (2)

where,

α = upstream weir face slope, and

υ = kinematic viscosity.

Using Buckingham Pi-theorem and after certain permissible manipulations, Eq.(2) becomes:

$C_D = f(H_e / P_1, \alpha, R_e)$ …… (3)

Where, Re = Reynolds number.

Reynolds number will have very large values and hence its effect on CD will be very little, therefore, Re can be dropped and Eq.(3) can be written as:

$C_D = f(H_e / P_1, \alpha)$ ……. (4)

3. EXPERIMENTAL STUDIES

[Farhoudi and Alami (2005)] produced a notable paper on the flow features over a broad-crested weir in which they described a comprehensive experimental campaign using a horizontal rectangular channel which was 0.6 m wide and 0.7 m high. A broad-crested weir of height 0.155 m and length 0.36 m was placed in the channel, which had a total length of 8 m. The upstream slope of the weir, ranging from 23 to 90 degrees, was modified by a separate sloping piece which could be replaced in each run. The upstream face of the weir was water tightened using water proof glue with special care. The flow was lead to the flume through upstream tank which was fed from the main reservoir. The flow was controlled by an adjustable valve and re-circulated to the main reservoir passing though the flume, over the weir crest, and downstream tank. The flow depth was controlled at downstream of the weir by means of a hinged gate and measured using a pre- calibrated sharp crested V-notch located at the end of downstream tank. The pressure head was measured taking the readings of 25 piezometers along the experimental reach. This model is used to simulate the numerical Fluent model.

4. Numerical Modelling

The numerical modelling involves the solution of the Navier-Stokes equations, which are based on the assumptions of conservation of mass and momentum within a moving fluid. In the absence of sources of mass and momentum, the conservation of mass is described by the differential equation, [Ferziger and Peric (1997]):

$$\frac{\partial \rho}{\partial t} + \nabla \cdot (\rho \mathbf{v}) = 0 \quad \text{….. (5)}$$

where ρ is the density and v is the velocity of the fluid. The conservation of momentum is similarly described by the equation:

$$\frac{\partial}{\partial t}(\rho \mathbf{v}) + \nabla \cdot (\rho \mathbf{v}\mathbf{v}) = -\nabla p + \nabla \cdot \boldsymbol{\tau} \quad \text{……. (6)}$$

where p is the pressure and $\boldsymbol{\tau}$ is the stress tensor. In order to represent the effects of turbulence on the flow, additional transport equations are solved for various turbulence quantities. To represent the sharp interface between the air and water, the Volume of Fluid (VOF) method of [Hirt and Nichols (1981)] is used. In this approach, the interface is tracked by introducing the volume fraction, αi, where i refer to the phase. The volume fraction for the i th phase is the fraction of the volume of a cell occupied by that phase. When modelling the free surface between water and air, a transport equation is solved for the water phase,

$$\frac{\partial \alpha_w}{\partial t} + \nabla \cdot (\mathbf{v}\alpha_w) = 0 \quad \text{…. (7)}$$

which holds in the absence of any inter-phase mass transfer and where α_w is the volume fraction of water. The Finite Volume method is used to solve the above equations and relies on the flow domain being divided into a grid consisting of a large number of cells. In each cell, if it contains only water, then $\alpha_w = 1$; if none, then $\alpha_w = 0$. For cells that span the interface between the air and water, $0 < \alpha_w < 1$. Various algorithms have been developed to sharpen the interface between the two phases because the interface tends to be smeared if Equation (7) is used alone.

In the present work, the *geometric reconstruction* method of [Youngs (1982)] was employed. To model upstream and downstream boundaries, CFD software includes boundary conditions that are specific to the open channel case, at which the upstream and downstream water levels can be specified. At a vertical upstream boundary, a pressure inlet is used. A pressure outlet is applied for downstream.

5. CFD MODEL

The simulations model used version 6.2 of FLUENT, Fluent Inc. (2005) applied on a hydraulic model produced by [Farhoudi and Alami (2005)]. The use of a 2D model can be justified on the grounds that indicated by [Hager and Schwalt (1994)] that said their experiments were essentially 2D in nature and only took measurements on the centerline in the channel. With a 2D model it is possible to produce a grid that resolves the vertical and stream wise directions with sufficient accuracy. A transient numerical model was applied owing to the use of the geometric reconstruction surface tracking algorithm. The Re-Normalized Group theory (RNG) *k*-ε turbulence model of [Yakhot and Orsag (1986)] was used with standard wall functions. This is one of a range of turbulence models classed as Reynolds-Averaged Navier-Stokes (RANS) models as defined by [Ferziger and Peric (1997)]. They are time-averaged approximations that are widely used in industrial applications. The (RNG) *k*-ε has known advantages when there is strong curvature in the streamlines, as is the case with the accelerating flow over the weir therefore was used. To complete the description of the CFD modelling: the *body force-weighted* pressure discretization scheme was used because of the presence of gravity; second-order discretization schemes were used for the momentum, turbulence kinetic energy and dissipation equations; and the PISO pressure velocity coupling algorithm was used, purely because it is

designed specifically for transient simulations. A time step of 1.0×10^{-4} s was used throughout to keep the simulation stable because of the demands of the VOF model. Since the flow fields being modelled take of the order of 10 s to establish, it can be appreciated how many time steps are required to reach steady-state conditions. Fig. (1), shows the dimensions of the domain and position of the boundary conditions used in the modelling. At inlet the upstream boundary pressure inlet was used. When modelling a free surface in FLUENT, the user specifies the free surface height relative to the datum, which in this case was set at the weir crest. FLUENT then internally calculates the volume fraction and static pressure at the inlet based on the position of the face, relative to the free surface position. At the downstream pressure outlet, only the free surface height (or tail water) height was required. The upper boundary above the air phase was specified as a symmetry condition, which enforces a zero normal velocity and a zero shear stress. Use of a symmetry boundary condition in this way is a standard practice for such distant, open boundaries. All other unmarked boundaries are set as walls. On the walls, the no-slip condition was applied and the walls were assumed to be smooth, since the experimental channel was constructed of PVC and glass.

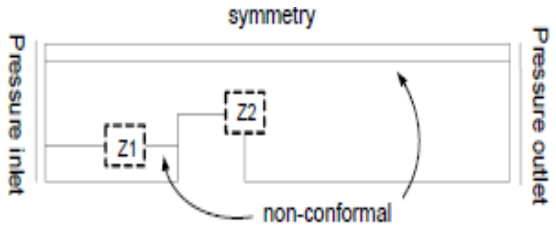

Fig. (1) Schematic of CFD domain showing: boundary conditions.

The mesh used in CFD can have a dramatic effect on the accuracy of the solution. In this work there were two sets of unmatched or non-conformal grid interfaces in the domain are used, as indicated in Fig. (2). At such an interface, the cell faces do not match up exactly as they would at a conformal interface. To demonstrate this, Fig. (2), shows the mesh used. The use of such boundaries in regions of the flow main in which flow gradients are low allows abrupt changes in the cell size. This means that the overall cell count can be reduced (here the grid consisted of 21,375 quadrilateral cells). Extensive use was made of geometric progressions in the meshing of the domain.

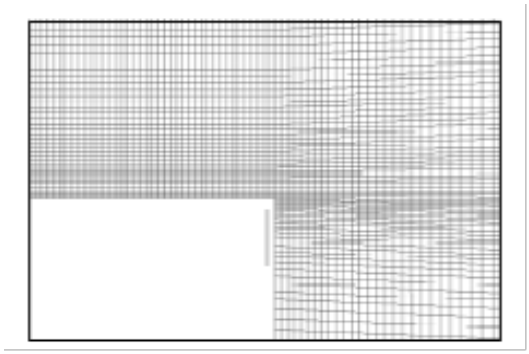

Fig. (2) Zoomed mesh regions from CFD model.

6. RESULTS

Under usual weir conditions, since the free surface level and total energy head upstream were fixed, the predicted discharge and free surface shape were the chief measures of accuracy. To see the extent to which the former measure compared, Fig. (3), show the velocity distribution predicted by the CFD modelling. For those simulations using the (RNG) k -ε model, the CFD predictions and experimental data agreed very well.

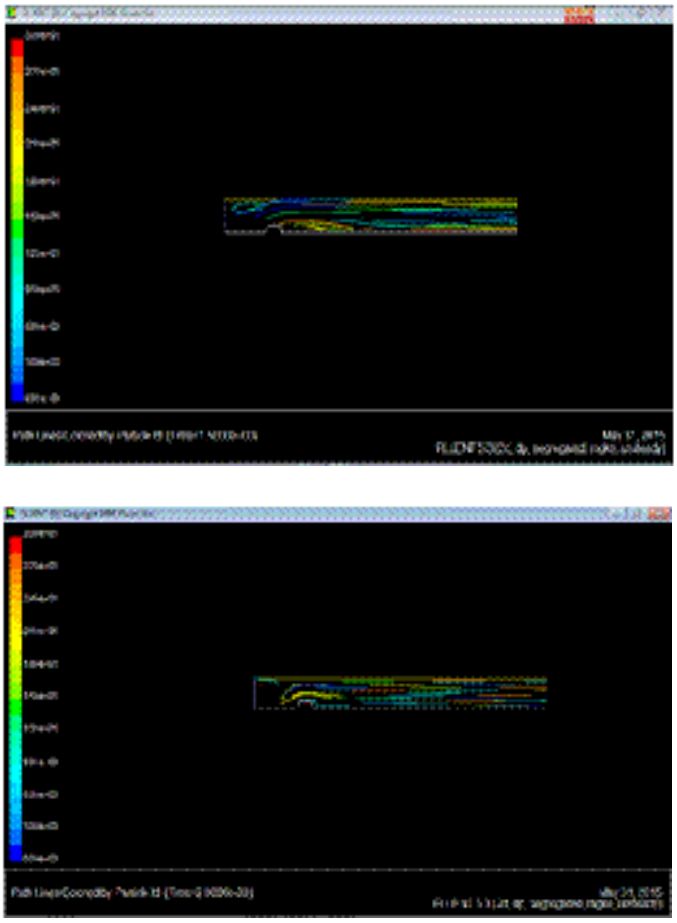

Fig. (3) Velocity Distribution over Broad Crested Weir

7. ANALYSIS OF RESULTS

A. Upstream Face Slope

A way of improving the performance of broad crested weir is to introduce an upstream face slope to the upstream square

edge. The effect of upstream face slope on the behavior of broad crested weirs was studied by testing five weir models of different cases, the first weir model was broad crested with vertical upstream face(square edge), i.e., with slope $\alpha = 90^o$, while, the other four were of slopes($\alpha = 60^o, 45^o, 30^o$ and 23^o).

B. Empirical Expressions of Discharge Coefficient

All numerical model results of broad crested wires of vertical upstream face and with different slope face were used as input data in a regression analysis computer program to obtain an empirical power expression for the variation of C_D with both (He/P_1) and α.

$C_D = 2.615\ [H_e/P_1]^{0.949}$ ……. (8)

with a correlation coefficient =0.976.

Another empirical expression for the variation of C_D with both (He/P_1) and α can written,

$C_D = - 0.21 – 0.912\ Sin\ (\alpha) + 0.993\ (H_e/P_1)$ ……. (9)

with a correlation coefficient = 0.985.

8. CONCLUSION

This paper discusses the accuracy of CFD in being able to predict the important flow variables over a broad-crested weir. By using a published experimental dataset as a validation set, it has been shown that it is possible to build a CFD model that replicates the findings to acceptable levels of accuracy. The driver behind this paper was to test the free surface modelling capabilities of version 6.2 of FLUENT and in that it proved successful. The time taken to produce steady-state free surface flows, even in 2D, is prohibitive when compared with other modelling techniques that are routinely applied to modelling hydraulic structures. However, for the detailed prediction of flow around hydraulic structures, CFD is increasingly becoming the most reliable and accurate modelling option.

Within the numerical modelling results of the present work, the following main conclusions can be summarized as:

1. The discharge coefficient related to overflow energy heads varies with the relative upstream slope. Decreasing upstream face slope makes the water surface profile fall into smooth curvature and become flatter. Also, the discharge coefficient tends to increase with decreasing upstream weir slope. Thus, weirs with upstream face slopes of 90^o and 23^o have the smallest and largest discharge coefficient, respectively. The weir discharge coefficient value at a 23^o slope is about 22% higher than for a weir with a 90^o upstream face slope. In addition, new empirical expressions were presented to estimate the discharge coefficient of rectangular broad-crested weirs with different upstream face slopes.

2. Flow separation occurs at the edge of rectangular broad-crested weirs and extends to a certain point over the crest. Regarding the separation, flow velocity becomes negative through this zone. Decreasing upstream face slope reduces the separation zone and so the negative velocity would not occur at the weir entrance. Hence, there was no negative velocity in weirs with upstream slopes of less than 45^o.

Notation

The following symbols are used in this paper:

C_D = dimensionless weir discharge coefficient,
g = acceleration due to gravity,
H_1 = upstream head above crest,
H_e = effective upstream head above crest,
L = weir length,
P_1 = weir height,
q = flow rate over the weir per unit width,
R_e = Reynolds number,
α = upstream weir face slope, and
υ = kinematics viscosity.

9. REFERENCE

[1]. Bos, M. G.: Discharge measurement structure, Laboratorium voor hydraulic an afvoerhydrologie, LandbouwhogeschoolWageningen,The etherland,rapport 4, 1976.

[2]. Hager, W.H.: Discharge measurement structure, Communications I, chairs de construction hydrauliques, department de genie Civil, EPFL,Lausanne, , 1986.

[3]. Fritz, H. M. and Hager,W. H. : Hydraulic of embankment weirs, journal of hydraulic research, 1998,124(9),963^971.

[4]. Azimi A. H. and Rajaratnam, N.: Discharge characteristics of weir of finite crest length, journal of hydraulic engineering, 2009, 135(12), 1081^1085.

[5]. Bazin, H.: Experiences nouvelles sur l'ecoulement en d'eversoir,Annales des ponts et chausses, 1898, 68(2),151^265.

[6]. Hager, W. H. and Schwalt, M.: Broad crested weir, Journal of irrigation and drainage engineering, 1994, 120(1), 13^26

[7]. Sarker M. A. and Rhodes, D. G.: Calculation of free surface profile over a rectangular broad crested weir, Flow measurement and instrumentation, 2004, 15,215^219.

[8].Hargreaves, D. M., Morvan, H. P. and Wrigth, N. G. : Validation of the volume of fluid method for free surface calculation, the broad crested weir, engineering applications of computational fluid dynamics, 2007, 1(2),136^147.

[9]. Boiten, W.: Flow measurement structures. *Flow Measurement and Instrumentation*, 2002, 3:203^207.

[10]. Farhoudi, J. and Alami, S. : Slope effect on discharge efficiency in rectangular broad crested weir with slope upstream face, International Journal of Civil Engineering, March 2005, Vol. 3, No. 1, 58^65.

[11]. Ferziger J and Peric M : Computational Methods for Fluid Dynamics. Springer, Verlag, Berlin, 1997.

[12]. Hirt, C. W. and Nicholas, B. D.: Volume of fluid (VOF) method for the dynamics of free boundaries, Journal computational physics, 1998, 39,201^225.

[13]. Youngs, D. L. : Time-dependent multimaterial flow with large fluid distortion. Num. Meth. for Fluid Dynamics. Academic Press.

[14]. Fluent Inc. (2005). Fluent v 6.2, Lebanon, NH, USA.

[15]. Yakhot, V. and Orsag, S.: Renormalisation group analysis of turbulence. Journal of Science and Computing, 1986, 1:3^51.

1. Researcher Dr. **Shaymaa Abdul Muttaleb Hashim** ; Assistant Professor in Civil Engineering Dept.; College of Engineering ; Al-Mustansiriyh University; Baghdad; Iraq.

e-mail: shyabed@yahoo.com ; shyabed1976@gmail.com;

2. Researcher Dr. **Sadeq A. Sulaiman** ; Assistant Professor in Civil Engineering Dept.; College of Engineering; Al-Anbar University; Al-Anbar; Iraq.

e-mail: **sadiq1969@yahoo.com**

3. Researcher Dr. **Huda Mahdi Madhloom**; Lecturer in Civil Engineering Dept.; College of Engineering ; Al-Mustansiriyh University; Baghdad; Iraq.

e-mail: adam_202077@yahoo.com

Reuse of Treated Wastewater for Irrigation
(March 2015)

Ibtisam R. Karim
University Of Technology
Building&Construction Eng.Dept

Karim K. EL- Jumaily,
University Of Technology
Building&Construction Eng.Dept

Mohammed Jallel Al- Janabi
University Of Technology
Building&Construction Eng.Dept

***Abstract*— Reusing of treated wastewater effluent is normally reliable alternative solution for water scarcity. The effluent from municipal wastewater treatment plants is an increasing attention as a reliable water resource. Wastewater reuse for agriculture needs to be planned with attention to type of crops and existing water irrigation methods. Domestic and municipal wastewaters contain the macronutrients nitrogen, phosphorous, zinc, boron and potassium, and micronutrients such as calcium and magnesium, all of which are vital to plant and soil health. Its use can supplement or even replace commercial fertilizer inputs, saving farmers money. Wastewater reuse also benefits the environment because it allows these valuable nutrients to be diverted from the waste stream and recycled, instead of released into watercourses where they can become significant pollutants.**

This research studied the possibility of using treated wastewater for irrigation purposes, AL Rustumiya station as a case study, laboratory tests were then compared to the special determinants of water allowed to be used for irrigation. On the whole all the results of treated water were fall in the allowable limitations, and the effluent from AL Rustumiya station certain for irrigation using.

***Index Terms*- raw, effluent, BOD, COD, SS, Ph, TDS.**

I. INTRODUCTION

WASTEWATER reuse is a useful tool in minimizing waste quantity in the environment. The inclusion of planned water reclamation, recycling, and reuse in water resource systems reflects the increasing scarcity of water sources to meet societal demand technological advancements ,increased public acceptance, and improved understanding of public health risks. As the link between wastewater, reclaimed water, and water reuse has become delineated more clearly, increasing smaller recycle loops are possible (Metcalf and Eddy, 2002). The link between water and food is strong. Each is consume, on average, nearly 4 liters of water per day in one form or another, while the water required producing the daily food totals at least 2,000 liters, 500 times as much. This helps explain why 70 percent of all water use is for irrigation. Another 20 percent is used by industry, and 10 percent goes for residential purposes. With the demand for water growing in all three categories, competition among sectors is intensifying, with agriculture almost always losing. While most people recognize that the world is facing a future of water shortage, not everyone has connected the dots to see that this also means a future of food shortages **(EPI, 2008)**.

A. OBJECTIVES

The objectives of this work consist of the followings:

1. Evaluation of (Potentiality of wastewater reuse in Iraq).
2. Specifying the beneficial of wastewater reuse as additional resources.
3. Evaluation of quantitative and qualitative of wastewater in AL Rustumiya.
4. Finding out the data base for designing wastewater reuse system in the city of Baghdad to be used for modern techniques conveyance reused water.
5. Finding out some useful recommendations that help to apply wastewater reuse in Iraq, as this technique is not used yet.

B. Approaches to Wastewater Reuse for Irrigation:

The methods employed to reuse wastewater for irrigation vary considerably, depending on the volumes of water and areas of land available, the level of treatment employed, the types of crops to be irrigated, the level of technical capacity and investment of the farmers and environmental considerations. Thus, the scale ranges from localized, per urban, often informal irrigation of small gardens by collected but untreated wastewater, with simple irrigation methods and few controls, to the large, canal commanded irrigation schemes of thousands of hectares, but still using untreated wastewater, to highly sophisticated, heavily controlled and managed soil aquifer treatment in which the re abstracted, fully treated effluent can be used to grow any type of crop using sophisticated and efficient irrigation techniques **(UNE, 2003**).

C. Irrigation of Agricultural Crops

The oldest and largest reuse of wastewater is for irrigation of agricultural crops. However, many research studies have proved that in addition to providing a low cost water source, other side benefits of using wastewater for irrigation include increase in crop yields, decreased reliance on chemical fertilizers, and increased protection against frost damage. Modern reuse for irrigation of agricultural purposes in

developed countries was the result of two pioneering studies that were conducted in California during the 1970s and 1980s: The Pomona virus study and the Monterey wastewater reclamation study for agriculture. The Pomona virus study was conducted in Los Angeles in an effort to determine the degree of treatment necessary to minimize potential transmission of waterborne diseases via surface water. The study concluded that complete virus removal is possible through tertiary treatment of wastewater by either direct filtration or activated carbon followed by adequate disinfection, thus proving the possibility for reclamation of microbiologically risk free water from wastewater. These results of this study have opened up the possibilities of wastewater reuse for various applications. Based on biological, bacteriological, and chemical results from sampled tissues of vegetables grown using wastewater as irrigate, the study established the safety of this type of reuse. Both studies demonstrated conclusively that even food crops that are consumed uncooked could be successfully irrigated with reclaimed municipal wastewater without adverse environmental or health effects. In many countries in the Mediterranean region, spanning from Spain to Syria, shortage of water has been the main driving force for wastewater reuse. Wastewater from Tunis, the capital city of Tunisia, has been used to irrigate citrus fruit orchards since the 1960s. From 1989 onwards, secondary treated wastewater has been allowed for growing all types of crops, except vegetables. In countries like Morocco, Jordan, Egypt, Malta, Cyprus, and Spain, several large scale wastewater irrigation schemes are already in operation or under planning. In occupied Palestine, the percentage of wastewater reused for irrigation purposes is highest in the region, at 24.4%, which is expected to be increased to 36% by the year 2010. In temperate zones of Australia, reclaimed water is being used to irrigate a variety of crops including sugarcane. A recent development is the use of reclaimed water for irrigation of tea-tree plantations, which will produce tea-tree oil as a cash crop. Eucalyptus forestry also is a major reuse option followed in Australia, which provides timber for a number of purposes including pulp wood and fire wood **(ELOSS, 2004**). Table (1) an indicator on the reuse wastewater in irrigation in many countries.

Table (1) Wastewater reuses applications in many countries.

No.	year	Location	Wastewater reuse application
1.	1989	Tunisia	Irrigation with reused wastewater for citrus plants and ground water recharge (Metcalf and eddy, 2002).
2.	1984	Japan	Irrigation rice farms with treated wastewater (UNEP, 2007).
3.	1980	Texas	Using treated wastewater in irrigation (TWDB, 2011).
4.	1890	Mexico	Drain canal were built to take untreated waste wastewater to irrigate 90000 ha (Metcalf and eddy, 2002).
5.	1997	Arab World	48 percent of treated wastewater used in the agricultural irrigation (Khaled, 2009).
6.	1911	Egypt	Begun to use the sewage is treated in the irrigation of agricultural crops (Abdel Gawad, 1998).
7.	1894	Florida	Using reclaimed wastewater in irrigation was more feasible and cost effective than advanced treatment (UDWR, 2005).
8.	1994	Saudi Arabia	Irrigate about 90 km2 of agricultural land by with treatment wastewater (Saif, 2000).
9.	1918	California	In 1997 practiced reused wastewater in agricultural irrigation 4.45 mg/d (UDWR, 2005).
10.		Syria	2.6 percent of irrigated area used treatment wastewater (Mohammed, 2014).
11.	2013	Iraq	No actual purpose yet.

II. Description of AL Rustumiya project:

Rustumiya project is located on the banks of the old Diyala River south of the city of Baghdad in the area at the end of the line Rustumiya Baghdad. The main carrier of the sewage project serves areas of Baghdad, the army channel between the east and west of the Tigris River, professionals starting from the AL Adhamiya district in the north down to the south Rustumiya area **(Baghdad Sewage Board, 2013).**

The most important laboratory tests are:

1-Biological oxygen demand (BOD).
2-Chemical oxygen demand (COD).
3-Suspended solid material (SS).
4-Acidic function (PH).
5-Total dissolved solid (TDS).
6-Tests of oil and grease.

III. Evolution of Samples of Al-Rustamiya Old Treatment Plant

The characteristic of wastewater of Al-Rustimya old treatment plant for the Winter and Summer seasons and range for one year are shown in table (2).

Table (2): Characteristics of wastewater in Al-Rustaimya old treatment plant, for one Year period **(Baghdad Sewage Board, 2013)**.

Teste	BOD ppm		COD ppm		SS ppm	
Sample	Inf.	Eff.	Inf.	Eff.	Inf.	Eff.
Standars		40		100	60	
Junuary	233	21	369	65	309	41
Febreuary	241	14	444	56	279	34
March	226	13	334	39	248	28
April	240	17	490	40	241	31
May	252	23	371	45	275	30
June	298	19	396	210	236	32
July	241	19	400	34	270	23
August	213	19	291	46	179	30
September	193	20	379	63	167	28
October	168	16	468	41	145	27
novemper	165	18	445	44	291	25
Decemper	---	---	---	---	---	---
Average	224	18	399	62	240	30

cont…

PH		Chloride ppm		T.D.S		Oil	
Inf.	Eff.	Inf.	Eff.	Inf.	Eff.	Inf.	Eff.
	6.5..8.5		600				
7.4	7.5	351	310	1713	1560	16	2.6
7.3	7.5	367	327	1936	1809	7.7	2.1
7.2	7.5	325	277	1582	1340	9.2	0.7
7.3	7.5	334	280	1541	1064	4	
7.2	7.4	327	278	1359	1314	7.3	1
	8.6	320	274				
7.2	7.5	325	251				
	7.5	343	274	1224	1181	15	2
7.3	7.5	321	270	1206	1226	7.1	0.8
7.2	7.5	319	257	1240	1119	14	0.7
7.3	7.5	359	296	2024	1837	19	1
---	---	---	---	---	---	---	---
7.3	7.6	335	281	1536	1383	11	1.4

Eff: effluent, Inf: influent.

Concerning average values of the B.O.D in raw level, it was 224 ppm then and after treatment to the concentration falls to 14 in winter season as shown in table (2). Also, by comparing these results to its results in summer season of the same stage, it is obvious that the treatment in winter season more efficiencies than treatment in summer. Also table (2) shows that during holydays and rainy days some measurements are not carried out, especially when overflows are experienced and the required test kits are not available. For this the related result are not shown in this table. Table (2) shows the annual results and its averages. as a result of present tested and its result that give idea all the results falls in the allowable range and can use this effluent in irrigation, in other words potentially of reuse treatment wastewater.

IV. Results of Analysis

Figure (1) shows BOD concentration in raw sewage which was at a peak from about June, and was also a steep decline over the next 4 months, and a corresponding steady increase in the effluent curve in May as a whole, there was a steady rise in Summer.

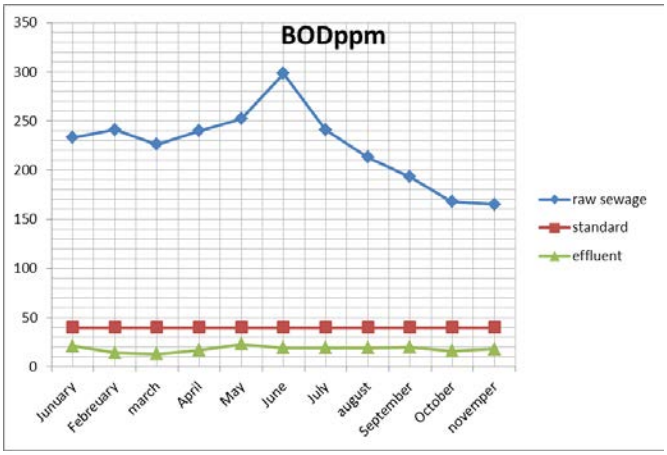

Figure (1): AL-Rustumiya BOD Treatment Curve, Stage (2) for One Year Period

The COD raw curves, fig.(2) shows that the concentration was between 500 ppm and 300 ppm while effluent curve illustrate the minimum value in Summer, but the effluent curve decrease in Summer and gradually increase in Winter.

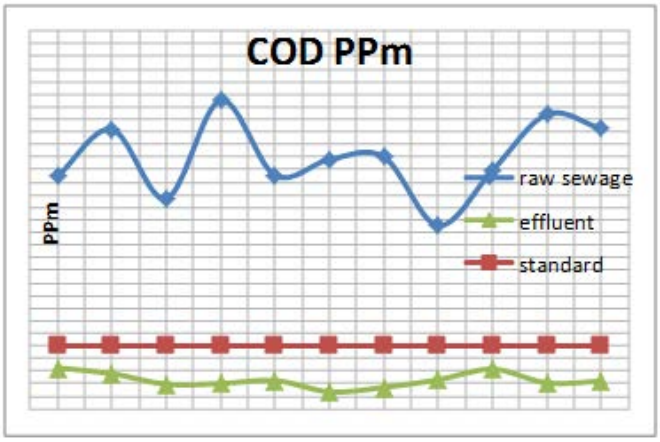

Fig.(2): AL-Rustumiya COD Treatment Curve, Stage (2) for One Year Period

Figure (3) shows that raw sewage SS was unstable, and the effluent to the river after treatment is slightly decreasing in Summer.

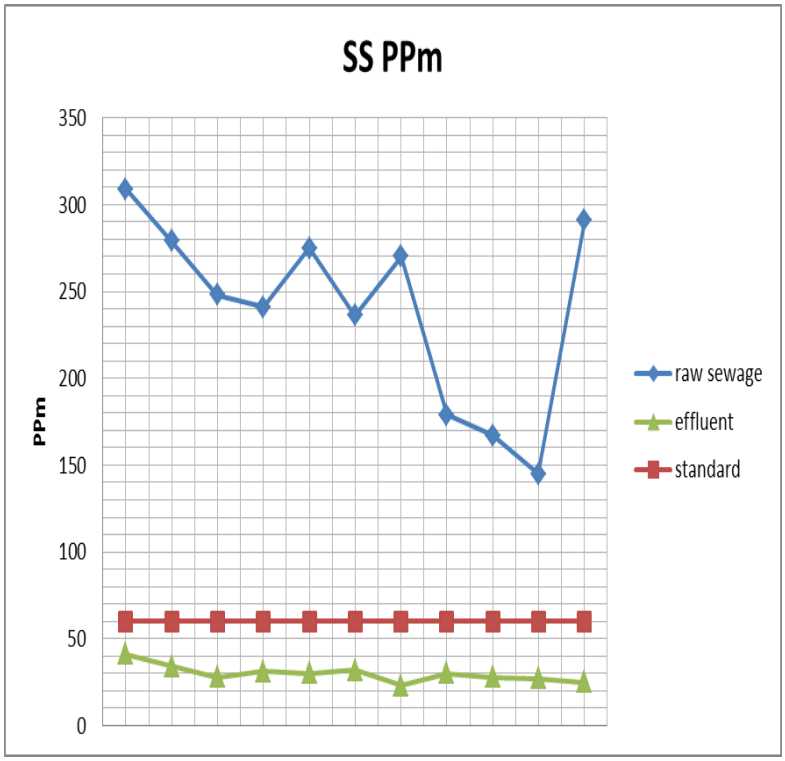

Figure (3): AL-Rustumiya SS Treatment Curve, Stage (2) for One Year Period

The PH curve illustrate that there was a small gap between raw and effluent, and all fall in the allowable values, fig. (4).

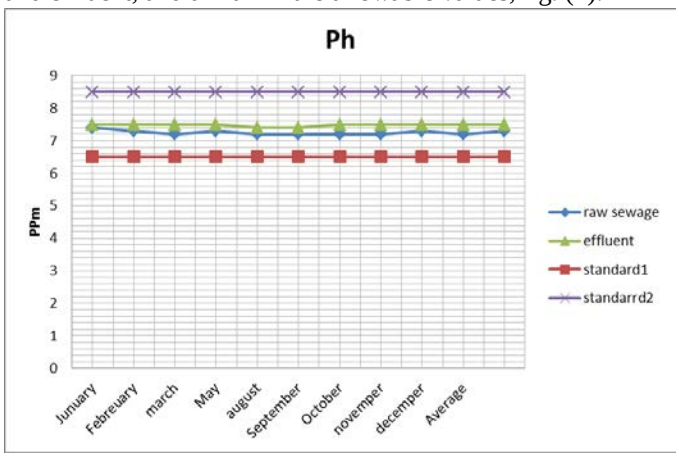

Fig (4): AL-Rustumiya Ph Treatment Curve, Stage (2) for One Year Period

The figures (5) and (6) illustrate raw sewage and effluent curves for TDS and Chloride respectively. Both figures show their fall in allowable limitation.

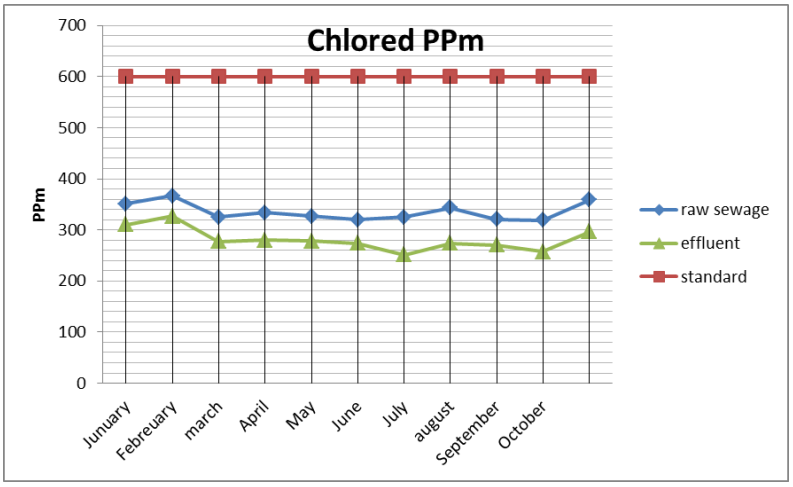

Figure (5): AL-Rustumiya Chloride Treatment Curve, Stage (2) for One Year Period

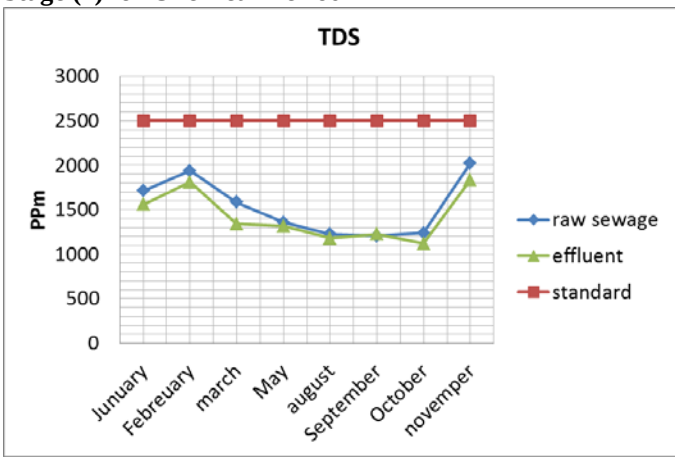

Figure (6): AL-Rustumiya TDS Treatment Curve, Stage (2) for One Year Period

Figure (7) shows the important of treatment and the ratio of grease and oil in the effluent to river.

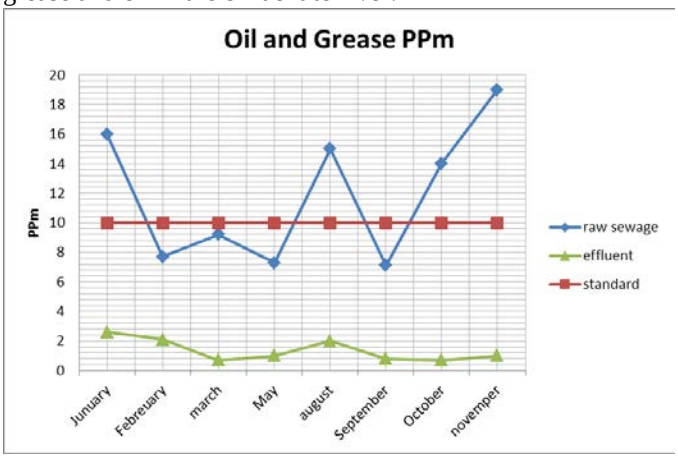

Figure(7): AL-Rustumiya Oil & Grease Treatment Curve,Stage (2) for One Year Period

V. CONCLUSIONS

The following conclusions can be drawn based on the analysis and the results in this study as follow

1. Wastewater reuse for irrigation apparently not applied yet in Iraq.

2. Average results of AL Rustumiya laboratory tests showed correspond to the Iraqi limitation requirement for irrigation after tertiary treatment, except for oil and grease.
3. Irrigation of land with treated wastewater increases the adhesive among soil molecules and this is clearly useful in sandy soils.
4. The pollution status of Diyala River has been a result of untreated surplus wastewater received by AL Rustumiya WWTP.
5. The favorite tool for treating wastewater is by adopting decentralized system after separating graywater at the source.
6. The drip irrigation system is an appropriate method for treated wastewater, as direct contact with such water may be avoided; in addition this approach represents the optimal use of water amount.

REFERENCES

[1] Baghdad sewage Board, 2013, wastewater treatment plant, operation section.
[2] EPA. Washington, DC. , 2004, "Primer for Municipal Wastewater Treatment Systems." Document no. EPA 832-R-04-001.
[3] EPI Earth Policy Institute, 2008, http://www.earth policy.org.
[4] Khaled, 2009."Use of non-conventional water in the Arab world", experience Arab Center for the Studies of Arid Zones and Dry Land ,ACSAD 41.
[5] Metcalf & Eddy, 1991"Wastewater Engineering Treatment, Disposal and Reuse". New York, McGraw-Hill.
[6] NSFC, National Small Flows Clearing House 1999. "Pipeline", West Virginia University.
[7] Saif, 2000. "Evaluation of Irrigation Water Quality and Its Effect on Soil Infiltration Rate" Riyadh Region. Research to the Ministry of Planning Saudi Arabia.
[8] UDWR, 2005. The Utah Division of Water Resources, "water reuse in Utaha", April 2005.
[9] UNEP, 2003. "Wastewater reuse for agriculture". Economic And Social Commission For Western Asia03-0695 United Nations New York.
[10] UNEP, 2007,"water and wastewater reuse", An Environmentally Sound Approach for Sustainable Urban Water Management, United Nations environment program.

Variation Effect of Discharge on Total Dissolved Solid in Shatt Al-Arab River

Dr. AHMED NASEH AHMED HAMDAN
Dept. Of Civil Engineering, College of Engineering , University of Basrah
009647801129130 / 009647713554287
E-Mail : ahmed_n_ahmed2005@yahoo.com

***Abstract*—There is a water shortage problem in Shatt al Arab river in addition to the water quality problem because the total dissolved solid (TDS) values are higher than the permissible. The quality of Shatt al Arab river water is high in salinity because the annual average of TDS is greater than 1500 mg/L. Therefore its water is considered impermissible for irrigation and drinking because it is brackish water. The aim of this study is to explain the effect of the discharge of Shatt Al-Arab river on total dissolved solid. Six water years have been chosen to study this effect (from October of 2009 up to end of 2014). Also the study includes a comparison between the TDS of Tigris and Euphrates in relation to that of Shatt al Arab river. The results display that the Ebb discharge is higher in comparison to Flood discharge. The high values of TDS in Shatt Al-Arab river are due to: the low river water discharge of the sources, the drainage water from agricultural and industrial lands beside Shatt al Arab river that discharge into it and the sewage and polluted water that pour into it. Also, TDS seems almost higher in case of Flood because of the effects of Arabian Gulf. There are also differences in the yearly and monthly averages of these characteristics because of the water balance effect from river sources of Shatt Al-Arab river in addition to the progress of salt wedge intrusion from the Arabian Gulf. The study concludes that the greatest rate of the discharge that comes to Shatt al Arab river was from Tigris and that the rivers of the source were not responsible of Shatt al Arab high TDS values.**

Keywords (TDS, Discharge, River, Shatt Al Arab)

I. INTRODUCTION

The Shatt al Arab River is formed after the confluence of the Euphrates and the Tigris Rivers near the city of Qurnah in southern Iraq (see Fig.1). The southern part of the river constitutes the border between Iran and Iraq until it discharges into the Gulf. With a total length of 192 km, the Shatt al Arab widens over its course, expanding from a width of 250-300m near the Euphrates-Tigris confluence to almost 700 m near the city of Basrah and about 2 Km as it approaches the river mouth, and a depth of between 8-15 m, considering tides[1]. An area of 145.190 km^2 drains directly to the Shatt al Arab region downstream of the Euphrates-Tigris confluence (excluding the Euphrates and Tigris Basin areas). Several tributaries join the Shatt al Arab during its course, most importantly the Karkheh and the Karun Rivers. But now there was diversion of the water of Karun and Karkheh tributaries inside the Iranian borders that's were caused very high increase of the salinity in Shatt Al-Arab River [2].

The Total dissolved solid (TDS) of the Shatt Al-Arab River water is of great importance in designing the future usage of this water for irrigation, municipal and industrial purposes, [3].

The main reason of TDS in the Shatt Al-Arab river near to the estuary is due to intrusion of salt water from Arabian Gulf in the flood tide case, the intrusion of the sea water actually may reach the distance of a few kilometers upstream of the mouth, but not farther than Abadan (about 50 km inland, halfway to Basrah) [4], the river water rises and falls as far north as Qurnah due to the dynamic tide influence.

There is limited information on water resource development projects in the Shatt al Arab region. However, in 2011 the Iraqi Ministry of Water Resources announced plans to construct a 129 km channel to divert water from the Shatt al Arab River for irrigation purposes. The irrigation channel will transfer about 30 m^3/s of water for use on agricultural land in Basrah Governorate.

The salinization of the Shatt al Arab first became an issue in the 1960s. The situation further deteriorated from the 1970s onwards with the construction of dams and reservoirs on the Euphrates and Tigris Rivers. The regulation of the Euphrates and, to a lesser extent, the Tigris, led to a decrease in runoff, which eventually resulted in the degradation of the delta, as accumulated salt was no longer adequately drained. Low river runoff and high evaporation rates up to 41% in the extreme north-western part of the Gulf further contribute to high salinity. In Turkey, the TDS was about 260 mg/L which is suitable for irrigation while TDS values in Shatt al Arab reach as high as 3500 mg/L [5].

The aims of the study is to make a knowledge about the main reasons of high increase of TDS in Shatt al Arab river for the latest years and by take mainly the effect of discharge variation into it. Site measurements of TDS, discharge and water level for the latest 6

years has been measured to study this effect in different locations.

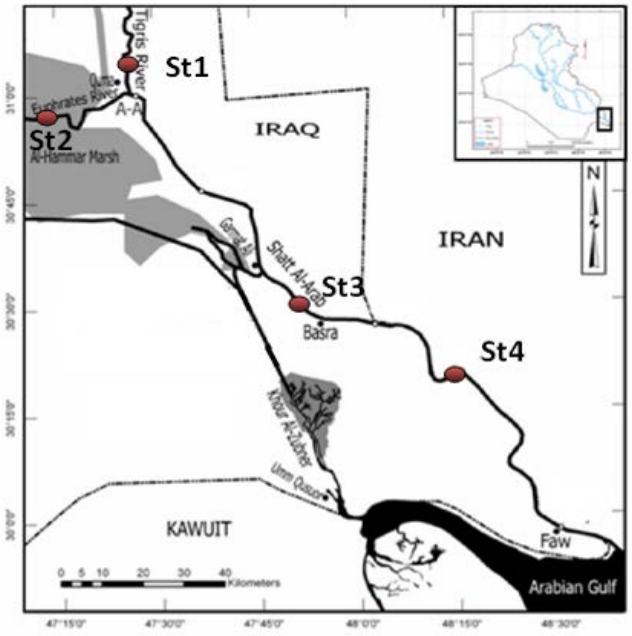

Fig. 1. Location map of study area, show the three stations of sampling

II. LITERATURE REVIEW

The prior studies which Interest in the reasons of increasing values of TDS in Shatt al Arab river, Hassan and Jasim [6] which conclude that the paper factory, Al-Hartha electric station and Al-Najebiah electric station on Shatt Al-Arab that pour a drainage water to it caused high values of TDS.

Mahmood, et al. [7] study on Shatt al Arab river from 2009 to 2011 and get the results show that the quality of water in the north part of Shatt Al- Arab affected by the discharge and human control like establishing dams and barrages on the Tigris River. and In the south part of Shatt Al-Arab, the effect of the water from the Arabian Gulf during the tide is the main factor effect the quality of water. Also the water influenced by agricultural activities, sewage water and waste from plants in addition to marine incursion of salt water. As well as they conclude that the fresh water from Shatt Al-Arab which takes water from Tigris only in the present.

Fawzi, and Mahdi [4] study on Tigres, Euphrates and Shatt al Arab, and they get a result that Salinity ranged from 1300 to 2100 mg/L at lower regions of Shatt Al-Arab, due to the effect of the Gulf water. And they conclude that the salinity of Shatt Al-Arab shows higher values even in the upper parts, due to the agricultural runoff, industrial and other disposal.

Al- Mahmood [8] study the role of the discharge of Shatt Al-Arab River on TDS, two years (2006 and 2007) include in the study to show this effect. The results display that the ebb discharge is high in comparison with flood discharge, (TDS) and salinity is a high in comparison with last studies, and there are a variance between ebb and flood characteristics due to different effects such as a water source and the progress of Salt Wedge procession in Shatt Al-Arab from Arabian Gulf with shortage discharge.

III. MATERIALS AND METHODS

Study area and sampling sites

The hydrological condition of the Shatt Al-Arab River basin is affected by several factors including conditions at the upper reaches of the Tigris and Euphrates rivers, the status of advancing flood tides from the Arabian Gulf, seepage of saline ground water into the basin, as well as the impact of climate conditions prevailing in the region on discharge rates and the payload of the river.

There was no systematic evaluation of water quality for irrigation in Iraq during the past century, However, the Directorate of Water Resources in Basra started to evaluate the values of TDS, discharge, and water levels in cases of ebb and flood. Four sampling stations were established along the river course in order to obtain a good knowledge to the TDS, discharge and water level. The locations of these station were in Tigris (near to Al- Quarna), Euphrates rivers (near to Al- Medainah), Al Ashar (center of Basrah), and Sehan (South of Abu Al Khaseeb). (As shown in Fig.1).

Station number	Station name	Longitude	Latitude
St. 1	Tigris	47° 20 37. 39	31° 07 29.85
St. 2	Euphrates	47° 00 10. 11	30° 58 22.13
St. 3	Al- Ashar	47° 51 29.10	30° 30 12.43
St. 4	Sehan	48° 12 51.29	30° 18 53.43

Field Sampling and procedures

The measurements was taken daily (except Friday and Saturday due to holiday) from October of 2009 up to end of 2014, which include the measure of water level, case of tide ((St.3) and (St.4)), measure the river velocity, and water samples collected for analysis of TDS.

The field sampling is as shown:-

1. The samples were collected from water to measure the TDS(mg/l) using Multi-Probe System (MPS).
2. Using Echo Sounder to draw a cross section of the rivers.
3. Using Current meter to measure the rivers velocity.

The discharge was measured by using the equation.

Discharge (m^3/s) = Average velocity (m/s) * Area (m^2) (1)

IV. TOTAL DISSOLVED SOLIDS (TDS)

Water used for irrigation can vary greatly in quality depending upon type and quantity of dissolved salts. Salts are present in irrigation water in relatively small but significant amounts. They originate from

dissolution or scouring of the rocks and soil, including dissolution of lime, gypsum and other slowly dissolved soil minerals. These salts are carried with the water to wherever it is used. In the case of irrigation, the salts are applied with the water and remain behind in the soil as water evaporates or is used by the crop. Water with TDS less than 450mg/L is considered good and that with greater than 2000 mg/L is unsuitable for irrigation purpose.

River Water can be classified by the amount of TDS as [9] :

- fresh water < 1500 mg/L TDS
- brackish water 1500 to 5000 mg/L TDS
- saline water > 5000 mg/L TDS

V. RESULTS AND DISCUSSION

In this study, by taking station St.3 as an average discharge of Shatt Al Arab in the upstream of it, the values of discharge show to be high in ebb cases as compared with its values in flood cases (see Fig.2 to Fig.7), the reasons is due to the effect of river flow with hydraulic gradient from upstream to downstream in ebb cases as compared with the obstruction of flow due to salt wedge intrusion into Shatt al Arab river from Arabian Gulf in the case of flood. Also it's seems a noticeable increase of discharge in the recent years (See Fig.8).

For the years of study, the highest value of average discharge in upstream of Shatt al Arab river in ebb case was in February for the year of 2014, and it's value was 79.43 m^3/s, and The highest value of average discharge in upstream of Shatt al Arab in flood case was in same month and year, and it's value was 76.67 m^3/s.

The highest values of average discharge in upstream of Shatt al Arab river was in spring season (see Figs. 2 to 7) that's due to increase the average values of Precipitation. Also it can be noticed that increase the values of discharge in start of Autumn season for the water year 2011, 2013 and 2014.

The lowest value of average discharge in upstream of Shatt al Arab river in ebb case was in December for the year of 2011, and it's value was 29.64 m^3/s, and the lowest value of average discharge in flood case was in November for the year of 2012, and it's value was 21.04 m^3/s. (see Fig.8), and that's may be due to the decrease of water supply from the source.

Generally it's noticed a decrease of discharge for ebb and flood cases in the months June and July as compared with other months discharge values for the same year, that's due to increase of evaporation in that's months, and human being water demand and the increase of plants demand in the summer season for the agricultural regions crossed by Shatt al Arab river.

From (Fig. 9) it can be shown that almost the flow of Shatt al Arab river was coming from Tigris and most of the water which is coming from Euphrates was gone to Al Hammar marshes that's consists with Mahmood, et al. [7].

The variance of discharge in Shatt al Arab river was due to the source of water was depend on precipitation and snow melt which is depend on the nature of the year. So it can be noticed from Figs 2 to 7 that there are a decrease of TDS in the cases of high discharge and vise versa.

The lack of discharge lead to increased the ability to carry the water soluble substances, where it can be noticed that the concentration of dissolved substances in the city of Basra record high values during the driest years.

From Figs. 2 to 7 and Fig.10, TDS values in upstream of Shatt al Arab was shown to be exceed the value of 7000 mg/L in October of the year of 2009 and there are a variance of TDS from 1300 mg/L to about 2500 mg/L, from January 2010 to July 2012, TDS values then suffer of noticeable rise in TDS values especially in February and March of 2013 and 2014 that reach a value of 5000 mg/l, then there a noticeable decrease in TDS especially in Autumn season which reach to about 1000 mg/L in October 2013.

By studying TDS values in upstream of Shatt al Arab river from 2009 to 2014 it can be shown that TDS values in the flood was great than TDS in the Ebb, and the greatest value of TDS in the case of Ebb was in November 2009 and it was 6812 mg/L and the discharge was 30.45 m^3/s. And the greatest value of TDS in the Flood case was 7081 mg/L and was occurred in October of 2009, the discharge was 46.85 m^3/s, while TDS values when compared with Tigris river values in October and November 2009 it seems that values not exceed 1000 mg/L.

The lowest value of TDS in Shatt al Arab river was in June 2012 in the case of ebb and it was 1050 mg/L and the discharge was 53.68 m^3/s. And the lowest value of TDS in the flood case was 1083 mg/L and was occurred in November 2013, the discharge was 50.09 m^3/s, while TDS values when compared with Tigris river values in June 2012 and November 2013 it was 758 mg/L and 698.42 mg/L respectively.

From Fig.(10), it can be noticed that TDS values in Tigris which have the greatest contribution of Shatt al Arab discharge don't exceed 1400 mg/L in the worse condition for the past years 2009 to 2014, and it was often don't exceed 1000 mg/L. This is evidence that the reason of Shatt al Arab high TDS values in upstream of Shatt al Arab was not from the rivers of the source (Tigris and Euphrates), So Tigris is considered good water quality for irrigation until when connected with Shatt al Arab river which is suffer from increasing in TDS values due to effect of drainage water from tributaries, sewage water that pure into it and shortage of river discharge.

By taking station St.4 as an average of Shatt Al Arab river flow in the downstream, and from Fig.11, it can be shown,

that maximum TDS value was 10089 mg/L in Ebb case and 12079 mg/L in Flood case which occurred in October of 2009 and November of the same year respectively.

The minimum value of TDS was 1560 mg/L in Ebb case and 1619 mg/L in Flood case which occurred in May of 2013.

From Fig. 11, it can be shown that all TDS values of downstream is greater than complementary values of it in the upstream, the possible of TDS increase in the downstream is due to effect of salinity intrusion wedge from Arabian Gulf. Also the value of TDS in the Flood case is greater than the values of it in the ebb case due to the same reason.

VI. CONCLUSIONS AND RECOMMENDATIONS

- **Conclusions**

1- It shown a little increase of discharge in latest years .
2- The highest values of discharge was almost in spring season. And was increased also in some times of the year especially in September and October.
3- Reduction of discharge in both cases of ebb and flood in Shatt al Arab river in Summer season.
4- There are a decrease of TDS in the cases of high discharge and vise versa, the lack of discharge lead to increased the ability to carry the water soluble substances, where it can be noticed that the concentration of dissolved substances in the city of Basra record high values during the driest years.
5- The results show that the year of 2009, was suffer of high TDS due to low discharge.
6- The study indicated that the increase of TDS was due to deterioration the quality of Shatt al Arab river, where the values of TDS exceed the acceptable limit for all the months which is 1500 mg/L.
7- The study concludes that the greatest rate of the discharge that comes to Shatt al Arab river was from Tigris and that the rivers of the source were not responsible of Shatt al Arab high TDS values.
8- The values of TDS in flood cases was greater than ebb cases that's due to effect of saline wedge intrusion from Arabian Gulf.
9- Shatt al Arab river is considered as a brackish water that's due to the values of TDS was greater than 1500 mg/L in the almost of the months in the years under study.
10- Shatt al Arab river in the upstream was considered as a saline water in the months October, November and December of the year of 2009 that's due to exceed the value of 5000 mg/L, also the months of February and March of the year of 2013.
11- The values of TDS in the downstream of Shatt Al Arab was greater than complementary values of it in the upstream that's due to the effect of salinity wedge intrusion from Arabian Gulf.

- **Recommendations**

1. Convert the agricultural drainage water from the lands beside Tigris, Euphrates and Shatt al Arab river to drainage channel far from these rivers.
2. Negotiate with turkey to increase the water share incoming to Iraq (from Tigris and Euphrates).
3. Negotiate with Iran to increase the pure water incoming to Iraq that have a good and unpolluted water quality. Also to prevent drained water that incoming to Iraq from Iran side.
4. Prevent sewage and polluted water that pour to Shatt al Arab river.
5. Prevent agricultural and industrial water discharge into Shatt al Arab river unless treated by the method that trust the requirement of environmental standards.

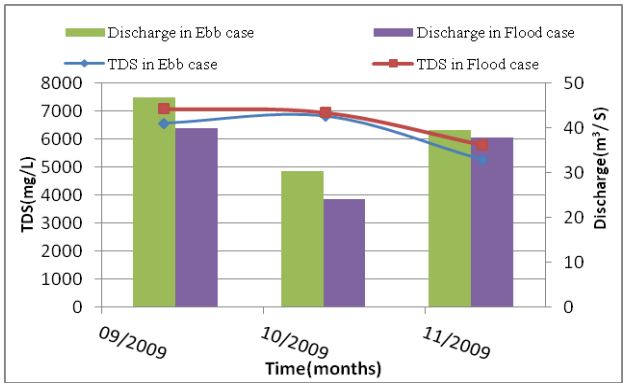

Fig. 2. TDS/ Discharge diagram in Shatt al Arab River 2009

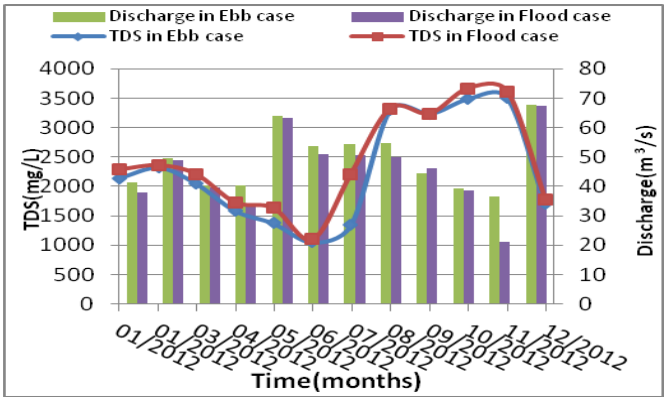

Fig. 5. TDS/ Discharge diagram in Shatt al Arab River 2012.

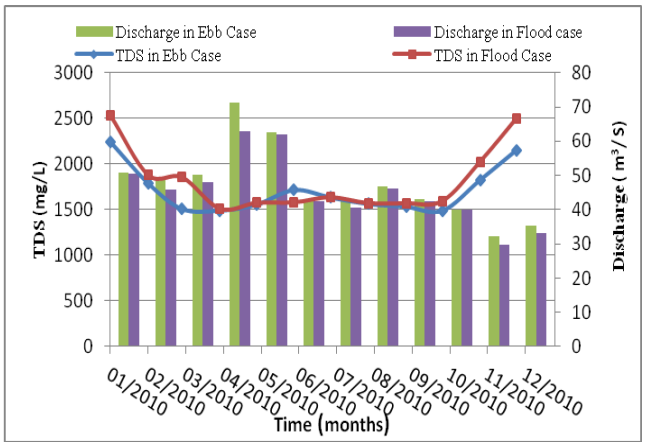

Fig. 3. TDS/ Discharge diagram in Shatt al Arab River 2010

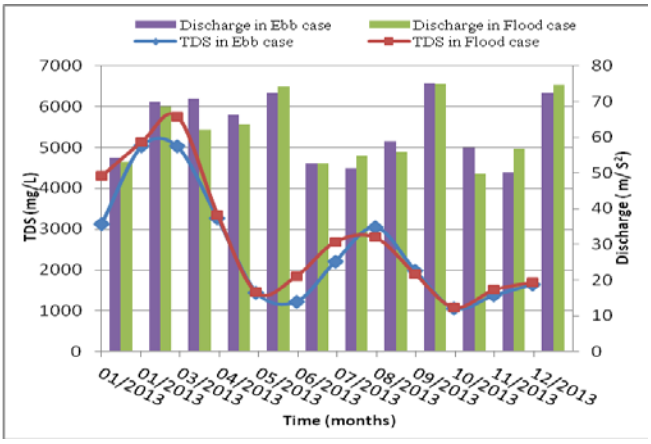

Fig. 6. TDS/ Discharge diagram in Shatt al Arab River 2013.

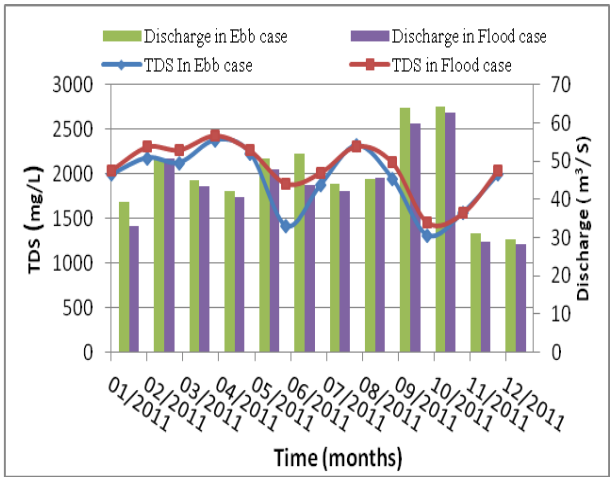

Fig. 4. TDS/ Discharge diagram in Shatt al Arab River 2011.

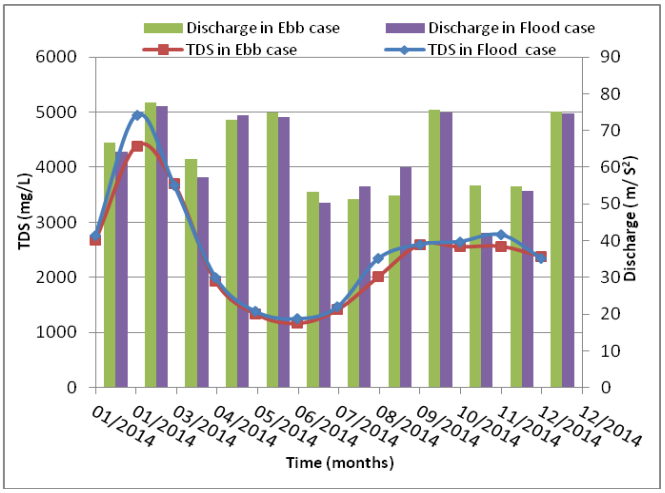

Fig. 7. TDS/ Discharge diagram in Shatt al Arab River 2014.

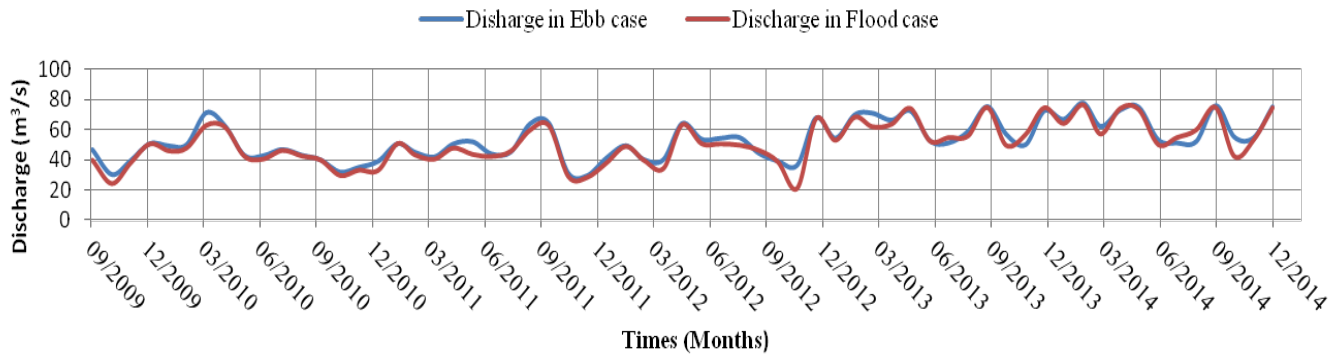

Fig. 8. Discharge diagram in Shatt al Arab River for the year 2009 to 2014.

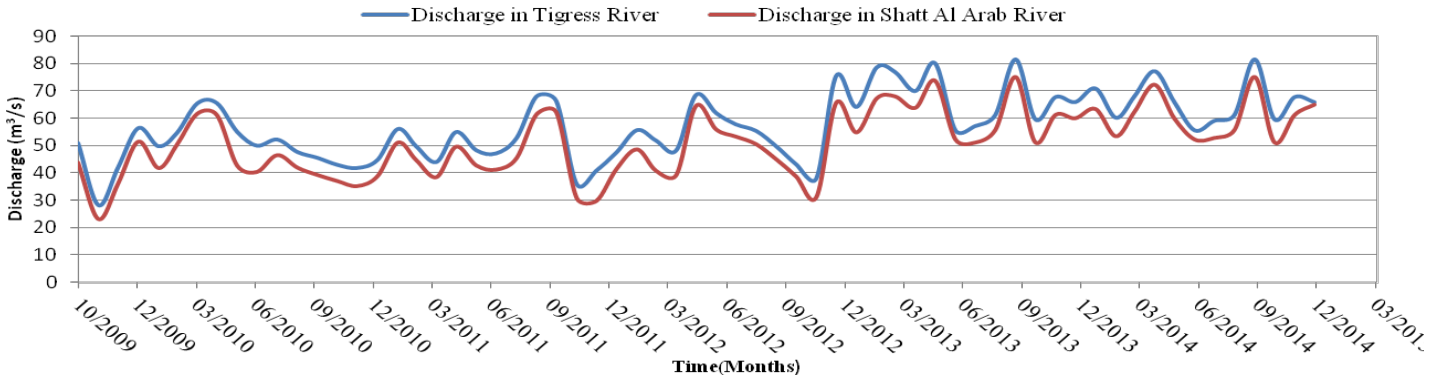

Fig. 9. Discharge diagram in Shatt al Arab River and Tigris for the year 2009 to 2014.

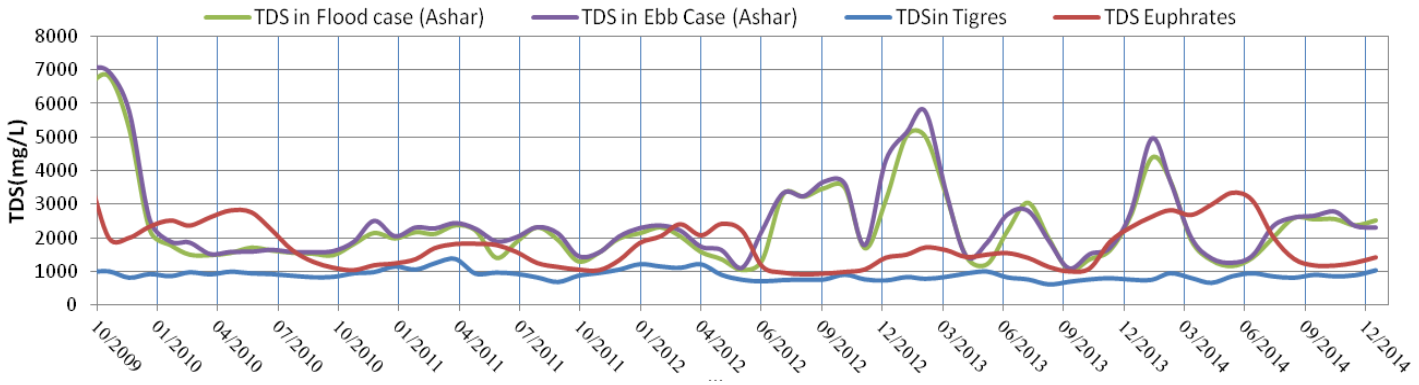

Fig. 10. TDS diagram in Shatt al Arab River, Tigris and Euphrates for the year 2009 to 2014.

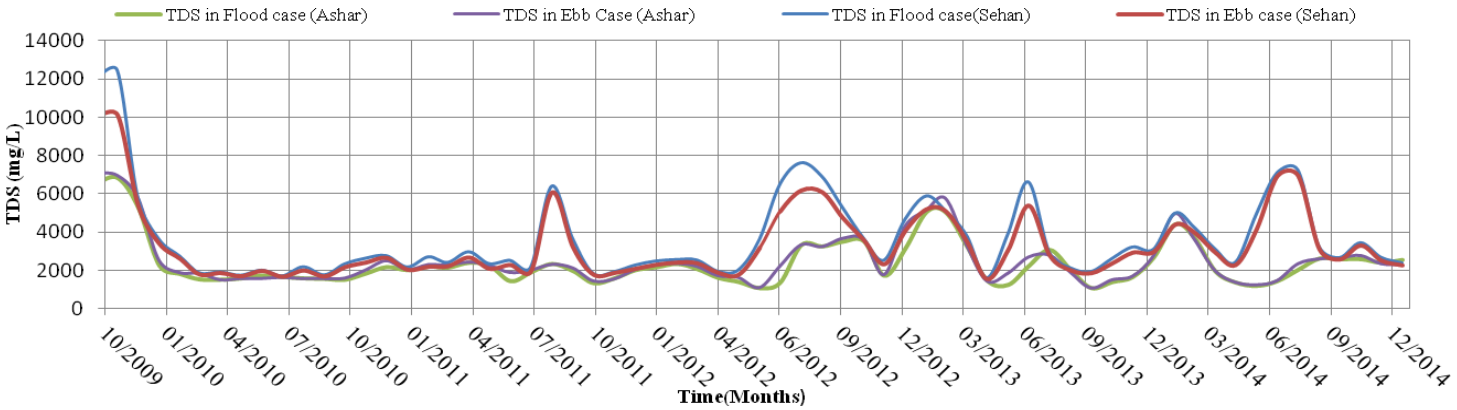

Fig. 11. TDS diagram in Shatt al Arab River, upstream and downstream for the year 2009 to 2014.

REFERENCES

[1] Hamdan, A., "2d sediment transport modelling to the Shatt al-Arab river estuary," Journal of Basrah Researches (Sciences), vol.34, no.4, pp50-59, 2008.

[2] Al-Ansari, N., Ali, A. and Knutsson, S. " Present Conditions and Future Challenges of Water Resources Problems in Iraq," Journal of Water Resource and Protection, no. 6, pp 1066-1098, 2014.

[3] Al-Kazaeh, D."Chemical and Physical properties of common water in area and evaluation degree for Irrigation in Basra/ Iraq," Journal of Basrah researches (Sciences),vol.40 , no.2, pp 26-44, 2014.

[4] Al-Mudaffar, N. and Mahdi, B., "Iraq's inland Water quality and their impact on the North- Western Arabian Gulf," Marsh Bulletin Journal, vol.9, no.1, pp 1-22, 2014.

[5] Al-Murib, M., "Application of CE-QUAL-W2 on Tigris River in Iraq, " M.Sc Thesis, Portland State University, USA, 2014.

[6] Hassan, W., Hassan, I. and Jasim, A." The Effect of industrial effluents polluting water near their discharging in Basrah Governorate /Iraq," Journal of Basrah researches (Sciences), vol. 37, no.1, pp 21-32, 2011.

[7] AL- Mahmood, H., Hassan,W., AL-Hello, A., Hammood, O., and Muhson, N. "Impact of low discharge and drought on the water quality of the Shatt al-Arab and Shatt al-Basra rivers (south of iraq)," Journal of international academic research for multidisciplinary, vol.3, no.1, pp 285-296, 2015.

[8] Al- Mahmood, H." The monthly variations of discharge and effect that on a total dissolve suspended and salinity in Shatt al-Arab river (south of Iraq)," Journal of Iraq sciences, vol.50, No.3, pp 355-368, 2009.

[9] Ela, W. P. "Introduction to Environmental Engineering and Science, Prentice Hall," 3rd ed. ISBN 0-13-148193-2, 2007.

[10] Water Resources Ministry, Water Resources Directorate in Basrah, "Discharge, TDS, and levels records from 2009 until 2015", unpublished works.

Evaluation of the Radiological Contaminated Area in Al Tuwaitha Nuclear Site, Iraq

Hisham M. J. Al Sharaa, Dr. AbdolRazak T. Zaboon., and Dr.AbdulHameed M. Jawad Al Obaidy
Building and Construction Engineering Department, University of Technology/Baghdad

***Abstract*— In this paper, the authors aim to introduce contaminated area in Al Tuwaitha nuclear site, Iraq using GIS and statistical techniques. This contamination problem draws attention to the new result of radioactive contamination found in part of the country. The area are characterized into{ equivalent dose (effective dose), ^{40} K, $^{(234, 235,238)}$U , ^{60}Co,^{137}Cs and ^{90} Sr}. the represent area contaminated by equivalent dose that directly reflect measured values of contaminants in mrem/hr and percentage of contaminated area and by Bq/g as radionuclide concentrations activity in Al Tuwaitha soil. Most areas have value around (0.01) mrad/hr or less do not appear as effective level The results show that 35% from contaminated area (7 km^2) has value from (0.01-0.1) and only 2% found in the range between (40-105) mrem/hr. The contaminated area above normal concentration of U sum in soil having about 65% from total contaminated area (0.87 km^2) Where for ^{40}K found near to the background level and UNSCEAR (2000), between (0.2-0.4) Bq/g have area about 74% . Serious contamination with ^{137}Cs found in total area of about (0.29 km^2). While the area classified as 57% from (0.02-2) Bq/g, 21% for (2-8) Bq/g, 9% for (8-16) Bq/g, 7% for (16-28) Bq/g and 6% for (28-56) Bq/g. The total estimated contaminated area with (^{60}Co) is about (0.14 km^2) while 33% from contaminated area have concentration level between (0.05-10) Bq/g. The Strontium-90 (90Sr) having almost the same contaminated area with ^{60}Co and ^{137}Cs (0.21Km^2) as 6% from contaminated area having concentration level between (0.005-0.10) Bq/g.**

I. INTRODUCTION

The information of radionuclide distribution and radiation levels in the environment is important for assessing the terrestrial radiation exposure affects due to, cosmogenic and human activities. The principal nuclear site is Al Tuwaitha nuclear research center which contains about 18 facilities. Al Tuwaitha site considered as unique case most of its facilities suffer substantial physical damage during the Gulf Wars and have been subjected to subsequent looting. Despite the long history of nuclear programs at Al Tuwaitha no significant radioactive contamination as a result of normal operations has been officially reported for the site or surrounding communities Radionuclide's are present in the environment and within the remaining structures. ([1]) Location of these facilities are shown in fig.1

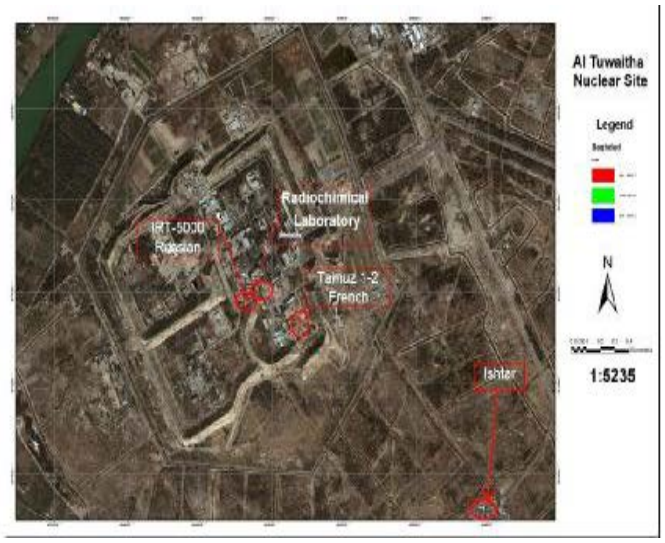

Fig. 1: Map of Al Tuwaitha nuclear site Facilities

Radionuclide and radioactive sources are the main reason to cause cancer in humans and can also cause other adverse health effects, including genetic defects in the children of exposed parents or mental retardation in the children of mothers exposed during pregnancy. The contaminated area was identified and contoured according to the measured dose and analyzes samples taken from such area. The GIS and the statistical software used to characterize the contaminated areas based on the dose and radioactive concentration levels.[1]

This study introduces the contaminated area in Al Tuwaitha nuclear site and the GIS analysis. introduces more information about radioactivity dose in Al Tuwaitha site. This study goes, also, with the other studies which were done at different areas in Al Tuwaitha nuclear site like ([2],[3],[4],[5])

II. AL TUWAITHA SITE DESCRIPTION

Al Tuwaitha Nuclear Research Center covers an area about 1.3 km^2 and is located approximately 1 km east of the Tigris River 18 km south of Baghdad. This site is fortified by large earthen beams around the key facilities which cover over one km^{2}which includes two research reactors (Osiraq and IRT-5000) a fuel fabrication facility, plutonium separation uranium enrichment, waste storage facilities and many other facilities, ([6],[7]). The nuclear research facilities at Al Tuwaitha were built by various companies during the development of the Iraq's peaceful nuclear program. Therefore, the area inside the earthen beam is divided into many sectors. French, Italian, and

Russian sectors are so named according to the nationality of the companies that designed and built the nuclear research facilities. Fig (1) illustrates the buildings layout within Al Tuwaitha region and the associated sector names. At gulf wars, the IRT 5000, Tammuz-2, radiochemistry and nuclear physics laboratories, fuel fabrication laboratories, the radioactive waste treatment station, and nuclear material stores were seriously destroyed. In late-April 2003, a documented radioactive dispersal occurred ([7]). Iraqi civilians looted perimeter storageareas at Al Tuwaitha and dumped more than 200 barrels of uranium compounds in the form of yellowcake near the village of Ishtar. The barrels, still containing more than 10 kilograms of yellowcake residue, were transferred to nearby villages and used for household storage. Uranium residue from the looted barrels was likely dumped in residential areas prior to recovery of the containers. Coalition forces, IAEC hazmat teams, and others recovered most of the barrels and dumped yellowcake by June 2003. Also, they recovered numerous cesium and cobalt sources that possessed acute danger to surrounding communities. Subsequently, all high-level radioactive materials at the site were secured and transported out of Iraq. Remaining sources and unsecured radioactive materials were consolidated into on-site bunkers and storage buildings ([1]).

III. MATERIALS AND METHODS

In this paper, total of 201 soil samples were analyzed. The radioactivity data samples used in this paper were collected in 2009 were provided by of Science Ministry and Technology (MOST). They were collected locations with effective gamma and beta dose rates were measured (1-meter heigh) at same locations, they were collected from inner and outer Tuwaitha site (Fig. 2). The output digital map layer includes contours for exposures dose radioactive maps were created by additive interpolation. While the background levels defined from soil samples collected within Baghdad city 18 km far from Al-Tuwaitha site (Fig. 3). Soil samples were analysis for gamma, beta and Alfa spectra.

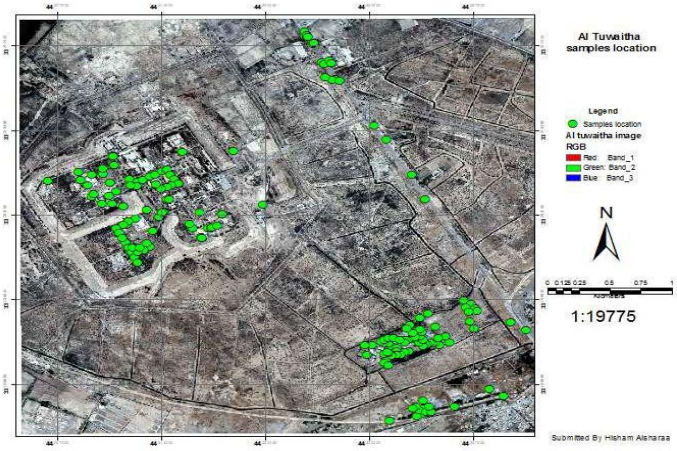

Fig 2: Photo map of samples locations

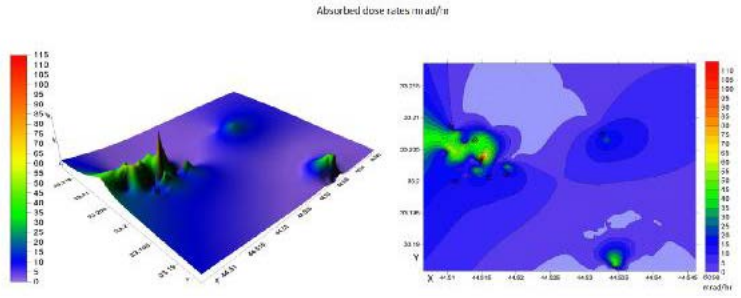

Fig. (3) Dose rate contour and 'mountain range' plots.

IV. RESULTS AND DISCUSSION

The area are characterized into equivalent dose (effective dose), ^{40}K, Usum, ^{60}Co, ^{137}Cs and ^{90}Sr. the area represent area contaminated by equivalent dose that directly reflect measured values of contaminants in mrem/hr and percentage of contaminated area and by Bq/g as radionuclide concentrations activity in Al Tuwaitha soil. Most areas have value around (0.01) mrad/hr or less do not appear as effective level. about 35% from contaminated area (7 km^2) has value from (0.01-0.1) mrem/hr,exposure doses change into range between (0.1-0.5) mrad/hr have about 30% from contaminated area, this values rise between (0.5-40) mrem/hr and have 33% contaminated area and 2% contaminated area from (40-105) mrem/hras in Figure 4. The contaminated area has normal concentration of Usum in soil having about 65% from contaminated area (0.87km^2) between (0.08-0.2)Bq/g , 23% (0.2-0.4) Bq/g, 6% between (0.4-0.7) Bq/g, 5% between (0.7-2.5) Bq/g and 1% between (2.5-4.5) Bq/g as the highest concentration level in the study area as in Figure 5.

For **^{40}K**can see normal levels near to the background level and UNSCEAR (2000), with level between (0.2-0.4) Bq/g have area about 74% from^{40}K totalcontour area (1.4 km^2), 22% between (0.4-0.52)Bq/g and 4% between(0.52-0.64)Bq/g Fig.6.

It is shown in Fig.(7) that for Cesium-**137** (^{137}Cs) contaminated area with (0.29 km^2),57% from (0.02-2) Bq/g, 21% between (2-8)Bq/g, 9% between (8-16) Bq/g, 7% between (16-28) Bq/g and 6% between (28-56) Bq/g. While for ^{60}Co as nuclear reactor waste, contaminate area with (0.139 km^2) 33% from contaminated area have concentration level between (0.05-10) Bq/g, 27% having concentration level between (10-30)Bq/g, 15% having concentration level between (30-50) Bq/g, 17% having concentration level between (50-100) Bq/g and 8% as the highest concentration between (100-180) Bg/g Figure 8.

Finally,Strontium-90 (^{90}Sr) having almost the same contaminated area with ^{60}Co and ^{137}Cs (0.21 km2) as 6% from contaminated area having concentration level between (0.005-0.10) Bq/g, 75% having concentration level between (0.1-0.5) Bq/g, 15% having concentration value between (0.5-1) Bq/g and 4% having concentration level between (1-1.4) Bq/g (Fig. 9).

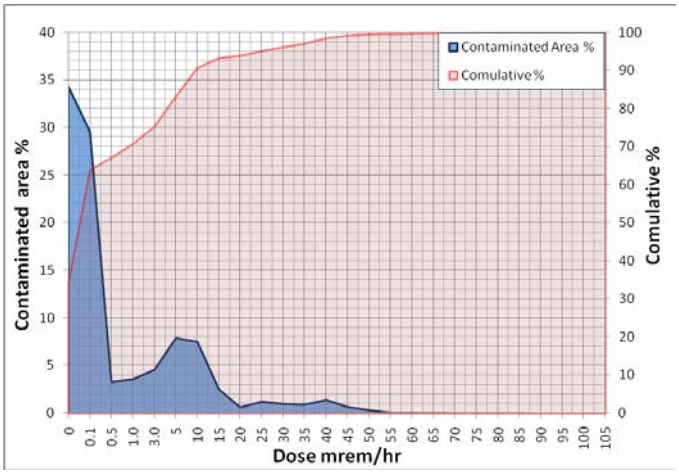

Fig 4: Contaminated area with measured dose

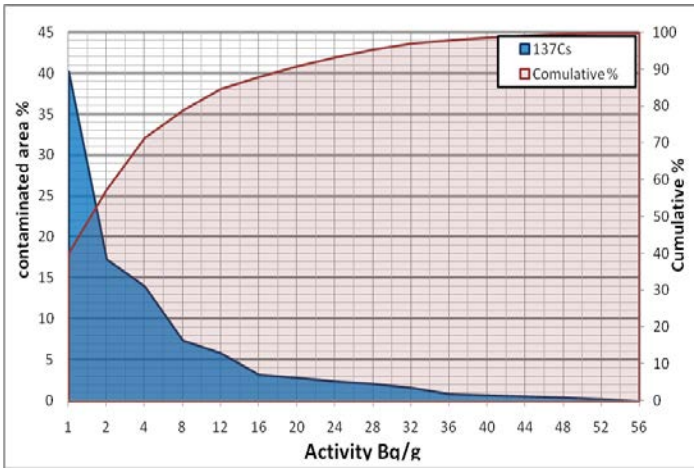

Fig. 7: Contaminated area with Caesium-137

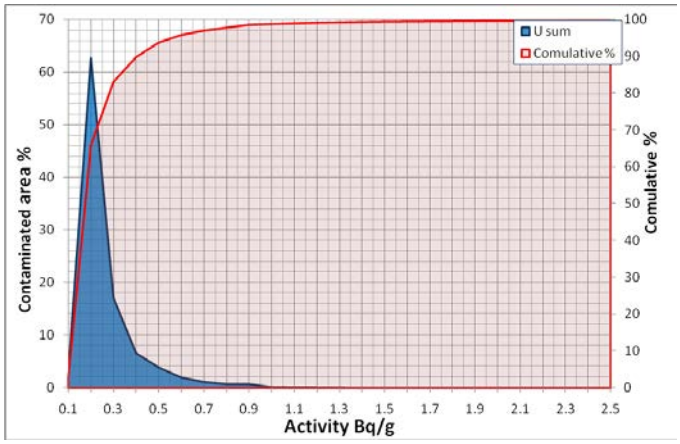

Fig. 5: Contaminated area with uranium

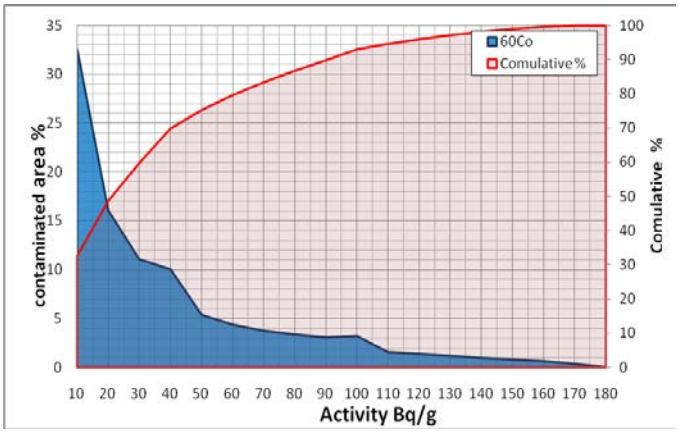

Fig. 8: Contaminated area with Cobalt-60

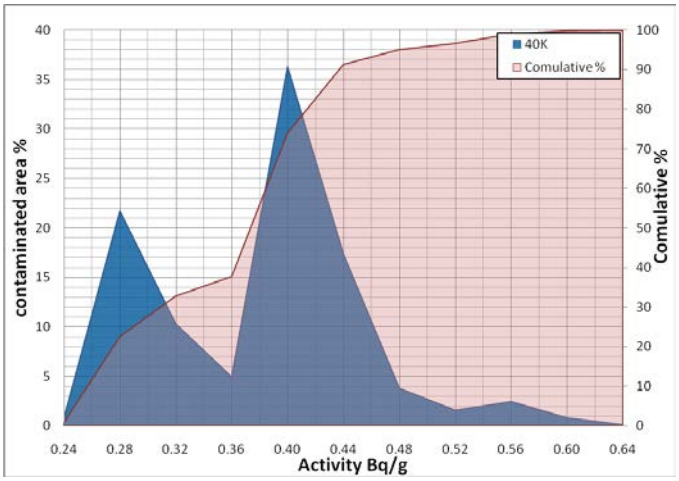

Fig. 6: Contaminated area with Potassium-**40**

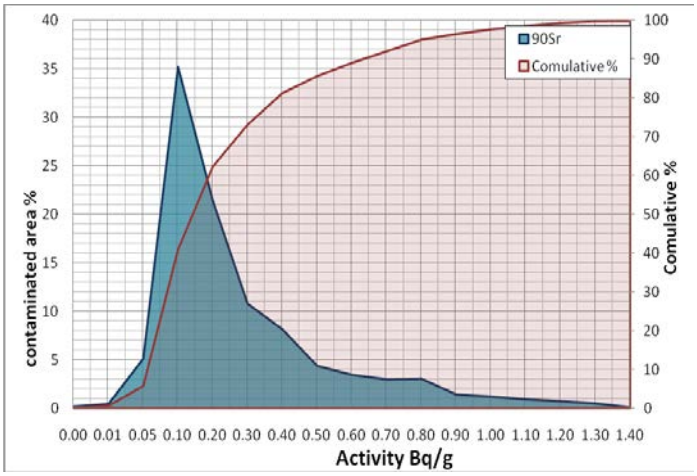

Fig. 9: Contaminated area with **Strontium-90**

V. CONCLUSIONS

Relationship holds (external radiation pathway). For example, the Contours are designed to be Base for area calculation in NRC and area surrounding, regulators and the regulated community for evaluating the environmental progress are used to set the contamination level. The contamination area based on contaminant values are also being used as a part of statistical and GIS programs. These areas estimate the rate of continuing sources of contaminants soil and facilities the represent area contaminated by equivalent dose that directly reflect measured values of contaminants in mrem/hr and percentage of contaminated area and by Bq/g as radionuclide concentrations activity in Al Tuwaitha soil. Most areas have value around (0.01) mrad/hr or less do not appear as effective level The results show that 35% from contaminated area (7 km^2) has value from (0.01-0.1) and only 2% found in the range between (40-105) mrem/hr.

The contaminated area above normal concentration of U sum in soil having about 65% from total contaminated area (0.87 km^2) Where for ^{40}K found near to the background level and UNSCEAR (2000), between (0.2-0.4) Bq/g have area about 74% . Serious contamination with ^{137}Cs found in total area of about (0.29 km^2). While the area classified as 57% from (0.02-2) Bq/g, 21% for (2-8) Bq/g, 9% for (8-16) Bq/g, 7% for (16-28) Bq/g and 6% for (28-56) Bq/g.

The total estimated contaminated area with (^{60}Co) is about (0.14 km^2) while 33% from contaminated area have concentration level between (0.05-10) Bq/g.

The Strontium-90 (90Sr) having almost the same contaminated area with ^{60}Co and ^{137}Cs (0.21Km^2) as 6% from contaminated area having concentration level between (0.005-0.10) Bq/g.

REFERENCES

[1] Al Sharaa Hisham "Evaluation of Radioactive Contamination at Al Tuwaitha Nuclear Site Using Gis" M SC. Thesis submitted to Building and Construction Engineering Department of the University of Technology. (2012).

[2] Abdol Razak T. Zaboon ,Abdul Hameed M. J. Al Obaidy,Hisham M. J. Al Sharaa " Cobalt-60 And Cesium-137 Soil Contamination In Al Tuwaitha Nuclear Site, Using GIS Technique" Eng. &Tech. Journal, Vol.32, Part (A), No.13, 2014

[3] Abdol Razak T. Zaboon ,Abdul Hameed M. J. Al Obaidy,Hisham M. J. Al Sharaa " Radioactive Doses Contamination in Al-Tuwaitha Nuclear Site, Using GIS Techniques" Eng. &Tech. Journal, Vol.31, Part (A), No.9, 2013

[4] Abdul Hameed M. J. Al Obaidy, Bashair AR Mohammed, Hisham M.J. Al Sharaa"Radiological risk assessment for Al-Twuaitha nuclear site in Iraq" (IJEE), Volume 4, Issue 3, 2013, pp.409-414

[5] Jarjies Adnan, Mohammed Abbas, Horst Monken Fernandes, Melanie Wong and Roger Coates "Prioritization methodology for the decommissioning of nuclear facilities: a study case on the Iraq former nuclear complex", Journal of Environmental Radioactivity doi: 10.1016/j.jenvrad.2012.01.001. (2012).

[6] Cochran, J.R., and J.J. Danneels,"Sandia National Laboratories Support of the Iraq Nuclear Facility Dismantlement and Disposal Program", SAND2009-1732, Sandia National Laboratories, Albuquerque, NM. , (2009).

[7] Chesser Ronald K., Brenda E. Rodgers, Mikhail Bondarkov, Esmail Shubber and Carleton J. Phillips, "Piecing together Iraq's nuclear legacy," Bulletin of the Atomic Scientists, May/June, vol. 65, no. 3, pp.19–33. (2009).

[8] United Nations Scientific Committee on Effects of Atomic Radiation UNCEAR Report of UNSCEAR to the general assembly, United Nations, New York, USA. PP. 111-125. (2000).

The fate of Some Emerging Contaminants in conventional Wastewater treatment plants

Hussein Janna and Mark D. Scrimshaw

Abstract— **Over the past decade, the occurrence and removal of emerging contaminants in the environment has received much attention. Both natural and synthetic progestogens are two examples of such emerging contaminants. Sewage treatment works are recognised as one of the main routes of these compounds to the environment. Low concentrations (nanograms per litre) of biologically active chemicals may exhibit an impact on aquatic organisms and human health. This study was undertaken to determine the occurrence and removal of these chemicals at sewage treatment works. Therefore, field-based sampling campaigns were undertaken at a sewage treatment works, to achieve this study. Solid phase extraction and LC/MS/MS were used in order to analyse the samples from these different locations.**

The results have demonstrated that progestogens are in the sewage system; the natural hormone (progesterone) was the most predominant compound (46.9 ng/l) among the progestogens in the influent. The conventional sewage treatment works were, to some extent, able to remove these compounds from wastewaters. However, this may not be adequate to afford protection to the environment.

Key words **— Emerging Contaminants, Liquid Chromatography, Progesterone, PPCPs.**

I. Introduction

MANY researchers, around the world, are finding out the trace levels of some emerging contaminants in water related with wastewater treatment plants effluents [1, 2]. One of the [3] earliest reports published was in 1965 by Stumm-Zollinger, showing that the wastewater treatment process was not reducing the concentration of steroids [4]. An issue began to receive more attention by environmenlist scientists in the late 1990s when these pollutants linked to toxicological effects in fish [5].

There are a very large number of possible emerging contaminants, from industrial chemicals to the category known as pharmaceuticals and personal care products (PPCPs), Progestogens One obvious group would be the synthetic progestogens, which are the other active ingredient of many contraceptives (at doses higher than EE2) and are also used in hormone replacement therapy [6]. Endogenous (natural) progesterones play important roles in reproduction in fish, controlling maturation of the gametes (sperm and oocytes) in both sexes. Synthetic progestogens target the progesterone receptor in women, and as fish also have this receptor, so it seems likely that synthetic progestogens will target these receptors. All of this information suggests that synthetic progestogens may have effects on fish reproduction and the key issue is really at what concentration do synthetic progestogens cause adverse effects, and how different is this concentration to those in the aquatic environment [7]. There is some evidence that natural progesterone and synthetic progestogens are present in wastewaters in Europe at up to 40 ng/L [8] and that advanced treatment, such as ozonation will effectively remove progesterone [9]. However, there is no comparison of removal in such advanced treatment processes with what may be achieved in biological processes, and in particular, evidence that nitrifying bacteria enhance removal rates of other hormonally active compounds with similar structures, such as the steroid estrogens [10,11,12].

The overall aim of this paper is to determine the occurrence and fate of progestogens in wastewaters in the UK, comparing two types of biological treatment processes (trickling filters and nitrifying activated sludge).

Hussein Janna ,Civil Engineering Dept., Al-Qadisiyah University, Al-Diwaniyah, Iraq (corresponding Author e-mail: hussein.janna@ qu.edu.iq).

Mark D. Scrimshaw, Institute for the Environment, Brunel University, Uxbridge, UB8 3PH, UK.

II. Materials and Methods

A. Sampling Sites

Two sewage treatment works were selected for the study, both discharging into a tributary of the River Trent near Nottingham, UK. One was trickling filter (TF) plant, with a rapid sand filter, and dry weather flow (DWF) of 13,000 m^3/day. The other site was a nitrifying activated sludge (N/AS), again with a sand filter treating a DWF of 11,000 m^3/day. For progestogens, all samples were 1L, except settled sewage was (500ml). Samples were collected in 2.5L amber glass bottles and filtered by (GF/C, Whatman, UK) directly after collection. Samples were extracted onto SPE directly. Sampling regime achieved at conventional STWs was at 9:00 am and 2:00 PM at Hallam Field STW while was at 12:00Pm at Newthorpe STW. During the sampling, there was no rain or wet weather; as a result the concentrations of the chemicals of interest in the influent would be expected to be at relatively high concentrations due to the lack of dilution, giving high loadings to the STWs.

B. Reagents, chemicals, and method

The purity of all progestogens are more than 98%, were purchased from (QMx and LGC, UK). Organic solvents with HPLC grade, methanol (MeOH), dichloromethane (DCM), and MTBE were purchased from Rathburn Chemicals (walkerburn, UK). Cyproterone–acetate (CPA), megetsrel–acetate (MTA), medroxyprogesterone (MDP), and progesterone (PGT) were purchased from QMx, (Essex, UK). Norethindrone (NTD), drosprinone (DSP), dydrogesterone (DHG), norgestrel (NGL), tibolone (TBL), and medroxyprogesterone–acetate (MPA) were obtained from LGC (Exeter, UK). Deutrated Norethindone_d6, and Progesterone-d9 were obtained from (Aldrich and QMx) with >98% chemical purity. For solid-phase extraction (SPE), Oasis HLB (500mg/6cm3) cartridges were obtained from Waters (watford,UK). Calibration standard solutions were prepared from individual stock solutions. Around 1000 ng/ml individual stock solution of each compound (deuterated and non-deuterated) was prepared in methanol. A series of mixed calibration standards containing all ten analytes in MeOH/H_2O (50/50), at a concentration range 0.5-500 ng/ml, and deuterated internal standards at 100 ng/ml were prepared from the stock solution

The method followed Vanderford et al, [13]. The extraction was performed by using 12-port vacuum extraction manifold with a -15 Hg (-0.5 bar). Cartridges were preconditioned with 5mL of methanol, followed by 5ml of reagent grade 18MΩ water (Milli-Q, Millipore, Watford, UK) before loading the sample with a 10 ml/min flow rate. After extraction, the cartridges were rinsed with 5mL of reagent water and the dried with a stream of air for about 3hrs. Cartridges were then eluted with 5 ml (90% of MTBE, 10% MeOH) followed by 5 ml of MeOH. These elutes were collected in 15 ml polypropylene tubes, and were subsequently evaporated on a miVac concentrator at 35 ºC on the [-OH] programme setting for 65 minutes and then evaporated to dryness with nitrogen. Samples were re-dissolved in 50:50 (MeOH / H_2O) prior to quantification by LC/MS/MS.

The concentration of analytes were determined using LC/APCI (+)/MS/MS consisting of an HPLC (Hewlett Packard 1050) coupled to a Perkin Elmer Series 200 auto sampler and a PESciex API 365 triple quadruple mass spectrometer with APCI source. Analytes were separated using an Ascentis c18 (10cm x 2.1mm) 2.7µm column, (Ascentis, Bellefonte, USA). The total run time was 44 minutes, with data acquisition over a methanol/water (+0.4% formic acid) for 5% MeOH for 2 minutes, linear gradient to 80% MeOH over 25 minutes and held at 80% for 5 minutes, followed by a column wash for 1 minute and equilibration back to starting conditions for 13 minutes for a 44 minutes cycle time. The mass spectrometer was operated in a positive APCI mode using multiple reactions monitoring (MRM).

III. Results and Discussion

The concentrations of progestogens after each process at Hallam Fields and Newthorpe STWs are shown in Figure (1). Concentrations of the chemicals of interest in the settled sewage, rapid gravity filter (RGF) feed, and final effluent are described below:

A. Settled sewage.

The concentrations of progestogens after the primary settling tank at Hallam Fields and Newthorpe STWs are shown in Figure (1-A). The natural hormone, progesterone (PGT), was detected in all the samples at this stage at both STWs. It can be seen that there was an abundance of progesterone, where the mean concentration was 46.9 ng/l at Hallam Fields STW and was 41.6 ng/l at Newthorpe STW, no significant difference had occurred between both STW. Many compounds concentrations at both STW were similar, DHG and TBL mean concentrations in settled sewage at Hallam Fields STW was 35.4 and 29.4 ng/l, while at Newthorpe STW the mean concentrations of them were 35.2 and 15.9 ng/l. The cyproterone acetate (CPA) was quantified in seven out of eight samples with a mean concentration of 18.0 ng/l at Hallam Fields STW, and detected in all samples with a mean of 13.5 ng/l at Newthorpe STW. MPA and DSP were detected only in 25% of the samples of the settled sewage at Hallam Fields STW and 50% of the samples at Newthorpe STW, while NTD was quantified in half of the number of the samples and 75% of the sample at Hallam Fields and Newthorpe STWs. MPA, DSP, and NTD show again no significant difference in concentrations for each individual compounds at each STWs, and the mean concentration of each individual compound was below 10 ng/l in both STWs.

For a few compounds, significant differences (p=0.05) in concentrations were observed, Norgestrel in settled sewage at Hallam Fields STW 23 ng/l was a significantly above the concentration at Newthorpe STW of 6.1 ng/l. Conversely, MDP 6 ng/l and MTA 6 ng/l were significantly less at Hallam Fields STW than at Newthorpe STW of 23.9 ng/l and 17 ng/l respectively.

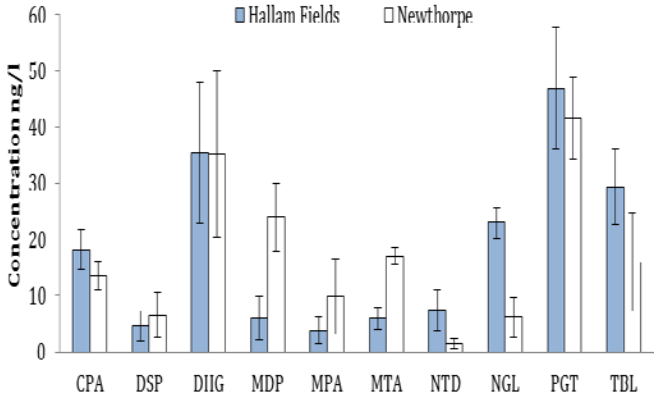

(A) Settled Sewage

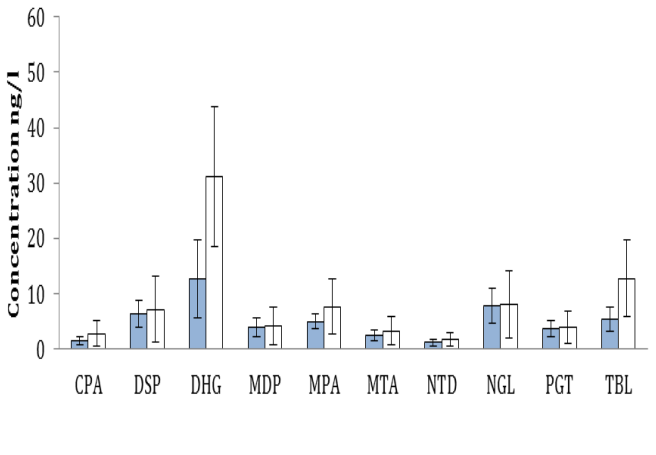

(B) RGF Feed

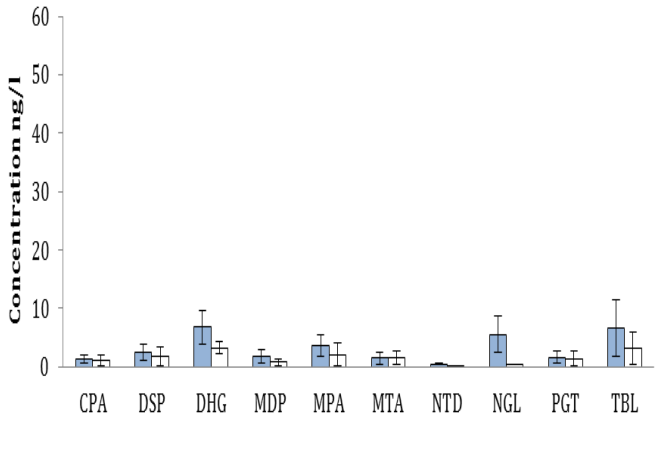

(C) Final Effluent

Fig.1: Concentrations of progestogens in ng/l (A. Settled Sewage. B. RGF Feed. C. Final Effluent) of two sewage treatment works.

B. Rapid gravity filters (RGF) feed.

The concentrations of progestogens after the biological treatment (N/AS or TF) at Hallam Fields and Newthorpe STWs are shown in the Figure (1-B). It can be seen that significant difference (p=0.05) for progesterone had occurred between the settled sewage and the RGF feed indicating a removal of 92% and 90% for Hallam Fields and Newthorpe STWs respectively. According to Figure (1-B), it apparent that CPA, NTD, NGL and TBL show significant removal had occurred during the N/AS process at Hallam Fields STW, while these chemicals apart from CPA show no removal had occurred during the TF process at Newthorpe STW. This indicates that the activated sludge process (ASP) may be more efficient to remove these compounds than the TF process.

Conversely, medroxyprogesterone (MDP) and MTA present a significant difference had occurred during TF as a biological process at Newthorpe STW, but there was no evidence for removal during N/AS and perhaps this because of these compounds had low concentrations entering the ASP at Hallam Fields STW.

For a few compounds, Drosprinone (DSP), DHG, and MPA show no significant removal was observed during the biological treatment at both STWs. It is possible that more removal could occurred , but not statistically observed in this study and that probably due to the number of samples limits statistical power. Generally, removal of compounds can be achieved by either adsorption or degradation and the range of Log Kow (3.87±0.68) was similar for all progestogens. This means similar removals were expected in terms of adsorption and the differences in the removal might be resulted from the degradation.

C. Final effluent.

Figure (1-C) shows the concentrations of progestogens after the RGFs at Hallam Fields STW and Newthorpe STW. From Figure (1-C), it can be seen that all compounds demonstrated removal through the STW. Although it appears that the performance of the RGF at Newthorpe STW was better than the performance of that at Hallam Fields STW, however there was no significant difference (p=0.05) had occurred across the RGF's for either STWs. Whereas the RGF at Newthorpe STW removal efficiency was between 53%-94%, and it was lower at Hallam Fields STW (0-62%). This difference in removal efficiencies may be real or might be biased because of the sampling strategy.

The effluent mean concentration of each individual compound at Hallam Fields STW was below 7 ng/l, while the concentrations of the final effluents at Newthorpe STW were below 3.5 ng/l. Most of the final effluent samples concentrations were below their limit of quantification in both STWs, half of LOD value was taken to calculate the mean concentration of each compound. For example, there were only two values at Hallam Fields STW were above the quantification limit and these values had possibly influenced the results for DSP, MDP, MTA, NTD, PGT, and TBL, therefore it is possible that the performance of the RGF at Hallam Fields STW looked less efficient than the RGF at Newthorpe STW.

The overall removal efficiency of progestogens during all the processes at each STW is illustrated in Figure (2). It is apparent that the natural hormone, progesterone, was the easiest compound which could be removed with 96% and 97% removal efficiency at Hallam Fields and Newthorpe STWs respectively. At Hallam Fields STW, the removal efficiency for most of the compounds were above 70% and only DSP and MPA were removed at 48% and 5% removal efficiencies, this is perhaps due to the low initial concentrations of these chemicals which were just above the limit of quantification. Newthorpe STW presented a very good removal for all compounds and the removal efficiencies were between 71% and 97%. In general, the ASP would be expected to give more removal than the TF process, however Hallam Fields STW looked less efficient to remove these compounds than Newthorpe STW and as mentioned this may be due to sampling strategy. Therefore, it is possible that the removal efficiencies at Hallam Fields STW were more realistic than at Newthorpe STW.

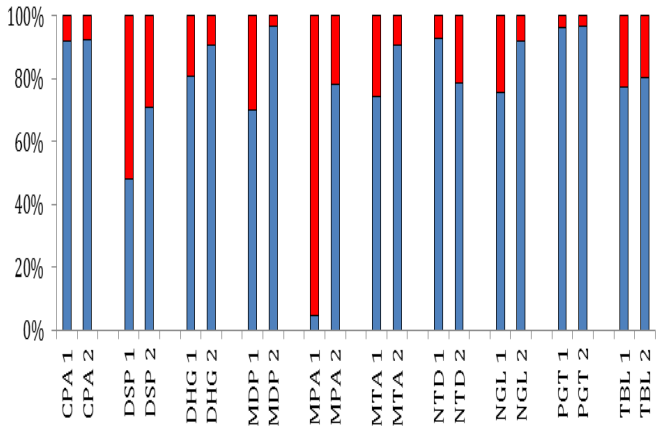

Fig.2 Percentage removal efficiencies of progestogens through the conventional treatment works. (1) Hallam Fields STW, (2) Newthorpe STW. □ % removed during STW, ■ % Discharged to the surface water.

IV. CONCLUSION

The conclusions obtained throughout this research are:

1. Progestogens were present in the sewage system. In terms of predominance, the natural hormone, progesterone, was the most predominant progestogens.

2. Both the ASP and TF plant partially removed the compounds, and at both sites the sand filters contributed to improving overall removal.

3. Although sand filter was not designed to remove emerging contaminants from wastewater, however, removal of progestogens did occur in this study with removal efficiency rate from 53 - 94% in trickling filter STW and from no removal to 62% at the activated sludge STW. Therefore the performance of the sand filter at the TF plant appeared better than that one of ASP sewage work although there was no significant difference. There is very limited information available to demonstrate the performance of sand filter in terms of removing emerging contaminants from wastewaters. However, the results achieved by Gunnarsson et al. exhibited that estrone (E1) and bisphenol A (PBA) had reduced from 6.3 ng/l to 0.67 ng/l and from 780 ng/l to 420 ng/l respectively due to the fact that the sand filter demonstrated biological activity (nitrification)[14].

REFERENCES

[1] Halling-Sorensen, B., Nielsen, S.N., Lanzky, P.F., Ingerslev, F.,Lutzhoft, H.C.H., Jorgensen, S.E., 1998. Occurrence, fate and effect of pharmaceutical substances in the environment—a review. Chemosphere 36 (2), 357–393.

[2] Ternes, T.A., Kreckel, P., Mueller, J., 1999a. Behaviour and occurrence of estrogens in municipal sewage treatment plants—II. Aerobic batch experiments with activated sludge. Sci. Total Environ. 225, 91–99.

[3] Kim, S.D., Cho, J., Kim, I.S., Vanderford, B.J. & Snyder, S.A. 2007, "Occurrence and removal of pharmaceuticals and endocrine disruptors in South Korean surface, drinking, and waste waters", Water Research, vol. 41, no. 5, pp. 1013-1021.

[4] Stumm-Zollinger, E., Fair, G.M., 1965. Biodegradation of steroid hormones. J. Water Pollut. Cont. Fed. 37, 1506–1510.

[5] Jobling, S., Noylan, M., Tyler, C.R., Brighty, G., Sumpter, J.P., 1998. Widespread sexual disruption in wild fish. Environ. Sci.Technol. 32, 2498–2506.

[6] Bromley, S.E., de Vries, C.S. and Farmer, R.D.T. (2004). Utilisation of hormone replacement therapy in the United Kingdom. A descriptive study using the general practice research database. BJOG Int. J. Obstet. Gynaecol., 111, 369-376.

[7] Sumpter, J.P. (2008). The ecotoxicology of hormonally active micropollutants. Water Sci. Technol., 57, 125–130.

[8] Vulliet, E., Baugros, J.B., Flament-Waton, M.M. and Grenier-Loustalot, M.F. (2007). Analytical methods for the determination of selected steroid sex hormones and corticosteriods in wastewater. Anal. Bioanal. Chem., 387, 2143-2151.

[9] Snyder, S.A., Wert, E.C., Rexing, D.J., Zegers, R.E. and Drury, D.D. (2006). Ozone oxidation of endocrine disruptors and pharmaceuticals in surface water and wastewater. Ozone Sci. Eng., 28, 445-460.

[10] Vader, J.S., van Ginkel, C.G., Sperling, F., de Jong, J., de Boer, W., de Graaf, J.S., van der Most, M. and Stokman, P.G.W. (2000). Degradation of ethinyl estradiol by nitrifying activated sludge. Chemosphere, 41, 1239-1243.

[11] Leusch, F.D.L., Chapman, H.F., Korner, W., Gooneratne, S.R. and Tremblay, L.A. (2005). Efficacy of an advanced sewage treatment plant in southeast Queensland, Australia, to remove estrogenic chemicals. Environ. Sci. Technol., 39, 5781-5786.

[12] Ren, Y.X., Nakano, K., Nomura, M., Chiba, N. and Nishimura, O. (2007). Effects of bacterial activity on estrogen removal in nitrifying activated sludge. Water Res., 41, 3089-3096.

[13] Vanderford, B.J., Pearson, R.A., Rexing, D.J. & Snyder, S.A. (2003) "Analysis of endocrine disruptors, pharmaceuticals, and personal care products in water using liquid chromatography/tandem mass spectrometry", Analytical Chemistry, vol. 75, no. 22, pp. 6265-6274.

[14] Gunnarsson, L., Adolfsson-Erici, M., Bjorlenius, B., Rutgersson, C., Forlin, L. & Larsson, D.G.J. (2009) "Comparison of six different sewage treatment processes-Reduction of estrogenic substances and effects on gene expression in exposed male fish", Science of the Total Environment, vol. 407, no. 19, pp. 5235-5242.

Advective Transport of Trace Elements Pollution in the Shallow Groundwater of Baghdad Area

Sawsan M. Ali and Qusay Al-Suhail

***Abstract*—Groundwater flow of the shallow aquifer of Baghdad area was simulated by a mesh of 2096 non-uniform cells in order to use it later for tracing the advective transport of some trace elements. Two potential waste dumping sites at both sides of Baghdad area were used as a point source pollution spots. Numerical flow model results show good matching between the observed and calculated heads for both steady and unsteady state stages. Advective transport model based on particle tracking scheme of Fe, Mn, Pb and Br elements shows that the possible pollutant plume extension of these elements was slight where the maximum travelled distance after 25 years of the model operation are 1000 and 750 m for Rasafa and Karkh sides respectively. This is mainly due to the low velocities of the groundwater in the study area. Proximity of Karkh pollution site to the River Tigris make the problem more series and all the required measurements should be taken to prevent polluted groundwater approaching River Tigris at this area.**

***Index Terms*—Baghdad, Flow, Modeling, Trace Elements, Transport .**

I. Introduction

Pollution transport in surface and groundwater aquifers is one of the most critical environmental issues that facing the decision makers especially in the urbanized areas where the locals depend on these sources for different uses. The situation becomes more series if there is a connection between the surface and groundwater. Baghdad City, a heavily populated area, with a total area of about 1200 km2, is characterized by passing of the River Tigris dividing the city into two sides, Karkh and Rasafa,(Figur-1).The study area is also characterized by shallow groundwater aquifer system. This aquifer extends within the Quaternary deposits composing mainly from the alternation of sand, silt and clays in some places,[1] rendering it unconfined aquifer through the most parts of the study area. It transforms into semi-unconfined at the areas of dispersion of silt and clay layers. The depth of water table ranges from 1 to 9 meters above sea level, where there multi-flow direction on the both sides of the City. In the Karkh side, the main direction is from the western to the eastern direction, i.e. towards Tigris River. Another direction from River Tigris towards the southwest can be observed.. At Rasafa side the main direction is from the northeast towards the southern west which is also towards Tigris River, (Figur-2). The flow direction may explain temporal changes depending upon the recharge nature and fluctuation of the River Tigris levels as well the anthropogenic effects,[2]and [3]. Several studies have been conducted where most of these studies show variable and complex relation between Tigris River and the shallow aquifer of Baghdad area,[4],[5].

Two waste dumping sites on both sides of the City were established since the seventies of the last century and since that time the population has been rapidly increased and the urbanized areas were extended near to these sites. Now aday , they represent a possible pollution sources especially at the last years where the waste treatment became inefficient due to the war conditions and embargo imposed on the country at the beginning of the nineties. Waste leachate represents the most dangerous form of the pollution due to its variety and ease to access the water table especially in the areas of shallow groundwater system as the case of Baghdad City where the depth to the groundwater table ranging from 0.5 to 12 meters. Accordingly, preventing of leachate approaching the groundwater aquifer or surface water is of prime importance to maintain these waters from the pollution sources. The present study goal is to evaluate the groundwater aquifer pollution by trace elements and then after tracing these elements transport by using numerical flow simulation and advective transport modeling.

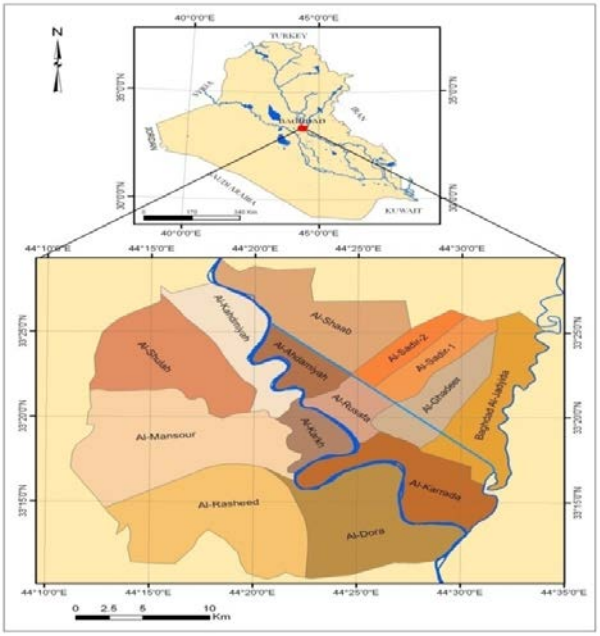

Fig.1 : .Location map of Baghdad City.

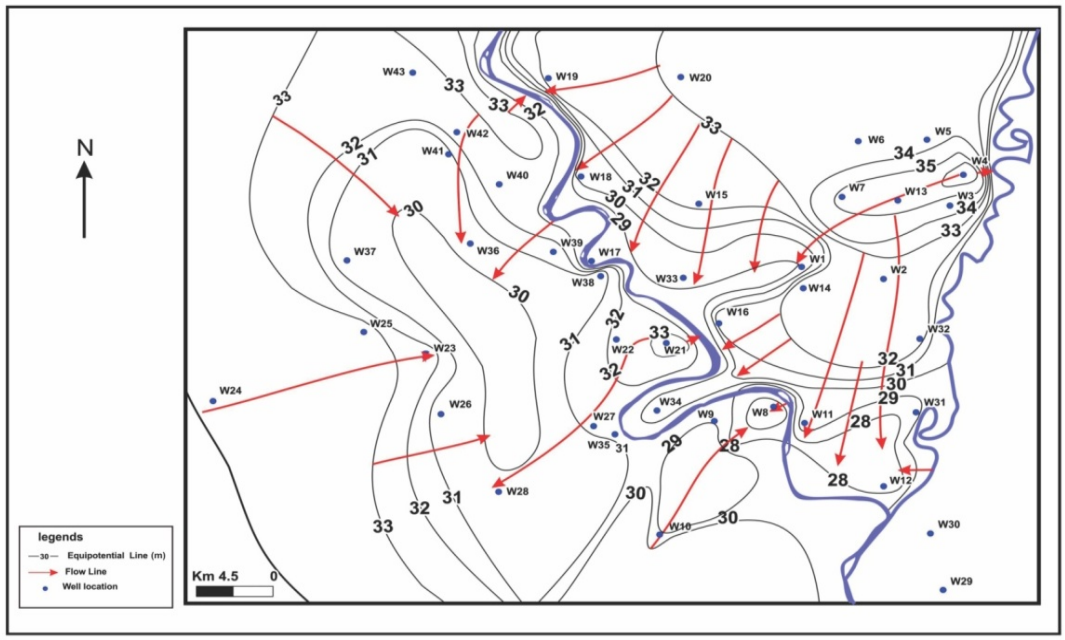

Fig. .2. Groundwater flow map of Baghdad area.

II. MODELING FRAMEWORK

A. Flow model:

The partial differential equation describing the flow in groundwater system is based on Darcy' s law and the law of mass conservation and it can be expressed in three dimensions as [6].

$$\frac{\partial}{\partial x}\left[K_{xx}\frac{\partial h}{\partial x}\right]\frac{\partial}{\partial y}\left[K_{yy}\frac{\partial h}{\partial y}\right]+\frac{\partial}{\partial z}\left[K_{zz}\frac{\partial h}{\partial z}\right] - w = Sc\frac{dh}{dt} \quad \text{---------- (1)}$$

Where:

K_{xx}, k_{yy} ,k_{zz} are hydraulic conductivities along x ,y and z directions (M/T).

h: hydraulic head (L).

w: volumetric flux per unit volume(sink and/or source) (T^{-1}).

Sc: specific storage of the porous media (L^{-1}), and t: time (T).

The above equation applies for the homogenous and isotropic porous media where it describes the distribution of the hydraulic head and flow through continuous region. Practically, this equation can be solved numerically by replacing the continuous system by set of spatially and temporally discrete points using numerical methods, in which the set of the simultaneous algebraic equations that describe the head and flow at each point can be solved using matrix operation. Certain initial and boundary conditions should be imposed depending on the nature of the groundwater system being considered, [7].

B. Transport model:

This model simulates the movement and the chemical alteration of the contaminants as they move through the subsurface. Transport model requires the development of a calibrated flow model or at minimum an accurate determination of the flow velocity which has been based on the field data. The generalized form of the solute transport equation is presented by [8], in which terms are incorporated to represent chemical reactions and solute concentration both in the pore fluid and on the solid surface as [8]:

$$\frac{\partial(\varepsilon C)}{\partial t}=\frac{\partial}{\partial xi}\{\varepsilon D_{ij}\frac{\partial C}{\partial xj}\}-\frac{\partial}{\partial xi}(\varepsilon CV_i)-C'W^* + CHEM \text{ ---------- (2)}$$

Where, CHEM equal one or more of the following:-

- $\rho_b\frac{\partial \bar{C}}{\partial t}$ for linear equilibrium controlled sorption or ion-exchange

$\sum_{k=1}^{g} R_k$ for s chemical rate–controlled reactions and (or) $\lambda(\varepsilon C+\rho_b \bar{C})$ for decay reactions.

D_{ij} : Coefficient of hydrodynamic dispersion, L^2T^{-1}.

C'W*: Solute concentration in the source or sink fluid (mass of solute / mass of solid).

$\bar{C}$: is the concentration of the species absorbed on the solid (mass of solute/ mass of solid).

ρ_b : Bulk density of the sediments ML^{-3}.

R_k : Rate of production of the solute in reaction K, ML^{-3}.

λ : Decay constant, ε: Effective porosity, V: Seepage velocity, LT^{-1}.

C. Study area and conceptual model:

As previously stated, the shallow aquifer of the study area extends within the Quaternary deposits of clastic nature, it is mostly of unconfined type and transforms into semi-unconfined at many locations. Tigris River represents natural internal boundary significantly affects the groundwater flow regime especially near the surrounding areas. According to water table map (figure-2), there are two main flow directions, the first in Rasafa side is from the northeast towards the southwest, i.e. Tigris River whereas the second direction at Karkh side is from the west to the east. Local directions at some locations are also noticed.

The shallow aquifer extends many kilometers away from the study area, therefore, the modeled area is restricted to the coordinates: Latitudes:33º 10′ -33º 29′N and longitudes: 44º 09′- 44º33′E .For the purpose of the present model application, the study area was simulated by mesh of non-uniform 2096 cells where these cells area ranged from 750*750m to 1500*1500m. The central part of the present area was refined into finer cells in order to used it later for transport simulation. The boundary conditions were depicted as follows: for steady state simulation, all the model boundaries as well as the River Tigris and Dyala River cells were regarded as constant head cells whereas for unsteady state simulation, the northern and southern boundaries are regarded as no flow boundaries since they parallel to the flow lines, the eastern and western boundaries were considered as variable head boundaries. Tigris River cells were treated as constant head but with variable monthly heads levels in the unsteady state. MODFLOW,2006 code developed by [9], was used for this purpose.

III. APPLICATION OF THE MODELING PROCESS:

A. Flow model:

Steady state simulation results show good agreement between the calculated and observed head distribution for the entire model cells, where the differences ranged from 0.10 to 1.3 meter at the cells 3,14 and 5,23 respectively. The resulted head distribution are used later as an initial head input values for unsteady state simulation. As stated earlier, the northern and southern boundaries were regarded as no flow while the remaining cells are of variable head. The Rivers Tigris and Dyala cells were treated as variable head cells using the levels record supplied by the Ministry of Water Resources for the study year. Monthly observations of head levels of 12 monitoring wells for one year period are used for unsteady state model calibration. Total of 43 wells dispersed through both sides of the City are pumped with a rate ranging from 5 to 10 liter/second, while the recharge rate (coming from direct rainfall) for the entire model cells is 2.19*10-5 m/day which concentrated in the months of September to April,[5]. The calculated head distribution of 12 months is exhibited in Figures 3 where gradual decrease of the water table of the model cells as compared with the initial head can be noticed. Matching between the calculated and observed head values of the selected 12 wells are explained by figures-4. This figure shows acceptable matching between the two head values where the weak matching at some locations can be attributed to the complex flow behavior resulted from the natural and anthropogenic effects. Lack of detailed storage coefficient values that cover the entire model area where the general value, (with certain error) is an additional factor. However, the present model is acceptable and could be used later for prediction and transport calculation purposes.

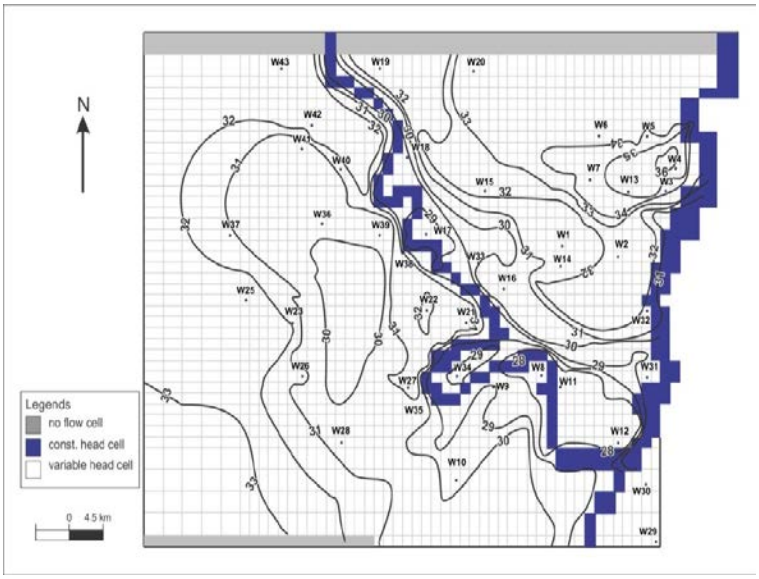

Fig.3: Calculated unsteady state of 12 months model operation.

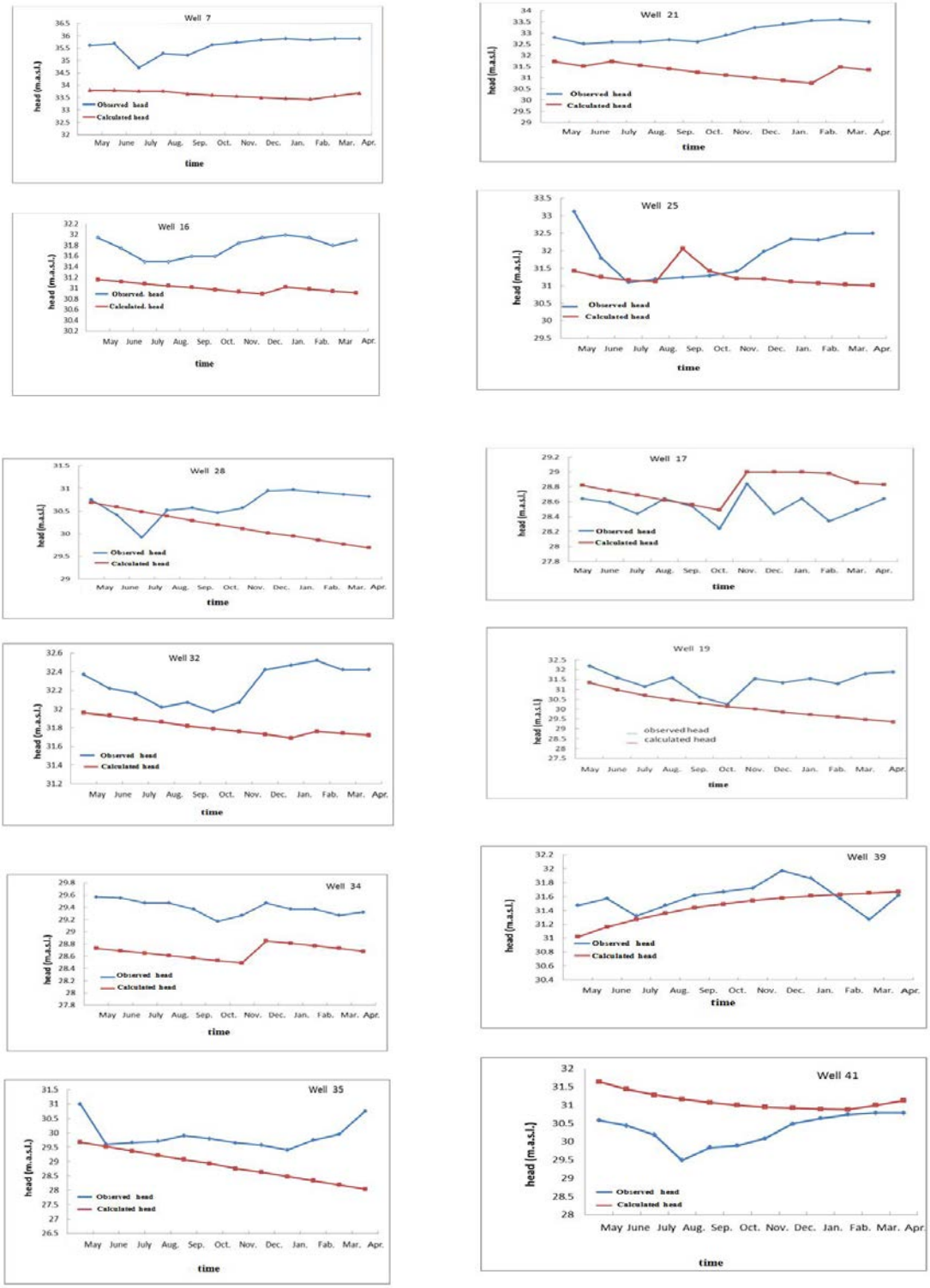

Fig. 4: Matching between calculated and observed heads of the selected wells.

B. Transport Model:

This model calculates the contaminant concentration that are in equilibrium with the groundwater system and geochemical conditions of the modeled area, [10]and [11]. As stated previously, the abnormal concentrations of some trace elements were observed at the two dumping sites, i.e. wells 6 and 42 where the range values of Pb, Fe , Mn and Br(in ppm), are 2-7, 2-7, 1.7-2 and 19.7-22.7 at well site 6 and 4.1-7,4.12-11.9, 1.8-2 and 15.8-18.8 at well 42 respectively. These values are above the permissible limits of the Iraqi, 2009,[12] and WHO, 2008,[13] standards and representing potential health hazard specifically when the transported with the groundwater. The above two points are modeled as starting point for the pollution and that the pollutant mass plume extends from these points with the dominant groundwater flow direction. As the trace elements are conservative, i.e. they move with water by the bulk velocity of the fluid, only advective transport is simulated in this study. For this purpose, PMPATH, 2006, code for particles tracking is used regardless of the trace element type. In particle tracking method of mass transport, the mass of the contaminant is divided into specific number of particles and the movement of these particles from cell to cell is traced. This method is originally developed by [14] and then enhanced by [15]. The same flow grid is used for the advective transport tracing in the study area where the calibrated unsteady state flow model was used as starting head for the simulation process.

FIgur-5 shows the resulted velocity vectors map in which the relatively high velocity zones are concentrated in the western and middle parts of the study area near River Tigris at Rasafa side. As shown by this figure, it is clear that the pollutants move towards River Tigris which acting as sink where significant velocity variations among the model cells can also be observed. This velocity distribution and presence of the pollution spots (well6 and 42) will highly affect the pollution movement. No clear movement from the above two points after model operation for one year period can be noticed. Increasing of the model operation time to 5, 10, 15, 20,and 25 years,(Figures5 and 6), show that the maximum distance passed by the pollutant mass is about 1000 and 750 meters in Rasafa and Karkh sides respectively. The situation in Karkh is more complex since the pollution source site just five kilometers away from River Tigris, therefore the risk possibility will be increased.

According to the above mentioned results, tenths of years may be needed for the pollutants to reach River Tigris from both dumping sites at wells 6 and 42. However, taking measurements such as lining the dumping area and finding other new dumping sites may greatly assisted solving this problem.

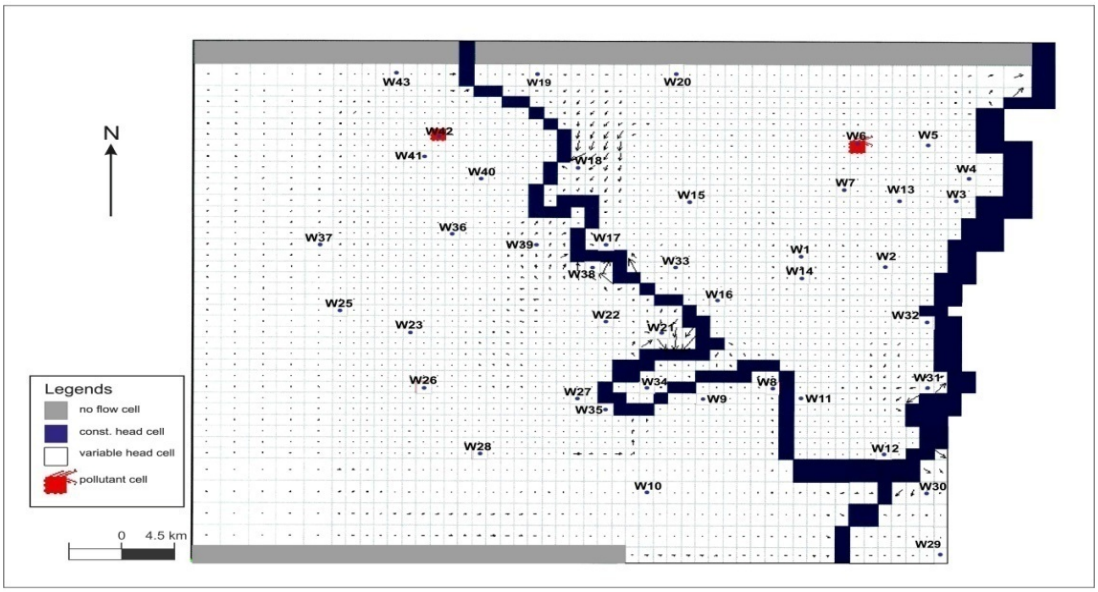

Fig. 5: Extension of pollutant plume after five-years model operation, showing the velocity vector distribution.

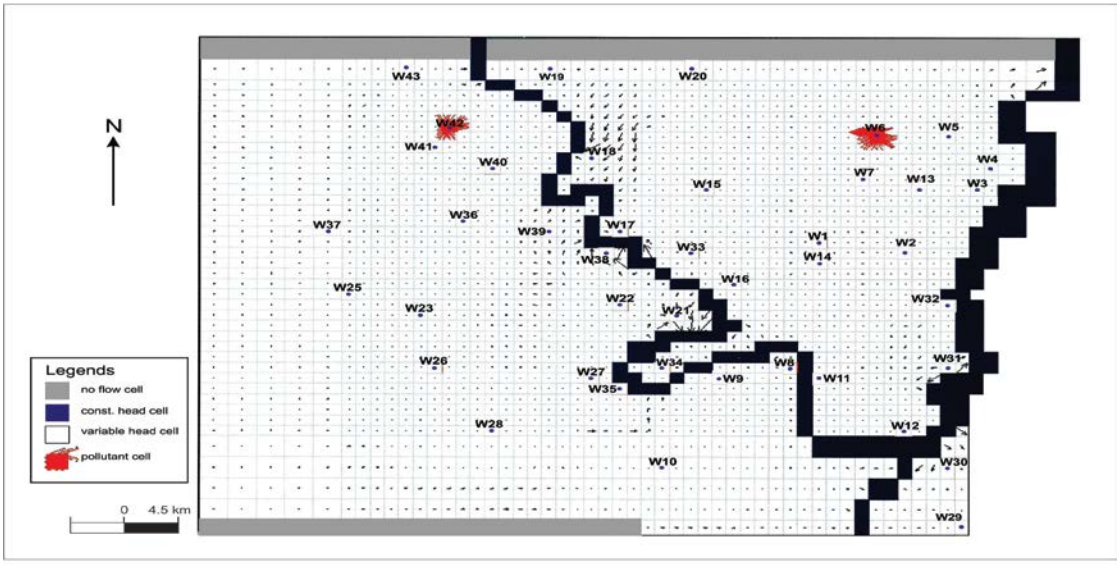

Fig. 6: Extension of pollutant plume after twenty five- years model operation.

IV. CONCLUSIONS

-The shallow aquifer of Baghdad City is of variable nature due to the variations in the sedimentary environment. It is hydraulically connected with River Tigris at the surrounding zones. This relation is variable and depends on the recharge rates incoming from the available sources,(i.e. natural and anthropogenic).

-Flow model of both steady and unsteady state stage show good agreement between the calculated and observed heads where it is sensitive to the changes in hydraulic conductivity and storage coefficient values for the steady and unsteady state respectively. The calibrated flow model is then acceptable for tracing the pollutant transport.

Some of the trace elements of the shallow aquifer show abnormal concentrations where they regarded as conservative pollutant and then traced at the two dumping sites of Karkh and Rasafa sides. Pollution transport model based on particle tracking method is highly related to the nature of velocities variations through the study area.

-Due to the nature of the aquifer being considered, no five years can be noticed where the maximum travelled distances at Karkh and Rasafa sides after 25 years of the model operation are 750 and 1000 meters respectively.

-The situation in Karkh side is more difficult and complex due to the proximity to the River Tigris which represents sink for the groundwater flow, and also when there is a need for using groundwater for different purposes at these two locations. This urges the need for alternative dumping sites away from the present ones.

- REFERENCES:

[1] Buday, T., ; The Regional Geology of Iraq, Vol. 1, Stratigraphy and Paleogeography, I.I.M. Kassab and S.Z. Jassim (eds.),SOM, Baghdad, Dar EL kutib publ. house, Univ. of Mosul, 445p.,1980.

[2] Al-Hiti, B.M., ; Ground water quality within Baghdad area, M.Sc. thesis, College of Science, University of Baghdad, 235p,(in Arabic).1985

[3] Salman, A., Sultan, S. A. and Ibrahim, I. M., The study of groundwater level and engineering characteristics of Baghdad Soil, Amanat Baghdad, Rep. of Iraq, 382p,1990.

[4] Al-dili, A.S., Geotechnical Evaluation of Baghdad Soil Subsidence and their Treatments , Ph.D. Thesis , Univ. of Baghdad , 150 p .,1998.

[5] Bashoo, D. , Lazim, S. and Alwan, M., Hydrogeology of Baghdad province, General Directorate of Water Well Drilling, Baghdad , (internal report), 51p.,2005.

[6] Kinzelbach, W., 1986; Groundwater Modeling; an Introduction with Sample Programs in Basic, Elsevier, NY, 333p.

[7] Frank. L., Reilly, T. E. and Bennette, G.D., 1986; Definition of boundary and initial conditions in the analysis of saturated groundwater flow systems, an introduction, U.S. Geological Survey, Techniques of water resources investigation, book 3, chapter-B5,15p.

[8] Konikow, L. F. and Grove, D. B.; Derivation of equation describing solute transport and dispersion in groundwater, U.S. Geological Survey, Water Resources Investigation, 77-19, 30p.,1977.

[9] McDonald, M.C. and Harbough, A.W; MODFLOW, A modular three dimensional finite difference ground water flow model, U. S. Geological Survey, open file report 83-875.,1988.

[10] Bear, J. and Verruijt, A., Modeling Groundwater Flow and Pollution, D. Reidel publ. comp., 414,1987.

[11] Konikow, L. and Reilly; Groundwater Modeling: The Handbook of Groundwater Engineering by J. W. Delleur, (editor); CRC press, Chapter 20, 969p.,1999.

[12] Iraqi Standard, 2009; Iraqi standard of drinking water No.417; modification No.2.

[13] WHO, 2008; Guidelines for drinking water quality.3rd ed.,vol.1, recommendations, Geneva, 516p.

[14] Pollock D.W; Semi-analytical computation of path lines for finite difference model, Ground Water, Vol. 26, No. 6, pp: 743-750.,1988.

[15] Zimmermann, S., Koumoutsakos, and Kinzelbach, W; Simulation of pollutant transport using a particle method, Journal of Computational Physics, Vol. 173, pp: 322-347, 2001.

Environmental Change Detection of the Main Drain Area, Iraq

Qusay Al-Suhail, Inass Al-Mallah, Adel Albadran

***Abstract*— Main Drain is a longest canal constricted from the middle to the southern parts of Iraq for transporting the agricultural and saline waters of the areas between Tigris and Euphrates Rivers via well- linked drainage networks. Multi-temporal satellite Images of the periods, 1990, 2001 and 2013are used for assessment the environmental change detection of the area restricted between Tigris and Euphrates Rivers, where the used indicators includes: Normalized Differential Vegetation Index (NDVI), Normalized Differential Water Index (NDWI), and Salinity Index(SI). ERDAS V. 11.1 and ARC GIS-10 software's are used to conduct and process all the required calculations. NDVI and NDWI results show similar behavior where they explain decreasing patterns at the year 2001 and then slightly increasing at the year 2013, this is due to the decreasing of the available water quantities and hence the vegetation cover at 2001due to the drought condition at that year. Salinity Index (SI) shows growing increase reflecting the continuous deterioration of agricultural land in the study area. The drought conditions, misuses of the irrigation water, and mismanagement of some secondary drains considered as the main degrading factors affecting the Main Drain area. Protecting of the Main Drain and surrounding areas by completing the lands reclamation plan in association with a proper operation scheme of the Main and secondary drains is of prime importance in this regard.**

***Key words*—Iraq, Main Drain , Change detection, NDVI, NDWI, SI, TM, ETM, OLI8.**

I. INTRODUCTION

Image classification is one of the most important steps in processing remote sensing imagery and provides important input data for Geographic Information Systems (GIS). Land cover characteristics are utilized to assess the environmental impact resulting from the development of energy resources, also to manage wildlife resources and minimize man- wildlife ecosystem conflicts, in addition to preparing the current environmental influence statements and predict future impacts on environment. The land cover monitoring is the registration process variables that occurred over long-time period. This monitoring represents the important factors required for natural resources management and development operations manager of any area [1].

Change detection is the process of identifying differences in the state of an object or phenomenon by monitoring that object at different times [2]. It involves the ability to quantify temporal effects using multi-temporal data-sets [3]. Remote sensing has the capability of capturing such changes, where extracting the change information from satellite data requires effective and automated change detection techniques [4].

II. STUDY AREA

The Main Drain is located in the middle of the Mesopotamia and limited by the coordinates: latitudes (30˚2̀36.098"E) (33˚5̀4̀47.421"E), and Longitude (43˚5́57.918"N) (47˚52́1.706"N) with total area of 60340.590km^2,(Figure.1).Iraq's Main Drain Project (Third River) was considered as one of the most important strategic projects as a downstream drainage line designed primarily to wash the salty soils of the Mesopotamia, and to transport the drainage waters from the catchment area between the Tigris and Euphrates Rivers, and as a border/barrier against the expansion of sand dunes towards the irrigated lands. Additionally, it acts as a navigable waterway for inland transportation between the Gulf and Baghdad, [5].This water course has, in fact, caused significant changes to the environmental, hydrological, and hydrogeological conditions in the areas along its way.

The total length of the Main Drain is about 565 km and consists of Northern, Middle, and Southern main sectors. The pumping station near Nassiriya City is designed for twelve pumps, ten of them operate at a time and two are in standby. The flow through the siphon was by gravity, to be of at (80-110m^3/Sec). Then, it was under rehabilitation since 2005 and then completed in 2009.The Main Drain water is therefore discharged to the nearby marshes by the emergency outlet, where a discharge of approximately 25-30 m^3/Sec was released through the (Dutch canal) which is connected to one of the branches in Gelween and then released to Al-Hammar marshes in Mujammar[5].In order to benefit from the Main Drain water, it has been linked to Al-Hammar marsh to avoid its drying again by Al-Khamisiyah Canal in which its entrance located at 140 km from the Main Drain. This canal has been implemented at the end of year 2009 with a capacity of (40 m^3/Sec) [6]. One of the best ways for studying the above mentioned changes along the Main Drain canal is by using of satellite imagery and classification of these images. In this respect, the change detection procedure is the main tool for observing the temporal and spatial changes of the land cover and other geological phenomena.

Qusay Al-Suhail, Prof. of Water Resources, Geology Dept., College of Science, University of Basrah (email: quab1965@hotmail.co.uk).

Inass Al-Mallah, Lecturer of Hydrogeology, Geology Dept., College of Science, University of Basrah (email: anosa1974@yahoo.com) .

Adel Albadran, Ass. Prof. of Engineering Geology, Geology Dept., College of Science, University of Basrah (email: adelalbadran@gmail.com).

The aim of the present work is to identify the environmental changes for three periods namely: 1990, 2001 and 2013 by using of some the environmental idiocies such as Normalized Differential Vegetation (NDVI), Normalized Differential Water (NDW), and Salinity Index,(SI) with the aid of the remote sensing and Geographic Information System techniques.

III. GEOLOGIC AND GEOMORPHOLOGIC SETTING

The study area is located within the Mesopotamia which is flood plain subsiding basin since the Pliocene [7], with more than 250m thickness consisting of complex alternating sequence from sand, silt, and clay sediments accumulated during the quaternary period, and brought by the rivers Tigris, Euphrates and tributaries from adjacent mountains area to the central parts of Mesopotamia [8]. Terraces, alluvial fans, and fluvial sediments represent the main Pleistocene sediments. The Pleistocene – Early Holocene units include sheet runoff, gypecrete, and slope sediments. While the Holocene units include sediments of different origin like fluvial, lacustrine, marine, estuarine, Aeolian, and anthropogenic [9](Figure.2).Geomorphologically, it is a huge aggradation (accumulation) geomorphological unit, where the fluvial, lacustrine, and aeolian landforms prevail. Estuarine and marine forms also exist, but these are restricted to the extreme southeastern reaches of the plain.

IV. HYDROLOGIC SETTING

Rainfall of the study area occurs in the months extending from October to April ranged from (0,007 – 31.69 mm), while the months of June to September are almost dry. High temperature values are concentrated in January and July in rage of (9.94 – 36 ˚C). The global warming as a whole, as well as the increasing of anthropogenic effects mainly cause increasing of temperature. General decrease of rainfall during the last years was also noticed.

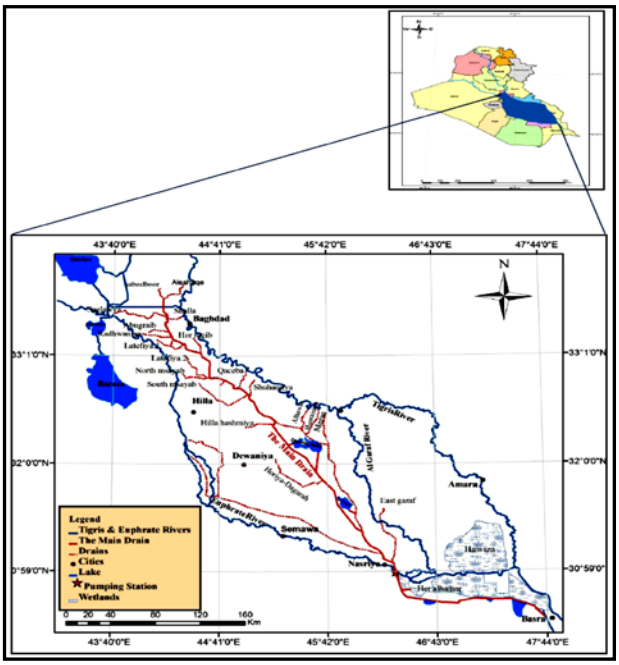

Figure (1): Location map of the study area (Prepared by the authors).

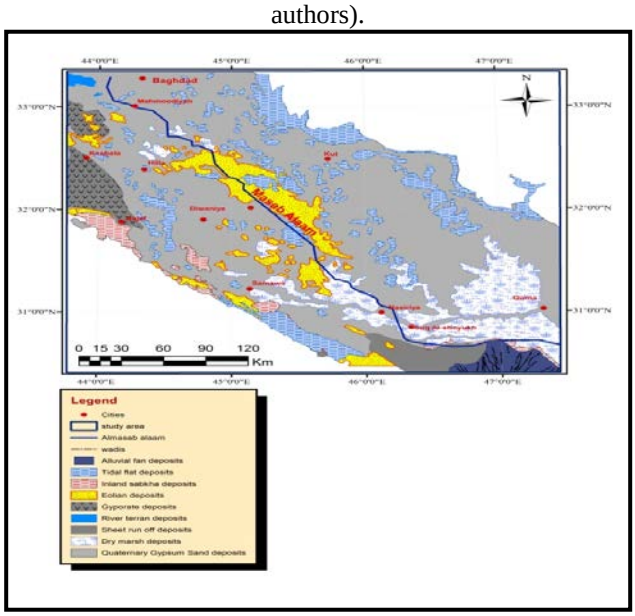

Figure (2): Geological map of the study area modified from [10].

Mean monthly values of the discharges of the Euphrates and Tigris Rivers of four stations namely, Baghdad, Shat Al-Gharaf, Hindiya barrage, and Shat Al-Hilla are used to investigate the trends at these stations for the period 1980 – 2013 in the Main Drain area, (Figure.3). All of the four stations of both Tigris and Euphrates Rivers show remarkable decreasing trends specifically for the periods after the year 1990. Decreasing of precipitation at the upper parts of the two rivers catchment area is the main reason for these trends. Controlling of discharge through dams construction by riparian countries (Turkey and Syria) is an additional factor in lowering the incoming water quantities.Discharges of the Main Drain at two stations, the first is Numaniya-Shomaly at the kilometer 731 and the second is the pumping station at the

kilometer 160 for the period 2011-3013 were used to explain the nature of flow rates changes [11]. Figure (4) shows that the above two stations have slight increasing trends. Extensive application of irrigation without strict control leads to the increasing of water discharge to the Main Drain canal.

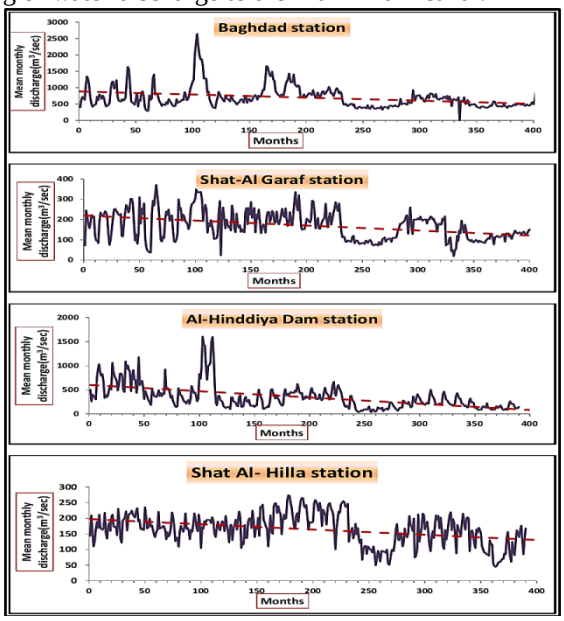

Figure (3): Mean monthly discharges of the present study stations for the period (1980 – 2013).

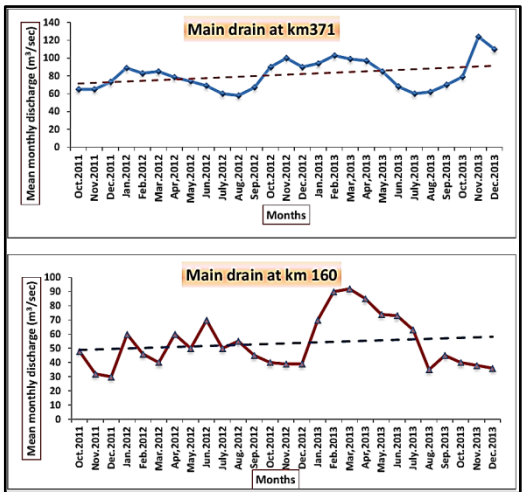

Figure (4): Mean monthly discharge of two stations at the Main Drain for the period 2011-2013.

V. METHODS OF THE STUDY

Three sets of Landsat satellite images are prepared, they are; Landsat type Thematic Mapper (TM-1990), Enhanced Thematic Mapper (ETM+-2001), and Landsate8 Operational Land Image (OLI8-2013) with spatial resolution of 30m, Figure (5), these images were taken at different acquisition dates, all of them are free from cloud and dust effects, therefore they are regarded suitable for processing and change detection purposes. These images have beentreated by using the specialized software's, such as ERDAS V. 11.1 and ARC GIS-10for classifying them and plotting the final maps of the land cover categories.

The images were geometrically corrected and projected (WGS84 datum and UTM 38N projection) using nearest neighbor resampling. The results are layout with the aid of ArcGIS 10 software. Post-processing technique results allowed the production of thematic maps and thus the quantification of changes for each phenomenon in the study area.

Image Indices: Indices are used to create output image by mathematically combining the DN (Digital Number of each pixel) values for different bands [12]. The following indices are applied in the present study, which can be regarded as the most indices used in the environmental studies worldwide.

Normalized Difference Vegetation Index (NDVI): Vegetation indices derived from the satellite data are one of the primary sources of information for the operational monitoring of the earth vegetation cover [13]. Vegetation indices combine reflectance measurements from different portions of the electromagnetic spectrum to provide information about vegetation cover on ground [14].

The Normalized Difference Vegetation Index (NDVI) can be calculated by dividing the difference between infrared and red reflectance measurements by their sum, equation 1, which provides the effects measure of the photosynthetic active biomass [15]. It is an effective indicator to show the surface coverage conditions of the vegetation.

$$NDVI = \frac{NIR-R}{NIR+R} \qquad \text{----------(1)}$$

Where NIR= near infrared band (band 4 in TM) and R= red band (band 3 in TM, ETM+ data, and band 4 in OLI8).

Normalized Differential Water index (NDWI): Normalized Differential Water Index (NDWI) is used to oversee the situation of water in the map area. Water index was computed by the average of summing the NIR and SWIR bands, where SWIR indicating short wave infrared band [16] as shown in the equation below:

$$NDWI = \frac{NIR+SWIR}{2} \text{-------} (2)$$

The idea of the NDWI is based on the nature of the very high contrast between water and land. The low reflections of SWIR and NIR bands of the water allow for their detection [17].

Salinity index (SI): Salinity Index of soil can be computed by making use of the green and red bands, as follows:

$$SI = \frac{Green+Red}{2} \quad \text{------} (3)$$

Where the high reflections of the green and red bands of the salts and saline soil allow for their detection [17]. Salinity index of equation (3) is applied on the three period's images, where the high reflection represents high saline soil. All raster data of SI were converted to vector data.

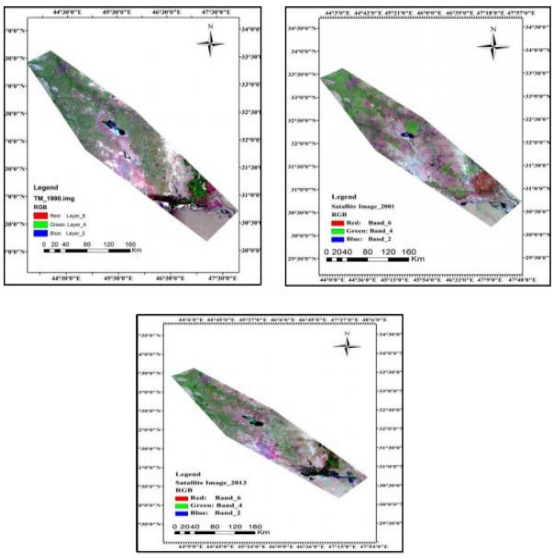

Figure (5): Satellite images used in the present study.

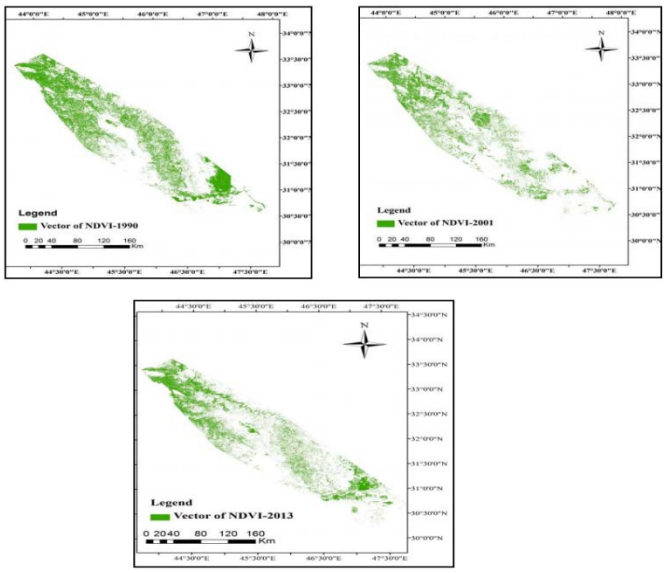

Figure (6): Vectors of the NDVI of the used images for the study period.

RESULTS AND DISCUSSION

The images of three periods (Landsat TM-1990, ETM+-2001, and OLI8-2013) data are used in this study for assessing the changes in the vegetated lands in the study area. The raster maps resulting from NDVI model running is divided by using a threshold, and then all raster data of NDVI are then converted to vector data. The distribution of vegetation covers, which is extracted from NDVI of the above three images, is shown in Figure (6).

Table (1) shows the calculated area covered by vegetation by the three acquisition dates. The results show that the vegetation cover is decreased in ETM+-2001 (9002.25km^2) as compared with TM1990 (14338.38km^2), and then tend to increase in the year 2013 (9635.87km^2)(Figure.7). This slight increase of the NDVI reflects local increasing of the vegetation in the southern marshes area due to available water.Equation (2) was applied on the presently used three satellite images for the same three periods; and the results of the water index distribution of the three periods are shown in Figure (8).The NDWI of the study area shows the same pattern as that for NDVI results where there is a decrease of the water area from (4357.40km^2) in TM-1990 to (1036.15Km^2) in ETM+-2001 while there is an increasing in water index area about (6394.29km^2) in OLI8-2013 image, (Figure.9).

The most increasing of the water area is concentrated in the southern parts as a result of marshes re-flooding and increasing of the water logging around the Main Drain specifically in the central parts. Salinity index areas, (SI) of the three study periods show significant increasing in its value from 2754.85 km^2 to 18760.23 km^2 in TM-1990 to OLI8-2013 images respectively, Figures (10 and 11).

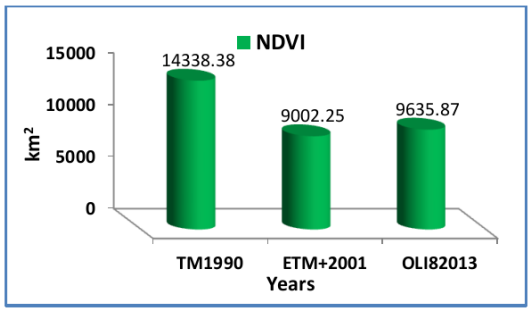

Figure (7): Variation of NDVI of the three study periods.

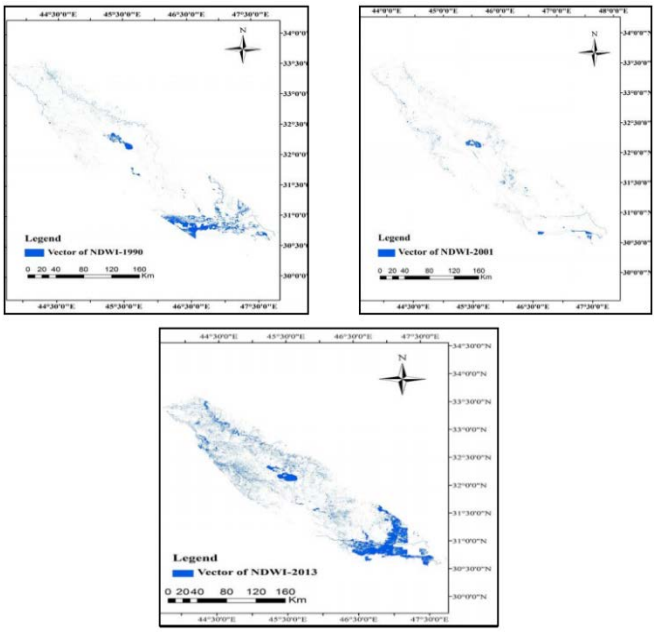

Figure (8): Vectors of the NDWI of the used images for the study period.

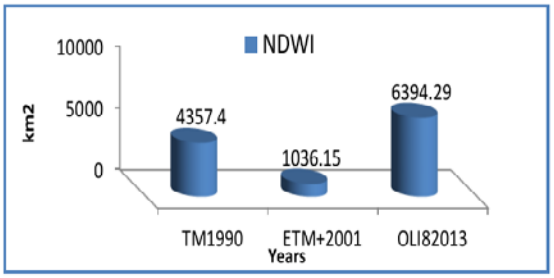

Figure (9): Variation of NDWI area of the three study periods.

Table-1: Image indices of TM-1990, ETM+-2001, and OLI8-2013.

Images Indices	Date		
	TM1990 image	ETM+ 2001 image	OLI8 2013 image
	Area (km^2)		
NDVI	14338.38	9002.25	9635.87
NDWI	4357.40	1036.15	6394.29
SI	2754.85	14031.91	18760.23

Table-2: Change detection results of the three studied periods .

Class name	Area (km^2)		
	TM1990 –ETM+2001	ETM+2001-OLI8 2013	TM1990-OLI8 2013
NDVI	-5336.13	+633.62	-4702.51
NDWI	-3321.25	+5358.14	+2036.89
SI	+11277.0	+4728.32	+16005.38
+ Refers to an increase in the class area, - Refers to a decrease in the class area			

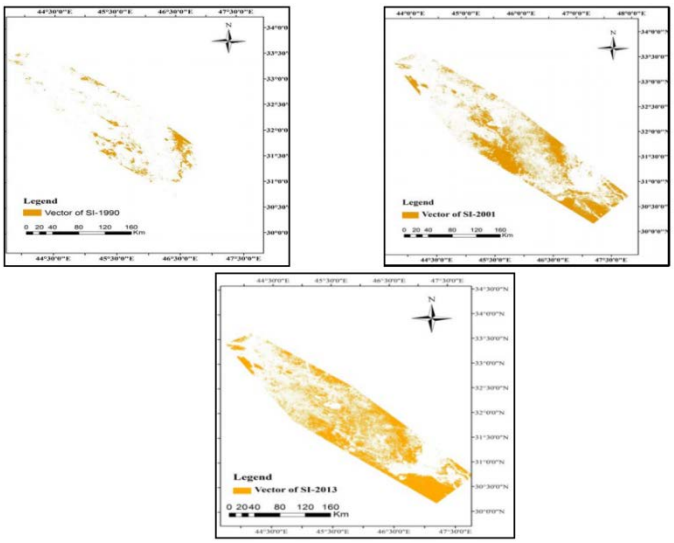

Figure(10): Vectors of SI of the used images for the study period.

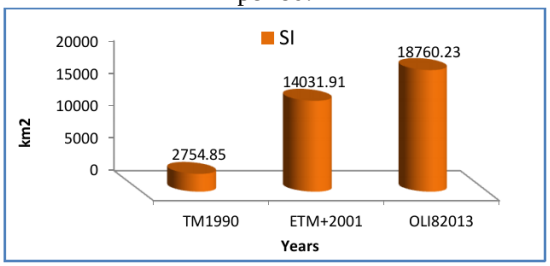

Figure (11): Variation in SI area of three present study periods.

VI. CONCLUSIONS

-Many environmental indices such as NDVI, NDWI and SI are used to show the nature of environmental changes of the Main Drain area for the last 23 years where many natural and anthropogenic factors affect this area.

-Shortage of water due to drought conditions, increasing of hydraulic projects in the riparian countries reflected in NDVI and NDWI indices values assuring no systematic changes in the environmental conditions.

-Disturbance of the land reclamation plans that assumed to be associated with the operation of the Main Drain and the secondary drains have lead to an improper operation and then after deterioration of the Main Drain water.

-Linking of the southern parts of the Main Drain with the marshes to release excess water at sometimes should be under strict monitoring to avoid undesirable environmental changes.

REFERENCES

[1] Mehmood, M.A.,.Classification and monitoring landuse of Mosul city and surrounded areas using the available remote sensing data. Unpubl. MSc. thesis, Remote sensing center, University of Mosul, 1990.

[2] Singh, A., Review Article, Digital change detection techniques using remotely- sensed data.Int. J.Remote Sensing, Vol.10, No.6, pp: 989-1003, 1989.

[3] Khairy, M.A., Spectral mixture for monitoring and mapping desertification processes in Semi- Arid area in North Kordofan State, Sudan. H. D. thesis, Univ. off Dresden, 126p, 2007.

[4] Roy D.P.; Lewis, P.E., Justice, C.O., Burned area mapping using multi-temporal moderate spatial resolution data- a bi- directional reflectance model- based expectation approach. Remote Sensing Environment, Vol 83, pp: 263-286, 2002.

[5] UNEP (United Nation Environmental Programme, Environmental Monitoring and Main Drain Wetland Pilot Project. Final Technical Report. Support for the environmental management of the Iraqi marshlands, 2009.

[6] Engineering report,.Study of processing Al-Masab Al-Aam water\ middle of Iraq.Finalreport.Office of engineering consultants, Univ. of Baghdad, College of Science.,2010

[7] Al-Bassam, K.S.,Yousif, M. A., Geochemical distribution and background values of some minor and trace elements in Iraq soils and recent sediments. Second Iraqiconference on the mineral investment, Baghdad. 51p, 2012.

[8] Jassim, S. Z, and Goff, J. C, .Geology of Iraq, Dolin Prague and Moravian Museum, Brno, 341p,2006.

[9] Yacoub, S.Y.,Stratigraphy of the Mesopotamia Plain. Iraqi Bull. Geol. Min. Special Issue, No.4. p 47-82, 2011.

[10] GEOSURV.The Geological Map of Iraq. Scale 1:1000000.,2011.

[11] NCWRM, The final yearly report results from water control center. National Center for Water Resources Management, Ministry of water resources,2011

[12] Al-Saady, Y.I., Al-Obadi, M.M., and Ahmed, M.A.,. Monitoring of aeolian deposits and environmental changes detection of Ali-Al-Gharbi area, south east Iraq, using remote sensing and GIS techniques. Iraqi Bulletin of Geology and Mining. Vol.9, No.2, pp: 47-79.,2013

[13] Gilaberd, M.A., Gonza'lez-Piqueras, F.J., Garci'a-Haro, F.J. and Melia, J., Ageneralized soil- adjustec vegetation index. Remote Sensing of Environment, Vol.82, pp: 303-310,2002.

[14] Campbell, J.B, .Introduction to remote sensing, 2nd edit., Guilford Press, New York,1996.

[15] Lunetta, R.S., Knight, J.F., Ediriwickrema, J., Lyon, J.G. and Worthy, L.D., Land- cover change detection using multi-temporal MODIS NDVI data. Remote Sensing of Environment, Vol.105, pp: 142-154, 2006.

[16] Al-Jaf A.A., and Al-Saady, Y.I.,.Integration of remote sensing data and GIS application for land cover land use and environmental change

detection in Razaza Lake Bahr Alnajaf area, GEOSURV int. rep.no.3150, 2009.

[17] Othman, A.A.; Al-Saady, Y.I; Al-Khafaji, K., and Gloaguen, R., Environmental change detection in the central part of Iraq using remote sensing data and GIS.Arabian Journal of Geosciences.ISSN 1866-7511.Springer. 12p, 2013.

Effect of Particle Floc Size on Water Treatment by Coagulation–Flocculation Process

Prof. Dr Thamer J.Mohammed* & Mohanad I.Farhan

Corresponding Author* Chemical Engineering Department/University of Technology-Iraq, Email:thamer_jasim58@yahoo.com

Abstract - Several experimental runs were carried out to investigate the effect of flocculation times (1,6 and 20) min. coagulants dose and Camp No .on the residual turbidity or removal efficiency ,floc size or floc formation formed that have (greater Intensity, floc strength and recovery factor, largest volume, greater surface area and the most number) and properties of electrical particle such as (zeta potential ,mobility , frequency) . The floc growth, breakage floc size and regrowth of different type of coagulant were investigated by a laser diffraction particle sizing device (zeta plus) .The coagulants used were alum, $FeCl_3$, polyelectrolyte (PE), alone or in combination of them. Experiments were conducted using a sample of natural water 55NTU turbidity of Tigris River. Jar – test was used to carry out coagulation, flocculation and sedimentation. The results were presented graphically in two dimensional co-ordinates showing the residual turbidity or removal efficiency as a function of coagulant dose to locate the appropriate coagulant type and coagulant dose which it gives higher efficiency (>91%, <5 NTU). The results are also plotted to show the required floc size, zeta potential (0 mv) and others parameters as a function of optimum coagulant dose and flocculation time (1, 6, 20) min., to locate the overall optimum working conditions.

Keywords: Water treatment, Particle size, Zeta potential meter

I.INTRODUCTION

With relatively few exceptions, surface waters require some kind of treatment before distribution to the consumers; surface water is generally more turbid than ground water. Furthermore, river water, which is the major source of water supplies in Iraq, is more turbid than lake and reservoir water [1]. Suspended solids and colloids cause turbidity. Suspended particles in raw water are of large variety in types and characteristics. The removal of suspended impurities from water in conventional water treatment can be performed by two different principles:

(a) By clarification (coagulation-flocculation) and settling process which makes use of the type and concentration of suspended impurities using flocculation agents.

(b) By filtration process through which the remaining unsettled impurities are removed by the filters [1].

The two stages mentioned above are complementary to each other, and consequently, the design, operation and efficiency of filters depend to a large extent on the method and efficiency of the clarification process previously given to the raw water [1]. The type of treatment selected depends on the size of particles present in the surface water. In practice, treatment efficiency also depend on particle size. Thus, for a given water, the optimal condition is inter – related with various parameters such as residual turbidity as suspended solid, flocculation doses and type of coagulant and the condition of mechanical mixing (velocity gradient).The key to effective coagulation and flocculation is an understanding of how individual colloids interact with each other. Turbidity particles range from about (0.01 to 100) microns in size. Contaminated surface water contains particles of different size which can be classified as dissolved (< 0.08) µm, colloidal (0.08-1) µm supracolloidal (>1-100) µm and settable (>100) µm, [2]. The larger fraction is relatively easy to settle or filter. The behavior of colloids in water is strongly influenced by their electrokinetic charge.

Each colloidal particle carries a like charge, which in nature is usually negative. This like charge causes adjacent particles to repel each other and prevents effective agglomeration and flocculation. As a result, charged colloids tend to remain discrete, dispersed, and in suspension. On the other hand, if the charge is significantly reduced or eliminated, then the colloids will gather together. First forming small groups, then larger aggregates and finally into visible floc particles which settle rapidly and filter easily. [3]. Little attention is paid to details of the particle size distribution or floc size and the morphology of the aggregates that are formed through coagulation and flocculation of surface water treatment. These physical properties can strongly influence the efficiency of downstream processes (e.g., sedimentation granular media filtration . and membrane filtration). [4]. The smaller particles, which are classified as colloidal (the colloidal size range is generally regarded to extend from 1nm to 1µm) will remain suspended for very long times. Most attention has therefore been directed toward the use of coagulation for enhancing sedimentation of colloidal material, although this process removes the larger particles, it is so important to remove small particles because of their ability to protect bacteria and viruses from the effects of disinfection [5].

They are chemicals dosed to rapid mixing basins, which are capable of destabilization of colloidal suspensions. The coagulant is usually a metal salt, which reacts with alkalinity in the water to produce an-insoluble metal hydroxide floc, which incorporates the colloidal particles. This fine precipitate is then flocculated to produce settable solids. Coagulants are usually added as concentrated solution which can be dosed accurately using a positive displacement-metering pump [6]. The most effective coagulant is based on the reduction of turbidity, conductivity, cationic demand and total solids. Tests were performed according to the standard jar-test procedure [7], [8] Coagulant aids are substances added to water in addition to the primary coagulant to enhance the coagulation process [9]. A great variety of materials have been used to aid clarification, the most

widely used materials may be roughly classified as [10], [11]-[12]:-
Aluminum sulphate, Poly aluminum chloride PAC, Polyelectrolyte and Titanim tetrachloride.. Oxidants. Absorbents-weighting agents (clay and powdered silica, alkalinity addition such as lime).
Therefore the aim of the present work is study the effect of multi variables on the residual turbidity , floc size distribution and other electrical properties as zeta potential, such as coagulant type, flocculation time.

II.EXPERIMENTAL WORK

In this research, raw water was taken from Tigris River location, AL Sarrafia Bab Almoatham in Baghdad . Conducted laboratory tests on natural water turbidity to Tigris River. Its standard equipment used to study the effect of particle size and Floc size at the time of sintering without coagulants however added coagulants to remove the turbidity of the river water to different levels, and change the velocity gradient.

III.EQUIPMENT

A .Electrical Balance

Equipment model PW 184 with a capacity of Max 210 g and sensitivity of 0.1mg (0.0001g).

B. Floccuator Test (Jar -Test)

The Flocculator/SW6 jar tester used in the experiments has six-stainless steel paddles and two operator programmable memories, each memory may be programmed with paddle speeds between 25 and 250 rpm and time, which can be set to count down from 1 to 99 minutes.

C. Turbidity Meter device

Use the device for measuring the turbidity of the type of HACH -2100Q. Turbidity was measured primitive models raw water and after the addition of coagulants units (N.T.U).

D. pH/Temperature Meter

The pH values and temperature were measured by WTW SERIES pH 720 instrument model Lab 850. Its capacity of measuring is 0 to 14pH and temperature 0-100^{o}C

E. Zeta Plus (Zeta Potential Analyzer and Measure Particle Size) :

Zeta Plus, The Brookhaven Zeta Plus is the simplest, most accurate particle electrophoresis system available. The Zeta Plus measures complete electrophoretic mobility distributions in seconds, including multi-modals, from which zeta potential distribution is calculated. And as the name implies, the Zeta Plus is more than just a zeta potential analyzer. It also measures particle size distributions. The Zeta Plus software will tabulate or graph any appropriate pair of parameters, allowing the determination of the isoelectric point. Statistical process control software is standard. The Zeta Plus is truly cost effective. Its capabilities offer you competitive advantages and savings in both time and labor. Best of all, the Zeta Plus has the highest performance/price ratio of any zeta potential analyzer [13].

F. Measure Zeta Potential

Zeta potential is a measure of the charge on a particle surface in a specific liquid medium. This value of surface charge is useful for understanding and predicting interactions between particles in suspension. Manipulating zeta potential is a method of enhancing suspension stability for formulation work, or speeding particle flocculation in applications such as water treatment. Zeta potential is defined as the potential measured in mV at the slipping plane distance from the particle surface. It is calculated from the following.

G .Intensity Distribution

The first order result from a DLS experiment is an intensity distribution of particle sizes. The intensity distribution is naturally weighted according to the scattering intensity of each particle fraction or family. For biological materials or polymers the particle scattering intensity is proportional to the square of the molecular weight. As such, the intensity distribution can be somewhat misleading, in that a small amount of aggregation/agglomeration or presence or a larger particle species can dominate the distribution. However this distribution can be used as a sensitive detector for the presence of large material in the sample [13].

H. Volume Distribution

Although the fundamental size distribution generated by DLS is an intensity distribution, this can be converted, to a volume distribution or a distribution describing the relative proportion of multiple components in the sample based on their mass or volume rather than based on their scattering (Intensity.) When transforming an intensity distribution to a volume/mass distribution, there are 4 assumptions that must be accepted.

- All particles are spherical.
- All particles are homogeneous.
- There is no error in the intensity distribution.

An understanding of these assumptions is particularly important since the DLS technique itself produces distributions with inherent peak broadening, so there will always be some error in the representation of the intensity distribution. As such, volume and number distributions derived from this intensity distribution are best used for comparative purposes, or for estimating the relative proportions where there are multiple modes, or peaks, and should never be considered absolute. It is therefore good practice to report the size of the peak based on an intensity analysis and report the relative percentages only (not size) from a Volume distribution analysis[13].

L.Floc Strength Factor and Recovery Factor

Floc strength factor (S_f) and recovery factor (R_f), which have previously been used to compare the relative breakage and regrowth of flocs, were calculated as follows [14] .

$$Sf = [d2/d1] * 100 \quad (1)$$

$$Rf = [d3 - d2/d1 - d2] * 100 \quad (2)$$

Where d1 is the average floc size of the plateau before breakage, d2 is the floc size after floc breakage period, and d3 is the floc size after regrowth to the new plateau.

MATERIALS

The coagulants and flocculants used in this study are: Alum $(Al_2SO_4)_3 14H_2O$, Ferric chloride $(FeCl_3.6.H_2O)$, and Cationic polyelectrolyte.

EXPERIMENTAL PROCEDURE

Experiments were performed using the conventional Jar-test procedure. River water sample 55NTU turbidity were collected from Tigris River for experimental work. Sample were transferred to the Jar-test apparatus. Immediately , coagulant (alum, ferric chloride ,or polyelectrolyte as alone or combination between them) were added at various dosage with rapid mixing at 150 s^{-1} velocity gradient for 1min., and flocculation was followed at different times t_f (1-20min.) with kept constant velocity gradient 50 s^{-1}. Settling periods was kept constant 20 min. [15]. At the end of settling periods, samples of 100ml were with drawn from 1cm below the liquid surface by means of suction apparatus connected to a vacuum source. The residual turbidity (C) was measured to determine removal efficiency by using Eqn.3

$$R\% = [C_0 - C/C_0] * 100 \quad (3)$$

where C_o initial turbidity.

The other parameters of particle and floc size were measured at optimum coagulant dose by zeta-potential meter. All details of the equipment and procedure was shown in[15].

RESULTS and DISCUSSION

Optimum Coagulant Dose

The removal turbidity as a function of various kind of coagulants {alum, $FeCl_3$, PE, (alum+PE), ($FeCl_3$+PE)} as alone and combination between them in the following operation coagulation, flocculation and sedimentation is shown in Figs. 1&2. The best coagulant which gave a great removal efficiency and optimum condition (residual turbidity less than (5) NTU, according to standard water quality**.**

These figures show the removal efficiency of turbidity increase with coagulant dose increase until reaching the optimum dose, then removal efficiency decrease if increasing dose of coagulant because the over dosing causes reverse flocculation process and destabilization of the colloidal particles. The best results were obtained with flocculation using $FeCl_3$ 2ppm and polyelectrolyte (0.2-1.2ppm) dose gives R% 94.77 (2.8NTU) as shown in Figs1 &2. These results are in agreement with those suggested by [16], [17].

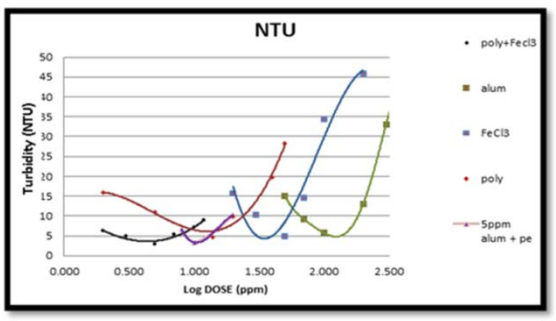

Fig.1 The relationship between turbidity and dose additive and show optimum dose

EFFECT DIAMETER of PARTICLE AND FLOC SIZE in COAGULATION and FLOCCULATION

Several experimental runs were carried out to investigate the effect of natural of particle size of raw water turbidity (55) NTU ,flocculation time ,coagulants dose and camp No. on the floc size or floc formation ,volume, number, surface

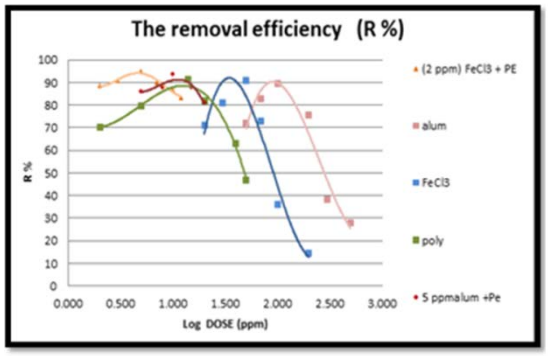

Fig.2 The relationship between removal efficiency R% and dose additive

area, and intensity of floc .

EFFECT DIAMETER of PARTICLE SIZE and FLOC on INTENSITY

The first order result from a DLS experiment is an intensity distribution of particle sizes. The intensity distribution is naturally weighted according to the scattering intensity of each particle fraction or family. For biological materials or polymers the particle scattering intensity is proportional to the square of the molecular weight. As such, the intensity distribution can be somewhat misleading, in that a small amount of aggregation/agglomeration or presence or a larger particle species can dominate the distribution.

This Fig.3 shows the effect of diameters particle and floc size have higher intensity in the solution at 1, 6, 20 min of the formed as a result of added coagulant dose.

The results at twenty-minute of flocculation time were indicated in a simple and remarkable stability of coagulation and the regrowth capacity of the flocs was in the following order:

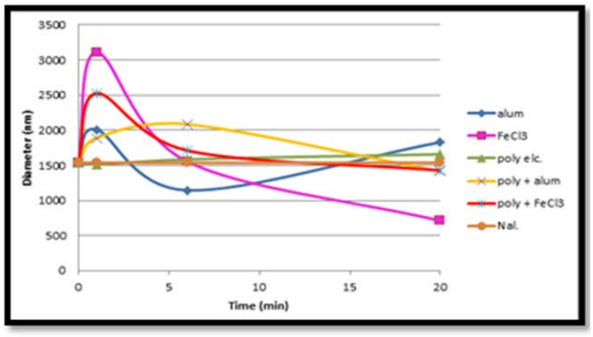

Fig.3 The effect of diameters particle and floc size based on intensity in the solution with time

Alum (1829.11) nm > PE (1657.174) nm > PE+$FeCl_3$ (1427.472) nm > PE+ Alum (1415.448) nm > $FeCl_3$ (711.52) nm respectively this results agreement with , Zhao, et, al, [14].

The result in Fig.3 clearly show that the shear force, flocculation time and breakage period significantly affected the floc breakage and regrowth in the (55) NTU natural turbidity of raw water with $Fecl_3$, Alum, PE and combination between them. Analysis of coagulation – flocculation mechanic can give importer interpreting of the difference in floc breakage and regrowth property.

EFFECT DIAMETER of PARTICLE SIZE and FLOC on VOLUME

It is found that the results at the particle size and Floc size formed in solution in the final flocculation minute, the volume of particles formed after the addition of coagulants smaller than the size of the particles natural water before added where as follows:

PE (1004) nm^3 > (PE + $FeCl_3$) (782) nm^3 > (PE + Alum) (684) nm^3 > Alum(480) nm^3> $FeCl_3$ (368.33) nm^3 respectively.

The results in Fig.4 were noted to show and help the analysis of followed filtration processes and sedimentation which it is required pore size of filter and the capacity of tank settler.

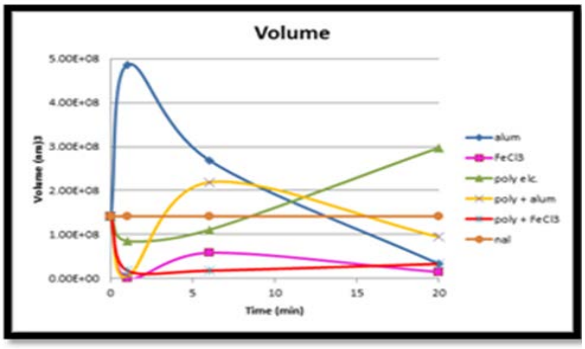

Fig 4 The volume of particle and floc size in the solution with flocculation time

EFFECT DIAMETER of PARTICLE SIZE AND FLOC SIZE IN SURFACE AREA

The results showed in Fig.5 that surface area of the particles and floc size in the solution formed in the final minute after the addition of coagulants where as the following range order

(2.432E+06) nm^2 > Alum(1.601E+06)nm^2 > (PE + $FeCl_3$) (1.411E+06) nm^2 > (PE + Alum) (1.286E+06) nm^2 > $FeCl_3$(1.520E+05)nm^2 respectively.

The advantage of the measuring the surface area of the particles after the addition of coagulants is to the possibility to choose and know the type of filters and pore size required for filtration process and sedimentation.

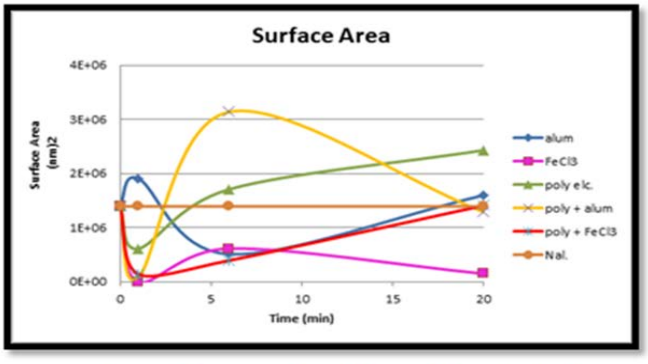

Fig 5 the surface area of particle and floc size in the solution with time

THE EFFECT of PARTICLE DIAMETER and FLOC SIZE BASED on NUMBER

The maximum mean diameter of floc size (2000)nm was observed at flocculation time 6min with (PE + alum) and the diameter of floc decreases at (20) min because breakage floc as shown in Fig.6. This may be due to the fact that the alum and PE combination would improve floc growth and their numbers.

The PE added would shift the size floc from (218) nm at alone alum curve to larger size at (PE+ alum) with the time of (6) min. Therefore adding PE forms stray flocs as a result of reducing the energy of repulsion between colloidal suspended matter and results in an increased number of particles adsorbing on the polymer.

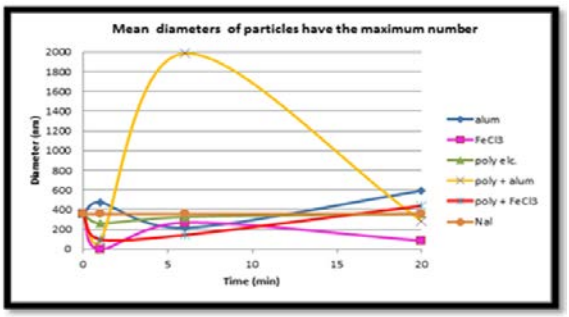

Fig 6 the effect of diameters particle and floc size based on the maximum number in the solution with flocculation

THE COAGULATION - FLOCCULATION EFFECT ON ZETA POTENTIAL

Figure 7 show the effect of flocculation time on zeta potential for each coagulant in time 1,6,20min.

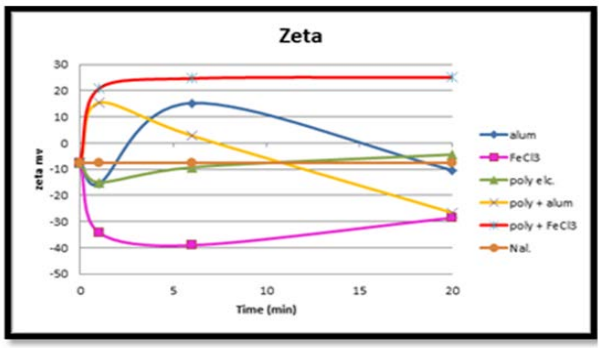

Fig 7 values of the zeta potential in the solution with flocculation time

The results at (20) min. were tabulated in Table (1) for each coagulants be as follows:

Table (1) the values best (zeta potential) for each coagulant at 20 min

doees/time	zeta mv
20min/poly	-4.35
20min/alum	-10.37
20min/poly+$FeCl_3$	25.092
20min/poly+alum	-26.612
20min/$FeCl_3$	-28.518

And arranged values (Zeta potential) in the Table (1,2) in order of preference, where the values of (zeta potential) for the best **{(PE) (-4.35)}, {(alum) (-10.37)}, {(PE+FeCl3) (25.092)}, {(PE+ alum) (-26.612)}, {(FeCl3) (-28.518)}** respectively, to be close to the it (zero). And where it is less voltage differential between the charge particles, and needed to shake shipments within the solution which reduce turbidity in the solution. Produced weaker flocs and have lower zeta potential, indicating that the surface charge of particles and colloids were not effectively neutralized here. The stronger internal electrostatic repulsive force may be another possible reason .The coagulant which generated a zeta potential more close to zero also gave stronger floc. This result corresponds well with the findings of, Zhao et al., [14]

Table (2) the values of: Optimum dose, residual turbidity (NTU), removal efficiency, zeta potential (mv) at (20) min. with flocculation time

Coagulant	Optimum dose	NTU	R%	Zeta potential (mv)
Alum	10	5.73	89.310	-10.37
FeCl3	5	4.86	90.933	-28.518
PE	1.4	4.71	91.213	-4.35
Alum+PE	1	3.4	93.657	-26.612
FeCl3+PE	0.5	2.8	94.776	25.092

The Coagulation - Flocculation Effect on Mobility

Arranged values (mobility) in the Fig.8 in order of preference, respectively, to be close to the it (zero). And where it is directly proportional to the mobility of her relationship with Zeta potential and work in the same work potential Zeta.

CONCLUSIONS

The experimental study on water treatment of the Tigris River, which owns 55 N.T.U turbidity that, some basic information, is extracted the following conclusions from this study:

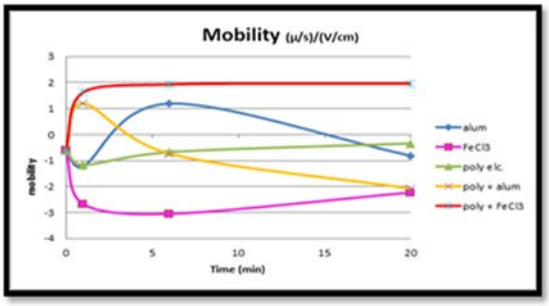

Fig 8 values of the mobility in the solution with flocculation time

1-For coagulation-flocculation treatment, (Alum, $FeCl_3$, Polyelectrolyte, (Polyelectrolyte + alum), (Polyelectrolyte + $FeCl_3$)) are used as coagulants. The optimum of alum dosage is 10 ppm, the optimum of $FeCl_3$ dosage is 5 ppm , the optimum of polyelectrolyte optimum dosage is 1.4 ppm, Polyelectrolyte and alum optimum dosage to ((5) ppm Alum + PE(1)ppm) and Polyelectrolyte and $FeCl_3$ optimum dosage is ((2)ppm Alum + PE(0.5) ppm).

2- The optimum combination coagulant doses and turbidity removal efficiency for coagulation and flocculation treatment are alum (89.3)% , $FeCl_3$(90.93)% , Polyelectrolyte(91.21)% , (Polyelectrolyte + alum) (93.65)% , (Polyelectrolyte + $FeCl_3$)(94.77)% .

3- Cationic polyelectrolyte -when used as coagulant aid- reduces the required dosage of alum to (5 ppm) and increase the turbidity removal efficiency to (94%).Using cationic Polyelectrolyte as a coagulant aid with alum and $FeCl_3$ accelerates the formation of flocs and increases the sedimentation rate. The coagulation power of $FeCl_3$ when used as a primary coagulant seems to be more effective than alum.

4- The value of the Diameter (nm) of particles and floc size have largest intensity with alum (1829.11) , $FeCl_3$(711.52) ,Polyelectrolyte (1657.17) , (Polyelectrolyte + alum)(1415.45) , (Polyelectrolyte + $FeCl_3$)(1427.47) at 20 min.

5- The value of the Diameter (nm) of particles and floc size have maximum number with alum (591.800) , $FeCl_3$(86.667) ,Polyelectrolyte (360.000) , (Polyelectrolyte + alum)(286.000) , (Polyelectrolyte + $FeCl_3$)(440.006) at 20 min.

6- The value of volume $(nm)^3$ with alum (1.41E+08) , $FeCl_3$(9.42E+07) ,Polyelectrolyte (2.98E+08) , (Polyelectrolyte + alum)(1.47E+07) , (Polyelectrolyte + $FeCl_3$)(3.26E+07) at 20 min.

7- The value of surface area $(nm)^2$ with alum (1.601E+06) , $FeCl_3$(1.520E+05) , Polyelectrolyte (2.432E+06) , (Polyelectrolyte + alum)(1.286E+06) , (Polyelectrolyte + $FeCl_3$)(1.411E+06) at 20 min.

8- The value of zeta potential (mv) with alum (-10.37) , $FeCl_3$(-28.518), Polyelectrolyte (-4.35), (Polyelectrolyte + alum) (-26.612) , (Polyelectrolyte + $FeCl_3$)(25.092) at 20 min

REFERENCES

[1]. ***Hammer*** M.J and Hammer M.J. Jr (2008) "Water and Wastewater Technology" 6th Edition, Pearson Education, Inc., New Jersey. http://www.quantumltnx.com/water

[2]. ***Levine*** , L., Taicheng, A., Jiaxin, C., Guoying, S., Jiamo, F., Fanzhong, C., Shanqing, Z., and Huijun, Z., 1991.

[3]. ***Zeta-meter Inc*** (1993). "Everything You Want to Know about Coagulation & Flocculation" fourth edition guide, Middle brooks avenue Staunton, Virginia

[4]. ***Maguire ,Ian R***., 2010 "the effect of coagulation condition on floc size Distribution and morphology

:implications for downstream treatment processes ".URI:htp//hdi.handle.Net/1957/13872

[5]. ***Degremont***, 1991, "Water Treatment Hand Book", 6th ed. Distributed by Halsted Press, NY.

[6]. ***Metcalf*** and Eddy Inc. revised by George Tchobanoglous, 2003, "Wastewater Engineering Treatment and Reuse", Fourth Edition. Published by McGraw-Hill

[7]. ***Bruno Chabot***, Gopal A. Krishnagopalan, and Said Abubakr, 1999, "Coagulation Pretreatment for Ultrafiltration of Deinking Effluents Containing Flexographic Inks", Progress in Paper Recycling

[8]. ***Kim*** J. and Kang L., 1997, "Investigation of Coagulation Mechanism with Fe(III) Salt Using Jar Tests and Flocculation Dynamics", Environ. Eng. Res. Vol.3, No.1, pp.11-19

[9]. Alley E.R.(2000) "Water Quality Control Handbook " Mc Graw-Hill , Inc. NewyYork.

[10]. McGhee, T.J.,(1991), "Water Supply and Sewage" 6th Ed.

[11]. ***Scribd***, 2011, "Coagulation-Flocculation of SugarIndustry Wastewater Using: Ferric Chloride (Fecl3),Calcium Hydroxide ($Ca(OH)_2$), and Poly-aluminum chloride (PAC)", Undergraduate thesis, Available at: http://www.scribd.com/doc/59437185/Thesis

[12]. ***Hudson***, H. E., Jr.(1981)"Conduct and Uses of Jar Test. J.AWWA, Vol. 73, No. 3.

[13]. ***Brookhaven*** Instruments Corporation(2012), 90Plus Zeta 'Particle Size & Zeta Potential Analyzer', Available at:http://www.brookhaveninstruments.com/products/particle_sizing/NanoBrook-90Plus-Zeta.html

[14]. ***Zhao, Y.X.*** B.Y. Gao, H.K. Shon, B.C. Cao, J.-H. Kim(2011), Coagulation characteristics of titanium (Ti) salt coagulant compared with aluminum (Al) and iron (Fe) salts, J. Hazard. Mate.

[15]. Mohanad, I.Farhan,2014."Effect of Particle Floc Size on Water Treatment by Physico-Chemical Process". M.Sc Thesis University of Technology.

[16].***Al-Shuwaiki*** N.M. (2009) "Utilization of Magnesium Oxide for the Industrial Wastewater Treatment and Re-use" Ph.D. Thesis, University of Technology.Article 20 (http://www.aapsi.org)

[17]. ***Roaa A.M.***, (2012), "Removal of Water Turbidity by Different Coagulants",M. Sc. Thesis, University of Baghdad, Iraq.

Analysis and Design of Infiltration Basins in Agriculture Area of Bahr Al-Najaf

Namir K. S. Al-Saoudi, Mohammed Shaker Mahmood, Mustafa M. Abdal Husain

Abstract— **During the last decade, Iraq experienced gradual shortage in the volume of water flowing in Tigris and Euphrates rivers due to natural and environmental effects. Shortage of rainfall in the basin areas, lack of snow cover over the catchment areas and reduction in water released downstream from dams constructed in the riparian state in Turkey are the major causes of the current shortage. The present paper focuses on the possibility of constructing an infiltration basin in Najaf governorate, to benefit from the recharged overflow water in agricultural areas and to sustain ground water. Field and laboratory geotechnical and hydrological tests were performed in selected agriculture area in Bahr Al Najaf, including field infiltration, field permeability and soil classification. The analysis of the tests revealed that the development of design charts and equations that facilitate the design process of infiltration basin. Accordingly the selected site is found to match with the requirements of the infiltration basins, and the recommended area of the infiltration basin is 9% of the irrigated area with depth of 0.35m.**

Index Terms— **Infiltration, Bahr Al-Najaf, Al-Najaf, Infiltration rate, Agriculture Area, infiltration basin.**

I. Introduction

The Soil water infiltration is controlled by the rate and duration of water application, soil physical properties, slope, vegetation, and surface roughness. Beyond the wetting front, there is no visible penetration of water. [1] Many Best Management Practices (BMPs) have been developed for on-site disposal of storm water. As a storm water quality control facility, an infiltration basin is often designed for micro events at the level of daily runoff, but not for the minor (5-year) or major (100-year) events. When the basin is loaded with storm water, the soil medium between the basin and the groundwater table will first undergo a storage process in which the soil water moisture varies from an unsaturated to a saturated condition. As soon as the infiltrating water reaches the groundwater table, the saturated soil medium will act as a conduit to pass the water flow. The conveyance capacity in a saturated soil medium depends on the hydraulic gradient and the soil conductivity. If the underground seepage flow through the soils cannot sustain the surface infiltrating water, the soil-water system will be backed up and a water mound will begin to build up. The shape and growth of water mound depends on the rate of infiltrating flow, size of basin, and hydraulic properties of the soil mediums. [2] The infiltration rate is generally the highest when the soil is dry and slows down gradually as the soil becomes more wet. Infiltration rates decline as water temperature approaches freezing. Little or no water penetrates the surface of frozen or saturated soils. [3]

Infiltration basin is a facility constructed within highly permeable soils that provides temporary storage of storm water runoff. An infiltration basin does not normally have a structural outlet to discharge runoff from the storm through the surrounding soil. An infiltration basin may also be combined with an extended detention basin to provide additional runoff storage for both storm water quality and quantity management. [4]

Al Saoudi et. al., 2010 and Al Saoudi et. al., 2013 investigated the infiltration characteristics in Al Najaf city soil in two non-agriculture locations, they found close agreement with the ideal shape of infiltration characteristics for both locations. [5&6]

The design of infiltration facilities is particularly challenging because of the large uncertainties associated with predictions of both short-term and long-term infiltration rates. These uncertainties in infiltration rates translate into uncertainties in the area and volume that is required for infiltration ponds. Under-sized ponds may result in flooding, while over-sized ponds may be inefficient in terms of land use and expensive in terms of property acquisition. [7]

The present paper illustrates the main steps to design an infiltration basin in a selected agricultural area of Bahr Al Najaf in Iraq.

II. Specifications for Infiltration Basins

Infiltration basins must not be used in industrial and commercial areas where contaminated are loaded, unloaded, stored, these materials if present in large quantities are hazardous to the surrounding environment. The bottom of the infiltration basin must be at least 0.6 m above seasonal high water table or bedrock. While for surface basins, this distance must be measured from the bottom of the sand layer. The basin bottom must be as level as possible to uniformly distribute runoff infiltration over the subgrade soils.[4]

Manuscript received October 9, 2001. (Write the date on which you submitted your paper for review.) this paper is a part of M.Sc. thesis in Faculty of Engineering, University of Kufa.

Namir K. S. Al-Saoudi, Professor, Ph.D., [1]Iraqi Cultural Attaché in Aus & NZ, Embassy of Republic of Iraq- Canberra- Australia. namirks@yahoo.com

Mohammed Shaker Mahmood, Asst. Professor, Faculty of Engineering/University of Kufa. mohammedsh.alshakarchi@uokufa.edu.iq

Mustafa M. Abdal Husain, ***M.Sc. Candidate***. Al_esawy_1988@yahoo.com

All infiltration basins should be designed to infiltrate or empty within 24 to 72 hours.[4&7] The minimum permeability rate is 0.12 m/day for subsurface basins and maximum is 0.3 m/day for surface basins.[4]

Construction of an infiltration basin must be done without compacting the basin's subgrade soils. Excavation must be performed by equipment placed outside the basin whenever possible to keep the base of the basin in its natural state. This requirement should be considered when designing the dimensions and total storage volume of an infiltration basin.[4]

III. SIZING OF INFILTRATION BASINS

To estimate the dimensions of infiltration basin (length, width, and depth), first, the maximum depth is determined using Eq. 1. [8]

$$d_{max} = f * T_p \quad \dots (1)$$

Where: dmax is the depth of the basin, f is the final infiltration rate of the trench area,$T_p$is the maximum allowable ponding time in hours.

An infiltration basin is sized to accept the design volume that enters the basin (V_W) plus the volume of rain that falls on the surface of the basin (PA_b) minus the exfiltration volume (fTA_b) out of the bottom of the basin. Based on the SCS hydrograph analysis, the effective filling time for most infiltration basins will generally be less than two hours therefore (use T = 2 hours). The volume of water that must be stored in the trench (V) is defined in Eq. 2 (neglecting the evaporation). [8]

$$V = V_W + PA_b - fTA_b \quad \dots (2)$$

Where: Ab is the base area of the basin, Vw is the total runoff from irrigation and rainfall and P is the rainfall depth.

For most design storm events, the volume of water due to rainfall on the surface area of the basin (PA_b) is small when compared to the design volume (V_W) of the basin and may be ignored with little loss in accuracy to the final design. The volume of rainfall and runoff entering the basin can be defined in terms of basin geometry. The geometry of a basin will generally be in the shape of an excavated trapezoid with specified side slopes. The volume of a trapezoidal shaped basin may be approximated calculated by Eq. 3.[8]

$$V = \frac{(A_t + A_b)d_b}{2} \quad \dots (3)$$

Where A_t the top surface area of the basin, A_b is the bottom surface area of the basin, and $d_b$is the basin depth. By setting Equations 2 and 3 equal the following equation may be used to define the bottom area (A_b), as in Eq. 4. [8]

$$A_b = \frac{2V_w - A_t d_b}{(d_b - 2P + 2fT)} \quad \dots (4)$$

If a rectilinear shape is used, the bottom length and width of the basin may be defined in terms of the top length and width as in Eqs. 5&6:

$$L_b = L_t - 2Zd_b \quad \dots (5)$$

$$W_b = W_t - 2Zd_b \quad \dots (6)$$

Where Z is a specified side slope ratio (1:Z). By substituting the above relationships for L_b and W_b into Eq. 4, Eq. 7 is derived for the basin top length:

$$L_t = \frac{V_w + Zd_b(W_t - 2Zd_b)}{W_t(d_p - P) - Zd_b^2} \quad \dots (7)$$

The Fig. (1) shows the parameters of infiltration basin.

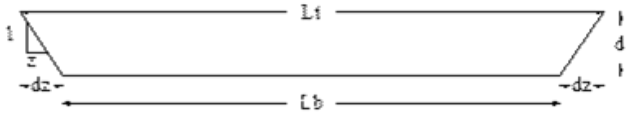

Fig. 1. parameters of infiltration basin.

The rainfall-runoff relationship based on daily rainfall as in Eq. 8. [10]

$$Q = \frac{\left[P - 0.2\left(\frac{1000}{CN} - 10\right)\right]^2}{P + 0.8\left(\frac{1000}{CN} - 10\right)} \quad \dots (8)$$

Where: Q is the runoff depth (in); P is the Rainfall (in) and CN is the curve number related to the type of plants cover.

To estimate the runoff from irrigation process, the potential available water capacity (PAWC) will be adopted to identify the amount of water that can infiltrate into soil, so the runoff water volume from irrigation process will be the difference between the applied irrigated water and the PAWC with effect of irrigation efficiency.[11]Surface irrigation systems are usually designed to have a percentage (up to 30%) of the applied water lost as runoff. [12]Table 1 presents the soil water capacity for a range of soil texture classes. [11]

To estimate the volume of required water in litters per square meter of soil:[11]

- Estimation of soil water (liter/m^2)
  = soil water capacity factor (PAWC) x expected rooting depth
- Estimation of water for certain area (m^2)
  = estimated soil water (liter/m^2) x Area
- Estimation of required water (liter)
  = Estimated water for certain area (m^2) x (1+Efficiency)

TABLE 1
Soil Water Capacity (mm water/cm soil) Estimates For a Range of Soil Texture Classes.[11]

Texture class	Estimated PAWC, mm water/cm soil
Sand	0.5
Sandy Loam to Clay Loam	0.8-1.2
Heavy Clay	1.5-2.0

IV. METHODOLOGY AND SITE PROPERTIES

A. Selection of The Site and Test Pits

The agricultural area of Bahr Al Najaf was selected For the purpose of designing of an infiltration basin. Three pits (3, 4 and 5) were excavated to cover the selected location (south of Bahr Al-Najaf), representing area about 5000 hectares, in addition, results of two pits (1 and 2) tested previously by the authors [13]. These locations were determined by available Global Position System device (GPS). The coordinates (x,y) of the pits are (435143, 3538380), (433473, 3535848), (431149, 3533320), (435904, 3532708), (437581, 3535911) respectively as shown in the Plate (1). The first two locations are continuous irrigation (cultivated) area and the other three locations are with no irrigation (not cultivated) area.

The dimensions of tested pits are 2 meter in length, 1.5 meter in width, and 0.5 meter in depth. The base area of the pit (2m*1.5m) was selected randomly, while .The depth of the pit 0.5m, in accordance with the specifications of infiltration basin.

The width of Bahr Al Najaf ranges between (6-60) km, covering an area about 2700 km2 (about 250,000 hectares). The area available for agricultural purposes is about 40,000 hectares (or 16% of Bahr Al- Najaf area), but currently only 15000 hectares are used for planting. [14]

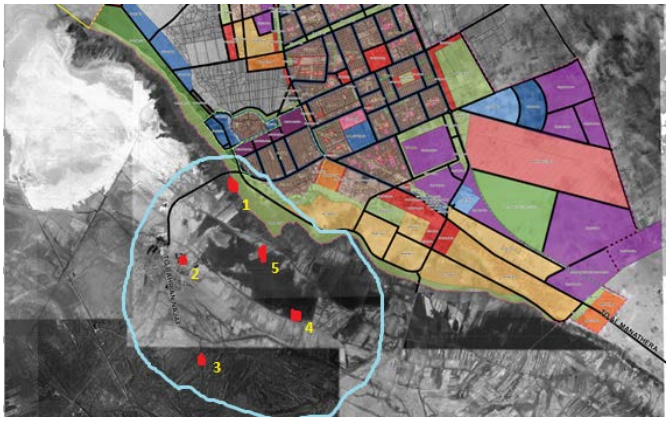

Plate 1. Locations of Tested Pits.

B. Soil Classification

The results of grain size distribution are presented in Fig. (2). The analysis of the results are outlined in Table 2. The general description of the soil is medium to coarse sand with some gravel.

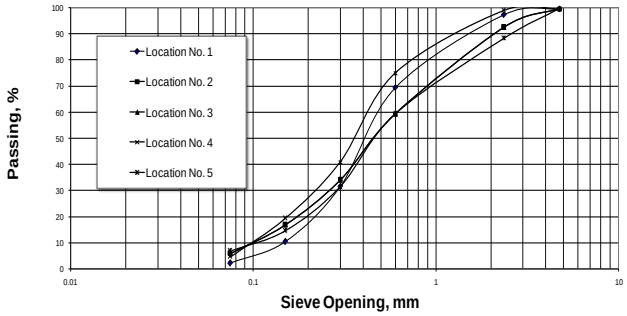

Fig. 2. Grain Size Distribution Curves of the Five Soil Samples.

TABLE 2
The Classification of The soil.

Pit No.	Sand %	d_{10}, mm	Soil Classification According to USCS	Soil Classification According to USDA	Soil Classification According to HST
1	95*	0.15*	SP*	Sand	B
2	87*	0.1*	SP*	Sand	B
3	95	0.1	SW	Sand	A
4	93	0.105	SW-SM	Sand	A
5	90	0.071	SW-SM	Sand	A

* from Authors published work [13].

C. Soil Permeability

The coefficient of permeability (hydraulic conductivity) was determined using "inversed auger-hole method". A borehole of 0.30 m in diameter and 0.60 m in depth was made in the selected five locations within the tested area; five boreholes were selected for determining the coefficient of permeability. The borehole was completely filled with water and level of water in each borehole was recorded at various time intervals.

The value of k was determined from Eq. (9):[14]

$$k = 1.15 \,.\, r \,.\, tan(\alpha) \qquad \ldots (9)$$

Where tan α is the slope of the best linear relationship between log (h+r/2) and time . The typical steps for calculating the permeability are as following:

1. The observed time-water depths (h) as a result of inversed auger-hole method test for each borehole, as in Table 3,
2. Figures 3illustrates the relationship between log (h+r/2) and time in addition to the best line passing through points for all boreholes with R^2 between 0.94 to 0.99,
3. Determine the slope of the predicted curve,$tan(\alpha)$, as in Table 4,
4. using Eq. 5 to predict k, as in Table 4.

TABLE 3
Observed Water Depth in Inversed Auger-Hole Method for the Five Boreholes.

Time from start of test, min.		0	1	2	3	4	6	8	10
Water height in pit (h), cm	B.H.1	60	59	57	55	54	51	49	45
	B.H.2	60	58	56	54	53	51	49	45
	B.H.3	60	52	48	47	43	36	33	28
	B.H.4	60	55	50	45	40	35	32	27
	B.H.5	60	55	51	44	42	33	22	11

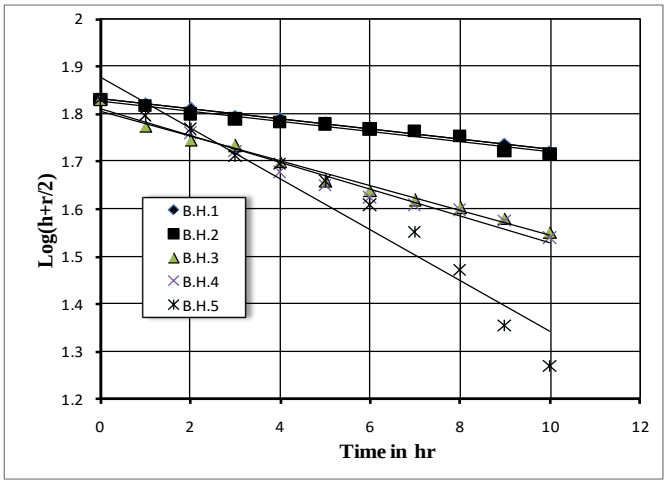

Fig. 3. Relationship between log (h+r/2) and Time for all Locations Boreholes.

TABLE 4
Coefficient of Permeability for all Locations Boreholes.

B.H. No.	B.H.1	B.H.2	B.H.3	B.H.4	B.H.5
$tan(\alpha)$	0.0105	0.0105	0.0263	0.0283	0.0535
k, m/day	2.6082	2.6082	6.5329	7.0297	13.289

The coefficient of permeability remains constant in locations 1 & 2 and increased for the other three locations, and this may reflect the situation of the saturation, the first two locations still irrigating, while the others no more irrigation (dry).

V. INFILTRATION CHARACTERISTICS OF THE SOIL

For each pit, infiltration process was made to determine the infiltration characteristics. This process started with flooding of the pit, recording the variation of water level (height) in pit with time and repeating of flooding. The infiltration process was repeated four times in pits 1 and 2,[13] while this process was repeated three times in pits 3, 4 and 5. Figures 4, 5 and 6 present the results of the infiltration rate for the three locations. It can be noticed that the values of infiltration rate demonstrate peak values at the beginning stage of flooding and gradually leveled off with time.

The average infiltration rate at steady state remains constant in pits 1 & 2, while this rate is different in the other three pits, as shown in Table 5, and this may be caused by the difference in saturation, the first two locations within the irrigated area while the others are not.

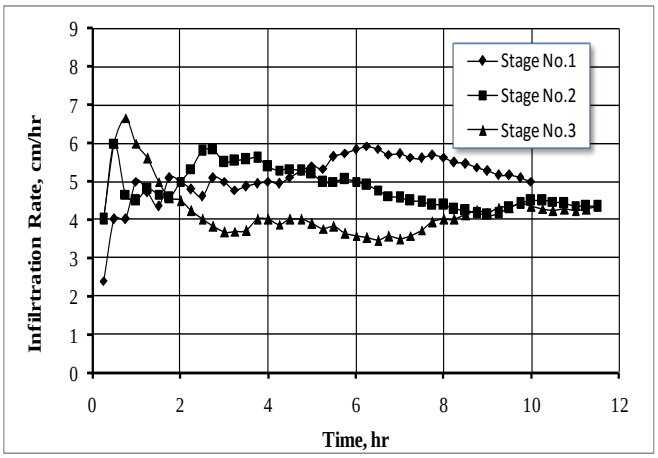

Fig. 4. Results of Infiltration Rate for the Location No.3.

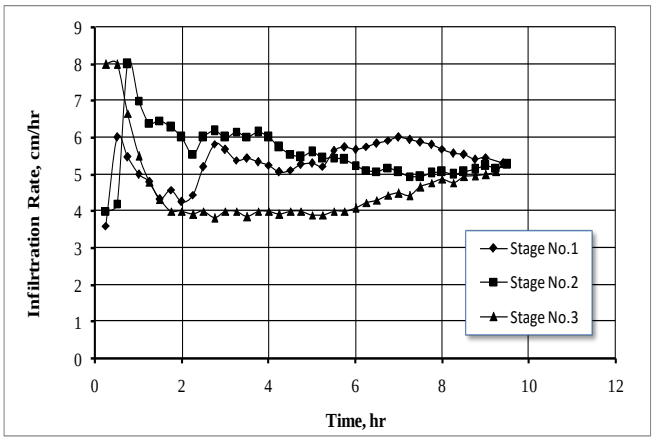

Fig. 5. Results of Infiltration Rate for the Location No.4.

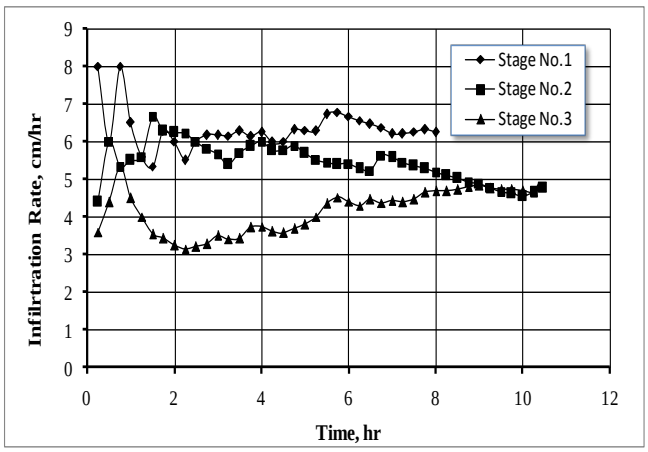

Fig. 6. Results of Infiltration Rate for the Location No.5.

TABLE 5
Summary of the Average Infiltration Rate at Steady State.

Pit No.	1*	2*	3	4	5
Average infiltration rate, cm/hr	1.34	1.35	4.25	5.4	6.25

* from Authors published work [13].

VI. WATER RESOURCES AND LOSES

A. *Irrigation Method and Water Source*

Almost 70% of the country's cultivated area is under irrigation while the remaining 30% are under rain fed cultivation. Of the areas under irrigation, 62.8% receives water through gravity irrigation projects, 36% pumped from rivers and major channels and 1.2% from ground water aquifers and springs.[15] In Bahr Al-Najaf agriculture area, the border irrigation method (the area was divided into borders) was adopted by farmers depending on two rivers, Al Gazi (previously named Al Sadeer) with discharge of 3.28 m3/s, and Al Bedairiyah with discharge of 3.28m3/s. [16]

The dimensions of borders are 10m*5m. The water volume of irrigation is 35m3 per 5 hrs per half hectares per day.

B. *Rainfall Depth*

Through the analysis of Table 6 for the monthly rates for the amount of rainfall in the study area, the rainfall is concentrated during the winter months (November, December, January, February) and extended to March, dry season summer months (June, July, August) and little rain is in autumn.[16]

TABLE 6
Average rainfall for Al-Najaf station, mm/month (1970-2004).[14]

Jan.	Feb	Mar	Apr	May	Jun	Jul	Aug	Sep	Oct	Nov	Dec
19.8	16.9	15.4	12.2	4.6	0.04	-	-	0.04	4.3	13.5	15.4

C. *Evaporation*

Depending on the information recorded in Najaf climate station (the General Authority for Meteorology Iraqi) andAl-Janabi work,the evaporation was calculated as in Table 7.

VII. ANALYSIS AND DISCUSION

A. *Verification of Site Selection*

The following points were considered in the selection process of the site:

i. Soil Investigation: The results of soil classification tests at different locations were performed according to USCS, USDA.

ii. Permeability of the Site: According to five field permeability tests performed, the coefficient of permeability of the selected site is approximately 2.6082 m/day (3.02*10-5 m/s) which is higher than the minimum required permeability (0.3m/day) in infiltration basin specifications.

iii. Groundwater Level: The groundwater level in the selected site is about 2m below the ground surface and this level is deeper than the required minimum level suggested in the infiltration basin specifications (0.6m).

TABLE 7
Calculated Value of Daily Evaporation for Each Month.[14]

Month	Daily Evaporation, mm/day
Jan.	2.81
Feb.	4.66
Mar.	7.97
April	13.63
May	22.84
June	37.26
July	46.40
Aug.	38.36
Sep.	25.56
Oct.	14.79
Nov.	6.26
Dec.	3.12

B. *Modeling Charts*

Volume of recharged water

The volume of water that is expecting to enter into the infiltration basin in the selected site is from rainfall and the irrigation processes neglecting the evaporation process.

Modeling of runoff from rainfall: Figure 7 was developed using equation 8 to estimate the runoff depth from the rainfall depth for different curve numbers.

Modeling of runoff from irrigation process: Figure 8 shows the estimated PAWC in L/m^2 related to the different root zone and soil texture depending on table 1 and followed steps.

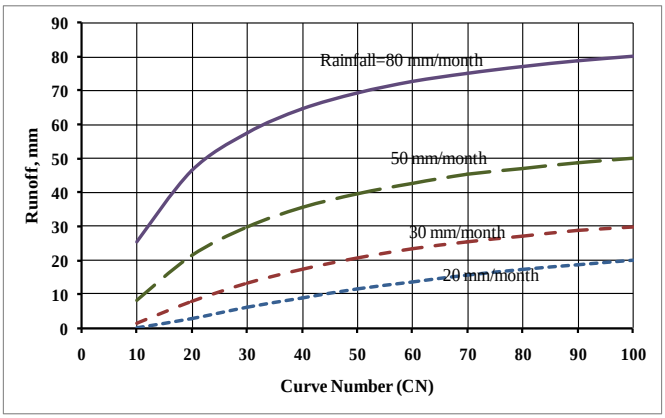

Fig. 7. Runoff From Rainfall With Curve Number (CN) for Different Rainfall Depths.

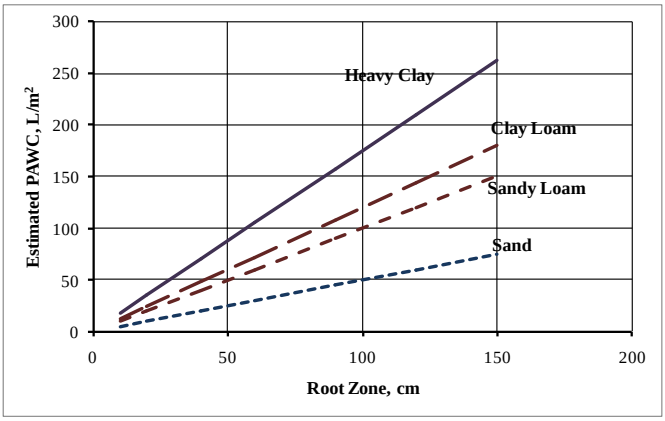

Fig. 8. Estimated PAWC with Root Zone Depth for Different Soil Texture.

VIII. APPLICATION OF DESIGN EXAMPLE

The estimation of the basin area for the selected area (2 hectares agriculture area), the following steps are followed (neglecting the evaporation depth for larger infiltration basin):

- Step 1: Runoff from the max. Rainfall as a single event:
  - From table 6, max. Rainfall = 19.8 mm/month
  - Curve number, CN = 90(row crops) [17]
  - From figure 7, the runoff = 5 mm/month
  - Runoff volume from rainfall for 2 hectares = 0.005m*20000m^2 = 100m^3
- Step 2: the estimation of runoff from the irrigation consists of the following steps:
  - Volume of water from the irrigation process by the farmer: 5*35*4 = 700m^3 for 2 hectares
  - Volume of water (PAWC) from figure 8 for root zone of 10cm =(5*20000)/1000 = 100m^3
  - Volume of water from the efficiency of irrigation for 20% selected efficiency = 0.2*700=140
  - Volume of runoff from irrigation = 700 – 100 – 140 = 460m^3
- Step 3: From Eq. 1, f=1.35 cm/hr (irrigated), Tp = 24 (minimum), dmax≅ 35cm,
- Step 4: the top length (Lt) of infiltration basin using Eq. 7, taking Wt = 20m and Z=2

The total volume of runoff water = 100 + 460 = 560m^3

$$L_t = \frac{560+2*0.35(20-2*2*0.35)}{20(0.35-19.8/1000)-2*(0.35)^2} = 90\text{m}$$

Or, At = 20*90 = 1803 m^2

Or, $\frac{1803}{20000} \times 100 = 9\%$ of the selected area (2 hectars)

IX. CONCLUSIONS

The study demonstrates that 9% of the agriculture area is required to be used as infiltration basin for Bahr Al-Najaf based on the developed charts in figures7 and 8. These can be used directly for the design of the infiltration basin in this area.

REFERENCES

[1] United States Environmental Protection Agency (EPA), Estimation of Infiltration Rate in the Vadose Zone: Application of Selected Mathematical Models, Volume II", USA,1998. (www.epa.gov)

[2] Guo, James C.Y. Design of Infiltrating Basin, Department of Civil Engineering, University of Colorado at Denver, Denver,2003.

[3] Yong, Raymond N. and Warkentin, Benno P. Soil Properties and Behavior, Book of Development in Geotechnical Engineering, Elsevier Scientific Publishing Company, Amsterdam, Netherlands, 1975, Vol. 5, pp. 141^195

[4] New Jersey Department of Environmental Protection (NJDEP), New Jersey Stormwater Best Management Practices Manual,USA, 2004.

[5] Al Saoudi, Namir K. S. and Al Shakerchy, Mohammed Sh. M. Water Infiltration Characteristics Of Al Najaf City Soil. In Proceeding of the 4th International Conference on Geotechnical Engineering and Soil Mechanics, Tehran, Iran, November 2-3, 2010, p.p. 1^8.

[6] Al Saoudi, Namir K. S., Al Shakerchy, Mohammed Sh. M. and Al Janabi, Salam A. Abbas. Water Infiltration Characteristics for Artificial Lake In Bahr Al-Najaf. In Proceeding of the 1st International Conference on Geotechnical and Transportation Engineering ICGTE, 14 to 15 of April, Baghdad, Iraq, Eng. & Tech. Journal, 2013, Vol.31, Part (A), No. 19, p.p. 1^12.

[7] Massmann, Joel W. October. A Design manual For Sizing Infiltration Ponds, Washington State Department of Transportation, USA, 2003.

[8] Maryland Stormwater Design Manual, Appendix D.13. Method for Designing Infiltration Structures, Vol. I & II, Maryland, USA 2009. (www.mde.state.md.us).

[9] Tennessee BMP Manual Stormwater Treatment. Infiltration Basin,Tennessee, USA. 2002. (http://eerc.ra.utk.edu/divisions/wrrc/)

[10] Ponce, Victor M. and Hawkins, Richard H. Runoff Curve Number: Has it Reached Maturity. Journal of Hydrologic Engineering, 1996, No. 1, Vol. 1, p.p. 11^19.

[11] Burk, L. and Dalgliesh, N. Estimating Plant Available Water Capacity - a Methodology. Canberra: CSIRO Sustainable Ecosystems. Australia, 2008, ISBN 0977517004, Version 1.1.

[12] U.S. Environmental Protection Agency, Office of Water (4503T). National Management Measures to Control Nonpoint Pollution from Agriculture, USA, July, 2003.

[13] Al-Saoudi, Namir K. S., Al-Shakerchy, Mohammed Sh. M., and Abdal Husain, Mustafa M. Infiltration Characteristics In Agriculture Area of Bahr Al Najaf, Journal of Babylon University, Babylon, Iraq, 2014, No. 4, Vol. 22,p.p. 971^978.

[14] Al Fartosy, AbdulHady, Bahr Al Najaf: Eye on The History of Al Najaf City, 2005. (http://www.iraqalyoum.net/archf/515/iraq/p3.htm) (In Arabic).

[15] AlEsawy, Mustafa Mohammed AbdalHusain. Hydraulic Design of Infiltration Basins in Bahar Al-Najaf, M.Sc. Thesis, Civil Engineering Department, University of Kufa, Kufa, Iraq, 2013.

[16] Al-Janabi, S., A., A. Effect of Water Seepage on Nearby Structures A Case Study of SayfThulfiqar Artificial Lake in Bahr Al-Najaf, M.Sc. Thesis, Civil Engineering Department, University of Kufa, Kufa, Iraq, 2012.

[17] United States Department of Agriculture. Urban Hydrology for Small Watersheds, Technical Release 55 (TR-55), 2nd Edition, Natural Resources Conservation Service, Conservation Engineering Division, USA,1986.

Factors affecting aerobic granulation process of activated sludge

* Ghufran F.J, ** Talib R.A, *** Mohammed A.I.A.H.

Abstract---- Aerobic granular activated sludge is an attractive and promising process for intensive and high-rate biological nutrient removal from wastewater. This work reports the effect of air superficial velocity and type of carbon source on the granulation process using synthetic wastewater. Four sequential batch reactors (SBR) have been used. They operated for 100 days with the range of air superficial velocity (1-5) cm/s. Sodium acetate and sucrose were used as carbon source. The influent COD was 1000 mg/l. The results showed that the maximum granules size was achieved in the reactor with superficial velocity was 3.5 cm/s and fed with sodium acetate. The dominant granules size was (4-10) mm. The removal efficiency of COD, NH_4 and TN was 97%, 98% and 92%, respectively. Sludge volume index (SVI) and MLSS were 26 ml/g, 4,900 mg/l respectively. After 100 days the reactor fed with sucrose achieved smaller granules size and less removal rates in comparison with that of rectors fed with sodium acetate under same operating conditions due to bulking and instability. Optical microscope images showed that the surfaces of granules fed with sodium acetate were rich with ciliates and rotifers while those fed with sucrose was rich with yeast and ciliates.

Key words: Granular sludge, Activated sludge, Wastewater, SBR

AUTHORS

*Ghufran Farooq Jumaha ,, Lecturer in Building and Construction Engineering Department,Universityof Technology /Baghdad; e-mail: ghofranf@ymail.com

** Talib Rashid Abaas , D r in Environment and Water Directorate, Ministry of science and Technology, Baghdad, Iraq(e- mail talibrshd@yahoo.com).

*** Mohammed Ali Ibrahim Al- Hashimi , Prof. D r. in Building and Construction Engineering Department, University of Technology /Baghdad. And Head of Building and Construction Engineering Department, Dijlah University College E-mail: mohashimi2003@yahoo.com

I.INTRODUCTION

Aerobic granular activated sludge is an attractive and promising process for intensive and high-rate biological nutrient removal from waste water [1, 2, 3]. Compared with conventional flocculent sludge, it has good settling ability and ability to maintain high biomass concentration and achieve high organic load treatment. Whereas in conventional activated sludge process, microorganisms accommodated in wastewater exist in the form of desultory flocs. These flocs are composed of filamentous matrixes and zoogloea, thus the structure of activated sludge has low biomass concentration, bad settling ability and poor ability against impact. The land area needed for a municipal aerobic granular sludge wastewater treatment plant could be reduced by 80%, and accordingly the construction investment would be cut down [4, 5, 7]. Furthermore aerobic granular sludge can resist the effect of toxic substances [4, 6].

Sequencing batch reactors (SBR) commonly used for the granulation of activated sludge [7, 8]. Aerobic-granule-based SBRs have been proven to be applicable for treating wastewaters from various industries, such as malting , dairy , and soybean-processing [9, 10, 11] as well as municipal wastewater [7, 8]. Studies show that many factors are affecting the granulation process of activated sludge include carbon source, hydrodynamic shear force, feast–famine regime, feeding strategy, dissolved oxygen concentration, reactor configuration, pH, temperature, volume exchange ratio and applied selection pressures in the forms of settling time [12, 13, 14, 15] and type of carbon source. Air superficial velocity play two important roles in the formation of granules: firstly it imposes the dissolved oxygen (DO) concentration, and secondly it determines the hydrodynamic shear forces [14].

In many previous studies, microscopic observations show that the formation of aerobic granules is a gradual process from seed sludge to compact aggregates, further to granular sludge and finally to mature granules. It has been reported that mature granules arrange their structure to protect against environmental attacks [16, 17, 18]. For instance, mature granules have special heterogeneous structure with compact outer layer and loose inner layer [16]. In granulation system the most recognized sessile states of microorganisms are biofilm and bio-granule forming microorganisms. Biofilm is a kind of microorganisms attached to the inert support whereas a bio-granule is completely self-immobilization of microorganisms without any carrier [15]. Compact structured, biologically efficient aerobic sludge granules with diverse microbial species, excellent settling capabilities, an excellent feature of nitrogen and phosphorus removal in the degradation of organic carbon at the same time have been developed in sequencing batch reactors [5, 15].

Unlike the conventional biological nutrient removal (BNR) process which is based on several bioreactors where aerobic, anoxic and anaerobic zones are separately provided, granular structure provides different spatially distributed redox zones, due to substrate mass transfer limitations, inside the granule. Moreover, operation in sequencing batch mode allow the introduction of periods with and without aeration that is necessary for nitrification and denitrification processes. The microbial consortia in the aerobic granule consist of two main different microbial groups, i.e., autotrophic and heterotrophic bacteria. The autotrophs are responsible for nitrification, whereas the heterotrophs are responsible for organic carbon oxidation and denitrification. Both of them play a vital role in

the removal of nitrogen and conversion of a wide diversity of organic matters present in wastewater [19]. The aim of this study is to investigate the effect of carbon source and air superficial velocity inside the reactor on the granulation process and the performance of aerobic granular sludge SBR.

II. Materials and Methods

Four laboratory batch reactors R1, R2, R3 and R4 were used for growing aerobic sludge granules. Each reactor was a graduated glass cylinder with a working volume of 1 liter and dimensions of (40 cm length x 6 cm I.D.). These reactors were seeded with flocculated activated sludge collected from AL-Rustumiya wastewater treatment plant in Baghdad. The seeded activated sludge was filtered through 0.2 mm screen to remove large debris. Initial mixed liquor suspended solids (MLSS) was about 3500 mg/l. Synthetic waste was used as feed influent composed of distilled water with 191 mg/l NH_4C, 27.2 mg/l K_2HPO_4, 18.7 mg/l $NaH_2PO_4 \cdot 2H_2O$, 29.6 mg/l $CaCl_2$, 54.2 mg/l $MgCl_2 \cdot 6H_2O$, and 1.0 mL of a trace element solution. The carbon source was 1282 mg/l CH_3COONa for R1 ,R2, R3 while sucrose was used for R4 to get COD concentration of 1000 mg/l and the corresponding volumetric organic loading of the reactor was about 1 g COD/l/d. Aeration was supplied from the bottom of the reactors through an air diffuser supplied from an air pump with air flow rate so that the resultant air superficial velocity of 5, 1, 3.5, 3.5 cm/sec for R1, R2, R3, R4, respectively. The reactors were operated on 12 hr. cycles. Each cycle includes different phases: 2 min influent feeding, aeration period (> 11.5 hr.), settling and discharge periods at the end of the cycle. Settling period was 30 min for the first 15 days to reduce biomass washing out and then reduced gradually to be 5 min at day 30 and to 1 min at day 90 from the beginning of reactor operation. Discharging period was 2 min by using siphon after a sludge settling period through a rubber tube withdraw the effluent from a point located at mid height of the reactor so that the volumetric exchange ratio was 50% per cycle . The pH value is controlled at 7.0~8.0 by addition of acid and base solutions .The reactors were operated at room temperature is room temperature which was in the range 25-35ºC [15].

III. Analytical Methods

COD was measured using a spectrophotometer, lovibond. NH_4-N, TN were measured using DR-5000 spectrophotometer, Hatch. MLSS were measured according to Standard Methods [20]. Settling velocity of sludge was estimated by measuring the time taken for individual granules to drop from height of 40 cm in a measuring cylinder. Dissolved oxygen (DO) and pH were measured by CX-401 multifunction meter, Eutech instrument.. Sludge volume index (SVI) was monitored at the end of aeration phase. This was done by determining the volume of the granules after 30 min of settling and dry weight of the separated biomass was measured after drying at 105°C for 24 h**.** The experiments were done during the period from15/3/2014 to 30/6/2014

IV. Morphology observation

The morphology of the flocculated sludge and the aerobic granule was observed using an optical microscope and stereomicroscope equipped with a digital camera. The microstructure of granules was examined with Scanning Electron Microscope (SEM). The size distributions of the aerobic granules were determined by analysis of images taken by a digital camera for random samples of granules groups collected in Petri dishes.

V. Results and discussion

Granulation process involves growing of compacted biological structure (granule) which contain great diversity of microorganisms that are responsible for nutrient removal [15]. Heterotrophic microorganisms is normally dominant in the aerobic outer layer of the granule while autotrophic microorganism dominate the deeper anoxic layer. Depending on granule size the inner zone of granule may provide anaerobic conditions for facultative heterotrophic microorganisms, so that nutrient removal efficiency depends on the competition between these layers which is governed by the granule size [21]. Fig's (1) & (2) illustrate that granules size range in R1, R2, R3 and R4 were 0.4-7 mm, 0.25-3 mm, 4-10 mm and 0.25-2 mm, respectively. It is clear that maximum granular size was obtained in reactor R3 where the air superficial velocity was 3.5 cm/s and CH_3COONa was used as carbon source.

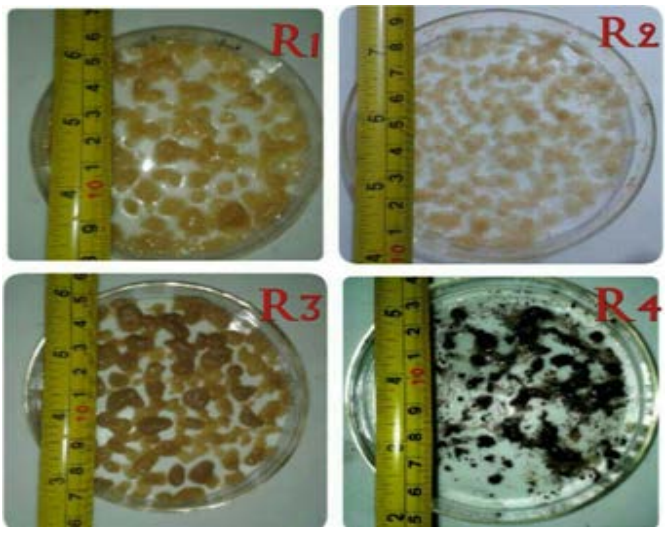

Fige (1): Granules after 100 days of cultivation in R1, R2, R4

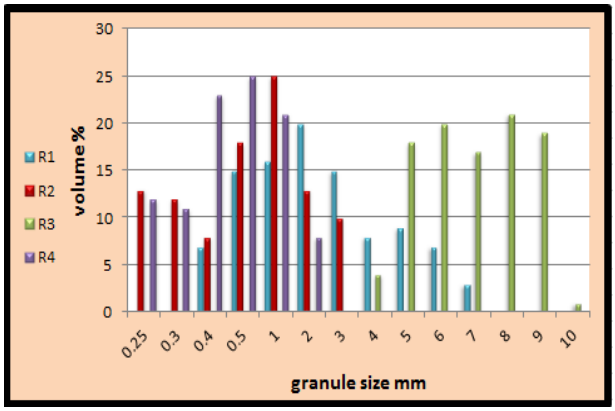

Fig (2): Size distribution of granules for R1, R2, R3and R4

Fig. (3) shows the variation of removal efficiencies of COD, NH4 and TN in the reactors after 100 days of operation. These result indicate that aeration rate and type of substrate play main role in nutrient removal efficiency, so that after 100 days of system operation, the COD, NH_4, TN removal efficiencies for R4 were 89%, 78%, 55% , respectively. The larger granules size in R3 provided sufficient layers for more efficient simultaneous nutrient removal. For R3 the removal efficiencies of COD, NH_4, TN were 97%, 98%, 92, respectively.

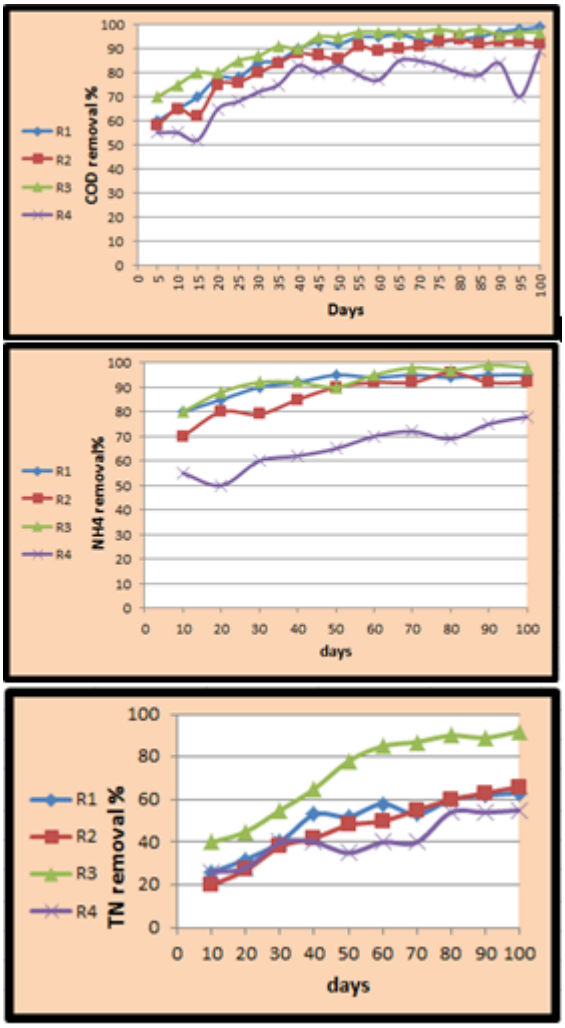

Fig (3): COD, NH4, TN removal inR1,R2,R3 and R4 during 100 days of operation

Fig. (4) shows the variation of DO, COD and NH_4 inside the reactors during one typical operation cycle. It is clear that the majority of the oxidation of COD and NH_4 occur during the first two hours of operation cycle in the reactors R1, R2 and R3, while it take more time in R4 which may attribute to the less biodegradability of sucrose than acetate.

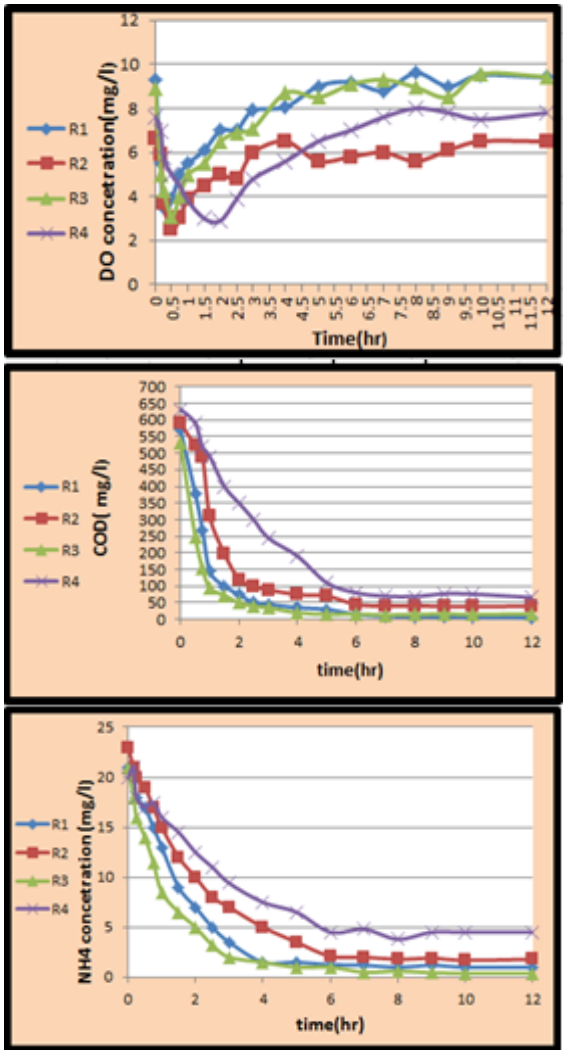

Fig (4): DO, COD, NH_4 variation with time during typical reactor operation cycle.

VI. Granules Settling Velocity and Sludge Properties

Due to microorganisms selection pressure imposed by short settling period, sludge concentration and other properties were improved gradually during cultivation process within 100 days of R1, R2, R3 reactors operation, while the reactor R4 show noticeable biomass washout. Fig. (5) illustrates decreasing in the MLSS all reactors in the first 15 days due to severe washout of sludge. After 60 days MLSS concentration began to increase in R1, R2 and R3 due to granules formation and consequently immobilization of biomass, so that MLSS reached 3500, 3400, 4900 mg/l for R1, R2 and R3, respectively after 90days. MLSS in reactor R4 decreased gradually from 3500 mg/l to 2100mg/l during the 100 days operation due to unstable operation caused by filamentous bulking and consequently continuous biomass washout. Fig. (6) presents the variation in settling velocity of granules in these reactors which increased as granules size increased,.Fig. (7) shows the improvement in sludge settlability in terms of reduction in SVI which was about 26 ml/g for reactor R3.

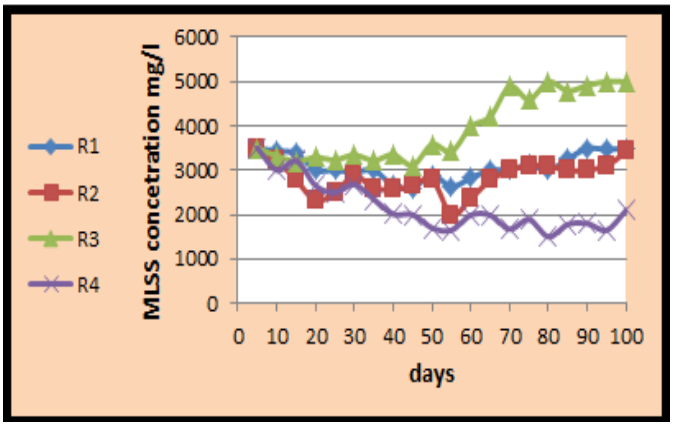

Fig (5): MLSS concentration during 100 day for R1, R2, R3 and R4.

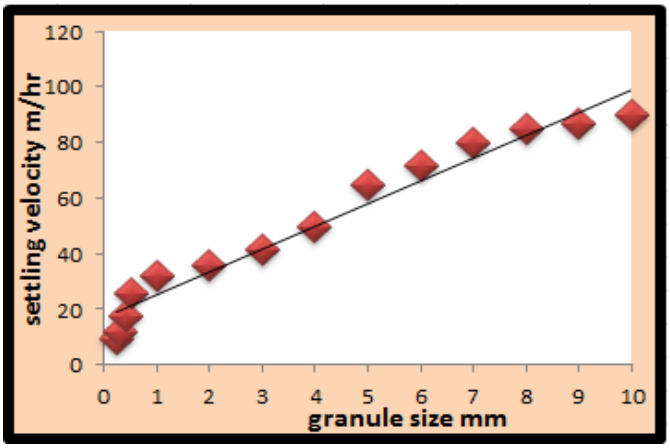

Fig (6): variation of granule settling velocity with granules size

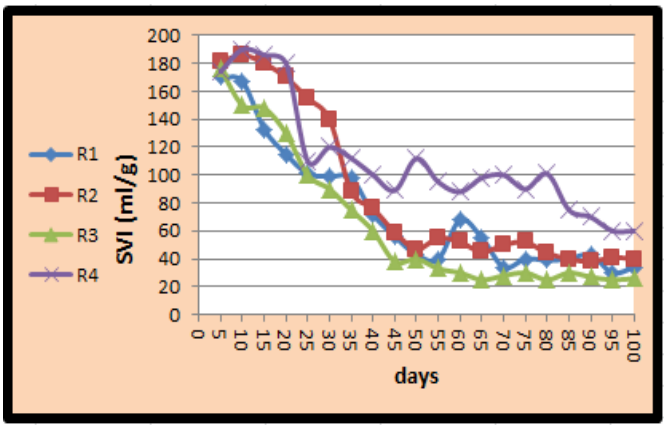

Fig (7): SVI development during operation time for R1, R2, R3 and R4.

VII. Granules Morphology

Using optical microscope, Fig. (8) shows that the granules in the reactors R1, R2, R3 and R4 are compact and the granules surface were rich with higher order microorganisms. The abundant existence of these microorganisms indicates a good bio-activity of the reactors. In R1, R2, R3, most of these microorganisms were rotifers while most of them in R4 were

yeast. The presence of rotifers in activated sludge indicated good and stable sludge because rotifers have the ability to control filamentous bacteria growth and consequently cause improvement in settling properties and SVI value, while presence abundant of yeast on the surface of the granules and in the bulk activated sludge liquor causes undesirable effect including bulking due to inter-floc bridging. Under aerated conditions with high BOD (primarily composed of simple sugars such as sucrose, maltose, glucose, and fructose, or carbohydrates) yeast proliferates rapidly, converting these easy-to-use substrates into biomass and causing an increase in sludge volume and/or total suspend solid levels [22]. Therefore, R4 had less quality activated sludge performance in comparison with other reactors R1, R2 and R3. On the other hand Fig. (9) shows SEM images of the microstructure of granules in these reactors which illustrates that most of them consist of (rod, coccus and irregular morphologies of filament bacteria covered with extra cellular polymeric substances (EPS) which play main role in maintaining granule robustness [12].

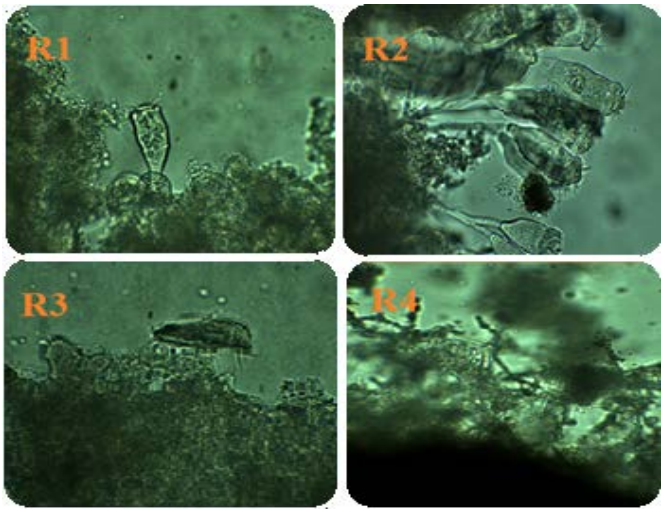

Fig (8): Optical microscope images shows microorganisms grown on the granules surfaces

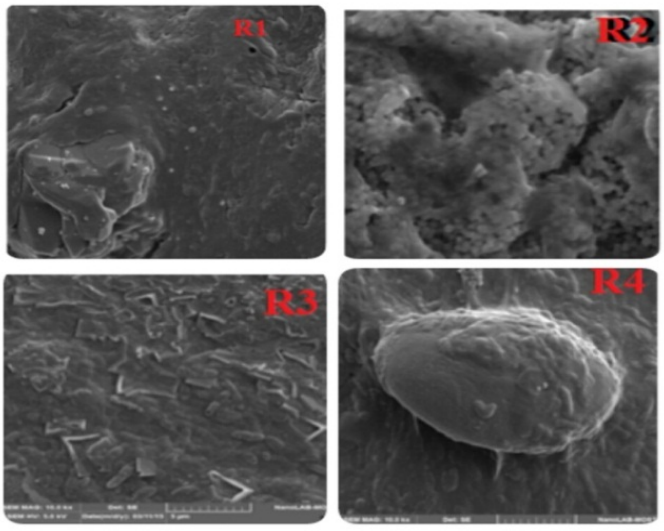

Fige (9): SEM images for granules after 100 days.

VIII. Conclusions

This study showed that;

1- Successful granulation of activated sludge was achieved in a pilot-scale SBR system with maximum granules size was achieved in the reactor with superficial velocity was 3.5 cm/s and fed with sodium acetate. After 100 days, the dominant granules size was 4-10 mm with high settling velocity and high biomass retention.

2- Aerobic granule technology can achieve successful and feasible simultaneous removal organic carbon and nitrogen from wastewater.

3- Aeration rate and type of substrate are significant factors affecting granulation process and reactor performance.

4- A study deals with granulation of flocculated activated sludge using municipal wastewater instead of synthetic wastewater as an influent is needed.

References

[1] Adav S, Lee D., Show K.and Tay J.: Aerobic granular sludge. Recent Advances. Biotechnology, 2008, 26, 411^23.

[2] Arrojo B., Mosquera-Corral A., Garrido J. M., and Mendez R. R.: Aerobic Granulation with Industrial Wastewater in Sequencing Batch Reactors. Water Res., 2004, 38, 3389^3399..

[3] Bing-Jie N. and Han-Qing Y. : Mathematical Modeling of Aerobic Granular Sludge. Biotechnology Advances, 2010, 28, 895^909B. Smith, "An approach to graphs of linear forms (Unpublished work style)," unpublished.

[4] Bing-Jie N., Wen-Ming X., Shao-Gen L., Han-Qing Y., Ying-Zhe W., Gan W. and Xian-Liang D.: Granulation of Activated Sludge in a Pilot-Scale Sequencing Batch Reactor for the Treatment of Low-Strength Municipal Wastewater. Water Res, 2009, 43, 751^761.

[5] Beun, J. J., Heijnen, J. J. and Van Loosdrecht, M. C. M : N-Removal in a Granular Sludge Sequencing Batch Airlift Reactor. Biotechnol.Bioeng., 2001, 75, 82^92.

[6] De Bruin, L. M. M., De Kreuk, M. K., Van Der Roest, H. F. R., Van Loosdrecht, M. C. M. and Uijterlinde, C.: Aerobic Granular Sludge Technology, Alternative for Activated Sludge Technology. Water Sci. Technol., 2004, 49, 1^9.

[7] Beun, J. J., Hendriks, A., Van Loosdrecht, M. C. M, Morgenroth, E., Wilderer, P. A. and Heijnen, J. J. ;Aerobic Granulation in Sequencing Batch Reactor. Water Res.,1999, 33, 10, 2283^2290.

[8] De Kreuk, M. K.: Aerobic Granular Sludge Scaling Up, a New Technology. Ph.D. thesis, Delft University of Technology, Delft, The Netherland. 2006.

[9] Su, K. Z. and Yu, H. Q.: Formation and Characterization of Aerobic Granules in a Sequencing Batch Reactor Treating Soyabean-Processing Wastewater. Environ. Sci. Technol., 2005, 39, 2818^2827.

[10] Thamera,M. : aerobic Granular Sludge - Study of Applications for Industrial and Domestic of Wastewater.MSC. thesis,Chalmers University Of Technology. Department of Civil and Environmental Engineering ,Division of Water Environment Technology ,2014.

[11] Khlida M.,; Bioremediation of Color Contaminant for Textile Dying Wastewater Using Aerobic Granular Sludge, University Technology Malaysia, 2007, vot75221.

[12] Xiaoling, Z., Shan L.: Effect of Shear Stress on Granular Activated Sludge in Sequencing Batch Reactor**,** International Conference on Biology, 2010, Environment and Chemistry IPCBEE, 2011, Vol. 1. IACSIT Press, Singapore.

[13] Bindhu, B. K. and Madhu, G.: Influence of Organic Loading Rates on Aerobic Granulation Process for the Treatment of J. P. Wilkinson,

Wastewater.,Journal of Clean Energy Technologies, 2013, Vol. 1, No.2..

[14] Nor-Anuar, A., Ujang, Z., Van Loosdrecht, M. C. M., de Kreuk, M. K. and Olsson, G.: Strength Characteristics of Aerobic Granular Sludge.Water Science & Technology, 2012, 65.2.

[15] Jakub, K., Piotr, A. and Łukasz, R.: Long Term Cultivation of an Aerobic Granular Activated Sludge.Electronic Journal of Polish Agricultural Universities, 2012, Volume 15 Issue 1, Topics in Environmental Development.

[16] Yangm Q., Li X. and Zeng G.: Cultivation of Aerobic Granular Sludge for Simultaneous Nitrification and Denitrification in SBR System. Chinese Journal of Environmental Science, 2003, Vol. 24, No. 4, 94^99.

[17] Marta, C. B. : Biological Nutrient Removal in SBR Technology: From Floccular to Granular Sludge. PhD thesis, University De Giroa, 2011.

[18] Monica, F. L.: Aerobic Granular Systems for Biological Treatment of Industrial Wastewater: Operation and Characterization of Microbial Population. PhD Thesis, University De Santiogo, 2011.

[19] Guo-ping, S., An-jie, L., Xiao-yan, L. and Han-qing Y.: Effects of Seed Sludge Properties and Selective Biomass Discharge on Aerobic Sludge Granulation. Chemical Engineering Journal, 160, 108^114.

[20] APHA, Standard Methods for Examination of Water and Wastewater, 19th ed., American Public Health Association, Washington, DC, 1995.

[21] Ni, B. J., Yu, H.Q. and Sun, Y. J.: Modeling Simultaneous Autotrophic and Heterotrophic Growth in Aerobic Granules. Water research, 2008, 42, 1583^1594.

[22] ZH, Li, Kuba, T., Kusuda, T. and Wang X. C.: Effect of Rotifers on the Stability of Aerobic Granules. Environ Technol., 2007, 28, 235^42.

Ground Water Assessment and Management at Khaniqeen area, Diyala Governorate, Iraq

M. Al-Dabbas, Q. Al-Kubaisi, T. Hussein and A. Al-Kafaji

***Abstract*-The climate parameters data for more than sixty years for Khaniqeen meteorological station were studied .The results show good evidence of climate change indicated by the remarkable decrease of the average means annual rainfall in the studied stations, with the remarkable increase of the average mean annual temperature. MODFLOW program is applied. GIS, 3D spatial analyst is used to prepare future planning to drill more water wells. The Storage and recharge measurements reflects that it is possible to drill 330 wells in the future and it is considered of about 300-500 m to be very suitable distances more than the effective well radius. To simulate for 20 years, the stress period were divided to 40 stress periods, one year simulation divides into 2 period lengths, 1 for wet period represented by 60 days, while another for dry period represented by 300 days. The calculated head values after 5, 10 and 20 years were indicated. Groundwater Flow Model of at Khaniqeen basin reflects that Well Module increase flow from Diyala River to the underlying aquifer, due to groundwater pumping near River. For these simulations, pumping is assumed to be from aquifer by wells, and the pumping rate is set to be continuous in dry period, an up rise in head in the lower part of the basin, while draw down in the upper part will happen. Therefore, It is recommended for Khaniqeen basin to drill wells within the middle and western side of the secondary basin (below isopotential line 200 m) this will not leave bad impact on aquifer storage with keeping acceptable distance between wells at least 500 m.**

Keywords: **Climate change, Groundwater Modeling, Khaniqeen - Iraq.**

I. INTRODUCTION

Major areas in the middle of Iraq are depending on the groundwater, for both domestic and the agricultural sectors. In order to conserve, protect, and develop water resources in the area in sustainable manner, it is essential to adopt an integrated water resources management approach taken in consideration the role of economical, societal and cultural status in implementation of future plans [1], [2].

M. Al-Dabbas is with the College of Science, University of Baghdad (corresponding author to provide mobile: 009647902290029;

E-mail : profaldabbas@yahoo.com

Q. Al-Kubaisi, is with the College of Science, University of Baghdad (e-mail:qusaikubs@yahoo.com).

T. Hussein is with the Building & Construction Engineering Department, University of Technology, Baghdad, Iraq(e-mail: tariqabed67@yahoo.com).

A. Al-Kafaji is with the Water Management Research Centre, Ministry of Water Resources, Baghdad (e-mail: alimjawad55@yahoo.com).

Quantity of groundwater has been badly changes through increasing of total soluble salts. This might be developed due to many new wells, new farms, and heavy population, improperly drilled and created with no previous recommendation and attention [3], [4] . Groundwater flow models are used to calculate the rate and direction of movement of groundwater through aquifers and confining units in the subsurface. The selected study area, Khaniqeen area is situated between 45^{o} $09^{/}$ – 45^{o} $36^{/}$ E and 34^{o} $12^{/}$ –34^{o} $39^{/}$ N within Diyala governorate, (Figure 1) [1], [2]. Its total area is equal to 1100 $Km^{2.}$ Al-Wand River is a permanent stream passed through the area; and drained its water to Diyala River [2]. Khaniqeen is the main city in the basin which has a total population of 15000 persons; most of them are occupied in agriculture . The area is considered as a secondary basin due to its location inside Diyala River
Basin, (Figure 1).

The quality and quantity groundwater of the study area has been recently appeared in the last two decade to suffer pollution, depletion, bad quality and quantity of groundwater, due to heavy and excessive pumping of groundwater and planting the area, especially during the dry long period (April – October) in Iraq. Pollution mainly comes from human activities, such as irrigation water that mixed with fertilizes and from the waste disposal (solid or liquid).

The area is divided into two parts having significant differences in geology, topography, and ground-water conditions. These are the low Folds province of long ridges and intervening valleys where water occurs in the Bai Hassan, Mukdadia, Injana and Fatha Formations, and older Tertiary strata as well as in alluvial deposits, and, the Delta Plains province where it's nearly flat or gently sloping surface is underlain by alluvium that completely covers the older beds. The Delta Plains province is the major ground-water basin. The major portion of the area is flat and featureless and lies with minor and unimportant exceptions at an elevation of less than 83 meters above sea level. Relief is low with only a few isolated hills rising above the general level of the plain in the east. The area is characterized by low anticlinal folds with intervening synclinal valleys. The elevations in this eastern zone vary from approximately 250 meters in the south to as much as

135 m in the Khaniqeen area to the north. Relief is greater in this eastern part, reaching as much as 140 m. Drainage in the region is almost exclusively in a southwesterly direction. Soil types within this area are typical of an arid to semi- arid region.

Many groundwater wells had been drilled in Khaniqeen area (about 65 pipe wells and many hand dug shallow wells [1]. Several aquifers can be recognized in the area. :

1-The most promising one are those located in the quaternary deposits such as the alluvial fan, Terraces, Natural Levee deposits, such as sand, gravel, silt and clay deposits. The drilled wells within the quaternary deposits considered to be of high production with low salinity, ranging in depth from 5 to 40 m.

2- Bai Hassan aquifer which is of good quality water(With 1750 ppm),and discharge, with sand and large gravels of Bai Hassan Formation .The drilled wells within this deposits, ranging in depth from 50 to 100 m .

3- Mukdadia Formation aquifer which is of wells depth that reach more than 100 m deep with 1000 ppm TDS with 7 liter/sec productivity. This aquifer considered to be with Bai Hassan aquifer of great importance in the area, and for deeper one Injana Formation.

Wells penetrate the aquifers can discharge around (5 – 10) l/s with salinity varies between (500 – 2500ppm) TDS. [5].

This study is performed to determine quantity and quality for ground water and prepare an initial study to available consequences in order to forming a complete idea to prepare a brief study in the future depends mainly about planning to drill more water wells in the region .

II. Materials and Methods

A. Climatic parameter analysis

Khaniqeen meteorological station was chosen in order to analyze the general climatic elements. The available data for more than sixty years (1938 t0 2009) records of the climatic elements were studied, such as temperature, evaporation and rainfall [6]

B. Groundwater Flow Modeling of Khaniqeen shallow aquifer

Groundwater flow model of [7], which was based on finite difference method of implicit solution, was applied. The use of this model is to develop a numerical quasi three dimensional groundwater flow of the shallow aquifer in the studied basin within the U. Pliocene,Pleistocene-Quaternary sediments.

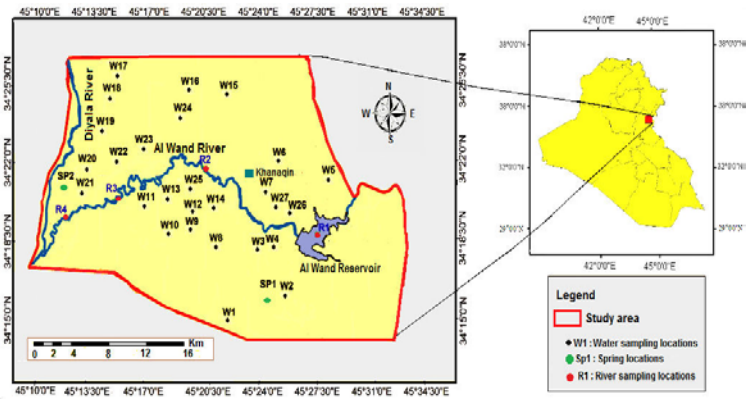

Figure 1: location map of the selected wells and Al- wand River sampling of the studied area [2].

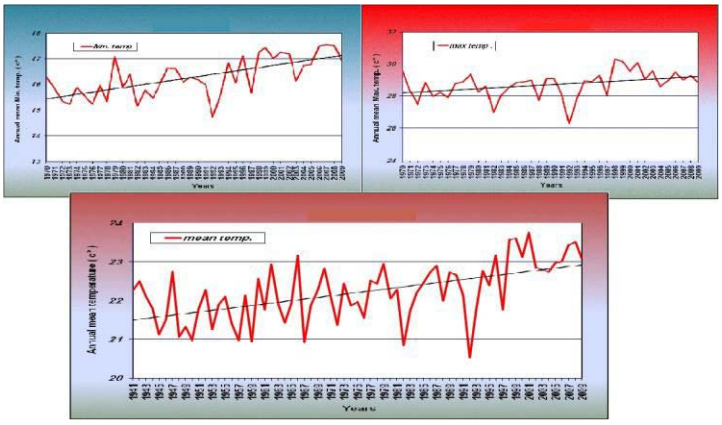

Figure 2: The Linear trend of annual mean temperature, mean annual minimum temperature and mean annual maximum temperature (^{o}C) time series of Khaniqeen meteorological stations for years 1941–2009 [6]

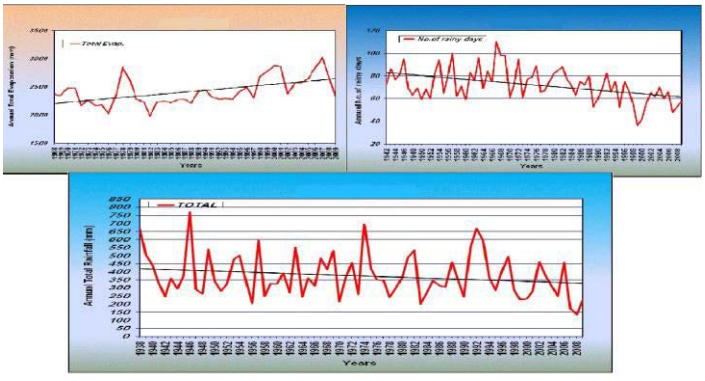

Figure 3: The Linear trend of annual total Rainfall , Number of rainy days and annual total Evaporation (mm) time series of Khaniqeen meteorological stations for years 1938–2009 (Iraqi Meteorological Organization, 2013).

III. Results and discussion

Climate:

The mean annual temperature: The mean monthly minimum and maximum temperature of of Khaniqeen meteorological station for the year from 1941–2009 (°C) frequency curves were studied for available data. The relationship between temperature and time seems positive with remarkable increase in temperature values were indicating from the general trend line, (Fig. 2).

The Rainfall Analysis: The mean annual rainfall (mm) frequency curves for the years 1938–2009, were studied for available data of Khaniqeen meteorological station. The relationship between rainfall and time seems negative, (Fig. 3). Remarkable decrease in rainy days, with increase in annual total evaporation was indicating as well from the general trend line (Fig. 3).

The hydraulic properties of Khaniqeen ground water aquifer:

The results of the hydraulic properties of Khaniqeen area reflect that their specific capacity varies due to the lithological variations of the rock beds within the groundwater aquifer that reach more than 200 m3/day to the south and east of Wand River, while less specific capacity values wells are located to the north of Wand River. The most important hydraulic properties of the groundwater aquifer are the Transmssivity coefficient (T) and Storage coefficient (S):

These Hydraulic parameters are the Transmssivity (T) in m2/day or it represent the hydraulic conductivity times the saturated thickness, it is ranging in the area of study from less than 50 m2/day at the north part of the study area to more than 300 m2/day at the south part of the study area south of Wand River. Also, the transmssivity coefficient (T) contour map indicate that there are two sub basins in the study area the first at the south of wand river ,where the transmssivity are ranging from (150 – 350 m2/day) ,the second sub basin located to the east of the study area with transmssivity ranging from (50 to 100 m2/day). Infact, the transmssivity coefficient depends on the following parameters: the permeability coefficient (K) and the saturated thickness of the water bearing bed rock (B), where: $T = K \times B$

Storage coefficient(S) and called Specific yield (SY) for the unconfined aquifers, it is estimated to be 0.1 in the study area taken into consideration the nature of the similar geological formations. Hydraulic conductivity (K) is representing the moving water volume per time unit trough unit area with hydraulic slope.

Modeling of Groundwater Flow in Khaniqeen Secondary Basin

Mathematical model is constructed for simulation of groundwater flow in Khaniqeen secondary basin. An understanding of groundwater flow is necessary to develop an efficient program for future. Model was constructed in stepwise fashion, beginning with single layer and model domain extension .The primary source of groundwater to the model is recharge, primary sinks for groundwater within the model area are wells. Calibration targets were hydraulic heads, water fluxes. In this investigation the model was constructed to simulate the Pliocene aquifer which is a single layer, important hydrologic feature (river) is represented in the model. The model domain is discredited into a grid; therefore a solution for the flow equation can be calculated at any point in the domain. After construction of conceptual model and selection of the modeling software, [PMWIN pro] [8], the features of the conceptual model are transferred to an input file that defines the mathematical model. The Boundary condition, grid dimensions and spacing, initial aquifer properties, and time steps features are specified as the basic components of the model. Model grids discrete the continuous natural system into segments (cells) that allow numerical solution to be calculated. The spacing between nodes called grid resolution should be responsive to sharp changes. The overall size of grid (total number of nodes) should be adequate to define the problem and procedure results consistent with modeling objectives, but not so large to cause excessive run preparation and computation requirements. The model grid consist of (44) columns and (47) rows and the cell dimension are 900 by 900 m, the total number of grid cells is (2068) of which (1105) are active cells within the study area.

Boundary Conditions (IC BOUND) have great influence on the computation of flow velocities and heads within the modeled area .Two types of boundary conditions are used in Khaniqeen groundwater flow model, specified head positive values (+1) in the I Bound array defines an active cells when expressing the domain inside. A (0) value defines inactive cells (no flow) taken place within the cells I Bound defines any outer flow boundary cells, While the river (Diyala River) is represented as a flow package with different hydraulic conductance and head.

Initial Hydraulic Head at constant head cells are used as specified head values of these cells. For steady state simulation the initial heads are used as starting values .Actual, confidential head values derived from the hydrogeological data bank of groundwater studies center. (Figure 4), shows the isopotential lines of the aquifer, the same values were loaded to the model as initial heads.

Aquifer Material Properties: The top elevation and the bottom elevation of the layer were also loaded, the values of the top of aquifer were derived from (Figure 5), and the values of the bottom of the aquifer were derived from Figure 6. Transmissivity is one of the input readings required in the model; the distribution of transmissivity is also prepared (Figure 7), and the values were loaded in each cell. Flow packages represented by recharge (L/T) positive values and wells (L3/T) negative values will added to the model .Recharge is defined by assigning the data to each vertical column of cells. The input parameters are assumed to be

constant during a given stress period, negative values indicate pumping wells; MODFLOW assumes that a well penetrates the full thickness of the cell (Processing Modflow pro V.7). To calculate heads in each cell in finite difference grid, PMWIN pro prepares one finite difference equation for each cell. Expressing the relationship was indicated between the head at a node and the heads at each of the six adjacent nodes at the end of time step.

SIP (strongly implicit procedure) package is used to solve the system of finite difference equation.

Time Stepping:

Time stepping is desicretizing of flow equation through time and is used in transient simulation (coming next) while in steady state simulation time variation is not included.

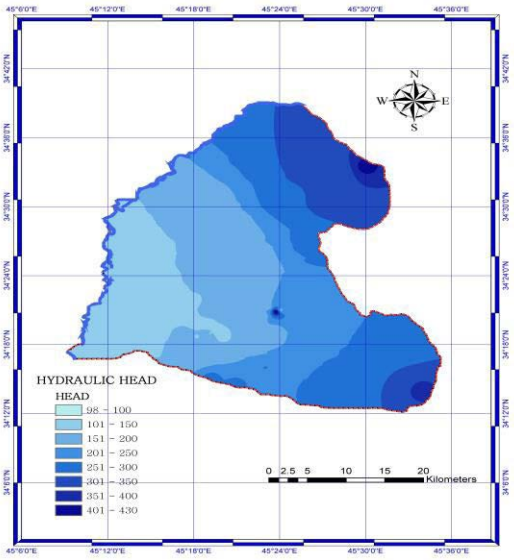

Fig. 4: Isopotential Lines (Initial heads) m.

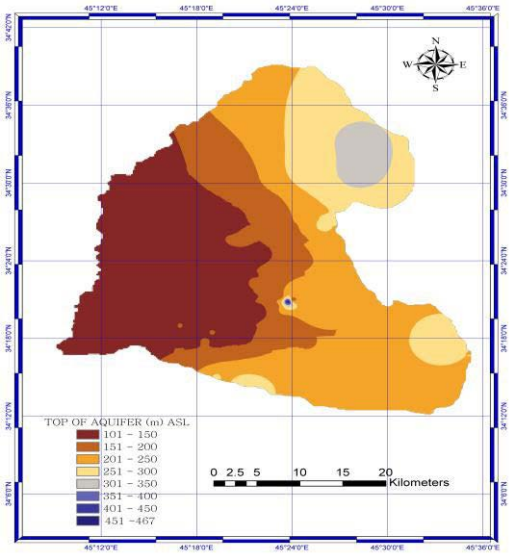

Fig. 5: Top Elevation of the Aquifer calculated hydraulic heads (Figure 10) shows the draw downs

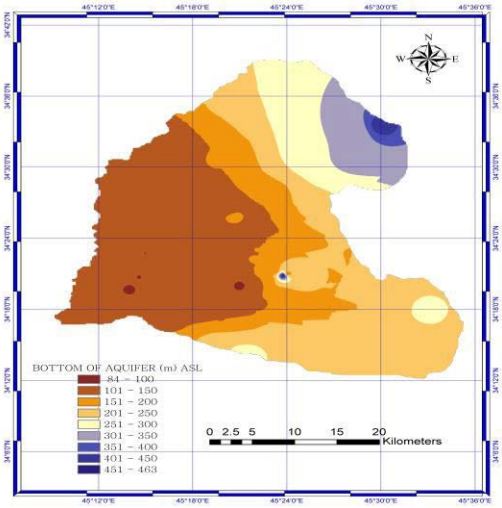

Fig. 6:Bottom Elevation of the Aquifer

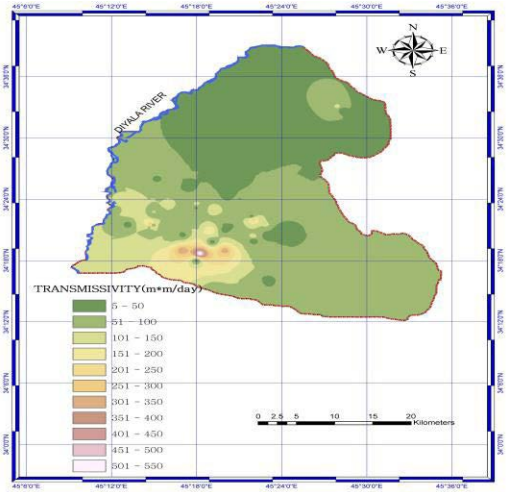

Fig. 7: Transmissivity Values

Steady state simulation is required for time-dependent modeling of groundwater flow. After input of the data and after running the model hydraulic heads are the primary results of MODFLOW as a steady state simulation will appear as in (Figure 8). Calibration is the process of adjusting model inputs to achieve a desired degree of correspondence between the model simulations and the natural groundwater flow system [7]. In other words, calibration methods are used until the solution matches the known (usually hydraulic heads) .For this model calibration is made for hydraulic heads inputs (manual calibration) to reach the matching between inputs and model simulation. After all of these hydraulic heads are the primary results of MODFLOW simulation (Figure 9). Draw down is the differences between the initial hydraulic heads and the

which are mostly below than 1 m.; this means that there is a good matching between observed and calculated heads. PMWIN pro calculates water budget for each sub region in each time step, the percent of discrepancy [100*(IN-OUT) / (IN+OUT)/2] In this step (steady state simulation) the percent discrepancy was 0.47% this means that the model equation has been correctly solved.

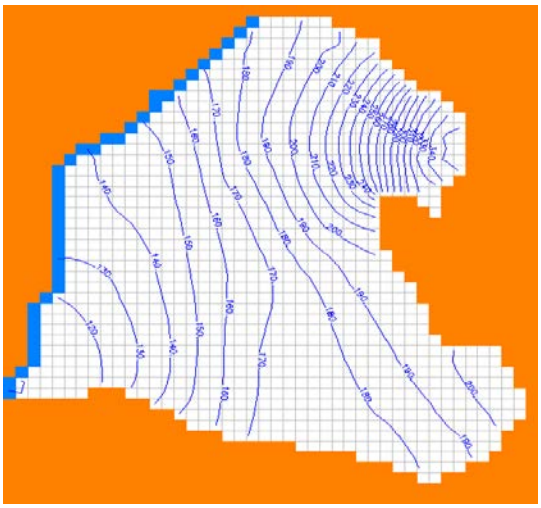

Fig.8: Calculated Head Values (m.)

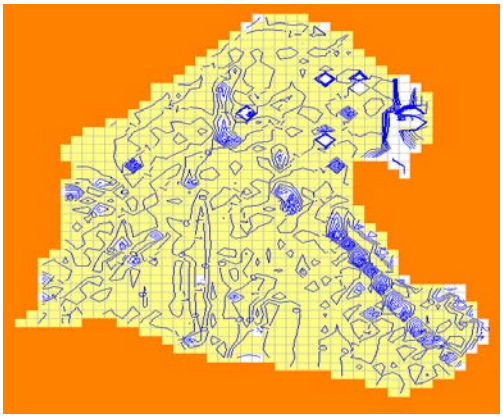

Fig.9: Drawdown values m.

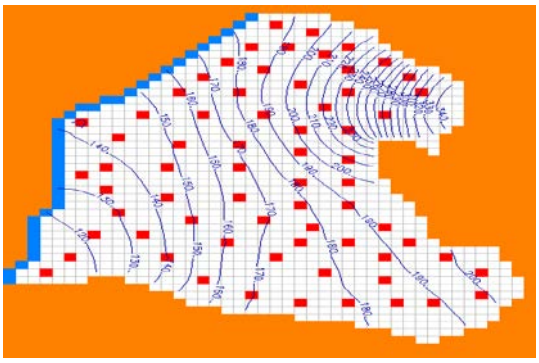

Fig. 10: Calculated head values through the end simulation (January)m.

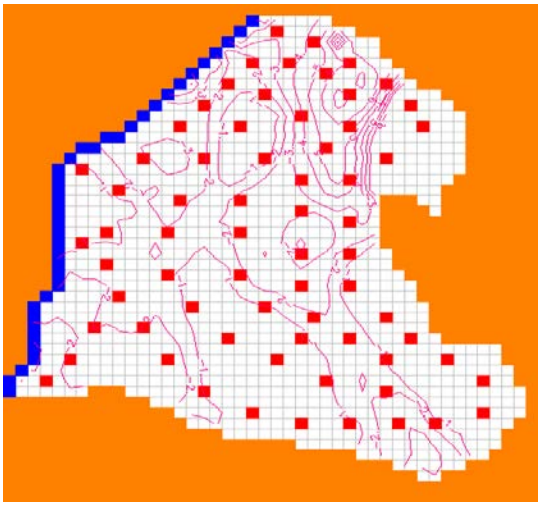

Fig. 11: Drawdown values (20 years later

Transient Simulation and Model Development: The applicability of groundwater model to a real situation depends on the accuracy of the input data, the determination of these requires considerable study, and like the collection of hydrological data (rainfall, evapotranspiration, surface runoff, and soil moisture) Groundwater recharge was evaluated based on these calculations. For transient calculations of groundwater flow, a stable initial condition which is created from a steady state simulation is undertaken in this simulation, beside sinks (wells) and sources (recharge). The initial base line condition is simulated with no pumping wells, while recharge is modeled as a source. [3] calculated the water surplus (Groundwater recharge + Surface runoff). The aquifer receives 39.11 mm/year as areal recharge; the mentioned value is a groundwater recharge during two months, 17.19 mm in February and 21.92 mm in March. Since the model used (L/T) as units for recharge, the values changed to 0.000614 m/day and 0.000707 m/day respectively for the two months. These two values are included in the groundwater model in development as transient simulation.

Time stepping in transient simulation: The time for one year simulation without sinks (wells) is divided to 12 stress periods, each stress period represents a month ,while the period length of each stress period are divided into days . So the total time steps equal to 12 months, while the total simulation time equals to 3.65e+2 days. The model is output in the monthly flow map depending on the variation of the above package (groundwater recharge). The calculated head values for each step are noticed showing slight differences in head contours. Figure 10 shows the calculated heads for the last step in this simulation (January). One of the most basic ways to evaluate quantitatively the movement of groundwater through aquifer system is the water budget [8]. The fundamental equation of a water budget (or water balance) is the sum of

inputs minus the sum of outputs equals the change in storage of the system: ∑ Inputs - ∑ Outputs = Δ Storage

Water budget calculation in Modflow calculates a volumetric water budget for the entire model at the end of each time step. In numerical solution techniques, the system of the equations solved by the model actually consist of a flow continuity statement for each model cell. Continuity should also exist for the total flows of the entire model or sub region. This means that the difference between total inflow and total outflow should equal the total change in the storage [9]. Another simulation with sinks (wells) is divided to 12 stress periods, each stress period represents a month ,while the period length of each stress period are divided into days . 68 wells are suggested to drill in the area to know the difference in heads. (Figure 11), shows the calculated head values of the last step for the suggested simulation. From the two mentioned (Figures 10and 11), it is well noticed that there are a changes in isopotential lines; indicating a change in flow direction besides uprising in water level and hydraulic gradient at the start point.

Predictive simulation: A model may be used to predict future groundwater flow conditions, such simulation estimates the hydraulic response of an aquifer, and also it can predict the pumping rate needed to monitor the hydraulic heads. A pumping strategy (groundwater management) is a set of spatially and possibly temporary distributed rates of extracting water from aquifer [10]. To predict the simulation for 20 years, the stress period were divided to 40 stress periods, one year simulation divides into 2 period lengths ,1 for wet period represented by 60 days while the another one for dry period represented by 300 days. A continuous uprising in groundwater level is happened in many parts of the area beside drawdown in others depends upon the situation of location of pumping.

IV. CONCLUSIONS:

1 - The results of this research revealed that the modeling and using the MODFLOW modeling program, based on the different aspects of a natural hydro geological system to simulate groundwater flow in three dimensions is very useful for groundwater basins in Iraq. Also, GIS, 3D spatial analyst is important to draw isopotential lines of the groundwater aquifers in Iraq.

2- Well Module increase flow from Diyala River to the underlying aquifer, due to groundwater pumping near River, is tested with this model by placing a simulated pumping well at alternate cell locations, operating the model for a 20 years period at each location, and calculating the change in the water budget when compared with the baseline condition (The initial baseline condition is simulated with no pumping well). For these simulations, pumping is assumed to be from aquifer by wells, the volume of water pumped is set at -600 m^3 per day, and the pumping rate is set to be continuous in dry period ,An up rise in head in the lower part of the basin, while draw down in the upper part will happen. It is recommended to drill wells within the middle and western side of the secondary basin (below isopotential line 200 m) this will not leave bad impact on aquifer storage with keeping acceptable distance between wells at least 500 m.

VI. REFERENCES:

[1] Jassim, A., S., and Ismael, S., K.: Hydrogeological study of Khaniqeen Basin, unpub. Internal report, Water Wells Drilling Co., Ministry of Water Resources, Iraq, 2005.

[2] Oleiwi A.S.,: *Hydrogeological and Environmental study of Khanaqin area, Northeastern of Iraq*, unpub. Thesis, College of Science, University of Baghdad, 2015.

[3] Al-Tamimi , O .S., : Water resources evaluation in Diyala river basin. Ph.D. thesis, College of Science , University of Baghdad , 2007,235 P.

[4] Al-Jiburi, H. K. S: Summary of hydrogeological and hydrochemical study of Khanaqin Quadrangle sheet (NI-38-7) GEOSURV. Baghdad,Iraq , 2009, 26 p.

[5] Ahmed A.M., Mummad, A.A., and Dawood, K.S.,: Hydrogeological study of upper part of Diyala Basin, Ministry of Water Recourse, General Commission of Groundwater , 2005,150p.

[6] Iraqi Meteorological Organization,: Climatical Data for Khanaqin Station, for period (1990-2013), 2013.

[7] Arlen H. W.: MODFLOW-2005, The U.S. Geological Survey Modular Ground-Water Model—the Ground-Water Flow Process, Techniques and Methods 6–A16. U.S. Geological Survey. 2005.

[8] Wen-Hsing C.: *3D-Groundwater Modeling with PMWIN*, Second edition, Springer, 2005, 397 p.

[9] Al_Zubari, W.:*Numerical Groundwater Flow Model MODFLOW, MODFLOW Exercises*, UNESCO Iraq Project :(Capacity Building of Water Institution in Iraq) ,2004.

[10] Parelta,R.C.,:*Optimization modeling for groundwater and conjunctive water policy*) Water dynamic laboratory ,Utah state university foundation,Utah state university,2004.

The Impact of using BIM-based building performance analysis for housing projects in Iraq

Hussaen A. Kahachi, Architectural Engineering Department, University of Technology

***Abstract*— The development of computer application for engineers and architects from the basic Computer Aided Drawing system (CAD) to Building Information Modeling system (BIM) not only allowed designers and architects to visualize buildings but also to analyze and estimate their performance in a virtual environment. This enabled designers to maximize building's efficiency, performance and reduce building's carbon footprint along the whole building lifecycle.**

This research is looking at the potential impacts of using BPA and BIM technologies to achieve better building performance with special focus on the housing system in Iraq. The impact, nevertheless, applies to other types of buildings as well. The research will achieve its goal via the following objectives:

- **What is BIM?**
- **How could BPA be applied through BIM? And the main differences compared to the traditional methods.**
- **What are the main advantages and disadvantages of using BIM for building performance?**
- **The Impact of using BIM for building performance analysis of affordable housing projects.**

***Index Terms*— Building Information Modeling (BIM), Building Performance Analysis (BPA), Housing in Iraq, Environmental Impacts, Affordable Housing.**

I. INTRODUCTION

The advancements in environmental science lead to the realization of the huge impact of buildings on the environment. Housing is considered one of the most important types of buildings as it is directly associated with people's lives and any improvements could have huge effects on the environment in the long term [1]. Engineers and designers used to estimate environmental impact of buildings through conventional analysis tools that was based on specific mathematical expressions which was handled manually. The introduction of advanced computer-based system facilitated the analysis of buildings' design and helped estimating its environmental impacts. With the rising complexity of building's design and environmental requirements as well as the need for more accurate, fast and reliable analysis made the use of advance computerized systems such as CAD-based and BIM systems a necessity these days, especially when analyzing large developments such as mega redevelopment and housing projects.

This research is concerned with the impact of using Building Information Modeling (BIM) and Building Performance Analysis (BPA) on housing projects in Iraq. It will start by defining BIM system and giving a brief background about its origins and development. Following that, the research will analyze BIM system process for analyzing building performance during building's lifecycle. While comparing BIM to the traditional methods usually used in Iraqi organization such as CAD-based systems. Then, the research will critically discuss the main advantages and disadvantages of implementing BIM system for handling building performance analysis. Following that, the research will highlight the potential benefits of using BIM for decreasing housing costs especially for affordable housing projects. Finally, the research will highlight some key points in the conclusions.

II. THE DEVELOPMENT OF COMPUTER-BASED BUILDING DESIGN SYSTEMS

The revolution of computer systems during the last century meant the ability to handle complex mathematical calculation faster, easier and more reliable. Amongst many computer applications, Computer Aided Design (CAD) applications allowed engineers to draw 2D drawings of the building's design, its structure and the associated support systems. This made it much easier to do complex calculations of the building design [2]. Additionally, the 3D visualization of the building in a virtual environment provided a new mechanism to understand buildings construction. It allowed engineers to better estimate the area and volume of the building, handle light and sun analysis, estimate heating and cooling loads, and many other aspects which all helped towards understanding the environmental impact of a building [3, p. 3]. However, Computer Aided Design applications could not cover all of the different aspects of environmental analysis, also CAD based applications where never inclusive in terms of environmental analysis and the user was required to have a very deep understanding of the tools and the use of a number of applications to be able to analyze the building [4, p. 3]. In addition, most CAD-based applications did not have the options to include the physical information of the materials such as heat resistant (R-value), heat storage, weight and density, thus requiring the user to transfer the completed 3D Visualization of the building to another application and enter the physical data to be able to analyze its environmental impacts.

Building Information Modeling (BIM) was first introduced in the 1970s [2, 5], nevertheless, it was first implemented in Graphisoft's ArchiCAD in 1987 under the name "Virtual Building" [6, 7]. The term "BIM" became popular after

Autodesk's published a report explaining the system [8] as well as several web articles explaining why BIM should be the industry term for the system [9].

III. WHAT IS BUILDING INFORMATION MODELING (BIM)

BIM has gone through many improvements and developments since it was first introduced, thus its definition has gone through some changes and researchers have different definitions. According to Hergunsel (3 p. 5) "BIM is a three dimensional digital representation of a building and its intrinsic characteristics". The National BIM Standards in the United States defines BIM as "a digital representation of physical and functional characteristics of a facility. A BIM is a shared knowledge resource for information about a facility forming a reliable basis for decisions during its life-cycle" (10 p. 1). Steel et al and others (11; 12) define BIM as "an independent network of policies, processes and technologies. Which together constitute a methodology to manage the essential building design and project data in digital format throughout the buildings' lifecycle". Although these definitions differ in some aspects, they all define BIM as a system with virtual environment for modeling the building. They all consider that system a building specific running alongside building's lifecycle from planning to operation. Finally, they all focus on Information as being the new added dimension that allows engineers to further evaluate building's construction, processes and operation within the virtual environment. Autodesk defines BIM as "an intelligent model-based process that provides insight to help you plan, design, construct, and manage buildings and infrastructure" (13). This definition directly highlight the four stages of buildings' lifecycle covered by BIM that are Planning, Design, Construction and Operation. Although some researchers have different division of BIM workflow phases. They are, in most cases, just including sub-division to the general division and stages of BIM workflow (14), Hergunsel and many other researchers agree with this division of stages although they might differ in naming these stages (3 p. 9; 15) see Figure 1.

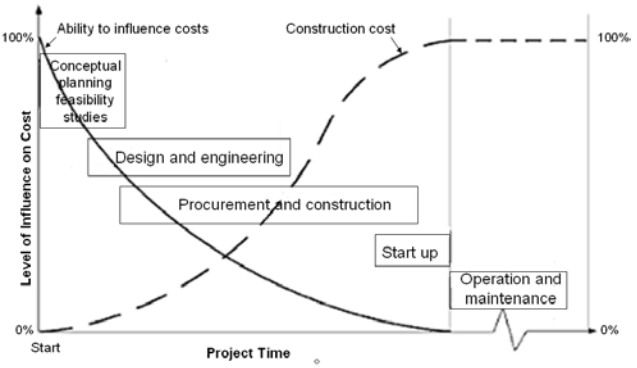

Figure 1: BIM project's lifecycle by Hergunsel *[3, p. 9]*

Since this research is concerned with the Building Performance Analysis in BIM and to the complexity and variety of subdivisions of these stages, the research will only discuss the general division and stages here but will go in further depth later on in the research when needed.

- According to Hergunsel (3), in the "Conceptual Design stage" and "Planning stage", the lead designer or architect and his/her team review the proposed project and the required resources and skills. They also start the legal contracts and understand them to ensure the deliverables they put for the project could be met. Additionally, the architect and the team build a simple representation for the design of the building to do some rough analyses.
- The "Design and Engineering stage" is where the team of engineers and architects design the building in full, ending with the full set of work-drawings and schedules such as quantities/specifications schedule. By the end of this stage, the building documentation provide full information about the project specification and design and the team have tackled most of the problems and issues in the design. This phase also include different analyses to justify and test the design of the building to the miner level possible and eliminate conflict (16).
- During the "Procurement and Construction stage" the procurement of the different resources including mechanical, human and materials starts. The delivery of these resources to the building site and initiation of the construction phase indicates the start for turning the design from the virtual environment to reality (2).
- The "Operation and Maintenance stage" is where a building start to perform its roles and objectives. The users start using the building, the different supportive systems start performing. BIM is beneficial in this phase through the ability to help in managing the building's users, users' needs, and systems more efficiently and effectively (3).

It could be argued here that a fifth stage could be added. This stage is associated with the end of building's lifecycle, BIM could help in the decision for the appropriate demolish approach, quantities and type of materials to result from demolish. Moreover, estimating the impact of removing the building on its surrounding buildings and area.

IV. THE APPLICATION OF BUILDING PERFORMANCE ANALYSIS (BPA) THROUGH BIM

According to Schlueter and Thesseling buildings in the United States alone account for almost 40% of energy consumption in the US, also buildings' energy consumption around the world accounts for about 40% of global CO2 emissions (17). The rising demand on energy and the growing awareness of the effects of CO2 emissions, as well as, the raising awareness of designers/engineers responsibility for minimizing the environmental impact of buildings. All that have pushed designers/architects and engineers to design more environmentally sensitive buildings to decrease its environmental impact (18).

Governments and professional organizations started putting building design criteria/codes and required planners, architects and engineers to apply them in their designs in order to minimize the environmental impacts of these designs. Such governments are the United States (19) and the United Kingdom (14). With the rising demand on building designs

that comply with environmental impacts codes, architects planners and engineers required a method to estimate buildings' environmental impact and try to minimize it through changes in design, material, and systems. Building Information Modeling provided the best environment to analyze building performance and make design changes virtually for the building (18). According to Autodesk, Building Performance Analysis (BPA) is “the process that uses BIM to driving a more efficient overall design through iteratively test, analyze, and improve building's design” (20). Although it should be highlighted here that all results are approximations of reality and hugely dependent on the accuracy of the building model used in the analysis and the knowledge of the user who interpret them. Building performance analysis deals with several aspects that all relate to building design. Kriegel and Nies (21) highlighted several aspects taken into consideration in BPA; first is the selection of Building Orientation that results in the minimum energy consumption possible. Second is analyzing Building Massing to optimize building envelope performance. Third is Daylighting Analysis that have impact on lighting and HVAC system. Fourth is Water Harvesting which could help reducing water needs. Fifth is Energy Modeling which could help in the reduction of energy requirements and analyze renewable energy systems such as windmills and solar panels. The sixth and final aspect is the use of Sustainable Materials by reducing materials needs and the usage of recycled materials.

Because all of above in addition to the fact that BIM links all buildings components with their physical properties, BIM is by far the best option to apply building performance analysis. According to Azhar et al. BIM is the perfect environment for building design analysis as all buildings components are five dimensional. Meaning that building objects and components in the representation do not have height, width and length properties only, additionally they are part of specific schedule of construction (time) and have physical properties such as heat resistant important for handling building performance analysis (16).

The default methodology/workflow for BIM and BPA design team as explained by Autodesk is as follows; first, the architect builds the basic geometry of the building in one of BIM virtual environment applications. Then another architect or engineer creates the energy model for the building geometry (Energy Analytical Model EAM). MEP engineer/s will create a design model for the piping, HVAC and electrical systems. Following that, the entire design team will start improving the design of building using building performance analysis of the now detailed building representation (20; 3).

Based on that it is possible to conclude that Building Performance Analysis could be applied in two stages:

A. The first is through the "Conceptual Planning/Design stage", in which simple representation of the building with low level of details is analyzed to estimate its environmental impact and make big changes to the building design in early stages before adding other details. The application of building performance analysis in this stage could dramatically decrease the time required for making big changes to the design such as building orientation, shading and construction materials which otherwise might require a lot of time in later stages of building the virtual model in BIM as it directly affect supporting systems design (22).
B. The second stage is "Design and Engineering stage", in which fully detailed representation of the building is analyzed with all its supporting systems including HVAC, electrical and plumbing systems. This stage provides fully detailed analysis of the virtual model and the supporting system, thus allowing making changes to the minor levels. This could dramatically affect building performance in reality especially if changes are made to the heating and cooling systems, lighting of different spaces, design of windows and doors and other aspects of design (7).

It could be argued here that Building Performance Analysis could have direct impacts during other stages as well. For instance, in the "Procurement and Construction stage", BPA could help architects/contractors decide the building materials and components to use and their suppliers/fabricators, as it will raise their awareness to direct environmental impacts of the construction processes of the building. As for the "Operation and Maintenance stage", BPA estimations of space use and energy consumption could help better manage the building during operation, for example benefiting from the cool night to lower space temperature in advance before having heat-generating activity in the afternoon that follows for a specific hot day in the year. Another example is making sure future expansions and systems does not have bad influence on the overall building performance.

V. THE ADVANTAGES AND DISADVANTAGES OF BIM-BASED BUILDING PERFORMANCE ANALYSIS

Based on what was discussed earlier it is possible to conclude that BIM is a much better environment than CAD and other traditional systems when it comes to Building Performance Analysis (BPA). *Ajila* [10] concludes that traditional systems have deficiencies as they are associated with simplified assumptions made by the designer and engineers that is, in most cases, based on rules-of-thumb thus the results could be widely misleading and inaccurate. Additionally, traditional methods may force some aesthetic features that could have large impact on the building performance hence the environment. Lastly, traditional methods does not provide, in any term, an effective and efficient approach for measuring building design options performance thus making objective judgments and comparisons is not possible.

The building performance analysis with BIM can more accurately estimate the impact of design options as it is based on calculations of actual quantifiable data rather than rule-of-thumb assumptions. Furthermore, as BIM uses detailed building models in simulations, it could better analyze and represent the behavior of the building and its supporting systems. Finally, BIM-based building performance analysis provides a method for measuring the performance of the different alternatives and design options for the building as it is based on systems such as Level of Development (LOD) with LEED system, thus allowing comparison that is more objective and accurate [10, 11]. See figure 2.

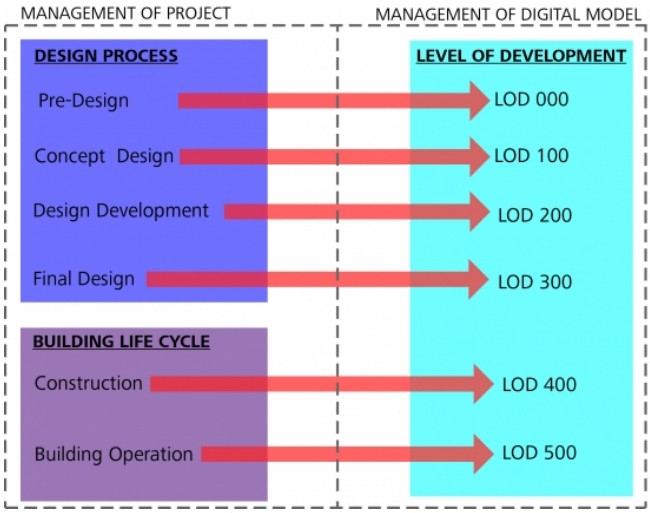

Figure 2: Level of Development and BIM project phase source: *[12]*

It could be argued here that although BIM-based building performance analysis has many advantages over traditional methods, it requires all engineers to have good understanding of the tools required for analysis to produce accurate and complete results. Otherwise, the analysis could end with misleading results that could affect the building performance hugely. Furthermore, although building performance covers the analysis of building design and operation that is responsible for the most environmental impact as many researchers say [13, 14]. It still misses building impacts during the fabrication and production of building elements, transportation of resources, construction of the building and other aspects, which still accounts for a respectable amount of building impacts on the environment. Finally, the implementation of building performance analysis may require some changes in national laws, institutional structures, design teams, contracts and other related factors to successfully implement this system in the building design, construction and operation which could require a lot of time and effort especially for countries that did not experience such laws like Iraq. As an example, while design team members structure and relation in both CAD and BIM-based systems are very similar as they both include architects, civil and structural engineers, systems engineers (Mechanical, Electrical and Plumping/Piping) as well as other member and engineers, the relation and responsibilities' allocation between teams may differ [15]. In the traditional CAD system -widely used in Iraq- team members work consequently meaning that architects will produce their plans then give them to the civil and structural engineers to design the structural system, and then MEP engineers will consequently design the supporting systems of the building. The traditional workflow involves a lot of going back and forth and the engineers have worked their way around it for years. In BIM, design team members start consequently but could work in parallel thus saving a lot of time and effort while improving the results and minimizing overlap work and collision in design [8, 15]; however, this change requires major changes in the structure of institutions, laws and standards especially when including Building Performance Analysis in the equation.

VI. BIM-BASED BUILDING PERFORMANCE ANALYSIS AND AFFORDABLE HOUSING IN IRAQ

Housing is the first type of buildings made by humans. Providing shelter against the different environmental factors as well as providing safety are some reasons to why this type of buildings are essential for human lives. Up to these days, housing form the majority of buildings built around the world not only in number but also in their land usage, resources and time requirements, thus they have huge impact on the environment beside their other impacts (27). Due to the rapid population growth, urbanization, migration, rising health needs, and modernization, the requirements of housing units dramatically increased in terms of the number and the standards of housing units (28; 29). Governments around the world started taking important role in the provision of housing units especially for low-income workers, as they are the most effected and incapable for producing housing units with good standards. This especially after the industrial revolution in Europe where large numbers of workers were brought to work in factories in industrial cities (29). In developing countries like Iraq, this notion was transferred over after the end of colonization era. This is because of modernization notions transferred from developed countries that caused developing countries to have similar problems (29; 30). In addition, religious and social factors promoted this notion as a way of providing justice and equity (31; 32).

Although Iraq has one of the first housing systems in the area (33). Presently, the country suffers from one of the most severe housing crisis (1). This could be attributed to a number of reasons such as political instability, wars, economic blockade, administrative corruption, absence of private sector affordable housing, Ill-considered laws and legislations, security crisis and many more factors (34). In 2003, the Iraqi Ministry for Construction and Housing estimated that Iraq need about 2.5 million housing units by 2016. The ministry put a strategic plan to fulfill that need via mega and big housing projects (35).

Just like in most counties, the rising demand on housing with higher standards and the outbreak of economic, environmental, social, planning, health and security problems in housing areas (36). All that required Iraqi government like many governments to put down a set of standards for housing planning and construction to guarantee the new housing units meet these standards (37; 38). However, as seen in other countries, the main problem facing the housing system particularly these days are derived not from putting these standards; rather it is associated with the implementation of these standards and making sure they are met in housing units. In short, governmental organizations associated with housing, need a method for; first, analyzing the housing units and check if they meet the standards, second monitoring and controlling the housing units to guarantee that they keep meeting these standards in the long term. Although, BPA in BIM cannot fully tackle the second problem in the environmental context, it can be extremely beneficial in addressing the first problem. There are a number of potential advantages from implementing BPA in housing projects especially for

affordable housing. This includes:

- More sustainable buildings/housing as BPA allow engineers to analyze housing buildings' design then making changes/choices for the design to be more sustainable such as decreasing power consumption, lowering waste producing and CO2 emissions. BPA could also raise awareness of the building design impact on the environment between engineers and people. This could help to improve the sustainability of other buildings' types in the future thus lowering the environmental impacts of buildings and new developments.
- BIM-based BPA have the ability to analyze new materials in a virtual environment. This allows engineers to test the impact of using local materials, recycled materials, or other materials that are more sustainable in the design of the building or any part of it to maximize sustainability without the need to test them in actual construction from the beginning. This does not mean eliminating the need for physical testing in the actual environment; rather it allows engineers to do these tests and analysis easier and at lower cost especially in first stages.
- Reducing costs in the short term. BPA could help reducing the costs of housing in the short term in many ways. For example, BPA could help designers to estimate the actual performance of the building and its components. This could help them identify where specific amount or type of materials are not needed in the building design thus eliminating it or changing it to a lower-cost material. Thus reducing the overall cost of the housing unit in the short term. For instance, based on BPA for a building, designers could decide to eliminate the insulation material from one side of the building, as it does not make meaningful improvements for its cost. Furthermore, the implementation of BPA could reduce building support systems and infrastructure. For example decreasing the size of air-conditioning units due to the improvements in passive cooling systems for the building. An example for the benefits of BPA for infrastructure is that by deciding to use water-recycling systems, the infrastructure size could be reduced and/or be more sustainable.
- Making housing more affordable in the long term. By implementing BPA, better choices of the infrastructure, systems, and building design could be made. These choices does not only result in decreasing power and water consumption, but it could also help by producing some or all of the required water and electricity locally. This would result in a huge power and water savings in the long term thus lowering the running costs of the housing units overall. Additionally, having such choices usually means lower spending on maintenance of the infrastructure and local systems, as they get smaller and more efficient. All this could result dramatic decrease of housing units costs in the long term.
- There are other advantages of implementing BPA in the national housing system. This include, enabling universities and professional organizations and bodies to monitor and track buildings performance thus cities' planning and the potential common issues facing it in the long term, thus helping future researchers, professionals and planners to find solutions for these issues or make improvements to the design of buildings and the planning of cities. Other advantages are derived from producing building that are more sustainable such as better health, better self-esteem and social awareness of the global and local environmental challenges.

All these potential advantages of implementing BPA in design could have major impact in Iraq if applied through the national housing system. This is particularly because the country's housing laws and standards are undergoing huge changes and improvement as stated in the National Housing Policy in Iraq by the Ministry of Construction and Housing (MOCH) and UN-Habitat in 2010 (35). Another reason why this change could result in rapid improvements is the large number of mega redevelopment and housing programs that could amplify the good impact of implementing BPA for housing systems by a huge amount. Such projects are the 10x10 project and Bismayah in Baghdad as well as many other similar projects in other Iraqi governorates (39; 35; 40). From all that it is possible to foresee the potential impact of implementing Building Performance Analysis in the national housing standards in Iraq. However, to achieve the best results from BPA implementation, few housing and building standards should be changed. Another limitation is the institutional structure which need to be refined to allow the successful implementation of building performance analysis. The final limitation is derived from not having enough experience and knowledge in this section which could cause misleading results.

VII. CONCLUSION

The research gave a brief background about the advancement of computer applications in design and the role of Building Information Modeling in satisfying many aspects in design. These aspects are derived from Building Information Modeling being a five-dimensional system specified for building design and analysis. In addition to the three dimensions in older systems, BIM also included time and physical properties of building's components in building design. This allowed engineers and architects to analyze the building different criteria in a virtual environment and make modifications to improve the design before constructing it. This is the main reason why Building Performance Analysis (BPA) is much more feasible through BIM and it is the reason why BPA could have more accurate results than traditional methods.

The implementation of Building Performance Analysis carries many benefits. Beside the big improvements in the sustainability context such as reducing CO2 emissions and lowering power and water consumption, BPA could result in major short and long term cost savings for the users and the government. In addition, BPA could make design analysis and researches more feasible as it could serve as a tool for measuring the performance of building and the potential benefits of specific improvements. Likewise, BPA could be

used as a tool to enable future planning and ensure buildings and cities have acceptable performance and environmental impacts. The implementation of BPA in the Housing System in Iraq especially affordable housing could magnify these benefits especially because Iraq is undergoing major improvements in tis housing standards and laws. In addition, the housing crisis and the strategic plan made by the government to overcome this crisis through mega redevelopment and housing projects like the 10x10 and Bismayah project in Baghdad could facilitate the implementation of BPA and maximize its potential benefits. However, this implementation does not come without limitations; BPA implementation requires changes to some housing laws and standards. It also need modifications to the organizational structure and development of staff and tech in these organizations to make it work. Keeping all that in mind, BPA implementation in the Housing System in Iraq could still make huge changes for present and future generations faster and easier than in many countries and should be considered further by the different governmental and non-governmental organizations and researchers.

REFERENCES

[1] UN HABITAT, "The State of Arab Cities 2012: Challenges of Urban Transition," Habitat Publications, Worldwide, 2012.

[2] P. T. R. S. K. L. Chuck Eastman, BIM Handbook: A Guide to Building Information Modeling for Owners, Managers, Designers, Engineers and Contractors, Hoboken - New Jersey: Wiley & Sons, 2011.

[3] M. F. Hergunsel, "BENEFITS OF BUILDING INFORMATION MODELING FOR CONSTRUCTION MANAGERS AND BIM BASED SCHEDULING (Master's Thesis)," WORCESTER POLYTECHNIC INSTITUTE, May 2011.

[4] I. F. C. S. Simon F. Bailey, "Case-Based Preliminary Building Design," Journal of Computing in Civil Engineering, vol. 8, no. 4, p. 454–468, October 1994.

[5] C. Eastman, D. Fisher, G. Lafue, J. Lividini, D. Stoker and C. Yessios, An Outline of the Building Description System, Institute of Physical Planning-Carnegie-Mellon University, September 1974.

[6] Dice, "ArchiCAD," [Online]. Available: https://www.dice.com/skills/ArchiCAD.html. [Accessed 25 4 2015].

[7] I. Howell and B. Batcheler, "Building Information Modeling Two Years Later –Huge Potential, Some Success and Several Limitations," Worldwide, 2011.

[8] Autodesk, "Building Information Modeling," CA, 2003.

[9] J. Laiserin, "Comparing Pommes and Naranjas," Laiserin, [Online]. Available: http://www.laiserin.com/features/issue15/feature01.php. [Accessed 24 4 2015].

[10] A. Aksamija, "BIM-Based Building Performance Analysis: Evaluation and Simulation of Design Decisions," in 2012 ACEEE Summer Study on Energy Efficiency in Buildings, 2012.

[11] W. A. C. D. O. I. A. Salman Azhar, "Building information modeling for sustainable design and LEED® rating analysis," Automation in Construction, vol. 20, no. 2, p. 217–224, March 2011.

[12] Autodesk, "Project Phases & Level of Development," Autodesk, [Online]. Available: http://sustainabilityworkshop.autodesk.com/buildings/project-phases-level-development. [Accessed 15 5 2015].

[13] Autodesk, "Building Information Modeling for Sustainable Design," Autodesk Inc. White Paper, Worldwide, 2005.

[14] R. Brahme, A. Mahdavi, K. Lam and S. Gupta, "COMPLEX BUILDING PERFORMANCE ANALYSIS IN EARLY STAGES OF DESIGN: A solution based on differential modeling, homology-based mapping, and generative design agents," in Seventh International IBPSA Conference, Rio de Janeiro, August 13-15, 2001.

[15] M. Ibrahim, R. Krawczyk and G. Schipporeit, "Two Approaches to BIM: A Comparative Study," Illinois Institute of Technology.

[16] J. B. R. F. Salman Azhar, "BIM based Sustainability Analysis : An Evaluation of Building Performance Analysis Software," Worldwide.

[17] F. T. Arno Schlueter, "Building information model based energy/exergy performance assessment in early design stages," Automation in Construction, vol. 18, no. 2, p. 153–163, MARCH 2009.

[18] Autodesk, "Improving Building Industry Results through Integrated Project Delivery and Building Information Modeling," Autodesk Inc. White Paper, Worldwide, 2008.

[19] IBM, "Building Information Modelling," IBM - UK, [Online]. Available: https://www.ibm.com/smarterplanet/global/files/building_information_modelling_ibm_pov.pdf. [Accessed 15 4 2015].

[20] Autodesk, "Building Performance Analysis (BPA)," Autodesk, [Online]. Available: http://sustainabilityworkshop.autodesk.com/buildings/building-performance-analysis-bpa. [Accessed 2 5 2015].

[21] E. Kriegel and B. Nies, "Green BIM," 2008.

[22] R. HARRIS, "Learning from the past: international housing policy since 1945," Habitat International, vol. 27, pp. 163-166, 2003.

[23] P. JENKINS, H. SMITH and Y. P. WANG, Planning and Housing in the Rapidly Urbanising World, UK, USA and Canada: Routledge, 2007.

[24] R. HARRISA and C. GILES, "A mixed message: the agents and forms of international housing policy, 1945–1973," Habitat International, vol. 27, pp. 167-191, 2003.

[25] G. K. PAYNE, Urban Housing in the Third World, UK and USA: Great Britain and Routledge, 1977.

[26] M. A. H. AHMAD, Studies in Islamic culture (Dirasat fe Al-thaqafa Al-Islamia) [Arabic], Egypt, Lebanon and Iraq: Dar-Al-Fikr, 2004.

[27] B. AL-ARABI, "Construction and housing issues in Islamic law (Qathaia Al-Aumran wa Al-Iskan fe Al-Sharia Al-Islamia) [Arabic]," Al-Tafahum, vol. 12, pp. 2-10, 2011.

[28] Z. HONKE, Arab's sun shining on the West: impact of Arabic civilization in Europe (Shams Al-Arab tastu'a ala al-garb: Athar al-hathara al-arabia ala al-garb) [Arabic translated from German], Beirut: Dar Al-jeel, 1993.

[29] H. Kahachi, "State-Led Low-cost housing in Iraq in the political and social context (Master's thesis)," Cardiff University, Cardiff - UK, 2013.

[30] Iraqi Ministry of Construction and Housing; UN Habitat, "National housing policy in Iraq," Iraqi Ministry of Construction and Housing, Baghdad, October 2010.

[31] A. D. LASSERVE and L. ROYSTON, "International Trends and Country Contexts - From Tenure Regularization to Tenure Security," in Holding Their Ground: Secure Land Tenure for The Urban Poor in Developing Countries, D. A. and L. ROYSTON, Eds., 2002.

[32] A. KAMI, "Iraq needs billions to meet growing housing shortage," Reuters, 2011 . [Online]. Available: http://www.derechos.org/nizkor/econ/irq1.html. [Accessed 23 4 2015].

[33] P. MARR, The Modern History of Iraq Third edition, Westview Press, 2012.

[34] Baghdad Mayor's Office, "Ten by Ten plan for the development of Sadr City (Khutat Ashra fe Ashra li A'amar Madenat Al-Sadr)," Unpublished, Baghdad, 2008.

[35] National Investment Commission, "NIC and Hanawah South Korean Company sign Bismayah New City infrastructure contract," National Investment Commission, 4 8 2015. [Online]. Available: http://investpromo.gov.iq/newsticker/nic-and-hanawah-south-korean-company-sign-bismayah-new-city-infrastructure-contract/. [Accessed 4 5 2015].

GIS MODEL FOR PRODUCING HSG CLASSIFICATION DIGITAL MAP OF BAGHDAD CITY

Ahmed A.M. Ali, Professor, Water Resources Eng. Dept./ University of Baghdad,
Mahmoud S. Mahdi, Assistant Professor, Building and Construction Eng. Dept./University of Technology-Linoxer@Gmail.com
Nuha Jamal Abdullah M. Sc., Water Resources Eng. Dept./ University of Baghdad.

Abstract— **The Geographical Information System (GIS) was used to produce a major United States Department of Agriculture (USDA) textural soil classification digital map and subsequently produce the Hydrologic Soil Groups (HSG) classification digital map for Baghdad City. The produced map can be considered as baseline data for estimating runoff using the Natural Resources Conservation Service (NRCS) runoff curve number (CN) method.**

Soil investigation reports for the 23years (1990 to 2013) were adopted as a reference for 362 boreholes spread randomly within Baghdad City. The soil data of these boreholes and a digital map of Baghdad City were used for estimating HSG.

GIS techniques were integrated with the geo-statistics to analyze the spatial variability in soil properties within the city, where the shape files of soil separates are interpolated using kriging combined with semi-variogram parameters to generate digital maps of sand, silt and clay which are used in preparing major USDA textural soil model.

Digital maps of soil separates were used for applying percentage criteria of the twelve major USDA textural soil classes as rules within knowledge based classification model in ERDAS Imagine 11.2 software to predict the required soil characteristics digital map.

The soils within the city were assigned to HSG according to Technical Release 55 (TR55) of USDA-NRCS criteria, by using knowledge based classification model to predict the HSG map.

The overall accuracy of HSG model produced from knowledge-based classification is 97.93 % with Kappa coefficient of 0.916 indicate that the produced HSG map was at high level of accuracy.

The produced soil textural map shows that among twelve classes, seven classes of soil texture appeared within the area of study which are: Loam, Silt Loam, Sandy Clay Loam, Clay Loam, Silty Clay Loam, Silty Clay and Clay. Whereas, the produced HSG digital map shows that most of the area of study covered with D class (89%) followed by B class (10%) and very small part of C class (1%). The results of accuracy assessment and the produced digital maps show that the implemented model and the produced digital maps can be effectively used for estimation runoff within Baghdad City.

Index Terms— GIS, HSGs model , USDA textural soil classes.

I. INTRODUCTION

Many urban drainage systems constructed under minimal levels of urbanization are now frequently operating under increased levels of urbanization and have inadequate capacity for controlling storm waters. Predicting runoff with respect to changing land use allows planners to design sufficient capacity of minor drainage structures and place appropriately sized culverts, sewer pipes, and storm drains to assure effective storm water flow out of an area. Effective sizing of storm water structures without overdesign is important if one is to develop economic and well designed structures. Failure to do this can lead to considerable damage, ranging from major infrastructure flooding to minor issues such as flooding cellars.

The United States Department of Agriculture (USDA), Natural Resources Conservation Service (NRCS), formerly the Soil Conservation Service (SCS) runoff curve number (CN) method [1] is the most widely used procedures for storm water calculation in drainage design and analysis. In this method, the runoff index is the critical parameter.

The NRCS runoff index is known as the curve number, CN. In general, the runoff index, CN, represents how the combined hydrologic effect of soil, land cover, hydrologic condition, and antecedent moisture condition control the amount of precipitation that becomes runoff.

The NRCS runoff curve number, CN is an index that is a function of three factors: Hydraulic Soil Groups (HSG) , cover-complex classification, and antecedent moisture condition.

Measurement of soil properties is time and cost prohibitive, especially in remote areas with limited access and rapid urbanized areas. Soil survey has traditionally provided the most comprehensive soil datasets; however, recent advances in Geomatic technologies (remote sensing and computing potential) have fostered the development of digital

soil mapping. Integrating Remotely-Sensed (RS) data with Geographical Information System (GIS) techniques through digital soil mapping presents a unique opportunity to improve quantitative estimation of soil properties at landscape and regional scales and then overcome labor intensive procedures necessary to estimate the runoff index.

This research aims to utilizing the GIS to produce a major United States Department of Agriculture (USDA) textural soil classification map and subsequently estimate the Hydrologic Soil Groups (HSG) classification map for Baghdad City. This map can be effectively used to estimate the runoff using the NRCS -CN method.

II. AREA OF STUDY

The city of Baghdad is the economic, cultural and political capital of Iraq, situated on the banks of Tigris River at the northwest end of the alluvial plain. It covers 4555km^2 which represented 1% from total area of Iraq, 435052 km^2, [2].

According to the Central Organization for Statistics (COS), [3], the number of housing units of Baghdad City expanded from about 618285 in 1997 to 1064175 in 2009, as such its population in 1997 and 2009 was approximately 5365989 and 6702538 inhabitants respectively. In 2011, Baghdad's population became nearly 7055196 inhabitants; about 21 % of Iraq's population , [3], which is making it the largest city in Iraq, the second largest city in the Arab World after Cairo, Egypt and the second largest city in Western Asia after Tehran, Iran.

Since Baghdad is the fastest growing city and urban drainage problems sometimes occur, it is very relevant to be as a study area. About 1090Km^2 of Baghdad City was chosen to be the area of study. Fig. (1) shows the location of the study area with respect to Iraq and to Baghdad City respectively. The study area bounded by the coordinates from 424329 to 460548 m easting and from 3702154 to 3671966m northing in zone 38N. Its dimensions of about 36.2km length and 30.1 km width.

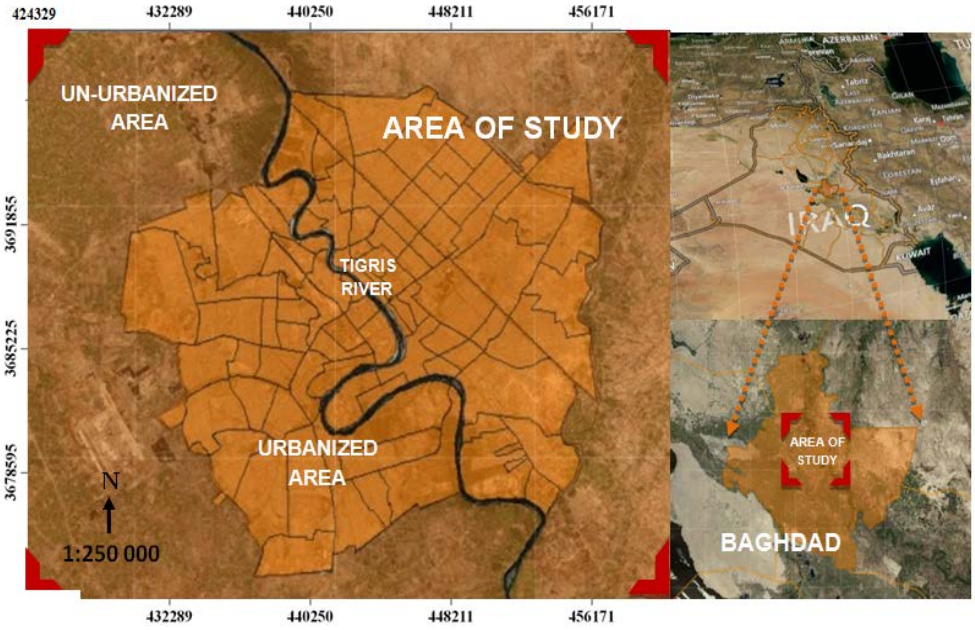

Fig. 1. Area of Study.

A. Administrative Divisions

Tigris River splits Baghdad in half, with the eastern half being called 'Rusafa' and the western half known as 'Karkh' which are connected by several modern bridges. The borders of the municipality of Baghdad encompass fourteen administrative units, eight in Rusafa and six in Karkh, they are, [4]:

9-Nissan, Al-Adhamiyah, Al-Doura, Al-Mansour, Al-Sha'ab, Al-Shula, Al-Kadamiyah, Al-Karada, Al-Karkh, Baghdad Al-Jadida, Al-Rasheed, Al-Rusafa, Al-Sadr City 1 and Al-Sadr City 2.

These fourteen districts are subdivided into 90 smaller neighborhoods according to Ministry of Municipalities and Public Works (GIS Department),which may make up sectors of any above districts, Table (I).

B. Land Use and Land Cover

Results of unsupervised classification using French SPOT 5 satellite, 5 m Spatial resolution, (acronym for System Pour l' Observation dela Terre 5) that is acquired in May 15, 2011 showed that the initial land use and land cover (LULC) map of the study area is mainly consisted of four classes: soil, water, vegetation and impervious. While, The final LULC map of supervised classification for the same classes was as shown in Fig. (2), [5].

Table (I): Neighborhoods Baghdad City.

ID	Neighborhood	ID	Neighborhood	ID	Neighborhood	ID	Neighborhood
1	14-July	24	Hadar	47	MuthanaZayuna	70	Sha'ab
2	6-Kanun	25	Hateen	48	Neel	71	Shamasiya
3	Aadhamiya	26	Huriya	49	Nidal	72	ShawraWa Um Jidir
4	Aamel	27	Idrissi	50	Oubaidy	73	Sheik Junaid
5	Abu Nuwas	28	Jamia	51	Qadisiya	74	Sheik Marouf
6	Adl	29	Janain	52	Qahira	75	Sheik Umar
7	Al Tib	30	Jazeera	53	Rabi	76	Shulla
8	Al Ulum	31	Jihad	54	Rasheed	77	Shurta
9	Ameriya	32	Jumhuriya	55	Risalah	78	Sindabad
10	Amin	33	Kadhimiya	56	Riyadh	79	Sumer Al-Ghadier
11	Andalus	34	Kamaliya	57	Saadoun	80	Tashree
12	Atifiya	35	Karada	58	Sadr 1	81	Tunis
13	Babil	36	KarbDejla	59	Sadr 2	82	Ur
14	Baghdad Al-Jadida	37	Karkh	60	Sadr 3	83	Washash
15	Baladiat	38	Keeylani	61	Sadr 4	84	Waziriya
16	Basateen	39	Khadra	62	Sadr 5	85	Wehda
17	Bayaa	40	Kindi	63	Sadr 6	86	Yarmouk
18	Beida	41	Maghrib	64	Sadr 7	87	Zafaraniya
19	Diyala	42	Mansour	65	Sadr 8	88	Zahra'a
20	Fajr	43	Masafee	66	Sadr 9	89	Zawra'a
21	Furat	44	Mashtal	67	Salaam	90	Zubaida
22	Ghartan	45	Mustansirya	68	Salhiya		

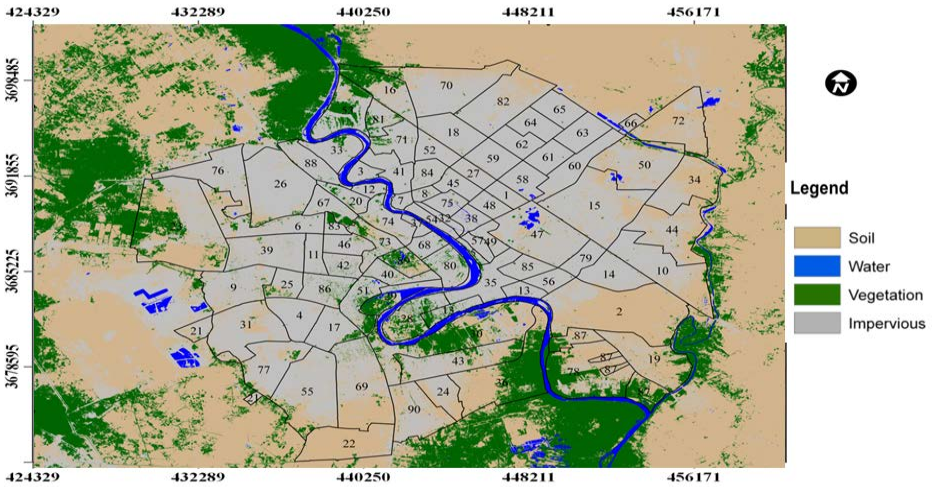

Fig. 2. Supervised classification of LULC with four classes, May 15, 2011.

C. Soil Properties

According to the geological surveys, the whole area is covered by recent sediments of alluvial origin, deposited by repeated floods of Tigris River and by wind action. The characteristics of the soil layers are basically derived from three origins namely, the mountains and foot-hills, the deserts, and the central Mesopotamian plain [6]. The soil stratification in Baghdad area is defined by three major layers, as reported by Hattab and Kachachiin 1986, [7]. The top layer consists of cohesive fill material occasionally containing lenses of gravel, bricks and organic matter underlain by the upper natural subsoil stratum which is basically silty clay or clayey silt with pockets of sand and gravel, followed by silty sand to sandy layer forming the lower natural soil stratum [7].

The general description of Baghdad soil profile is done by Buringh in 1960 as follow [8]:

- 0-20 cm, dark grey-brown, angular blocky porous Silt Loam, hard when dry, friable when moist.
- 20-75 cm, dark brown, sub-angular blocky, porous Silty Clay, hard when dry, very friable when moist.
- 75-135 cm, brown, sub-angular blocky, porous Silty Clay Loam, friable.
- 135-225 cm, dark yellowish-brown Silty Clay, friable and porous.
- 225-285 cm, brown, friable, porous Loam.
- 285-350 cm, dark brown, friable, porous Clay Loam and
- water table at 340 cm.

D. Soil Data

Soil investigations reports for the 23years period 1990-2013 that provided by Mayoralty of Baghdad, Ministry of Construction and Housing (National Center for Construction Labs and Research and State Commission for Buildings) and Ministry of Agriculture (Department of Agro-Ecological Zones) were adopted as a reference for 362 boreholes spread randomly within Baghdad City with different depths of soil layers which ranged between 0 to 3 m generally and between 3 to10 m specifically in some locations.

These reports included soil investigations for various types of structures (e.g., schools, mosques, police stations, water treatment stations, colleges, commercial buildings, hospitals, health centers, etc.). The location of each borehole is determined either from the test reports if available or by searching WEKIMAPIA website for well-known structures with the aid of boreholes plans.

E. Maps

In February 10, 2006, National Geospatial-Intelligence Agency (NGA) [9] produced second edition of digital map for Baghdad City at scale 1:40000, Fig. (3). Mainly usage of this map was to define the boundary of the area of study and secondly considering it as an Administrative Divisions Map (ADM) for districts and neighborhoods digitizing.

Fig. 3. Digital map of Baghdad City, February 10, 2006.

III. HSG CLASSIFICATION MODEL

A. Data Base Construction

The Borehole points are linked to their geographic locations through ArcGIS10 to build a GIS database consisting of the percentages of soil separates which are obtained from the collected tests results of the study area. Fig. (4) shows the distribution of boreholes locations in the study area and the percentages of soil separates within each borehole.

B. Interpolation and Mapping

GIS combined with geo-statistics was applied to analyze the spatial variability in soil properties for all of the study area, where the shape files of soil separates are interpolated using kriging combined with semi-variogram parameters to generate detailed maps of sand, silt and clay which are used in preparing major USDA textural soil model.

C. USDA Textural Soil Model

Based on percentage criteria of the twelve major USDA textural soil classes, digital maps of soil separates were used for applying these criteria as rules within knowledge based classification model to predict the required soil map. All of these processes performed using knowledge engineer tool, Fig. (5), available in ERDAS Imagine 11.2.

D. HSG Model

Taking advantage of the previous rules of the major USDA textural soil model, soils were assigned to HSG according to TR55 of USDA-NRCS criteria, by using knowledge based classification model of ERDAS Imagine 11.2. were used to predict the HSGs map.

E. Evaluation of the HSG Model

Like other traditional classifiers, providing proper testing samples is an important aspect of evaluating HSGs model. Thus, the sample size was selected based on binomial probability theory to provide a statistically sound assessment of accuracy.

Over 144 sample points were generated throughout the thematic map within ERDAS Imagine 11.2 using the stratified random sampling approach to insure good distribution of samples per each class of HSG within the study area.

Since the study concentrates on classifying HSG model at the same rules of classifying major USDA textural soil model, so accessing the accuracy of HSG model is considered sufficient for evaluating both of these models.

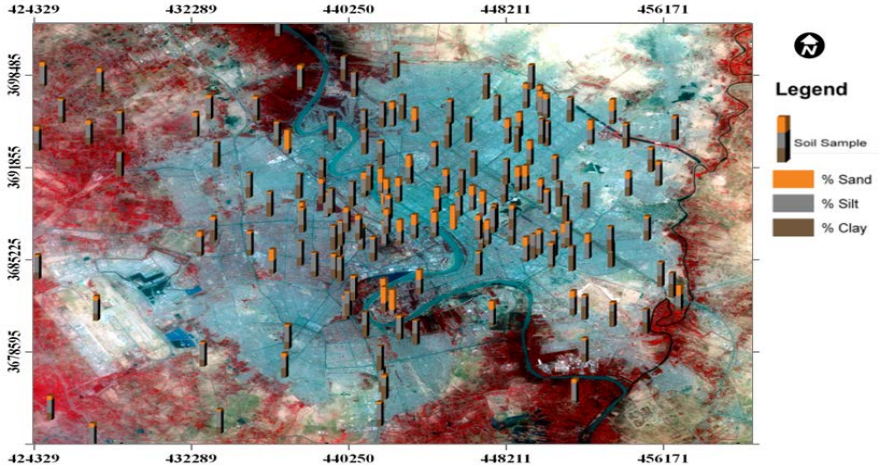

Fig. 4. The percentages of soil separates per boreholes (0 to 10 m depth).

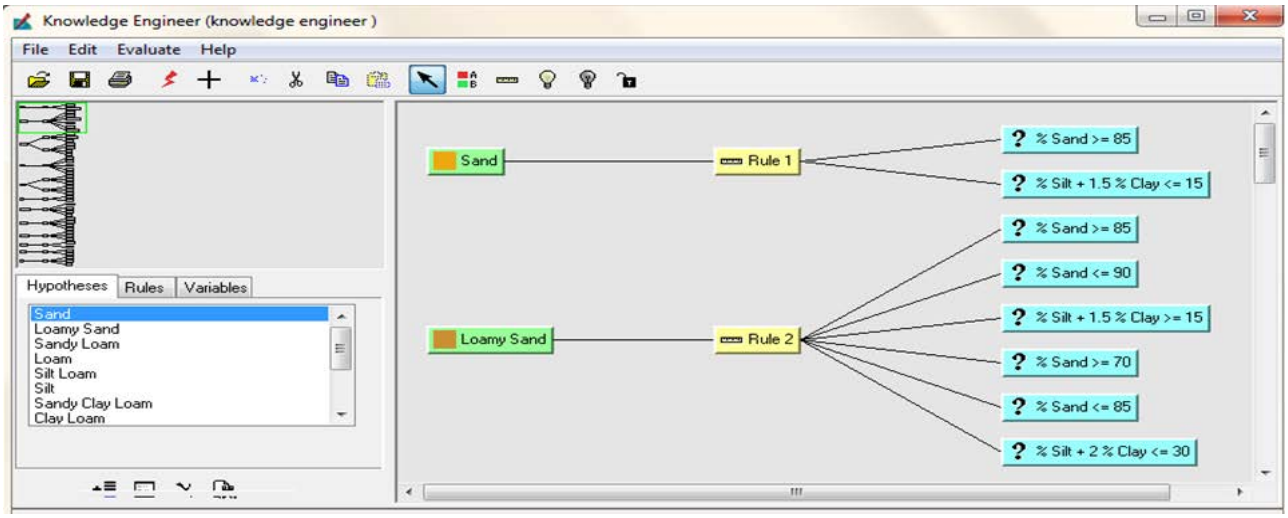

Fig. 5.The knowledge engineer tool in ERDAS Imagine 11.2.

IV. RESULTS ANALYSIS AND DISCUSSIONS

A. Soil Separates

The interpolated maps of sand, silt and clay, Fig.s (6) to (8) that generated using ArcGIS 10 were at the same scale and equal number of classes in order to allow easier comparison. These maps showed gradual spatial variability with significantly different values across the study area.

B. Major USDA Textural Soil

The textural soil map resulted from classifying the soil separates within knowledge engineer tool, based on major USDA textural soil rules, is shown in Fig. (9).

Among twelve classes, seven classes of soil texture appeared within Baghdad City which were: Loam, Silt Loam, Sandy Clay Loam, Clay Loam, Silty Clay Loam, Silty Clay and Clay.

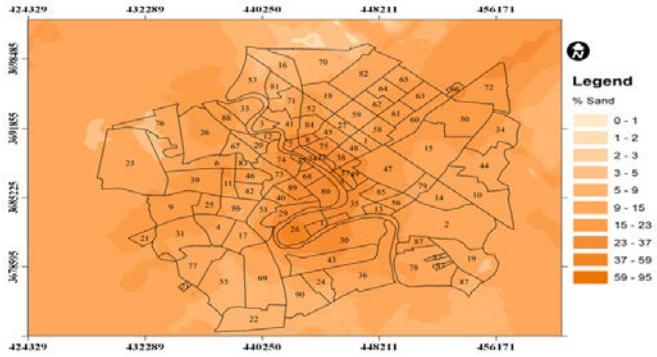

Fig. 6. Soil separates of the study area (Sand).

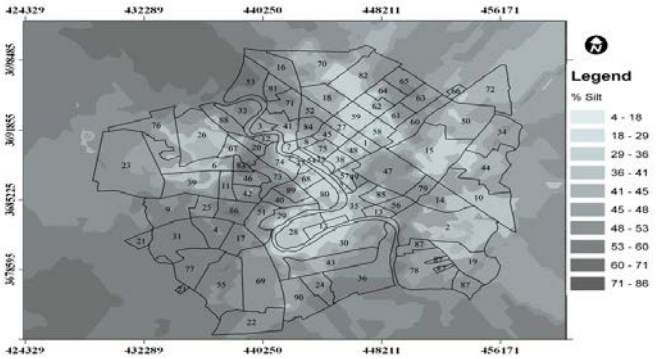

Fig. 7. Soil separates of the study area (Silt).

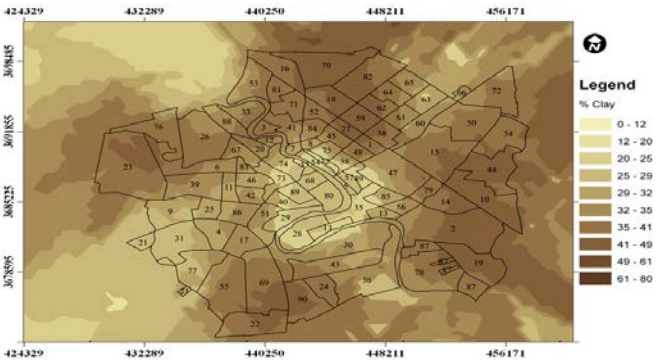

Fig. 8. Soil separates of the study area (Clay).

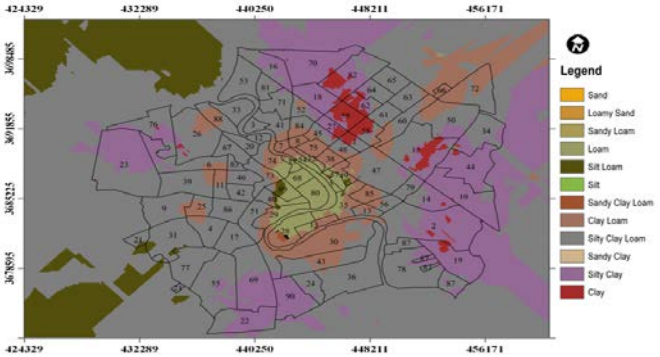

Fig. 9. The major USDA textural soil map with seven classes.

C. HSG Classification

The HSG map resulted from classifying the soil separates according toTR55 of USDA-NRCS criteria within knowledge engineer tool, basing on major USDA textural soil rules, is shown in Fig. (10). This figure shows that most of the study area covered with D class (966.896 km^2) followed by B class (123.977 km^2) and very small part of C class (0.435 km^2).

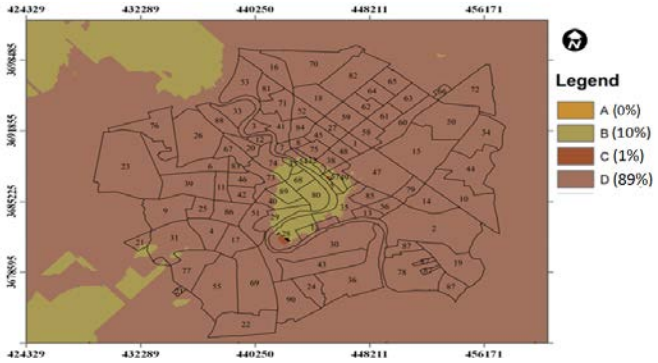

Fig. 10. The HSG map with B, C and D classes.

Analysis HSG within the area of study and for neighborhood areas is performed utilizing the LULC digital maps, Fig. (2), to extract three layers (B, C and D) instead of four layers (soil, water, vegetation and impervious surface). Accordingly, the effectively analysis tool of this model is produced by specifying five model parameters (P1,P2, P3,P4 and P5) as shown in Fig. (11). The results of extracted HSG classes per the area of study are shown in Fig. (12). While, the results of HSG analysis per neighborhoods area is listed in **Table (II)**.

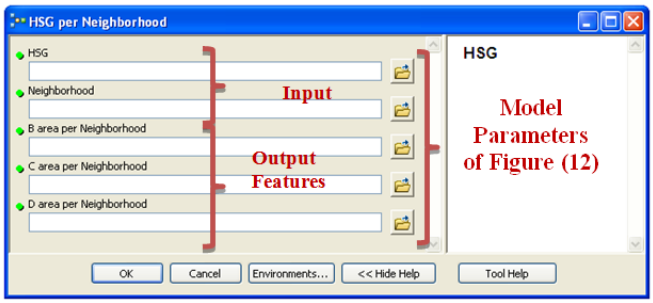

Fig. 11. Converting HSG analysis per neighborhood area model to effective tool through ArcGIS 10.

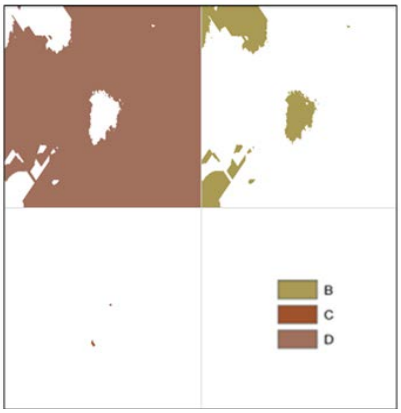

Fig. 12. The extracted three HSG classes of the area of study.

Table (II): Analysis of the HSG areas per ninety neighborhoods of the area of study.

ID	Neighborhood	Area, Km^2	HSG Area,Km^2			ID	Neighborhood	Area, Km^2	HSG Area,Km^2		
			B	C	D				B	C	D
1	14-Jul	1.87	0.00	0.00	1.87	46	Mutanabi	7.84	0.00	0.00	2.86
2	6-Kanun	20.41	0.00	0.00	20.41	47	MuthanaZayuna	11.28	0.10	0.00	11.73
3	Aadhamiya	1.54	0.00	0.00	1.54	48	Neel	2.51	0.00	0.00	2.10
4	Aamel	5.04	0.00	0.00	5.04	49	Nidal	1.20	0.69	0.00	1.12
5	Abu Nuwas	0.75	0.72	0.03	0.00	50	Oubaidy	3.89	0.00	0.00	10.82
6	Adl	7.94	0.00	0.00	7.94	51	Qadisiya	5.47	0.00	0.00	4.42
7	Al Tib	0.94	0.00	0.00	0.94	52	Qahira	15.16	0.00	0.00	2.88
8	Al Ulum	0.99	0.00	0.00	0.99	53	Rabi	6.25	0.00	0.00	6.89
9	Ameriya	7.84	0.00	0.00	7.84	54	Rasheed	4.77	0.99	0.00	0.64
10	Amin	11.28	0.00	0.00	11.28	55	Risalah	5.40	0.00	0.00	13.13
11	Andalus	2.51	0.00	0.00	2.51	56	Riyadh	8.71	0.00	0.00	2.21
12	Atifiya	1.20	0.00	0.00	1.20	57	Saadoun	2.30	1.23	0.06	0.01
13	Babil	3.89	0.86	0.00	3.03	58	Sadr 1	2.13	0.00	0.00	3.53
14	Baghdad Al-	5.47	0.00	0.00	5.47	59	Sadr 2	8.95	0.00	0.00	4.05
15	Baladiat	15.16	0.00	0.00	15.16	60	Sadr 3	22.31	0.00	0.00	5.46
16	Basateen	6.25	0.00	0.00	6.25	61	Sadr 4	3.77	0.00	0.00	3.04
17	Bayaa	4.77	0.00	0.00	4.77	62	Sadr 5	2.91	0.00	0.00	3.14
18	Beida	5.40	0.00	0.00	5.40	63	Sadr 6	12.49	0.00	0.00	3.87
19	Diyala	8.71	0.00	0.00	8.71	64	Sadr 7	2.07	0.00	0.00	3.37
20	Fajr	2.30	0.00	0.00	2.30	65	Sadr 8	5.49	0.00	0.00	3.58
21	Furat	2.13	0.20	0.00	1.92	66	Sadr 9	3.81	0.00	0.00	0.92
22	Ghartan	8.95	0.00	0.00	8.95	67	Salaam	15.76	0.00	0.00	3.37
23	Ghazaliya	22.31	0.00	0.00	22.31	68	Salhiya	9.96	2.12	0.00	0.00
24	Hadar	3.77	0.00	0.00	3.77	69	Saydiyah	1.11	0.00	0.00	13.72
25	Hateen	2.91	0.00	0.00	2.91	70	Sha'ab	3.99	0.00	0.00	12.70
26	Huriya	12.49	0.00	0.00	12.49	71	Shamasiya	8.00	0.00	0.00	4.35
27	Idrissi	2.07	0.00	0.00	2.07	72	ShawraWa Um	5.25	0.00	0.00	9.36
28	Jamiat	5.49	3.29	0.40	1.75	73	Sheik Junaid	13.85	0.31	0.00	3.40
29	Janain	3.81	2.24	0.00	1.57	74	Sheik Marouf	0.90	1.31	0.00	2.82
30	Jazeera	15.76	0.00	0.00	15.76	75	Sheik Umar	2.22	0.00	0.00	2.22
31	Jihad	9.96	0.70	0.00	9.26	76	Shulla	8.59	0.00	0.00	8.59
32	Jumhuriya	1.11	0.52	0.00	0.59	77	Shurta	8.09	0.25	0.00	7.84
33	Kadhimiya	3.99	0.00	0.00	3.99	78	Sindebad	12.08	0.00	0.00	12.08
34	Kamaliya	8.00	0.00	0.00	8.00	79	Sumer Al-	2.47	0.00	0.00	2.47
35	Karada	5.25	2.24	0.00	3.01	80	Tasheer	3.92	3.92	0.00	0.00
36	KarbDejla	13.85	0.00	0.00	13.85	81	Tunis	2.71	0.00	0.00	2.71
37	Karkh	0.90	0.80	0.00	0.10	82	Ur	10.27	0.00	0.00	10.27
38	Keeylani	1.87	0.15	0.00	1.87	83	Washash	1.16	0.00	0.00	1.16
39	Khadra	20.41	0.00	0.00	8.18	84	Waziriya	2.58	0.00	0.00	2.58
40	Kindi	1.54	1.54	0.00	1.37	85	Wehda	2.62	0.00	0.00	2.62
41	Maghrib	5.04	0.00	0.00	3.96	86	Yarmouk	4.43	0.00	0.00	4.43
42	Mansour	0.75	0.00	0.00	2.65	87	Zafaraniya	6.29	0.00	0.00	6.29
43	Masafee	7.94	0.00	0.00	8.79	88	Zahra'	3.90	0.00	0.00	3.90
44	Mashtal	0.94	0.00	0.00	10.16	89	Zawrar	2.70	2.29	0.00	0.41
45	Mustansirya	0.99	0.00	0.00	2.59	90	Zubaida	7.82	0.00	0.00	7.82
							Total	**506.432**	**26.45**	**0.435**	**506.432**

D. Accuracy Assessment of the HSG Classification Model

The results of the accuracy assessment for HSGs model produced from knowledge-based classification is listed in **Table (III)** . This classification produce an overall all accuracy of 97.93 % and Kappa coefficient of 0.916 indicating that HSG map was at high level of accuracy.

Table (III): Accuracy report of the HSG classification.

Class	Reference Totals	Classified Totals	Number Correct	Producer's Accuracy	User's Accuracy	Kappa Coefficient
A	0	0	0	-	-	-
B	18	21	18	100.00 %	85.71 %	0.837
C	1	1	1	100.00 %	100.00 %	0.100
D	126	123	123	97.62 %	100.00 %	0.100
Total	145	145	142	-	-	-
Overall Classification Accuracy = 97.93 %				Overall Kappa Statistics = 0.916		

V. CONCLUSIONS

The results of analysis and evaluation of the HSG classification model shows that the HSG classification model provides an effective means to map the distribution of soil properties across the area of study, at a particular depth based on ground truth in a simple manner at the lowest possible cost and time being based on laboratory tests prepared previously for other purposes, the overall classification accuracy of HSG is 97.93 %.

According to the USDA textural soil classes rules, the soil texture of Baghdad City consisted of seven classes: Loam, Silt Loam, Sandy Clay Loam, Clay Loam, Silty Clay Loam, Silty Clay and Clay. While, there are three types of HSG: B, C and D within Baghdad City which cover about 10% (123.977 km^2), 1% (0.435 km^2), 89% (966.896 km^2) of the study area, respectively. Most of the class B located at the central and upper left and lower left zones of the city. Most of this class extended within un-urbanized area.

The developed ArcGIS tools for each of: HSG analysis per the area of study and per neighborhood area can be effectively used that allow repeatability and consistency of the results per any specified zone within the area of study by removing human error factors while increasing speed and potentially reducing costs by specifying model parameters within the model builder.

REFERENCES

[1] USDA-NRCS, United States Department of Agriculture, Natural Resources Conservation Service, 2003."NRCS National Engineering Handbook", Part 630, Hydrology, Directives (Electronic Directives System), URL: http://directives.sc.egov.usda.gov/viewerFS.aspx?hid=21422 (last date accessed: September, 13 2013).

[2] Saleh, S. A. H., 2011. "Impact of Urban Expansion on Surface Temperature in Baghdad, Iraq, using Remote Sensing and GIS Techniques", Canadian Journal on Environmental, Construction and Civil Engineering.

[3] COS, Central Organization for Statistics, 2011. "Iraq - Household Socio-Economic Survey" 3 Vols, Baghdad-Iraq.

[4] Ahmmed, A. M., 2010. "Digital Map Preparation of Subgrade and Soil Profile Using GIS Techniques", Unpublished M.Sc. Thesis, Department of Highway and Transportation, College of Engineering, Al-Mustansiriya University, Baghdad, Iraq.

[5] Abdullah, N.J., 2013. "Impervious Surface Mapping by Using Satellite Imageries for Baghdad City", Unpublished M.Sc. Thesis, Department of Water Resources Engineering, College of Engineering, University of Baghdad, Baghdad, Iraq.

[6] Ramiah, B.K., and Ovanessian, R.A., 1982. "Engineering Properties of Sub-soils in Baghdad Area", a report by the Building Research Center, Baghdad.

[7] Hattab, T.N., and Kachachi, J., 1986. "A Study of The Engineering Soil Characteristics of Baghdad Area", A Report Prepared by the National Center for Construction Laboratories.

[8] Buringh, P., 1960. "Soils and Conditions in Iraq", Ministry of Agriculture, Baghdad, Iraq.

[9] NGA, National Geospatial-Intelligence Agency, 2006."Baghdad", digital map, 2nd edition, USA, URL: http://www.mapcruzin.com/free-iraq-maps.htm(last date accessed: February 10, 2013).

Evaluation Of Gases Emissions From Automobiles Exhaust In Baghdad City

Ammar A. F. Al-Sultan*

Abstract: **The increase number of non thoughtful imported automobiles to Baghdad city in Iraq especially after year 2003, in view of the poor quality of many of these vehicles because reformatted for service in developed countries and imported by developing countries, including Iraq, as well as others which is a modern-made but characterized by poor technical specifications and commercial licenses because of the low price of production and sale, a lot of importing cities has become a moving graveyard for these automobiles. The emitted gases from the automobiles exhaust are an important source of air pollutants, especially in congested traffic intersections in Baghdad city. Given the lack of quality control of the relevant authorities in the reduction of import these vehicles, especially in the past decade and the lack of activation of environmental legislation in addition to the absence of the green belt in the city, we'll prepare of this analytical study on the evaluation of gaseous pollutants namely (NO_2, %LEL, CO, CO_2, H_2S, SO_2, O_3 and VOCs) resulting from vehicles exhaust to enrich researchers in the future in order to reach the task of engineering solutions and come up with optimal recommendations to service of Baghdad city.**

***Keywords**:* gases emissions, gaseous pollutants, automobiles exhaust, environmental legislation

I. INTRODUCTION

The geographical coordinates of Baghdad city in Iraq are (33° 20' 19" North, 44° 23' 38" East) (Maplandia, 2015), the features of weather Baghdad city are high temperature and lack of rain, especially in the summer (CSO, 2015), This climate is a good environment for the spread of air pollutants resulting from the vehicle exhaust, the figure (6) shows the increasing of temperature degree during the study period. Known as polluted air that any material in the air that can cause harm to humans and the environment. It is possible that these pollutants in the form of solid particles or droplets of liquid or gas. This, in addition to that it may be natural or caused by human activity (EPA, 2000). The sources of air pollution reflect to the sites and activities various factors responsible for the leakage of contaminated material to the atmosphere. These sources can be classified into two types: the first one is human sources (i.e. relating to human activity that including fix sources such as manufactures, electrical power plant and mobiles sources such as vehicles, trains & ships, these activities burn different types of fuel), and the second one is natural sources such as dust, NH_4 gas, eruption activities, CO & smoke (Sher, 1998). The main air pollutants in most urban areas such as carbon monoxide (CO), nitrogen oxides (NO_2) and sulfur oxides (SO_2), hydrocarbons (H-C-H), and particulate matter (PM_x) (both solid and liquid). These pollutants are deployed in all parts of the atmosphere in the world in high concentrations, including enough to cause serious health problems gradually. can occur serious health problems quickly when high concentration of air pollutants, as is the case when the enormous injection of gas emitted sulfur dioxide particulates outstanding volcanic eruption by large (Sher, 1998). Today the major sources of man–made air pollution are motorized street traffic (especially exhaust gases and tire abrasion). The burning of fuels, and larger factory emissions. Depending on the pollutant particles size, they can be carried for distances of several thousand miles (Hasson, F., 2015). Since the breathing of polluted air may have severe health effects such as asthma, or increased cardiovascular risks (Gauderman,W.J., 2007). Thus air pollution has presented one of the major environmental issues and is becoming a very important factor of the quality of life in urban areas, posing a risk both to human health and to the environment (Hoffmann, B., 2007). According to the directive on ambient air quality assessment and management, ozone (O_3) nitric oxide (NO), nitrogen dioxide (NO_2), sulfur dioxide (SO_2), and carbon monoxide (CO) are target species, due to their negative effects on human health and vegetation (Fleming, J., 2005). Ozone a secondary air pollutant has gained extensive attention in the literature due to its harmful effects in vegetation during the growing period. Emission of nitrogen oxides (NO_X = NO + NO_2), volatile organic compounds (VOC_S) and sulfur compounds (including SO_2) can lead to complex series of chemical and physical transformations such as the formation of O_3 in urban and regional areas (NRC, 1991). Meteorological conditions (temperature, relative humidity, wind speed, rainfall and atmospheric pressure) strongly influence the efficiency of photochemical processes leading to the ozone formation and destructions (Vukovich, F., 2003) & (Markovic, D. M., 2005). The understanding of the O_3 behavior near surface layers is essential for a study of pollution oxidation processes in urban areas. Concentration of atmospheric trace

gasses involved in forming O_3 and NO_X change rapidly accompanied by a change of wind speed and wind direction, temperature, humidity and solar radiation. All these factors play crucial role in production and destruction of O_3 (Minoura, H., 1999). Usually NO_2 in the atmosphere comes from two sources, either directly from emission sources (primary pollutant) or from chemical reactions in the atmosphere (Han, X., 2006). Proxy radicals are produced mostly by the reactions of hydroxyl radical (OH) with reactive hydrocarbons and CO and photolysis of aldehydes which have both natural and anthropogenic origins (Hassone. F., 2015). Nitrogen dioxide is then photolysis in the atmosphere, and the released atomic oxygen combines with molecule O_2 to form O_3 (Aneja, P. V.,1996). High concentrations of CO generally occur in areas with heavy traffic and congestions. The point sources of CO emission also include industrial processes. Non transportation fuel combustion (Han, X., 2006). The present of sulphur dioxide in air is related to the fuel combustion and industrial processes. Primary pollutant (CO, SO_2) concentrations are usually higher in cold months (winter) than in hot months. Where the concentrations of the secondary pollutants (NO_2 and O_3) are higher in summer than in winter months (Barrero, M. A., 2006). Overall all these pollutant concentrated in crowed street where the United Nation estimated that over 600 million people worldwide in urban areas are exposed to dangerous levels of traffic generated air pollutants (Caciola, R. R., 2002). In present work analyzes the temporal variation of measurements CO, CO_2, SO_2, NO_2, H_2S, O_3, VOCs, concentrations were performed for the periode from January 2015 to June 2015 and the results are present in this paper to find simple evaluate the state of ambient air in urban area of Baghdad city – Iraq.

The mainly objectives for this study are in the following:

1. Measurement of the air pollutions components SO_2, NO_2, CO, CO_2, H_2S, VOCs and O_3.
2. Evaluation and compression of these pollutants with global standards.

II. METHODOLOGY AND SAMPLING

In this study, three traffic intersections has been selected, two in Al-Resafa sector (Al-Nidaa intersection and Al-Arasat intersection) and anther one in Al-Karkh sector (Adan Cycle intersection) as shown in figures (1), (2) & (3) respectively. The reason for choosing these sites that it's characterized by high traffic volume and small or gasoline fuel vehicles and large or diesel fuel vehicles. The research for the purpose of study within a wide range of pollutants it has been the used of device (GIG-6 gases) and (GIG-2 gases) that shown in the figure (4), the first device used to measurement the pollutants (NO_2, %LEL[1], CO, CO_2, H_2S and SO_2 - Worldwide manufacturer of gas detection solutions GFG instrumentation) and the second one used for (O_3, VOCs) measurement. The sampling has been measured at the peck time of the traffic volume in between of (1:00 to 2:00 after noon), because the peak time represents the worst case in the diffusion of gaseous pollutants as results of high traffic volume and highest value for the daily temperature. As the temperature of the main factors affecting the heterogeneity inspected the air pollutants, the study was conducted for a period of 6 months of continued from January 2015 to June 2015.

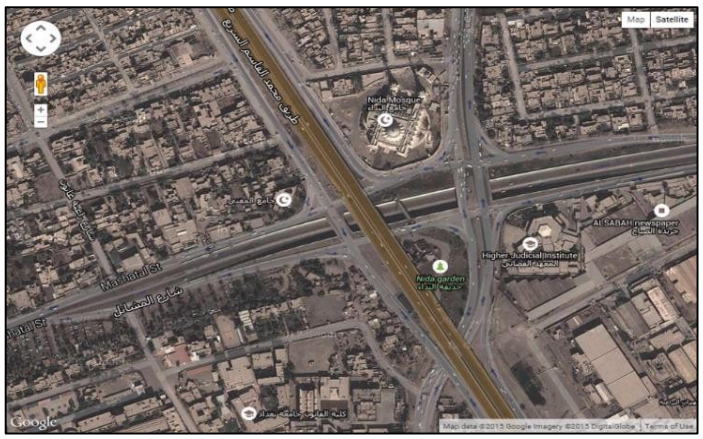

Fig (1): Al-Nidaa traffic Intersection

Fig (2): Al-Arassat traffic intersection

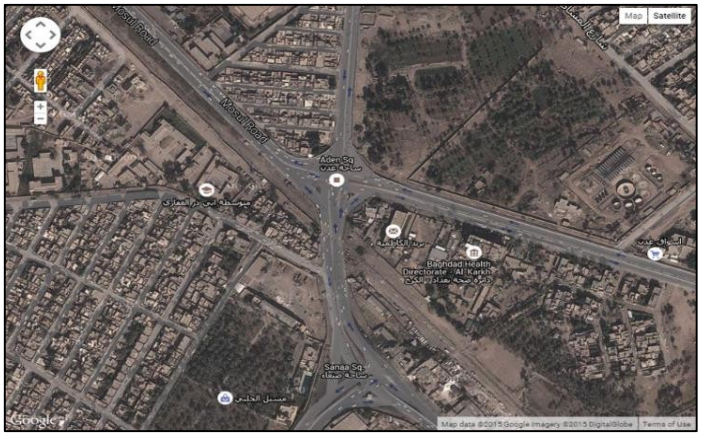

Fig (3): Adan cycle intersection

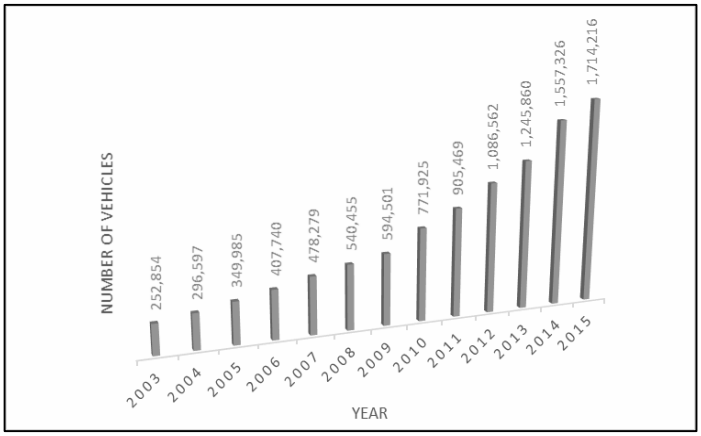

Fig (5): The increasing of number of automobiles in Baghdad city at the last twelve years

Fig (4): GIG-6 gases and GIG-2 gases Worldwide manufacturer of gas detection solutions GFG instrumentation

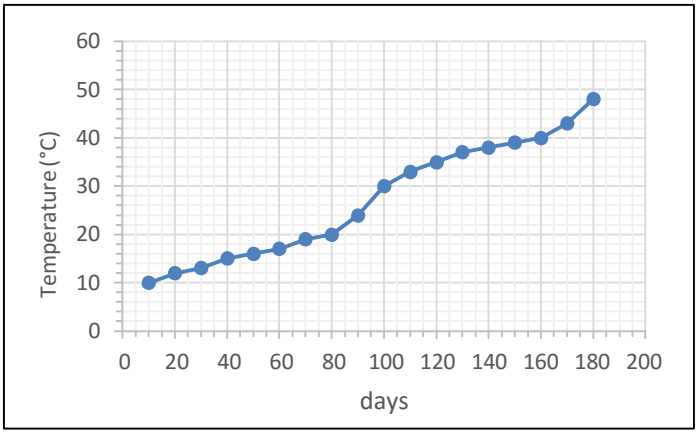

Fig (6): The increasing of temperature (ºC) during the period of research

In the year 2003 the number of vehicles in the whole of Iraq was equal to 665,404 and in the city of Baghdad was 252,854, this number was increased arrived in the city of Baghdad to 1,714,216 vehicles with an average annual increase is equal to 17.3%, and the proportion of the number of vehicles in the city of Baghdad is 38.2% of the total vehicles entering to the whole of Iraq (General Director of Traffic in Iraq, 2015), please see figure (5). This research has been studying within a wide range of temperatures degree. We note increase in temperature to reach a temperature of 48°C in June, 2015 (Yahoo weather), where is the temperature of the important factors in controlling the volatility speed and diffusion of the gaseous pollutants in air (Lawrence K. Wang, etal, 2005), kindly see the figure (6).

III. LITERATURE REVIEW

The researcher Timothy V. Johnson in 2006 presented a research paper, this paper deals with of summarizes the key developments in diesel emission control, generally for 2005. Regulatory targets for the next 10 years and projected advancements in engine technology are used to estimate future emission control needs. Recent NO_x control developments on selective catalytic reduction (SCR), lean NO_x traps LNT and lean NO_x catalysts (LNC) are then summarized. Likewise, the paper covers important recent developments on diesel particulate filters (DPFs), summarizing regeneration strategies, new filter and catalyst materials, ash management, and PM measurement. Recent developments in diesel oxidation catalysts are also briefly summarized. Finally, the paper discusses examples of how it is all pulled together to meet the tightest future regulations (Johnson, 2006). In 2012 the researchers Allaa M. Aenab, S. K. Singh and et al studied a statistical approach to stationary air monitoring stations to air quality assessment in Baghdad city, Samples were collected from

two stations in Baghdad city for 2 years (2012 & 2013). The study assesses levels and variations of Ozone (O_3), carbon Dioxide (CO_2) and the Temperature, using stationary environmental monitoring stations in Baghdad, Iraq. Analysis of variance (ANOVA) Two way confirmed significant variations in monthly observations. They founded that The Ozone (O_3) was with the limits of WHO and Iraqi standards and the student t-test shows in Al-Andulis air quality monitoring station and Al-Allawi air quality monitoring station no significant differences. Also Ozone shows in ANOVA two-way test (space and time) in 2012, except for the months of January, February, March, July, October and November all the other months show consistent values. All the results are consistent with respect to time. In 2013 shows, except for the months of February, April and May all the other months show consistent values. All the results are consistent with respect to time. The carbon Dioxide CO_2 was out of the limits of WHO and Iraqi standards and the student t-test shows in Al-Andulis air quality monitoring station significant differences and Al-Allawi air quality monitoring station no significant differences. In ANOVA two-way test in 2012 shows except for the months of September and October and all the other months show consistent values. All the results are consistent with respect to time. In 2013 shows, except September all the other months show consistent values. The results are inconsistent with respect to time.

The researcher Shukri I. Al-Hassen and et. al in 2013 deals with an experimental study on the determination of air pollutant concentrations released from selected outdoor gaseous emission sources in basra city, southern raq Air pollutant concentrations were measured by using the portable detection instrument Drager CMS. The measured air pollutants were CO, CO_2, NO_2, NO_x, SO_2, HCs, and H_2S. The selected emission sources divided into a variety of stationary and mobile sources. The obtained results indicated that mean concentrations for CO, CO_2, NO_2, NO_x, SO_2, HCs, and H_2S were ≥ 150, 2426, ≤ 0.5, 12.6, 0.7, 42.0, and ≤ 0.2 ppm, respectively. Most of these concentrations exceeded the maximum permissible limits for National Emission Standards in Iraq. As well, some of the recorded emission concentrations at this experimental study are higher than those that at other studies which dealt with ambient air pollution, because effect of diffusion and dispersion on the ambient air pollutants. The recorded values of gaseous pollutants in this study can be used as the background level for the next studies. The researcher conclude the most of the concentrations measured in the experimental study exceeded the maximum permissible limits for National Emission Standards. As well, some of the recorded emission concentrations at this experimental study are higher than those that at other studies which dealt with ambient air pollution, because effect of diffusion and dispersion on the ambient air pollutants. The recorded values of gaseous pollutants in this study can be used as the background level for the next studies.

Janice J. Kim, et. al, was prepared the study in 2004 about Traffic-related Air Pollution near Busy Roads, they are conducted a school-based, cross-sectional study in the San Francisco Bay Area in 2001. Information on current bronchitis symptoms and asthma, home environment, and demographics was obtained by parental questionnaire (n = 1,109). Concentrations of traffic pollutants (particulate matter, black carbon, total nitrogen oxides [NO_x], and nitrogen dioxide [NO_2]) were measured at 10 school sites during several seasons. Although pollutant concentrations were relatively low, we observed differences in concentrations between schools nearby versus those more distant (or upwind) from major roads. Using a two-stage multiple logistic regression model, we found associations between respiratory symptoms and traffic-related pollutants. Among those living at their current residence for at least 1 year, the adjusted odds ratio for asthma in relationship to an interquartile difference in NO_x was 1.07 (95% confidence interval, 1.00–1.14). Thus, they found spatial variability in traffic pollutants and associated differences in respiratory symptoms in a region with good air quality. The researcher findings support the hypothesis that traffic-related pollution is associated with respiratory symptoms in children. According to researchers knowledge, this is the first epidemiologic study in the United States to evaluate relationships between measured traffic-related pollutants and respiratory symptoms. For children residing at their current address for at least 1 year, they found modest but significant increases in the odds of bronchitis symptoms and physician-diagnosed asthma in neighborhoods with higher concentrations of traffic pollutants. They found increased association with asthma (but not bronchitis) with exposure to traffic air pollutants for girls who had lived at their current addresses at least 1 year compared with boys . Several investigators have also reported greater traffic associated effect estimates for girls versus boys. Previous air pollution studies examining the sex-specific effects of air pollution on lung function and lung function growth have been mixed. The reasons for the observations in this study are unclear and deserve attention in future studies.

IV. Results And Discussion

The components air pollutions components SO_2, NO_2, CO, CO_2, H_2S, VOCs and (O_3 indirectly) are considerd one of the outputs of the combustion gasoline and diesel fuel which emmesion from automobiles exhaust (Austin J., 2002).

4.1. Volatile Organic Components (VOCs): The term Volatile Organic Compounds (VOCs) considered one of the outputs of the combustion of vehicles fuel and it is used to describe organic material in the vapor phase excluding methane, there are many non-combustion sources of VOC emission of which the most important is the use of solvents, including those released from paints. Evaporative losses of gasoline during storage and distribution are also significant (Nagendra S. , 2002). The figure (7) noting the average seasonal variation of VOCs in the traffic intersection, obviously a significant increase in the concentrations of VOCs as result of increasing the temperature degree, the increase in temperatures is directly proportional to the speed of the resulting volatility organic compounds and the presence of high concentrations of VOCs for vehicles in his intersection traffic areas of negative impact on the health of the human being is the cause of the generation of ground-level ozone that affecting the lungs especially below the ages of 15 years (Sher, 1998), but the wind speed as resulting from the movement of vehicles cause the dispersing concentrations of VOCs and thus are within permitted by the border of EPA (EPA, 2000).

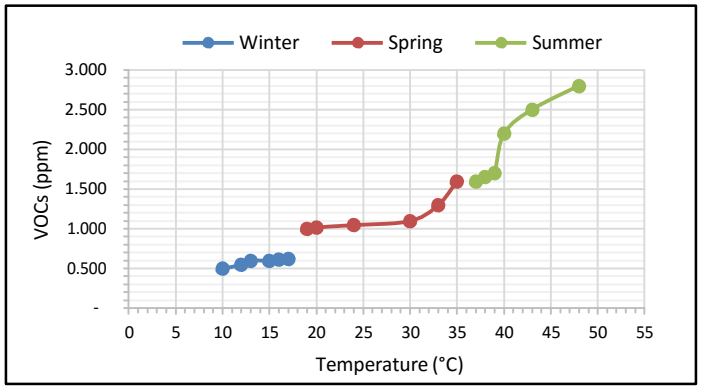

Fig (7): Seasonal variation of VOCs concentration

4.2. Nitrogen Dioxide (NO_2) and Sulfate Dioxide (SO_2): The figures (8) and (9) explain the relationship of the seasonal variation of NO_2 and SO_2 concentrations respectively, Nitrogen oxides (NOx) and sulfur oxides (SOx) emissions including of NO_2 and SO_2 are primary contributors to acid rain, which is associated with a number of effects including acidification of lakes and streams, accelerated corrosion of buildings, and visibility impairment. Among the various nitrogen oxides emitted from stationary combustion, nitrogen oxide (NO), nitrous oxide (N_2O) and nitrogen dioxide (NO_2) and nitrogen dioxide (NO_2) are stable, and NO predominates. In health effects, NO_2 can irritate the lungs and lower resistance to respiratory infection (Wang L. K., et.al, 2005). The range of NO_2 emission was (0.200 – 0.272) ppm, this result larger than the standard value set by the WHO which is (1- hour mean 200 $\mu g/m^3$ = 0.134 ppm) (WHO, 2005). The emission of SO_2 was in between of range values (0.008 – 0.651) ppm, the minimum value in the winter season was less than the standard emission value (10 minutes mean, 500 $\mu g/m^3$ = 0.335 ppm) (WHO, 2005), but the maximum concentration in the summer season was larger than the standard emission value. These values refer to the increasing the harmful effect of SO_2 with increasing the temperature degree. The values of NO_2 & SO_2 give us a clear indication of the relative increasing of high pollution at selected traffic intersections which directly affect the human respiratory tract (WHO, 2005).

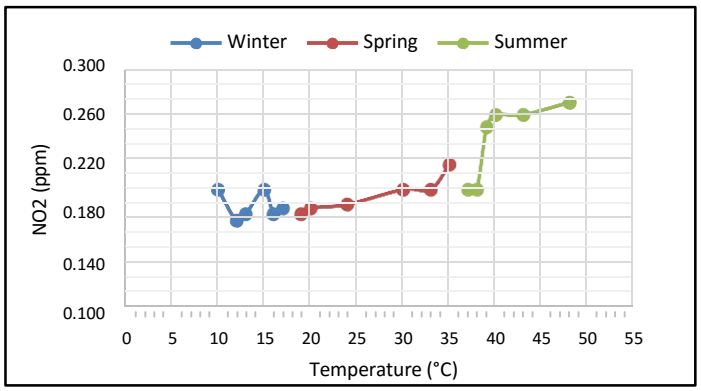

Fig (8): Seasonal variation of NO_2 concentration

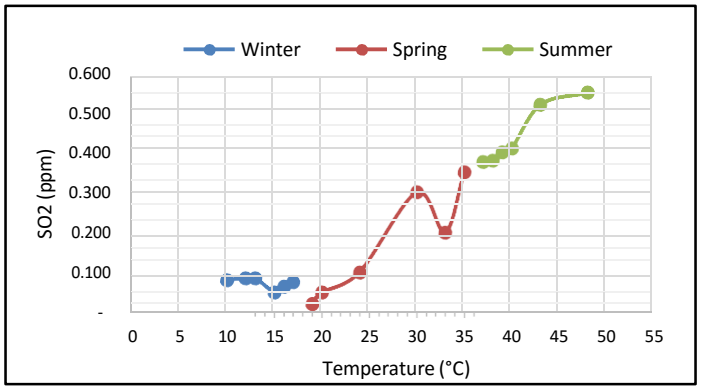

Fig (9): Seasonal variation of SO_2 concentration

4.3. Hydrogen Sulfide (H_2S): Hydrogen sulfide (H_2S) is a colorless gas, soluble in various liquids including water and alcohol (WHO, 2000). H_2S occurs around sulfur springs and lakes, and is an air contaminant in geothermal active areas, saline marshes can also produce sulfide (Steudler, P.A. 1985). The figure (10) shows the seasonal variation of H_2S during the period of study, the gas emission values was in between (0.0005 – 0.005 ppm) which is less than the standard concentration of emission (0.001ppm) (WHO, 2000). At concentrations of 15 mg/m^3 (10.05 ppm) and above, hydrogen sulfide causes conjunctival irritation, because sulfide and hydrogen sulfide anions are strong bases (Savolainen, H., 1982) & (WHO, 2000).

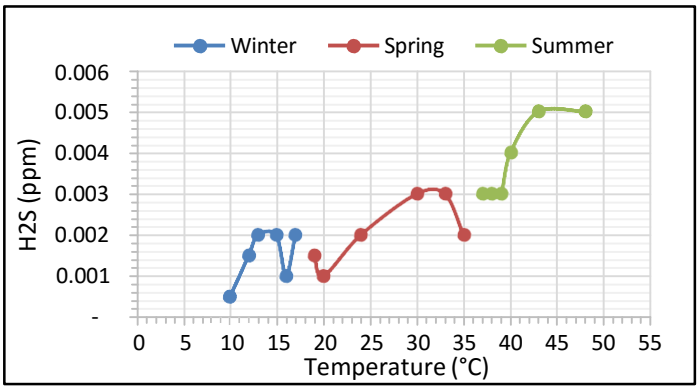

Fig (10): Seasonal variation of H_2S concentration

4.4. Carbon Monoxide (CO) and Carbon Dioxide (CO_2): CO is a colorless gas odorless and does not cause any irritation of the object that breathes but the poisonous gas, automobile exhaust is one of the main sources to be CO (EPA, 2000) & (WHO, 2005). The figure (11) describe the seasonal variation of CO concentration, there is a clear increase in the CO concentration when increasing temperature, the range of values from winter, spring and summer days was (9.95 – 30.20 ppm) which is in the allow value (maximum daily 1-hour mean = 52.238 mg/m^3 or 35 ppm), but these values are larger than the standard limits which is (maximum daily 8-hour mean = 9.00 ppm) (EPA, 2000). The CO_2 gas is an important gas plant, one of the components of the atmosphere (WHO, 2005), the figure (12) shows the seasonal variation of CO_2 concentrations during the period of study which was between of (0.398 – 0.610 ppm).

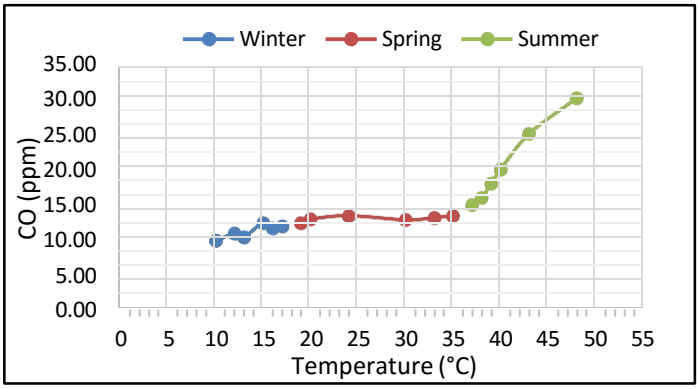

Fig (11): Seasonal variation of CO concentration

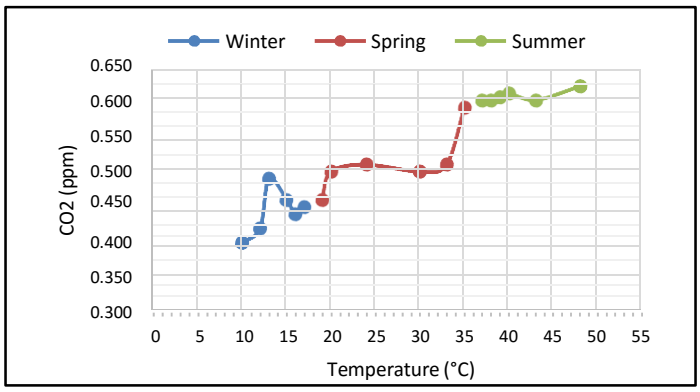

Fig (12): Seasonal variation of CO_2 concentration

4.5. Ozone (O_3): Ozone is a secondary pollutant formed through photochemical reactions and can have a harmful effect on human health causing respiratory problems, it's result from reaction between NOx and VOCs (EPA, 2000). O_3 is a one of the basic components of the troposphere in the atmosphere (as it also represents one of the basic components of certain areas in the stratosphere and is generally known as the ozone layer these areas), The chemical reactions associated with this optical gas control many of the chemical processes that occur in the atmosphere day and night (WHO, 2005). When O_3 concentrations unusually rises through human activities which contribute to burning fossil fuels, a large proportion of them, it becomes one of air pollutants as it represents one of the components of smog (Perera E. M., 2011). The figure (13) explain the seasonal variation for the O_3 during 180 days, we show the concentrations during the winter and spring months (0.000 – 0.0028 ppm) which was less than the standard level (112 mg/m^3 or 0.075 ppm) according to the (EPA, 2000) and the O_3 concentration in the summer specially at the end of May was equal to (0.008 – 0.01 ppm), these values larger than the standard level (112 mg/m^3 or 0.075 ppm) that wrote by (EPA, 2000). The reason for the high ozone concentrations at the beginning of the summer due to high temperatures and that work on breaking down the bonds of VOCs and with a

NOx it's lead to made of ground-level ozone (Perera E. M., 2011).

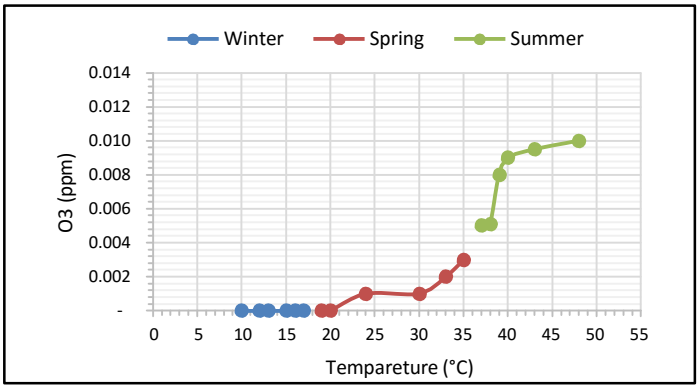

Fig (13): Seasonal variation of O_3 concentration

V. CONCLUSIONS

1. The increase of temperature as result of seasonal variation lead to increasing of air pollutants (VOCs, NO_2, SO_2, H_2S, CO, CO_2, and O_3).
2. The emission of NO_2 was larger than the WHO standard value.
3. The emission of SO_2 in the summer days was larger than the WHO standard value.
4. H_2S emission was less than the WHO standard value.
5. The emission of CO was in the allow limited values by WHO.
6. The emission of O_3 than in the summer days was larger than the WHO standard value

REFERENCES

[1] Web site of http://www.maplandia.com/, 2015.

[2] Ministry of Planning, Central Statistical Organization (CSO), 2015.

[3] Environmental Protection Agency (EPA), *National Ambient Air Quality Standards (NAAQS) 2000.*

[4] Wang, L. K., et. al.: *Advanced Air and Noise Pollution Control, Volume 2, Handbook of Environmental Engineering. In: INC., H. P. (ed.), 2005.*

[5] Austin, J. B., Sturges, W. P.: *Air Pollution Science for the 21st Century In: LTD., E. S. (ed.). Amsterdam - Boston - London - New York - Oxford, 2002.*

[6] Hasson, A. F.: Assessment of air pollution elements concentrations in Baghdad city from periods (May-December) 2010 *International Journal Of Energy And Environment 6, 10, 2015.*

[7] *Johnson, T. V.:* Diesel Emission Control in Review. SAE *International Organization Journal, Detroit, Michigan, USA, 18, 2006.*

[8] Nagendra, *S.: Line Source Emission Modelling, 2002.*

[9] Sher, E.: *Handbook of Air Pollution from Internal Combustion Engines Pollutant Formation and Control.* Boston, San Diego, New York, 1998.

[10] Gauderman, W. J., et. al.: Effect of exposure to traffic on lung development from 10 to 18 years of Age: *A-Cohort Study*, 369 (9561): 571-577, lancet 2007.

[11] Hoffmann, B., et. al.: Residential exposure to traffic is associated with coronary *Atherosclerosis, 116 (5) : 489-496, circulation, 2007.*

[12] Fleming, J., Stern R. & Yamartino, R. J.: A new air quality regime classification scheme for O3, NO2 , SO2 and PM10 Observations Site, *Atmospheric Environment, 39, 2005.*

[13] National Research Council, us Rethinking the ozone problem in urban and regional air pollution, Washington DC. *National Academy Press*. 1991.

[14] Vukovich, F. M. & Sherewell, *J.:* An examination of the relationship between certain Meteorological parameters and surface ozone variations in the Baltimore–Washington corridor, *Atmospheric Environment*, 37,971-981, 2003.

[15] Markovic, D. M. & Markovic, A. M.: The relationship between some meteorological parameters and the tropospheric concentrations of ozone in the urban area of Belgrade. *Journal of the Serbian chemical society, 70, 1478-1495, 2005.*

[16] Minoura, H., Some Characteristics of surface ozone concentrations observed in an urban atmosphere, *Atmospheric Research, 51, 153-169, 1999.*

[17] Han, X. & Naeher, P. L., A review of traffic-related air pollution exposure assessment studies in the developing world, *Environment International, 32, 106-120, 2006.*

[18] Aneja, P. V., Kim, D. S. & Chameides, *W. L., Trends and analysis of ambient NO, NOX, CO, and*

ozone concentrations in Raleigh, North Carolina, Chemosphere, 34, 611-623, 1996.

[19] Barrero, M, A., Grimalt, J., O., & Canton, L. *Prediction of daily ozone concentrations and maxima in urban atmosphere, chemo metrics and intelligent laboratory systems, 80, 67-76, 2006.*

[20] Caciola, R. R., Sarva, M., & Pasola, *R.* Adverse respiratory effects and allergic susceptibility in relation to particulate air pollution : *flirting with disasters. Allergy, 657-281, 2002.*

[21] General Director of Traffic in Iraq, http://www.itp.gov.iq, 2015.

[22] Johnson, T. V.: Diesel Emission Control in Review. SAE *International Organization Journal, Detroit, Michigan, USA, 18, 2006.*

[23] Web site of https://weather.yahoo.com/iraq/baghdad, 2015. [24] Lawrence K. W.: *Advanced Air and Noise Pollution Control, Volume 2, Handbook of Environmental Engineering. In: INC., H. P. (ed.), 2005.*

[25] Nagendra S. & el. al,: *An Introduction to Pollution Science, 2006.*

[26] Austin J., P. B. P., Sturges W.: *Air Pollution Science for the 21st Century In: LTD.,* E. S. (ed.). Amsterdam - Boston - London - New York – Oxford, 2002.

[27] Would Health Organization (WHO), Air quality guidelines, 2005.

[28] Would Health Organization (WHO), Regional Office for Europe, Copenhagen, Denmark, 2000. [29] Steudler, P.A. & Peterson, B.J.: Contribution of gaseous sulphur from salt marshes to the global sulphur cycle. *Nature, 311: 455-457 (1984).*

[30] Perera, E. M., & et. al.: Rising Temperatures, Worsening Ozone Pollution. *Union of Concerned Scientists. National Headquarters, Cambridge, 2011.*

Note:

Convert values:

[1 $\mu g/m^3 = 1x10^{-3}$ $mg/m^3 = 0.67$ ppm]*

***WHO, Regional Office for Europe, Copenhagen, Denmark, 2000.**

[1] LEL%: Low Exclusive Limited, it's express to the lowest level for combustion for the Volatile Gases, that's may by selected sing (↑↑) to express to the possibility of fire or (↓↓).

This paper has been written in Baghdad – IRAQ, 2015.

Effect of Wastewater on Concrete Tanks in Wastewater Plants

Dr. Mohammed Ali I. Al-Hashimi, Sameh Badry Tobeia, Ayat Hussein Mahdi,and Hadel A. Ibrahim

Abstract— **Sulfates found in wastewater have a great effect on concrete properties in wastewater plants, concrete compressive strength adversely affected by sewage aggressive environment due to the sulfate attack. In order to investigate this action several concrete cubs has been made and cured with ordinary water as well as sewage water taken from different stages of Al-Rustamiyah wastewater plant (grit removal tank, primary sedimentation tank and secondary sedimentation tank). Cubes made in four groups, all samples cured by using ordinary water for 28-days followed by another 28-days curing with sewage water except the reference group.**

Concrete compressive strength test shows a significant descending with concrete compressive strength of 20.1 MPa and 21.2 MPa for cubs curd with sewage water taken from grit removal and primary sedimentation tank respectively(descending ratio 25.6% and 21.5% respectively), in comparing with 27.0 MPa concrete compressive strength of reference group .

Keywords: **Wastewater Plants, Salt effect, Sulfate, Concrete compressive strength.**

I. INTRODUCTION

Concrete is a construction material, consist of a mix almost homogenous. This mix contains solid particles with different sizes called aggregate bonding with hardening cement paste. Concrete also contain gaps fill with air [(1)]. The durability of concrete is one of its most important properties due to its essential that concrete should be capable of withstanding the conditions for which it has been designed throughout the life of structure. Lack of durability can be caused by external agents arising from the environment or by internal agents within the concrete this action can be depend on the salts (sulfates, chloride and others) ability to dissolve in water and their concentrations. Other factors like in (pH) and temperature affect the sulfate attack and its results on concrete, especially for concrete structures exposed to sewage like treatment tanks and sewage transpose pipes. Usually sulfates and chloride found in solid case and has no effect on concrete but in presence of water these salts begin to dissolve and attack the cement paste in concrete [(2,3&4)].

Dr. Mohammed Ali I. Al-Hashimi,Building and Construction Engineering Department, University of Technology /Baghdad. And Head of Building and Construction Engineering Department, Dijlah University College. e-mail:mohashimi2003@yahoo.com.
Sameh Badry Tobeia, Building and Construction Engineering Department, University of Technology /Baghdad.
Ayat Hussein Mahdi, Building and Construction Engineering Department, University of Technology /Baghdad.
Hadel A. Ibrahim Building and Construction Engineer.

II. AIM OF WORK

This work aimed to experimentally investigate the effects of salts (sulfate, chloride, and some other salts) present in wastewater on the concrete compressive strength of Wastewater Plants Concrete Tanks. In order to reach this goal several concrete cubes has been made, cured and tested for compressive strength.

III. SULFATE EFFECT ON CONCRETE

Sulfate effect on concrete occurred as internal or external attacks. Internal attack occurred due to internal agents as sulfates present in concrete materials (cement, aggregate and water), in this case the reaction occurs fast and quick and concrete strength adversely affected even at three days age. Where sulfate found in sand is more dangerous on concrete than those found in gravel due to the fineness of the practical[(1)]
On the other hand external attack started when concrete exposed to sewage or soil or groundwater, and the mechanism of sulfate attack is similar to the internal attack but its effect take longer time to be obvious. In this type of attacks sulfate concentration still approximately constant due to the continuous compensate. The two major factors affected sulfate attack intensity are: sulfate concentration in solution and the movement of solution, the adversely effects are obvious with the increase of these factors [(1)].
Also, Chlorides, particularly calcium chloride and (to a lesser extent) sodium chloride have been shown to leach calcium hydroxide and cause chemical changes in concrete, leading to loss of strength, as well as attacking the steel reinforcement [(1)].

IV. TREATMENT TANKS CONCRETE IN WASTEWATER PLANTS

Generally, the durability of concrete structures decreases due to several chemical and physical factors. Concrete in wastewater plants exposed to a combination of chemical and physical factors leading to rapid concrete deterioration represented by lack in strength, disintegration, cracks and reinforcing steel corrosion. Since concrete in wastewater plants exposed to sulfate from its environment (external attack), therefore the durability and permeability of concrete have significant effect on deterioration and lake in concrete properties. Municipal wastewaters contain different types of materials like: fats, oil, detergents, organic matters, human excreta, food wastes, industrial wastes and different

types of material which cause concrete deterioration like sulfates, chlorides, nitrogen and phosphate. Variations in pH and biological reactions in wastewater also effect on concrete strength [2&4].

V. Mechanism of Sulfate Attack

Sulfate in sewage, groundwater or soil usually found in form of calcium sulfate (gypsum), magnesium sulfate and sodium sulfate which they react with calcium hydroxide $Ca(OH)_2$ and tricalcium aluminate to produce gypsum and calcium sulfoalminate respectively. Calcium sulfate attack only the calcium aluminate and produce calcium sulfoalminate, while magnesium sulfate attack calcium silicate in addition to calcium aluminate and calcium hydroxide as in Eq.1. These reactions accompanied by volumetric increase causing disintegration of concrete.

$MgSO_4.7H_2O+3CaO.2SiO2.aq. \rightarrow CaSO_4.2H_2O+Mg(OH)_2+SiO_2.aq.$ ------- (1)

Magnesium sulfate has more damaging effect than other sulfates because it leads to the decomposition of the hydrated calcium silicate as well as of calcium hydroxide and calcium aluminate. The sulfate attack becomes more aggressive as their concentration increase as well as concrete permeability [1].

VI. Wastewater Treatment Stages

Wastewaters must be treated from different types and sizes of particles, fats removal (skimming) before disposal to the rivers. Wastewater treatment plants usually consist of screens, comminutor, grit removal, grease removal, flotation, primary sedimentation tank, secondary sedimentation tank [5,6&7].

In this work wastewater used for curing concrete cubes taken from three different stages from Al-Rustamiyah wastewater treatment plant as follows:

1) Grit Removal Tank: this tank is the first part of wastewater treatment plant used for separation of large particles with different densities [5,6&7].

2) Primary Sedimentation Tank: used to separate suspended organic matter, chemicals and may be used to enhance removal of colloids and small particles and to precipitate phosphor [5,6&7].

3) Secondary Sedimentation Tank: used to remove small particles that did not removed in the first stage [5,6&7].

VII. Experimental Work

In order to simulate the effects of sulfate and other compositions (chlorides, magnesium and calcium) usually found in wastewater, concrete cubes has been made and cured in ordinary water as well as sewage. The materials properties used in this work included materials used in concrete in addition to the sewage as follows:

1) Ordinary Portland cement used to made concrete cubes with initial and final setting time of 112 minute and 210 minute respectively, cement compressive strength 24.1 MPa at one week and slump value of 10 mm. Where these result satisfy the requirements of Iraqi Standard Specification 1984[8].

2) Wastewaters experiments have been used to measure wastewater parameters taken from Al-Rustamiyah wastewater treatment plant like: (sulfate, chloride, and magnesium). Table (1), represents experiments results for different wastewater stages.

Table (1): Wastewater parameters used for concrete cubes curing

Sewage tank type	Sulfates mg/L	Chlorides mg/L	Magnesium mg/L	Calcium mg/L	Hardness mg/L	Turbidity (NTU)	pH
Grit chamber tank	570	494.84	146.74	701.4	100	171	7.91
Primary sedimentation tank	303.66	414.87	114.4	621.24	152	91.1	7.95
Secondary sedimentation tank	266.66	364.88	63.47	280.56	20.4	80	8.52

Sulfates, Chlorides and other parameters relationship illustrated in Fig. (1), all parameters decreased gradually except hardness which increased in the primary sedimentation tank this may be occurred due to the sediments that are agitated by influent wastewater velocity.

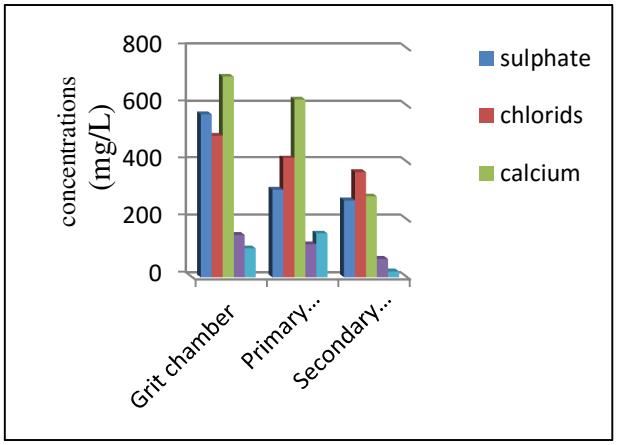

Fig. (1) Concentrations in wastewater treatment plant units

In this work 12 concrete cube with 150 mm has been made, concrete mix ratio 1:1.5:3. These cubes divided to four groups according to the water and wastewater type used in curing process as follows:

A) First group (group A): concrete cubes cured with ordinary water for 28 days.
B) Second group (group B): divided into two stages, first stage curing with ordinary water for 28 days, second stage partial immersing for the same cubes with wastewater from grit chamber tank for another 28 days in order to simulate the same conditions which the concrete exposed like high concentration of sulfates, and chlorides.
C) Third group (group C): Also consists of two stages, first stage full immersing with ordinary water for 28 days, and in the second stage the cubes partial immersing with wastewater taken from primary sedimentation tank for 28 days.
D) Fourth group (group D): first stage is curing with ordinary water for 28 days and second stage is partial immersing for the concrete cubes with wastewaters taken from secondary wastewater tank for another 28 days.

VIII. CONCRETE COMPRESSIVE STRENGTH TEST RESULTS

In structural design concrete usually assumed to resist compressive strength only, therefore Concrete compressive strength considered the basic criteria to determine the concrete type, durability for concrete structures. Also tensile strength and flexural strength can be measured as a percentage of compressive strength. Therefore, in this work 12 concrete cubes tested for compressive strength by using hydraulic test machine (ELE International ADR 3000) as appear in Fig.(2)

Fig.(2) Compressive strength test machine

All concrete cubes has been tested for compressive strength, group A tested at 28 day other groups tested after curing of 56 day divided in to two stages at first curing with ordinary water for 28 day followed by another 28 day with partial immersing in sewage taken from different tanks of wastewater treatment plant. Fig.(3) through Fig.(6) show the concrete cubes during test procedure and test results can be summarized as in table (2).

Fig.(3) Group A concrete cubes

Fig.(4) Group B concrete cubes

Fig.(5) Group C concrete cube during the test

Fig.(6) Group D concrete cube during the test

Table (2): Concrete compressive strength test results

No.	Group	Concrete cube name	Concrete compressive strength MPa	Concrete compressive strength average for each group MPa,	Concrete compressive strength descending ratio corresponding to group A
1	A	RC1	27.3	27.0	-
2		RC2	26.3		
3		RC3	27.2		
4	B	S1-1	20.4	20.1	25.6 %
5		S1-2	20.6		
6		S1-3	19.4		
7	C	S2-1	22.1	21.2	21.5 %
8		S2-2	20.6		
9		S2-3	21.0		
10	D	S3-1	28.9	27.1	≈ 0 %
11		S3-2	26.1		
12		S3-3	26.4		

The relationship of concrete compressive strength versus sulfate and chlorides concentration illustrated in Fig.(7) and Fig.(8), as well as Fig.(9) show the effect of the increased in magnesium concentration.

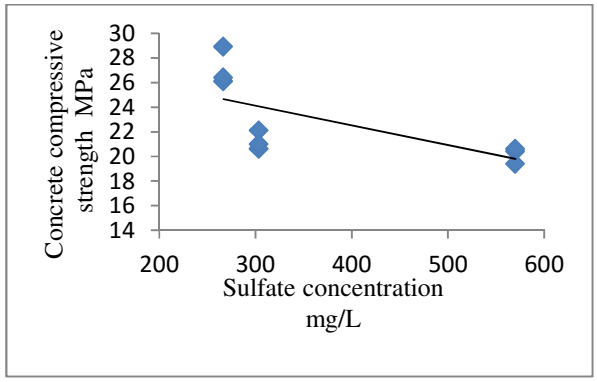

Fig.(7) Concrete compressive strength VS. sulfate concentration

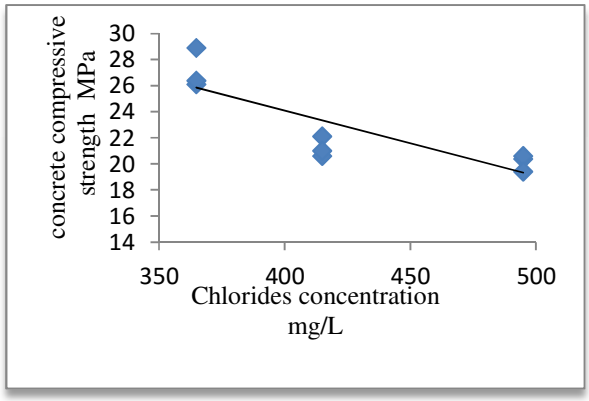

Fig.(8) Concrete compressive strength VS. Chlorides concentration

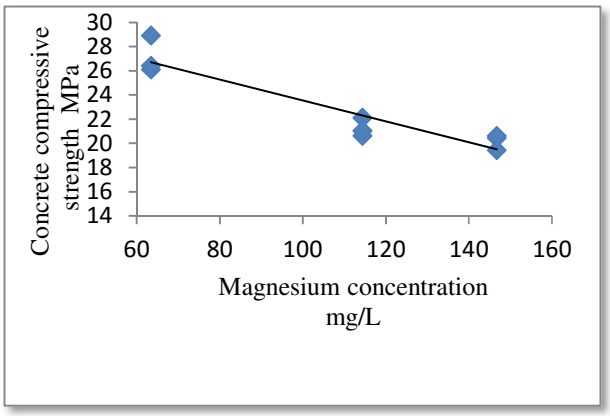

Fig.(9) Concrete compressive strength VS. magnesium concentration

IX. RESULTS AND DISCUSSION

In this work, four groups of concrete cubes have been made the first group (group A) cured in ordinary water for 28-days. The other three groups (group B, group C and group D) cured in two stages, the first curing stage done by using ordinary water only for 28-days. The second stage done by using sewage water taken from Grit Removal tank, Primary Sedimentation tank and Secondary Sedimentation tank from Al-Rustamiyah wastewater plant in order to simulate concrete behavior in wastewater plant concrete tanks. Curing in wastewater done by partial immersing of the concrete cubes for 28-days because the worst salts attack occur due to the repeated cycles of wet/dry concrete which cause sulfate, chloride and other salts deposition inside concrete pores after water evaporation continuously and leading to disintegration of concrete. The concrete compressive strength test shows that group (A) (cured only with ordinary water) gave the highest compressive strength with average of 27 MPa this value decreased to 20.1 MPa and 21.2 MPa with compressive strength descending ratio of 25.6% and 21.5% for group (B) (cured with ordinary water and sewage from Grit Removal tank) and group (C) (cured with ordinary water and sewage from Primary Sedimentation tank) respectively. The significant reduction in concrete compressive strength occurred for group (B) because this part of wastewater plant does not remove salts or acids therefore, chemical added usually used to reduce the organic materials. On the other hand group (D) cubes (cured with ordinary water and sewage from Secondary Sedimentation tank) gave high concrete compressive strength because most concentrations of sulfate, chloride and other salts have been reduced before this stage.

X. CONCLUSIONS

From the results of experimental work the following facts can be concludes:

1. Concrete grit removal tanks highly affected by the presence of sulfate, chloride and other salts in high concentrations which reduce compressive strength of tank concrete structure, in compare with other steps of wastewater plants.
2. The concrete of Grit Removal and Primary Sedimentation tanks deterioration in similar manner due to high concentrations of salts.
3. Secondary Sedimentation concrete tanks in wastewater treatment plants are less affected by the presence of sulfate, chloride and other salts due to the reduction in their concentrations in the first stage of treatment.

XI. REFERENCES

1-A. M. Neville and J. J. Brooks, "Concrete Technology", Second Edition, Prentice Hall, 2010.

2- WEI Chao-hai., WANG Wen-xiang, DENG Zhi-y iand WU Chao-fei, "Characteristics of high-sulfate wastewater treatment by two-phase anaerobic digestion process with Jet-loop anaerobic fluidized bed", Journal of Environmental Sciences,No.3, V.19,2007 , pp. 264–270.

3- A. K. Parande , P. L. Ramsamy, S. Ethirajan , C. R. K. Rao and N. Palanisamy, “Deterioration of reinforced concrete in sewer Environments”, Institution of Civil Engineers, March 2006 Issue ME, pp. 11–20.

4- Coatings manual, "Basic on corrosion in wastewater collection and treatment system ",2011,pp. 25, Internet.

5-E.W.Steel, "Water Supply and Sewerage ", McGraw-Hill, fifth Edition, 1979.

6- Howard S. Peavy, Donald R. Rowe & George Tchobanoglous, ”Environmental Engineering”, McGraw-Hill, First Edition, 1985.

7- Syed R. Qasim, "Wastewater Treatment Plants: Planning, Design, and Operation", College Publishing, International Edition, 1986.

8- Iraqi standards (No.5)-1984, central organization for standardization and quality control (COSQC) ,Baghdad 1984.

Pollution Status Analysis of Diyala River, Baghdad, Iraq

A. Abbas Al-Samawi[1] and S. Nasser Hassan Al-Hussaini[2]

Abstract— The last part of the reach of the River Diyala just before its confluence with the river Tigris south of the capital city Baghdad is taken as a case- study. It is about 15 km in length .Its aquatic physicochemical characteristics is investigated and its pollution status is assessed in this study.

This segment of Diyala River is exposed to multiple points of treated and raw municipal waste water discharges. These are represented by the outfalls and bypass of three wastewater treatment plants of Al-Rustimiyah. These discharges are overloading Diyala River's self – purification capacity.

Diyala River's aquatic parameters as represented by DO, BOD, COD, pH, and others were monitored and measured at nine stations along the river reach for a period of one year to assess seasonal variations.

The reaeration coefficient, K_2, was calculated from field data of DO concentration along the river reach. It ranged from ($0.35\ d^{-1}$) to ($1.1\ d^{-1}$) having its lowest value during the cold season while the highest occurred during the warm dry weather season.

The deoxygenation constant, K_1, was computed by monitoring the BOD of samples taken along the river segment. K_1 ranged from a minimum value of ($0.16\ d^{-1}$) , which occurred during the cold weather months while a maximum value ($0.63\ d^{-1}$) occurred during the warm dry weather months. Based on the maximum value of K_1, the river may be classified within the untreated wastewater category during the warm dry weather seasons, while its average values (K_1) for the other months of the year categorize the river to be between the polluted river and the treated wastewater.

The self-purification factor, or Fair's factor, (*f*) for the river Diyala was determined. It classifies the river as a sluggish during the summer.

The research results have shown that the natural self - purification process of the river water body is rather slow or absent due to the heavy pollution loads. It is concluded that full recovery of the river from pollution is only possible via human intervention.

The need for an urgent makeover of the water body characteristics of the river Diyala via mechanically assisted methods is necessary to restore its original usages and ensure public health safety.

Keywords Deoxygenation, Diyala River, Reoxygenation, Self-purification

Manuscript received March 20, 2015.

1. Adnan Abbas Ali Al- Samawi: Alumni Professor Emeritus of Environmental Engineering, University of Technology, Baghdad, Iraq.

2. Safaa Nasser Hassan Al-Hussaini: Lecturer at the Department of Environmental Engineering, College of Engineering, University of AL-Mustansiriyah, Baghdad, Iraq, PhD student at the Department of Building and Construction Engineering, College of Engineering, University of Technology, Baghdad, Iraq.
(Corresponding author: e-mail: eng.safa74@yahoo.com, Mobile Number: 07709278690).

I. Introduction

Water pollution is one of the major problems facing manhood nowadays. Surface water, being the first source of water, should be protected against pollution since water is the most important resource in the world and no life is kept without it.

Nature fortunately provides a mechanism for counteracting the effects of deoxygenation by reoxygenation, a means were by oxygen as well as other gaseous components of air is renewed in flowing stream water [1].

Wastes are most often discharged into the receiving water bodies with little or no regard to their assimilative capacities [2]. To protect the aquatic life of any receiving water body it is essential to determine its capacity to accommodate wastes.

Many parameters can be used to trace pollution in rivers, the dissolved oxygen (DO) and the biological oxygen demand (BOD) being the most useful ones, can be used in monitoring the self purification of the receiving river. The BOD defines the amount of oxygen required by bacteria to stabilize decomposable matter; therefore BOD measures the capacity of oxygen absorption of an effluent.

DO on the other hand, measures the amount of dissolved or free oxygen present in water; therefore, it represents the capacity of the water to assimilate the pollution load.

The deoxygenation coefficient (K_1) and the reoxygenation coefficient (K_2) of a river can both be calculated depending on BOD and DO measurements respectively. Both K_1 and K_2 are used to determine the self purification factor of a river.

The present study is concerned in making an assessment of the pollution status of Diyala River, Baghdad, Iraq.

II. Materials and Methods

A. The study area

Diyala River is one of the tributaries of Tigris River. In the past, it contributed in about 11% of River Tigris's total water income. Unfortunately, know it is considered an effluent receiving water body.

The current study is carried out on the last part of Diyala River just before its confluence with the Tigris River in about 15 km. It is located within the capital city of Baghdad, Iraq.
This segment of the River Diyala is exposed to multiple points of treated and raw municipal waste water discharges. These are represented by the outfalls and bypass of three wastewater treatment plants (WWTP) of Al-Rustimiyah. The WWTP's mentioned above are over loaded with influent that exceeds their operational capacities which in turn, affects the aquatic life of the receiving river represented by the River Diyala.
Fig. 1 illustrates the zone of the study area and the location of the WWTP's in the vicinity as well. Several studies have been done to identify different types of pollution loads in the River Diyala [3]-[5].

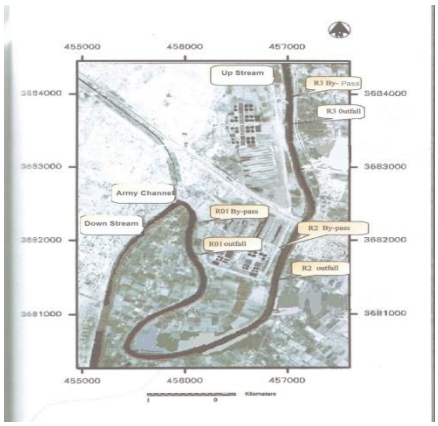

Fig. 1: The study area and the locations of the WWTP's along the reach.

B. *Field Sampling*

Nine stations were taken along the reach of the river with interest, the first station is located upstream of all three WWTP's while the further stations are located after each point of pollution submitted to the river, in an adequate distance to insure the mixing of pollutant with the river water. The final and ninth station is located downstream the last point of pollution were no other point inters the river till it pours into the River Tigris. **Fig. 2** shows the locations of the stations and their profile in kilometers along the river reach.
The field sampling was carried out during a whole year starting from April 2014 till March 2015 in order to cover all seasonal variation that may occur in the region.

A polyethylene bottle was used to collect the samples of TSS and TDS, while BOD glass bottles were used for the samples of BOD and COD. All bottles were rinsed with deionized water before usage. During sampling, the bottles were rinsed with the river water at points of collecting samples three times before taking any sample. Afterwards, all samples were preserved at a temperature of 4˚C and transferred to laboratory.

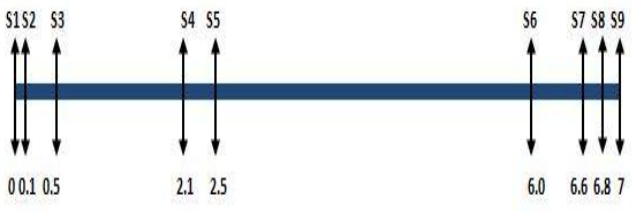

Fig. 2: Stations location and sampling profile in kilometers along Diyala River in Baghdad.

C. *Field and laboratory analysis*

The measurements were classified into two categories; Field and in lab measurements. The field measurements were represented by DO, pH, EC, and Temperature. On the other hand, the in lab measurements were TDS, TSS, BOD and COD.
Devices such as DO meter and pH meter were taken each trip to measure DO, pH, EC and Temperature onsite, duo to the wild variation in their values if they were to be measured in lab.
The in lab measurements were conducted following the standard analysis methods (APHA 1999) [6]. The results obtained were evaluated by using standard statistical methods.
Owens, Edward and Gibbs model [7] and Churchill Nomagraph [8] were used to predict the reaeration coefficient, K_2, based on the similarity in the determinants ranges and conditions with the case of study.

III. THEORETICAL CONCEPT

A. *Deoxygenation Coefficient, K_1*

The deoxygenation coefficient of a river, K_1, depends on the water condition and the characteristics of the waste induced to it. The most affecting character is the value of BOD and temperature. **Equation "(1)"** is usually used to determine the value of K_1 as shown below.

$$BOD_t = BOD_u (1-e^{-K1t}) \quad \text{.....(1)}$$

Where, BOD_t is the amount of carbonaceous BOD at any time (t) in mg/l, BOD_u is the ultimate carbonaceous BOD in mg/l, K_1 is the first order reaction rate constant in $days^{-1}$ [9].
The effect of temperature is introduced in **"(2)"** below.

$$K_{1_T} = K_{1_{20}} \theta^{T-20} \quad \text{.....(2)}$$

Where, K_{1_T} is the reaction rate at any temperature (T) in d^{-1}, $K_{1_{20}}$ is the reaction rate at 20ºC, and θ is the temperature activity coefficient varying from 1.056 in the temperature range between 20 and 30 ºC to 1.135 in the temperature range between 4 and 20 ºC [9].

Typical deoxygenation constants for different types of rivers are given in literature [10].

B. *Reoxygenation Coefficient, K_2*

The re-aeration or reoxygenation coefficient of a river, K_2, depends on the characteristics of the river itself such as steam velocity, depth and temperature.
Several models have been proposed by different researchers to determine K_2 each having its own limitations [7],[8],[11],[12], [13], and [14].
Two models were chosen, based on similarity in sampling conditions and limitations, to determine and compare K_2 values for the reach of interest.
The first model is Owens at el 1964 [7] which gave the closest limitations to the case study taken in this research, were the stream velocity variation in this model ranged from 0.1 to 5.0 ft/sec. and depths from 0.4 to11.0 feet. The model is represented by **"(3)"** below.

$$K_2(20\ ^oC) = 9.4\ V^{0.67}\ h^{-1.85} \quad \text{.....(3)}$$

Where, V is the mean stream velocity in ft/sec, h is the mean depth in feet, and K_2 is the reoxygenation coefficient in days^{-1}.
Churchill at el 1962 [8] on the other hand developed 19 equations and decided that the most useful one is given by **"(4)"** below.

$$K_2(20\ ^oC) = 5.026\ \frac{V^{0.969}}{R^{1.673}} \quad \text{.....(4)}$$

Where, V is the mean stream velocity in fps, and R is the mean stream depth in feel.
The minimum value of K_2 is given in **"(5)"** [10].

$$K_2(20\ ^oC) = 0.6/H \quad \text{.....(5)}$$

Where, H represents the mean stream depth in meters.
As in K_1, K_2 also is affected by the variation in water temperature and **"(2)"** can be used to determine the value of K_2 at different temperatures (T).

C. *Self-Purification factor, f*

Self-purification factor, and so known as Fair ratio, *f*, is defined by the ratio between K_2 and K_1 [15]. Dean Fair 1939 gave different values of *f* relating to the nature of receiving water body and by that classifying the type of the river duo to its' *f* factor. For example; sluggish streams has a value of *f* ranged between 1 to 2 at 20 ºC while large streams of normal velocities has the range of 2 to 3 at 20 ºC. Fair has found that there is a decrease in the value of *f* of about 3% for each one degree rise in temperature [15].

IV. Results and Discussion

The field results of DO in mg/l for a whole year along the river reach is illustrated in **Fig. 3**. As shown from **Fig. 3**, the DO trend has nearly the same pattern during different months of sampling with a variety in its value, for that reason one can replace this figure by **Fig. 4,** which represents the average value of DO during a year along the river reach.

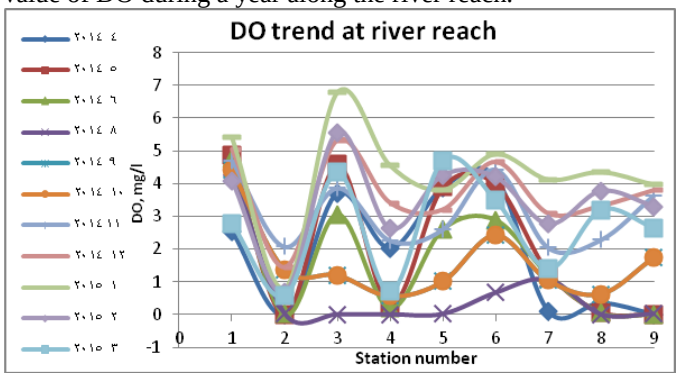

Fig. 3: Dissolved Oxygen (DO) trend for a whole year along the river reach in mg/l.

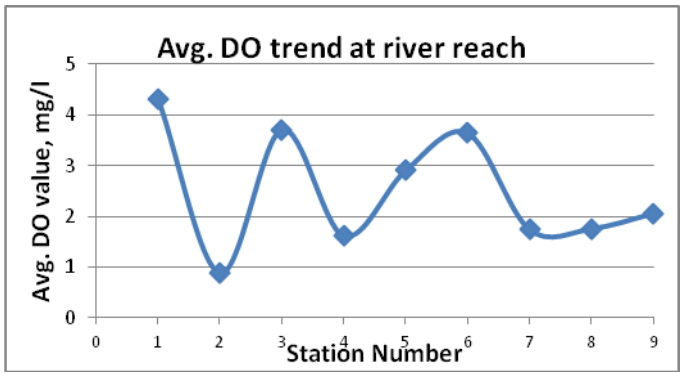

Fig. 4: Average DO values for a year along the river reach in mg/l.

Fig. 5 depicts the relation between the average values of COD, BOD_5 and TSS with the segment of the river to be studied. The average value of each test, for each station, was taken for the results of the whole period of study in order to simplify the display.

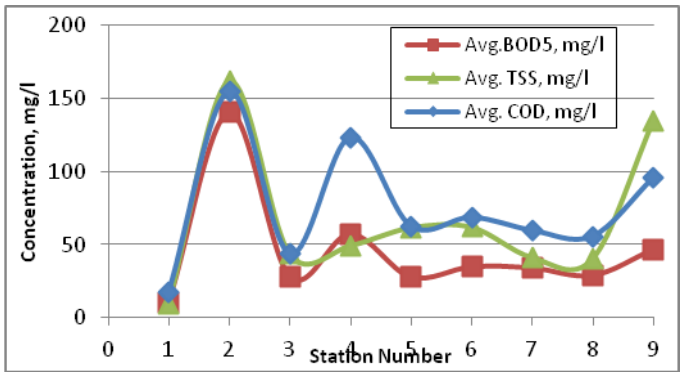

Fig. 5: Trend of COD, BOD_5, and TSS along the river reach.

From **Fig. 5** it can be concluded that the pollutants are at their highest values at station 2, which lies downstream the bypass of R3, afterwards the concentrations vary along the river reach depending on the location of stations taken. The converse can be said on **Fig. 4** were the DO value is at its highest at station1

before any pollutions from the WWTP's fall into the river, while the lowest concentration of DO is at station 2 which has the highest concentration of pollutants.

The concentration of TDS in mg/l along the segment of the river is illustrated in **Fig. 6.** This figure shows the maximum concentration of TDS to occur at station 1. This can be explained precisely duo to the existence of several drains upstream the river such as Al- khalis North and south outfall drains, Al-Nahrawan outfall drain and others, which contributes with high concentrations of dissolved solids.

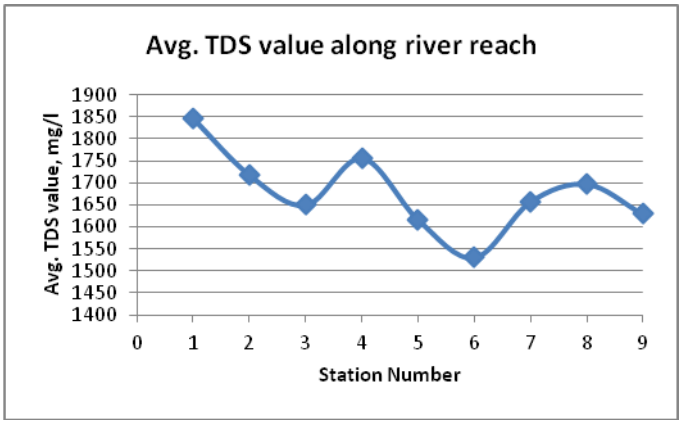

Fig. 6: Average TDS values for a year along the river reach in mg/l.

Table (1), at the end of this research, gives a description of the selected parameters studied in this paper and their statistical analysis.

The calculations of K_2 constant in both modals selected gave convergent results with a minimum value of 0.35 d^{-1} during the cold weather season, and a maximum value of 1.1 d^{-1} during the worm weather season. This is expected duo to the reliance of both models on the depth and velocity of water body in calculating the value of K_2. The average value of K_2, for each month, was considered in the comparison above. The results were compared with the minimum allowable value of K_2 given by Chin [10] and all were found to be within the criteria.

The values of K_1 were also calculated, and a minimum value was found to be 0.16 d^{-1} during the cold weather season and a maximum value of 0.63 d^{-1} during the worm weather season, which classifies the river into the polluted river class during the winter and an untreated wastewater class during the summer depending on the typical deoxygenation constant classifications given by Chin [10].

Both K_2 and K_1 constants were adjusted to the water temperature measured at the time of sampling by using **"(2)".**

The self purification constant for the river was found to have a minimum value of 1.7 during the worm season which classifies the river into a sluggish stream during the summer, depending on Fair classifications [15], and a maximum value of 2.19 during the cold weather, which classifies the river into large streams of low to normal velocities during the winter [15], this is duo to the presence of excessive rainfalls during the cold season which would increase the dilution capacity of the river. The relation between the self purification factor and the period of study was depicted in **Fig. 7.**

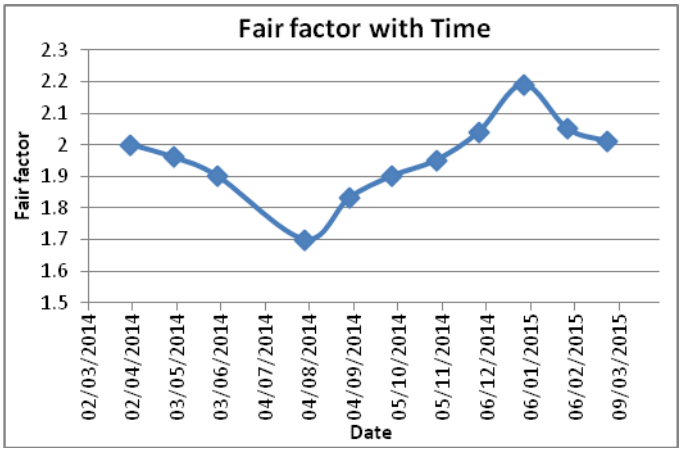

Fig. 7: Fair factor, f, annual pattern for Diyala River.

The value of f for each point in **Fig. 7** represents the average of nine stations for the time of sampling. As for the relation between f and the sampling stations along the river reach, it was found to have the same trend with a difference in its value with time. **Fig. 8** gives an example for such a relation. From this figure, it can be seen that f value is at its highest value at station 2, this is duo to having the lowest depth at this station beneath all which will give the highest value of K_2 and the same for f.

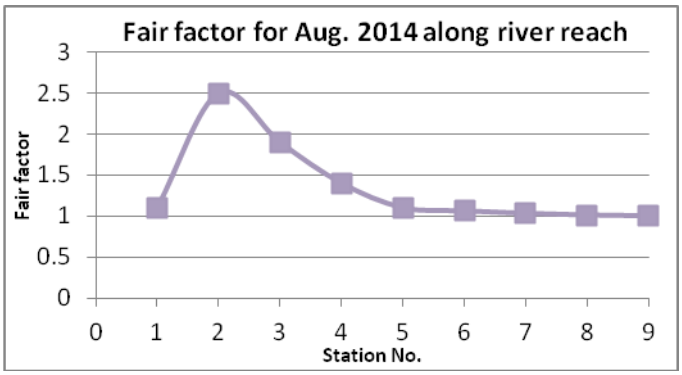

Fig. 8: Fair factor, f, trend along the river reach for August, 2014.

V. CONCLUSIONS

The self-purification of Diyala River at its last reach opposite Al-Rustimiyah WWTP's was found to be rather slow or absent due to the heavy pollution loads applied on it. Hence, the river may be classified as sluggish during the summer. However, the river was classified as a large stream with low to normal velocities during the winter.

The deoxygenation coefficient categorizes the river water into untreated wastewater class during the summer and as a polluted river class during the winter season. Both indicators prove that the condition of the river being at its worst during the summer.

Diyala River is no longer used as a river, not for fishing, swimming, irrigation, and other usages.

It was found that the applied pollution loads are beyond the river's assimilative capacity, and a full natural recovery of the river is never an option.

An urgent need for human intervention using mechanically assisted methods is necessary to restore the original clean environment and the usages of the river.

ACKNOWLEDGMENT

The authors are so grateful to the management of The Environmental Research Center, University of Technology in Baghdad, Iraq for all the help given by them to conduct this research.

Table (1): Statistical analysis of the parameters studied in this paper.

Parameter	Unit	Min	Max	Mean	Standard Deviation	Variance	Range	Standard Error
pH	—	6.9	9.5	7.6	0.34	0.11	2.6	0.034
EC	mS/cm	2.14	3.12	2.48	0.17	0.03	0.98	0.02
Temp.	˚C	11.8	34.1	22.2	2.24	5.03	22.3	0.23
DO	mg/l	0.01	6.78	2.51	1.76	3.1	6.77	0.18
COD	mg/l	7.2	520	75.67	71.97	5180	512.4	7.23
BOD5	mg/l	2	253	45.47	50.6	2560	251	5.09
TSS	mg/l	3	390	67.08	74.34	5525.8	387	7.47
TDS	mg/l	1380	2158	1678.4	137.8	18981.8	778	13.85

REFERENCES

[1] N. L. Nemerow, "Scientific Stream Pollution Analysis" Scripta Book Company, Washington, D.C., 1974.

[2] E. O. Longe, and D.O. Omole, " Analysis of Pollution Status of River Illo, Ota, Nigeria" Environmentalist 11/2008; 28(4):451-457. Springer Science + Business Media, LLC 2008.

[3] H. M. Faris "Effect of Rustimiyah Treatment Plants Effluents on Diyala river Sanitation" M.Sc. Thesis, University of Baghdad, Iraq, 1985.

[4] H. A. Riyad, and F. J. Ghufran, "The Evaluation of Heavy Metals Pollution in Agricultural Lands in Jisser Diyala District" Iraqi Journal of Market Research And Consumer Protection, University of Baghdad ,Iraq,vol.2, no.3, 2010.

[5] M. J. Maha, "Environmental Auditing of Rustimiyah Wastewater Treatment plant Effluents Based on the World Bank Requirements using Remote Sensing Technology" Ph.D. Dissertation, University of Technology, Iraq, 2010.

[6] American Public Health Association (APHA), Standard methods for the examination of water and wastewater, 20th edition, 1999.

[7] M. Owens, R. W. Edward, and J. W. Gibbs " Some Reaeration Studies in Streams" Int. J. Air Water poll., 8:90)469, 1964.

[8] M. A. Churchill, H. L. Elmore, and R. A. Buckingham, " The Prediction of Stream Reaeration Rates" J. San. Eng. Div. (ASCE), SA4, July 1962, paper 3199.

[9] T. George, L. B. Franklin, and H. S. David, "Wastewater Engineering Treatment and Reuse" Metcalf and Eddy Inc. Fourth Edition, 2004.

[10] D. A. Chin, "Water Quality Engineering in Natural Systems" John Wiley and sons, Inc., 2006.

[11] H. Streeter, " The Rate of Atmospheric Reaeration of Sewage Pollutes Streams" Reprint 1063, Public Health Reports, 1926.

[12] D. O'Connor, and W. Dobbins, "The Mechanism of Reaeration in Natural Streams" J. San. Eng. Div. (ASCE) SA6, 1115-1-1115-30, Dec. 1956.

[13] W. P. Isaacs, "Atmospheric Oxygenation and Biological Deoxygenation in an idealized Stream Flow Model" Ph.D. Dissertation, Oklahoma State University, Stillwater, Oklahoma, May, 1967.

[14] P. A. Krenkel, and G. T. Orlob, "Turbulent Diffusion and the Reaeration Coefficient" J. San. Eng. Div. (ASCE), 3(88):SA2, p.53, March, 1962.

[15] G. H. Fair, " The Dissolved Oxygen Sag-Analysis" Sewage Works J., 11(0):445, 1939.

WETLAND SYSTEM FOR WATER QUALITY IMPROVEMENT IN RURAL AREAS

Prof. Dr. Alaa H. Wadie Al-Fatlawi

Abstract: **This paper highlights the use of a pilot-scale surface-flow constructed wetland (SFW) consists of a septic tank, and wetland cell, for removal of biochemical oxygen demand (BOD), chemical oxygen demand (COD), total suspended solids (TSS), nitrite (NO2), nitrate (NO3), ammonia (NH3), phosphate (PO4), hydrogen ion concentration (pH), oil and grease (O&G), sulfate (SO4), hydrogen sulfide (H2S), and temperature (T), from a pretreated residential wastewater. The primary treated wastewater in a household septic tanks hauled by a tank to the proposed site. The constructed wetland is a surface type consists of emergent and floating plants.**

The scale plant was constructed at rural area (Alkhairat Village) of Al-Hilla province/Iraq. Two types of macrophytes, viz. Typha latifolia and Phragmites carca, were planted. The treatment wetland is composed of five rows of a 30 m long wetland channel. The BOD of the effluent concentrations was varied between 4 to 38 mg/l, with average concentration of 22 mg/l, and removal efficiency of 88.3% .

The average removal efficiencies of COD and TSS were 77.11 % and 80.8% respectively. As depicted from the results, the COD:BOD5 ratio of influent wastewater was 1.44. The average measured concentration of in the effluent was 35.8mg/L with an average removal efficiency equal to

During the monitoring period, the NO2, NO3, NH3, PO4, pH, O & G, SO4, and H2S, average effluent concentrations were 0.5, 31.65, 2.29, 1.02, 7.5, 47.76, 887.62 mg/l, respectively, with an effluent temperature of 24.45 oC.

According to these results, it can be concluded that the wetland system utilized in this research could be a suitable solution for raw wastewater as a stand-alone treatment, although a pre-treatment in order to remove grit, heavy solids and floatable materials would be necessary.

Index Terms— **pilot-scale, SFW; septic tank; BOD; COD; TSS; nitrogen content; phosphate.**

I. INTRODUCTION

IN both developed and developing countries the quality of water is deteriorating from time to time in two different angles. The problems are not the same. In developed countries eutriphication is the prominent problem but the main problem of developing country is lack of sanitation and water supply for drinking and other purposes. Wastewater treatment is a problem that has plagued man ever since he discovered that discharging his wastes into surface waters can lead to many additional environmental problems. Today, a wide range of treatment technologies are available for use in our efforts to restore and maintain the chemical, physical, and biological integrity of the nation's waters. During the past 20 years, considerable interest has been expressed in the potential use of a variety of natural biological systems to help purify water in a controlled manner. These natural biological treatment systems include various forms of ponds, land treatment and wetlands systems. As a result of both extensive research efforts and practical application of these technologies, considerable insight has been gained into their design, performance, operation and maintenance, [1].

Constructed wetlands are artificial wetlands, designed to utilize natural aquatic plants and organisms to improve water quality, retain storm water for flood control during heavy rain events, and provide wildlife habitat. Treatment of storm water and wastewater occurs in constructed wetlands by a number of processes. A constructed wetland can also serve as habitat for wildlife, and potentially as a recreational site if it is designed to maintain its principal functions while safeguarding public health. Wetlands designed for effluent polishing typically receive disinfected secondary effluent and rely on the wetland system to accomplish the equivalent of tertiary treatment. Constructed wetland systems require more space than mechanized treatment processes, but use little or no energy for operation, [2].

Constructed wetland treatment systems are engineered systems that have been designed and constructed to utilize the natural processes involving wetland vegetation, soils, and their associated microbial assemblages to assist in treating wastewater. They are designed to take advantage of many of the processes that occur in natural wetlands, but do so within a more controlled environment. Synonymous terms to *constructed* include *manmade, engineered* or *artificial* wetlands.

Wetlands have been used to provide tertiary treatment to municipal wastewater as an alternative to conventional methods. Wetland utilization generates economic savings: because they rely on more natural methods, they are less expensive to build and operate than conventional sewage treatment (e.g., less electricity consumption); furthermore the purified water is suitable for reuse, [3].

Nitrogen removal in wastewater treatment is important because of the potential hazard it causes to both living things and the ecosystem. For example, high nitrogen concentrations in water can directly affect human health, as when nitrate in drinking water causes methemoglobinemia in infants, commonly known as 'blue baby syndrome' [4]. However, the primary impact of nitrogen is due to its role as a limiting nutrient in many aquatic environments. Nitrogen is the limiting nutrient in most marine environments. Elevated nitrogen inputs into bodies of water can result in increased plant growth and

Manuscript received June 29, 2015.
Prof. Dr. Alaa H. Wadie Al-Fatlawi , College of Engineering / Babylon University, Iraq (phone: +9647801595607; e-mail: dr_ahw@yahoo.com).

eutrophication. Eutrophication due to nitrogen inputs have been implicated in loss of species diversity [5], and increased occurrence of harmful algal blooms such as red tide, which threaten both human and ecosystem health [6], [7]. Excessive nutrients in aquatic systems cause eutrophication, which can lead to decreased dissolved oxygen levels and fish kills [1].

Constructed wetlands can be built with a much greater degree of control than natural systems, thus allowing the establishment of experimental treatment facilities with well-defined composition of substrate, type of vegetation, and flow pattern. In addition, constructed wetlands offer several additional advantages compared to natural wetlands including site selection, flexibility in sizing, and most importantly, control over the hydraulic pathways and retention time, [8].

The major types of constructed wetlands are: [2]

- *Free-water-surface [FWS) constructed wetlands*. Wetland systems with open water areas containing submerged, floating, and emergent vegetation. FWS systems, or soil substrate systems, consist of aquatic plants rooted in a soil substrate within a constructed earthen basin that may or may not be lined depending on soil permeability and groundwater protection requirements [9]. FWS systems are designed to accept preliminary-treated, low-velocity wastewater, in plug flow, over the top of the soil media or at a depth between 1 and 18 inches.
- *Subsurface-flow (SF) constructed wetlands.* Wetland systems composed of bed of gravel or other granular support packing containing emergent plants. The water to be treated flows through the packing and plant roots during operation. SFS are typically gravel substrate systems that are similar to FWS systems, however, aquatic vegetation is planted in gravel or crushed stone and wastewater flows approximately 6 inches below the surface of the media. The aggregate typically has a depth between 12 and 24 inches. No visible surface flow is evident in SF [9].
- *Floating aquatic plant systems(APS).* Engineered wetland system consisting of a channel with floating plants with high surface area roots of varying lengths. APS also are similar to FWS systems, but the water is located in deeper ponds and aquatic floating aquatic plants or submerged plants are used [10].
- *Combination systems.* Various arrangements of the systems described above, Because constructed wetlands are engineered systems, the earthwork for these systems includes the construction of berms to contain the wetland area and an impermeable clay or plastic liner to prevent water exchange with groundwater.

2. Advantages & Disadvantages

Some Advantages and Disadvantages are listed below, [11].

Advantages:

1. Constructed wetlands are typically inexpensive to build and maintain.
2. They require little or no energy to operate.
3. They can provide effective tertiary treatment.
4. They can provide additional wildlife habitat.
5. They can be aesthetically pleasing additions to homes and neighborhoods.
6. They are viewed as an environmentally friendly technology and are generally well received by the public.

Disadvantages:

1. Constructed wetlands require more land area than many other treatment options.
2. Surface flow wetlands can attract mosquitoes and other pests.
3. Wetlands are not appropriate for treating some wastewater with high concentrations of certain pollutants.
4. The performance of wetlands may vary based on usage and climatic conditions.
5. There may be a prolonged initial start-up period before vegetation is adequately established.

3. Study Area

The pilot scale treatment wetland is built and constructed in the Rural Municipality of Hilla province (Alkhairat Village). The wetland receives rural wastewater from a septic tanks. Most septic tanks are approximately 3m length by 2m width and 2.5m in depth, with a total storage volume of 15 m^3 [12]. There are no direct sewage lines into the wetland facility, so sewage is aged for an unknown length of time in septic tanks before hauling by septic trucks to the wetland. The treatment wetland is composed of a 30 m long wetland channel "rows". The five rows were intended to achieve a 'snaking' configuration whereby water would enter the wetland at a single point and exit after passing through all of the rows. The wetland was designed to retain water at a depth of 15 to 30 cm throughout the year (Fig. 1). In reality, the residence time in the wetland is likely much shorter than originally anticipated (five to ten days). This is due to water entering the wetland via all of the rows and flowing directly through to drainage.

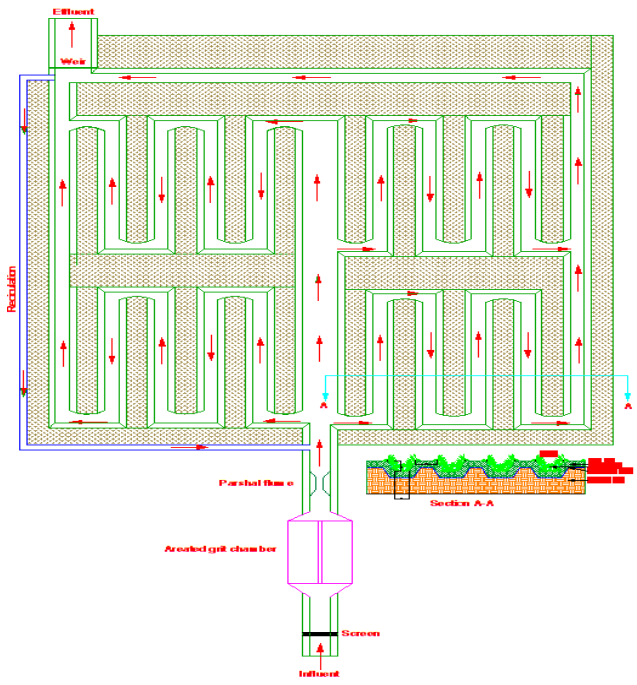

Fig. 1: Plan and section of scale plant wetland used in the study.

4. Conceptual Framework of the Design of Constructed Wetlands System Constructed wetlands are designed to mimic natural wetlands and use plants and microorganisms to treat effluent. [13] suggests the following guidelines for creating successful constructed wetlands: keep the design simple. Complex technological approaches often invite failure. design for minimal maintenance. design the system to use natural energies, such as gravity flow. design for the extremes of weather and climate, not the average. Storms, floods, and droughts are to be expected and planned for, not feared. design the wetland with the landscape, not against it. Integrate the design with the natural topography of the site. avoid over-engineering the design with rectangular basins, rigid structures and channels, and regular morphology. Mimic natural systems. give the system time. Wetlands do not necessarily become functional overnight and several years may elapse before performance reaches optimal levels. Strategies that try to short-circuit the process of system development or to over-manage often fail. 1 design the system for function, not form. For instance, if initial plantings fail, but the overall function of the wetland, based on initial objectives, is intact, then the system has not failed. A constructed wetland system consists of a septic tank, the wetland cell(s), and a method for returning the treated wastewater back to the environment, through a drainage system. In the septic tank, wastewater receives initial treatment. Anaerobic bacteria begin to break down wastes, and solids settle to form a sludge layer, while greases and oils float to form a scum layer. The clarified middle layer (effluent) travels to the constructed wetland cell.

From the wetland, effluent goes through a water-level control weirs that allows the wetland water level to be adjusted. The size and configuration of surface flow systems are based on estimates and strengths of the influent, climatic factors: (temperatures, evapotranspiration rates, and precipitation amounts to predict and maintain the level of water in the system). The design include multiple cells each providing the same level of treatment that may be operated simultaneously or independently. The inlet and outlet are located on opposite sides.

The bottom has a slight downgrade (approximately 0.5 percent) to assist the flow of wastewater through the cell by gravity (common slopes in residential systems range from 0 to 1 percent).

Cells usually was excavated by hand. Slightly sloping the wetland bottom helps gravity move effluent through the cell. The size of the system was determine based on temperature, which affects how fast the wetland can remove nutrients and other pollutants, and the amount of effluent that needs treatment, typically determined by the number of bedrooms in the home. This information is used to determine hydraulic retention time (the amount of time effluent needs to stay in the wetland for proper treatment). The longer the effluent stays in the wetland, the more time microorganisms and plants have to treat the water. Generally, effluent should stay in the wetland system for five days. After treatment in the wetland cell, effluent travel to a drainage system.

The cell bottom prevent wastewater from seeping into the groundwater below and the surrounding environment by using a polyethylene liner. Soil placed on top of the lining to form a substrate that will support the growth of wetland plants.

To prevent short-circuiting of the wastewater flow, the wastewater enter the channel of each cell. Wastewater enters surface flow cells by means of weirs at the inlet. At the outlet, the system has control weir to help operators adjust the water level.

The system was designed for the wastewater to flow once through the system. However, systems was designed to re-circulate all or a portion of the effluent to treat the wastewater more than once.

Fig. 2: Scale plant wetland used in the study in different configurations.

5. Samples Collection

Sampling was performed both before and after wetland release during the period from March to June of 2014. There were a total of two sampling sites in the wetland, (Fig. 1). The two sites were selected at the influent entry point and the outlet into the surrounding drainage.

Grab samples for nutrient analyses, total suspended solids (TSS), were collected using sterile 500 ml polyethylene bottles and 4 l amber glass bottles, as required for the analytical procedures. Each bottle and cap was rinsed three times with sample water.

6. Analytical Methods and Equipment's

A brief description of the methods and equipment's used to measure the considered parameters were performed following the methods described in Environmental Chemistry, [14].

BOD COD, Temperature, pH, NO_3, NO_2, were monitored. For each of the parameters, samples were analyzed in duplicates in order to minimize errors. The samples were only filtered for ammonium and nitrate analyses. Total suspended solids (TSS) were quantified according to a modified procedure based on Standard Methods for the Examination of Water and Wastewater.

7. Results

The standard BOD for typical constructed wetland influent from septic tank ranges between 310 to 344 mg/l [15]. The BOD of the effluent concentrations was varied between 4 to 38 mg/l. The measured average concentration of BOD_5 in the effluent was 22 mg/l. The average BOD_5

removal wetlands was 88.3% this is agreed with the findings of [16], that the treatment efficiency of wetlands for BOD_5 is very high.

The COD of the effluent concentrations was varied between 166 to 412 mg/l. effluents had average COD removal efficiencies of 77.11 %. As depicted from the results, the COD:BOD_5 ratio of influent wastewater was 1.44. Total suspended solids (TSS) of the effluent concentrations was varied between 21 to 60 mg/l. The measured average concentration of TSS in the effluent was 35.8mg/l with an average removal efficiency equal to 80.8%.

Nitrogen in wastewater exists in many forms. Each of the nitrogen forms is inter convertible and they are components of the nitrogen cycle. During the monitoring period, the NO_3 average effluent concentrations was 31.6 mg/l. There was a scarce of dissolved oxygen level in the wetland system. Even though NH_3 concentration in the wetlands was sufficient but the absence of oxygen in the wetland hinders the nitrification activity. The NH_3 effluent concentrations varied between 1.1 and 6 mg/l with an average of 2.3 mg/l. The concentration- based NH_3 removal efficiencies was 86.2%. The variation of the other parameters are illustrated in Figs. 3 to 14.

During the monitoring period, the NO_2, NO_3, PO_4, pH, O&G, SO_4, and H_2S, average effluent concentrations were 0.5, 31.65,2.29, 7.5, 47.76and 887.62, respectively, with an effluent temperature of 24.45 ^oC.

According to these results, it can be concluded that the wetland system utilized in this research could be a suitable solution for raw wastewater as a stand-alone treatment, although a pre-treatment in order to remove grit, heavy solids and floatable materials would be necessary.

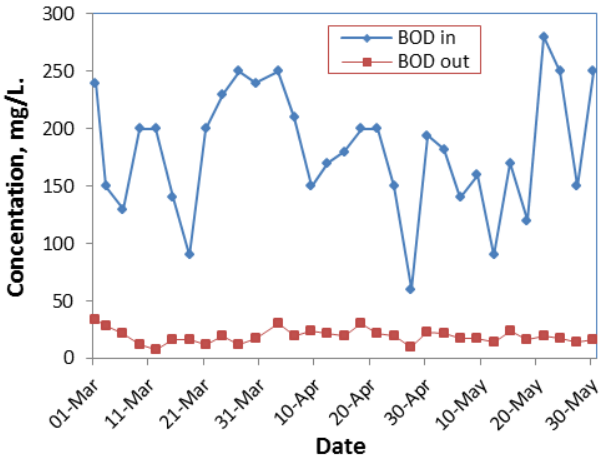

Fig. 3: Variation of BOD with time through the pilot scale-wetland

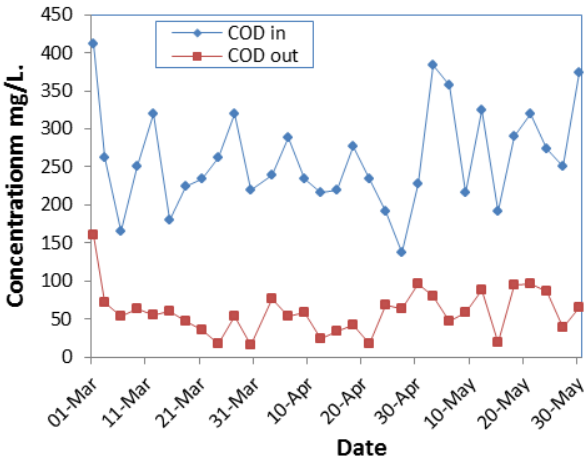

Fig. 4: Variation of COD with time through the pilot scale-wetland

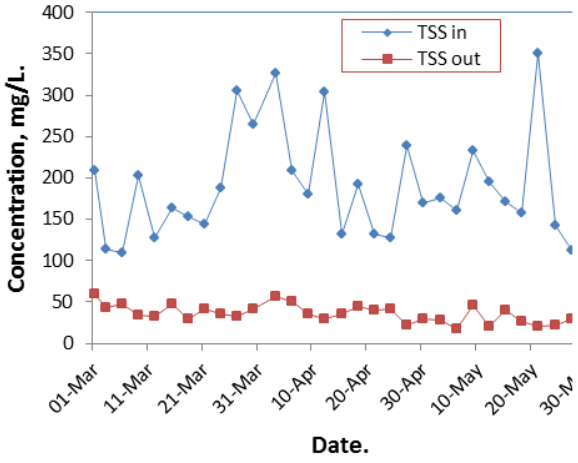

Fig. 5: Variation of TSS with time through the pilot scale-wetland

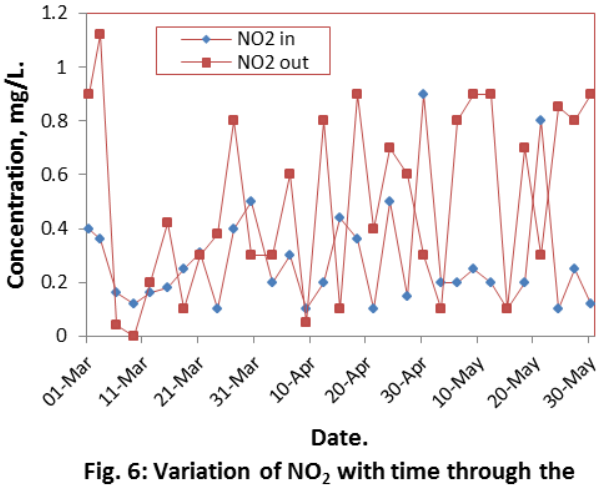

Fig. 6: Variation of NO_2 with time through the pilot scale-wetland

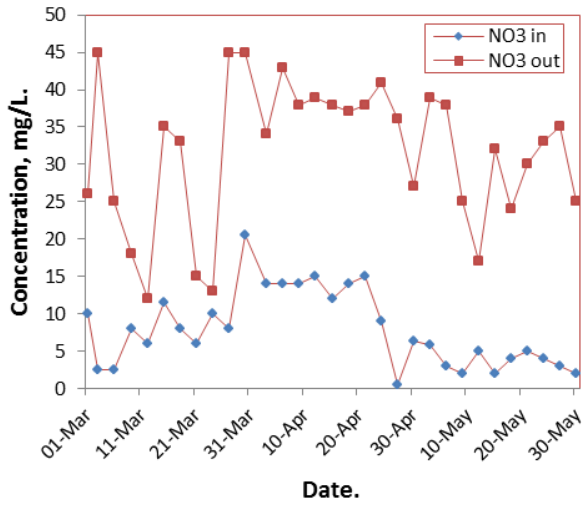

Fig. 7: Variation of NO_3 with time through the pilot scale-wetland

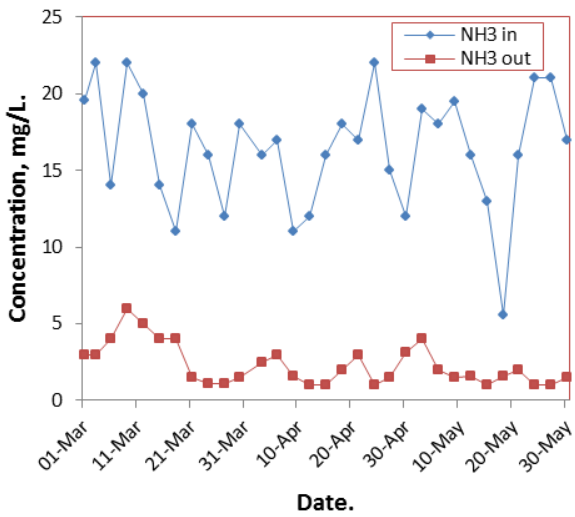

Fig. 8: Variation of NH_3 with time through the pilot scale-wetland

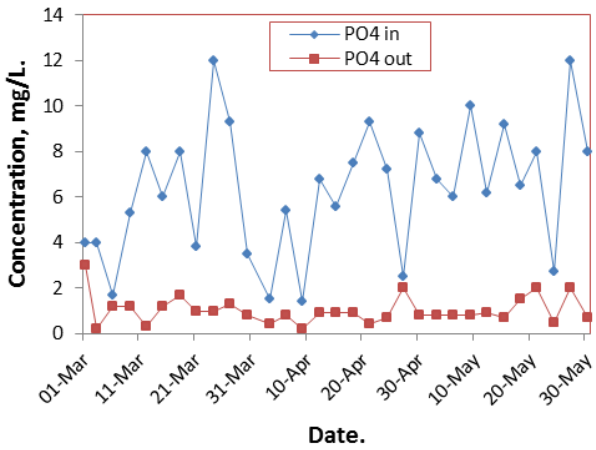

Fig. 9: Variation of PO_4 with time through the pilot scale-wetland

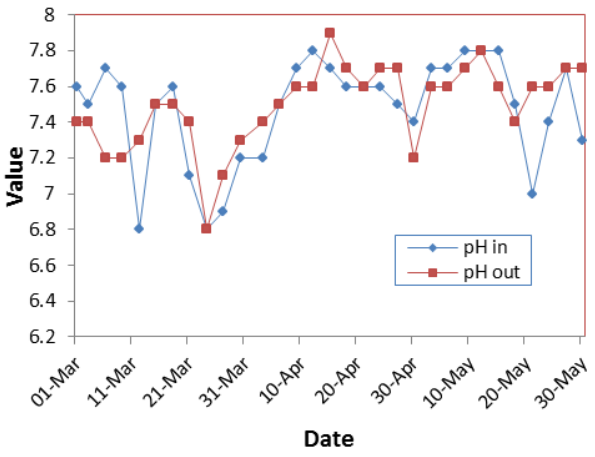

Fig. 10: Variation of pH with time through the pilot scale-wetland

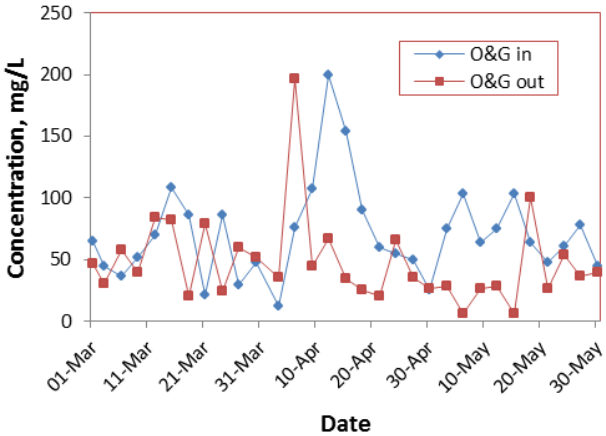

Fig. 11: Variation of oil (O) and grease (G) with time through the pilot scale-wetland

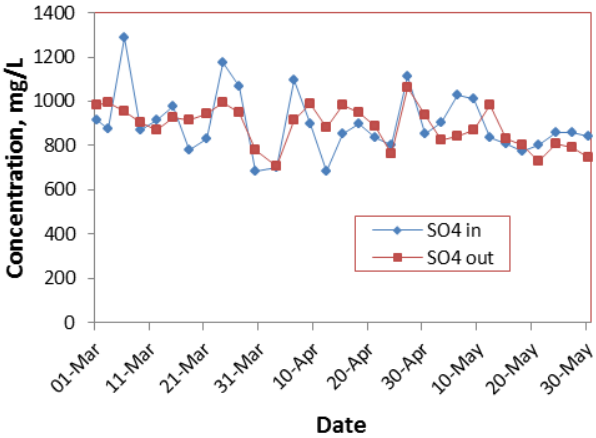

Fig. 12: Variation of SO_4 with time through the pilot scale-wetland

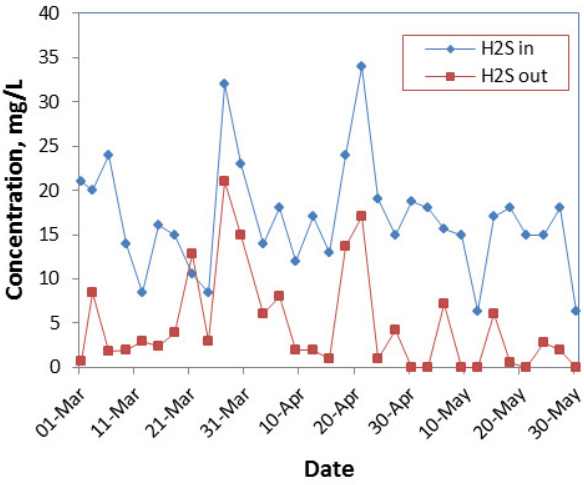

Fig. 13: Variation of H_2S with time through the pilot scale-wetland

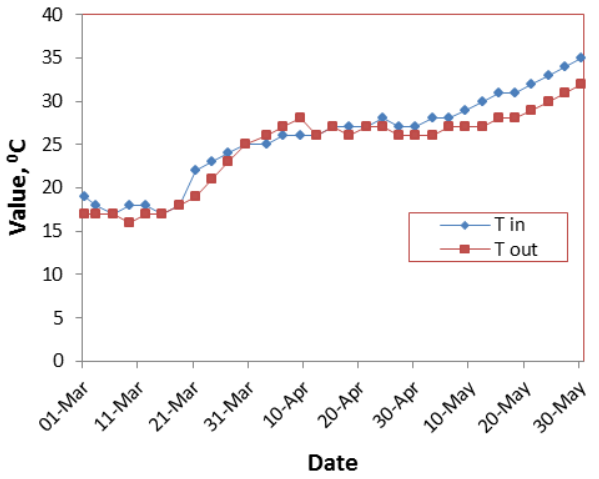

Fig. 14: Variation of Temperature (T) with time through the pilot scale-wetland

8. Conclusions

The constructed wetland treatment was found to be efficient in removal of BOD, and economically viable. The system, being easy to operate and low cost, can provide an economical viable solution for wastewater management in rural areas.

According to these results, it can be concluded that the wetland system utilized in this research could be a suitable solution for raw wastewater as a stand-alone treatment, although a previous pre-treatment is required to remove grit, heavy solids and floatable materials.

- The findings of this research showed that there was a significance removal efficiency for BOD and COD.
- These systems offer an effective means of integrating wastewater treatment and resource enhancement, often at a cost that is competitive with conventional wastewater treatment alternatives.
- The results show that the growing interest in the use of constructed wetlands as a part of water treatment offers considerable opportunity for realizing sizable future savings in wastewater treatment costs for small communities and for upgrading even large treatment facilities.
- Water surface systems, remove pollutants from the wastewater effluent. These systems affect water quality through a variety of natural processes that occur in wetlands.
- There is an obvious need for further study to improve our understanding of the internal components of these systems, their responses and interactions, in order to allow for more optimum project design, operation and maintenance.
- The use of wetlands for treatment can significantly lower the cost of wastewater treatment because the systems rely on plant and animal growth instead of the addition of power or chemicals.

References

[1]Abira M. A., 2008, "A pilot constructed treatment wetland for pulp and paper mill waste water", Unpublished PhD dissertation. Delft, The Netherlands.

[2]Metcalf and Eddy Inc., 1991, "Wastewater engineering: treatment, disposal and reuse", 3rd ed. McGraw Hill, New York, p. 1334.

[3] Siracusa, G., La Rosa, A.D, 2006, "Design of a constructed wetland for wastewater treatment in a Sicilian town and environmental evaluation using the energy analysis, ecological modeling", 1 9 7 490–497.

[4]Bastviken, S., 2006, " Nitrogen removal in treatment wetlands- Factors influencing spatial and temporal variations", Linkoping Studies in Science and Technology. Linkoping, Sweden, Linkoping University, Institute of Technology: 34.

[5]Joseph, K., 2005, "Optimizing processes for nitrogen removal in Nakivubo wetlands", Uganda. Stockholm, Royal Institute of Technology: 57.

[6]Anderson, D. M., P. M. Gilbert, et al., 2002, "Harmful algal blooms and eutrophication: Nutrient sources, composition, and consequences", Estuaries Vol. 25, No.4b, p 704726.

[7]Kangas, P., 2004, "Ecological engineering: principles and practice", Boca Raton, Florida, Lewis Publishers.

[8]Brix, H. ,1998, "Constructed wetlands for wastewater treatment in Europe", Leiden, Backhuys publishers.

[9]Freeman, R.J. Jr, 1993, "Constructed wetlands experience in the southeast, in constructed wetlands for water quality and improvement", Chapter 6, G.A. Moshiri, ed., CRC Press, Boca Raton, FL.

[10] Witthar, S.R., 1993, "Wetland water treatment systems, in constructed wetlands for water quality and improvement", Chapter 14, G.A. Moshiri, ed., CRC Press, Boca Raton, FL.

[11] Bruggen, J. J. A. v., 2007, "Wetland for water quality", Delft, UNESCO-IHE Institute for Water Education.

[12] Municipality of Hilla, 2014, "septic tanks design

data" unpublished data.
[13] Mitsch, W. J. 1992. Landscape design and the role of created, restored and natural riparian wetlands in controlling nonpoint source pollution. Ecological Engineering l(1992): 27-47.
[14] Kruis, F., 2005, "Environmental chemistry: selected analytical methods", Delft : IHE.
[15] U.S Environmental Protection Agency (USEPA), 2000, "Technology Transfer, Process Manual for Sludge Treatment and Disposal", Washington D.C.
[16] Kadlec, R. H., and R. L. Knight,1996, "Treatment wetlands", Boca Raton, CRC Press, Inc.

رقم الايداع في دار الكتب والوثائق 161 لسنة 2016

المؤتمر الدولي الثاني لهندسة البناء والإنشاءات والبيئة

17-18 تشرين الأول 2015

BCEE2

بيروت - لبنان

الجزء 5: محور الهندسة الصحية والبيئية والموارد المائية